

PHYTOCHEMICALS WITH α -GLUCOSIDASE INHIBITORY ACTIVITY FROM *CISSUS JAVANA*,
DENDROBIUM CHRISTYANUM, *GASTROCHILUS BELLINUS* AND *HUBERANTHA JENKINSII*



A Dissertation Submitted in Partial Fulfillment of the Requirements
for the Degree of Doctor of Philosophy in Pharmacognosy
Department of Pharmacognosy and Pharmaceutical Botany
FACULTY OF PHARMACEUTICAL SCIENCES
Chulalongkorn University
Academic Year 2019
Copyright of Chulalongkorn University

สารพจนานุกรมที่มีฤทธิ์ยับยั้งแอลฟาไกลูโคซิเดสจากดาตตะกัวเถา เอื้องชะงูกระดิ่ง เสือดำ
และตั้งงาขาว



วิทยานิพนธ์นี้เป็นส่วนหนึ่งของการศึกษาตามหลักสูตรปริญญาวิทยาศาสตรดุษฎีบัณฑิต
สาขาวิชาเภสัชเวช ภาควิชาเภสัชเวชและเภสัชพฤษศาสตร์
คณะเภสัชศาสตร์ จุฬาลงกรณ์มหาวิทยาลัย
ปีการศึกษา 2562
ลิขสิทธิ์ของจุฬาลงกรณ์มหาวิทยาลัย

ยะตุ ดินท์ ชัน : สารพฤกษเคมีที่มีฤทธิ์ยับยั้งแอลฟาไกลูโคซิเดสจากตาดตะกั่วเถา เอื้องแซะภูกระดึง เสือดำ และดั่งงาขาว. (PHYTOCHEMICALS WITH α -GLUCOSIDASE INHIBITORY ACTIVITY FROM *CISSUS JAVANA*, *DENDROBIUM CHRISTYANUM*, *GASTROCHILUS BELLINUS* AND *HUBERANTHA JENKINSII*) อ.ที่ปรึกษาหลัก : ศ. ภก. ดร.กิตติศักดิ์ ลิขิตวิทยาวุฒิ, อ.ที่ปรึกษาร่วม : รศ. ภก. ดร.บุญชู ศรีตุลารักษ์

การศึกษาพฤกษเคมีของต้นตาดตะกั่วเถา *Cissus javana* DC., เอื้องแซะภูกระดึง *Dendrobium christyanum* Rchb. f., เสือดำ *Gastrochilus bellinus* Rchb. f. Kuntze และดั่งงาขาว *Huberantha jenkinsii* (Hook. f. & Thomson) Chaowasku สามารถแยกสารได้ทั้งสิ้น 27 ชนิด ในจำนวนนี้เป็นสารธรรมชาติใหม่ 6 ชนิด โดยจากต้นตาดตะกั่วเถา *Cissus javana* แยกได้สาร 3 ชนิด ซึ่งมีโครงสร้างเป็นที่รู้จัก ได้แก่ bergenin, stigmast-4-en-3-one และ β -sitosterol จากต้นเอื้องแซะภูกระดึง *Dendrobium christyanum* แยกได้สารจำนวน 13 ชนิด ซึ่งมีโครงสร้างเป็นที่รู้จัก ได้แก่ *n*-eicosyl *trans*-ferulate, *n*-docosyl 4-hydroxy-*trans*-cinnamate, 4,5-dihydroxy-2-methoxy-9,10-dihydrophenanthrene, moscatilin, aloifol I, gigantol, batatasin III, dendrosinen B, coniferyl aldehyde, methyl haematommate, atraric acid, vanillin และ diorcinolic acid ส่วนต้นเสือด้า *Gastrochilus bellinus* แยกได้สารที่มีโครงสร้างใหม่จำนวน 4 ชนิด แบ่งเป็นสารในกลุ่ม phenanthropyrans จำนวน 3 ชนิด และสารอนุพันธ์ของ phenanthrene จำนวน 1 ชนิด และจากต้นดั่งงาขาว *Huberantha jenkinsii* แยกได้สารใหม่ที่มีโครงสร้างเป็น 8-oxoprotoberberine จำนวน 2 ชนิดและสารซึ่งเป็นที่รู้จักจำนวน 5 ชนิดคือ mangiferin, allantoin, oxylipinine, *N-trans*-feruloyl tyramine และ *N-trans-p*-coumaroyl tyramine การศึกษาโครงสร้างที่แยกได้เหล่านี้ใช้วิธีวิเคราะห์คุณสมบัติทางสเปกโทรสโกปีแบบ UV, IR, MS และ NMR ร่วมกับ การเปรียบเทียบกับ ข้อมูลที่มีรายงานมาก่อน เมื่อนำสารที่แยกได้มาศึกษาฤทธิ์ยับยั้งเอนไซม์ α -glucosidase พบว่ามีสารที่มีฤทธิ์แรงได้แก่ methyl haematommate (IC_{50} 18.7 \pm 2.1 μ M), *n*-docosyl 4-hydroxy-*trans*-cinnamate (IC_{50} 4.6 \pm 0.2 μ M), *N-trans*-feruloyltyramine (IC_{50} 30.6 \pm 2.9 μ M) และ *N-trans-p*-coumaroyl tyramine (IC_{50} 0.6 \pm 0.1 μ M) เมื่อเทียบกับ ยา acarbose (IC_{50} 724.7 \pm 46 μ M) นอกจากนี้ ได้ทำการศึกษาเพิ่มเติมเกี่ยวกับฤทธิ์การกระตุ้นการนำกลูโคสเข้าสู่เซลล์ L6 ของสารบางชนิดที่แยกได้ พบว่าสาร *N*-docosyl 4-hydroxy-*trans*-cinnamate (0.212 mM) กระตุ้นการนำกลูโคสเข้าสู่เซลล์เพิ่มขึ้นร้อยละ 31.6 \pm 4.4 สาร mangiferin สามารถยับยั้งเอนไซม์ α -glucosidase ในระดับปานกลาง (IC_{50} 253.6 \pm 14.2 μ M) และแสดงฤทธิ์กระตุ้นการนำกลูโคสเข้าสู่เซลล์ (เพิ่มขึ้นร้อยละ 208.1 \pm 10.7 ที่ความเข้มข้น 0.237 mM) โดยเปรียบเทียบกับ insulin (เพิ่มขึ้นร้อยละ 146.6 \pm 35.8 ที่ความเข้มข้น 500 nM).

สาขาวิชา เภสัชเวท
ปีการศึกษา 2562

ลายมือชื่อนิสิต
ลายมือชื่อ อ.ที่ปรึกษาหลัก
ลายมือชื่อ อ.ที่ปรึกษาร่วม

6076457433 : MAJOR PHARMACOGNOSY

KEYWORD: α -glucosidase, *Cissus javana*, *Dendrobium christyanum*, *Gastrochilus bellinus*,
Huberantha jenkinsii, glucose uptake

Htoo Tint San : PHYTOCHEMICALS WITH α -GLUCOSIDASE INHIBITORY ACTIVITY FROM *CISSUS JAVANA*, *DENDROBIUM CHRISTYANUM*, *GASTROCHILUS BELLINUS* AND *HUBERANTHA JENKINSII*. Advisor: Prof. KITTISAK LIKHITWITAYAWUID, Ph.D. Co-advisor: Assoc. Prof. BOONCHOO SRITULARAK, Ph.D.

Phytochemical investigations of *Cissus javana* DC., *Dendrobium christyanum* Rchb. f., *Gastrochilus bellinus* Rchb. f. Kuntze and *Huberantha jenkinsii* (Hook. f. & Thomson) Chaowasku led to the isolation of twenty-seven compounds, six of which were new naturally occurring compounds. From *Cissus javana*, three known compounds were isolated, including bergenin, stigmast-4-en-3-one, and β -sitosterol. From *Dendrobium christyanum*, thirteen known compounds were identified, namely, *n*-eicosyl *trans*-ferulate, *n*-docosyl 4-hydroxy-*trans*-cinnamate, 4,5-dihydroxy-2-methoxy-9,10-dihydrophenanthrene, moscatilin, aloifol I, gigantol, batatasin III, dendrosinen B, coniferyl aldehyde, methyl haematommate, atraric acid, vanillin and diorcinolic acid. From *Gastrochilus bellinus*, four new compounds, comprising three phenanthropyrans and a phenanthrene derivative, were isolated and structurally characterized. From *Huberantha jenkinsii*, two new alkaloids of 8-oxoprotoberberine type were isolated along with five known compounds including mangiferin, allantoin, oxylopinine, *N-trans*-feruloyl tyramine and *N-trans-p*-coumaroyl tyramine. The structures of these compounds were determined by UV, IR, MS and NMR spectroscopic methods, and comparison of the data with literature values. Methyl haematommate (IC_{50} $18.7 \pm 2.1 \mu M$), *n*-docosyl 4-hydroxy-*trans*-cinnamate (IC_{50} $4.6 \pm 0.2 \mu M$), *N-trans*-feruloyl tyramine (IC_{50} $30.6 \pm 2.9 \mu M$) and *N-trans-p*-coumaroyl tyramine (IC_{50} $0.6 \pm 0.1 \mu M$) showed potent α -glucosidase inhibitory activity in comparison with the drug acarbose (IC_{50} $724.7 \pm 46 \mu M$). *N*-Docosyl 4-hydroxy-*trans*-cinnamate at 0.212 mM also displayed 31.6 ± 4.4 % enhancement of glucose uptake in L6 cells. Mangiferin showed moderate α -glucosidase inhibition (IC_{50} $253.6 \pm 14.2 \mu M$) and recognizable cellular glucose uptake stimulatory activity (208.1 ± 10.7 % enhancement at a concentration of 0.237 mM) as compared with insulin (146.6 ± 35.8 % at a concentration of 500 nM).

Field of Study: Pharmacognosy

Student's Signature

Academic Year: 2019

Advisor's Signature

Co-advisor's Signature

ACKNOWLEDGEMENTS

First and foremost, I owe a great debt of gratitude to my thesis advisor, Professor Dr. Kittisak Likhitwitayawuid and my co-advisor Associate Professor Dr. Boonchoo Sritularak, for their expert guidance, immense knowledge, encouragement and continuous optimism concerning the thesis research and endless support that lead to successful completion of this study.

I would like to express my profound thanks to the members of my thesis committee for their valuable suggestion, and would like to owe my gratitude to all teachers and staff members of the Department of Pharmacognosy and Pharmaceutical Botany, as well as the staff members of the Faculty of Pharmaceutical Sciences, Chulalongkorn University for provision of all facilities.

I would like to extend my sincere thanks to Graduate School, Chulalongkorn University for CU-ASEAN scholarship for my Ph. D. study.

I would like to thank the Rector of the University of Pharmacy (Yangon) and Dr. Su Su Yee (Head of Pharmacognosy Department, UOP, Yangon, Retired) for giving me permission to pursue this Ph.D. degree in Chulalongkorn University. A special thanks to my seniors and colleagues in Department of Pharamcognosy, UOP, Yangon for standing with me throughout my study.

I would like to appreciate all of my friends in Thailand for their warmest heart and kindest help to me during this time.

Finally, my greatest gratitude is also expressed to my parents for their love and mortal support throughout the course of this Ph.D degree to accomplish flawlessly.

Htoo Tint San

TABLE OF CONTENTS

	Page
ABSTRACT (THAI).....	iii
ABSTRACT (ENGLISH).....	iv
ACKNOWLEDGEMENTS.....	v
TABLE OF CONTENTS.....	vi
LIST OF TABLES.....	14
LIST OF FIGURES.....	17
LIST OF SCHEMES.....	25
ABBREVIATIONS AND SYMBOLS.....	26
CHAPTER I INTRODUCTION.....	29
CHAPTER II LITERATURE REVIEW.....	38
1. <i>Cissus javana</i> DC.....	38
1.1 Taxonomic considerations and traditional uses.....	38
1.2 Chemical studies.....	39
1.3 Biological studies.....	45
2. <i>Dendrobium christyanum</i>	46
2.1 Taxonomic considerations and traditional uses.....	46
2.2 Chemical studies.....	47
2.3 Biological studies.....	118
3. <i>Gastrochilus bellinus</i>	120
3.1 Taxonomic considerations and traditional uses.....	120
3.2 Chemical studies.....	121

3.3 Biological studies.....	121
4. <i>Huberantha jenkinsii</i>	122
4.1 Taxonomic considerations and traditional uses	122
4.2 Chemical studies.....	123
4.3 Biological studies.....	124
CHAPTER III EXPERIMENTAL.....	125
1. Source of plant materials	125
1.1 <i>Cissus javana</i>	125
1.2 <i>Dendrobium christyanum</i>	125
1.3 <i>Gastrochilus bellinus</i>	125
1.4 <i>Huberantha jenkinsii</i>	125
2. General techniques.....	126
2.1 Analytical thin-layer chromatography (TLC).....	126
2.1.1 Normal-phase thin-layer chromatography	126
2.1.2 Reverse-phase thin-layer chromatography.....	126
2.2 Column chromatography (CC).....	126
2.2.1 Vacuum liquid chromatography (VLC).....	126
2.2.2 Flash column chromatography (FCC), normal phase.....	127
2.2.3 Flash column chromatography (FCC), reverse phase	127
2.2.4 Gel filtration chromatography.....	128
2.2.5 Semi-preparative high-pressure liquid chromatography (HPLC).....	128
2.3 Spectroscopy	129
2.3.1 Mass spectra	129
2.3.2 Ultraviolet (UV) spectra	129

2.3.3 Infrared (IR) spectra	129
2.3.4 Proton and carbon-13 nuclear magnetic resonance (^1H and ^{13}C -NMR) spectra.....	129
2.3.5 Optical rotations	130
2.4 Solvents	130
3 Extraction and isolation.....	131
3.1 Extraction and isolation of compounds from <i>Cissus javana</i>	131
3.1.1 Extraction	131
3.1.2 Isolation	131
3.1.2.1 Isolation of compound CJ1 (bergenin).....	131
3.1.2.2 Isolation of compounds CJ2 (stigmast-4-en-3-one) and CJ3 (β -sitosterol).....	131
3.2 Extraction and isolation of compounds from <i>Dendrobium christyanum</i>	133
3.2.1 Extraction	133
3.2.2 Isolation.....	134
3.2.2.1 Isolation of compound DC1 (methyl haematommate)....	134
3.2.2.2 Isolation of compounds DC2 (<i>n</i> -eicosyl <i>trans</i> -ferulate) and DC3 (atraric acid)	135
3.2.2.3 Isolation of compound DC4 (<i>n</i> -docosyl 4-hydroxy- <i>trans</i> -cinnamate).....	135
3.2.2.4 Isolation of compound DC5 (vanillin).....	135
3.2.2.5 Isolation of compound DC6 (coniferyl aldehyde).....	135
3.2.2.6 Isolation of compound DC7 (4,5-dihydroxy-2-methoxy 9,10-dihydrophenanthrene).....	135
3.2.2.7 Isolation of compound DC8 (moscatilin).....	136

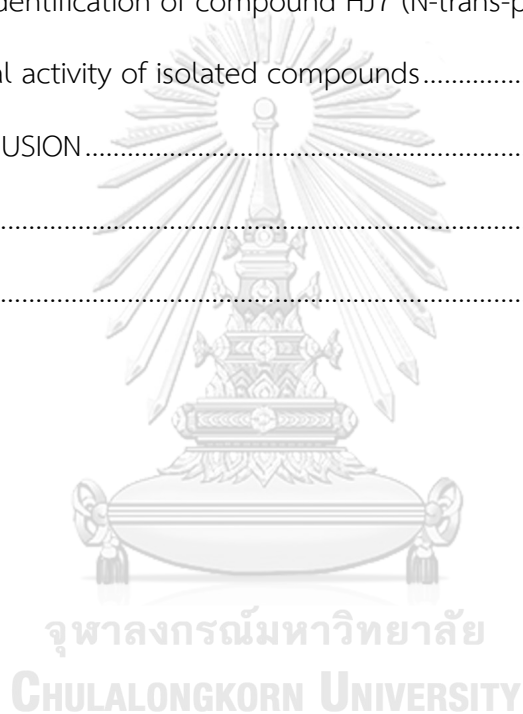
3.2.2.8 Isolation of compound DC9 (aloifol I).....	136
3.2.2.9 Isolation of compound DC10 (gigantol).....	136
3.2.2.10 Isolation of compound DC11 (batatasin III).....	136
3.2.2.11 Isolation of compound DC12 (dendrosinen B)	136
3.2.2.12 Isolation of compound DC13 (diorcinic acid)	137
3.3 Extraction and isolation of compounds from <i>Gastrochilus bellinus</i>	141
3.3.1 Extraction	141
3.3.2 Isolation.....	142
3.3.2.1 Isolation of compounds GB1	142
3.3.2.2 Isolation of compound GB2.....	142
3.3.2.3 Isolation of compounds GB3 and GB4	142
3.4 Extraction and isolation of compounds from <i>Huberantha jenkinsii</i>	144
3.4.1 Extraction.....	144
3.4.2 Isolation.....	145
3.4.2.1 Isolation of compound compounds HJ1 (mangiferin).....	145
3.4.2.2 Isolation of compounds HJ2, HJ3, HJ4 (allantoin) and HJ5 (oxylopinine).....	145
3.4.2.3 Isolation of compound HJ6 (<i>N-trans-feruloyl</i> tyramine). 145	
3.4.2.4 Isolation of compound HJ7 (<i>N-trans-p-coumaroyl</i> tyramine).....	146
4. Physical and spectral data of isolated compounds	148
4.1 Compound CJ1 (bergenin) [31]	148
4.2 Compound CJ2 (stigmast-4-en-3-one) [341]	148
4.3 Compound CJ3 (β -sitosterol) [33].....	148

4.4 Compound DC1 (methyl haematommate) [342]	149
4.5 Compound DC2 (<i>n</i> -eicosyl <i>trans</i> -ferulate) [343].....	149
4.6 Compound DC3 (atraric acid) [344].....	149
4.7 Compound DC4 (<i>n</i> -docosyl 4-hydroxy- <i>trans</i> -cinnamate) [345].....	149
4.8 Compound DC5 (vanillin) [274].....	150
4.9 Compound DC6 (coniferyl aldehyde) [346]	150
4.10 Compound DC7 (4,5-dihydroxy-2-methoxy-9,10- dihydrophenanthrene) [103]	150
4.11 Compound DC8 (moscatilin) [59].....	150
4.12 Compound DC9 (aloifol I) [38].....	151
4.13 Compound DC10 (gigantol) [54].....	151
4.14 Compound DC11 (batatasin III) [41].....	151
4.15 Compound DC12 (dendrosinen B) [73].....	151
4.16 Compound DC13 (diorcinic acid) [347]	152
4.17 Compound GB1 [348].....	152
4.18 Compound GB2 [349].....	152
4.19 Compound GB3 [350]	152
4.20 Compound GB4 [351].....	153
4.21 Compound HJ1 (mangiferin) [337]	153
4.22 Compound HJ2 [352].....	153
4.23 Compound HJ3 [353].....	153
4.24 Compound HJ4 (allantoin) [354]	154
4.25 Compound HJ5 (oxylopinine) [355]	154
4.26 Compound HJ6 (<i>N-trans</i> -feruloyltyramine) [10].....	154

4.27 Compound HJ7 (<i>N-trans-p-coumaroyl tyramine</i>) [356].....	154
5. Assay for α -glucosidase inhibitory activity.....	155
5.1 Materials and instruments.....	155
5.2 Determination of α -glucosidase inhibitory activity.....	155
6. Assay for glucose uptake stimulatory activity	156
6.1 Materials and instruments.....	157
6.2 Determination of glucose uptake stimulatory activity	157
6.3 Determination of cell viability.....	158
6.4 Statistical analysis	158
CHAPTER IV RESULTS AND DISCUSSION	159
1. Phytochemical and biological studies of <i>Cissus javana</i>	159
1.1 Preliminary biological activity evaluation	159
1.2 Chemical investigation	159
1.2.1 Identification of compound CJ1 (bergenin).....	160
1.2.2 Identification of compound CJ2 (stigmast-4-en-3-one)	165
1.2.3 Identification of compound CJ3 (β -sitosterol).....	167
1.3 Biological activity of isolated compounds.....	170
2. Phytochemical and biological studies of <i>Dendrobium christyanum</i>	174
2.1 Preliminary biological activity evaluation	174
2.2 Chemical investigation	175
2.2.1 Identification of compound DC1 (methyl haematommate).....	177
2.2.2 Identification of compound DC2 (<i>n</i> -eicosyl <i>trans</i> -ferulate).....	182
2.2.3 Identification of compound DC3 (atraric acid)	188

2.2.4 Identification of compound DC4 (<i>n</i> -docosyl 4-hydroxy- <i>trans</i> -cinnamate).....	194
2.2.5 Identification of compound DC5 (vanillin).....	198
2.2.6 Identification of compound DC6 (coniferyl aldehyde).....	203
2.2.7 Identification of compound DC7 (4,5-dihydroxy-2-methoxy-9,10-dihydrophenanthrene).....	208
2.2.8 Identification of compound DC8 (moscatilin).....	213
2.2.9 Identification of compound DC9 (aloifol I).....	216
2.2.10 Identification of compound DC10 (gigantol).....	221
2.2.11 Identification of compound DC11 (batatasin III).....	226
2.2.12 Identification of compound DC12 (dendrosinen B).....	232
2.2.13 Identification of compound DC13 (diorcinolic acid).....	237
2.3 Biological activity of isolated compounds.....	242
3. Phytochemical and biological studies of <i>Gastrochilus bellinus</i>	247
3.1 Preliminary biological activity evaluation.....	247
3.2 Chemical investigation.....	247
3.2.1 Structure elucidation of compound GB1.....	248
3.2.2 Structure elucidation of compound GB2.....	259
3.2.2 Structure elucidation of compound GB3.....	267
3.2.3 Structure elucidation of compound GB4.....	273
3.3 Biological activity of isolated compounds.....	282
4. Phytochemical and biological studies of <i>Huberantha jenkinsii</i>	282
4.1 Preliminary biological activity evaluation.....	282
4.2 Chemical investigation.....	283

4.2.1 Identification of compound HJ1 (mangiferin)	284
4.2.2 Structure elucidation of compound HJ2	291
4.2.3 Structure elucidation of compound HJ3	303
4.2.4 Identification compound HJ4 (allantoin).....	314
4.2.5 Identification of compound HJ5 (oxylopinine).....	319
4.2.6 Identification of compound HJ6 (<i>N-trans</i> -feruloyltyramine).....	323
4.2.7 Identification of compound HJ7 (<i>N-trans-p</i> -coumaroyl tyramine)....	329
4.3 Biological activity of isolated compounds.....	333
CHAPTER V CONCLUSION	337
REFERENCES	340
VITA.....	368



LIST OF TABLES

Table 1 Examples of α -glucosidase inhibitors from plants.....	32
Table 2 Distribution of secondary metabolites in the genus <i>Cissus</i>	40
Table 3 Distribution of secondary metabolites in the genus <i>Dendrobium</i>	48
Table 4 NMR spectral data of compound CJ1 as compared with bergenin	162
Table 5 NMR spectral of compound CJ2 as compared with stigmast-4-en-3-one	166
Table 6 NMR spectral data of compound CJ3 as compared with β -sitosterol.....	168
Table 7 α -Glucosidase inhibitory activity of compounds isolated from <i>C. javana</i> ..	172
Table 8 Glucose uptake stimulatory activity of compounds isolated from <i>C. javana</i>	173
Table 9 α -Glucosidase inhibitory activity of fractions.....	175
Table 10 NMR spectral data of compound DC1 as compared with methyl haematommate	179
Table 11 NMR spectral data of compound DC2 as compared with <i>n</i> -eicosyl <i>trans</i> - ferulate	184
Table 12 NMR spectral data of compound DC3 as compared with atraric acid.....	189
Table 13 NMR spectral data of compound DC4 as compared with <i>n</i> -docosyl 4- hydroxy- <i>trans</i> - cinnamate.....	196
Table 14 NMR spectral data of compound DC5 as compared with vanillin.....	199
Table 15 NMR spectral data of compound DC6 as compared with coniferyl aldehyde	204
Table 16 NMR spectral data of compound DC7 as compared with 4,5-dihydroxy-2- methoxy-9,10-dihydrophenanthrene.....	209
Table 17 NMR spectral data of compound DC8 as compared with moscatilin	214
Table 18 NMR spectral data of compound DC9 as compared with aloifol I.....	218

Table 19 NMR spectral data of compound DC10 as compared with gigantol	223
Table 20 NMR spectral data of compound DC11 as compared with batatasin III.....	228
Table 21 NMR spectral data of compound DC12 as compared with dendrosinen B233	
Table 22 NMR spectral data of compound DC13 as compare with diorcinolic acid	238
Table 23 α -Glucosidase inhibitory activity of compounds isolated from <i>D. christyanum</i>	243
Table 24 Glucose uptake stimulatory activity of compounds isolated form <i>D. christyanum</i>	245
Table 25 α -Glucosidase inhibitory activity of extracts from <i>Gastrochilus bellinus</i> ...	247
Table 26 NMR spectral data of compound GB1	250
Table 27 NMR spectral data of compound GB2	261
Table 28 NMR spectral data of compound GB3	268
Table 29 NMR spectral data of compound GB4	275
Table 30 α -Glucosidase inhibitory activity of compounds isolated from <i>Gastrochilus bellinus</i>	282
Table 31 α -Glucosidase inhibitory activity of extracts from <i>Huberantha jenkinsii</i> ...	283
Table 32 NMR spectral data of compound HJ1 as compared with mangiferin	287
Table 33 NMR spectral data of compound HJ2.....	293
Table 34 NMR spectral data of compound HJ3.....	305
Table 35 NMR spectral data of compound HJ4 as compared with allantoin	315
Table 36 NMR spectral data of compound HJ5 as compared with oxylopinine	320
Table 37 NMR spectral data of compound HJ6 as compared with <i>N-trans-feruloyltyramine</i>	325
Table 38 NMR spectral data of compound HJ7 as compared with <i>N-trans-p-coumaroyl tyramine</i>	330

Table 39 α -Glucosidase inhibitory activity of compounds isolated from *H. jenkinsii*
..... 334

Table 40 Glucose uptake stimulatory activity of compounds isolated from *H. jenkinsii*
..... 335



LIST OF FIGURES

Figure 1 Structures of α -glucosidase inhibitors from plants	34
Figure 2 <i>Cissus javana</i> DC.....	39
Figure 3 Structures of compounds from <i>Cissus</i>	42
Figure 4 <i>Dendrobium christyanum</i> Rchb. f.....	47
Figure 5 Structures of compounds from <i>Dendrobium</i>	85
Figure 6 <i>Gastrochilus bellinus</i> (Rchb.f.) Kuntze	121
Figure 7 <i>Huberantha jenkinsii</i> (Hook. f. & Thomson) Chaowasku.....	122
Figure 8 Structures of compounds from <i>Huberantha</i>	123
Figure 9 Rat skeletal (L6) myoblasts (a) and Rat skeletal (L6) myotubes (b).....	156
Figure 10 Structures of compounds isolated from <i>Cissus javana</i>	160
Figure 11 Mass spectrum of compound CJ1.....	163
Figure 12 $^1\text{H-NMR}$ (300 MHz) spectrum of compound CJ1 (DMSO- d_6)	163
Figure 13 $^{13}\text{C-NMR}$ (75 MHz) and DEPT-135 spectra of compound CJ1 (DMSO- d_6)....	164
Figure 14 HSQC spectrum of compound CJ1	164
Figure 15 HMBC spectrum of compound CJ1 (DMSO- d_6).....	165
Figure 16 Mass spectrum of compound CJ2.....	166
Figure 17 $^1\text{H-NMR}$ (300 MHz) spectrum of compound CJ2 (CDCl $_3$)	167
Figure 18 Mass spectrum of compound CJ3.....	169
Figure 19 $^1\text{H-NMR}$ (300 MHz) spectrum of compound CJ3 (CDCl $_3$)	170
Figure 20 Cytotoxicity (a) and glucose uptake stimulation (b) of MeOH extract, fractions and bergenin	174
Figure 21 Structures of compounds isolated from <i>Dendrobium christyanum</i>	176
Figure 22 Mass spectrum of compound DC1.....	180

Figure 23	$^1\text{H-NMR}$ (500 MHz) spectrum of compound DC1 (CDCl_3)	180
Figure 24	$^{13}\text{C-NMR}$ (125 MHz) spectrum of compound DC1 (CDCl_3)	181
Figure 25	HSQC spectrum of compound DC1	181
Figure 26	HMBC spectrum of compound DC1.....	182
Figure 27	Mass spectrum of compound DC2.....	185
Figure 28	$^1\text{H-NMR}$ (300 MHz) spectrum of compound DC2 (CDCl_3)	185
Figure 29	^{13}C NMR (75 MHz) and DEPT-135 spectra of compound DC2 (CDCl_3).....	186
Figure 30	NOESY spectrum of compound DC2	186
Figure 31	HSQC spectrum of compound DC2	187
Figure 32	HMBC spectrum of compound DC2.....	187
Figure 33	Mass spectrum of compound DC3.....	190
Figure 34	$^1\text{H-NMR}$ (300 MHz) spectrum of compound DC3 (acetone- d_6).....	191
Figure 35	$^{13}\text{C-NMR}$ (75 MHz) spectrum of compound DC3 (acetone- d_6).....	191
Figure 36	HSQC spectrum of compound DC3.....	192
Figure 37	NOESY spectrum of compound DC3	193
Figure 38	HMBC spectrum of compound DC3.....	194
Figure 39	Mass spectrum of compound DC4.....	197
Figure 40	$^1\text{H-NMR}$ (300 MHz) spectrum of compound DC4 (acetone- d_6).....	198
Figure 41	Mass spectrum of compound DC5.....	200
Figure 42	$^{13}\text{C-NMR}$ (75 MHz) spectrum of compound DC5 (acetone- d_6).....	201
Figure 43	$^1\text{H-NMR}$ (300 MHz) spectrum of compound DC5 (acetone- d_6).....	201
Figure 44	HSQC spectrum of compound DC5	202
Figure 45	HMBC spectrum of compound DC5.....	202
Figure 46	Mass spectrum of compound DC6.....	205

Figure 47 $^1\text{H-NMR}$ (300 MHz) spectrum of compound DC6 (acetone- d_6).....	205
Figure 48 COSY spectrum of compound DC6.....	206
Figure 49 $^{13}\text{C-NMR}$ (75 MHz) spectrum of compound DC6 (acetone- d_6).....	206
Figure 50 HSQC spectrum of compound DC6	207
Figure 51 HMBC spectrum of compound DC6.....	207
Figure 52 Mass spectrum of compound DC7.....	210
Figure 53 $^1\text{H-NMR}$ (300 MHz) spectrum of compound DC7 (acetone- d_6).....	211
Figure 54 $^{13}\text{C-NMR}$ (75 MHz) and DEPT-35 spectra of compound DC7 (acetone- d_6). 211	
Figure 55 HSQC spectrum of compound DC7	212
Figure 56 HMBC spectrum of compound DC7.....	212
Figure 57 Mass spectrum of compound DC8.....	215
Figure 58 $^1\text{H-NMR}$ (300 MHz) spectrum of compound DC8 (acetone- d_6).....	215
Figure 59 $^{13}\text{C-NMR}$ (75 MHz) spectrum of compound DC8 (acetone- d_6).....	216
Figure 60 Mass spectrum of compound DC9.....	219
Figure 61 $^1\text{H-NMR}$ (300 MHz) spectrum of compound DC9 (acetone- d_6).....	219
Figure 62 $^{13}\text{C-NMR}$ (75 MHz) spectrum of compound DC9 (acetone- d_6).....	220
Figure 63 HSQC spectrum of compound DC9	220
Figure 64 HMBC spectrum of compound DC9.....	221
Figure 65 Mass spectrum of compound DC10	224
Figure 66 $^1\text{H-NMR}$ (300 MHz) spectrum of compound DC10 (acetone- d_6)	224
Figure 67 $^{13}\text{C-NMR}$ (75 MHz) spectrum of compound DC10 (acetone- d_6)	225
Figure 68 NOESY spectrum of compound DC10	225
Figure 69 Mass spectrum of compound DC11	229
Figure 70 $^1\text{H-NMR}$ (300 MHz) spectrum of compound DC11 (acetone- d_6)	229

Figure 71 ^{13}C -NMR (75 MHz) and DEPT-135 spectra of compound DC11 (acetone- d_6)	230
Figure 72 HSQC spectrum of compound DC11	230
Figure 73 NOESY spectrum of compound DC11	231
Figure 74 HMBC spectrum of compound DC11	231
Figure 75 Mass spectrum of compound DC12	234
Figure 76 ^{13}C -NMR (75 MHz) and DEPT-135 spectra of compound DC12 (acetone- d_6)	234
Figure 77 ^1H -NMR (300 MHz) spectrum of compound DC12 (acetone- d_6)	235
Figure 78 NOESY spectrum of compound DC12	235
Figure 79 HSQC spectrum of compound DC12	236
Figure 80 HMBC spectrum of compound DC12	236
Figure 81 Mass spectrum of compound DC13	239
Figure 82 ^1H -NMR (300 MHz) spectrum of compound DC13 (acetone- d_6)	240
Figure 83 ^{13}C -NMR (75 MHz) spectrum of compound DC13 (acetone- d_6)	240
Figure 84 HSQC spectrum of compound DC13	241
Figure 85 HMBC spectrum of compound DC13	241
Figure 86 Cytotoxicity (a) and glucose uptake stimulatory activity (b) of extract and isolated compounds	244
Figure 87 Structures of compounds isolated from <i>Gastrochilus bellinus</i>	248
Figure 88 Mass spectrum of compound GB1	251
Figure 89 UV spectrum of compound GB1	252
Figure 90 IR spectrum of compound GB1	252
Figure 91 ^1H -NMR (300 MHz) spectrum of compound GB1 (acetone- d_6)	253
Figure 92 ^{13}C -NMR (75 MHz) and DEPT-135 spectra of compound GB1 (acetone- d_6)	253

Figure 93	HSQC spectrum of compound GB1	254
Figure 94	HMBC spectrum of compound GB1	255
Figure 95	NOESY spectrum of compound GB1	258
Figure 96	Mass spectrum of compound GB2.....	262
Figure 97	UV spectrum of compound GB2	263
Figure 98	IR spectrum of compound GB2	263
Figure 99	^1H -NMR (300 MHz) spectrum of compound GB2 (acetone- d_6).....	264
Figure 100	^{13}C -NMR (75 MHz) and DEPT-135 spectra of compound GB2 (acetone- d_6).....	264
Figure 101	HSQC spectrum of compound GB2	265
Figure 102	HMBC spectrum of compound GB2.....	265
Figure 103	NOESY spectrum of compound GB2	266
Figure 104	Mass spectrum of compound GB3	269
Figure 105	UV spectrum of compound GB3	270
Figure 106	IR spectrum of compound GB3.....	270
Figure 107	^1H -NMR (300 MHz) spectrum of compound GB3 (acetone- d_6)	271
Figure 108	^{13}C -NMR (75 MHz) and DEPT-135 spectra of compound GB3 (acetone- d_6)	271
Figure 109	HSQC spectrum of compound GB3	272
Figure 110	HMBC spectrum of compound GB3.....	272
Figure 111	NOESY spectrum of compound GB3	273
Figure 112	Mass spectrum of compound GB4	276
Figure 113	UV spectrum of compound GB4	277
Figure 114	IR spectrum of compound GB4	277
Figure 115	^1H -NMR (300 MHz) spectrum of compound GB4 (acetone- d_6)	278

Figure 116 ^{13}C -NMR(75 MHz) and DEPT-135 spectra of compound GB4 (acetone- d_6)	278
Figure 117 HSQC spectrum of compound GB4	279
Figure 118 HMBC spectrum of compound GB4.....	279
Figure 119 NOESY spectrum of compound GB4	281
Figure 120 Structures of compounds isolated from <i>Huberantha jenkinsii</i>	284
Figure 121 Mass spectrum of compound HJ1	288
Figure 122 ^1H -NMR (300 MHz) spectrum of compound HJ1 (acetone- d_6).....	288
Figure 123 COSY spectrum of compound HJ1	289
Figure 124 ^{13}C -NMR (75 MHz) spectrum of compound HJ1 (acetone- d_6).....	289
Figure 125 HSQC spectrum of compound HJ1.....	290
Figure 126 HMBC spectrum of compound HJ1	290
Figure 127 Mass spectrum of compound HJ2.....	294
Figure 128 UV spectrum of compound HJ2.....	294
Figure 129 IR spectrum of compound HJ2.....	295
Figure 130 ^1H -NMR (500 MHz) spectrum of compound HJ2 (acetone- d_6).....	295
Figure 131 COSY spectrum of compound HJ2	296
Figure 132 ^{13}C -NMR (125 MHz) spectrum of compound HJ2 (acetone- d_6).....	297
Figure 133 HSQC spectrum of compound HJ2.....	298
Figure 134 NOESY spectrum of compound HJ2.....	299
Figure 135 HMBC spectrum of compound HJ2	301
Figure 136 Mass spectrum of compound HJ3	306
Figure 137 UV spectrum of compound HJ3.....	306
Figure 138 IR spectrum of compound HJ3.....	307

Figure 139	COSY spectrum of compound HJ3	307
Figure 140	^1H -NMR (500 MHz) spectrum of compound HJ3 (acetone- d_6).....	308
Figure 141	^{13}C -NMR (125 MHz) spectrum of compound HJ3 (acetone- d_6).....	309
Figure 142	HSQC spectrum of compound HJ3.....	309
Figure 143	NOESY spectrum of compound HJ3.....	311
Figure 144	HMBC spectrum of compound HJ3	312
Figure 145	Mass spectrum of compound HJ4	315
Figure 146	^1H -NMR (300 MHz) spectrum of compound HJ4 (DMSO- d_6).....	316
Figure 147	^{13}C -NMR (75 MHz) spectrum of compound HJ4 (DMSO- d_6).....	316
Figure 148	HSQC spectrum of compound HJ4.....	317
Figure 149	HMBC spectrum of compound HJ4	317
Figure 150	NOESY spectrum of compound HJ4.....	318
Figure 151	Mass spectrum of compound HJ5	321
Figure 152	^1H -NMR (300 MHz) spectrum of compound HJ5 (acetone- d_6).....	321
Figure 153	^{13}C -NMR (75 MHz) spectrum of compound HJ5 (acetone- d_6).....	322
Figure 154	HSQC spectrum of compound HJ5.....	322
Figure 155	HMBC spectrum of compound HJ5	323
Figure 156	Mass spectrum of compound HJ6	326
Figure 157	^1H -NMR (300 MHz) spectrum of compound HJ6 (acetone- d_6).....	326
Figure 158	^{13}C -NMR (75 MHz) and DEPT-135 spectra of compound HJ6 (acetone- d_6)	327
Figure 159	HSQC spectrum of compound HJ6.....	327
Figure 160	HMBC spectrum of compound HJ6	328
Figure 161	NOESY spectrum of compound HJ6.....	328
Figure 162	Mass spectrum of compound HJ7	331

Figure 163 $^1\text{H-NMR}$ (300 MHz) spectrum of compound HJ7 (acetone- d_6).....	331
Figure 164 $^{13}\text{C-NMR}$ (75 MHz) and DEPT-135 spectra of compound HJ7 (acetone- d_6)	332
Figure 165 HSQC spectrum of compound HJ7.....	332
Figure 166 HMBC spectrum of compound HJ7	333
Figure 167 Cytotoxicity (a) and glucose uptake stimulatory activity (b) of isolated compounds.....	336



LIST OF SCHEMES

Scheme 1 Extraction steps for <i>Cissus javana</i>	131
Scheme 2 Isolation of compounds from fraction A of <i>Cissus javana</i>	132
Scheme 3 Isolation of compounds from fraction B of <i>Cissus javana</i>	133
Scheme 4 Extraction steps for <i>Dendrobium christyanum</i>	134
Scheme 5 Isolation of compounds from fraction A of <i>Dendrobium christyanum</i>	137
Scheme 6 Isolation of compounds from fraction B of <i>Dendrobium christyanum</i>	138
Scheme 7 Isolation of compounds from fraction C of <i>Dendrobium christyanum</i>	139
Scheme 8 Isolation of compound form fraction E of <i>Dendrobium christyanum</i>	140
Scheme 9 Extraction steps for <i>Gastrochilus bellinus</i>	141
Scheme 10 Isolation of compounds from EtOAc fraction of <i>Gastrochilus bellinus</i> ..	143
Scheme 11 Extraction steps for <i>Huberantha jenkinsii</i>	144
Scheme 12 Isolation of compound from BuOH fraction of <i>Huberantha jenkinsii</i>	146
Scheme 13 Isolation of compounds from EtOAc fraction of <i>Huberantha jenkinsii</i> ..	147

ABBREVIATIONS AND SYMBOLS

Acetone- d_6	=	Deuterated acetone
APCI-MS	=	Atmospheric Pressure Chemical Ionization Mass Spectrometry
br s	=	Broad singlet (for NMR spectra)
°C	=	Degree celsius
CC	=	Column chromatography
CDCl ₃	=	Deuterated chloroform
CH ₂ Cl ₂	=	Dichloromethane
cm	=	Centimeter
¹³ C-NMR	=	Carbon-13 Nuclear Magnetic Resonance
1-D NMR	=	One-dimensional Nuclear Magnetic Resonance
2-D NMR	=	Two-dimensional Nuclear Magnetic Resonance
d	=	Doublet (for NMR spectra)
dd	=	Doublet of doublets (for NMR spectra)
δ	=	Chemical shift
DEPT	=	Distortionless Enhancement by Polarization Transfer
DMSO- d_6	=	Deuterated dimethylsulfoxide
ϵ	=	Molar absorptivity
ESI-MS	=	Electrospray Ionization Mass Spectrometry
EtOAc	=	Ethyl acetate
FCC	=	Flash Column Chromatography
g	=	Gram
Gal	=	Galactose
GF	=	Gel Filtration
Glc	=	Glucose
HMBC	=	¹ H-detected Heteronuclear Multiple Bond Correlation

HR-ESI-MS	=	High Resolution Electrospray Ionization Mass Spectrometry
$^1\text{H-NMR}$	=	Proton Nuclear Magnetic Resonance
HSQC	=	^1H -detected Heteronuclear Single Quantum Coherence
Hz	=	Hertz
IC_{50}	=	Concentration exhibiting 50% inhibition
IR	=	Infrared
J	=	Coupling constant
Kg	=	Kilogram
L	=	Liter
λ_{max}	=	Wavelength at maximal absorption
$[\text{M-H}]^-$	=	Deprotonated molecular ion
$[\text{M+H}]^+$	=	Protonated molecular ion
$[\text{M+Na}]^+$	=	Sodium-adduct molecular ion
m	=	Multiplet (for NMR spectra)
MeOH	=	Methanol
mg	=	Milligram
μg	=	Microgram
min	=	Minute
ml	=	Milliliter
μl	=	Microliter
μM	=	Micromolar
mm	=	Millimeter
mM	=	Millimolar
MS	=	Mass spectrum
MW	=	Molecular weight
m/z	=	Mass to charge ratio

NA	=	Not applicable
nm	=	Nanometer
nM	=	Nanomolar
NMR	=	Nuclear Magnetic Resonance
NOESY	=	Nuclear Overhauser Effect Spectroscopy
ν_{\max}	=	Wave number at maximal absorption
OEt	=	Ethoxy group
OMe	=	Methoxy group
Rha	=	Rhamnose
<i>s</i>	=	Singlet (for NMR spectra)
<i>t</i>	=	Triplet (for NMR spectra)
TLC	=	Thin Layer Chromatography
UV-VIS	=	Ultraviolet and Visible spectrophotometry
VLC	=	Vacuum Liquid Column Chromatography
Xyl	=	Xylose

CHAPTER I

INTRODUCTION

Diabetes mellitus is a metabolic syndrome caused by defects in insulin secretion and action. Long-term complications of DM include cardiovascular disorders, nephropathy, neuropathy, and retinopathy, which can lead to failure of the organs and even death (Diabetes Control and Complications Trial Research Group, 1993). Insulin is an anabolic hormone secreted from the β -cells of the islets of Langerhans in the pancreas. It plays an essential role in blood glucose homeostasis by facilitating cellular glucose uptake and regulating the metabolism of protein, lipid and carbohydrate (Wilcox, 2005). In type 2 DM, impaired insulin secretion can lead to insulin resistance, which is a condition of low responsiveness of target tissues, such as liver, kidney, and adipose tissues, to circulating insulin, and this can result in postprandial hyperglycemia (Chiasson *et al.*, 2002; Sesti, 2006).

DM can be classified into 4 types according to Diabetes Canada Clinical Practice Guidelines Expert Committee (Punthakee *et al.*, 2018), as follows:

- Type 1 diabetes, which is related to absolute destruction of pancreatic β -cells of pancreas due to genetic disorder.
- Type 2 diabetes, which is commonly known as non-insulin dependent DM and caused by relative insulin deficiency which leads to insulin resistance.
- Gestational DM, which is recognized during pregnancy due to hormones released from placenta during pregnancy that can decrease the effect of insulin in the body.
- Other specific types, which are due to relatively uncommon causes such as diabetes associated with drugs or diseases.

Currently, anti-diabetic agents can be classified into several classes according to their chemical structures and mechanisms of action, including biguanides, incretin

mimetics, sodium-glucose co-transporter-2 (SGLT2) inhibitors, insulin, sulfonylureas, meglitinides, thiazolidinediones (TZDs), and α -glucosidase inhibitors (AGIs). These drugs have different targets that contribute to the regulation of glucose blood level. For example, metformin, a biguanide derivative, is the drug of choice for the management of type 2 DM. Metformin decreases hepatic gluconeogenesis and increases insulin sensitivity in peripheral tissues. Incretin mimetic compounds include GLP-1 (glucagon like peptide-1) receptor agonists which increase insulin secretion and decrease glucagon; and DPP-4 (dipeptidyl peptidase-4) inhibitors which slow the degradation of GLP. Inhibitors of SGLT2, also known as gliflozins, lower the reabsorption of glucose in the proximal renal tubule. Insulin is the last line therapy for type 1 DM and type 2 DM with inadequate glycemic control. Sulfonylureas and meglitinides stimulate the release of insulin from the pancreas by blocking the ATP-sensitive K^+ channels. TZDs are peroxisome proliferator-activated receptor (PPAR) agonists, and TZDs ameliorate insulin sensitivity in various target tissues such as liver, muscles and adipose tissues (Chaudhury *et al.*, 2017). AGIs are used in DM patients to control postprandial hyperglycemia. They inhibit α -glucosidase enzyme, which digests the dietary starch, and thereby suppress the glucose absorption in the intestine (Bischoff, 1994).

So far, only a few clinically useful AGI drugs are available, including acarbose and voglibose (Hakamata *et al.*, 2009; Yin *et al.*, 2014). However, these AGIs have some critical drawbacks. Studies have shown that 56 to 76% of patients who took AGIs suffered from side effects related to the digestive system such as bloating, flatulence, diarrhea and nausea (Du *et al.*, 2018; Mughal *et al.*, 2000). Besides, the chemical structures of these AGIs are mainly composed of sugar-like units, making their production processes quite complicated. In recent years, researchers have turned their attention to medicinal plants as an alternative source of anti-diabetic agents (Chatsumpun *et al.*, 2017; Panidthananon *et al.*, 2018).

Table 1 Examples of α -glucosidase inhibitors from plants

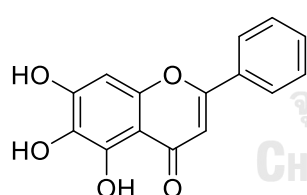
Structures	Category	Occurrence	Parts	Family
Baicalein [1]	flavonoid	<i>Scutellaria baicalensis</i> (Nishioka <i>et al.</i> , 1998)	roots	Lamiaceae
Kaempferol [2]	flavonoid	<i>Uvaria hamiltonii</i> (Meesakul <i>et al.</i> , 2018)	leaves	Annonaceae
Pinocembrin [3]	flavonoid	<i>Uvaria hamiltonii</i> (Meesakul <i>et al.</i> , 2018)	leaves	Annonaceae
Rutin [4]	flavonoid	<i>Annona macrophyllata</i> (Brindis <i>et al.</i> , 2013)	leaves	Annonaceae
Isoquercetin [5]	flavonoid	<i>Annona macrophyllata</i> (Brindis <i>et al.</i> , 2013)	leaves	Annonaceae
5-Hydroxy-3-methoxy-flavone-7-O- β -D-apiosyl-(1 \rightarrow 6)]- β -D-glucoside [6]	flavonoid	<i>Dendrobium devonianum</i> (Sun <i>et al.</i> , 2014b)	whole plant	Orchidaceae

Table 1 (continued)

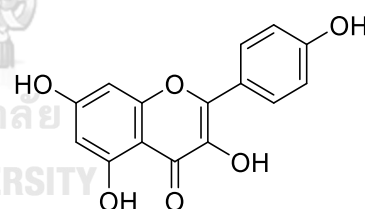
Structures	Category	Occurrence	Parts	Family
<i>trans</i> -Cinnamic acid [7]	phenylpropa- noid	<i>Drepananthus philippinensis</i> (Macabeo <i>et al.</i> , 2015)	leaves	Annonaceae
6- <i>O</i> -(<i>p</i> -Coumaroyl)-D-glucopyranoside [8]	phenylpropa- noid	<i>Vitis vinifera</i> (Sun <i>et al.</i> , 2016)	fruit	Vitaceae
Vasicine [9]	alkaloid	<i>Adhatoda vasica</i> (Gao <i>et al.</i> , 2008)	leaves	Acanthaceae
<i>N-trans</i> -Feruloyltyramine [10]	alkaloid	<i>Pseuduvaria fragrans</i> (Panidthananon <i>et al.</i> , 2018)	leaves and stem	Annonaceae
16-Hydroxycleroda-3,13-dien-15,16-olide [11]	diterpenoid	<i>Polyalthia longifolia</i> (Huang <i>et al.</i> , 2019)	leaves	Annonaceae
Oleanolic acid [12]	triterpenoid	<i>Xylopi aethiopica</i> (Mohammed <i>et al.</i> , 2019)	fruit	Annonaceae
Stigmasterol [13]	steroid	<i>Cissus populnea</i> (Nyemb, <i>et al.</i> , 2018)	root	Annonaceae

Table 1 (continued)

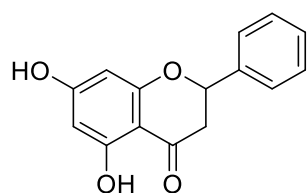
Structures	Category	Occurrence	Parts	Family
Dendrofalconerol A [14]	bibenzyl derivative (bisbibenzyl)	<i>Dendrobium tortile</i> (Limpanit <i>et al.</i> , 2016)	whole plant	Orchidaceae
5-Methoxy-7-hydroxy-9,10-dihydro-1,4-phenanthrenequinone [15]	bibenzyl derivative (phenanthrenequinone)	<i>Dendrobium formosum</i> (Inthongkaew <i>et al.</i> , 2017)	stem	Orchidaceae
Loddigesiinol J [16]	bibenzyl derivative (bisbibenzyl)	<i>Dendrobium loddigesii</i> (Lu, <i>et al.</i> , 2014)	stem	Orchidaceae



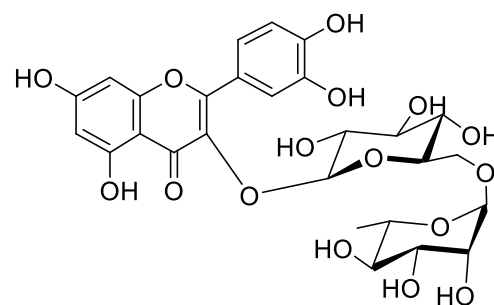
Baicalein [1]



Kaempferol [2]



Pinocembrin [3]



Rutin [4]

Figure 1 Structures of α -glucosidase inhibitors from plants

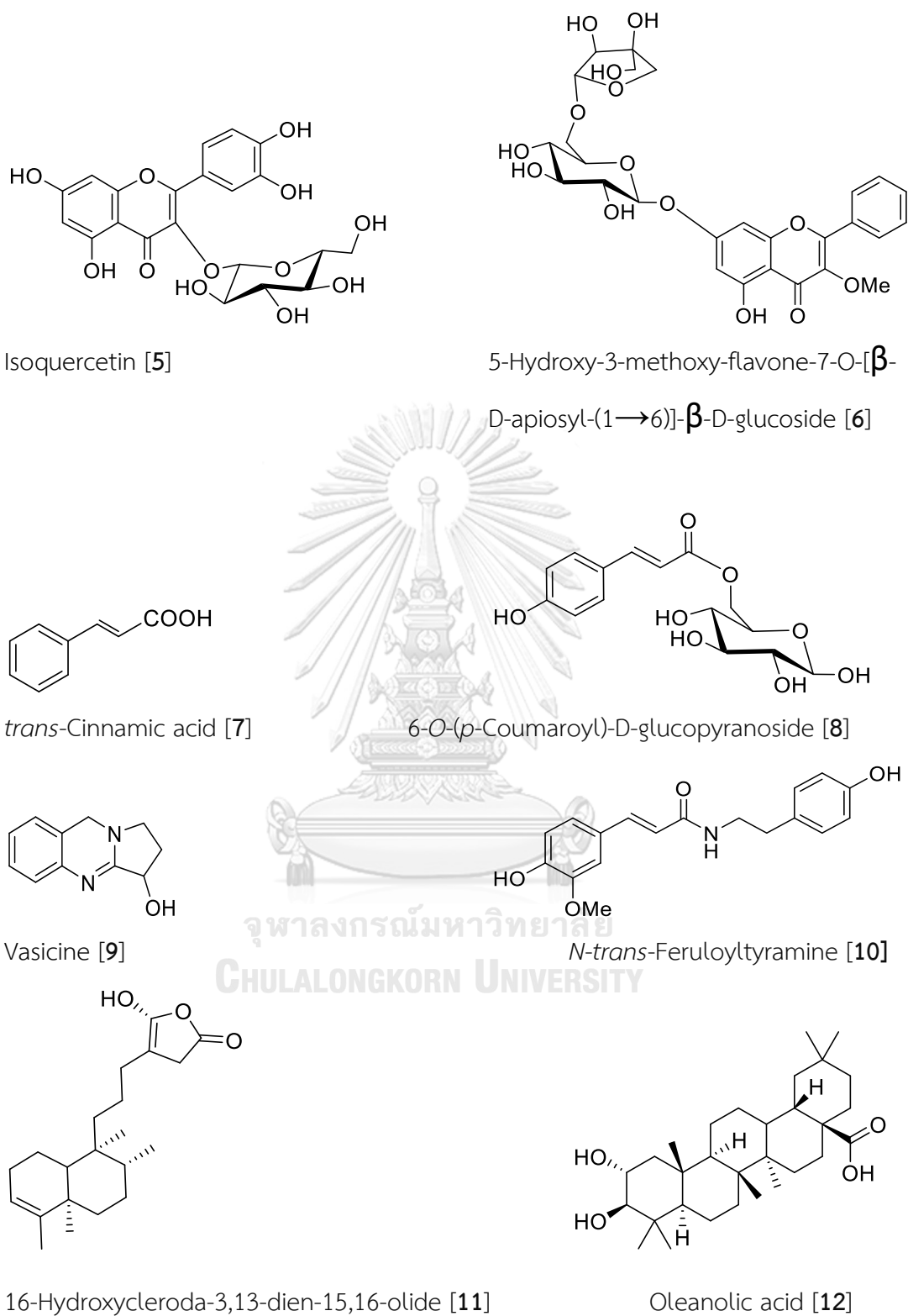


Figure 1 (continued)

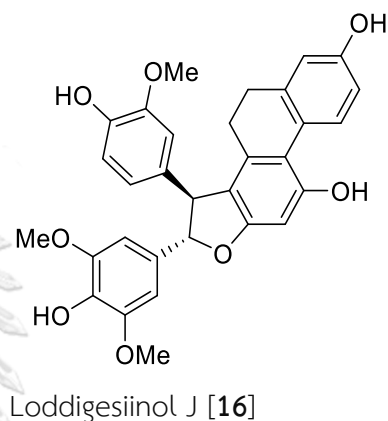
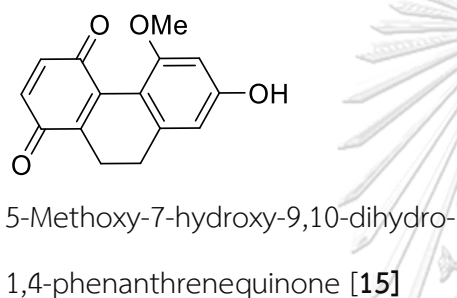
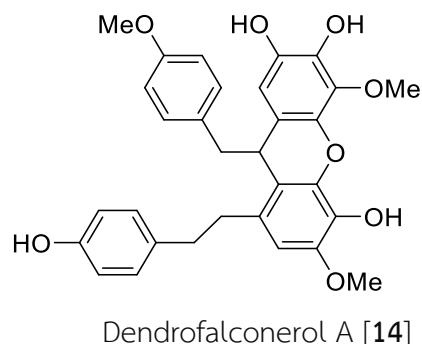
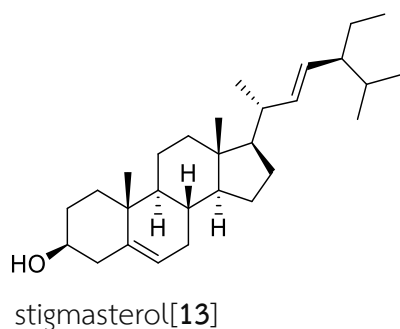


Figure 1 (continued)

It should be noted from **Table 1** that several of these AGIs are obtained from the plants in the families Annonaceae, Orchidaceae and Vitaceae. Based on these data the author decided to do preliminary screening of plants belonging to these three plant families for α -glucosidase inhibitory activity. The initial results revealed that the extracts prepared from *Cissus javana* (Vitaceae), *Dendrobium christyanum* (Orchidaceae), *Gastrochilus bellinus* (Orchidaceae) and *Huberantha jenkinsii* (Annonaceae) showed significant α -glucosidase inhibitory potential with percentage of inhibition of in the range of 70 - 100 % at a concentration of 100 μ g/ml (see the Results and Discussion). These results prompted the author to conduct chemical and biological investigations to identify the compounds responsible for the α -glucosidase inhibitory activity of these plants, and this is the primary goal of this research.

It should also be mentioned that, recently, some AGIs from plants have been shown to possess glucose-uptake stimulatory potential (Inthongkaew *et al.*, 2017; Lee & Thuong, 2010). Stimulation of glucose-uptake into muscle and adipose tissues is one of the key hypoglycemic mechanisms of several anti-DM drugs. Thus, in this study, where possible, the author would carry out additional investigations on some of the isolated compounds for their glucose-uptake enhancement potential. This secondary biological activity may help augment the antidiabetic effects of the AGIs.

Therefore, the overall objective of the current study was to find naturally occurring compounds with α -glucosidase inhibitory potential, which might be used as lead compounds for the development of new anti-DM drugs. To achieve this goal, the following objectives were put forward:

1. To isolate and characterize the structures of the chemical constituents of *Cissus javana*, *Dendrobium christyanum*, *Gastrochilus bellinus* and *Huberantha jenkinsii*.
2. To evaluate the α -glucosidase inhibitory activity of each isolated compound.
3. To carry out additional investigations, where possible, on the isolated compounds for secondary biological activity, i.e. glucose-uptake stimulatory activity.

CHAPTER II

LITERATURE REVIEW

1. *Cissus javana* DC.

1.1 Taxonomic considerations and traditional uses

The genus *Cissus* belongs to the family Vitaceae, which is also known as the grape family. *Cissus* consists of 350 species, widely distributed in China, India, Bangladesh, Nepal, and South-east Asia (Fatma, 2013; Fernandes & Banu, 2012).

Cissus plants have long been used as traditional medicine for the treatment of various ailments. In India, the extract of *Cissus quadrangularis* is used to improve the healing of bone fractures (Brahmkshatriya *et al.*, 2015). In Brazil, *C. sicyoides* has been used to treat diabetes, rheumatism and epilepsy (Fernandes & Banu, 2012; Viana *et al.*, 2004). *C. assamica* has been known for anti-snake venom property in Thailand and Nepal (Yang *et al.*, 1998). *C. araloides* has been used in antimicrobial recipes in Cameroon (Assob *et al.*, 2011). In Australia, *C. hypoglauca* has been used by indigenous people to relieve sore throat discomfort (Lassak and McCarthy, 1997).

The plant *Cissus javana* DC. is known as “Tabin-Daing-Mya-Nann” in Myanmar or “Dat Takua Thao” in Thai. It is an herbaceous climber with distinct leaves. The leaves are mostly ovate shaped with a heart-shaped base and an apiculate apex (eFloras, 2008). The upper surface contains white patches, whereas the lower surface is purple (Figure 2). The plant has been traditionally used for treating diabetes and cancer (Khin *et al.*, 2000; Sabeerali *et al.*, 2016).



Figure 2 *Cissus javana* DC.

1.2 Chemical studies

The leaves of *Cissus javana* have been earlier chemically studied (Asem *et al.*, 2014), but the structures of isolated compounds were not reported clearly. However, the roots of this plant have not been investigated.

The phytochemical studies on the other *Cissus* species have revealed the presence of several classes of chemical constituents. Examples are iridoids, flavonoids, stilbenes and terpenoids, as shown in **Table 2** and **Figure 3**.

Table 2 Distribution of secondary metabolites in the genus *Cissus*

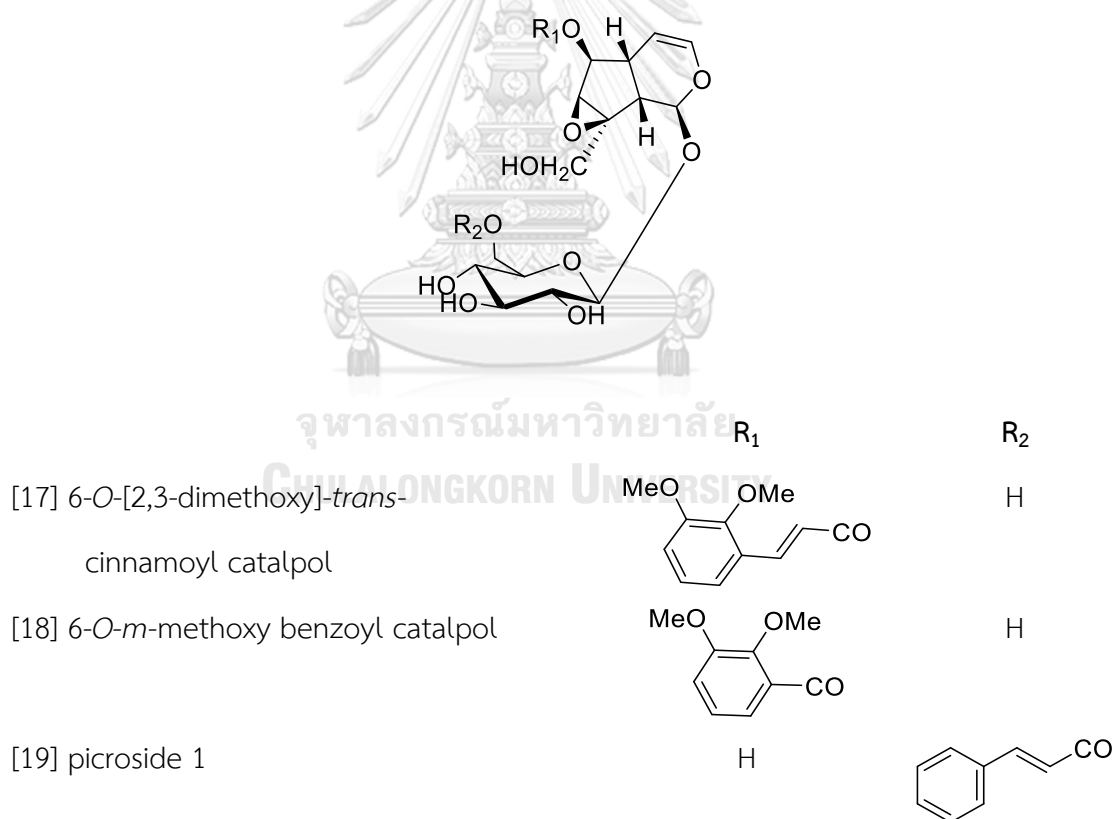
Category and compound	Plant	Plant part	references
Iridoids			
6- <i>O</i> -[2,3-Dimethoxy]- <i>trans</i> -cinnamoyl catalpol [17]	<i>C. quadrangularis</i>	stem	(Singh <i>et al.</i> , 2007)
6- <i>O</i> - <i>m</i> -Methoxybenzoyl Catalpol [18]	<i>C. quadrangularis</i>	stem	(Singh <i>et al.</i> , 2007)
Picoside 1 [19]	<i>C. quadrangularis</i>	stem	(Singh <i>et al.</i> , 2007)
Stilbenes and stilbene C-glycosides			
Quadrangularin A [20]	<i>C. quadrangularis</i>	stem	(Singh <i>et al.</i> , 2007)
Pallidol [21]	<i>C. quadrangularis</i>	stem	(Singh <i>et al.</i> , 2007)
<i>trans</i> -Resveratrol [22]	<i>C. repens</i> <i>C. vinifera</i>	aerial part fruit	(Wang <i>et al.</i> , 2007) (Langcake & Pryce, 1976)
<i>trans</i> -Resveratrol-2- <i>C</i> - β -glucoside [23]	<i>C. repens</i>	aerial part	(Wang <i>et al.</i> , 2007)
<i>trans</i> -3- <i>O</i> -Methyl-Resveratrol-2- <i>C</i> - β -glucoside [24]	<i>C. repens</i>	aerial part	(Wang <i>et al.</i> , 2007)
Cissuside A [25]	<i>C. repens</i>	aerial part	(Wang <i>et al.</i> , 2007)
Cissuside B [26]	<i>C. repens</i>	aerial part	(Wang <i>et al.</i> , 2007)
<i>cis</i> -Resveratrol-2- <i>C</i> - β -glucoside [27]	<i>C. repens</i>	aerial part	(Wang <i>et al.</i> , 2007)
<i>cis</i> -3- <i>O</i> -Methylresveratrol-2- <i>C</i> - β -glucoside [28]	<i>C. repens</i>	aerial part	(Wang <i>et al.</i> , 2007)

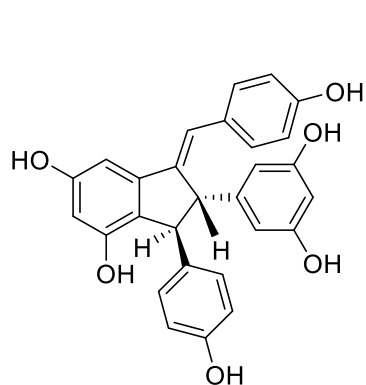
Table 2 (continued)

Category and compound	Plant	Plant part	references
Flavonoids and flavonoid glycosides			
Quercetin [29]	<i>C. quadrangularis</i>	stem	(Singh <i>et al.</i> , 2007)
Quercitrin [30]	<i>C. quadrangularis</i>	stem	(Singh <i>et al.</i> , 2007)
Isocoumarins			
Bergenin [31]	<i>C. populnea</i>	rhizomes	(Nyemb <i>et al.</i> , 2018)
	<i>C. assamica</i>	stem	(Chan <i>et al.</i> , 2018)
O-Acetylbergenin [32]	<i>C. repens</i>	rhizomes	(Nyunt <i>et al.</i> , 2012)
Steroids and steroidal glycosides			
β -Sitosterol [33]	<i>C. quadrangularis</i>	stem	(Singh <i>et al.</i> , 2007)
	<i>C. sicyoide</i>	aerial part	(Beltrame <i>et al.</i> , 2002)
	<i>C. populnea</i>	rhizomes	(Nyemb, <i>et al.</i> , 2018)
	<i>C. assamica</i>	stem	(Chan <i>et al.</i> , 2018)
β -Sitosterol glycoside [34]	<i>C. quadrangularis</i>	stem	(Singh <i>et al.</i> , 2007)
	<i>C. sicyoide</i>	aerial part	(Beltrame <i>et al.</i> , 2002)
	<i>C. populnea</i>	rhizomes	(Nyemb <i>et al.</i> , 2018)
Stigmasterol [13]	<i>C. assamica</i>	stem	(Chan <i>et al.</i> , 2018)
	<i>C. populnea</i>	rhizomes	(Nyemb <i>et al.</i> , 2018)
Stigmast-4-en-3-one [35]	<i>C. repens</i>	rhizomes	(Nyunt <i>et al.</i> , 2012)

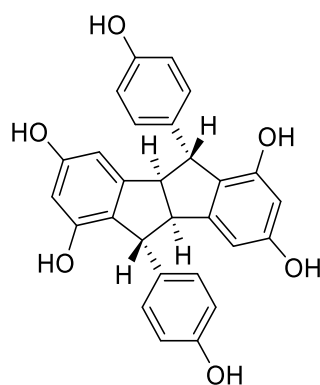
Table 2 (continued)

Category and compound	Plant	Plant part	references
Phenylpropanoids			
6- <i>O</i> -(<i>p</i> -Coumaroyl)-D-glucopyranoside [8]	<i>C. vinifera</i>	fruit	(Sun <i>et al.</i> , 2016)
Terpenoids			
Betulinic acid [36]	<i>C. assamica</i>	stem	(Chan <i>et al.</i> , 2018)
<i>epi</i> -Glut-5(6)-en-ol [37]	<i>C. assamica</i>	stem	(Chan <i>et al.</i> , 2018)
Oleanolic acid [12]	<i>C. assamica</i>	stem	(Chan <i>et al.</i> , 2018)

Figure 3 Structures of compounds from *Cissus*



[20] quadrangularin A



[21] pallidol

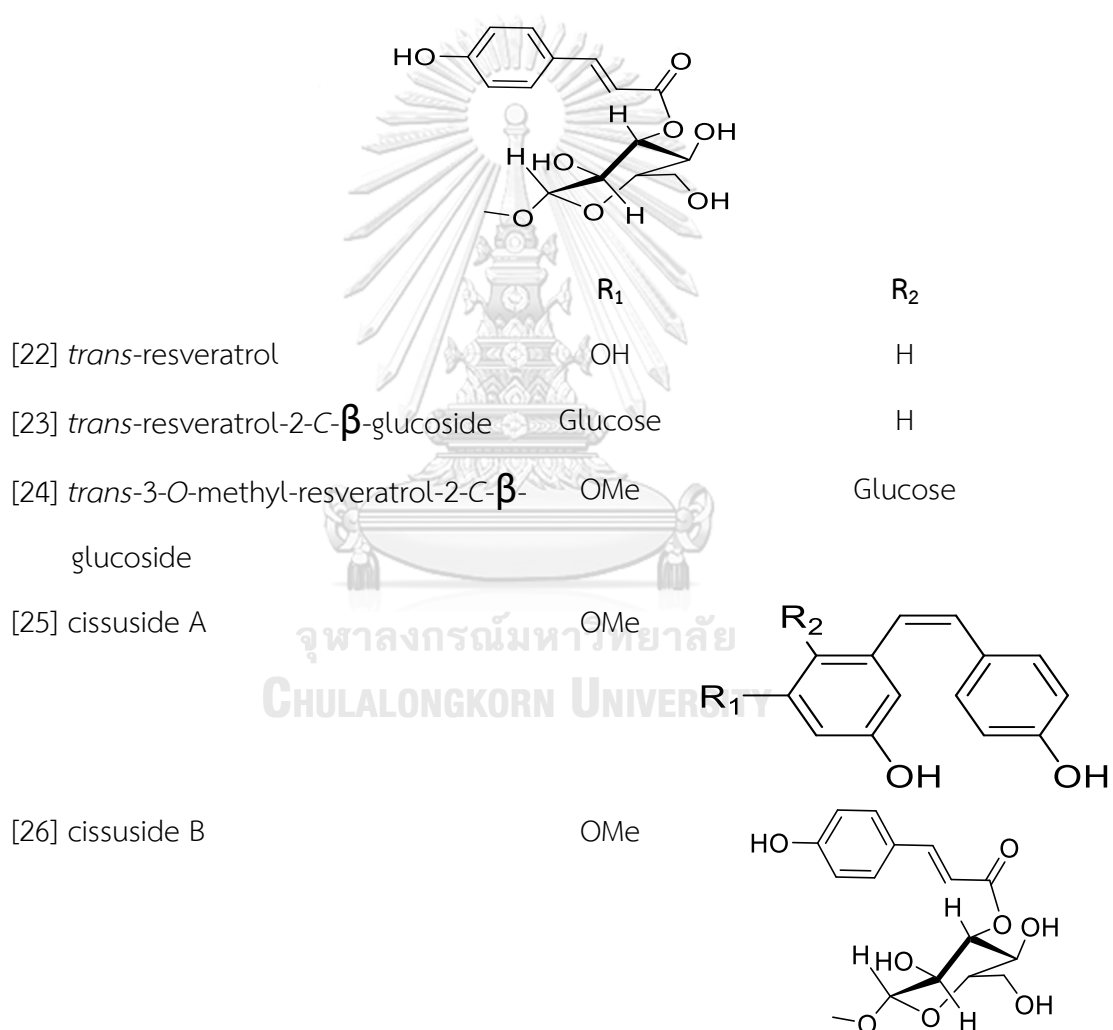
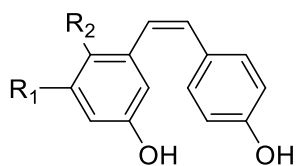
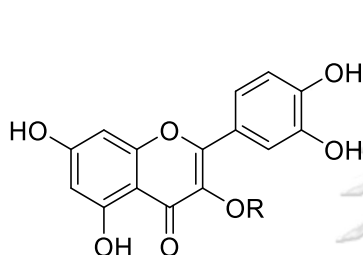


Figure 3 (continued)

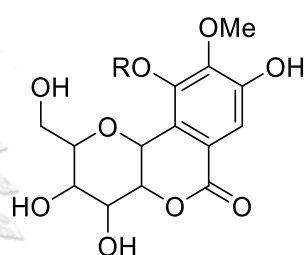


	R ₁	R ₂
[27] <i>cis</i> -resveratrol-2-C- β -glucoside	Glucose	H
[28] <i>cis</i> -3-O-methylresveratrol-2-C- β -glucoside	OMe	Glucose

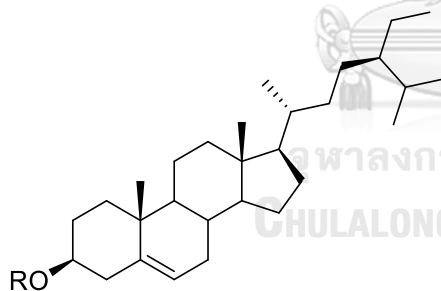
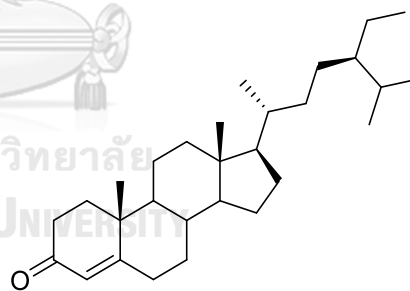


[29] quercetin R=H

[30] quercitrin R= rhamnose



[31] bergenin R= H

[32] O-acetylbergenin R= CH₃CO[33] β -sitosterol R=H[34] β -sitosterol glycoside R=glucose

[35] stigmast-4-en-3-one

Figure 3 (continued)

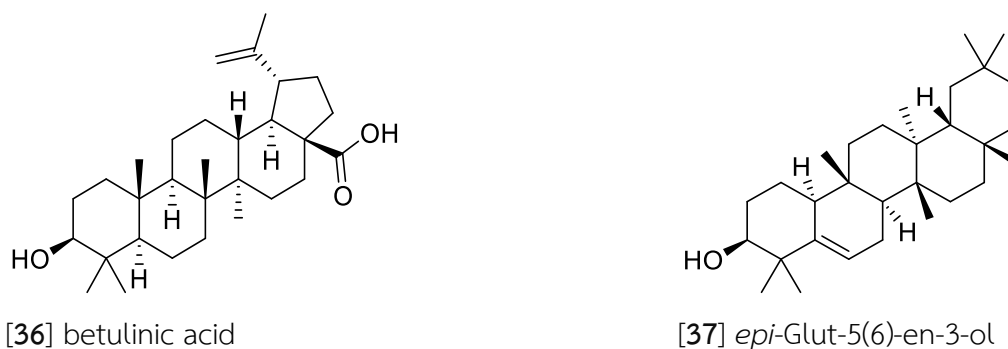


Figure 3 (continued)

1.3 Biological studies

Several plants in the genus *Cissus* have been studied for various biological activities. Examples are antidiabetic and anticancer [*Cissus vinifera* (L.) Kuntze, currently known as *Vitis vinifera* L. Kuntze (Suresh & Sunil, 2010)], antitrypanosoma [*C. repens* Lam. (Nyunt *et al.*, 2012)] and anti-osteoporotic [*C. quadrangularis* L. (Sawangjit *et al.*, 2017)] activities.

The most well-known chemical constituent reported for the *Cissus* genus is the polyhydroxy stilbene resveratrol. The compound has been considered as an important active principle of *Cissus vinifera* (which is now known as *Vitis vinifera*). It has been studied for a wide range of biological activities, including anti-diabetic, antibacterial, anticancer, anti-inflammatory and anti-oxidant activities, and cardiovascular and neuroprotective effects (Oyenihi *et al.*, 2016; Xia *et al.*, 2010). The steroids β -sitosterol and sitosterol- β -D-glucopyranoside from *Cissus sicyoides* showed antibacterial activity at 50 μ g/ml and 100 μ g/ml, respectively (Beltrame *et al.*, 2002). *Cissus repens* (also known as *Vitis repens*) showed *in-vitro* antitrypanosomal activity against trypomastigotes of *Trypanosoma evansi*, and the active principles were identified as resveratrol, 11-*O*-acetylbergenin and stigmast-4-en-3-one. Tyramine from *Cissus verticillata* displayed *in vivo* anti-diabetic activity in alloxan-induced diabetic rats (Lino *et al.*, 2007).

Regarding the biological activity of *Cissus javana*, so far, there have been no

previous reports.

2. *Dendrobium christyanum*

2.1 Taxonomic considerations and traditional uses

Dendrobium is a large genus in the family Orchidaceae. The genus consists of about 1,217 species, distributed in tropical and subtropical areas. In Thailand, about 170 species of *Dendrobium* have been identified (Nanakorn & Indharamusika, 1999; "The plant list ", 2010).

In traditional Chinese medicine, several members of *Dendrobium* collectively known as “Shihu” have been applied as a tonic to boost body fluid production, alleviate indigestion and enhance eyesight (Hu *et al.*, 2012).

Dendrobium christyanum Rchb. f. is known in Thai as “Ueang Sae Phu Kradueng” (Smitinand, 2001) or “Ngwe-Da-Nu” in Myanmar. It is an epiphytic plant, endemic to Southeast Asia (Worldview International Foundation, 2016). The leaf sheaths with black hairs and flowers with white lip with orange center are distinct characteristics of this plant (eFloras, 2008) (**Figure 4**). Although several species of *Dendrobium* are widely used in traditional Chinese medicine, *D. christyanum* has no record of traditional uses (Teixeira da Silva & Ng, 2017).



Figure 4 *Dendrobium christyanum* Rchb. f

2.2 Chemical studies

Bibenzyls are the major constituents of *Dendrobium*, existing as monomeric derivatives and dimeric analogues. Other types of phenolic compounds such as phenylpropanoids and flavonoids have also been found, but to a lesser extent. The presence of these phenolics and other constituents in the genus *Dendrobium* are summarized in **Table 3** and **Figure 5**. It should be mentioned that before the current investigation, *Dendrobium christyanum* has not been chemically studied.

Table 3 Distribution of secondary metabolites in the genus *Dendrobium*

Category and compound	Plant	Plant part	references
Bibenzyls and derivatives:			
<i>(a) Simple bibenzyls</i>			
Aloifol I [38]	<i>D. infundibulum</i>	whole plant	(Na Ranong <i>et al.</i> , 2019)
	<i>D. longicornu</i>	stem	(Hu <i>et al.</i> , 2008a)
	<i>D. williamsonii</i>	whole plant	(Yang <i>et al.</i> , 2017b)
	<i>D. scabrilingue</i>	whole plant	(Sarakulwattana <i>et al.</i> , 2018)
Amoenylin [39]	<i>D. amoenum</i>	whole plant	(Majumder <i>et al.</i> , 1999)
	<i>D. williamsonii</i>	whole plant	(Yang <i>et al.</i> , 2017b)
Batatasin [40]	<i>D. longicornu</i>	stem	(Hu <i>et al.</i> , 2008a)
	<i>D. plicatile</i>	stem	(Yamaki & Honda, 1996)
Batatasin III [41]	<i>D. aphyllum</i>	stem	(Yang <i>et al.</i> , 2015)
	<i>D. cariniferum</i>	stem	(Chen <i>et al.</i> , 2008c)
	<i>D. chrysotoxum</i>	whole plant	(Li <i>et al.</i> , 2009a)
	<i>D. draconis</i>	stem	(Sritularak <i>et al.</i> , 2011b)
	<i>D. formosum</i>	whole plant	(Inthongkaew <i>et al.</i> , 2017)

Table 3 (continued)

Category and compound	Plant	Plant part	references
Batatasin III [41] (continued)	<i>D. gratiosissimum</i>	stem	(Zhang <i>et al.</i> , 2008a)
	<i>D. infundibulum</i>	whole plant	(Na Ranong <i>et al.</i> , 2019)
	<i>D. loddigesii</i>	stem	(Ito <i>et al.</i> , 2010)
	<i>D. venustum</i>	whole plant	(Sukphan <i>et al.</i> , 2014)
	<i>D. scabrilingue</i>	whole plant	(Sarakulwattana <i>et al.</i> , 2018)
Brittonin A [42]	<i>D. secundum</i>	stem	(Sritularak <i>et al.</i> , 2011a)
Chrysotobibenzyl [43]	<i>D. aurantiacum</i>	stem	(Yang <i>et al.</i> , 2006b)
	var. <i>denneanum</i>		
	<i>D. capillipes</i>	stem	(Phechrmeekha <i>et al.</i> , 2012)
	<i>D. chrysanthum</i>	stem	(Yang <i>et al.</i> , 2006a)
	<i>D. chrysotoxum</i>	stem	(Hu <i>et al.</i> , 2012)
	<i>D. nobile</i>	stem	(Zhang <i>et al.</i> , 2007b)
	<i>D. pulchellum</i>	stem	(Chanvorachote <i>et al.</i> , 2013)
	<i>D. aurantiacum</i>	stem	(Yang <i>et al.</i> , 2006b)
	var. <i>denneanum</i>		

Table 3 (continued)

Category and compound	Plant	Plant part	references
Chrysotobibenzyl [43] (continued)	<i>D. chrysanthum</i>	stem	(Yang <i>et al.</i> , 2006a)
	<i>D. nobile</i>	stem	(Zhang <i>et al.</i> , 2007b)
	<i>D. pulchellum</i>	stem	(Chanvorachote <i>et al.</i> , 2013)
Crepidatin [45]	<i>D. aurantiacum</i>	whole plant	(Yang <i>et al.</i> , 2006b)
	<i>D. capillipes</i>	stem	(Phechrmeekha <i>et al.</i> , 2012)
	<i>D. chrysanthum</i>	stem	(Yang <i>et al.</i> , 2006a)
	<i>D. crepidatum</i>	whole plant	(Majumder & Chatterjee, 1989)
Cumulatin [46]	<i>D. cumulatum</i>	whole plant	(Majumder & Pal, 1993)
Dendrobin A [47]	<i>D. nobile</i>	stem	(Wang <i>et al.</i> , 1985); (Ye & Zhao, 2002)
Dendromonilaside E [48]	<i>D. nobile</i>	stem	(Miyazawa <i>et al.</i> , 1999)
3,3'-Dihydroxy-4,5-dimethoxybibenzyl [49]	<i>D. williamsonii</i>	whole plant	(Rungwichaniwat <i>et al.</i> , 2014)
3,4'-Dihydroxy-5-methoxybibenzyl [50]	<i>D. amoenum</i>	whole plant	(Majumder <i>et al.</i> , 1999)
3,4'-Dihydroxy-5,5'-dimethoxydihydrostilbene [51]	<i>D. nobile</i>	stem	(Hwang <i>et al.</i> , 2010)

Table 3 (continued)

Category and compound	Plant	Plant part	references
3,4'-Dihydroxy-3',4,5,2-trimethoxybibenzyl [52] Erianin [53] Gigantol [54]	<i>D. infundibulum</i>	whole plant	(Na Ranong <i>et al.</i> , 2019)
	<i>D. chrysotoxum</i>	stem	(Hu <i>et al.</i> , 2012)
	<i>D. aphyllum</i>	whole plant	(Chen <i>et al.</i> , 2008c)
	<i>D. aurantiacum</i>	whole	(Liu <i>et al.</i> , 2009)
	var. <i>denneanum</i>	plant	
	<i>D. brymerianum</i>	whole plant	(Klongkumnuankarn <i>et al.</i> , 2015)
	<i>D. densiflorum</i>	stem	(Fan <i>et al.</i> , 2001)
	<i>D. devonianum</i>	whole plant	(Sun <i>et al.</i> , 2014)
	<i>D. draconis</i>	stem	(Sritularak <i>et al.</i> , 2011b)
	<i>D. longicornu</i>	stem	(Hu <i>et al.</i> , 2008a)
	<i>D. nobile</i>	stem	(Zhang <i>et al.</i> , 2007b)
	<i>D. officinale</i>	stem	(Zhao <i>et al.</i> , 2018)
	<i>D. palpebrae</i>	whole plant	(Kyokong <i>et al.</i> , 2018)
	<i>D. polyanthum</i>	stem	(Hu <i>et al.</i> , 2009)
	<i>D. scabrilingue</i>	whole plant	(Sarakulwattana <i>et al.</i> , 2018)
<i>D. trigonopus</i>	stem	(Hu <i>et al.</i> , 2008b)	

Table 3 (continued)

Category and compound	Plant	Plant part	references
Gigantol [54] (continued)	<i>D. venustum</i>	whole plant	(Sukphan <i>et al.</i> , 2014)
	<i>D. wardianum</i>	stem	(Zhang <i>et al.</i> , 2017)
Gigantol-5-O- β -D-glucopyranoside [55]	<i>D. fimbriatum</i>	stem	(Xu <i>et al.</i> , 2017)
4-Hydroxy-3,5,3'-trimethoxybibenzyl [56]	<i>D. nobile</i>	stem	(Ye & Zhao, 2002)
5-Hydroxy-3,4,3',4',5'-pentamethoxybibenzyl [57]	<i>D. secundum</i>	stem	(Phechrmeekha <i>et al.</i> , 2012)
Isoamoenylin [58]	<i>D. amoenum</i>	whole plant	(Majumder <i>et al.</i> , 1999)
Moscatilin [59]	<i>D. amoenum</i>	whole plant	(Majumder <i>et al.</i> , 1999)
	<i>D. aurantiacum</i>	stem	(Yang <i>et al.</i> , 2006b)
	var. <i>denneanum</i>		
	<i>D. brymerianum</i>	whole plant	(Klongkumnuankarn <i>et al.</i> , 2015)
	<i>D. chrysanthum</i>	stem	(Yang <i>et al.</i> , 2006a)
	<i>D. densiflorum</i>	stem	(Fan <i>et al.</i> , 2001b)
	<i>D. ellipsophyllum</i>	whole plant	(Tanagornmeatar <i>et al.</i> , 2014)
	<i>D. formosum</i>	whole plant	(Inthongkaew <i>et al.</i> , 2017)

Table 3 (continued)

Category and compound	Plant	Plant part	references
Moscatilin [59] (continued)	<i>D. gratiosissimum</i>	stem	(Zhang <i>et al.</i> , 2008a)
	<i>D. infundibulum</i>	whole plant	(Na Ranong <i>et al.</i> , 2019)
	<i>D. loddigesii</i>	whole plant	(Chen <i>et al.</i> , 1994a); (Ito <i>et al.</i> , 2010)
	<i>D. longicornu</i>	stem	(Hu, <i>et al.</i> , 2008a)
	<i>D. moscatum</i>	whole plant	(Majumder & Sen, 1987)
	<i>D. nobile</i>	stem	(Miyazawa <i>et al.</i> , 1999); (Yang <i>et al.</i> , 2007)
	<i>D. palpebrae</i>	whole plant	(Kyokong <i>et al.</i> , 2018)
	<i>D. parishii</i>	whole plant	(Kongkatitham <i>et al.</i> , 2018)
	<i>D. polyanthum</i>	stem	(Hu <i>et al.</i> , 2009)
	<i>D. pulchellum</i>	stem	(Chanvorachote <i>et al.</i> , 2013)
	<i>D. secundum</i>	stem	(Sritularak <i>et al.</i> , 2011a)
	<i>D. wardianum</i>	stem	Zhang <i>et al.</i> , 2017)

Table 3 (continued)

Category and compound	Plant	Plant part	references
Moscatilin [59] (continued)	<i>D. williamsonii</i>	whole plant	(Yang <i>et al.</i> , 2017b)
Moscatilin diacetate [60]	<i>D. loddigesii</i>	stem	(Chen <i>et al.</i> , 1994)
3,3',4-Trihydroxy bibenzyl [61]	<i>D. longicornu</i>	stem	(Hu <i>et al.</i> , 2008b)
3,3',5-Trihydroxy bibenzyl [62]	<i>D. cariniferum</i>	whole plant	(Chen <i>et al.</i> , 2008c)
3,5,4'-Trihydroxy bibenzyl [63]	<i>D. gratiosissimum</i>	stem	(Zhang <i>et al.</i> , 2008a)
4,5,4'-Trihydroxy-3,3'-dimethoxy bibenzyl [64]	<i>D. ellipsophyllum</i>	whole plant	(Tanagornmeatar <i>et al.</i> , 2014)
	<i>D. palpebrae</i>	whole plant	(Kyokong <i>et al.</i> , 2018)
	<i>D. parishii</i>	whole plant	(Kongkatitham <i>et al.</i> , 2018)
	<i>D. secundum</i>	stem	(Sritularak <i>et al.</i> , 2011a)
4,3',4'-Trihydroxy-3,5-dimethoxybibenzyl [65]	<i>D. parishii</i>	whole plant	(Kongkatitham <i>et al.</i> , 2018)
Tristin [66]	<i>D. aphyllum</i>	stem	(Yang <i>et al.</i> , 2015)
	<i>D. chrysotoxum</i>	stem	(Hu <i>et al.</i> , 2012)
	<i>D. densiflorum</i>	stem	(Fan <i>et al.</i> , 2001b)
	<i>D. gratiosissimum</i>	stem	(Zhang <i>et al.</i> , 2008a)
	<i>D. longicornu</i>	stem	(Hu <i>et al.</i> , 2008a)

Table 3 (continued)

Category and compound	Plant	Plant part	references
Tristin [66] (continued)	<i>D. officinale</i>	stem	(Zhao <i>et al.</i> , 2018)
	<i>D. trigonopus</i>	stem	(Hu <i>et al.</i> , 2008b)
(b) Bibenzyls with substitution at ethylene bridge			
Dendrophenol [67]	<i>D. candidum</i>	stem	(Li <i>et al.</i> , 2008)
Dendrocandin A [68]	<i>D. candidum</i>	stem	(Li <i>et al.</i> , 2008)
	<i>D. wardianum</i>	stem	(Zhang <i>et al.</i> , 2017)
Dendrocandin C [69]	<i>D. candidum</i>	stem	(Li <i>et al.</i> , 2009c)
Dendrocandin D [70]	<i>D. candidum</i>	stem	(Li <i>et al.</i> , 2009c)
Dendrocandin E [71]	<i>D. candidum</i>	stem	(Li <i>et al.</i> , 2009c)
	<i>D. parishii</i>	whole plant	(Kongkatitham <i>et al.</i> , 2018)
Dendrosinen A [72]	<i>D. sinense</i>	whole plant	(Chen <i>et al.</i> , 2014)
Dendrosinen B [73]	<i>D. sinense</i>	whole plant	(Chen <i>et al.</i> , 2014)
	<i>D. infundibulum</i>	whole plant	(Na Ranong <i>et al.</i> , 2019)
3,4-Dihydroxy-5,4'-dimethoxybibenzyl [74]	<i>D. candidum</i>	stem	(Li <i>et al.</i> , 2008)
	<i>D. signatum</i>	whole plant	(Mittraphab <i>et al.</i> , 2016)
	<i>D. tortile</i>	whole plant	(Limpanit <i>et al.</i> , 2016)
	<i>D. wardianum</i>	stem	(Zhang <i>et al.</i> , 2017)
	<i>D. williamsonii</i>	whole plant	(Yang <i>et al.</i> , 2017b)

Table 3 (continued)

Category and compound	Plant	Plant part	references
4,4'-Dihydroxy-3,5-dimethoxybibenzyl [75]	<i>D. candidum</i>	stem	(Li <i>et al.</i> , 2008)
	<i>D. ellipsophyllum</i>	whole plant	(Tanagornmeatar <i>et al.</i> , 2014)
	<i>D. williamsonii</i>	whole plant	(Yang <i>et al.</i> , 2017b)
4-[2-(3-Hydroxyphenol)-1-methoxyethyl]-2,6-dimethoxyphenol [76]	<i>D. longicornu</i>	stem	(Hu <i>et al.</i> , 2008a)
	<i>D. loddigesii</i>	whole plant	(Ito <i>et al.</i> , 2010)
Loddigesiinol C [77]	<i>D. candidum</i>	stem	(Li <i>et al.</i> , 2008)
3-O-Methylgigantol [78]	<i>D. plicatile</i>	stem	(Yamaki & Honda, 1996)
	<i>D. nobile</i>	stem	(Zhang <i>et al.</i> , 2006)
Nobilin A [79]	<i>D. nobile</i>	stem	(Zhang <i>et al.</i> , 2006)
Nobilin B [80]	<i>D. nobile</i>	stem	(Zhang <i>et al.</i> , 2006)
Nobilin C [81]	<i>D. nobile</i>	stem	(Zhang <i>et al.</i> , 2006)
Nobilin D [82]	<i>D. nobile</i>	stem	(Zhang <i>et al.</i> , 2007b)
(c) Bibenzyls with other substitutions			
Dendrosinen C [83]	<i>D. sinense</i>	whole plant	(Chen <i>et al.</i> , 2014)
Loddigesiinol D [84]	<i>D. loddigesii</i>	whole plant	(Ito <i>et al.</i> , 2010)
Densiflorol A [85]	<i>D. densiflorum</i>	stem	(Fan <i>et al.</i> , 2001b)
Crepidatuol A [86]	<i>D. crepidatum</i>	stem	(Li <i>et al.</i> , 2013)
Crepidatuol B [87]	<i>D. crepidatum</i>	stem	(Li <i>et al.</i> , 2013)
Trigonopol B [88]	<i>D. chrysotoxum</i>	stem	(Hu <i>et al.</i> , 2012)

Table 3 (continued)

Category and compound	Plant	Plant part	references
Longicornuol A [89]	<i>D. longicornu</i>	stem	(Hu <i>et al.</i> , 2008a)
Trigonopol A [90]	<i>D. trigonopus</i>	stem	(Hu <i>et al.</i> , 2008b)
Dendrocandin B [91]	<i>D. candidum</i>	stem	(Li <i>et al.</i> , 2008)
	<i>D. signatum</i>	whole plant	(Mittraphab <i>et al.</i> , 2016)
	<i>D. officinale</i>	stem	(Yang <i>et al.</i> , 2015)
Dendrocandin T [92]	<i>D. officinale</i>	stem	(Yang <i>et al.</i> , 2015)
Dendrocandin U [93]	<i>D. officinale</i>	stem	(Yang <i>et al.</i> , 2015)
	<i>D. wardianum</i>	stem	(Zhang <i>et al.</i> , 2017)
Dendrocandin V [94]	<i>D. wardianum</i>	stem	(Zhang <i>et al.</i> , 2017)
Dendrowillol A [95]	<i>D. williamsonii</i>	whole plant	(Yang <i>et al.</i> , 2017b)
(d) Dihydrophenanthrenes			
1,5-Dihydroxy-3,4,7-trimethoxy-9,10-dihydro-phenanthrene [96]	<i>D. moniliforme</i>	whole plant	(Zhao <i>et al.</i> , 2016)
Coelonin [97]	<i>D. aphyllum</i>	whole plant	(Hu <i>et al.</i> , 2008a)
	<i>D. formosum</i>	whole plant	(Inthongkaew <i>et al.</i> , 2017)
	<i>D. nobile</i>	stem	(Yang <i>et al.</i> , 2007)
	<i>D. scabrilingue</i>	whole plant	(Sarakulwattana <i>et al.</i> , 2018)
Dendroinfundin A [98]	<i>D. infundibulum</i>	whole plant	(Na Ranong <i>et al.</i> , 2019)

Table 3 (continued)

Category and compound	Plant	Plant part	references
Dendroinfundin B [99]	<i>D. infundibulum</i>	whole plant	(Na Ranong <i>et al.</i> , 2019)
4,5-Dihydroxy-2,3-dimethoxy-9,10-dihydrophenanthrene [100]	<i>D. ellipsophyllum</i>	whole plant	(Tanagornmeatar <i>et al.</i> , 2014)
4,5-Dihydroxy-2,6-dimethoxy-9,10-dihydrophenanthrene [101]	<i>D. sinense</i>	whole plant	(Chen <i>et al.</i> , 2013)
4,5-Dihydroxy-2,6-dimethoxy-9,10-dihydrophenanthrene [101]	<i>D. chrysotoxum</i>	stem	(Hu <i>et al.</i> , 2012)
4,5-Dihydroxy-3,7-dimethoxy-9,10-dihydrophenanthrene [102]	<i>D. nobile</i>	stem	(Ye & Zhao, 2002)
4,5-Dihydroxy-2-methoxy-9,10-dihydrophenanthrene (Orchinol) [103]	<i>D. nobile</i>	stem	(Zhang <i>et al.</i> , 2007a)
9,10-Dihydromoscatin [104]	<i>D. polyanthum</i>	stem	(Hu <i>et al.</i> , 2009)
9,10-Dihydrophenanthrene-2,4,7-triol [105]	<i>D. officinale</i>	stem	(Zhao <i>et al.</i> , 2018)
	<i>D. polyanthum</i>	stem	(Hu <i>et al.</i> , 2009)

Table 3 (continued)

Category and compound	Plant	Plant part	references
2,7-Dihydroxy-3,4,6-trimethoxy-9,10-dihydrophenanthrene [106]	<i>D. densiflorum</i>	stem	(Fan <i>et al.</i> , 2001b)
2,8-Dihydroxy-3,4,7-trimethoxy-9,10-dihydrophenanthrene [107]	<i>D. nobile</i>	stem	(Yang <i>et al.</i> , 2007)
4,7-Dihydroxy-2,3,6-trimethoxy-9,10-dihydrophenanthrene [108]	<i>D. rotundatum</i>	whole plant	(Majumder & Pal, 1992)
3,4-Dimethoxy-1-(methoxymethyl)-9,10-dihydrophenanthrene-2,7-diol [109]	<i>D. hainanense</i>	aerial part	(Zhang <i>et al.</i> , 2018)
Ephemeranthol A [110]	<i>D. infundibulum</i>	whole plant	(Na Ranong <i>et al.</i> , 2019)
	<i>D. nobile</i>	stem	(Yang <i>et al.</i> , 2007); (Hwang <i>et al.</i> , 2010)
	<i>D. officinale</i>	stem	(Zhao <i>et al.</i> , 2018)
Ephemeranthol C [111]	<i>D. nobile</i>	stem	(Yang <i>et al.</i> , 2007); (Hwang <i>et al.</i> , 2010)
Erianthridin [112]	<i>D. nobile</i>	stem	(Hwang <i>et al.</i> , 2010)

Table 3 (continued)

Category and compound	Plant	Plant part	Reference
Erianthridin [112] (continued)	<i>D. formosum</i>	whole plant	(Inthongkaew <i>et al.</i> , 2017)
	<i>D. plicatile</i>	stem	(Yamaki & Honda, 1996)
Flavanthridin [113]	<i>D. nobile</i>	stem	(Hwang <i>et al.</i> , 2010)
Hircinol [114]	<i>D. aphyllum</i>	stem	(Yang <i>et al.</i> , 2015)
	<i>D. draconis</i>	stem	(Sritularak, <i>et al.</i> , 2011b)
	<i>D. formosum</i>	whole plant	(Inthongkaew <i>et al.</i> , 2017)
3-Hydroxy-2,4,7-trimethoxy-9,10-dihydrophenanthrene [115]	<i>D. nobile</i>	stem	(Yang <i>et al.</i> , 2007)
	<i>D. hainanense</i>	aerial part	(Zhang <i>et al.</i> , 2018)
7-Hydroxy-2,3,4-trimethoxy-9,10-dihydrophenanthrene [116]	<i>D. brymerianum</i>	whole plant	(Klongkumnuankarn <i>et al.</i> , 2015)
	<i>D. formosum</i>	whole plant	(Inthongkaew <i>et al.</i> , 2017)
	<i>D. palpebrae</i>	whole plant	(Kyokong <i>et al.</i> , 2018)

Table 3 (continued)

Category and compound	Plant	Plant part	Reference
Lusianthridin [117] (continued)	<i>D. plicatile</i>	stem	(Yamaki & Honda, 1996)
	<i>D. venustum</i>	whole plant	(Sukphan <i>et al.</i> , 2014)
	<i>D. scabrilingue</i>	whole plant	(Sarakulwattana <i>et al.</i> , 2018)
2-Hydroxy-4,7-dimethoxy-9,10-dihydrophenanthrene [118]	<i>D. nobile</i>	stem	(Yang <i>et al.</i> , 2007)
7-Methoxy-9,10-dihydrophenanthrene-2,4,5-triol [119]	<i>D. draconis</i>	stem	(Sritularak, <i>et al.</i> , 2011b)
2,5,7-Trimethoxy-4-methoxy-9,10-dihydrophenanthrene [120]	<i>D. formosum</i>	whole plant	(Inthongkaew <i>et al.</i> , 2017)
Plicatol C [121]	<i>D. plicatile</i>	stem	(Honda & Yamaki, 2000)
Rotundatin [122]	<i>D. rotundatum</i>	whole plant	(Majumder & Pal, 1992)
(S)-2,4,5,9-Tetrahydroxy-9,10-dihydrophenanthrene [123]	<i>D. fimbriatum</i>	stem	(Xu <i>et al.</i> , 2014)

Table 3 (continued)

Category and compound	Plant	Plant part	Reference
(e) Phenanthrenes			
2,5-Dihydroxy-3,4-dimethoxyphenanthrene [124]	<i>D. nobile</i>	stem	(Yang <i>et al.</i> , 2007)
2,5-Dihydroxy-4,9-dimethoxyphenanthrene [125]	<i>D. nobile</i>	stem	(Zhang <i>et al.</i> , 2008b)
	<i>D. palpebrae</i>	whole plant	(Kyokong <i>et al.</i> , 2018)
2,8-Dihydroxy-3,4,7-trimethoxyphenanthrene [126]	<i>D. nobile</i>	stem	(Yang <i>et al.</i> , 2007)
Epheranthol B [127]	<i>D. chrysotoxum</i>	stem	(Hu <i>et al.</i> , 2012)
	<i>D. plicatile</i>	stem	(Yamaki & Honda, 1996)
Fimbriol B [128]	<i>D. nobile</i>	stem	(Yang <i>et al.</i> , 2007); (Hwang <i>et al.</i> , 2010)
Flavanthrinin [129]	<i>D. brymerianum</i>	whole plant	(Klongkumnuankarn <i>et al.</i> , 2015)
	<i>D. venustum</i>	whole plant	(Sukphan <i>et al.</i> , 2014)
	<i>D. nobile</i>	stem	(Zhang <i>et al.</i> , 2008b)
	<i>D. parishii</i>	whole plant	(Kongkatitham <i>et al.</i> , 2018)

Table 3 (continued)

Category and compound	Plant	Plant part	Reference
Moscatin [130]	<i>D. aphyllum</i>	whole plant	(Hu <i>et al.</i> , 2008a)
	<i>D. chrysanthum</i>	stem	(Yang <i>et al.</i> , 2006a)
	<i>D. chrysotoxum</i>	whole plant	(Li <i>et al.</i> , 2009a)
	<i>D. densiflorum</i>	stem	(Fan <i>et al.</i> , 2001b)
	<i>D. polyanthum</i>	stem	(Hu <i>et al.</i> , 2009)
Loddigesiinol A [131]	<i>D. loddigesii</i>	whole plant	(Ito <i>et al.</i> , 2010)
	<i>D. wardianum</i>	stem	(Zhang <i>et al.</i> , 2017)
Dendroscabrol A [132]	<i>D. scabrilingue</i>	whole plant	(Sarakulwattana <i>et al.</i> , 2018).
Nudol [133]	<i>D. formosum</i>	whole plant	(Inthongkaew <i>et al.</i> , 2017)
	<i>D. nobile</i>	stem	(Yang <i>et al.</i> , 2007)
	<i>D. rotundatum</i>	whole plant	(Majumder & Pal, 1992)
Plicatol A [134]	<i>D. nobile</i>	stem	(Yang <i>et al.</i> , 2007)
	<i>D. plicatile</i>	stem	(Honda & Yamaki, 2000)
Plicatol B [135]	<i>D. plicatile</i>	stem	(Honda & Yamaki, 2000)
2,3,5-Trihydroxy-4,9-dimethoxyphenanthrene [136]	<i>D. nobile</i>	stem	(Yang <i>et al.</i> , 2007)

Table 3 (continued)

Category and compound	Plant	Plant part	Reference
3,4,8-Trimethoxyphenanthrene-2,5-diol [137]	<i>D. nobile</i>	stem	(Hwang <i>et al.</i> , 2010)
Bulbophyllanthrin [138]	<i>D. nobile</i>	stem	(Yang <i>et al.</i> , 2007)
Denthyrsinin [139]	<i>D. thyriform</i>	stem	(Zhang <i>et al.</i> , 2005)
5-Hydroxy-2,4-dimethoxyphenanthrene [140]	<i>D. loddigesii</i>	whole plant	(Ito <i>et al.</i> , 2010)
3-Hydroxy-2,4,7-trimethoxyphenanthrene [141]	<i>D. nobile</i>	stem	(Yang <i>et al.</i> , 2007)
Confusarin [142]	<i>D. chrysotoxum</i>	stem	(Hu <i>et al.</i> , 2012)
	<i>D. formosum</i>	whole plant	(Inthongkaew <i>et al.</i> , 2017)
	<i>D. nobile</i>	stem	(Zhang <i>et al.</i> , 2008c)
	<i>D. officinale</i>	stem	(Zhao <i>et al.</i> , 2018)
2,6-Dihydroxy-1,5,7-trimethoxyphenanthrene [143]	<i>D. densiflorum</i>	stem	(Fan <i>et al.</i> , 2001b)
	<i>D. palpebrae</i>	whole plant	(Kyokong <i>et al.</i> , 2018)
1,5,7-Trimethoxyphenanthren-2-ol [144]	<i>D. nobile</i>	stem	(Kim <i>et al.</i> , 2015)
(f) Phenanthrene-1,4-dione			
Cypripedin [145]	<i>D. densiflorum</i>	stem	(Fan <i>et al.</i> , 2001b)
Densiflorol B [146]	<i>D. densiflorum</i>	stem	(Fan <i>et al.</i> , 2001b)

Table 3 (continued)

Category and compound	Plant	Plant part	Reference
Densiflorol B [146] (continued)	<i>D. venustum</i>	whole plant	(Sukphan <i>et al.</i> , 2014)
Denbinobin [147]	<i>D. moniliforme</i>	stem	(Lin <i>et al.</i> , 2001)
	<i>D. nobile</i>	stem	(Yang <i>et al.</i> , 2007)
	<i>D. wardianum</i>	stem	(Zhang <i>et al.</i> , 2017)
(g) 9,10-Dihydrophenanthrene -1,4-dione			
Dendronone [148]	<i>D. chrysanthum</i>	stem	(Yang <i>et al.</i> , 2006a)
	<i>D. longicornu</i>	stem	(Hu <i>et al.</i> , 2008a)
Ephemeranthoquinone [149]	<i>D. plicatile</i>	stem	(Yamaki & Honda, 1996)
5-Methoxy-7-hydroxy-9,10-dihydro-1,4-phenanthrenequinone [15]	<i>D. draconis</i>	stem	(Sritularak, <i>et al.</i> , 2011b)
	<i>D. formosum</i>	whole plant	(Inthongkaew <i>et al.</i> , 2017)
Moniliformin [150]	<i>D. moniliforme</i>	stem	(Lin <i>et al.</i> , 2001)
(h) Phenanthropyran derivatives			
Amoenumin [151]	<i>D. amoenum</i>	whole plant	(Veerraju <i>et al.</i> , 1989)
Fimbriatone [152]	<i>D. nobile</i>	stem	(Zhang <i>et al.</i> , 2008b)
	<i>D. pulchellum</i>	stem	(Chanvorachote <i>et al.</i> , 2013)
Crystalltone [153]	<i>D. chrysotoxum</i>	stem	(Hu <i>et al.</i> , 2012)

Table 3 (continued)

Category and compound	Plant	Plant part	Reference
Loddigesiinol B [154]	<i>D. loddigesii</i>	whole plant	(Ito <i>et al.</i> , 2010)
Chrysotoxol A [155]	<i>D. polyanthum</i> <i>D. chrysotoxum</i>	stem stem	(Hu <i>et al.</i> , 2009) (Hu <i>et al.</i> , 2012)
Chrysotoxol B [156]	<i>D. chrysotoxum</i>	stem	(Hu <i>et al.</i> , 2012)
(i) 9,10-dihydrophenanthrodioxine			
Dendrocandin P2 [157]	<i>D. officinale</i>	stem	(Zhao <i>et al.</i> , 2018)
(j) Phenanthrodioxine			
Dendrocandin P1 [158]	<i>D. officinale</i>	stem	(Zhao <i>et al.</i> , 2018)
(k) Others			
Dendrochrysanene [159]	<i>D. chrysanthum</i>	stem	(Yang <i>et al.</i> , 2006a)
Aphyllone [160]	<i>D. nobile</i>	stem	(Hwang <i>et al.</i> , 2010)
9,10-Dihydro-aphyllone A-5-O- β -D-glucopyranoside [161]	<i>D. fimbriatum</i>	stem	(Xu <i>et al.</i> , 2017)
2,4,5,9S-Tetrahydroxy-9,10-dihydrophenanthrene -4-O- β -D-glucopyranoside [162]	<i>D. primulinum</i>	whole plant	(Ye <i>et al.</i> , 2016)
(l) Dimeric bibenzyls			
Dendrocandin I [163]	<i>D. candidum</i> <i>D. signatum</i>	stem whole plant	(Li <i>et al.</i> , 2009c) (Mitrphab <i>et al.</i> , 2016)

Table 3 (continued)

Category and compound	Plant	Plant part	references
Dendrocandin F [164]	<i>D. candidum</i>	stem	(Li <i>et al.</i> , 2009c)
Dendrocandin G [165]	<i>D. candidum</i>	stem	(Li <i>et al.</i> , 2009c)
Dendrosinen D [166]	<i>D. sinense</i>	whole plant	(Chen <i>et al.</i> , 2014)
Dendrofalconerol B [167]	<i>D. falconeri</i>	stem	(Sritularak & Likhitwitayawuid, 2009)
Nobilin E [168]	<i>D. nobile</i>	stem	(Zhang <i>et al.</i> , 2007b)
Dendroscabrol B [169]	<i>D. scabrilingue</i>	whole plant	(Sarakulwattana <i>et al.</i> , 2018).
Dengraol A [170]	<i>D. gratiosissimum</i>	stem	(Zhang <i>et al.</i> , 2008a)
Dengraol B [171]	<i>D. gratiosissimum</i>	stem	(Zhang <i>et al.</i> , 2008a)
Dencryol A [172]	<i>D. crystallinum</i>	stem	(Wang <i>et al.</i> , 2009)
Dencryol B [173]	<i>D. crystallinum</i>	stem	(Wang <i>et al.</i> , 2009)
2,2'-Dihydroxy-3,3',4,4',7,7'-hexamethoxy-9,9',10,10'-tetrahydro-1,1'-biphenanthrene [174]	<i>D. nobile</i>	stem	(Yang <i>et al.</i> , 2007)
2,2'-Dimethoxy-4,4',7,7'-tetrahydroxy-9,9',10,10'-tetrahydro-1,1'-biphenanthrene [175]	<i>D. plicatile</i>	stem	(Yamaki & Honda, 1996)

Table 3 (continued)

Category and compound	Plant	Plant part	references
Flavanthrin [176]	<i>D. aphyllum</i>	whole plant	(Chen <i>et al.</i> , 2008c)
Phoyunnarin C [177]	<i>D. venustum</i>	whole plant	(Sukphan <i>et al.</i> , 2014)
Phoyunnarin E [178]	<i>D. venustum</i>	whole plant	(Sukphan <i>et al.</i> , 2014)
Dendrosignatol [179]	<i>D. signatum</i>	whole plant	(Mittraphab <i>et al.</i> , 2016)
Dendroparishiol [180]	<i>D. parishii</i>	whole plant	(Kongkatitham <i>et al.</i> , 2018)
Dendrocandin H [181]	<i>D. candidum</i>	stem	(Li <i>et al.</i> , 2009c)
Loddigesiinol G [182]	<i>D. loddigesii</i>	stem	(Lu <i>et al.</i> , 2014)
Loddigesiinol H [183]	<i>D. loddigesii</i>	stem	(Lu <i>et al.</i> , 2014)
Loddigesiinol I [184]	<i>D. loddigesii</i>	stem	(Lu <i>et al.</i> , 2014)
Loddigesiinol J [16]	<i>D. loddigesii</i>	stem	(Lu <i>et al.</i> , 2014)
Dendropalpebrone [185]	<i>D. palpebrae</i>	whole plant	(Kyokong <i>et al.</i> , 2018)
Dendrofalconerol A [14]	<i>D. falconeri</i>	stem	(Sritularak & Likhitwitayawuid, 2009)
	<i>D. signatum</i>	whole plant	(Mittraphab <i>et al.</i> , 2016)
	<i>D. tortile</i>	whole plant	(Limpanit <i>et al.</i> , 2016)

Table 3 (continued)

Category and compound	Plant	Plant part	Reference
Flavonoids			
(a) Flavones			
Apigenin [186]	<i>D. crystallinum</i>	stem	(Wang <i>et al.</i> , 2009)
	<i>D. williamsonii</i>	whole plant	(Rungwichaniwat <i>et al.</i> , 2014)
apigenin 6-C-glucosyl-(1→2)- α -L- arabinoside [187]	<i>D. officinale</i>	leaves	(Zhang <i>et al.</i> , 2017)
6-C-(α -Arabinopyrano-syl)-8-C-[(2-O- α -rhamnopyranosyl)- β -galactopyranosyl] apigenin [188]	<i>D. huoshanense</i>	aerial part	(Chang <i>et al.</i> , 2010)
6-C-(α -Arabinopyrano-syl)-8-C-[(2-O- α -rhamnopyranosyl)- β -glucopyranosyl] apigenin [189]	<i>D. huoshanense</i>	aerial part	(Chang <i>et al.</i> , 2010)
6-C-[(2-O- α -Rhamnopyranosyl)- β -glucopyranosyl]-8-C-(α -arabinopyranosyl) apigenin [190]	<i>D. huoshanense</i>	aerial part	(Chang <i>et al.</i> , 2010)

Table 3 (continued)

Category and compound	Plant	Plant part	Reference
6-C-(β -Xylopyranosyl)-8-C- [(2-O- α -rhamnopyra-nosyl)- β -glucopyranosyl] apigenin [191]	<i>D. huoshanense</i>	aerial part	(Chang <i>et al.</i> , 2010)
5,6-Dihydroxy-4'- methoxyflavone [192]	<i>D. chrysotoxum</i>	stem	(Hu <i>et al.</i> , 2012)
6'''-Glucosyl-vitexin [193]	<i>D. crystallinum</i>	stem	(Wang <i>et al.</i> , 2009)
5-Hydroxy-3-methoxy- flavone-7-O-[β -D-aposyl- (1 \rightarrow 6)]- β -D-glucoside [6]	<i>D. devonianum</i>	whole plant	(Sun <i>et al.</i> , 2014)
Isoschaftoside [194]	<i>D. huoshanense</i>	aerial part	(Chang <i>et al.</i> , 2010)
Isoviolanthin [195]	<i>D. crystallinum</i>	stem	(Wang <i>et al.</i> , 2009)
Kaempferol [1]	<i>D. aurantiacum</i> var. <i>denneanum</i>	stem	(Yang <i>et al.</i> , 2006b)
Kaempferol-3-O- α -L- rhamnopyranoside [196]	<i>D. secundum</i>	stem	(Phechrmeekha <i>et al.</i> , 2012)
Kaempferol-3,7-O-di- α -L- rhamnopyranoside [197]	<i>D. secundum</i>	stem	(Phechrmeekha <i>et al.</i> , 2012)
Kaempferol-3-O- α -L- rhamnopyranosyl-(1 \rightarrow 2)- β -D-glucopyranoside [198]	<i>D. capillipes</i>	stem	(Phechrmeekha <i>et al.</i> , 2012)
Kaempferol-3-O- α -L- rhamnopyranosyl-(1 \rightarrow 2)- β -D-xylopyranoside [199]	<i>D. capillipes</i>	stem	(Phechrmeekha <i>et al.</i> , 2012)

Table 3 (continued)

Category and compound	Plant	Plant part	Reference
Luteolin [200]	<i>D. aurantiacum</i> var. <i>denneanum</i>	whole plant	(Liu <i>et al.</i> , 2009)
	<i>D. ellipsophyllum</i>	whole plant	(Tanagornmeatar <i>et al.</i> , 2014)
	<i>D. longicornu</i>	stem	(Hu <i>et al.</i> , 2008a)
Vicenin-2 [201]	<i>D. aurantiacum</i> var. <i>denneanum</i>	stem	(Xiong <i>et al.</i> , 2013)
Quercetin-3-O-L-rhamnopyranoside [202]	<i>D. secundum</i>	stem	(Phechrmeekha <i>et al.</i> , 2012)
Quercetin-3-O- α -L-rhamnopyranosyl-(1 \rightarrow 2)- β -D-xylopyranoside [203]	<i>D. capillipes</i>	stem	(Phechrmeekha <i>et al.</i> , 2012)
(b) Flavanones			
(2S)-Homoeriodictyol [204]	<i>D. densiflorum</i>	stem	(Fan <i>et al.</i> , 2001b)
	<i>D. ellipsophyllum</i>	whole plant	(Tanagornmeatar <i>et al.</i> , 2014)
Naringenin [205]	<i>D. aurantiacum</i> var. <i>denneanum</i>	stem	(Yang <i>et al.</i> , 2006b)
	<i>D. densiflorum</i>	stem	(Fan <i>et al.</i> , 2001b)
	<i>D. longicornu</i>	stem	(Hu <i>et al.</i> , 2008a)
(2S)-Eriodictyol [206]	<i>D. ellipsophyllum</i>	whole plant	(Tanagornmeatar <i>et al.</i> , 2014)
	<i>D. trigonopus</i>	stem	(Hu <i>et al.</i> , 2008b)

Table 3 (continued)

Category and compound	Plant	Plant part	Reference
(2S)-Eriodictyol [206] (continued)	<i>D. tortile</i>	whole plant	(Limpanit <i>et al.</i> , 2016)
Terpenoids			
Amoenin [207]	<i>D. amoenum</i>	whole plant	(Dahmen & Leander, 1978)
	<i>D. williamsonii</i>	whole plant	(Yang <i>et al.</i> , 2017a)
Asiatic acid [208]	<i>D. parishii</i>	whole plant	(Kongkatitham <i>et al.</i> , 2018)
Corchoionoside C [209]	<i>D. wardianum</i>	stem	(Fan <i>et al.</i> , 2013)
Crystallinin [210]	<i>D. wardianum</i>	stem	(Fan <i>et al.</i> , 2013)
(-)-(1R,2S,3R,4S,5R,6S, 9S, 11R)-11-Carboxy-methyl-dendrobine [211]	<i>D. nobile</i>	stem	(Meng <i>et al.</i> , 2017)
Dendrobine [212]	<i>D. nobile</i>	stem	(Wang <i>et al.</i> , 1985) (Meng <i>et al.</i> , 2017)
Dendrobane A [213]	<i>D. moniliforme</i>	stem	(Bi <i>et al.</i> , 2004)
Dendromoniliside A [214]	<i>D. nobile</i>	stem	(Zhang <i>et al.</i> , 2007a)
Dendromoniliside B [215]	<i>D. moniliforme</i>	stem	(Zhao <i>et al.</i> , 2003)
Dendromoniliside C [216]	<i>D. moniliforme</i>	stem	(Zhao <i>et al.</i> , 2003)

Table 3 (continued)

Category and compound	Plant	Plant part	Reference
Dendromoniliside D [217]	<i>D. moniliforme</i>	stem	(Zhao <i>et al.</i> , 2003)
Dendronobiloside A [218]	<i>D. moniliforme</i>	stem	(Zhao <i>et al.</i> , 2003)
	<i>D. nobile</i>	stem	(Zhao <i>et al.</i> , 2001); (Ye & Zhao, 2002)
Dendronobiloside B [219]	<i>D. nobile</i>	stem	(Zhao <i>et al.</i> , 2001); (Ye & Zhao, 2002)
Dendronobiloside C [220]	<i>D. nobile</i>	stem	(Zhao <i>et al.</i> , 2001); (Ye & Zhao, 2002)
Dendronobiloside D [221]	<i>D. nobile</i>	stem	(Zhao <i>et al.</i> , 2001); (Ye & Zhao, 2002)
Dendronobiloside E [222]	<i>D. nobile</i>	stem	(Zhao <i>et al.</i> , 2001); (Ye & Zhao, 2002)
Dendronobilin A [223]	<i>D. wardianum</i>	stem	(Zhang <i>et al.</i> , 2007a)
Dendronobilin B [224]	<i>D. wardianum</i>	stem	(Zhang <i>et al.</i> , 2007a)
	<i>D. nobile</i>	stem	(Wang <i>et al.</i> , 2009); (Meng <i>et al.</i> , 2017)
Dendronobilin C [225]	<i>D. crystallium</i>	stem	(Wang <i>et al.</i> , 2009)
Dendronobilin D [226]	<i>D. nobile</i>	stem	(Zhang <i>et al.</i> , 2007a)
Dendronobilin E [227]	<i>D. nobile</i>	stem	(Zhang <i>et al.</i> , 2007a)
Dendronobilin F [228]	<i>D. nobile</i>	stem	(Zhang <i>et al.</i> , 2007a)
Dendronobilin G [229]	<i>D. nobile</i>	stem	(Zhang <i>et al.</i> , 2007a)
Dendronobilin H [230]	<i>D. nobile</i>	stem	(Zhang <i>et al.</i> , 2007a)
Dendronobilin I [231]	<i>D. nobile</i>	stem	(Zhang <i>et al.</i> , 2007a)
Dendronobilin J [232]	<i>D. nobile</i>	stem	(Zhang <i>et al.</i> , 2007a)

Table 3 (continued)

Category and compound	Plant	Plant part	Reference
Dendronobilin K [233]	<i>D. wardianum</i>	stem	(Fan <i>et al.</i> , 2013)
Dendronobilin L [234]	<i>D. nobile</i>	stem	(Zhang <i>et al.</i> , 2007a)
Dendronobilin M [235]	<i>D. nobile</i>	stem	(Zhang <i>et al.</i> , 2008b); (Meng <i>et al.</i> , 2017)
Dendronobilin N [236]	<i>D. nobile</i>	stem	(Zhang <i>et al.</i> , 2008b)
Dendroside A [237]	<i>D. moniliforme</i>	stem	(Zhao <i>et al.</i> , 2003)
	<i>D. nobile</i>	stem	(Zhao <i>et al.</i> , 2001); (Ye & Zhao, 2002)
Dendroside B [238]	<i>D. nobile</i>	stem	(Ye & Zhao, 2002)
	<i>D. williamsonii</i>	whole plant	(Yang <i>et al.</i> , 2017a)
Dendroside C [239]	<i>D. moniliforme</i>	stem	(Zhao <i>et al.</i> , 2003)
	<i>D. nobile</i>	stem	(Ye & Zhao, 2002)
Dendroside D [240]	<i>D. nobile</i>	stem	(Ye & Zhao, 2002)
Dendroside E [241]	<i>D. nobile</i>	stem	(Ye <i>et al.</i> , 2002)
Dendroside F [242]	<i>D. moniliforme</i>	stem	(Zhao <i>et al.</i> , 2003)
Dendroside G [243]	<i>D. nobile</i>	stem	(Ye <i>et al.</i> , 2002)
Dendrowardol A [244]	<i>D. wardianum</i>	stem	(Fan <i>et al.</i> , 2013)
Dendrowardol B [245]	<i>D. wardianum</i>	stem	(Fan <i>et al.</i> , 2013)
Dendrowardol C [246]	<i>D. wardianum</i>	stem	(Fan <i>et al.</i> , 2013)
Amotin [247]	<i>D. amoenum</i>	whole plant	(Majumder <i>et al.</i> , 1999)
Dendrowillin A [248]	<i>D. williamsonii</i>	whole plant	(Yang <i>et al.</i> , 2017a)
Dendrowillin B [249]	<i>D. williamsonii</i>	whole plant	(Yang <i>et al.</i> , 2017a)

Table 3 (continued)

Category and compound	Plant	Plant part	Reference
α -Dihydropicrotoxinin [250]	<i>D. amoenum</i>	whole plant	(Majumder <i>et al.</i> , 1999)
Picrotin [251]	<i>D. williamsonii</i>	whole plant	(Yang <i>et al.</i> , 2017a)
Findlayanin [252]	<i>D. nobile</i>	stem	(Meng <i>et al.</i> , 2017)
	<i>D. polyanthum</i>	stem	(Hu <i>et al.</i> , 2009)
3-Hydroxy-2-oxodendrobine [253]	<i>D. findlayanum</i>	whole plant	(Qin <i>et al.</i> , 2011)
Wardianumine A [254]	<i>D. wardianum</i>	stem	(Zhang <i>et al.</i> , 2017)
Aliphatic acid derivatives			
Aliphatic acids [255]	<i>D. clavatum</i> var. <i>aurantiacum</i>	stem	(Chang <i>et al.</i> , 2001)
Aliphatic alcohols [256]	<i>D. clavatum</i> var. <i>aurantiacum</i>	stem	(Chang <i>et al.</i> , 2001)
Decumbic acid [257]	<i>D. nobile</i>	stem	(Zhou <i>et al.</i> , 2016)
Dimethyl malate [258]	<i>D. huoshanense</i>	aerial part	(Chang <i>et al.</i> , 2010)
Malic acid [259]	<i>D. huoshanense</i>	aerial part	(Chang <i>et al.</i> , 2001)
Isopentyl butyrate [260]	<i>D. huoshanense</i>	aerial part	(Chang <i>et al.</i> , 2010)
(-)-Shikimic acid [261]	<i>D. fuscescens</i>	whole plant	(Talapatra <i>et al.</i> , 1989)
	<i>D. huoshanense</i>	aerial part	(Chang <i>et al.</i> , 2010)
	<i>D. longicornu</i>	stem	(Hu <i>et al.</i> , 2008a)
	<i>D. pulchellum</i>	stem	(Chanvorachote <i>et al.</i> , 2013)

Table 3 (continued)

Category and compound	Plant	Plant part	Reference
Benzoic acid derivatives and phenolic compounds			
Antiarol [262]	<i>D. chrysotoxum</i>	stem	(Hu <i>et al.</i> , 2012)
Ethylhaematommate [263]	<i>D. longicornu</i>	whole plant	(Li <i>et al.</i> , 2009d)
Gallic acid [264]	<i>D. longicornu</i>	whole plant	(Li <i>et al.</i> , 2009d)
<i>p</i> -Hydroxybenzaldehyde [265]	<i>D. tortile</i>	whole plant	(Limpanit <i>et al.</i> , 2016)
<i>p</i> -Hydroxybenzoic acid [266]	<i>D. williamsonii</i>	whole plant	(Yang <i>et al.</i> , 2017b)
3-Hydroxy-2-methoxy-5,6-dimethylbenzoic acid [267]	<i>D. crystallinum</i>	stem	(Wang <i>et al.</i> , 2009)
Methyl 4-hydroxybenzoate [268]	<i>D. williamsonii</i>	whole plant	(Hu <i>et al.</i> , 2012)
Methyl β -orsellinate [269]	<i>D. longicornu</i> <i>D. williamsonii</i>	stem whole plant	(Li <i>et al.</i> , 2009d) (Rungwichaniwat <i>et al.</i> , 2014)
Protocatechuic acid [270]	<i>D. nobile</i>	stem	(Ye & Zhao, 2002)
Salicylic acid [271]	<i>D. huoshanense</i> <i>D. williamsonii</i>	aerial part whole plant	(Chang <i>et al.</i> , 2010) (Yang <i>et al.</i> , 2017b)

Table 3 (continued)

Category and compound	Plant	Plant part	Reference
Syringic acid [272]	<i>D. crystallinum</i>	stem	(Wang <i>et al.</i> , 2009)
Tachioside [273]	<i>D. denneanum</i>	stem	(Pan <i>et al.</i> , 2012)
Vanillic acid [274]	<i>D. crystallinum</i>	stem	(Hu <i>et al.</i> , 2012)
	<i>D. williamsonii</i>	whole plant	(Li <i>et al.</i> , 2009d)
Vanillin [275]	<i>D. williamsonii</i>	whole plant	(Yang <i>et al.</i> , 2018)
Vanilloside [276]	<i>D. denneanum</i>	stem	(Pan <i>et al.</i> , 2012)
Phenylpropanoids			
Alkyl 4'-hydroxy- <i>trans</i> -cinnamates [277]	<i>D. clavatum</i> var. <i>aurantiacum</i>	stem	(Chang <i>et al.</i> , 2001)
Alkyl <i>trans</i> -ferulates [278]	<i>D. clavatum</i> var. <i>aurantiacum</i>	stem	(Chang <i>et al.</i> , 2001)
Defuscin [279]	<i>D. aurantiacum</i> var. <i>denneanum</i>	stem	(Yang <i>et al.</i> , 2006b)
	<i>D. moniliforme</i>	stem	(Bi <i>et al.</i> , 2004)
<i>n</i> -Octacosyl ferulate [280]	<i>D. aurantiacum</i> var. <i>denneanum</i>	stem	(Yang <i>et al.</i> , 2006b)
	<i>D. moniliforme</i>	stem	(Bi <i>et al.</i> , 2004)
<i>n</i> -Triacontyl <i>p</i> -hydroxy- <i>cis</i> -cinnamate [281]	<i>D. moniliforme</i>	stem	(Bi <i>et al.</i> , 2004)
Tetratriacontanyl- <i>trans-p</i> -coumarate [282]	<i>D. williamsonii</i>	whole plant	(Rungwichaniwat <i>et al.</i> , 2014)
<i>n</i> -Docosyl <i>trans</i> -ferulate [283]	<i>D. longicornu</i>	whole plant	(Li <i>et al.</i> , 2009d)

Table 3 (continued)

Category and compound	Plant	Plant part	Reference
<i>trans</i> -Tetracosyl ferulate [284]	<i>D. tortile</i>	whole plant	(Limpanit <i>et al.</i> , 2016)
	<i>D. scabrilingue</i>	whole plant	(Sarakulwattana <i>et al.</i> , 2018)
Ferulaldehyde [285]	<i>D. longicornu</i>	whole plant	(Li <i>et al.</i> , 2009d)
Ferulic acid [286]	<i>D. secundum</i>	stem	(Sritularak <i>et al.</i> , 2011a)
2-(<i>p</i> -Hydroxyphenyl) ethyl <i>p</i> -coumarate [287]	<i>D. falconeri</i>	stem	(Sritularak & Likhitwitayawuid, 2009)
Coniferyl alcohol [288]	<i>D. trigonopus</i>	stem	(Hu <i>et al.</i> , 2008b)
Dendroside [289]	<i>D. nobile</i>	stem	(Zhou <i>et al.</i> , 2017)
<i>cis</i> -Hexacosanoyl ferulate [290]	<i>D. tortile</i>	whole plant	(Limpanit <i>et al.</i> , 2016)
<i>cis</i> -Tetracosanoyl ferulate [291]	<i>D. scabrilingue</i>	whole plant	(Sarakulwattana <i>et al.</i> , 2018)
Tetracosyl (<i>Z</i>)- <i>p</i> -coumarate [292]	<i>D. falconeri</i>	whole plant	(Sritularak & Likhitwitayawuid, 2009)
Dihydroconiferyl dihydro- <i>p</i> -coumarate [293]	<i>D. formosum</i>	whole plant	(Inthongkaew <i>et al.</i> , 2017)
	<i>D. nobile</i>	stem	(Zhang <i>et al.</i> , 2006)
	<i>D. williamsonii</i>	whole plant	(Yang <i>et al.</i> , 2017b)

Table 3 (continued)

Category and compound	Plant	Plant part	Reference
1-[4-(β -D-Glucopyranosyloxy)-3,5-dimethoxyphenyl]-1-propanone [294]	<i>D. aurantiacum</i> var. <i>denneanum</i>	stem	(Xiong <i>et al.</i> , 2013)
<i>p</i> -Hydroxyphenyl propionic methyl ester [295]	<i>D. aphyllum</i>	whole plant	(Chen <i>et al.</i> , 2008a)
Phloretic acid [296]	<i>D. ellipsophyllum</i>	whole plant	(Tanagornmeatar <i>et al.</i> , 2014)
Dihydroconiferyl alcohol [297]	<i>D. longicornu</i>	stem	(Hu <i>et al.</i> , 2008a)
Salidroside [298]	<i>D. chrysotoxum</i>	stem	(Hu <i>et al.</i> , 2012)
Shashenoside I [299]	<i>D. aurantiacum</i> var. <i>denneanum</i>	stem	(Xiong <i>et al.</i> , 2013)
Syringin [300]	<i>D. aurantiacum</i> var. <i>denneanum</i>	stem	(Xiong <i>et al.</i> , 2013)
Coumarins			
Ayapin [301]	<i>D. densiflorum</i>	stem	(Fan <i>et al.</i> , 2001b)
Coumarin [302]	<i>D. aurantiacum</i> var. <i>denneanum</i>	stem	(Yang <i>et al.</i> , 2006b)
	<i>D. clavatum</i> var. <i>aurantiacum</i>	stem	(Chang <i>et al.</i> , 2001)
Denthyrsin [303]	<i>D. thyrsiflorum</i>	stem	(Zhang <i>et al.</i> , 2005)
Scoparone [304]	<i>D. densiflorum</i>	stem	(Fan <i>et al.</i> , 2001b)

Table 3 (continued)

Category and compound	Plant	Plant part	Reference
Scoparone [304] (continued)	<i>D. palpebrae</i>	whole plant	(Kyokong <i>et al.</i> , 2018)
	<i>D. thyrsoiflorum</i>	stem	(Zhang <i>et al.</i> , 2005)
	<i>D. williamsonii</i>	whole plant	(Yang <i>et al.</i> , 2017b)
Scopoletin [305]	<i>D. densiflorum</i>	stem	(Fan <i>et al.</i> , 2001b)
Lignans and neolignans			
Dehydrodiconiferyl alcohol-4-O- β -D-glucoside [306]	<i>D. chrysanthum</i>	stem	(Ye <i>et al.</i> , 2004)
Balanophonin [307]	<i>D. williamsonii</i>	whole plant	(Yang <i>et al.</i> , 2017b)
Acanthoside B [308]	<i>D. chrysanthum</i>	stem	(Ye <i>et al.</i> , 2004)
Liriodendrin [309]	<i>D. aurantiacum</i>	stem	(Xiong <i>et al.</i> , 2013)
	var. <i>denneanum</i>		
	<i>D. pulchellum</i>	stem	(Chanvorachote <i>et al.</i> , 2013)
Syringaresinol [310]	<i>D. secundum</i>	stem	(Sritularak <i>et al.</i> , 2011a)
	<i>D. williamsonii</i>	whole plant	(Yang <i>et al.</i> , 2017b)
Syringaresinol-4-O-D-monoglucopyranoside [311]	<i>D. aurantiacum</i>	stem	(Xiong <i>et al.</i> , 2013)
	var. <i>denneanum</i>		

Table 3 (continued)

Category and compound	Plant	Plant part	Reference
Episyringaresinol [312]	<i>D. chrysotoxum</i>	stem	(Hu <i>et al.</i> , 2012)
	<i>D. longicornu</i>	stem	(Hu <i>et al.</i> , 2008a)
	<i>D. nobile</i>	stem	(Zhang <i>et al.</i> , 2008b)
Episyringaresinol 4''-O- β -D-glucopyranoside [313]	<i>D. moniliforme</i>	stem	(Zhao <i>et al.</i> , 2003)
(-)-(7 <i>S</i> ,8 <i>R</i> ,7' <i>E</i>) -4-Hydroxy-3,3',5,5'-tetramethoxy-8,4'-oxyneolign-7'-ene-7,9,9'-triol-7,9'-bis-O- β -D-glucopyranoside [314]	<i>D. aurantiacum</i> var. <i>denneanum</i>	stem	(Xiong <i>et al.</i> , 2013)
Lyoniresinol [315]	<i>D. chrysanthum</i>	stem	(Ye <i>et al.</i> , 2004)
(-)-Medioresinol [316]	<i>D. loddigesii</i>	whole plant	(Ito <i>et al.</i> , 2010)
(-)-Pinoresinol [317]	<i>D. loddigesii</i>	whole plant	(Ito <i>et al.</i> , 2010)
Dendrolactone [318]	<i>D. nobile</i>	stem	(Zhou <i>et al.</i> , 2016)
<i>Erythro</i> -1-(4-O- β -D-glucopyranosyl-3-methoxyphenyl)-2-[4-(3-hydroxypropyl)-2,6-dimethoxyphenoxy]-1,3-propanediol [319]	<i>D. longicornu</i>	stem	(Hu <i>et al.</i> , 2008a)

Table 3 (continued)

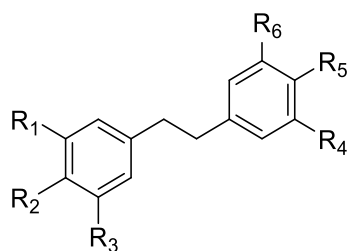
Category and compound	Plant	Plant part	Reference
(-)-(8 <i>R</i> ,7' <i>E</i>)-4-Hydroxy-3,3',5,5'-tetra-methoxy-8,4'-oxyneolign-7'-ene-9,9'-diol-4,9-bis- <i>O</i> - β -D-glucopyranoside [320]	<i>D. auranticum</i>	stem	(Li <i>et al.</i> , 2014)
(-)-(8 <i>S</i> ,7' <i>E</i>)-4-Hydroxy-3,3',5,5'-tetramethoxy-8,4'-oxyneolign-7'-ene-9,9'-diol-4,9-bis- <i>O</i> - β -D-glucopyranoside [321]	<i>D. auranticum</i>	stem	(Li <i>et al.</i> , 2014)
(-)-(8 <i>R</i> ,7' <i>E</i>)-4-hydroxy-3,3',5,5',9'-penta-methoxy-8,4'-oxyneolign-7'-ene-9-ol-4,9-bis- <i>O</i> - β -D-glucopyranoside [322]	<i>D. auranticum</i>	stem	(Li <i>et al.</i> , 2014)
Fluorenones			
Denchrysan A [323]	<i>D. chrysotoxum</i>	whole plant	(Li <i>et al.</i> , 2009a)
Dendroflorin [324]	<i>D. aurantiacum</i> var. <i>denneanum</i>	stem	(Yang <i>et al.</i> , 2006b)
	<i>D. brymerianum</i>	whole plant	(Klongkumnuankarn <i>et al.</i> , 2015)

Table 3 (continued)

Category and compound	Plant	Plant part	Reference
Dendroflorin [324] (continued)	<i>D. palpebrae</i>	whole plant	(Kyokong <i>et al.</i> , 2018)
Dengibsin [325]	<i>D. aurantiacum</i> var. <i>denneanum</i>	stem	(Yang <i>et al.</i> , 2006b)
	<i>D. chrysanthum</i>	stem	(Yang <i>et al.</i> , 2006a)
	<i>D. chrysotoxum</i>	whole plant	(Li <i>et al.</i> , 2009a)
Nobilone [326]	<i>D. brymerianum</i>	whole plant	(Klongkumnuankarn <i>et al.</i> , 2015)
	<i>D. nobile</i>	stem	(Zhang <i>et al.</i> , 2007b)
	<i>D. palpebrae</i>	whole plant	(Kyokong <i>et al.</i> , 2018)
1,4,5-Trihydroxy-7-methoxy-9H-fluoren-9-one [327]	<i>D. chrysotoxum</i>	whole plant	(Chen <i>et al.</i> , 2008b)
2,4,7-Trihydroxy-5-methoxy-9-fluorenone [328]	<i>D. chrysotoxum</i>	stem	(Yang <i>et al.</i> , 2004)
2,4,7-Trihydroxy-1,5-dimethoxy-9-fluorenone [329]	<i>D. chrysotoxum</i>	stem	(Yang <i>et al.</i> , 2004)
Denchrysan B [330]	<i>D. brymerianum</i>	whole plant	(Klongkumnuankarn <i>et al.</i> , 2015)
	<i>D. chrysanthum</i>	whole plant	(Ye <i>et al.</i> , 2003)

Table 3 (continued)

Category and compound	Plant	Plant part	Reference
Others			
3,6,9-Trihydroxy-3,4-dihydroanthracen-1-(2H)-one [331]	<i>D. chrysotoxum</i>	stem	(Hu <i>et al.</i> , 2012)
Palmarumycin JC2 [332]	<i>D. crystallinum</i>	stem	(Wang <i>et al.</i> , 2009)
Dehydrovomifoliol [333]	<i>D. loddigesii</i>	whole plant	(Ito <i>et al.</i> , 2010)
4-(2-Hydroxypropyl)-2(5H)-furanone [334]	<i>D. tortile</i>	whole plant	(Limpanit <i>et al.</i> , 2016)
5,7-Dihydroxychromen-4-one [335]	<i>D. ellipsophyllum</i>	whole plant	(Tanagornmeatar <i>et al.</i> , 2014)
RF-3192C [336]	<i>D. scabrilingue</i>	whole plant	(Sarakulwattana <i>et al.</i> , 2018)

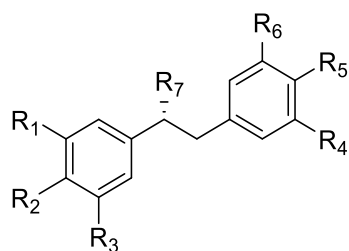


	R ₁	R ₂	R ₃	R ₄	R ₅	R ₆
[38] Aloifol I	OMe	OH	OMe	OH	H	H
[39] Amoenylin	OMe	OH	OMe	H	OMe	H
[40] Batatasin	OMe	H	H	OH	H	OH
[41] Batatasin III	OH	H	OMe	H	H	OH
[42] Brittonin A	OMe	OMe	OMe	OMe	OMe	OMe
[43] Chrysotobibenzyl	OMe	OMe	OMe	OMe	OMe	H
[44] Chrysotoxine	OMe	OH	OMe	OMe	OMe	H
[45] Crepidatin	OMe	OMe	OMe	OMe	OH	H
[46] Cumulatin	OMe	OMe	OH	OH	OMe	OMe
[47] Dendrobin A	OH	OH	OMe	H	H	OMe
[48] Dendromoniliside E	OGlc	OGlc	OMe	H	OMe	H
[49] 3,3'-Dihydroxy-4,5-dimethoxybibenzyl	OMe	OMe	OH	H	H	OH
[50] 3,4'-Dihydroxy-5-methoxybibenzyl	OH	H	OMe	H	OH	H
[51] 3,4'-Dihydroxy-5,5'-dimethoxydihydrostilbene	OH	H	OMe	OMe	OH	H
[52] 3,4'-Dihydroxy-3',4,5-trimethoxybibenzyl	OMe	OMe	OH	H	OH	OMe

Figure 5 Structures of compounds from *Dendrobium*

	R ₁	R ₂	R ₃	R ₄	R ₅	R ₆
[53] Erianin	OMe	OMe	H	OMe	OH	OMe
[54] Gigantol	OMe	H	H	H	OH	OMe
[55] Gigantol-5-O- β -D-glucopyranoside	OMe	H	OGlc	H	OH	OMe
[56] 4-Hydroxy-3,5,3'-trimethoxybibenzyl	OMe	OH	OMe	H	H	OMe
[57] 5-Hydroxy-3,4,3',4',5'-penta-methoxybibenzyl	OMe	OMe	OH	OMe	OMe	OMe
[58] Isoamoenylin	OMe	OMe	OMe	H	H	OH
[59] Moscatilin	OMe	OH	OMe	H	OH	OMe
[60] Moscatilin diacetate	OMe	OAc	OMe	H	OAc	OMe
[61] 3,3',4-Trihydroxybibenzyl	OH	OH	H	H	H	OH
[62] 3,3',5-Trihydroxybibenzyl	OH	H	OH	H	H	OH
[63] 3,5,4'-Trihydroxybibenzyl	OH	H	OH	H	OH	H
[64] 4,5,4'-Trihydroxy-3,3'-dimethoxybibenzyl	OMe	OH	OH	H	OH	OMe
[65] 4,3',4'-Trihydroxy-3,5-dimethoxybibenzyl	OMe	OH	OMe	H	OH	OH
[66] Tristin	OH	H	OH	H	OH	OMe

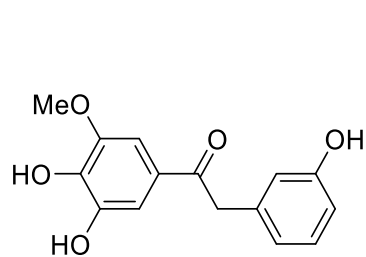
Figure 5 (continued)



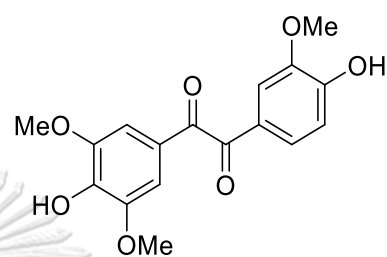
	R ₁	R ₂	R ₃	R ₄	R ₅	R ₆	R ₇
[67] Dendrophenol	OMe	OH	OMe	OH	H	OH	H
[68] Dendrocandin A	OMe	OH	OH	H	OMe	H	OMe
[69] Dendrocandin C	OMe	OH	OH	H	OH	H	OMe
[70] Dendrocandin D	OMe	OH	OH	H	OH	H	OEt
[71] Dendrocandin E	OMe	OH	OH	OH	OH	H	H
[72] Dendrosinen A	OMe	OMe	OH	H	OH	H	OH
[73] Dendrosinen B	OMe	OMe	OH	H	OH	H	H
[74] 3,4-Dihydroxy-5,4'- dimethoxybibenzyl	OH	OH	OMe	H	OMe	H	H
[75] 4,4'-Dihydroxy-3,5- dimethoxybibenzyl	OMe	OH	OMe	H	OH	H	H
[76] 4-[2-(3-Hydroxyphenyl)-1- methoxyethyl]-2,6- dimethoxyphenol	OMe	OH	OMe	H	H	OH	OMe
[77] Loddigesiinol C	OMe	OH	OMe	H	OH	OMe	OMe
[78] 3-O-Methylgigantol	OMe	H	OH	OMe	OMe	H	H
[79] Nobilin A	OMe	OH	OH	H	H	OMe	OMe

Figure 5 (continued)

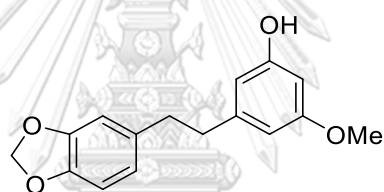
	R ₁	R ₂	R ₃	R ₄	R ₅	R ₆	R ₇
[80] Nobilin B	OMe	OH	OMe	H	OH	OMe	OMe
[81] Nobilin C	OMe	OH	OMe	H	OMe	OMe	OMe
[82] Nobilin D	OMe	OH	H	OMe	OH	OMe	OH



[83] Dendrosinen C

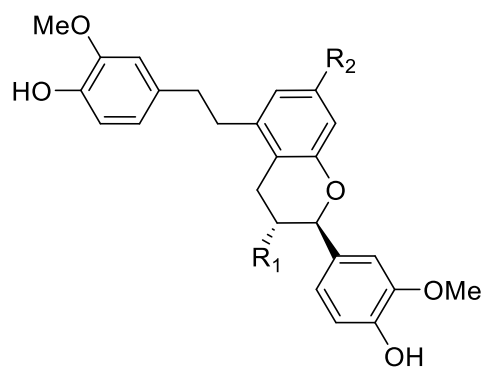


[84] Loddigesiinol D



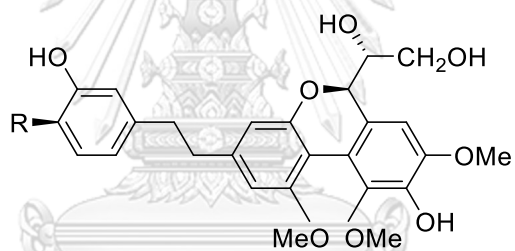
[85] Densiflorol A

Figure 5 (continued)



R₁ R₂

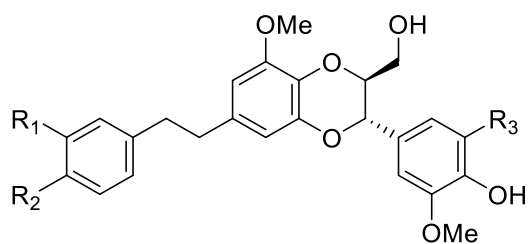
[86] Crepidatuol A	H	OMe
[87] Crepidatuol B	OH	OMe
[88] Trigonopol B	OH	OH



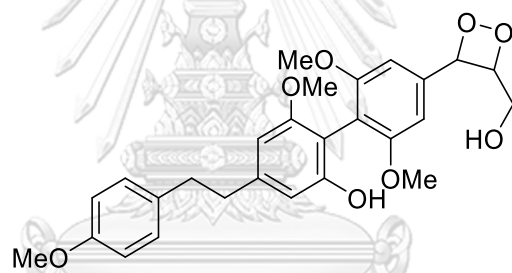
[89] Longicornuol A: R = H

[90] Trigonopol A: R = OMe

Figure 5 (continued)



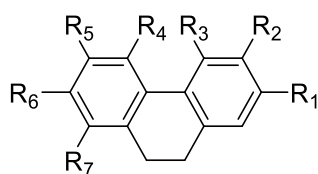
	R ₁	R ₂	R ₃
[91] Dendrocandine B	H	OMe	OMe
[92] Dendrocandine T	OMe	OH	OMe
[93] Dendrocandine U	H	OH	OMe
[94] Dendrocandine V	H	OMe	H



[95] Dendrowillot A

จุฬาลงกรณ์มหาวิทยาลัย
CHULALONGKORN UNIVERSITY

Figure 5 (continued)



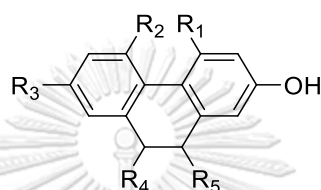
	R ₁	R ₂	R ₃	R ₄	R ₅	R ₆	R ₇
[96] 1,5-Dihydroxy-3,4,7-trimethoxy-9,10-dihydrophenanthrene	H	OMe	OMe	OH	H	OMe	H
[97] Coelonin	OH	H	OMe	H	H	OH	H
[98] Dendroinfundin A	OMe	OMe	OH	H	H	OMe	H
[99] Dendroinfundin B	OMe	OMe	OH	OH	H	H	OMe
[100] 4,5-Dihydroxy-2,3-dimethoxy-9,10-dihydrophenanthrene	OMe	OMe	OH	OH	H	H	H
[101] 4,5-Dihydroxy-2,6-dimethoxy-9,10-dihydrophenanthrene	OMe	H	OH	OH	OMe	H	H
[102] 4,5-Dihydroxy-3,7-dimethoxy-9,10-dihydrophenanthrene	H	OMe	OH	OH	H	OMe	H
[103] 4,5-Dihydroxy-2-methoxy-9,10-dihydrophenanthrene (Orchinol)	OMe	H	OH	OH	H	H	H

Figure 5 (continued)

	R ₁	R ₂	R ₃	R ₄	R ₅	R ₆	R ₇
[104] 9,10-Dihydromoscatin	H	H	OH	OMe	H	OH	H
[105] 9,10-Dihydrophenanthrene -2,4,7-triol	OH	H	OH	H	H	OH	H
[106] 2,7-Dihydroxy-3,4,6-trimethoxy-9,10-dihydrophenanthrene	OH	OMe	OMe	H	OMe	OH	H
[107] 2,8-Dihydroxy-3,4,7-trimethoxy-9,10-dihydrophenanthrene	OH	OMe	OMe	H	H	OMe	OH
[108] 4,7-Dihydroxy-2,3,6-trimethoxy-9,10-dihydrophenanthrene	OMe	OMe	OH	H	OMe	OH	H
[109] 3,4-Dimethoxy-1-(methoxymethyl)-9,10-dihydrophenanthrene-2,7-diol	OH	H	H	OMe	OMe	OH	CH ₂ OMe
[110] Ephemeranthol A	OH	H	H	OH	OMe	OMe	H
[111] Ephemeranthol C	OH	OH	OMe	OH	H	H	H
[112] Erianthridin	OH	OMe	OMe	H	H	OH	H
[113] Flavanthridin	OH	H	H	OMe	OH	OMe	H
[114] Hircinol	OH	H	OMe	OH	H	H	H

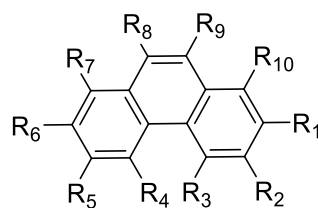
Figure 5 (continued)

	R ₁	R ₂	R ₃	R ₄	R ₅	R ₆	R ₇
[115] 3-Hydroxy-2,4,7- trimethoxy-9,10-dihydrophenanthrene	OMe	OH	OMe	H	H	OMe	H
[116] 7-Hydroxy-2,3,4-trimethoxy-9,10-dihydrophenanthrene	OMe	OMe	OMe	H	H	OH	H
[117] Lusianthridin	OMe	H	OH	H	H	OH	H



	R ₁	R ₂	R ₃	R ₄	R ₅
[118] 2-Hydroxy-4,7-dimethoxy-9,10-dihydrophenanthrene	OMe	H	OMe	H	H
[119] 7-Methoxy-9,10-dihydrophenanthrene-2,4,5-triol	OH	OH	OMe	H	H
[120] 2,5,7-Trihydroxy-4-methoxy-9,10-dihydrophenanthrene	OMe	OH	OH	H	H
[121] Plicatol C	OMe	OH	H	OMe	OMe
[122] Rotundatin	OMe	OH	H	OH	OH
[123] (S)-2,4,5,9-Tetrahydroxy-9,10dihydrophenanthrene	OH	OH	H	OH	H

Figure 5 (continued)

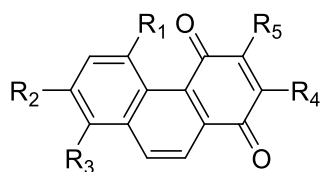


	R ₁	R ₂	R ₃	R ₄	R ₅	R ₆	R ₇	R ₈	R ₉	R ₁₀
[124] 2,5-Dihydroxy- 3,4- dimethoxy phenanthrene	OH	OMe	OMe	OH	H	H	H	H	H	H
[125] 2,5-Dihydroxy- 4,9-dimethoxy phenanthrene	OH	H	OMe	OH	H	H	H	OMe	H	H
[126] 2,8-Dihydroxy- 3,4,7- trimethoxy phenanthrene	OH	OMe	OMe	H	H	OMe	OH	H	H	H
[127] Epheranthol B	H	H	OMe	OH	H	OMe	H	H	H	H
[128] Fimbriol B	OH	OMe	OH	H	H	H	H	H	H	H
[129] Flavanthrinin	H	H	OMe	H	H	OH	H	H	H	H
[130] Moscatin	H	H	OH	OMe	H	OH	H	H	H	H
[131] Loddigesinol A	OH	H	OMe	OMe	H	H	H	OH	H	H
[132] Dendroscabrol A	OH	OMe	OMe	H	H	OMe	H	H	H	H
[133] Nudol	OH	OMe	OMe	H	H	OH	H	H	H	H
[134] Plicatol A	OH	H	OMe	OH	H	H	H	OMe	OMe	OH
[135] Plicatol B	OH	H	OMe	OH	H	H	H	H	H	H

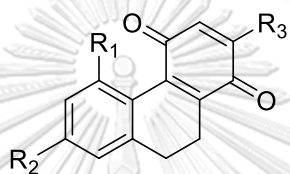
Figure 5 (continued)

	R ₁	R ₂	R ₃	R ₄	R ₅	R ₆	R ₇	R ₈	R ₉	R ₁₀
[136] 2,3,5-Trihydroxy-4,9-dimethoxyphenanthrene	OH	OH	OMe	OH	H	H	H	OMe	H	H
[137] 3,4,8-Trimethoxyphenanthrene-2,5-diol	OH	OMe	OMe	OH	H	H	OMe	H	H	H
[138] Bulbophyll-anthrin	OMe	OH	OMe	OH	H	H	H	H	H	H
[139] Denthyrsinin	OMe	OH	OMe	H	H	OH	OMe	H	H	H
[140] 5-Hydroxy-2,4-dimethoxyphenanthrene	OMe	H	OMe	OH	H	H	H	H	H	H
[141] 3-Hydroxy-2,4,7-trimethoxyphenanthrene	OMe	OH	OMe	H	OMe	H	H	H	H	H
[142] Confusarin	OH	H	H	OMe	OMe	OH	H	H	H	OMe
[143] 2,6-Dihydroxy-1,5,7-trimethoxyphenanthrene	OH	H	H	OMe	OH	OMe	H	H	H	OMe
[144] 1,5,7-Trimethoxyphenanthrene-2-ol	OH	H	H	OMe	H	OMe	H	H	H	OMe

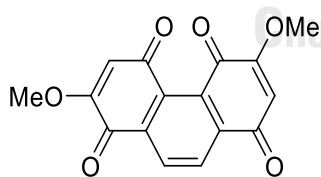
Figure 5 (continued)



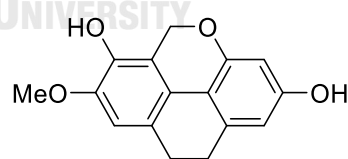
	R ₁	R ₂	R ₃	R ₄	R ₅
[145] Cypripedin	H	OH	OMe	OMe	H
[146] Densiflorol B	H	OH	H	OMe	H
[147] Denbinobin	OH	OMe	H	H	OMe



	R ₁	R ₂	R ₃
[148] Dendronone	OH	OMe	H
[149] Ephemeranthoquinone	H	OH	OMe
[15] 5-Methoxy-7-hydroxy-9,10-dihydro-1,4-phenanthrenequinone	OMe	OH	H

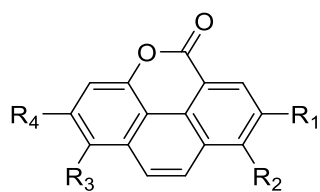


[150] Moniliformin



[151] Amoenumin

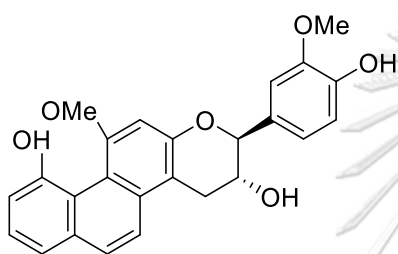
Figure 5 (continued)



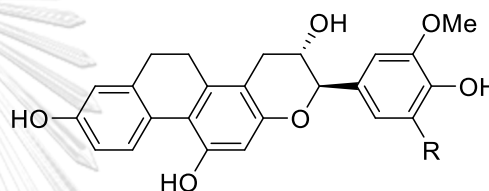
R₁ R₂ R₃ R₄

[152] Fimbriatone OH OMe H OH

[153] Crystalltone OMe H OH EtO

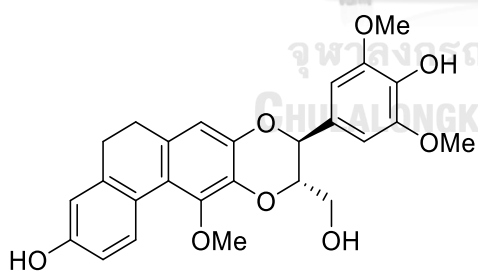


[154] Loddigesiinol B

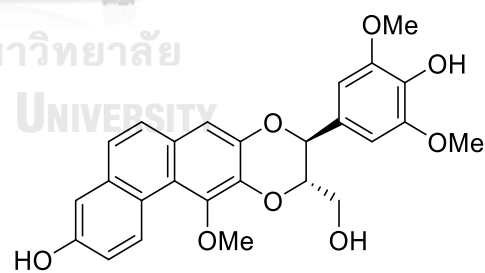


[155] Chrysotoxol A: R = H

[156] Chrysotoxol B: R = OMe

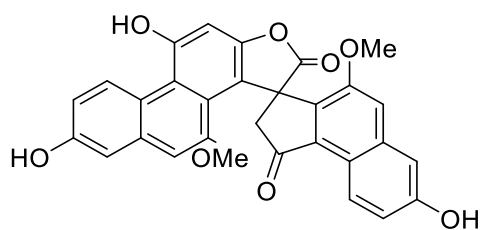


[157] Dendrocandin P2

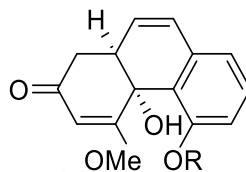


[158] Dendrocandin P1

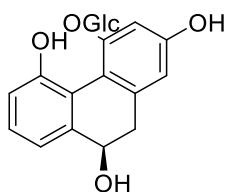
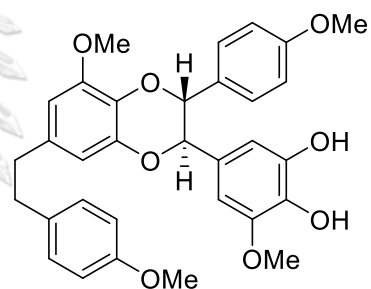
Figure 5 (continued)



[159] Dendrochrysanene



[160] Aphyllone: R = H

[161] 9,10-Dihydro-aphyllone A-5-O- β -D-glucopyranoside: R = Glc[162] 2,4,5,9S-Tetrahydroxy-9,10-dihydro-phenanthrene-4-O- β -D-glucopyranoside

[163] Dendrocandine I

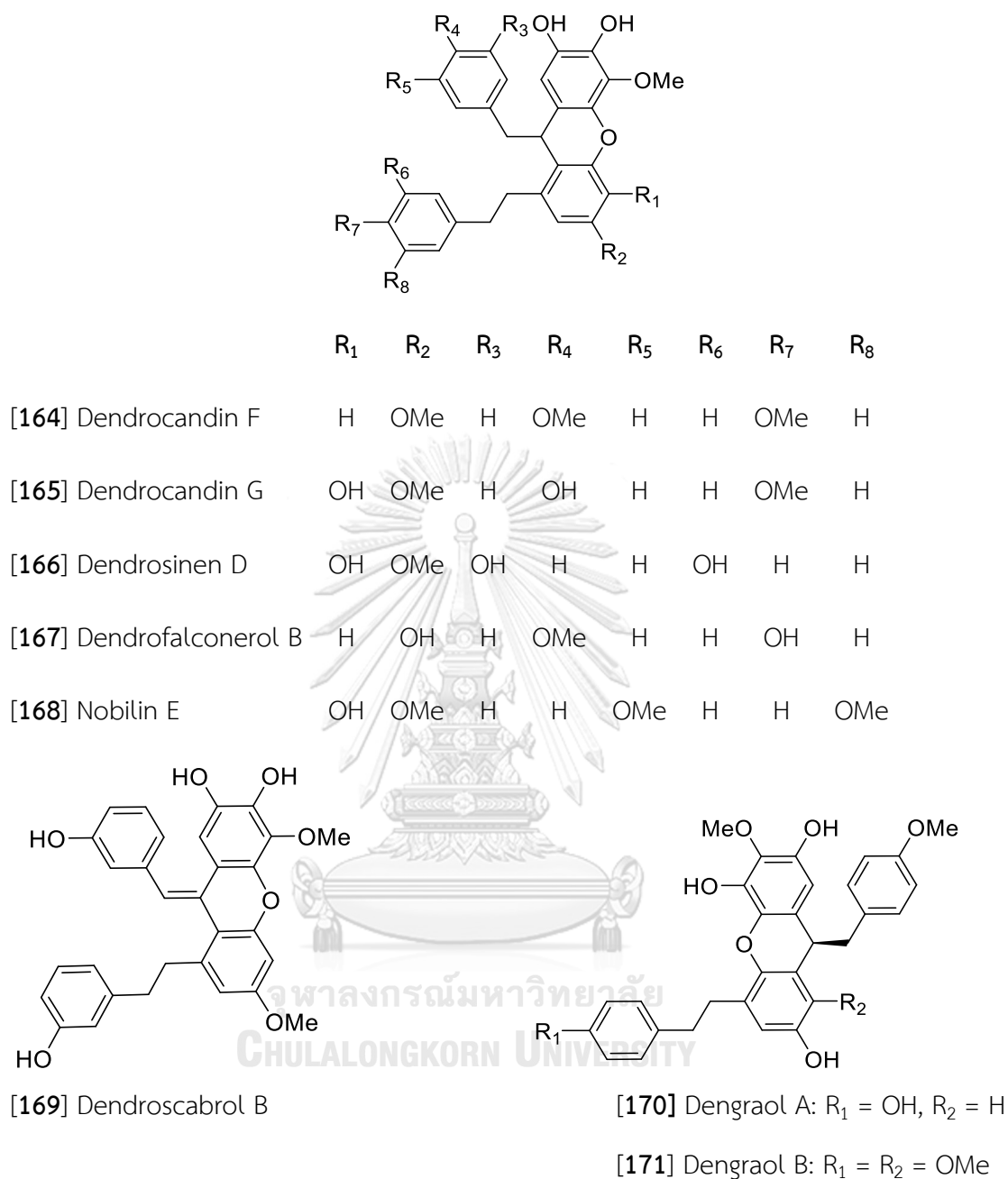
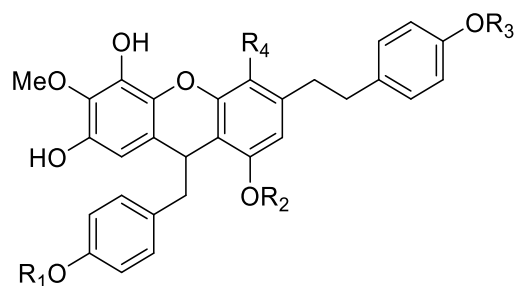


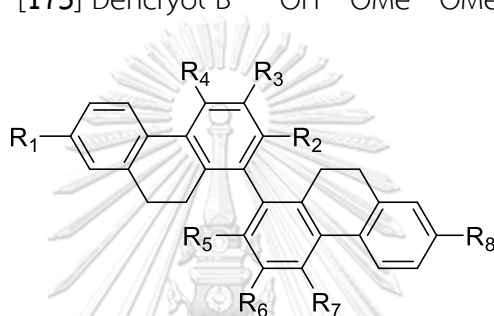
Figure 5 (continued)



R₁ R₂ R₂ R₄

[172] Dencryol A OMe OH OH H

[173] Dencryol B OH OMe OMe OH



R₁ R₂ R₃ R₄ R₅ R₆ R₇ R₈

[174] 2,2'-Dihydroxy-

3,3',4,4',7,7'-hexamethoxy-9,9',10,10'-

tetrahydro-1,1'-

biphenanthrene

OMe OH OMe OMe OH OMe OMe OMe

[175] 2,2'-Dimethoxy-4,4',7,7'-

tetrahydroxy-9,9',10,10'-

tetrahydro-1,1'-

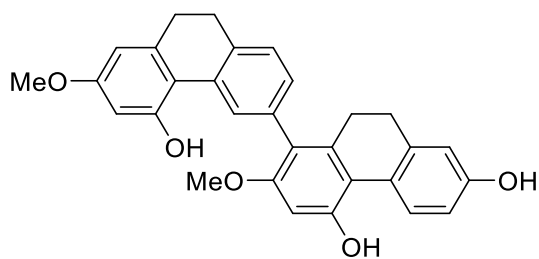
biphenanthrene

OH OMe H OH OMe H OH OH

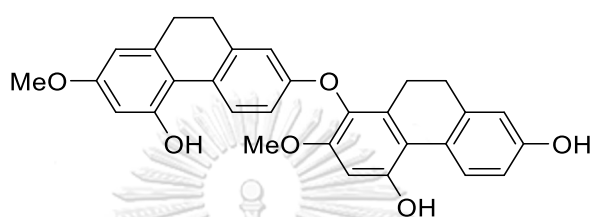
[176] Flavanthrin

OH OH H OMe OH H OMe OH

Figure 5 (continued)



[177] Phoyunnanin C



[178] Phoyunnanin E

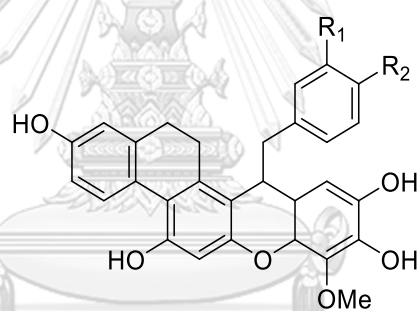
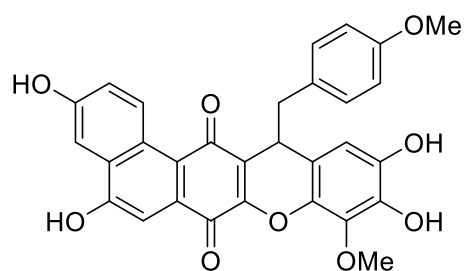
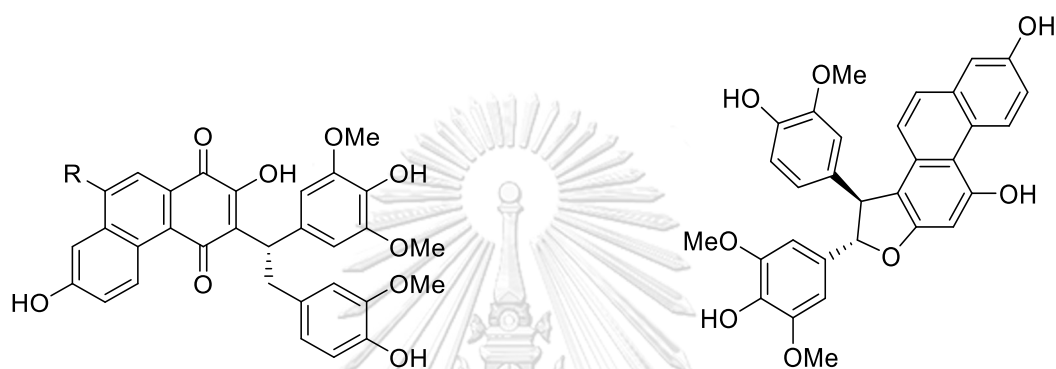
[179] Dendrosignatol: $R_1 = H$, $R_2 = OMe$ [180] Dendroparishiol: $R_1 = OMe$, $R_2 = OH$

Figure 5 (continued)



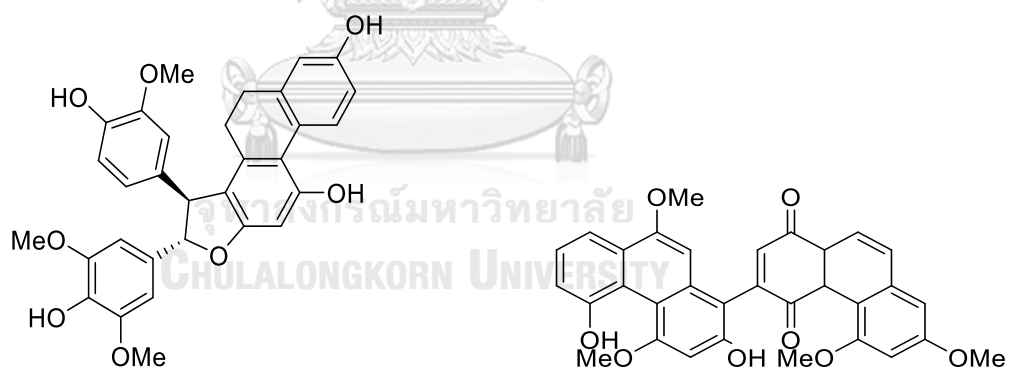
[181] Dendrocandine H



[182] Loddigesiinol G: R = H

[184] Loddigesiinol I

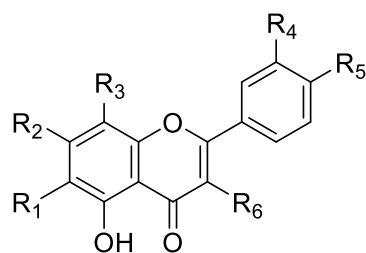
[183] Loddigesiinol H: R = OH



[16] Loddigesiinol J

[185] Dendropalpebrone

Figure 5 (continued)



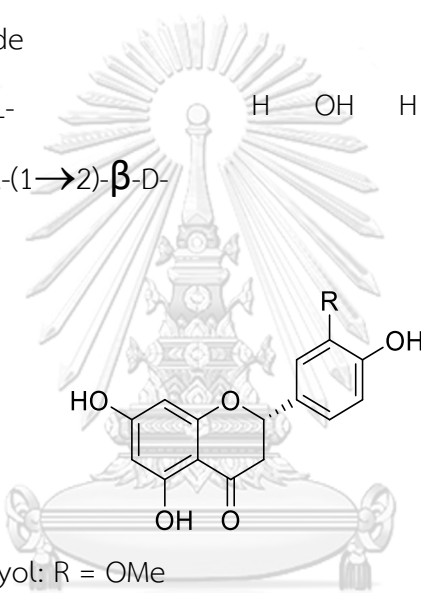
	R ₁	R ₂	R ₃	R ₄	R ₅	R ₆
[186] Apigenin	H	OH	H	H	OH	H
[187] Apigenin-6-C-glucosyl-(1→2)- α - L-arabinoside	[Ara-] ₂	OH	H	H	OH	H
[188] 6-C-(α -Arabinopyranosyl)-8-C-[(2- O- α -rhamnopyranosyl)- β - galactopyranosyl] apigenin	-Ara	OH	-Gal-Rha	H	OH	H
[189] 6-C-(α -Arabinopyranosyl)-8-C-[(2- O- α -rhamnopyranosyl)- β - glucopyranosyl]apigenin	-Ara	OH	-Glc- Rha	H	OH	H
[190] 6-C-[(2-O- α -Rhamnopyranosyl)- β - glucopyranosyl]-8-C- (α -arabino- pyranosyl)apigenin	-Glc-Rha	OH	-Ara	H	OH	H

Figure 5 (continued)

	R ₁	R ₂	R ₃	R ₄	R ₅	R ₆
[191] 6-C-(β -Xylopyrano-syl)-8-C- [(2-O- α -rhamno-pyranosyl)- β -glucopyranosyl]apigenin	-Xyl	OH	-Glc-Rha	H	OH	H
[192] 5,6-Dihydroxy-4'-methoxyflavone	OH	H	H	H	OMe	H
[193] 6'''-Glucosyl-vitexin	H	OH	-(Glc) ₂	H	OH	H
[6] 5-Hydroxy-3-methoxy-flavone-7-O-[β -D-apiosyl-(1 \rightarrow 6)]- β -D-glucoside	H	-Glc- Api	H	H	H	OMe
[194] Isoschaftoside	-Ara	OH	-Glc	H	OH	H
[195] Isoviolanthin	-Rha	OH	-Glc	H	OH	H
[1] Kaempferol	H	OH	H	H	OH	OH
[196] Kaempferol-3-O- α -L-rhamnopyranoside	H	OH	H	H	OH	O-Rha
[197] Kaempferol-3,7-O-di- α -L-rhamnopyranoside	H	O-Rha	H	H	OH	O-Rha
[198] Kaempferol-3-O- α -L-rhamnopyranosyl (1 \rightarrow 2)- β -D-glucopyranoside	H	OH	H	H	OH	O-Glc-Rha

Figure 5 (continued)

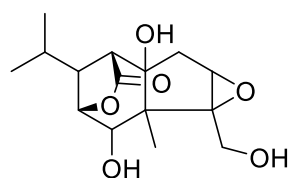
	R ₁	R ₂	R ₃	R ₄	R ₅	R ₆
[199] Kaempferol-3-O- α -L-rhamnopyranosyl(1 \rightarrow 2)- β -D-xylopyranoside	H	OH	H	H	OH	O-Xyl- Rha
[200] Luteolin	H	OH	H	OH	OH	H
[201] Vicenin-2	-Glc	OH	-Glc	H	OH	H
[202] Quercetin-3-O- α -L-Rhamnopyranoside	H	OH	H	OH	OH	-O-Rha
[203] Quercetin-3-O- α -L-rhamnopyranosyl(1 \rightarrow 2)- β -D-xylopyranoside	H	OH	H	OH	OH	-O-Xyl-Rha



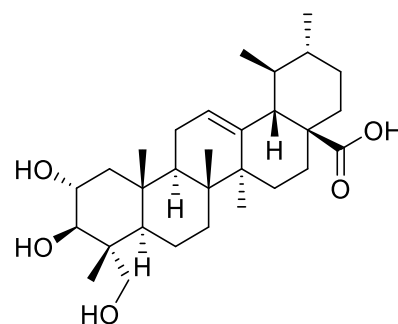
[204] (2S)-Homoeriodictyol: R = OMe

[205] Naringenin: R = H

[206] (2S)-Eriodictyol: R = OH

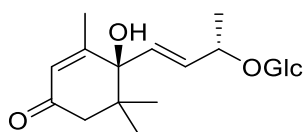


[207] Amoenin

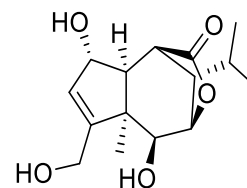


[208] Asiatic acid

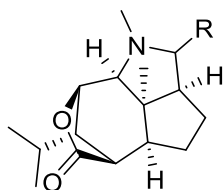
Figure 5 (continued)



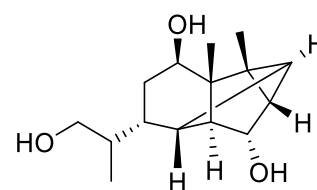
[209] Corchoionoside C



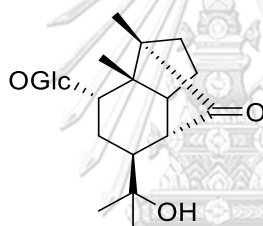
[210] Crystallinin

[211] (-)-(1*R*,2*S*,3*R*,4*S*,5*R*,6*S*,9*S*,11*R*)-11-Carboxymethyldendrobine: R = CH₂COOH

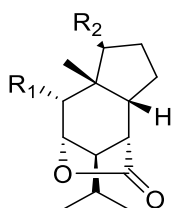
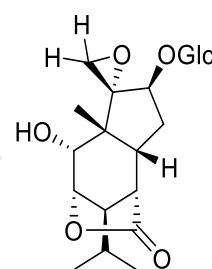
[212] Dendrobine: R = H



[213] Dendrobane A

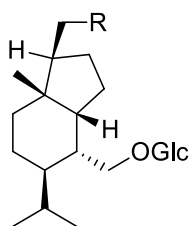


[214] Dendromonilide A

[215] Dendromonilide B, R₁ = OGlc, R₂ = COOH[217] Dendromonilide D, R₁ = OH, R₂ = OGlc

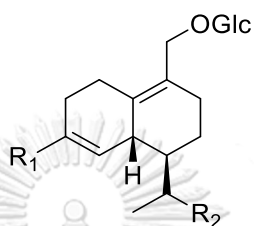
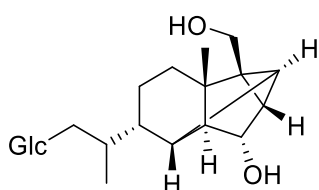
[216] Dendromonilide C

Figure 5 (continued)

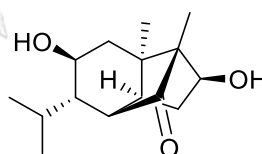


[218] Dendronobiloside A: R = OGlc

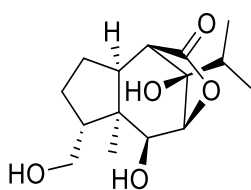
[219] Dendronobiloside B: R = OH

[220] Dendronobiloside C, R₁ = -CH₂OGlc, R₂ = H[221] Dendronobiloside D, R₁ = H, R₂ = OGlc

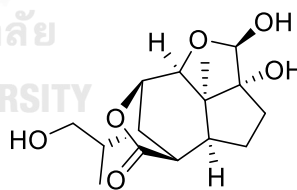
[222] Dendronobiloside E



[223] Dendronobilin A

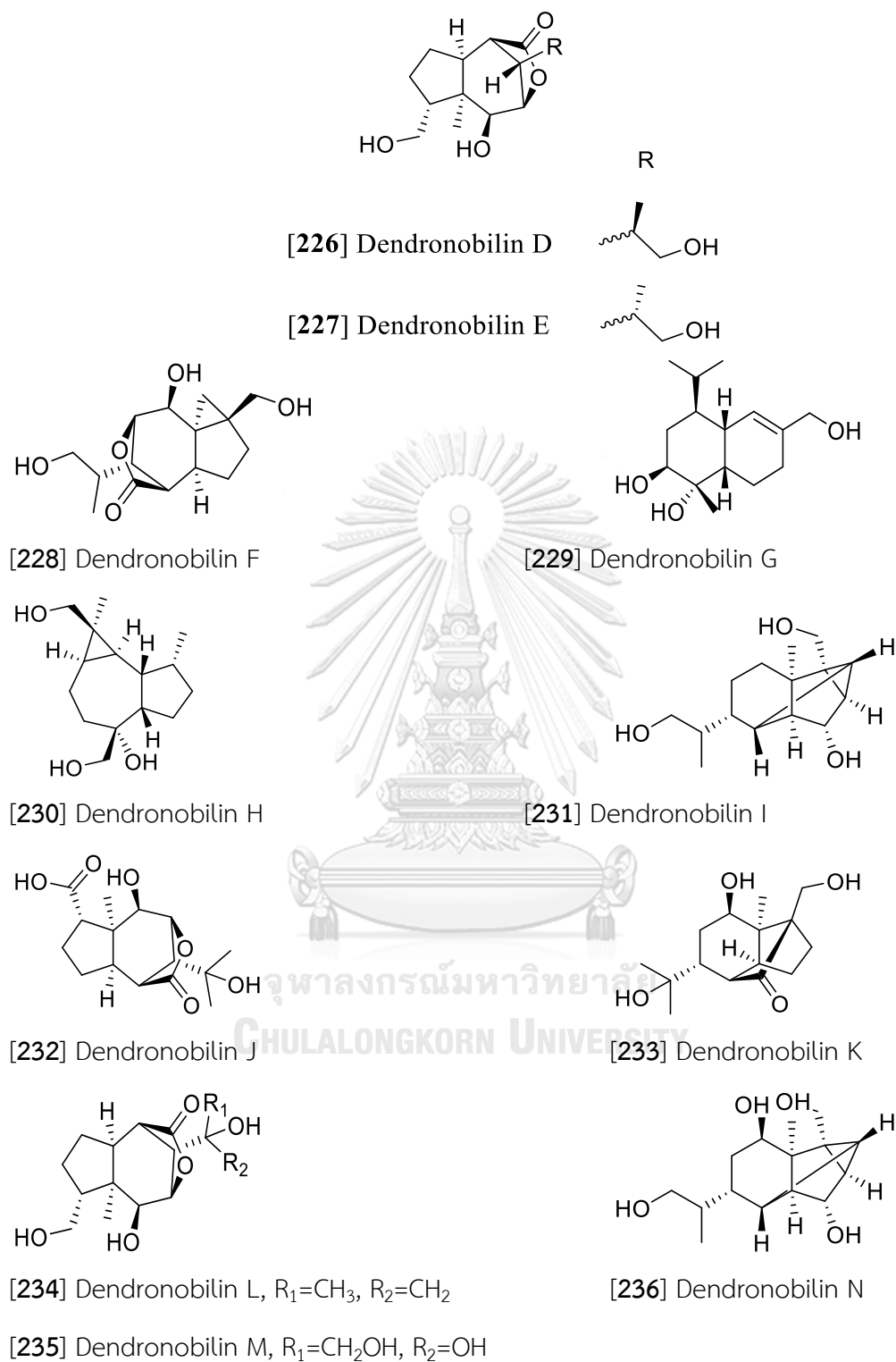


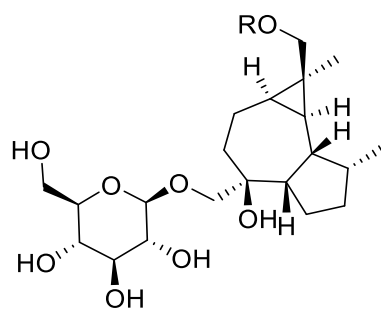
[224] Dendronobilin B



[225] Dendronobilin C

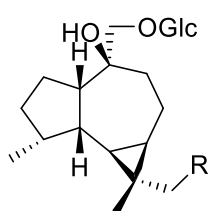
Figure 5 (continued)





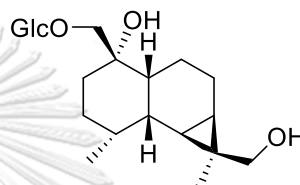
[237] Dendroside A : R = H

[238] Dendroside B : R = Glc

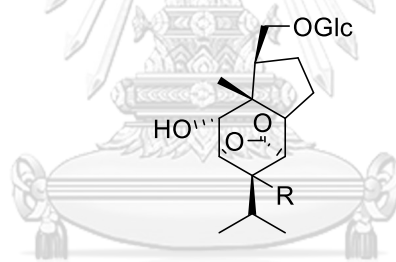


[239] Dendroside C; R = OH

[240] Dendroside D; R = OGlc

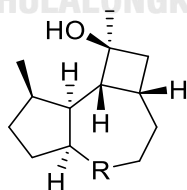


[241] Dendroside E



[242] Dendroside F; R = H

[243] Dendroside G; R = OH



[244] Dendrowardol A

[245] Dendrowardol B

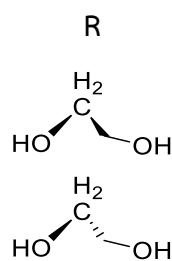
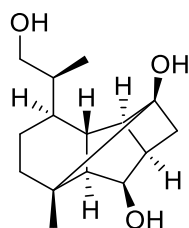
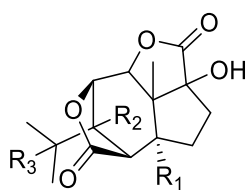
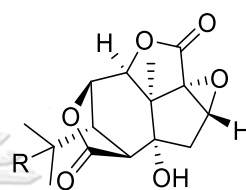
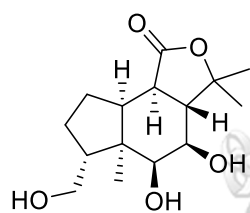


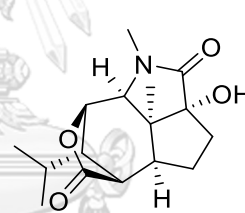
Figure 5 (continued)



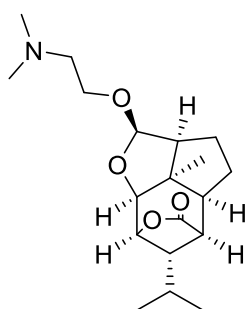
[246] Dendrowardol C

[247] Amotin: $R_1 = R_3 = H, R_2 = OH$ [248] Dendrowillin A: $R_1 = R_3 = OH, R_2 = H$ [249] Dendrowillin B: $R_1 = R_2 = H, R_3 = OH$ [250] α -Dihydropicrotoxinin: $R = H$ [251] Picrotin: $R = OH$ 

[252] Findlayanin



[253] 3-Hydroxy-2-oxodendrobine



[254] Wardianumine A

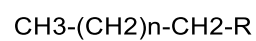
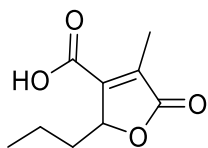
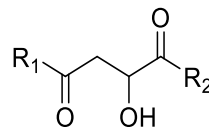
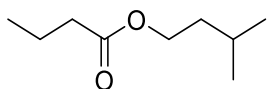
[255] Aliphatic acids: $R = COOH, n = 19-31$ [256] Aliphatic alcohols: $R = OH, n = 22-32$

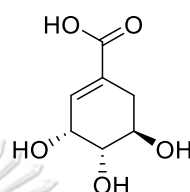
Figure 5 (continued)



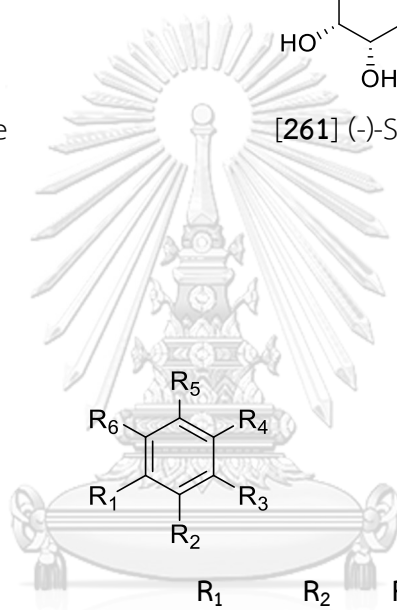
[257] Decumbic acid

[258] Dimethyl malate: $R_1 = R_2 = \text{OMe}$ [259] Malic acid: $R_1 = R_2 = \text{OH}$ 

[260] Isopentyl butyrate



[261] (-)-Shikimic acid



[262] Antiarol

[263] Ethylhaematommate

[264] Gallic acid

[265] *p*-Hydroxy-benzaldehyde[266] *p*-Hydroxybenzoic acid

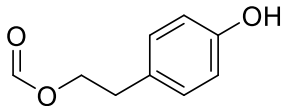
[267] 3-Hydroxy-2-methoxy-5,6-dimethylbenzoic acid

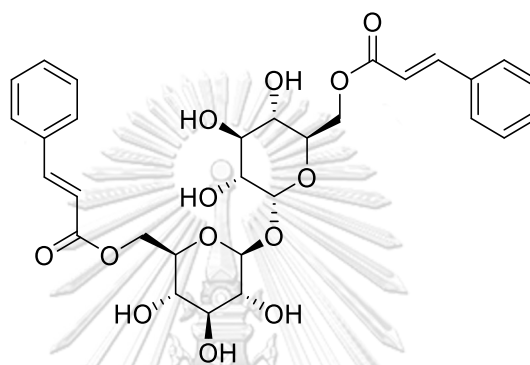
[268] Methyl-4-hydroxybenzoate

[269] Methyl β -orsellinate

	R_1	R_2	R_3	R_4	R_5	R_6
[262] Antiarol	OMe	OMe	H	OH	H	OMe
[263] Ethylhaematommate	H	CH ₃	COOC ₂ H ₅	OH	CHO	OH
[264] Gallic acid	OH	OH	OH	H	COOH	H
[265] <i>p</i> -Hydroxy-benzaldehyde	OH	H	H	CHO	H	H
[266] <i>p</i> -Hydroxybenzoic acid	H	OH	H	H	H	COOH
[267] 3-Hydroxy-2-methoxy-5,6-dimethylbenzoic acid	COOH	CH ₃	CH ₃	H	OH	OMe
[268] Methyl-4-hydroxybenzoate	H	H	COOMe	H	H	OH
[269] Methyl β -orsellinate	H	OH	COOMe	CH ₃	H	OH

Figure 5 (continued)

	R ₁	R ₂
[286] Ferulic acid	OMe	COOH
[287] 2-(<i>p</i> -Hydroxyphenyl)-ethyl- <i>p</i> -coumarate	OMe	
[288] Coniferyl alcohol	OMe	CHO



[289] Dendroside

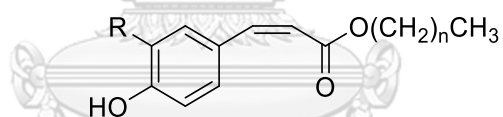
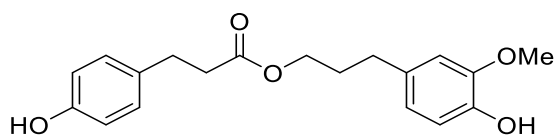
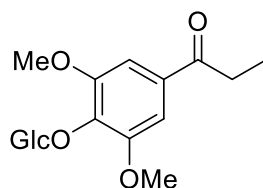
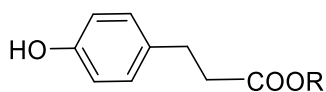
[290] *cis*-Hexacosanoyl ferulate: R= OMe, n=25[291] *cis*-Tetracosanoyl ferulate :R= OMe, n=22[292] Tetracosyl (*Z*)-*p*-coumarate: R= H, n=23[293] Dihydroconiferyl dihydro-*p*-coumarate

Figure 5 (continued)

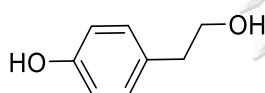


[294] 1-[4-(β -D-glucopyranosyloxy)-3,5-dimethoxyphenyl]-1-propanone

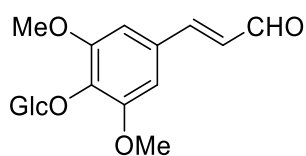


[295] *p*-Hydroxyphenyl propionic
methyl ester: R = CH₃

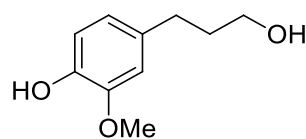
[296] Phloretic acid: R = H



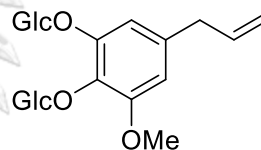
[298] Salidroslol



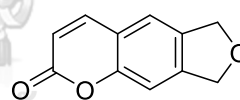
[300] Syringin



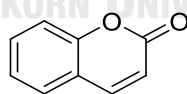
[297] Dihydroconiferyl alcohol



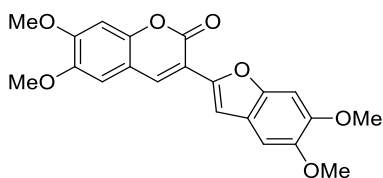
[299] Shashenoside I



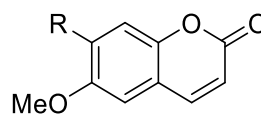
[301] Ayapin



[302] Coumarin



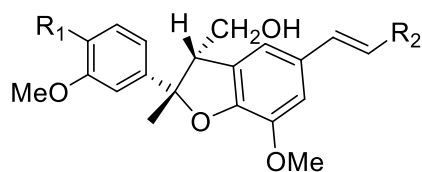
[303] Denthyrsin



[304] Scoparone: R = OMe

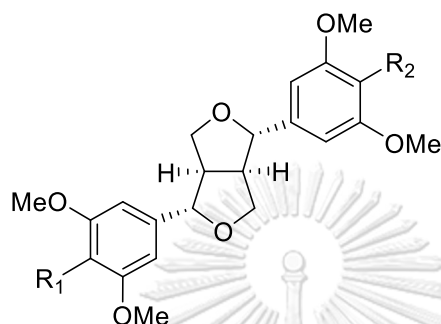
[305] Scopoletin: R = OH

Figure 5 (continued)



[306] Dehydrodiconiferyl alcohol-4- O - β -D-glucoside: $R_1=OGlc$, $R_2=CH_2OH$

[307] Balanophonin,: $R_1=OH$, $R_2=CHO$



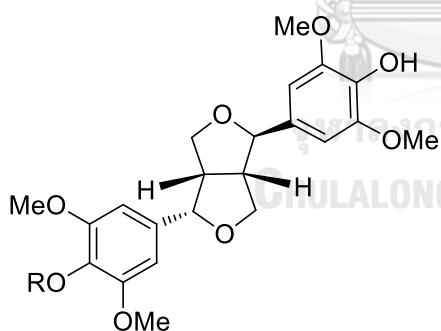
[308] Acanthoside B

[309] Liriodendrin

[310] Syringaresinol

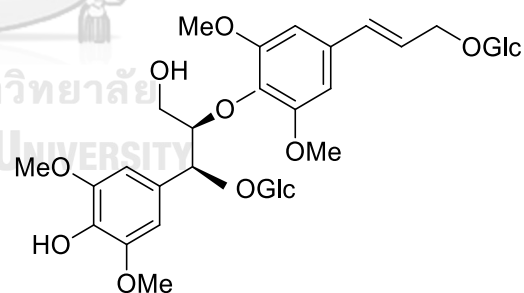
[311] Syringaresinol-4- O -D-monoglucopyranoside

R_1	R_2
OGlc	OH
OGlc	OGlc
OH	OH
OGlc	H



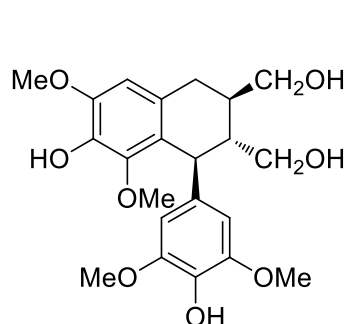
[312] Episyngaresinol: $R = H$

[313] Episyngaresinol 4''- O - β -D-glucopyranoside: $R = Glc$

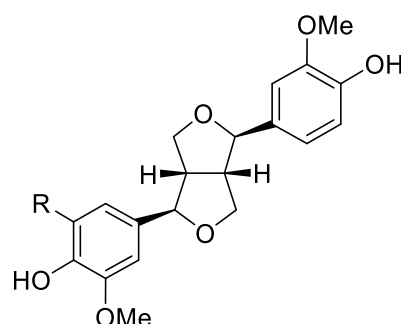


[314] (-)-(7S,8R,7'E)-4-Hydroxy-3,3',5,5'-tetramethoxy-8,4'-oxyneolign-7'-ene-7,9,9'-triol-7,9'-bis- O - β -D-glucopyranoside

Figure 5 (continued)

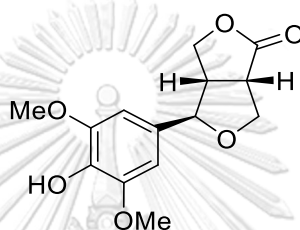


[315] Lyoniresinol



[316] (-)-Medioresinol: R = OMe

[317] (-)-Pinoresinol: R = H



[318] Dendrolactone

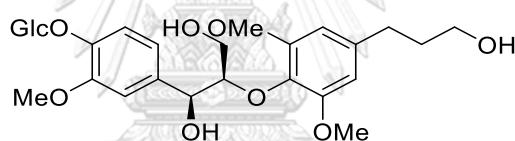
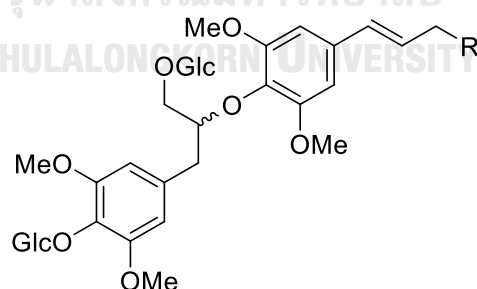
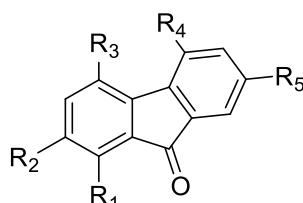
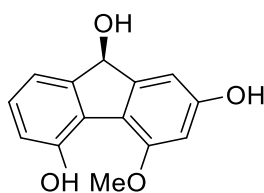
[319] *Erythro*-1-(4- O - β -D-glucopyranosyl-3-methoxyphenyl)-2-[4-(3-hydroxypropyl)-2,6-dimethoxyphenoxy]-1,3-propanediol[320] (-)-(8*R*,7'*E*)-4-Hydroxy-3,3',5,5'-tetramethoxy-8,4'-oxyneolign-7'-ene-9,9'-diol 4,9-bis- O - β -D-glucopyranoside: R = OH; 8*R*[321] (-)-(8*S*,7'*E*)-4-Hydroxy-3,3',5,5'-tetramethoxy-8,4'-oxyneolign-7'-ene-9,9'-diol 4,9-bis- O - β -D-glucopyranoside: R = OH; 8*S*

Figure 5 (continued)

[322] (-)-(8*R*,7'*E*)-4-Hydroxy-3,3',5,5',9'-pentamethoxy-8,4'-oxyneolign-7'-ene-9-ol
4,9-bis-*O*- β -D-glucopyranoside: R = OMe; 8*R*



	R ₁	R ₂	R ₃	R ₄	R ₅
[323] Denchrysan A	H	OH	OH	OMe	OH
[324] Dendroflorin	OH	H	OH	OMe	OH
[325] Dengibsin	H	OH	OMe	OH	H
[326] Nobilone	H	OH	H	OMe	OH
[327] 1,4,5-Trihydroxy-7-methoxy-9 <i>H</i> -fluoren-9-one	OH	H	OH	OH	OMe
[328] 2,4,7-Trihydroxy-5-methoxy-9-fluorenone	OMe	OH	OH	H	OH
[329] 2,4,7-Trihydroxy-1,5-dimethoxy-9-fluorenone	OMe	OH	OH	OMe	OH



[330] Denchrysan B

Figure 5 (continued)

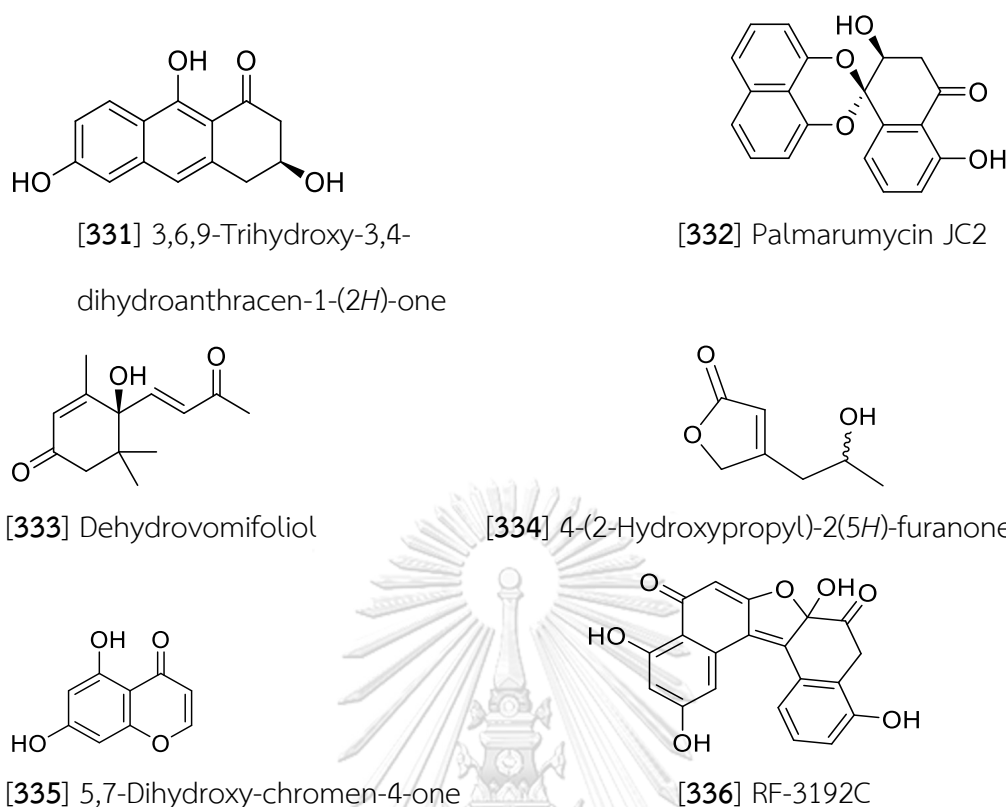


Figure 5 (continued)

2.3 Biological studies

Previous studies have shown that *Dendrobium* plants possess diverse biological activities. Examples are antioxidant [*D. nobile* (Zhang *et al.*, 2008c)], anticancer [*D. signatum* (Mitrphab *et al.*, 2016)], antimicrobial [*D. amoenum* (Paudel *et al.*, 2018)], antimalarial [*D. venustum* (Sukphan *et al.*, 2014)], antiherpes [*D. venustum* (Sukphan *et al.*, 2014)], anti-diabetes [*D. candidum* (Wu *et al.*, 2004)], anti-inflammatory [*D. crepidatum* (Hu *et al.*, 2016)], neuroprotective [*D. aurantiacum* var. *denneanum* (Xiong *et al.*, 2013)], immunomodulatory [*D. Officinale* (Wei *et al.*, 2016)] and antiplatelet aggregation [*D. loddigesii* (Chen *et al.*, 1994a); (Lam *et al.*, 2015)] effects.

Free radical scavenging and antioxidant activities of *Dendrobium* species have been reported in several investigations. Dendrocandin C [69], dendrocandin D [70]

and dendrocandin E [71] from *D. candidum* were reported as potential antioxidants with IC₅₀ values of 34.2, 34.5, and 15.6 mM, respectively, in comparison with vitamin C (IC₅₀ 23.2 μM) (Li *et al.*, 2009b).

In the investigation for antimalarial activity of *D. venustum*, densiflorol B [146] and phoyunnanin E [178] showed potent antimalarial activity with IC₅₀ values of 1.3 and 1.1 μM, respectively, while gigantol [54] (12.2 μM), batatasin III [41] (39.3 μM) and phoyunnanin C [177] (5.8 μM) exhibited moderate activity (Sukphan *et al.*, 2014).

D. candidum has been reported for *in vitro* anti-cancer and *in vivo* anti-metastatic activity in HCT-116 colon cancer cells (Zhao *et al.*, 2014). The ethanolic extract of *D. formosum* showed *in vitro* and *in vivo* anticancer activity in Dalton's lymphoma cells (Prasad & Koch, 2014). Several compounds from *D. brymerianum* exhibited cytotoxic activity against human lung cancer cell line (H46), including moscatilin [59] (IC₅₀ 196.7 μM), gigantol [54] (IC₅₀ 23.4 μM), lusianthridin [117] (IC₅₀ 65.0 μM) and dendroflorin [324] (IC₅₀ 125.8 μM) (Klongkumnuankarn *et al.*, 2015).

Regarding anti-diabetic activity, the polysaccharides from *D. chrysotoxum* (Zhao *et al.*, 2007) and *D. huoshanens* (Pan *et al.*, 2013) showed oral hypoglycemic activity in diabetic mice.

Phenolic glucosides from *D. aurantiacum* var. *denneanum*, for example liriodendrin [309] and (-)-(7*S*,8*R*,7'*E*)-4-Hydroxy-3,3',5,5'-tetramethoxy-8,4'-oxyneolign-7'-ene-7,9,9'-triol-7,9'-bis-*O*-β-D-glucopyranoside [314], showed neuroprotective activity against glutamate-induced neurotoxicity in PC12 cells (Xiong *et al.*, 2013).

With regard to immunomodulatory activity, dendroside A [212] and dendroside B [213] from *D. nobile* showed enhancement of *in vitro* proliferation of murine T and B lymphocytes (Zhang *et al.*, 2006).

Some chemical constituents of *D. densiflorum* namely gigantol [54], moscatilin [59], homoeriodictyol [192], moscatin [130], scoparone [304], displayed

platelet-aggregation activity (Fan *et al.*, 2001). *D. Loddigesii* also showed platelet aggregation activity, and the active principles were identified as moscatilin [59] and moscatin [130] (Chen *et al.*, 1994b).

It is interesting to note that a large number of α -glucosidase inhibitors have been identified from *Dendrobium* plants. Examples are loddigesiinols G-J [182-184, 16] from *D. loddigesii* (Lu *et al.*, 2014), 5-methoxy-7-hydroxy-9,10-dihydro-1,4-phenanthrenequinone [15] from *D. formosum* (Inthongkaew *et al.*, 2017), and dendrofalconerol A [14] from *D. tortile* (Limpanit *et al.*, 2016) and dendroscabrol B [169] from *D. scabrilinque* (Sarakulwattana *et al.*, 2018).

Prior to this study, there have been no reports on the biological activities of *Dendrobium christyanum*.

3. *Gastrochilus bellinus*

3.1 Taxonomic considerations and traditional uses

Gastrochilus, a small genus of monopodial herbs in the family Orchidaceae, is comprised of approximately 62 species. They have been found mainly in Southeast Asia (Liu *et al.*, 2020).

Gastrochilus bellinus (Rchb.f.) Kuntze (“Suea Dam” in Thai or “Wat-Won-Thit-Khwa” in Myanmar), has stems enclosed in basal sheaths of leaves. Its subumbellate inflorescence contains small flowers (2–3 cm in diameter). Each flower has pale yellow sepals and petals with brownish purple marking, and a central cushion on white lip epichile with a groove or cavity at base (Figure 6). These are the key characteristics of *G. bellinus* (Don *et al.*, 2009). Although a large number of orchids have been used in folk medicine, there has been no previous report for traditional use of *G. bellinus*.



Figure 6 *Gastrochilus bellinus* (Rchb.f.) Kuntze

3.2 Chemical studies

There is only one single report on the genus *Gastrochilus*, describing the preliminary phytochemical screening of *Gastrochilus acutifolius* and *G. distichus* (Chand *et al.*, 2016). The ethanolic extracts prepared from the leaves and roots of *G. acutifolius* showed the presence of alkaloids, flavonoids, saponins, steroids, terpenoids and tannins, whereas the ethanolic extract obtained from the whole plant of *G. distichus* displayed a similar chemical profile except for the absence of alkaloids. The flavonoid and phenolic contents of both plants were also quantitatively studied, but without detailed structural characterization.

For the plant *Gastrochilus bellinus*, neither chemical nor biological studies have been reported.

3.3 Biological studies

The above-mentioned phytochemical study on *Gastrochilus acutifolius* and *G. distichus* (Chand *et al.*, 2016) also reported the DPPH free radical scavenging activity of the plant extracts, in comparison with quercetin [29] (IC₅₀ 32.90 µg/ml). The ethanolic extracts of leaves and roots of *G. acutifolius* exhibited IC₅₀ values of 341.79 and 163.37 µg/ml, respectively, while that of *G. distichus* had an IC₅₀ value of 159.15 µg/ml.

4. *Huberantha jenkinsii*

4.1 Taxonomic considerations and traditional uses

The genus *Huberantha* Chaowasku (formerly known as *Hubera* Chaowasku) was established as a new genus in the family Annonaceae in 2012 (Chaowasku *et al.*, 2012; Chaowasku *et al.*, 2015). The genus contains 27 species, most of which have been segregated from the genus *Polyalthia*.

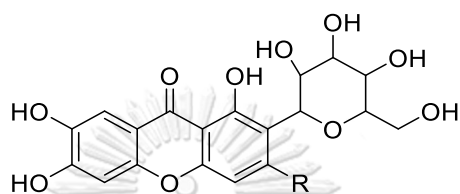
Huberantha jenkinsii is called “Dang nga khao” in Thai or “Taung-Kabut” in Myanmar (Kress *et al.*, 2003). The plant was previously known as *Hubera jenkinsii* (Hook. f. & Thomson) Chaowasku or *Polyalthia jenkinsii* (Hook. f. & Thomson) Hooker & Thomson (Chaowasku *et al.*, 2012; Chaowasku *et al.*, 2015). It shows morphological characters of the genus *Huberantha*, such as leaves with reticulate tertiary venation, single-ovule ovaries and axillary inflorescences (Chaowasku *et al.*, 2012). The most important characteristics of *Huberantha jenkinsii* are 3- mm long suborbicular sepals, with petals turning uniformly pale brown when dried (Turner & Utteridge, 2016). **Figure 7** (Chaowasku *et al.*, 2012) shows the fruit and flower of this plant.



Figure 7 *Huberantha jenkinsii* (Hook. f. & Thomson) Chaowasku

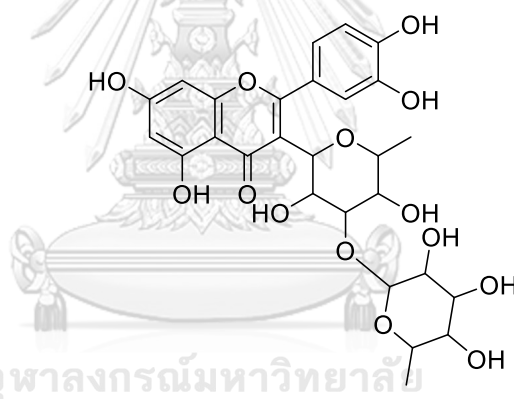
4.2 Chemical studies

Up to the present, there has been only one study on this genus, reporting the presence of C-glycosyl xanthenes, namely mangiferin [337] and homomangiferin [338] and quercetin glycosides [339 and 340] in *Huberantha nitidissima* (Dunal) Chaowasku (Toussirot *et al.*, 2014) (Figure 8).

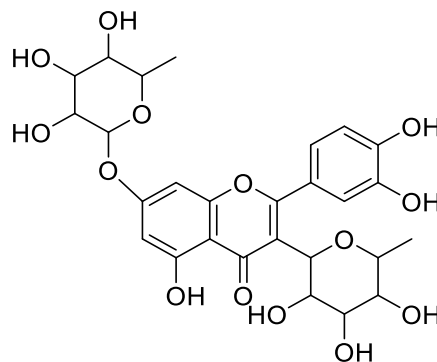


[337] Mangiferin R=OH

[338] Homomangiferin R=OCH₃



[339] Quercetin-3-O- α -L-rhamnopyranosyl-(1 \rightarrow 3)- β -D-glycopyarnoside]



[340] Quercetin-3,7-di-O- α -L-rhamnopyranoside

Figure 8 Structures of compounds from *Huberantha*

4.3 Biological studies

As the genus *Huberantha* has been recently established, there has been only one previous study, reporting the free radical scavenging potential and antioxidant activity of the 50% EtOH extract of *Huberantha nitidissima* (previous scientific name: *Hubera nitidissima*) (Toussirot *et al.*, 2014).



CHAPTER III

EXPERIMENTAL

1. Source of plant materials

1.1 *Cissus javana*

The roots of *Cissus javana* were collected from Shan State, Myanmar in July 2017 and authenticated by comparison with herbarium specimens at the University of Pharmacy, Yangon, Myanmar, where a voucher specimen of the plant materials has been kept.

1.2 *Dendrobium christyanum*

The whole plants of *Dendrobium christyanum* were purchased from Chatuchak market, Bangkok, in July 2015. Plant identification was done by Assoc. Prof. Dr. Boonchoo Sritularak through comparison with the database of the Botanical Garden Organization. A voucher specimen has been deposited at the herbarium of the Department of Pharmacognosy and Pharmaceutical Botany, Faculty of Pharmaceutical Sciences, Chulalongkorn University.

1.3 *Gastrochilus bellinus*

The whole plants of *Gastrochilus bellinus* were purchased from Chatuchak market, Bangkok, in March 2018. Plant identification was done by Assoc. Prof. Dr. Boonchoo Sritularak through comparison with the database of the Botanical Garden Organization. A voucher specimen of has been deposited at the herbarium of the Department of Pharmacognosy and Pharmaceutical Botany, Faculty of Pharmaceutical Sciences.

1.4 *Huberantha jenkinsii*

The stems of *Huberantha jenkinsii* were collected from Surat Thani province in September 2014. The plant was identified by Dr. Tanawat Chaowasku, and its herbarium specimens have been kept at the Faculty of Science, Chiang Mai University.

2. General techniques

2.1 Analytical thin-layer chromatography (TLC)

2.1.1 Normal-phase thin-layer chromatography

Technique	One-dimension ascending
Absorbent	Silica gel 60 F254 precoated plate (E. Merck)
Temperature	Laboratory temperature (30-35 °C)
Detection	1. Ultraviolet light at wavelengths of 254 and 365 nm. 2. Spraying with anisaldehyde reagent (<i>p</i> -anisaldehyde 15 g in ethanol 250 mL and concentrated sulfuric acid 2.5 mL) and heating at 105 °C for 10 minutes.

2.1.2 Reverse-phase thin-layer chromatography

Technique	One-dimension ascending
Absorbent	RP C-18 precoated on aluminum sheet (Anal Tech)
Temperature	Laboratory temperature (30-35 °C)
Detection	Ultraviolet light at wavelengths of 254 and 365 nm.

2.2 Column chromatography (CC)

2.2.1 Vacuum liquid chromatography (VLC)

Adsorbent	Silica gel 60 (No. 107734), size 0.063-0.200 mm (E. Merck)
Packing method	Dry packing
Sample loading	The sample was dissolved in a small volume of organic solvent, triturated with a small amount of the adsorbent, dried and then gradually placed on top of the column.

Detection Each fraction was examined by TLC under UV light at the wavelengths of 254 and 365 nm.

2.2.2 Flash column chromatography (FCC), normal phase

Adsorbent Silica gel 60 (No. 109385), size 0.040-0.063 mm (E. Merck)

Packing method Wet packing

Sample loading The sample was dissolved in a small volume of organic solvent, triturated with a small amount of the adsorbent, dried and then gradually placed on top of the column.

Detection Fractions were examined as described in section 2.2.1

2.2.3 Flash column chromatography (FCC), reverse phase

Adsorbent C-18 (No. 113900), size 40-63 μm (E. Merck)

Packing method Wet packing

Sample loading The sample was dissolved in a small volume of organic solvent, and then gradually loaded on top of the column.

Detection Fractions were examined as described in section 2.2.1

2.2.4 Gel filtration chromatography

Gel filter	Sephadex LH-20, particle size 25-100 μm (GE Healthcare)
Packing method	The gel filter was suspended in an appropriate solvent, left standing about 24 hours and then poured into the column and left to set tightly.
Sample loading	The sample was dissolved in a small volume of the eluent and then gradually distributed on top of the column.
Detection	Fractions were examined in a similar manner as described in section 2.2.1.

2.2.5 Semi-preparative high-pressure liquid chromatography (HPLC)

Column	COSMOSIL 5C ₁₈ -AR-II (10ID x 250 mm)
Flow rate	3 ml/min
Mobile phase	Isocratic 50% methanol in water
Sample preparation	The sample was dissolved in a small volume of the eluent and filtered through Millipore filter paper before injection.
Injection volume	1 ml
Pump	LC-8A (Shimadzu)
Detector	SPD-10A UV-Vis Detector (Shimadzu)
Recorder	C-R6A Chromatopac (Shimadzu)
Temperature	Room temperature

2.3 Spectroscopy

2.3.1 Mass spectra

Mass spectra (MS) were recorded on a Bruker micro TOF mass spectrometer (Department of Chemistry, Faculty of Science, Mahidol University).

2.3.2 Ultraviolet (UV) spectra

UV spectra were recorded on a Milton Roy Spectronic 3000 Array spectrophotometer (Pharmaceutical Research Instrument Center, Faculty of Pharmaceutical Sciences, Chulalongkorn University).

2.3.3 Infrared (IR) spectra

IR spectra were recorded on a Perkin-Elmer FT-IR 1760X spectrophotometer (Scientific and Technology Research Equipment Center, Chulalongkorn University).

2.3.4 Proton and carbon-13 nuclear magnetic resonance (^1H and ^{13}C -NMR) spectra

^1H NMR (300 MHz) and ^{13}C NMR (75 MHz) spectra were recorded on a Bruker Avance DPX-300 FT-NMR spectrometer (Faculty of Pharmaceutical Sciences, Chulalongkorn University).

^1H NMR (500 MHz) and ^{13}C NMR (125 MHz) spectra were recorded on a Bruker Avance III HD 500 NMR spectrometer (Scientific and Technology Research Equipment Center, Chulalongkorn University).

Solvents for NMR spectra were deuterated acetone (acetone- d_6), deuterated dimethyl sulfoxide (DMSO- d_6) or deuterated chloroform (CDCl_3). Chemical shifts were reported in ppm scale using the chemical shift of the solvent as the reference signal.

2.3.5 Optical rotations

Optical rotations were measured on a Perkin-Elmer 341 polarimeter (Pharmaceutical Research Instrument Center, Faculty of Pharmaceutical Sciences, Chulalongkorn University).

2.4 Solvents

All organic solvents employed throughout this work were of commercial grade and were redistilled prior to use.

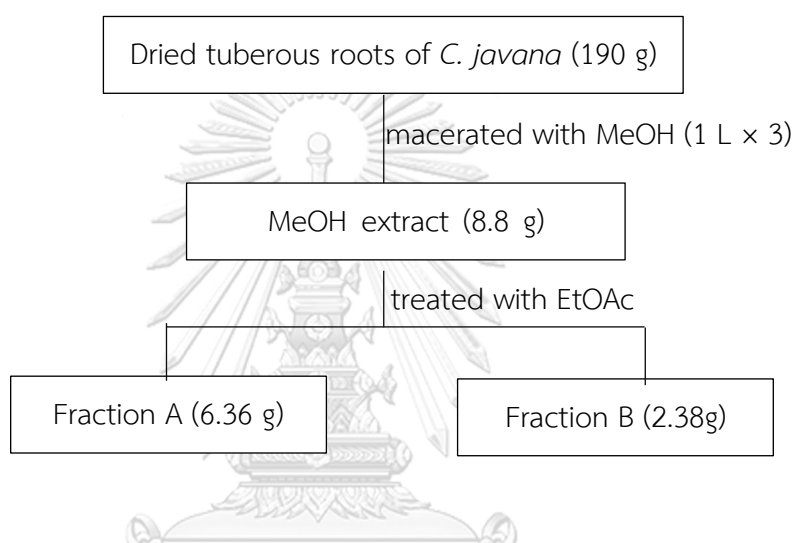


3 Extraction and isolation

3.1 Extraction and isolation of compounds from *Cissus javana*

3.1.1 Extraction

The dried tuberous roots of *Cissus javana* DC. (190 g) were chopped and macerated with MeOH (1 L × 3) (**Scheme 1**). The dried MeOH extract (8.8 g) was then treated with EtOAc to give EtOAc insoluble (6.36 g) and soluble (2.38 g) fractions after drying, and designated as fractions A and B, respectively.



Scheme 1 Extraction steps for *Cissus javana*

3.1.2 Isolation

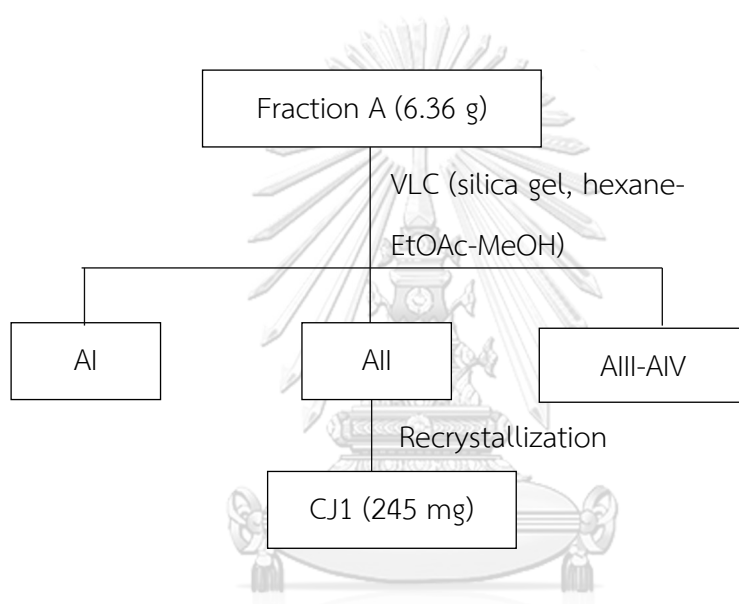
3.1.2.1 Isolation of compound CJ1 (bergenin)

Fraction A (6.36 g) was initially separated by vacuum liquid chromatography (silica gel, hexane-EtOAc-MeOH) to give five fractions (AI to AIV) (**Scheme 2**). Fraction AI, after drying, gave compound CJ1 (245 mg) as colorless crystals. CJ1 was further purified by recrystallizing from MeOH, and later identified as bergenin [31].

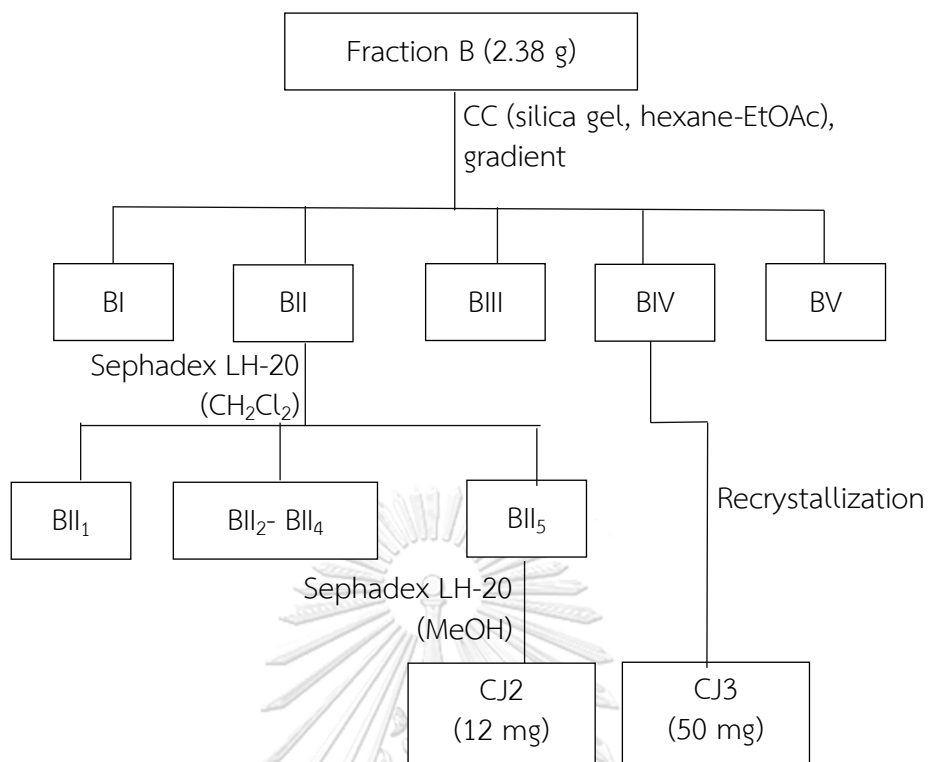
3.1.2.2 Isolation of compounds CJ2 (stigmast-4-en-3-one) and CJ3 (β -sitosterol)

Fraction B (2.38 g) was subjected to column chromatography (CC) on a silica gel column (hexane-EtOAc) (**Scheme 3**). Seven subfractions (BI to BV) were obtained.

Fraction BII was further fractionated on Sephadex LH-20 (CH_2Cl_2) to give fifteen fractions (BII₁-BII₅). Purification of BII₅ on a Sephadex LH-20 (MeOH) column yielded CJ2 (12 mg). Fraction BIV gave white precipitates after left standing at room temperature overnight. The precipitates were collected, washed with EtOAc and dried to give CJ3 (50 mg). Compounds CJ2 and CJ3 were identified as stigmast-4-en-3-one [35] and β -sitosterol [33], respectively.



Scheme 2 Isolation of compounds from fraction A of *Cissus javana*

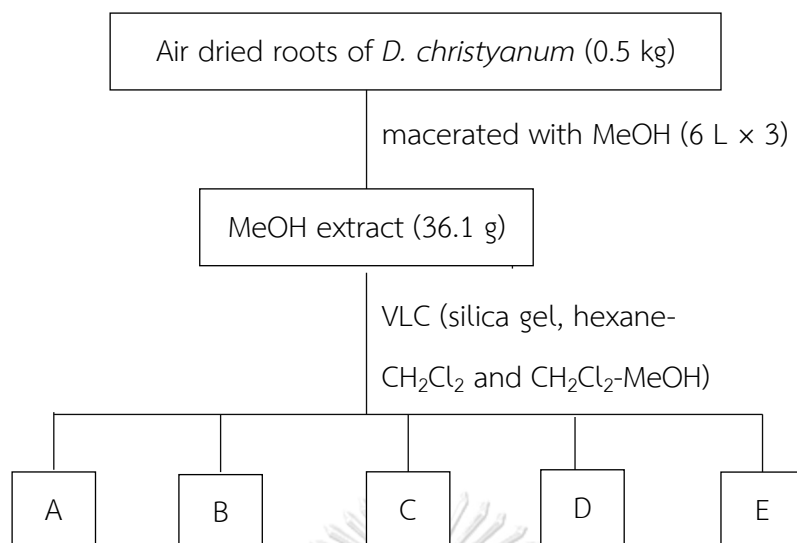


Scheme 3 Isolation of compounds from fraction B of *Cissus javana*

3.2 Extraction and isolation of compounds from *Dendrobium christyanum*

3.2.1 Extraction

The air-dried roots of *Dendrobium christyanum* (0.5 kg) were chopped and extracted with MeOH to give a MeOH extract after removal of the solvent (**Scheme 4**). The MeOH extract (36.1 g) was fractionated by vacuum-liquid chromatography (VLC) on silica gel (hexane-CH₂Cl₂ and CH₂Cl₂-MeOH, gradient) to give five fractions (A-E).



Scheme 4 Extraction steps for *Dendrobium christyanum*

3.2.2 Isolation

3.2.2.1 Isolation of compound DC1 (methyl haematommate)

Fraction A (479 mg) was separated by column chromatography (silica gel, hexane-acetone, gradient) to give five fractions (AI-AV) (**Scheme 5**). Fraction AI (155.2 mg) was further separated on Sephadex LH-20 (CH_2Cl_2) and then on silica gel (hexane-acetone, gradient) to give **DC1** (4mg), which was identified as methyl haematommate [342].

3.2.2.2 Isolation of compounds DC2 (*n*-eicosyl *trans*-ferulate) and DC3 (atraric acid)

DC2 (109 mg) and DC3 (5.9 mg) were purified from fractions AIII (138.9 mg) and AIV (38.6 mg) (**Scheme 5**) by chromatographic separation on Sephadex LH-20 (acetone) and identified as *n*-eicosyl *trans*-ferulate [343] and atraric acid [344], respectively.

3.2.2.3 Isolation of compound DC4 (*n*-docosyl 4-hydroxy-*trans*-cinnamate)

Fraction B (2.4 g) was fractionated by CC (silica gel, hexane-acetone, gradient) to give 17 fractions (BI-BXVII) (**Scheme 6**). Fraction BIV (348.8 mg) was purified on Sephadex LH-20 (CH₂Cl₂) to furnish DC4 (40.6 mg) which was identified as *n*-docosyl 4-hydroxy-*trans*-cinnamate [345].

3.2.2.4 Isolation of compound DC5 (vanillin)

Fraction BVIII (179.7 mg) was separated on Sephadex LH-20 (CH₂Cl₂) to give DC5 (29.1 mg) (**Scheme 6**), which was later identified as vanillin [274].

3.2.2.5 Isolation of compound DC6 (coniferyl aldehyde)

Fraction BIX (198.5 mg) was subjected to separation on Sephadex LH-20 (CH₂Cl₂) to give 12 fractions (BIX₁-BIX₁₂) (**Scheme 6**). Then, fraction BIX₇ (17.7 mg) was purified by CC (silica gel; hexane-acetone, gradient) to give DC6 (13.7 mg) which was subsequently identified as coniferyl aldehyde [346].

3.2.2.6 Isolation of compound DC7 (4,5-dihydroxy-2-methoxy-9,10-dihydrophenanthrene)

Fraction BIX₁₀ (190.5 mg) was purified on Sephadex LH-20 (CH₂Cl₂) to afford DC7 (20.8 mg) (**Scheme 6**), which was eventually identified as 4,5-dihydroxy-2-methoxy-9,10-dihydrophenanthrene [103].

3.2.2.7 Isolation of compound DC8 (moscatilin)

Fraction BX (556.7 mg) was separated on Sephadex LH-20 (CH_2Cl_2) to give 9 fractions ($\text{BX}_1\text{-BX}_9$) (**Scheme 6**). **DC8** (25.6 mg) was obtained from fraction BX_2 (90.8 mg) after separation by CC (silica gel, hexane-acetone, gradient) and was identified as moscatilin [59].

3.2.2.8 Isolation of compound DC9 (aloifol I)

DC9 (215.6 mg) was isolated from fraction BX_3 (361 mg) by CC (silica gel; hexane-acetone, gradient) (**Scheme 6**) and identified as aloifol I [38].

3.2.2.9 Isolation of compound DC10 (gigantol)

Fraction C (1.7 g) was fractionated by CC (silica gel; hexane-acetone, gradient) to yield 10 fractions (CI-CX) (**Scheme 7**). Fraction CVII (50.9 mg) was subjected to CC (silica gel, hexane-acetone, gradient) to yield **DC10** (3.3 mg) which was identified as gigantol [54].

3.2.2.10 Isolation of compound DC11 (batatasin III)

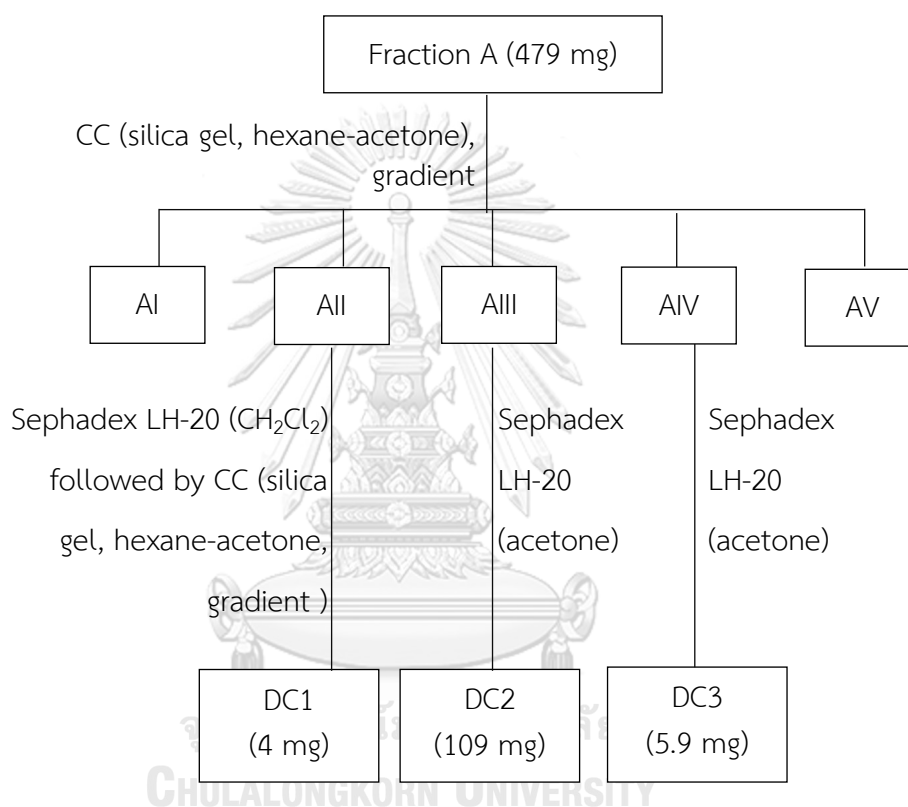
Fraction CIX (260 mg) was separated on Sephadex LH-20 (acetone) and then further purified by CC (silica gel, hexane-acetone, gradient) to give **DC11** (49.8 mg) (**Scheme 7**). It was identified as batatasin III [41].

3.2.2.11 Isolation of compound DC12 (dendrosinen B)

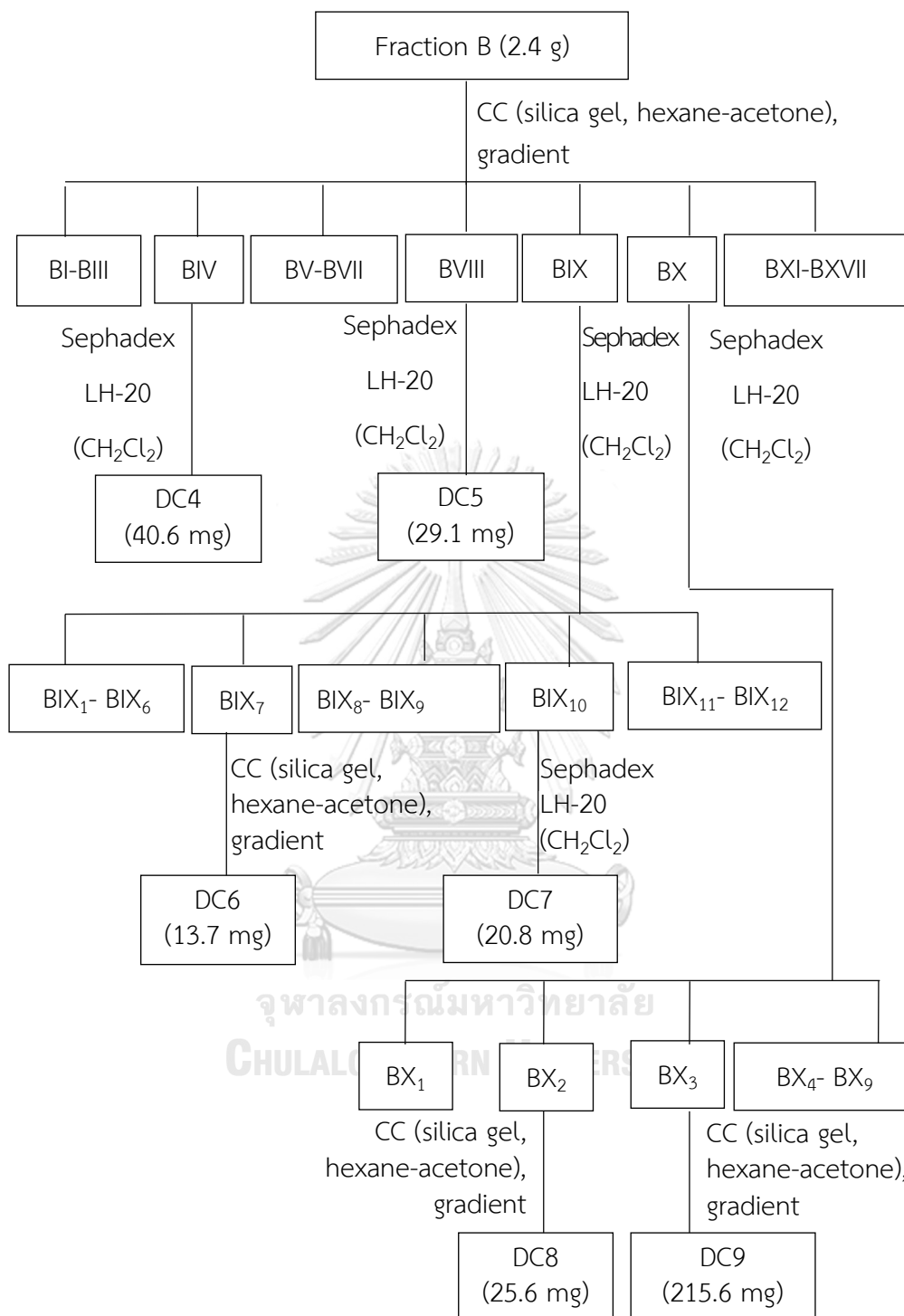
Fraction CX (884.9 mg) was fractionated by CC (silica gel, hexane-acetone, gradient) to give 13 fractions ($\text{CX}_1\text{-CX}_{13}$) (**Scheme 7**). Fraction CX_9 (57.7 mg) was further purified by CC (silica gel, hexane-acetone, gradient) and then by Sephadex LH-20 (acetone) to afford **DC12** (19.1 mg) which was identified as dendrosinen B [73].

3.2.2.12 Isolation of compound DC13 (diorcinolic acid)

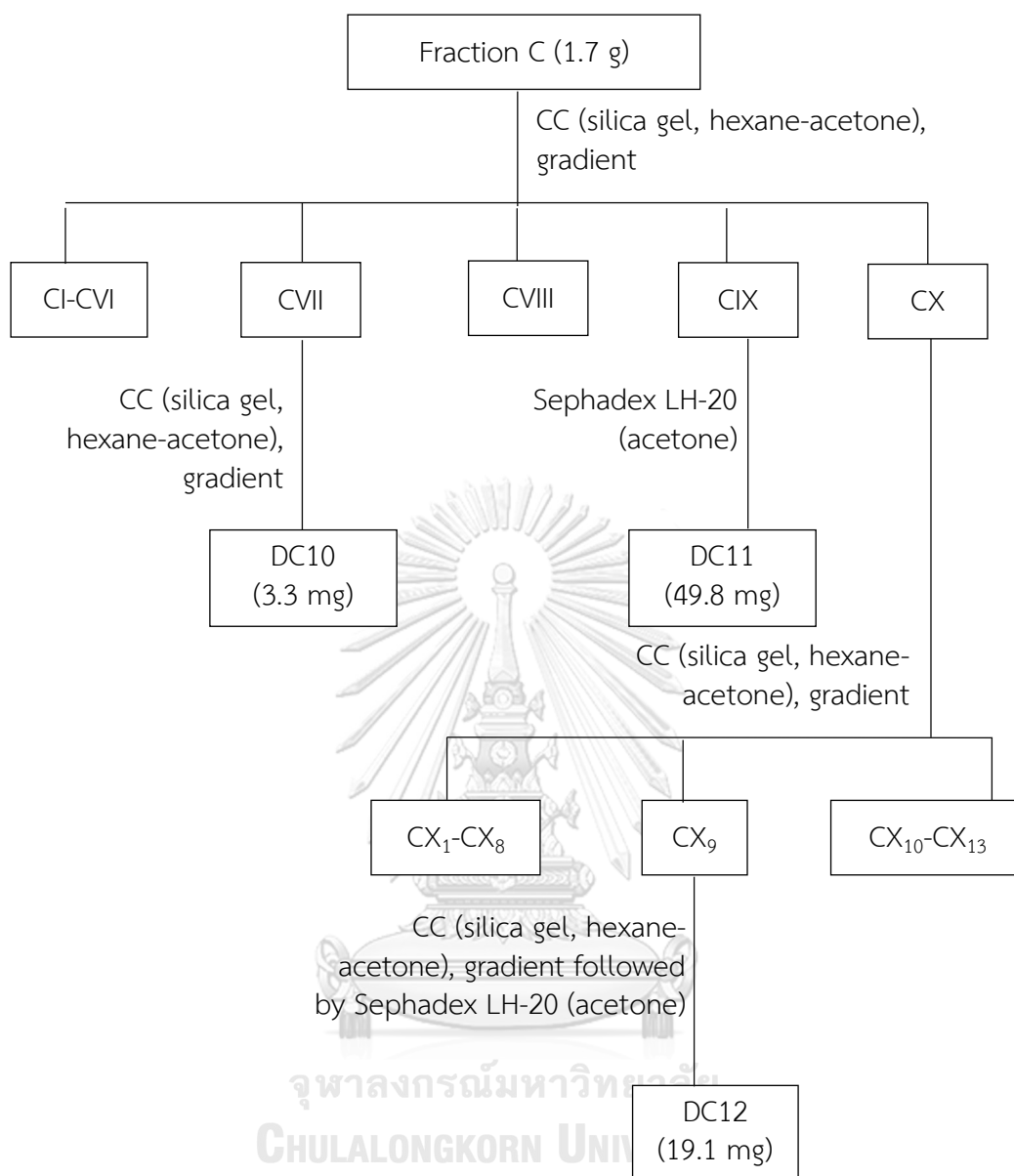
Fraction E (15.2 g) was separated on Diaion HP-20 (H₂O-MeOH, gradient) to give 5 fractions (EI-EV) (**Scheme 8**). Fraction EII (1.47 g) was separated by (C₁₈, acetonitrile-H₂O, gradient) and then further purified by CC (silica gel, hexane-acetone, gradient) to give **DC13** (7.1 mg) which was finally identified as diorcinolic acid [347].



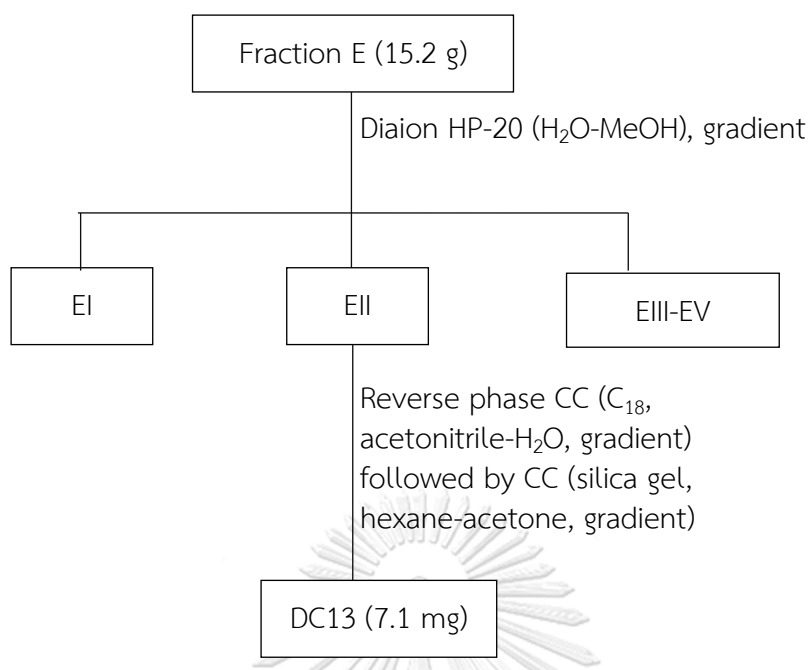
Scheme 5 Isolation of compounds from fraction A of *Dendrobium christyanum*



Scheme 6 Isolation of compounds from fraction B of *Dendrobium christyanum*



Scheme 7 Isolation of compounds from fraction C of *Dendrobium christyanum*



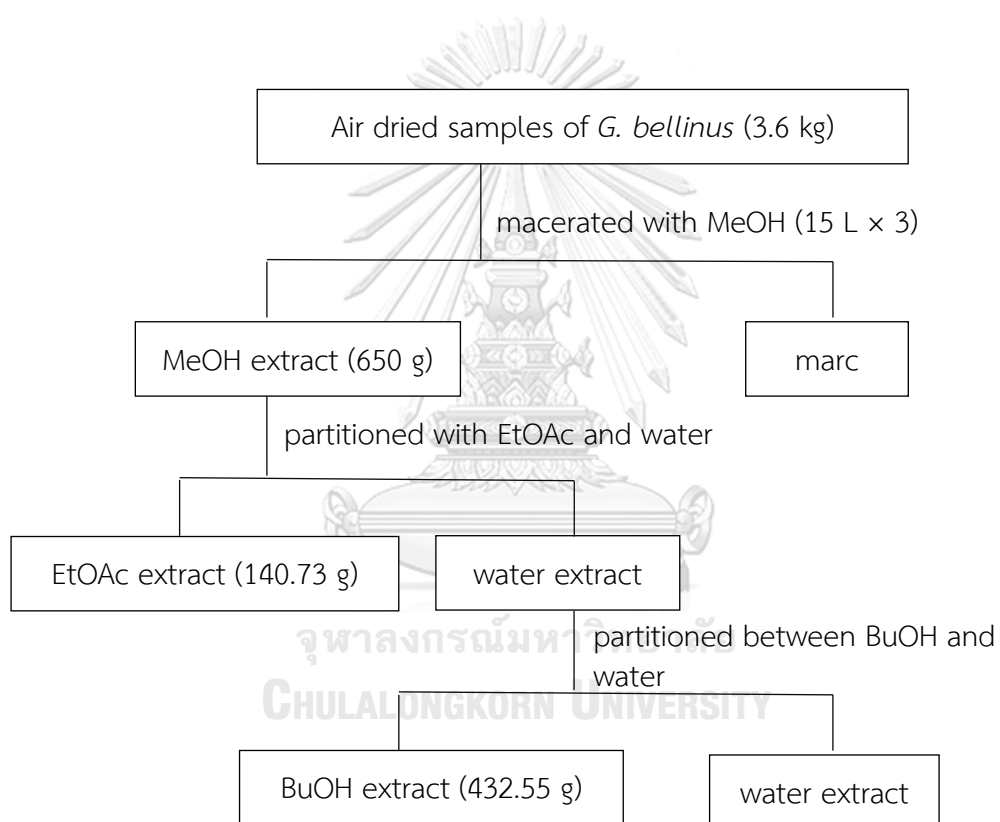
Scheme 8 Isolation of compound from fraction E of *Dendrobium christyanum*



3.3 Extraction and isolation of compounds from *Gastrochilus bellinus*

3.3.1 Extraction

The air-dried samples of *Gastrochilus bellinus* (3.6 kg) were chopped and extracted with methanol (MeOH) to give a MeOH extract after removal of the solvent. The MeOH was suspended in water and then partitioned with ethyl acetate (EtOAc) and *n*-butanol (BuOH) to give EtOAc, BuOH and water extracts, respectively (**Scheme 9**).



Scheme 9 Extraction steps for *Gastrochilus bellinus*

3.3.2 Isolation

3.3.2.1 Isolation of compounds GB1

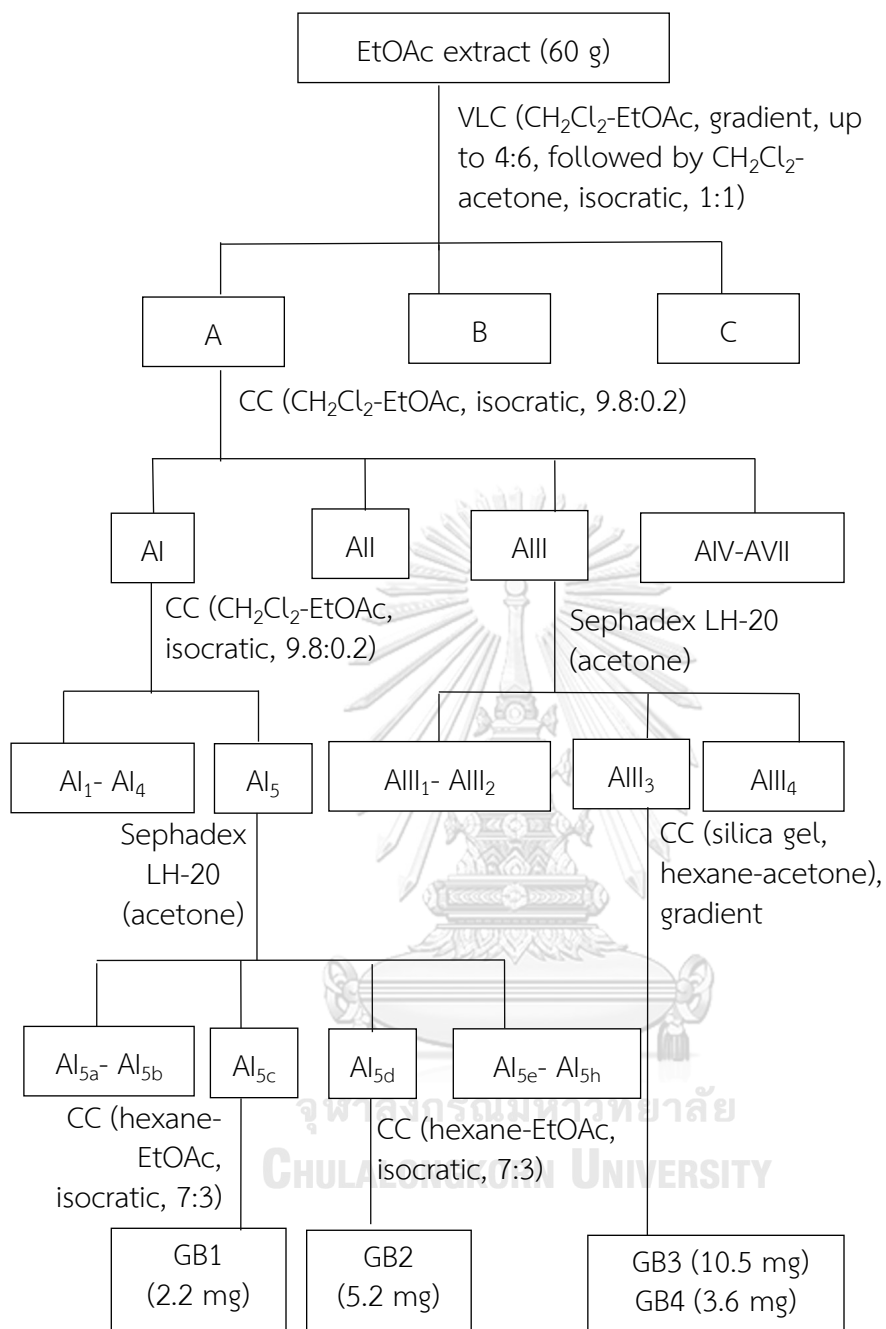
The EtOAc extract (60 g) was fractionated by vacuum-liquid chromatography (VLC) on silica gel (CH₂Cl₂-EtOAc, gradient up to 4:6 and then CH₂Cl₂-acetone, isocratic, 1:1) to give three fractions (A-C) (**Scheme 10**). Fraction A (32.2 g) was separated by CC (silica gel CH₂Cl₂-EtOAc, isocratic, 9.8:0.2) to give eight fractions (AI-AVIII). Fraction AI (560 mg) was re-separated by CC (silica gel CH₂Cl₂-EtOAc, isocratic, 9.8:0.2) to obtain five fractions (AI₁-AI₅). Fraction AI₅ was separated on Sephadex LH-20 (acetone) to give AI_{5a} to AI_{5h}. Compound **GB1** (2.2 mg) was obtained from fraction AI_{5c} by purifying on silical gel column (hexane-EtOAc, isocratic, 7:3). Compound **GB1** was later characterized as a new compound with the structure (3-(4'-hydroxybenzyl)-3-methoxy-2,7-dihydroxy-5H-phenanthro[4,5-bcd]pyran [348].

3.3.2.2 Isolation of compound GB2

Compound **GB2** (5.2 mg) was isolated from fraction AI_{5d} by purifying on CC (hexane-EtOAc, isocratic, 7:3) (**Scheme 10**) and characterized as a new compound, with the structure 1-(4'-hydroxybenzyl)-2,6-dimethoxy-,7-hydroxy-5H-phenanthro[4,5-bcd]pyran [349].

3.3.2.3 Isolation of compounds GB3 and GB4

Fraction AIII (105.7 mg) was separated on Sephadex LH-20 (acetone) to give four fractions (AIII₁ to AIII₄) (**Scheme 10**). Compounds **GB3** (10.5 mg) and **GB4** (3.6 mg) were collected from fraction AIII₃ by purifying on CC (silica gel, hexane-acetone, gradient). Their structures were hitherto unknown and subsequently determined as [350] and [351], respectively.

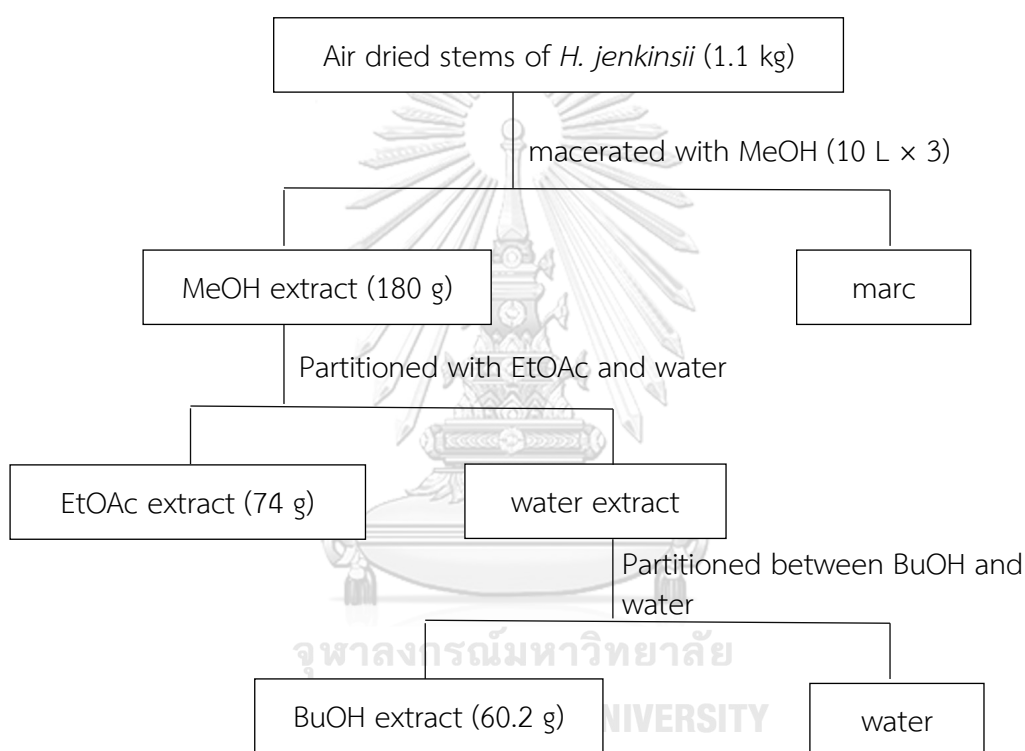


Scheme 10 Isolation of compounds from EtOAc fraction of *Gastrochilus bellinus*

3.4 Extraction and isolation of compounds from *Huberantha jenkinsii*

3.4.1 Extraction

The air-dried stems of *Huberantha jenkinsii* (1.1 kg) were chopped and extracted with MeOH to give a MeOH extract (180 g) after drying. The MeOH extract was suspended in water and treated with EtOAc and *n*-BuOH to give corresponding extracts after removal of the solvent as shown in **Scheme 11**.



Scheme 11 Extraction steps for *Huberantha jenkinsii*

3.4.2 Isolation

3.4.2.1 Isolation of compound compounds HJ1 (mangiferin)

Compound **HJ1** (1 g) was collected as white precipitates from BuOH extract (60.2 g) and re-purified on Sephadex LH-20 (MeOH) (**Scheme 12**). Compound **HJ1** was identified as mangiferin [337].

3.4.2.2 Isolation of compounds HJ2, HJ3, HJ4 (allantoin) and HJ5 (oxylopinine)

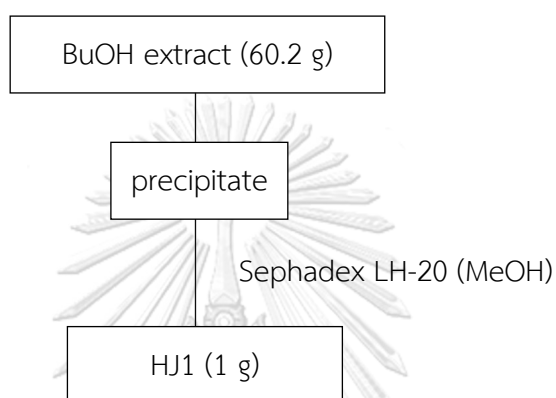
The EtOAc extract (74 g) was on fractionated by vacuum-liquid chromatography (VLC) on silica gel (hexane-CH₂Cl₂ and CH₂Cl₂-MeOH, gradient) to give five fractions (A-E) (**Scheme 13**). Fraction B was separated on Sephadex LH-20 (MeOH) to give five fractions (BI-BV). Separation of fraction BII (1.03 g) on reverse-phase CC (C18, MeOH-H₂O, gradient) followed by CC (silica gel; hexane-acetone, gradient) furnished **HJ2** (3.5 mg), **HJ3** (3.4 mg), **HJ4** (32.6 mg) and **HJ5** (6.5 mg). Compounds **HJ2** and **HJ3** were characterized as new alkaloids having structures **352** and **353**. The isolates **HJ4** and **HJ5** were identified as allantoin [354] and oxylopinine [355], respectively.

3.4.2.3 Isolation of compound HJ6 (*N-trans*-feruloyltyramine)

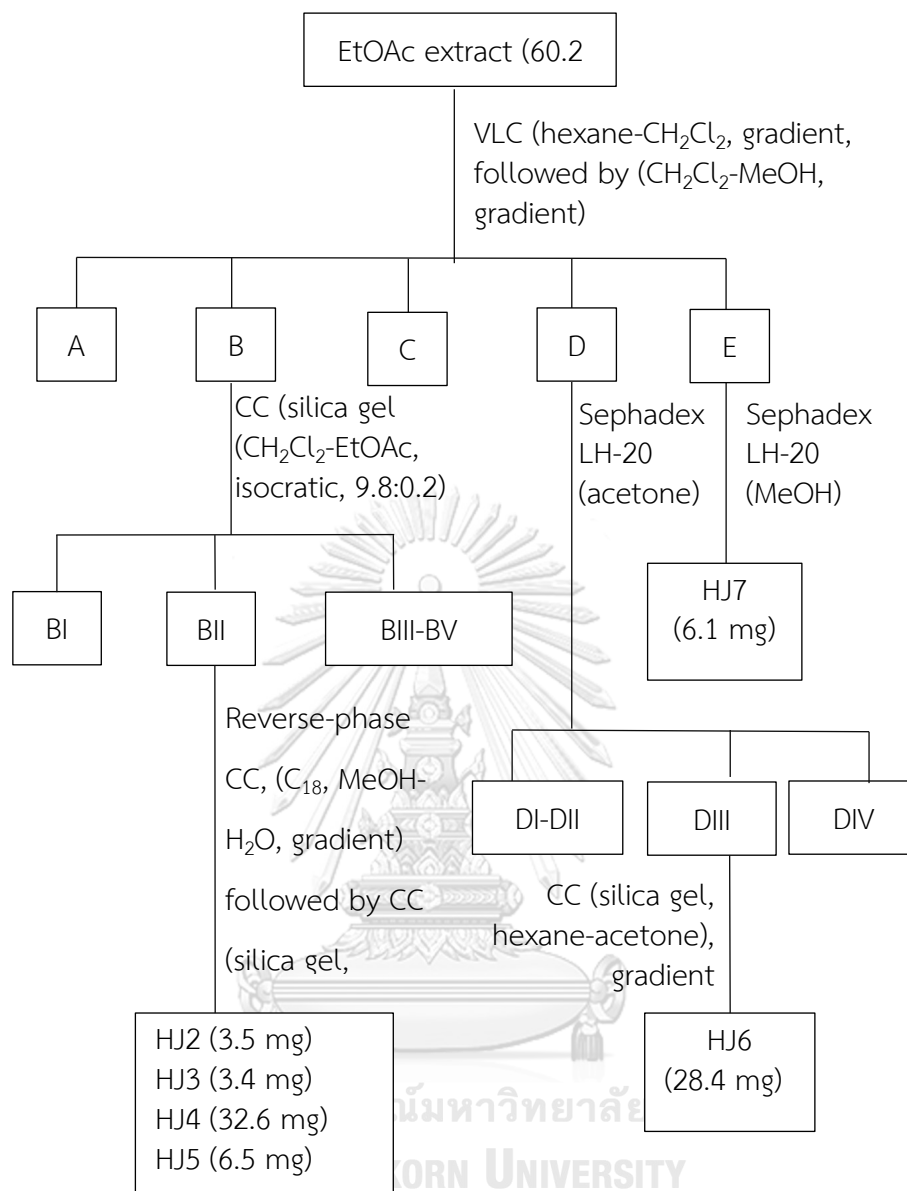
Fraction D was separated on Sephadex LH-20 (MeOH) to give four fractions (DI and DIV) (**Scheme 13**). Compound **HJ6** (28.4 mg) was isolated from fraction DIII by purifying on CC (silica gel; hexane-acetone, gradient). Compound **HJ6** was subsequently identified as *N-trans*-feruloyltyramine [10].

3.4.2.4 Isolation of compound HJ7 (*N-trans-p-coumaroyl tyramine*)

Compound **HJ7** (6.1 mg) was obtained from fraction E by purifying on Sephadex LH-20 (MeOH) (**Scheme 13**) and identified as *N-trans-p-coumaroyl tyramine* [356].



Scheme 12 Isolation of compound from BuOH fraction of *Huberantha jenkinsii*



Scheme 13 Isolation of compounds from EtOAc fraction of *Huberantha jenkinsii*

4. Physical and spectral data of isolated compounds

4.1 Compound CJ1 (bergenin) [31]

Compound **CJ1** was obtained as colorless crystals (245 mg, 0.1289% based on dried weight of root). It was soluble in DMSO.

MS [M-H]⁻ ion at *m/z* 327.0703 (C₁₄H₁₅O₉)

¹H NMR δ ppm, 300 MHz, in DMSO-*d*₆; **Table 4**

¹³C NMR δ ppm, 75 MHz, in DMSO-*d*₆; **Table 4**

4.2 Compound CJ2 (stigmast-4-en-3-one) [341]

Compound **CJ2** was obtained as white crystals (12 mg, 0.0063% based on dried weight of root). It was soluble in chloroform.

MS [M+H]⁺ ion at *m/z* 413.3781 (C₂₉H₄₉O)

¹H NMR δ ppm, 300 MHz, in CDCl₃; **Table 5**

4.3 Compound CJ3 (β-sitosterol) [33]

Compound **CJ3** was obtained as white crystals (50 mg, 0.0263% based on dried weight of root). It was soluble in chloroform.

MS [M+H]⁺ ion at *m/z* 415.3769 (C₂₉H₅₁O)

¹H NMR δ ppm, 300 MHz, in CDCl₃; **Table 6**

4.4 Compound DC1 (methyl haematommate) [342]

Compound **DC1** was obtained as a brownish white powder (4 mg, 0.0008% based on dried weight of root). It was soluble in acetone.

MS [M-H]⁻ ion at m/z 209.0441 (C₁₀H₉O₅)

¹H NMR δ ppm, 300 MHz, in CDCl₃; **Table 10**

¹³C NMR δ ppm, 75 MHz, in CDCl₃; **Table 10**

4.5 Compound DC2 (*n*-eicosyl *trans*-ferulate) [343]

Compound **DC2** was obtained as white crystals (109 mg, 0.0218% based on dried weight of root). It was soluble in acetone.

MS [M+Na]⁺ ion at m/z 497.3523 (C₃₀H₅₀O₄Na)

¹H NMR δ ppm, 300 MHz, in CDCl₃; **Table 11**

¹³C NMR δ ppm, 75 MHz, in CDCl₃; **Table 11**

4.6 Compound DC3 (atraric acid) [344]

Compound **DC3** was obtained as white crystals (5.9 mg, 0.0012% based on dried weight of root). It was soluble in acetone.

MS [M+H]⁺ ion at m/z 197.0838 (C₁₀H₁₃O₄)

¹H NMR δ ppm, 300 MHz, in acetone-*d*₆; **Table 12**

¹³C NMR δ ppm, 75 MHz, in acetone-*d*₆; **Table 12**

4.7 Compound DC4 (*n*-docosyl 4-hydroxy-*trans*-cinnamate) [345]

Compound **DC4** was obtained as a white powder (40.6 mg, 0.00812% based on dried weight of root). It was soluble in acetone.

MS [M+H]⁺ ion at m/z 473.4060 (C₃₁H₅₃O₃)

¹H NMR δ ppm, 300 MHz, in acetone-*d*₆; **Table 13**

4.8 Compound DC5 (vanillin) [274]

Compound **DC5** was obtained as yellowish white crystals (29.1 mg, 0.0058% based on dried weight of root). It was soluble in acetone.

MS [M-H]⁻ ion at *m/z* 151.0394 (C₈H₇O₃)

¹H NMR δ ppm, 300 MHz, in acetone-*d*₆; **Table 14**

¹³C NMR δ ppm, 75 MHz, in acetone-*d*₆; **Table 14**

4.9 Compound DC6 (coniferyl aldehyde) [346]

Compound **DC6** was obtained as a greenish yellow powder (13.7 mg, 0.0027% based on dried weight of root). It was soluble in acetone.

MS [M+Na]⁺ ion at *m/z* 201.0547 (C₁₀H₁₀O₃Na)

¹H NMR δ ppm, 300 MHz, in acetone-*d*₆; **Table 15**

¹³C NMR δ ppm, 75 MHz, in acetone-*d*₆; **Table 15**

4.10 Compound DC7 (4,5-dihydroxy-2-methoxy-9,10-dihydrophenanthrene) [103]

Compound **DC7** was obtained as a brown amorphous solid (20.8 mg, 0.0042% based on dried weight of root). It was soluble in acetone.

MS [M+Na]⁺ ion at *m/z* 243.1065 (C₁₅H₁₅O₃)

¹H NMR δ ppm, 300 MHz, in acetone-*d*₆; **Table 16**

¹³C NMR δ ppm, 75 MHz, in acetone-*d*₆; **Table 16**

4.11 Compound DC8 (moscatilin) [59]

Compound **DC8** was obtained as a brown amorphous solid (25.6 mg, 0.0051% based on dried weight of root). It was soluble in acetone.

MS [M+Na]⁺ ion at *m/z* 327.1215 (C₁₇H₂₀O₅Na)

¹H NMR δ ppm, 300 MHz, in acetone-*d*₆; **Table 17**

¹³C NMR δ ppm, 75 MHz, in acetone-*d*₆; **Table 17**

4.12 Compound DC9 (aloifol I) [38]

Compound **DC9** was obtained as a brown amorphous solid (215.6 mg, 0.0431% based on dried weight of root). It was soluble in acetone.

MS [M+Na]⁺ ion at *m/z* 297.1102 (C₁₆H₁₈O₄Na)

¹H NMR δ ppm, 300 MHz, in acetone-*d*₆; **Table 18**

¹³C NMR δ ppm, 75 MHz, in acetone-*d*₆; **Table 18**

4.13 Compound DC10 (gigantol) [54]

Compound **DC10** was obtained as a brown amorphous solid (3.3 mg, 0.0007% based on dried weight of root). It was soluble in acetone.

MS [M+Na]⁺ ion at *m/z* 297.1178 (C₁₆H₁₈O₄Na)

¹H NMR δ ppm, 300 MHz, in acetone-*d*₆; **Table 19**

¹³C NMR δ ppm, 75 MHz, in acetone-*d*₆; **Table 19**

4.14 Compound DC11 (batatasin III) [41]

Compound **DC11** was obtained as a brown amorphous solid (49.8 mg, 0.0099% based on dried weight of root). It was soluble in acetone.

MS [M+Na]⁺ ion at *m/z* 267.1024 (C₁₅H₁₆O₃Na)

¹H NMR δ ppm, 300 MHz, in acetone-*d*₆; **Table 20**

¹³C NMR δ ppm, 75 MHz, in acetone-*d*₆; **Table 20**

4.15 Compound DC12 (dendrosinen B) [73]

Compound **DC12** was obtained as a brown amorphous solid (19.1 mg, 0.0038% based on dried weight of root). It was soluble in acetone.

MS [M+Na]⁺ ion at *m/z* 283.0998 (C₁₅H₁₆O₄Na)

¹H NMR δ ppm, 300 MHz, in acetone-*d*₆; **Table 21**

¹³C NMR δ ppm, 75 MHz, in acetone-*d*₆; **Table 21**

4.16 Compound DC13 (diorcinolic acid) [347]

Compound **DC13** was obtained as a brownish white powder (7.1 mg, 0.0014% based on dried weight of root). It was soluble in acetone.

MS [M-H]⁻ ion at m/z 317.0752 (C₁₆H₁₃O₇)

¹H NMR δ ppm, 300 MHz, in acetone-*d*₆; **Table 22**

¹³C NMR δ ppm, 75 MHz, in acetone-*d*₆; **Table 22**

4.17 Compound GB1 [348]

Compound **GB1** was obtained as a brown amorphous solid (2.2 mg, 0.000061% based on dried weight of whole plant). It was soluble in acetone.

MS [M+H]⁺ ion at m/z 363.1260 (C₂₂H₁₉O₅)

¹H NMR δ ppm, 500 MHz, in acetone-*d*₆; **Table 26**

¹³C NMR δ ppm, 125 MHz, in acetone-*d*₆; **Table 26**

4.18 Compound GB2 [349]

Compound **GB2** was obtained as a brown amorphous solid (5.2 mg, 0.0001% based on dried weight of whole plant). It was soluble in acetone.

MS [M+H]⁺ ion at m/z 389.1351 (C₂₄H₂₁O₅)

¹H NMR δ ppm, 300 MHz, in acetone-*d*₆; **Table 27**

¹³C NMR δ ppm, 75 MHz, in acetone-*d*₆; **Table 27**

4.19 Compound GB3 [350]

Compound **GB3** was obtained as a brown amorphous solid (10.5 mg, 0.0001 % based on dried weight of whole plant). It was soluble in acetone.

MS [M+H]⁺ ion at m/z 375.1214 (C₂₃H₁₉O₅)

¹H NMR δ ppm, 300 MHz, in acetone-*d*₆; **Table 28**

¹³C NMR δ ppm, 75 MHz, in acetone-*d*₆; **Table 28**

4.20 Compound GB4 [351]

Compound **GB4** was obtained as a brown amorphous solid (3.6 mg, 0.0001% based on dried weight of whole plant). It was soluble in acetone.

MS [M+H]⁺ ion at *m/z* 363.1211 (C₂₂H₁₉O₅)

¹H NMR δ ppm, 300 MHz, in acetone-*d*₆; **Table 29**

¹³C NMR δ ppm, 75 MHz, in acetone-*d*₆; **Table 29**

4.21 Compound HJ1 (mangiferin) [337]

Compound **HJ1** was obtained as a white powder (1 g, 0.0909% based on dried weight of stem). It was soluble in DMSO.

MS [M+Na]⁺ ion at *m/z* 445.0747 (C₁₉H₁₈O₁₁Na)

¹H NMR δ ppm, 300 MHz, in DMSO-*d*₆; **Table 32**

¹³C NMR δ ppm, 75 MHz, in DMSO-*d*₆; **Table 32**

4.22 Compound HJ2 [352]

Compound **HJ2** was obtained as a white powder (3.5 mg, 0.0003% based on dried weight of stem). It was soluble in acetone.

MS [M-H]⁻ ion at *m/z* 338.1029 (C₁₉H₁₇NO₅)

¹H NMR δ ppm, 500 MHz, in acetone-*d*₆; **Table 33**

¹³C NMR δ ppm, 125 MHz, in acetone-*d*₆; **Table 33**

4.23 Compound HJ3 [353]

Compound **HJ3** was obtained as a brownish white powder (3.4 mg, 0.0003% based on dried weight of stem). It was soluble in acetone.

MS [M-H]⁻ ion at *m/z* 368.1129 (C₂₀H₁₈NO₆)

¹H NMR δ ppm, 500 MHz, in acetone-*d*₆; **Table 34**

¹³C NMR δ ppm, 125 MHz, in acetone-*d*₆; **Table 34**

4.24 Compound HJ4 (allantoin) [354]

Compound **HJ4** was obtained as yellowish-brown crystals (32.6 mg, 0.0029% based on dried weight of stem). It was soluble in DMSO.

MS [M+Na]⁺ ion at m/z 181.0330 (C₄H₆N₄O₃Na)

¹H NMR δ ppm, 300 MHz, in acetone-*d*₆; **Table 35**

¹³C NMR δ ppm, 75 MHz, in acetone-*d*₆; **Table 35**

4.25 Compound HJ5 (oxylopinine) [355]

Compound **HJ5** was obtained as white crystals (6.5 mg, 0.0006% based on dried weight of stem). It was soluble in acetone.

MS [M+H]⁺ ion at m/z 212.0693 (C₁₃H₁₀NO₂)

¹H NMR δ ppm, 300 MHz, in acetone-*d*₆; **Table 28**

¹³C NMR δ ppm, 75 MHz, in acetone-*d*₆; **Table 28**

4.26 Compound HJ6 (*N-trans*-feruloyltyramine) [10]

Compound **HJ6** was obtained as a brownish white powder (28.4 mg, 0.0026% based on dried weight of stem). It was soluble in acetone.

MS [M+H]⁺ ion at m/z 314.1395 (C₁₈H₂₀NO₄)

¹H NMR δ ppm, 300 MHz, in acetone-*d*₆; **Table 29**

¹³C NMR δ ppm, 75 MHz, in acetone-*d*₆; **Table 29**

4.27 Compound HJ7 (*N-trans-p*-coumaroyl tyramine) [356]

Compound **HJ7** was obtained as a brownish white powder (6.1 mg, 0.0006% based on dried weight of stem). It was soluble in acetone.

MS [M+H]⁺ ion at m/z 284.1277 (C₁₇H₁₈NO₃)

¹H NMR δ ppm, 300 MHz, in acetone-*d*₆; **Table 30**

¹³C NMR δ ppm, 75 MHz, in acetone-*d*₆; **Table 30**

5. Assay for α -glucosidase inhibitory activity

In this study, α -glucosidase inhibitory activity evaluation was based on the spectrophotometric measurement of the amount of *p*-nitrophenol (*p*NP) released from the hydrolytic reaction of *p*-nitrophenyl- α -D-glucopyranoside (*p*-NPG) catalyzed by α -glucosidase enzyme. *p*-NPG is a synthetic substrate that represents the α -linked terminal glucose of polysaccharide. The experiment was done at microscale *in vitro* in a 96-well plate following established protocols (Sun *et al.*, 2014; Inthongkaew *et al.*, 2017).

5.1 Materials and instruments

- *p*-Nitrophenyl- α -D-glucopyranoside (*p*NPG) (Sigma-Aldrich, USA)
- α -Glucosidase enzyme (Sigma-Aldrich, USA)
- Na₂CO₃ (Sigma-Aldrich, USA)
- Acarbose (Sigma-Aldrich, USA)
- Vortex mixer (Vortex-Genie2, Scientific industries)
- Ultrasonic bath (Transsonic 570/H, Elma)
- Incubator (BM500, Memmert)
- Microplate reader (CLARIOstar, BMG LABTECH)

5.2 Determination of α -glucosidase inhibitory activity

The sample was initially prepared in 50 % DMSO solution. The sample solution (10 μ l) was then mixed with 40 μ l of α -glucosidase enzyme (0.1 U/ml) in each well. The sample solution (10 μ l) with 40 μ l of phosphate buffer solution was used as the blank. Acarbose was used as the positive control. After the plate was pre-incubated at 37^o C for 10 min, the substrate (2 mM *p*NPG) 50 μ l was added into each well. The final concentration of DMSO was 5 % in each well. Then the plate was further incubated at 37^o C for 20 min. Finally, the reaction was stopped by the

addition of 100 μl of 1 M Na_2CO_3 , and the absorbance was measured at 405 nm using a microplate reader. The percentage of α -glucosidase enzyme inhibition was calculated as follows:

$$\% \text{ inhibition of } \alpha\text{-glucosidase enzyme} = \frac{(A_{\text{control}} - A_{\text{sample}}) \times 100}{A_{\text{control}}}$$

A_{control} : Absorbance of 5 % DMSO in H_2O (negative control)

A_{sample} : Absorbance of test sample or acarbose

* The final concentration of DMSO in each well was not more than 5%.

6. Assay for glucose uptake stimulatory activity

Glucose uptake stimulation assay was performed according to the method previously reported by Inthongkaew *et al.* (Inthongkaew *et al.*, 2017). The L6 rat skeletal muscle cells (myoblasts) were maintained in α -MEM containing 10 % fetal bovine serum (FBS) with 1 % penicillin-streptomycin at 37 $^{\circ}$ C in atmosphere of 5 % CO_2 . When the cells had the confluence around 90 %, the medium was switched to α -MEM with 2 % FBS and 1 % penicillin-streptomycin to facilitate the differentiation of myoblasts into myotubes (**Figure 9**). The medium was changed every 48 h during the differentiation period (5-7 days).

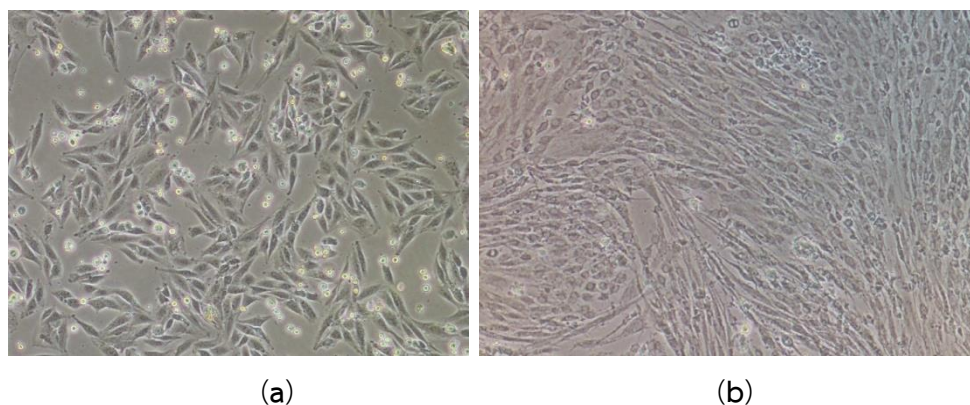


Figure 9 Rat skeletal (L6) myoblasts (a) and Rat skeletal (L6) myotubes (b)

6.1 Materials and instruments

- L6 Rat skeletal muscle (ATCC®CRL-1458) (Manassas, VA, USA).
- Penicillin-streptomycin (10000 IU/ml) (Thermo Fisher Scientific) (Grand Island, NY, USA)
- Fetal bovine serum (FBS) (Thermo Fisher Scientific) (Grand Island, NY, USA)
- Alpha minimal essential medium (α -MEM) (Thermo Fisher Scientific) (Grand Island, NY, USA)
- Glucose oxidase (GO) assay kit (Sigma Aldrich) (St Louis, MO, USA)
- Sodium dodecyl sulfate (SDS) (Sigma Aldrich) (St Louis, MO, USA)
- 3-(4,5-dimethyl thiazol-2-yl)-5-diphenyl tetrazolium bromide (MTT) (Sigma Aldrich) (St Louis, MO, USA)
- Insulin (100 IU/ml) (Biocon) (Bangalore, India)

6.2 Determination of glucose uptake stimulatory activity

The monolayer of L6 myotubes was cultured in growth medium containing α -MEM, supplemented with 2 % fetal bovine serum (FBS) and 1 % penicillin-streptomycin. The cells were maintained under the influence of 5 % CO₂. To determine the glucose uptake activity of the samples, the cells (myotubes) were seeded in 96-well plates at a density of 2×10^4 cells/well. After incubation at 37° C under 5 % CO₂ for 24 h, the myotubes were treated with the test compound (1, 10 and 100 μ g/ml) and incubated for 24 h. Insulin (500 nM) and metformin (2 mM) were used as positive controls, and the differentiation medium containing 0.1 % DMSO was used as a negative control. Finally, the medium was collected from the well, and the glucose level was determined using a glucose oxidase assay kit. A Biochom EZ Read 400 Microplate Reader was used to measure the absorbance of the microtiter plate (Biochrome, Cambridge) at 490 nm. The amount of glucose consumption by myotubes was determined by subtracting the glucose concentration of the blank

from the glucose in the well containing the sample. The amount of glucose uptake was described as percentage of glucose uptake, which was calculated as follows:

$$\text{Percentage of glucose uptake} = \frac{A \times 100}{B}$$

A = amount of glucose uptake in the presence of test compound

B = amount of glucose uptake with the medium containing 0.1 % DMSO

6.3 Determination of cell viability

Cell viability in each well was evaluated promptly after the determination of glucose uptake in L6 cells. MTT assay method was used to determine the cytotoxicity of each test compound. After removal of the medium for glucose uptake assay, fresh medium (100 μ l) and 10 μ l of MTT solution (5 mg/ml) were added into each well. The mixture was incubated for 2 h at 37 $^{\circ}$ C under 5 % CO₂. Then, a solubilization solution (100 μ l) [40 % dimethylformamide (DMF), 2% glacial acetic acid, 16 % w/v sodium dodecyl sulfate (SDS) in distilled water] was added to dissolve the formazan crystal, and the plate was shaken for 10 min. The supernatant was collected, and the absorbance was measured at 570 nm. The cytotoxicity was expressed as percentage of cell viability. The cell viability was calculated as follows:

$$\text{Cell viability} = \frac{A_{570} \text{ of treated well} \times 100}{A_{570} \text{ of medium containing 0.1 \% DMSO}}$$

6.4 Statistical analysis

The results of glucose uptake stimulation and cytotoxicity assays were described as the mean \pm standard deviation (SD). Analysis of variance (ANOVA) was performed using the GraphPad Prism Version 7.00 for Windows (GraphPad Software, Inc., San Diego, California USA). The Statistical analysis for evaluating the significance of the difference between means is performed by the uncorrected Fisher's LSD post hoc test. A *p* value < 0.05 was considered statistically significant.

CHAPTER IV

RESULTS AND DISCUSSION

In this study, four extracts were prepared from *Cissus javana* (Vitaceae), *Dendrobium christyanum* (Orchidaceae), *Gastrochilus bellinus* (Orchidaceae) and *Huberantha jenkinsii* (Annonaceae). They were found to possess significant α -glucosidase inhibitory potential and thus were subjected to further investigations to identify the active principles. This chapter is divided into four main sections. Each section describes the results and discussion on the phytochemical and biological studies of each plant.

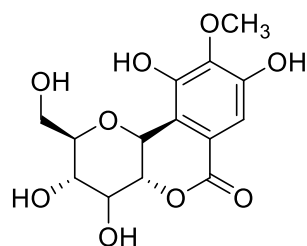
1. Phytochemical and biological studies of *Cissus javana*

1.1 Preliminary biological activity evaluation

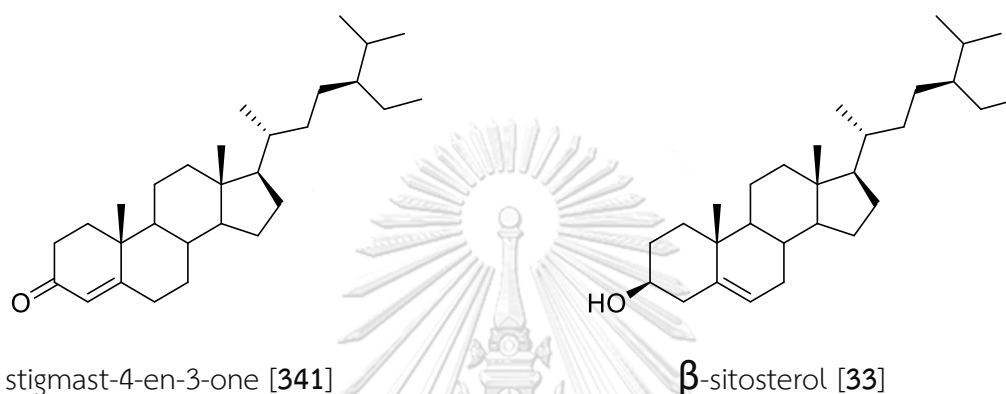
The MeOH extract prepared from the dried tuberous roots of *Cissus javana* at 100 $\mu\text{g/ml}$ exhibited 100 % inhibition of α -glucosidase enzyme. In addition, the extract at this concentration displayed glucose uptake stimulatory activity in rat L6 myotubes, with 70.9 % enhancement. Therefore, this MeOH extract was further investigated to identify the active principles.

1.2 Chemical investigation

The MeOH extract was separated into an EtOAc insoluble and soluble fraction, designated as fractions A (6.36 g) and B (2.38 g), respectively. From each fraction, the chemical components were isolated by chromatographic methods, and their structures were determined by spectroscopic analysis. This led to the isolation of three known compounds including the glycoside bergenin [31] and the phytosterols stigmast-4-en-3-one [341] and β -sitosterol [33] (Figure 10).



bergenin [31]



stigmast-4-en-3-one [341]

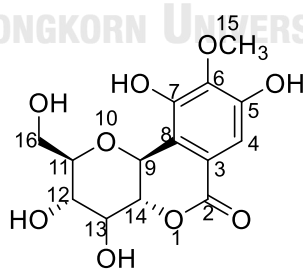
 β -sitosterol [33]**Figure 10** Structures of compounds isolated from *Cissus javana*

1.2.1 Identification of compound CJ1 (bergenin)

Compound CJ1 was obtained as colorless crystals. The high resolution ESI mass spectrum (**Figure 11**) showed a deprotonated molecular ion $[M-H]^-$ at m/z 327.0703 (calcd. for $C_{14}H_{15}O_9$, 327.0716), suggesting the molecular formula $C_{14}H_{16}O_9$. The 1H -NMR spectrum of CJ1 in $DMSO-d_6$ (**Figure 12** and **Table 4**) displayed signals for five aliphatic methine protons at δ 4.97 (1H, d, $J = 10.5$ Hz, H-9), 3.56 (1H, t, $J = 8.1$ Hz, H-11), 3.19 (1H, dd, $J = 9.6$ Hz, H-12), 3.63 (1H, m, H-13) and 3.98 (1H, dd, $J = 10.2, 9.6$ Hz, H-14) and two aliphatic methylene protons at δ 3.83 (1H, dd, $J = 11.7, 2.7$ Hz, H-16a) and 3.42 (1H, m, H-16b). In addition, signals for an aromatic proton at δ 6.98 (1H, s, H-4), and methoxyl protons at δ 3.67 (3H, s, H-15) were also observed. The ^{13}C NMR and DEPT spectra (**Figure 13** and **Table 4**) exhibited 14 carbon signals, which could be classified into five quaternary carbons [δ 118.5 (C-8), 116.4 (C-7),

141.0 (C-6), 148.5 (C-3) and 151.4 (C-5)], five methine carbons [δ 72.5 (C-9), 82.2 (C-11), 71.1 (C-12), 74.1 (C-13) and 80.2 (C-14)], a methylene carbon [δ 61.5 (C-16)], a methoxy group [δ 60.3 (C-15)] and a carbonyl carbon [δ 163.8 (C-2)].

The HSQC spectrum of CJ1 (**Figure 14**) showed correlation peaks for protonated carbons at δ_C 61.5 (C-16) / δ_H 3.83 (1H, dd, $J = 11.7, 2.7$ Hz, H-16a) and δ 3.42 (1H, m, H-16b); δ_C 72.5 (C-9) / δ_H 4.97 (1H, d, $J = 10.5$ Hz, H-9); δ_C 82.2 (C-11) / δ_H 3.56 (1H, t, $J = 8.1$ Hz, H-11); δ_C 71.1 (C-12) / δ_H 3.19 (1H, dd, $J = 9.6$ Hz, H-12); δ_C 74.1 (C-13) / δ_H 3.63 (1H, m, H-13); δ_C 80.2 (C-14) / δ_H 3.98 (1H, dd, $J = 10.2, 9.6$ Hz, H-14) and δ_C 109.9 (C-4) / δ_H 6.98 (1H, s, H-4). In the HMBC spectrum of CJ1 (**Figure 15**), the H-4 proton showed 3-bond couplings with C-2, C-6 and C-8. The HMBC correlation from the methoxyl protons to C-6 confirmed its location at this carbon. Additionally, H-9 showed 3-bond correlations with C-3, C-11 and C-13 and 2-bond correlation with C-14. Based on the aforementioned spectroscopic data, CJ1 was identified as bergenin [31]. The NMR data of **31** were in agreement with previously reported values (De Abreu *et al.*, 2008). However, the previous ^{13}C -NMR assignments for C-3, C-5, C-6, C-7 and C-8 should be revised, based on the HMBC correlations obtained in this study.



Bergenin [31]

Bergenin [31] has been previously isolated from several species of *Cissus*, for instance, *Cissus assamica* (M.A.Lawson) Craib, *C. populnea* Guill. & Perr., and *C. pteroclada* Hayata (Nyemb *et al.*, 2018; Sani *et al.*, 2015; Xie *et al.*, 2009).

Table 4 NMR spectral data of compound CJ1 as compared with bergenin

Position	Compound CJ1 (DMSO- <i>d</i> ₆)		Bergenin* (DMSO- <i>d</i> ₆)	
	δ_{H} (mult., <i>J</i> in Hz)	δ_{C}	δ_{H} (mult., <i>J</i> in Hz)	δ_{C}
1	-	-	-	-
2	-	163.8	-	163.4
3	-	118.6	-	150.9 [#]
4	6.98 (1H, s)	109.9	6.98 (1H, s)	109.4
5	-	151.4	-	140.6 [#]
6	-	141.0	-	148.1 [#]
7	-	148.2	-	115.9 [#]
8	-	116.4	-	118.1 [#]
9	4.97 (1H, d, 10.5)	72.5	4.96 (1H, d, 10.4)	72.1
11	3.56 (1H, m)	82.2	3.58 (1H, ddd, 7.6, 3.2, 1.9)	81.7
12	3.19 (1H, m)	71.1	3.20 (1H, ddd, 8.8, 7.6, 5.0)	70.7
13	3.63 (1H, m)	74.1	3.65 (1H, ddd, 9.5, 8.8, 5.3)	73.7
14	3.98 (1H, t, 10.5)	80.2	4.00 (1H, dd, 10.4, 9.5)	79.8
15	3.67 (3H, s)	60.3	3.78 (3H, s)	59.8
16a	3.83 (1H, br dd, 11.7, 2.7)	61.5	3.44 (1H, ddd, 10.9, 8.1, 1.9)	61.1
16b	3.42 (1H, m)		3.85 (1H, dd, 10.9, 3.2)	
5-OH	9.76 (1H, s)	-	9.76 (1H, s)	-
7-OH	8.44 (1H, s)	-	8.45 (1H, s)	-
13-OH	5.65 (1H, d, 4.8)	-	5.64 (1H, d, 5.3)	-
12-OH	5.43 (1H, d, 5.7)	-	5.42 (1H, d, 5.0)	-
16-OH	-	-	4.91 (1H, m)	-

* (De Abreu *et al.*, 2008), [#] assignments should be revised.

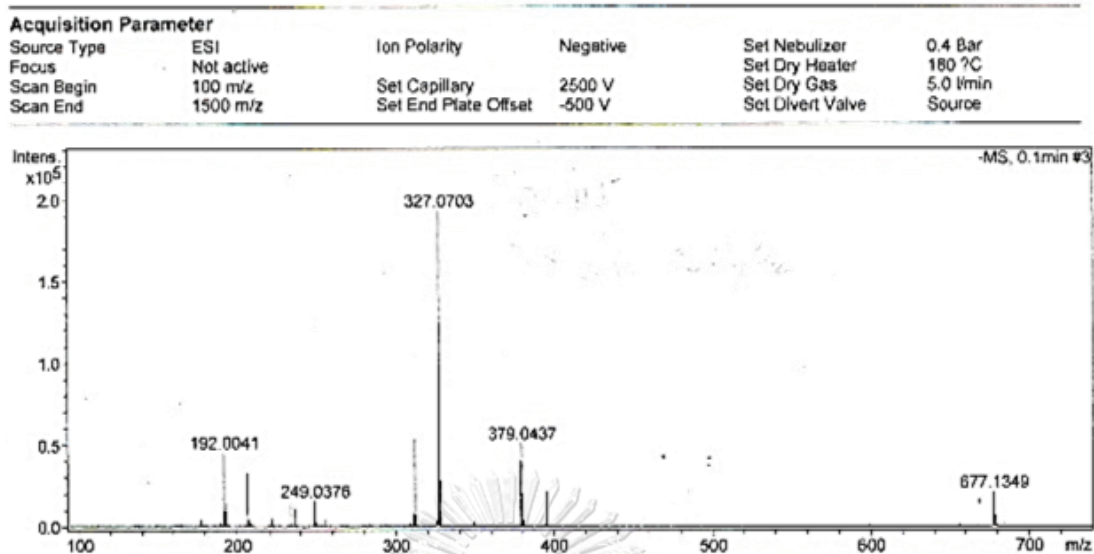
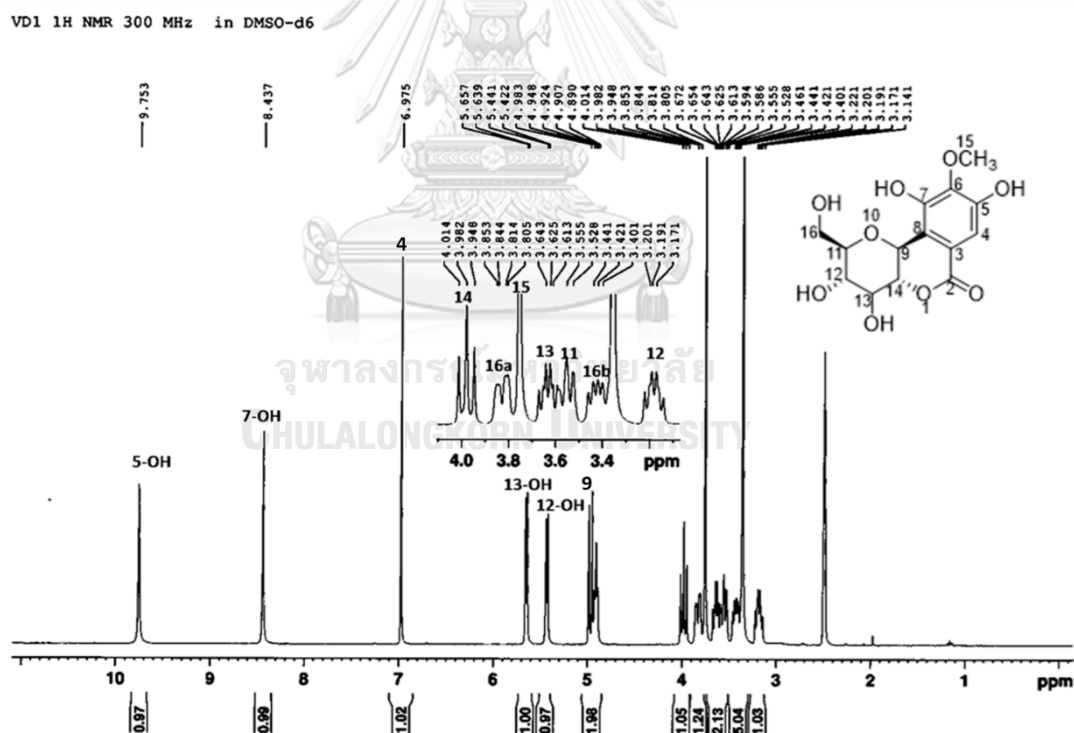


Figure 11 Mass spectrum of compound CJ1

Figure 12 ¹H-NMR (300 MHz) spectrum of compound CJ1 (DMSO-d₆)

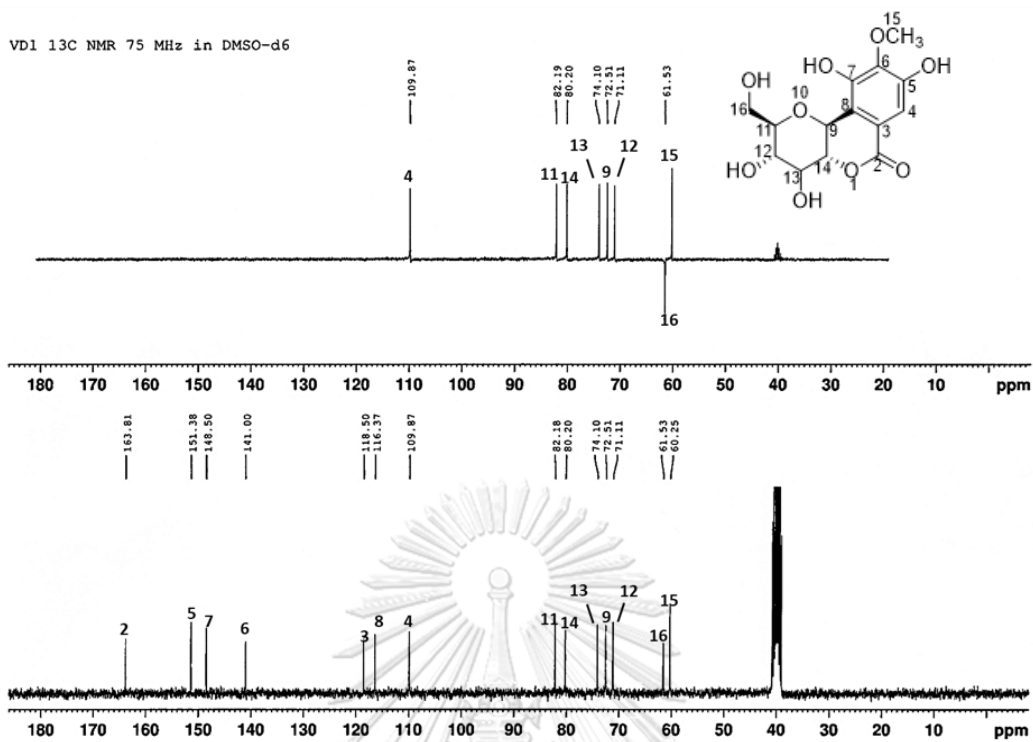


Figure 13 ¹³C-NMR (75 MHz) and DEPT-135 spectra of compound CJ1 (DMSO-*d*₆)

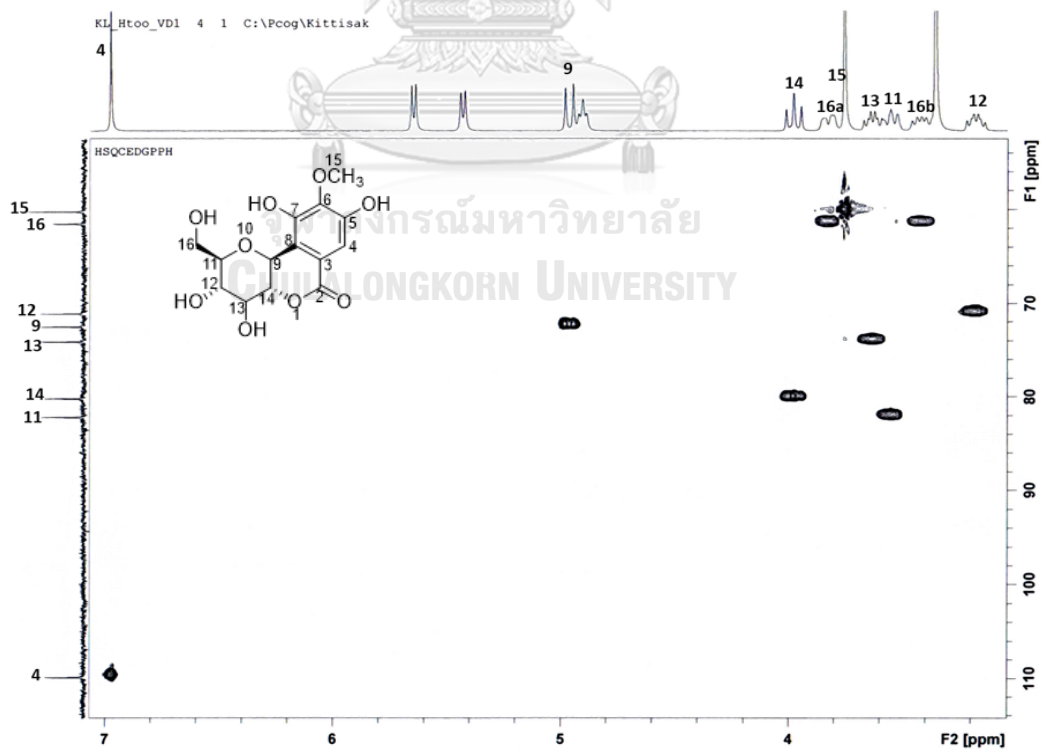


Figure 14 HSQC spectrum of compound CJ1

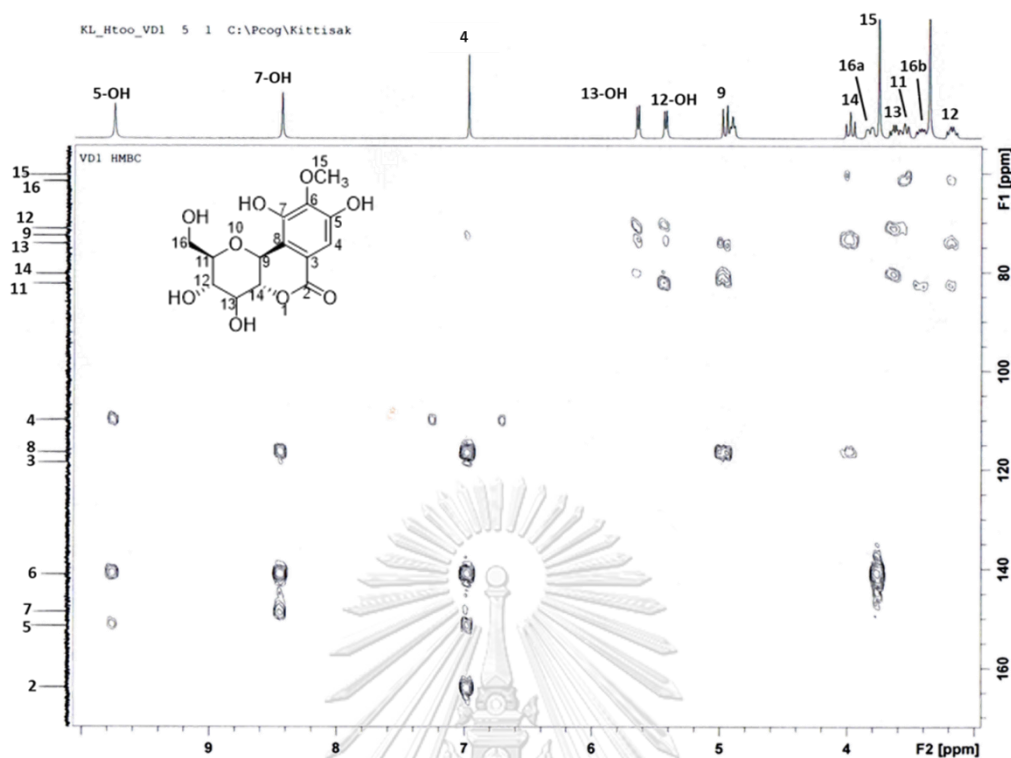
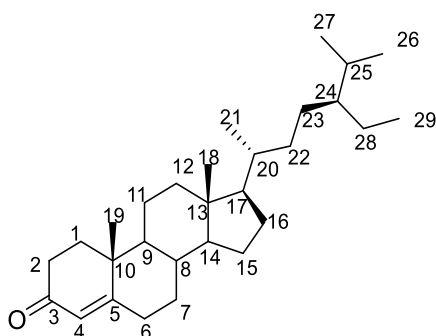


Figure 15 HMBC spectrum of compound CJ1 (DMSO- d_6)

1.2.2 Identification of compound CJ2 (stigmast-4-en-3-one)

CJ2 was collected as white crystals. The steroidal skeleton of the CJ2 was suggested from the purple spot on the TLC plate that developed after spraying with anisaldehyde reagent and heating. The high resolution ESI mass spectrum (Figure 16) showed a protonated molecular ion $[M+H]^+$ at m/z 413.3781 (calcd. for $C_{29}H_{49}O$ 413.3783), suggesting the molecular formula $C_{29}H_{48}O$. The 1H -NMR spectrum (Figure 17) displayed an olefinic proton signal at δ 5.73 (1H, s, H-4), and signals for six methyl groups at δ 0.72 (3H, s, H₃-18), 1.19 (3H, s, H₃-19), 0.93 (3H, d, J = 6.6 Hz, H₃-21), 0.83 (3H, d, J = 6.6 Hz, H₃-26), 0.87 (3H, d, J = 7.9 Hz, H₃-27) and 0.83 (3H, t, J = 6.6 Hz, H₃-29), respectively.

Through comparison with previously reported 1H -NMR and MS data (Kolak *et al.*, 2005) (Table 5), CJ2 was identified as stigmast-4-en-3-one [35]. The occurrence of 35 in *Cissus repens* Lam. was earlier reported (Nyunt *et al.*, 2012).



Stigmast-4-en-3-one [35]

Table 5 NMR spectral of compound CJ2 as compared with stigmast-4-en-3-one

Position	CJ2 (CDCl ₃)	stigmast-4-en-3-one (CDCl ₃)*
	δ_{H} (mult., <i>J</i> in Hz)	δ_{H} (mult., <i>J</i> in Hz)
H-4	5.73 (1H, s)	δ 5.74 (1H, s)
3-18	0.72 (3H, s,)	0.72 (3H, s)
H ₃ -19	1.19 (3H, s,)	1.19 (3H, s)
H ₃ -21	0.93 (3H, d, 6.6)	0.92 (3H, d, 6.4)
H ₃ -26	0.83 (3H, d, 6.6)	0.83 (3H, d, 6.8)
H ₃ -27	0.87 (3H, d, 7.9)	0.85 (3H, d, 7.8)
H ₃ -29	0.83 (3H, t, 6.6)	0.83 (3H, t, 6.8)

* (Kolak *et al.*, 2005)

Mass Spectrum List Report

Analysis Info

Analysis Name OSCUHTS06082019002.d
 Method Tune_wide_POS_Tawatchai_05Feb2016.m
 Sample Name VD.3
 06082019

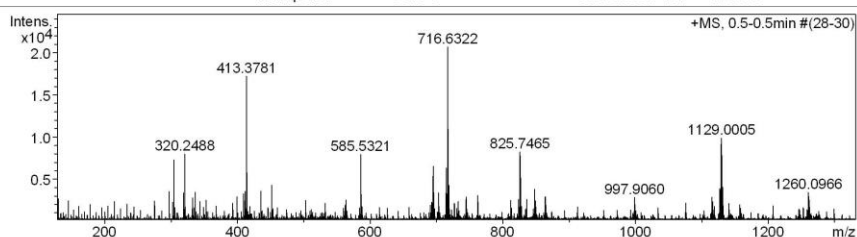
Acquisition Date 8/6/2019 2:30:25 PM
 Operator Administrator
 Instrument micrOTOF 72

Acquisition Parameter

Source Type ESI
 Scan Range n/a
 Scan Begin 50 m/z
 Scan End 3000 m/z

Ion Polarity Positive
 Capillary Exit 100.0 V
 Hexapole RF 400.0 V
 Skimmer 1 70.0 V
 Hexapole 1 25.0 V

Set Corrector Fill 50 V
 Set Pulsar Pull 337 V
 Set Pulsar Push 337 V
 Set Reflector 1300 V
 Set Flight Tube 9000 V
 Set Detector TOF 2295 V

**Figure 16** Mass spectrum of compound CJ2

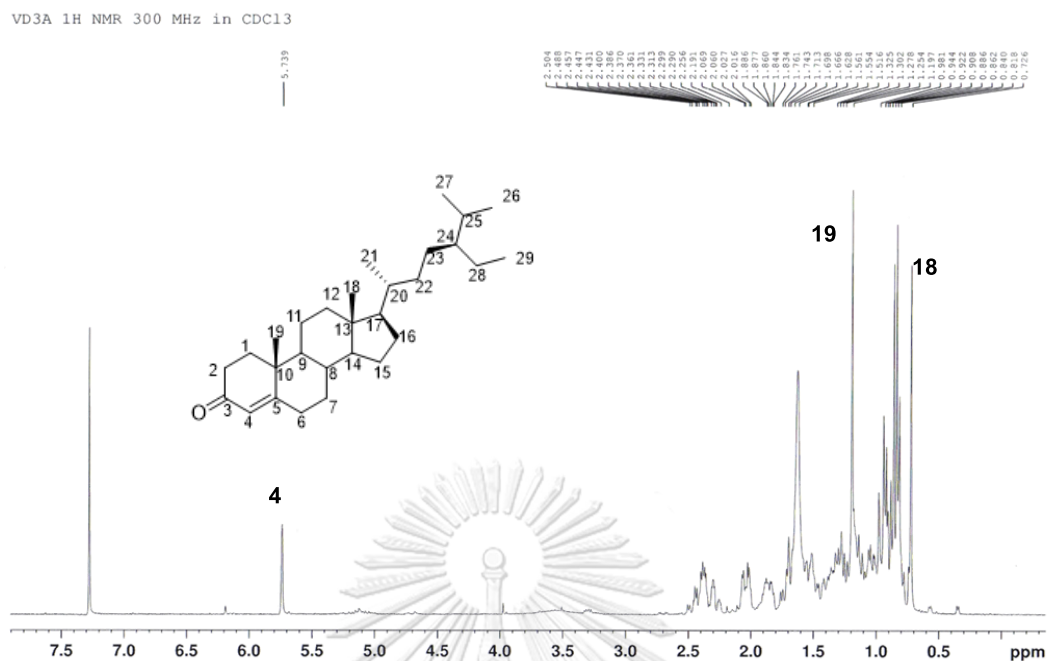


Figure 17 $^1\text{H-NMR}$ (300 MHz) spectrum of compound CJ2 (CDCl_3)

1.2.3 Identification of compound CJ3 (β -sitosterol)

Compound CJ3 was obtained as white needle-like crystals. Similar to CJ2, this compound possessed a steroid nucleus, giving a purple spot on the TLC plate after spraying with anisaldehyde reagent and heating. The high resolution APCI mass spectrum (Figure 18) showed a molecular ion $[\text{M}]^+$ at m/z 414.3830 (calcd. for $\text{C}_{29}\text{H}_{50}\text{O}$ 414.3862), suggesting the molecular formula $\text{C}_{29}\text{H}_{50}\text{O}$.

The $^1\text{H-NMR}$ spectrum (Figure 19) displayed an olefinic proton signal at δ 5.36 (1H, m, H-6), signals for six methyl groups at δ 0.69 (3H, s, H₃-18), 1.02 (3H, s, H₃-19), 0.94 (3H, d, $J = 6.6$ Hz, H₃-21), 0.83 (3H, d, $J = 6.9$ Hz, H₃-26), 0.87 (3H, d, $J = 6.3$ Hz, H₃-27) and 0.83 (3H, $J = 6.9$ Hz, H₃-29). The multiplet proton peak at δ 3.54 (H-3) represented a proton connected to an oxygen-bearing carbon.

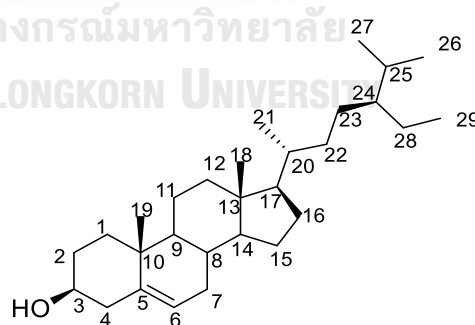
The results from comparison of the $^1\text{H NMR}$ data and MS data with literature values (Table 6) indicated that CJ3 was β -sitosterol [33] (Kolak *et al.*, 2005). This

steroid is ubiquitous in the plant Kingdom. In the genus *Cissus*, it has been found in *C. polyantha* (Sani *et al.*, 2015), *C. quadrangularis* (Singh *et al.*, 2007) and *C. trifoliata* (Méndez-López *et al.*, 2020).

Table 6 NMR spectral data of compound CJ3 as compared with β -sitosterol

Position	CJ3 (CDCl ₃)	β -sitosterol (CDCl ₃)*
	δ_{H} (mult., <i>J</i> in Hz)	δ_{H} (mult., <i>J</i> in Hz)
H-3	3.54 (m)	3.54 (m)
H-6	5.36 (1H, m)	5.35 (1H, m)
H ₃ -18	0.69 (3H, s,)	0.69 (3H, s,)
H ₃ -19	1.02 (3H, s,)	1.01 (3H, s,)
H ₃ -21	0.94 (3H, d, 6.6)	0.92 (3H, d, 6.4)
H ₃ -26	0.83 (3H, d, 6.9)	0.83 (3H, d, 6.8)
H ₃ -27	0.87 (3H, d, 6.3)	0.85 (3H, d, 7.8)
H ₃ -29	0.83 (3H, t, 6.9)	0.83 (3H, t, 6.8)

* (Kolak *et al.*, 2005)

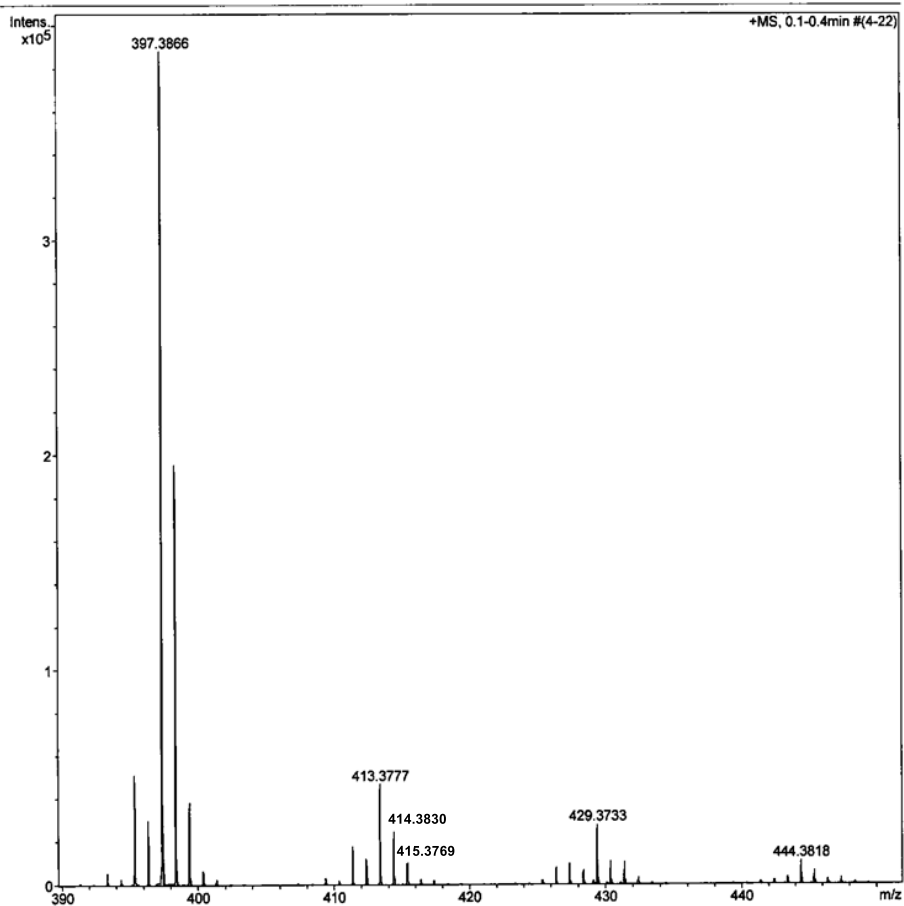


β -sitosterol [33]

Display Report

Analysis Info		Acquisition Date	3/24/2020 10:32:27 AM
Analysis Name	D:\Data\Yp sample\VD2.d	Operator	CTB
Method	tune_wide_pos.m	Instrument	micrOTOF-Q II 10414
Sample Name	VD2		
Comment			

Acquisition Parameter					
Source Type	APCI	Ion Polarity	Positive	Set Nebulizer	1.6 Bar
Focus	Not active	Set Capillary	4000 V	Set Dry Heater	200 °C
Scan Begin	50 m/z	Set End Plate Offset	-500 V	Set Dry Gas	8.0 l/min
Scan End	3000 m/z	Set Collision Cell RF	550.0 Vpp	Set Divert Valve	Waste



Bruker Compass DataAnalysis 4.0

printed: 3/24/2020 11:08:54 AM

Page 1 of 1

Figure 18 Mass spectrum of compound CJ3

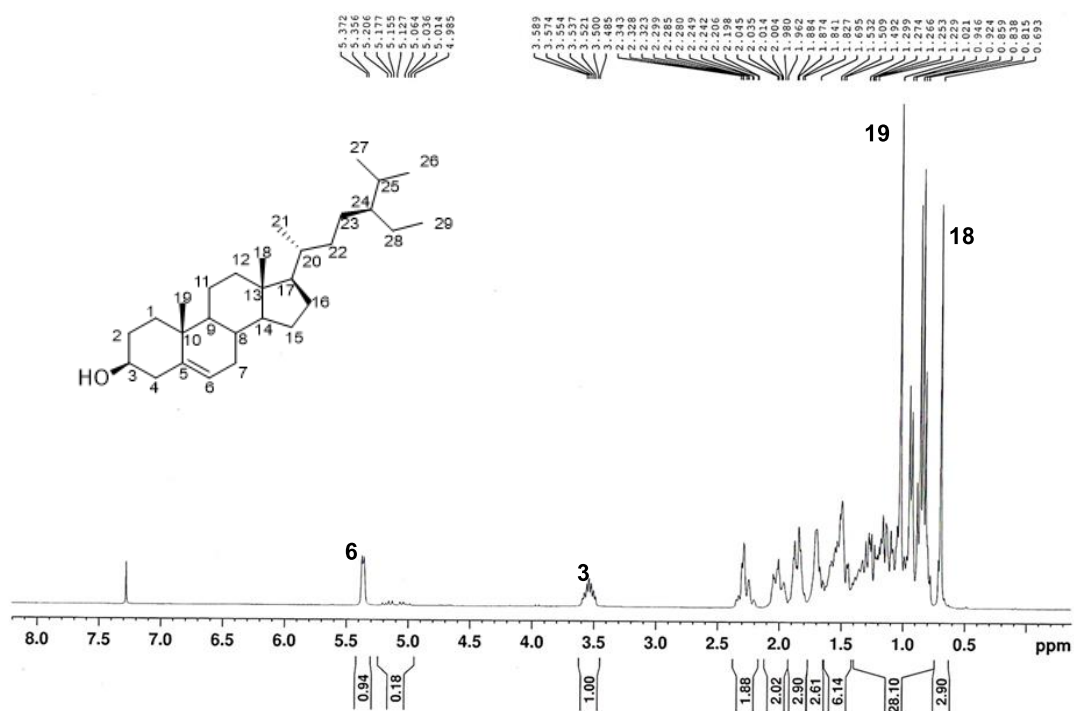


Figure 19 $^1\text{H-NMR}$ (300 MHz) spectrum of compound CJ3 (CDCl_3)

1.3 Biological activity of isolated compounds

In this study, the isolated compounds, bergenin [31], stigmast-4-en-3-one [35] and β -sitosterol [33], were evaluated for α -glucosidase inhibitory activity (Table 7). Bergenin [31] did not possess α -glucosidase inhibitory activity (2.2 % inhibition at 100 $\mu\text{g/ml}$), in agreement with a previous report (Kashima *et al.*, 2013). The two phytosteroidal compounds stigmast-4-en-3-one [341] and β -sitosterol [33] exhibited significant inhibitory effects (98.6 % and 40.6 % inhibition, respectively) in comparison with acarbose (21.9 % inhibition). These findings were consistent with earlier reported values (Nkobile *et al.*, 2011).

Recently, several α -glucosidase inhibitors (AGIs) derived from plants have been reported to also stimulate cellular glucose uptake (Inthongkaew *et al.*, 2017; Mitsumoto *et al.*, 1991). This supplementary activity may help augment the potential

of AGIs to lower the blood sugar level. With this hypothesis in mind, the author investigated the extracts and the compounds obtained from this plant (**31**, **33** and **341**) for their ability to enhance cellular glucose absorption, although this research direction was not originally in the scope of the study.

The test sample was prepared in three concentrations of 1, 10 and 100 µg/ml and evaluated for glucose uptake stimulatory activity and cytotoxicity in rat skeletal muscle cells (Inthongkaew *et al.*, 2017; Mitsumoto *et al.*, 1991).

The MeOH extract and fractions A and B showed no toxicity at these concentrations (cell viability > 80 %) (**Figure 20**). The MeOH extract at 10 and 100 µg/ml could stimulate glucose uptake by 41.8 and 70.9 %, respectively. Fraction A appeared to have stronger activity, with 52.0, 72.4 and 75.3 % enhancement at 1, 10 and 100 µg/ml, respectively, but fraction B displayed much less activity, showing only 57.8 % enhancement at 100 µg/ml (**Figure 20** and **Table 8**).

Regarding the isolated compounds, bergenin [**31**] showed 50.5 % glucose uptake enhancement at 100 µg/ml. The positive controls insulin and metformin exhibited 92.7 % enhancement at 500 nM and 118.9 % enhancement at 2 mM, respectively (**Figure 20**). It should also be noted that bergenin is structurally related to hydrolyzable tannins, and earlier studies suggested that tannins could stimulate glucose uptake and inhibit adipogenesis (Prasad *et al.*, 2010). In a previous study using streptozotocin-nicotinamide-induced type-2 diabetic rats, bergenin was found to reduce the fasting blood glucose level without effects on liver glycogen (Kumar *et al.*, 2012). Thus, the glucose uptake stimulatory potential of bergenin observed in this investigation may help explain the mechanism underlying the *in vivo* hypoglycemic action of bergenin.

For the steroids stigmast-4-en-3-one [**35**] and β -sitosterol [**33**], attempts to evaluate their activity in this L6 model were not successful. These two compounds

showed poor solubility in the test system, and this may partly account for the low glucose uptake stimulatory potential earlier observed for fraction B.

Table 7 α -Glucosidase inhibitory activity of compounds isolated from *C. javana*

compounds	% inhibition at 100 $\mu\text{g/ml}$	IC ₅₀ (μM)
bergenin [31]	NA	-
stigmast-4-en-3-one [341]	98.6 \pm 1.2	43.9 \pm 1.5
β -sitosterol [33]	40.6 \pm 4.2	-
acarbose	21.9 \pm 1.5	724.7 \pm 46



Table 8 Glucose uptake stimulatory activity of compounds isolated from *C. javana*

Sample	Percentage of glucose uptake	Percent enhancement
DMSO	100	0
Metformin (2 mM)	218.9 ± 4.4*	118.9 ± 3.6
Insulin (500 nM)	192.7 ± 13.1*	92.7 ± 10.7
MeOH extract		
1 µg/ml	102.5 ± 25.6	NA
10 µg/ml	141.8 ± 35.3*	41.8 ± 28.8
100 µg/ml	170.9 ± 15.1*	70.9 ± 12.3
Fraction A		
1 µg/ml	152.0 ± 10.9*	52.0 ± 9.0
10 µg/ml	172.4 ± 12.6*	72.4 ± 10.3
100 µg/ml	175.3 ± 23.1*	75.3 ± 18.9
Fraction B		
1 µg/ml	82.2 ± 11.0	NA
10 µg/ml	114.2 ± 24.3	NA
100 µg/ml	157.8 ± 24.3*	57.8 ± 19.8
Bergenin		
1 µg/ml (0.003 mM)	79.3 ± 19.0	NA
10 µg/ml (0.0304 mM)	124.3 ± 36.3	NA
100 µg/ml (0.304 mM)	150.5 ± 9.1*	50.5 ± 7.4

* $p < 0.05$; significantly different when compared to the control (DMSO)

NA = Not applicable

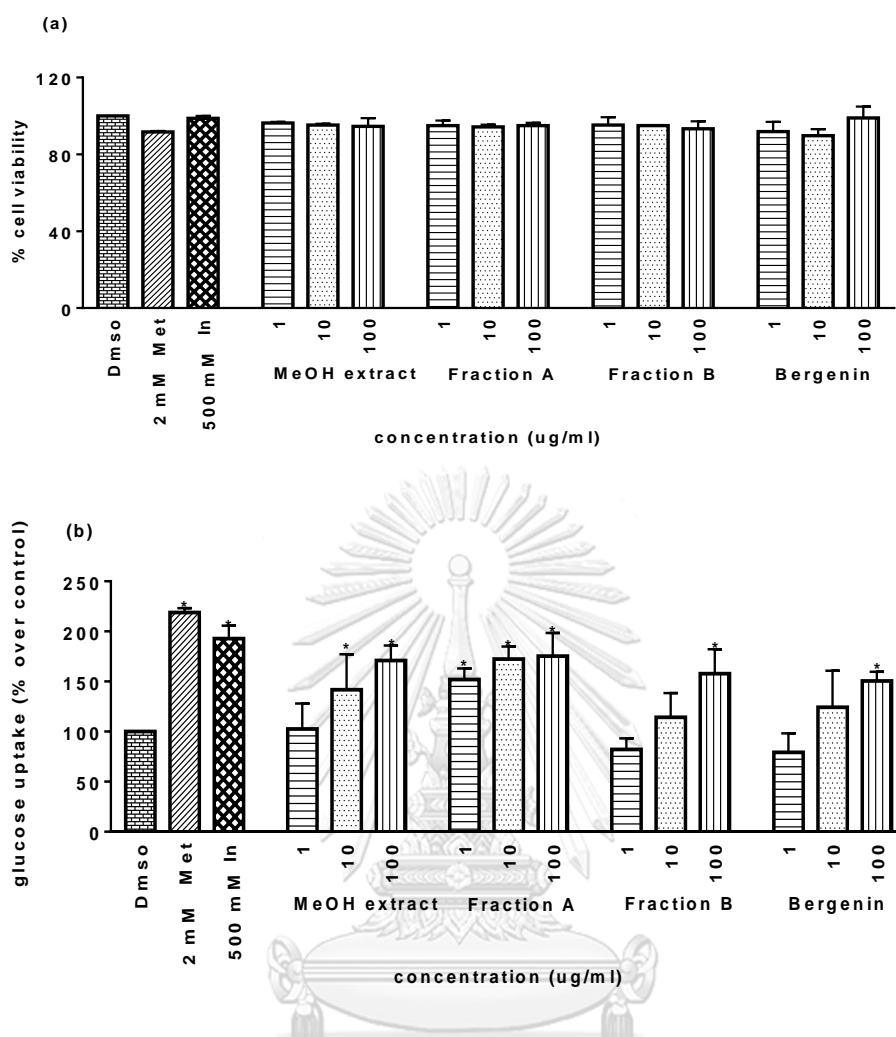


Figure 20 Cytotoxicity (a) and glucose uptake stimulation (b) of MeOH extract, fractions and bergenin

*($p < 0.05$) Significantly different when compared to the control (DMSO)

DMSO (control); Met = metformin, In = insulin (positive control)

2. Phytochemical and biological studies of *Dendrobium christyanum*

2.1 Preliminary biological activity evaluation

The air-dried roots of *Dendrobium christyanum* (0.5 kg) were extracted with MeOH to give a methanolic extract which showed 70 % inhibition against α -glucosidase enzyme at a concentration of 100 μ g/ml. The MeOH extract (36.1 g) was

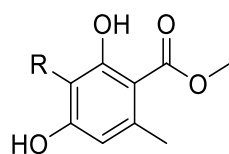
fractionated by vacuum-liquid chromatography (VLC). The obtained fractions (A-E) exhibited α -glucosidase inhibitory potential (Table 9) and were further investigated to identify the active compounds. The scope of this part of research was also expanded to include the investigation of the glucose uptake stimulatory activity of the MeOH extract in L6 myotubes (which later showed 56.4 ± 19.7 % enhancement of glucose uptake).

Table 9 α -Glucosidase inhibitory activity of fractions

Fraction	% inhibition at 100 μ g/ml
A	95.4
B	98.6
C	98.4
D	44.1
E	89.2
acarbose	21.9 ± 1.5

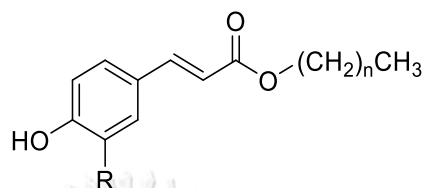
2.2 Chemical investigation

Repeated chromatographic separation of the MeOH extract of *D. christyanum* roots led to the isolation of thirteen compounds including two alkyl cinnamate esters (*n*-eicosyl *trans*-ferulate [343] and *n*-docosyl 4-hydroxy-*trans*-cinnamate [345]), a phenanthrene (4,5-dihydroxy-2-methoxy-9,10-dihydrophenanthrene [103]) and five bibenzyls (moscatilin [59], aloifol I [38], gigantol [54], batatasin III [41], dendrosinen B [73]), a phenylpropanoid (coniferyl aldehyde [346]) and four benzoic acid related compounds (methyl haematommate [342], atraric acid [344], vanillin [275] and diorcinolic acid [347]) (Figure 21).



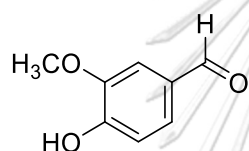
methyl haematommate [342]; R=CHO

atraric acid [344] R= Me

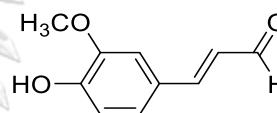


n-eicosyl *trans*-ferulate [343]; R=OMe, n=19

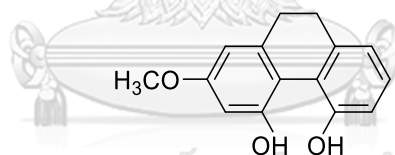
n-docosyl 4-hydroxy-*trans*- cinnamate [345]; R=H, n=21



vanillin [275]



coniferyl aldehyde [346]



4,5-dihydroxy-2-methoxy-9,10- dihydrophenanthrene [103]

Figure 21 Structures of compounds isolated from *Dendrobium christyanum*

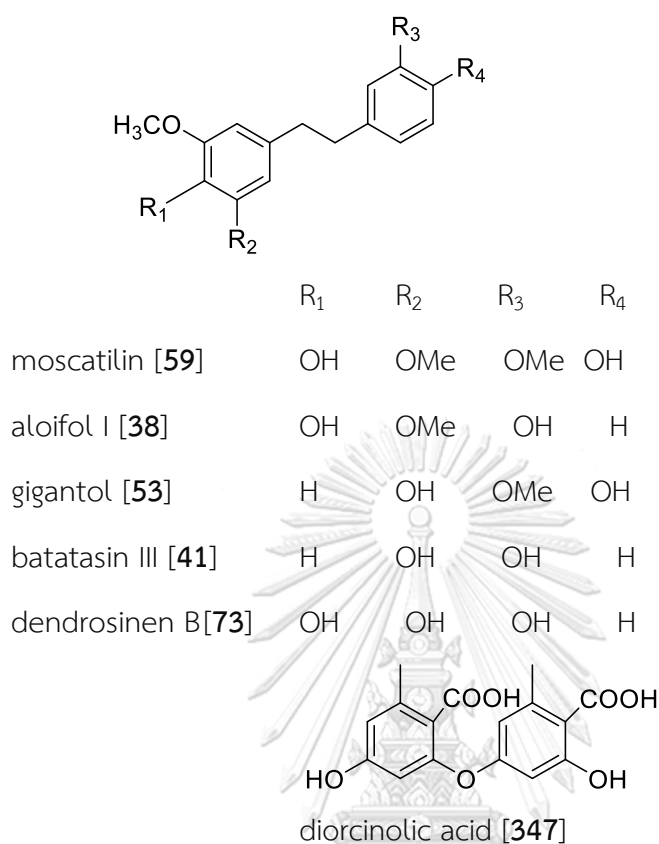


Figure 21 Structures of compounds isolated from *Dendrobium christyanum*
(continued)

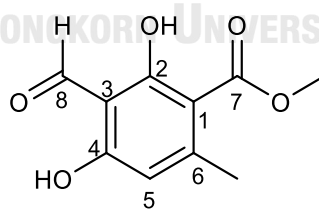
2.2.1 Identification of compound DC1 (methyl haematommate)

Compound DC1 was obtained as a brownish white powder. The high resolution ESI mass spectrum (**Figure 22**) showed a deprotonated molecular ion $[M-H]^-$ at m/z 209.0441 (calcd. for $C_{10}H_9O_5$ 209.0450), suggesting the molecular formula $C_{10}H_9O_5$.

The 1H -NMR spectrum (**Figure 23**) exhibited six singlet peaks representing a methyl group at δ 2.53 (3H, s, 6-Me), a methoxy group at δ 3.96 (3H, s, 7-OMe), an aromatic methine proton at δ 6.29 (1H, s, H-5), an aldehyde proton at δ 10.36 (1H, s, CHO), and two hydroxyl groups at δ 12.43 (1H, s, 2-OH) and 12.90 (1H, s, 4-OH). The

^{13}C -NMR and HSQC spectra (Figures 24 and 25) showed a penta-substituted aromatic ring displaying five quaternary carbon signals at δ 103.9 (C-1), 108.5 (C-3), 152.3 (C-6), 166.7 (C-4) and 168.3 (C-2), and a methine carbon signal at δ 112.1 (C-5). The remaining ^{13}C NMR signals represented a methyl group at δ 25.2 (6-Me), an aldehyde carbon at δ 193.9 (C-8), a methoxy group at δ 52.3 (7-OMe) and an ester carbonyl carbon at δ 172.0 (C-7). The aldehyde functionality was supported by the HSQC correlation peak at δ_{C} 193.9 (C-8) / δ_{H} 10.34 (Figure 25). The positions of the substituents were deduced through analysis of the HMBC spectrum (Figure 26). The cross peak at δ 172.0 (C-7) / δ 3.96 (3H, s, 7-OMe) linked the methoxy group to the ester carbonyl carbon. In addition, long range correlation from the proton at δ 25.2 (6-Me) to the carbons at δ 103.9 (C-1) and 112.1 (C-5) indicated the location of methyl group on aromatic ring. These spectroscopic data of compound DC1 were in accordance with the reported data for methyl haematommate [342] (Duong *et al.*, 2011).

It should be noted that methyl haematommate [342] has been reported as a typical depside-type constituent of lichens (Huneck & Yoshimura, 1996).



Methyl haematommate [342]

Table 10 NMR spectral data of compound DC1 as compared with methyl haematommate

Position	Compound DC1 (CDCl ₃)		methyl haematommate (CDCl ₃)*	
	δ_{H} (mult., <i>J</i> in Hz)	δ_{C}	δ_{H} (mult., <i>J</i> in Hz)	δ_{C}
1	-	103.9	-	103.9
2	-	168.3	-	168.3
3	-	108.5	-	108.5
4	-	166.7	-	166.7
5	6.29 (1H, s)	112.1	6.29 (1H, s)	112.1
6	-	152.3	-	152.3
7	-	172.0	-	172.0
8	10.36 (1H, s)	193.9	10.34 (1H, s)	193.9
6-Me	2.53 (3H, s)	25.2	2.53 (3H, s)	25.2
7-OMe	3.96 (3H, s)	52.3	3.96 (3H, s)	52.3
2-OH	12.43	-	12.40	-
4-OH	12.90	-	12.86	-

* (Duong *et al.*, 2011) จุฬาลงกรณ์มหาวิทยาลัย

CHULALONGKORN UNIVERSITY

Mass Spectrum List Report

Analysis Info

Analysis Name OSHTT26032019003_1.d
 Method Tune_low_Neg_PIN012018.m
 Sample Name Dvir 36
 Dvir 36

Acquisition Date 3/26/2019 2:58:29 PM
 Operator Administrator
 Instrument micrOTOF 72

Acquisition Parameter

Source Type ESI
 Scan Range n/a
 Scan Begin 50 m/z
 Scan End 3000 m/z
 Ion Polarity Negative
 Capillary Exit -90.0 V
 Hexapole RF 150.0 V
 Skimmer 1 -50.0 V
 Hexapole 1 -25.0 V

Set Corrector Fill 75 V
 Set Pulsar Pull 372 V
 Set Pulsar Push 372 V
 Set Reflector 1300 V
 Set Flight Tube 9000 V
 Set Detector TOF 2295 V

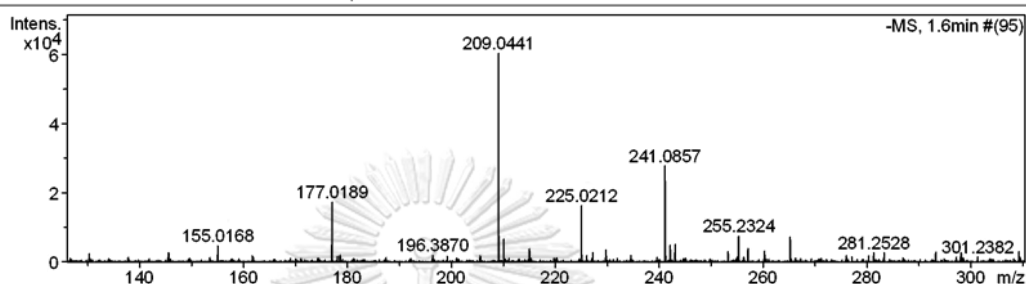


Figure 22 Mass spectrum of compound DC1

DC36 1H NMR 300 MHz in CDCl₃

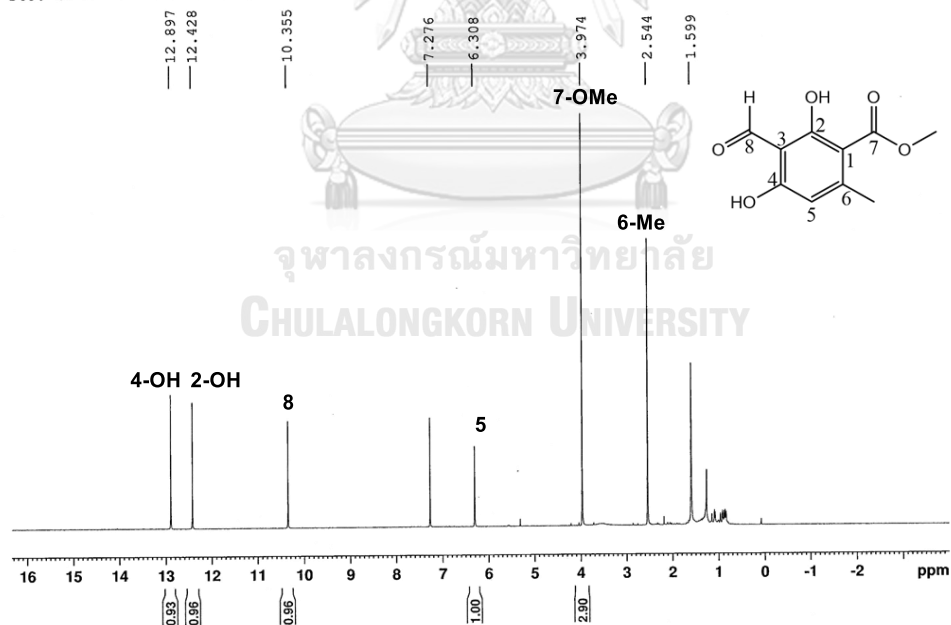


Figure 23 ¹H-NMR (500 MHz) spectrum of compound DC1 (CDCl₃)

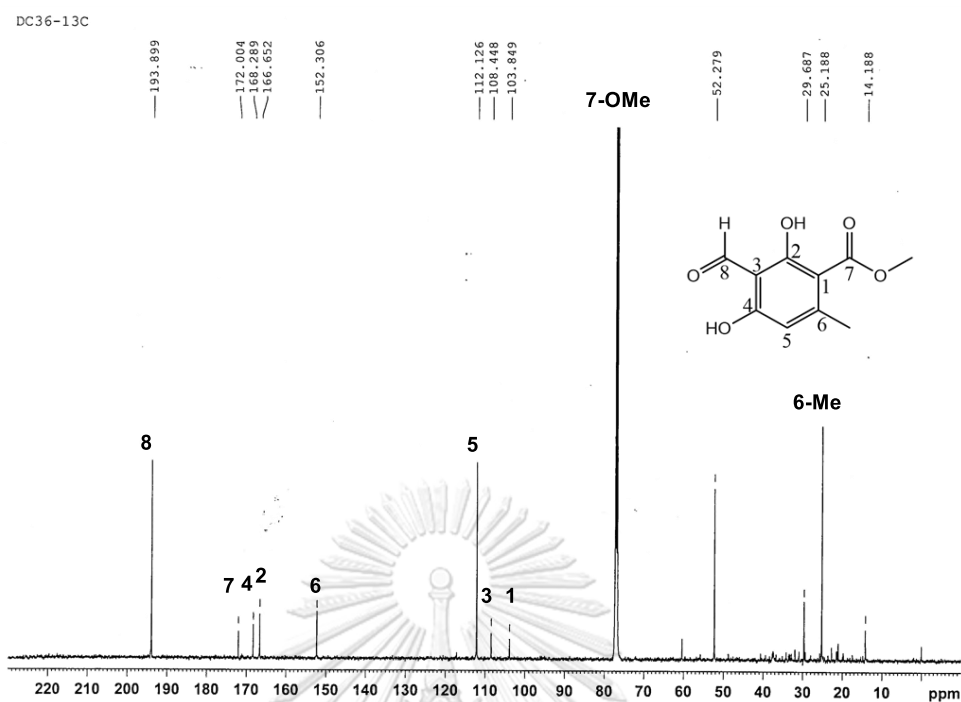


Figure 24 ^{13}C -NMR (125 MHz) spectrum of compound DC1 (CDCl_3)

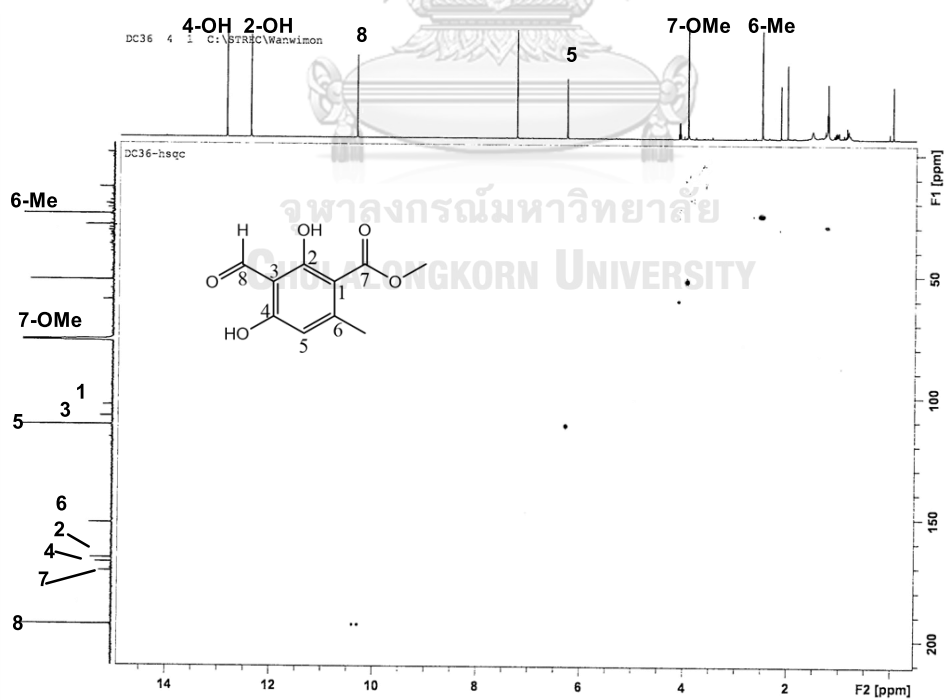


Figure 25 HSQC spectrum of compound DC1

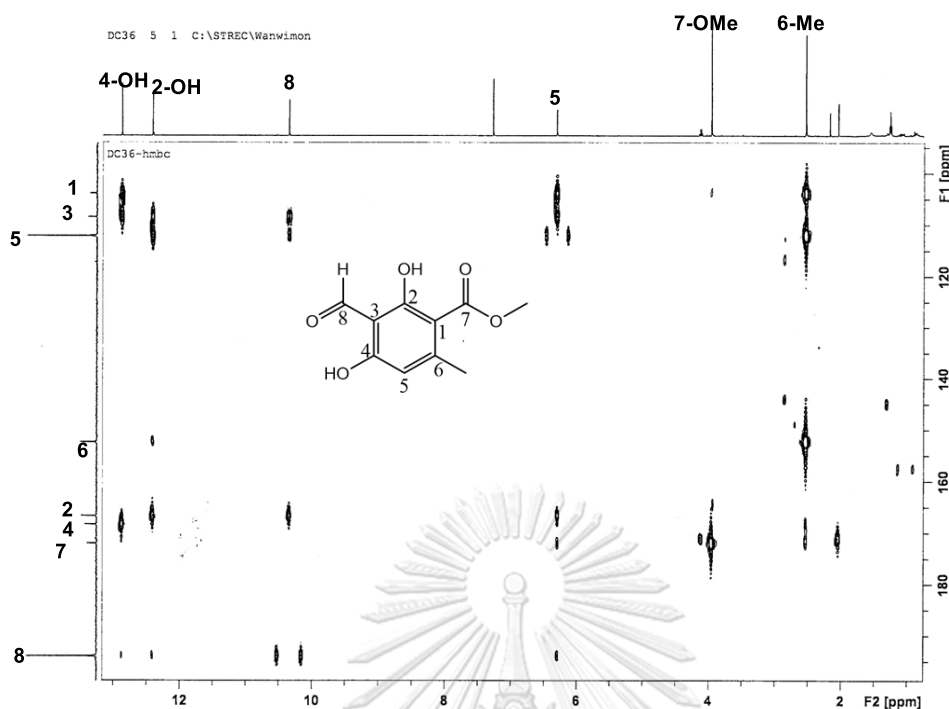


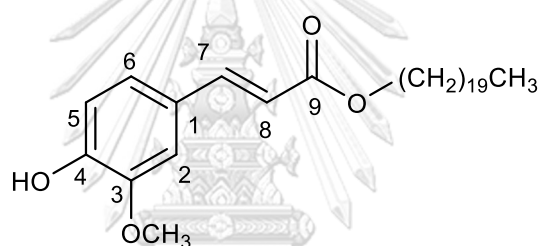
Figure 26 HMBC spectrum of compound DC1

2.2.2 Identification of compound DC2 (*n*-eicosyl *trans*-ferulate)

Compound DC2 was collected as a white powder. The high resolution ESI mass spectrum (Figure 27) showed a sodium adduct molecular ion $[M+Na]^+$ at m/z 497.3523 (calcd. for $C_{30}H_{50}O_4Na$ 497.3606), suggesting the molecular formula $C_{30}H_{50}O_4$. The 1H -NMR spectrum (Figure 28) indicated the presence of a feruloyl moiety, displaying two *trans* olefinic protons at δ 6.31 (1H, d, $J = 15.9$ Hz, H-8) and 7.62 (1H, d, $J = 15.6$ Hz, H-7), one methoxy group at δ 3.93 (3H, s, 3-OMe) and three aromatic protons at δ 6.93 (1H, d, $J = 8.1$ Hz, H-5), 7.05 (1H, s, H-2) and 7.08 (1H, d, $J = 8.1$ Hz, H-6). In the aliphatic region, eighteen pairs of methylene protons appeared as a complex multiplet at around δ 1.26, along with a pair of oxygen bearing methylene protons resonating at δ 4.20 (2H, t, $J = 6.6$ Hz, OCH_2). In addition, a triplet (3H, t, $J = 7.2$ Hz) at δ 0.89 in the 1H -NMR spectrum indicated presence of a terminal methyl

group. The ^{13}C -NMR and DEPT spectra (**Figure 29**) showed signals in support of the aliphatic methylene chain from δ 22.7 to δ 31.9 and the feruloyl moiety from δ 109.3 to δ 167.4 (**Table 11**). The location of the methoxy group at C-3 was deduced from the cross peak between H-2 (δ 7.05) and 3-OMe protons (δ 3.93) in the NOESY spectrum (**Figure 30**). Complete ^{13}C NMR assignments were obtained by analysis of HSQC and HMBC spectra (**Figure 31** and **32**). The NMR data of compound DC2 agreed with those of *n*-eicosyl *trans*-ferulate [**343**] in an earlier report (Baldé *et al.*, 1991).

Compound [**343**] has been earlier identified from several *Dendrobium* species, for example, *D. clavatum* var. *aurantiacum* (Chang *et al.*, 2001) and *D. brymerianum* (Klongkumnuankarn *et al.*, 2015).

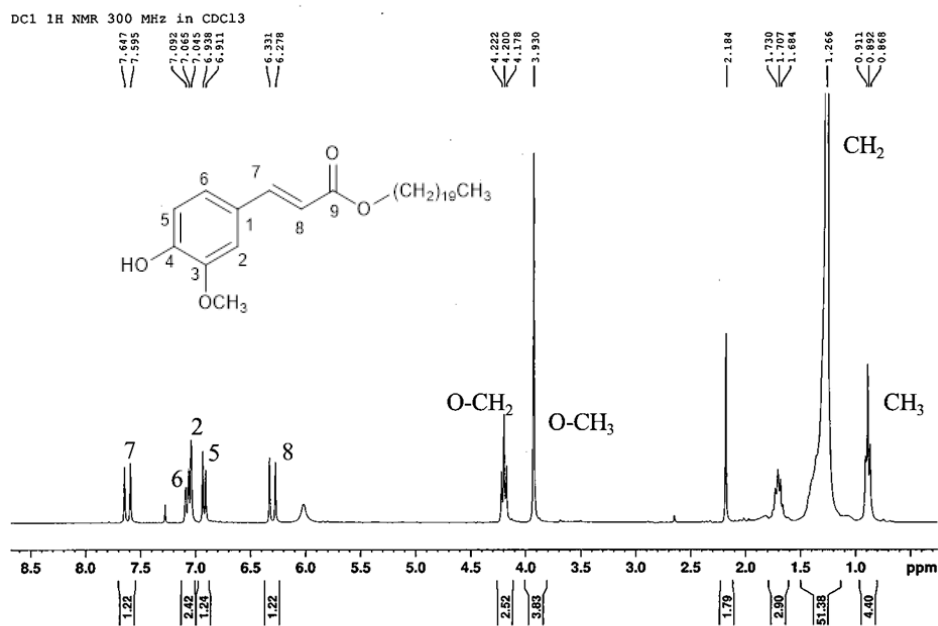
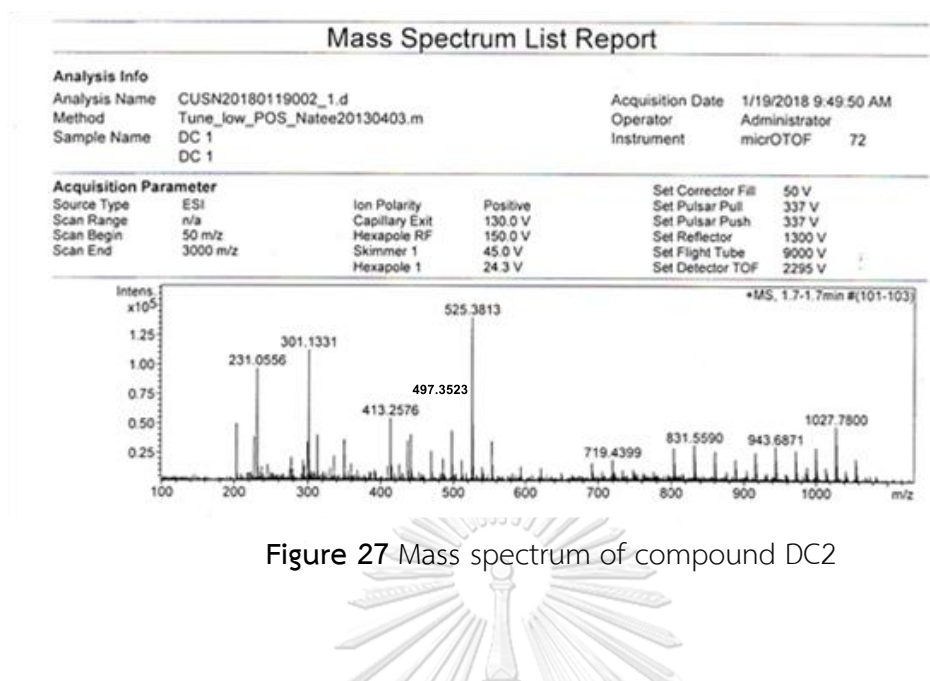


n-eicosyl *trans*-ferulate [**343**]

Table 11 NMR spectral data of compound DC2 as compared with *n*-eicosyl *trans*-ferulate

Position	Compound DC2 (acetone- d_6)		<i>n</i> -eicosyl <i>trans</i> -ferulate (CDCl $_3$)*	
	δ_H (mult., <i>J</i> in Hz)	δ_C	δ_H (mult., <i>J</i> in Hz)	δ_C
1	-	127.0	-	127.1
2	7.05 (1H, s)	109.3	7.03 (1H, d, 2)	109.3
3	-	146.8	-	147.8
4	-	147.9	-	146.7
5	6.93 (1H, d, 8.1)	114.7	6.91 (1H, d, 8)	114.6
6	7.08 (1H, d, 8.1)	123.0	7.07 (1H, d, 8)	122.9
7	7.62 (1H, d, 15.6)	144.7	7.61 (1H, d, 16)	144.6
8	6.31 (1H, d, 15.9)	115.6	6.29 (1H, d, 16)	115.6
9	-	167.4	-	167.3
3-OMe	3.93 (3H, s)	56.0	3.92(3H, s)	55.9
OCH $_2$	4.20 (2H, t, 6.6)	64.6	4.18 (2H, t)	64.6
(CH $_2$) $_{18}$	1.26 (m)	22.7-31.9	1.25 (m)	22.7-31.9
Me	0.89 (3H, t, 7.2)	14.1	0.86 (3H, t)	14.1

* (Baldé *et al.*, 1991)



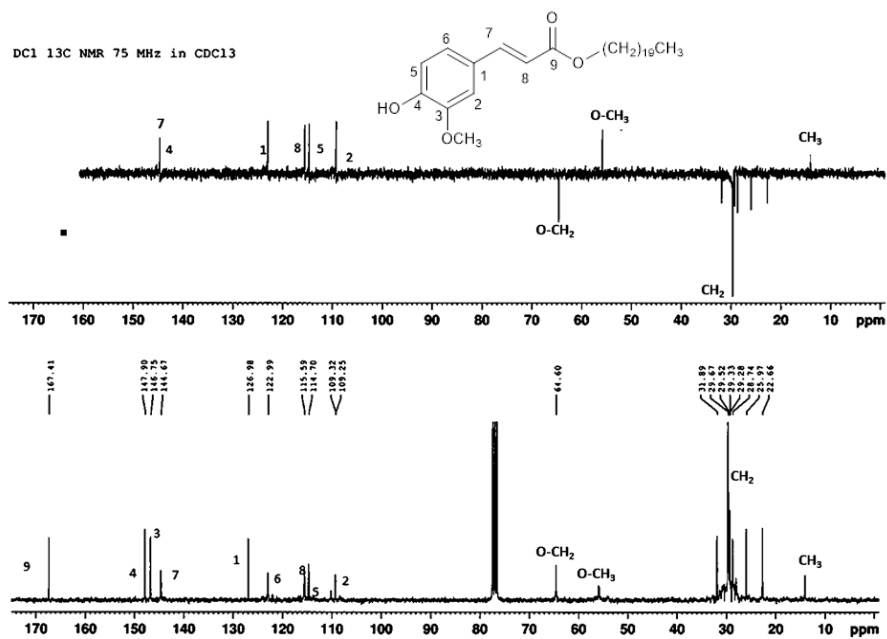


Figure 29 ^{13}C NMR (75 MHz) and DEPT-135 spectra of compound DC2 (CDCl_3)

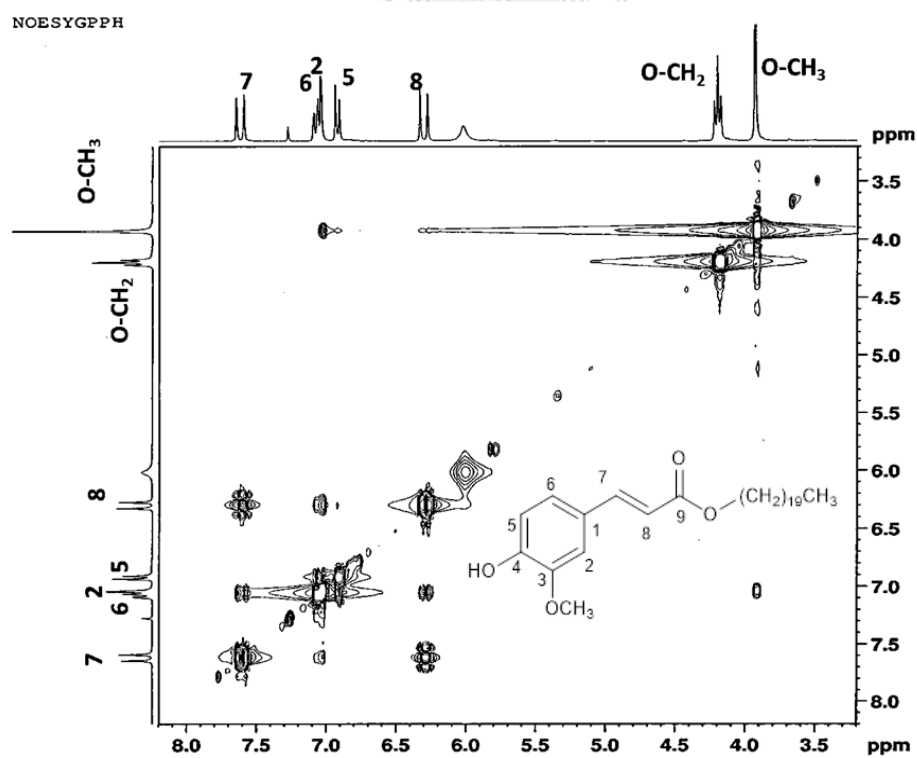


Figure 30 NOESY spectrum of compound DC2

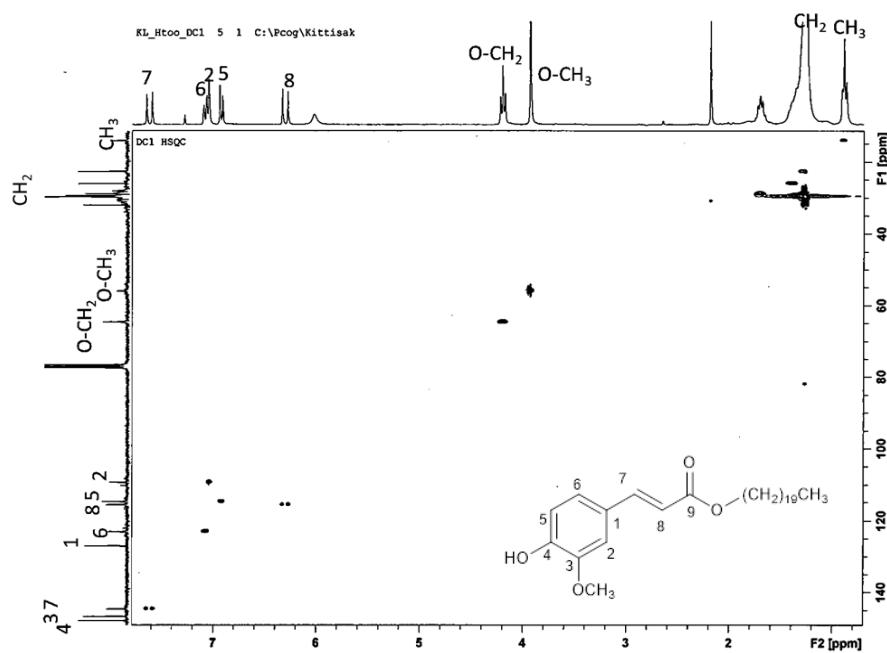


Figure 31 HSQC spectrum of compound DC2

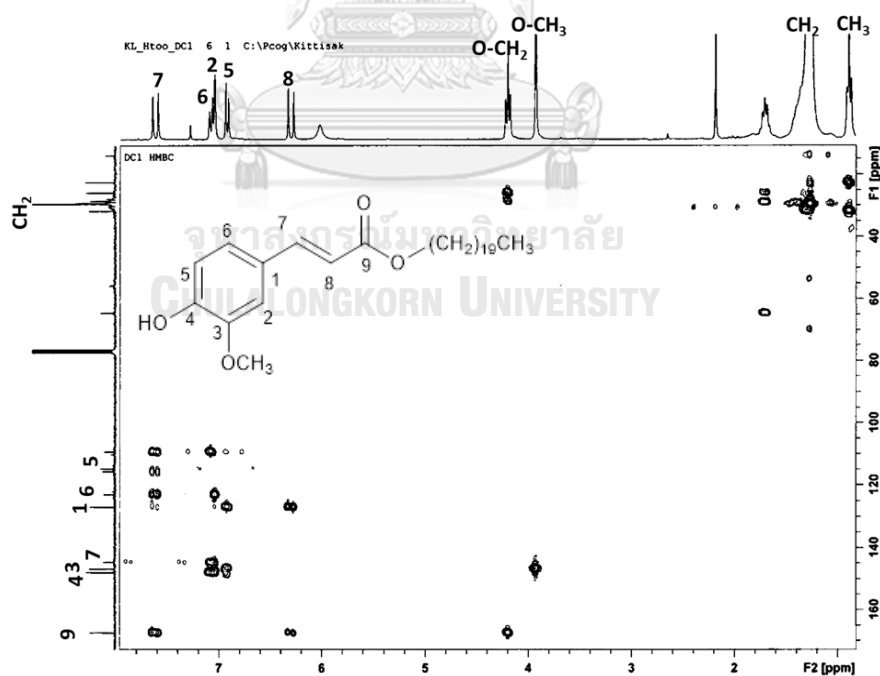
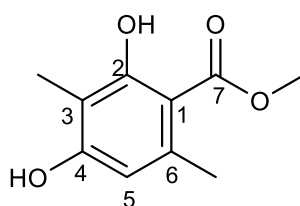


Figure 32 HMBC spectrum of compound DC2

2.2.3 Identification of compound DC3 (atraric acid)

The high resolution APCI mass spectrum of compound DC3 (**Figure 33**) showed a protonated molecular ion $[M+H]^+$ at m/z 197.0838 (calcd. for $C_{10}H_{13}O_4$ 197.0813), suggesting the molecular formula $C_{10}H_{12}O_4$. The 1H -NMR spectrum (**Figure 34**) exhibited an aromatic singlet signal at δ 6.32 (1H, s, H-5) suggesting a benzene ring with penta-substitution, which was supported by the signals for five quaternary carbons at δ 104.9 (C-1), 109.5 (C-3), 140.5 (C-6), 160.9 (C-4) and 164.1 (C-2) in the ^{13}C NMR spectrum (**Figure 35**) and a correlation peak for a methine carbon at δ 111.5 (C-5) in the HSQC spectrum (**Figure 36**). The methyl protons at δ 2.02 (3H, s, 3-Me) and 2.41 (3H, s, 6-Me) displayed HSQC correlations with the carbons at δ 8.0 (3-Me) and δ 24.2 (6-Me), respectively (**Figure 36**). The positions of these two methyl groups were deduced from the cross peak between the proton at δ 6.32 (1H, s, H-5) and the methyl protons at 2.41 (3H, s, 6-Me) in the NOESY spectrum (**Figure 37**). This was corroborated by the HMBC correlations from the 3-Me protons to the two oxygenated carbons at δ 160.9 (C-4) and 164.1 (C-2) (**Figure 38**). The placement of the carbomethoxy group [δ 173.5 (C-7) and 52.1 (7-OMe)] at C-1 was confirmed by the 3-bond coupling between 6-Me protons and C-1 in the HMBC spectrum (**Figure 38**).

On the basis of the 1H and ^{13}C NMR data (**Table 12**), compound DC3 was identified as atraric acid [**344**] (Wang *et al.*, 2005). Atraric acid has been reported in epiphytic lichens (Bourgeois *et al.*, 1999) and the stem bark of *Pygeum africanum* (Schleich *et al.*, 2006).



atraric acid [**344**]

Table 12 NMR spectral data of compound DC3 as compared with atraric acid

Position	Compound DC3 (acetone- d_6)		Atraric acid (CDCl ₃)*	
	δ_H (mult., J in Hz)	δ_C	δ_H (mult., J in Hz)	δ_C
1	-	104.9	-	105.3
2	-	164.1	-	163.1
3	-	109.5	-	110.5
4	-	160.9	-	158.0
5	6.32 (1H, s)	111.5	6.22 (1H, s)	108.5
6	-	140.5	-	140.1
7	-	173.5	-	172.6
3-Me	2.02 (3H, s)	8.0	2.12 (3H, s)	7.6
6-Me	2.41 (3H, s)	24.2	2.47 (3H, s)	24.0
2-OH	12.0 (1H, s)	-	12.03 (1H, s)	-
4-OH	9.0 (1H, s)	-	5.17 (1H, s)	-
7-OMe	3.91 (3H, s)	52.1	3.94 (3H, s)	51.8

* (Wang *et al.*, 2005)

Display Report

Analysis Info

Analysis Name D:\Data\Yp sample\DC35-5.d
Method tune_low_pos_infusion_20131014.m
Sample Name DC35-5
Comment

Acquisition Date 2/20/2019 3:43:27 PM

Operator CTB
Instrument micrOTOF-Q II 10414

Acquisition Parameter

Source Type	APCI	Ion Polarity	Positive	Set Nebulizer	1.6 Bar
Focus	Not active	Set Capillary	4500 V	Set Dry Heater	200 °C
Scan Begin	50 m/z	Set End Plate Offset	-500 V	Set Dry Gas	8.0 l/min
Scan End	1500 m/z	Set Collision Cell RF	150.0 Vpp	Set Divert Valve	Waste

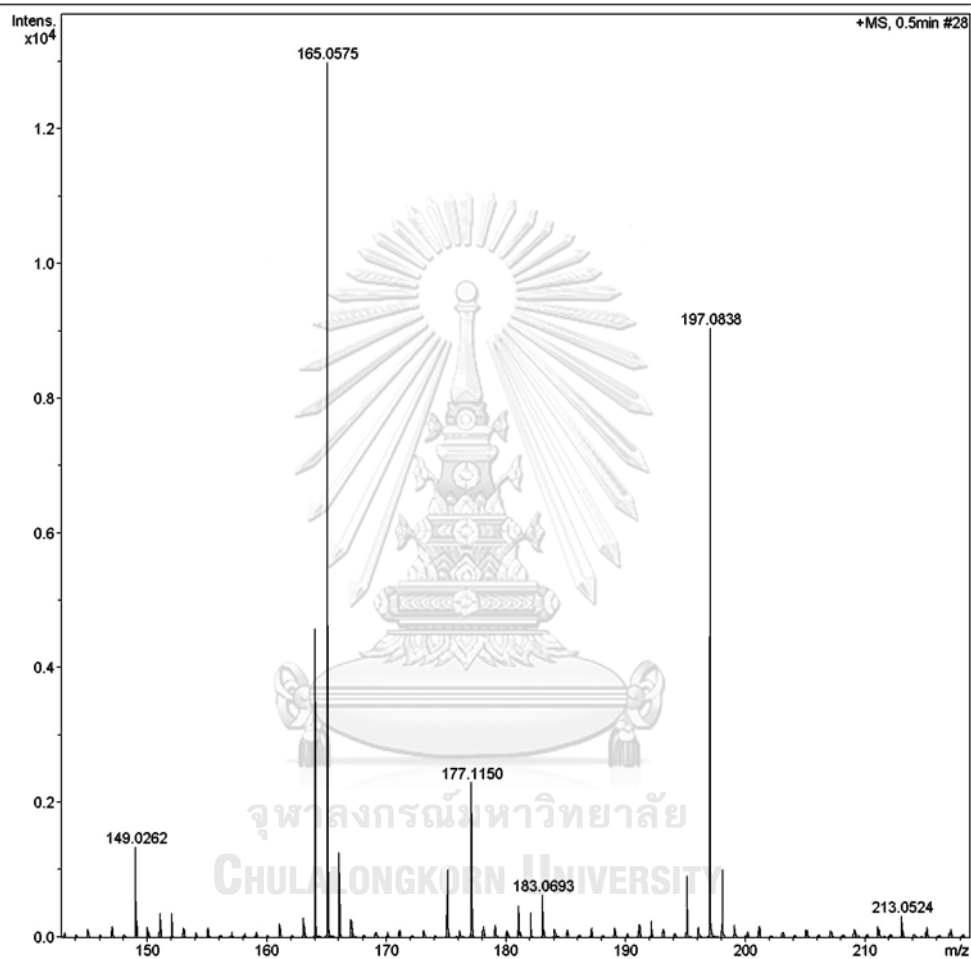


Figure 33 Mass spectrum of compound DC3

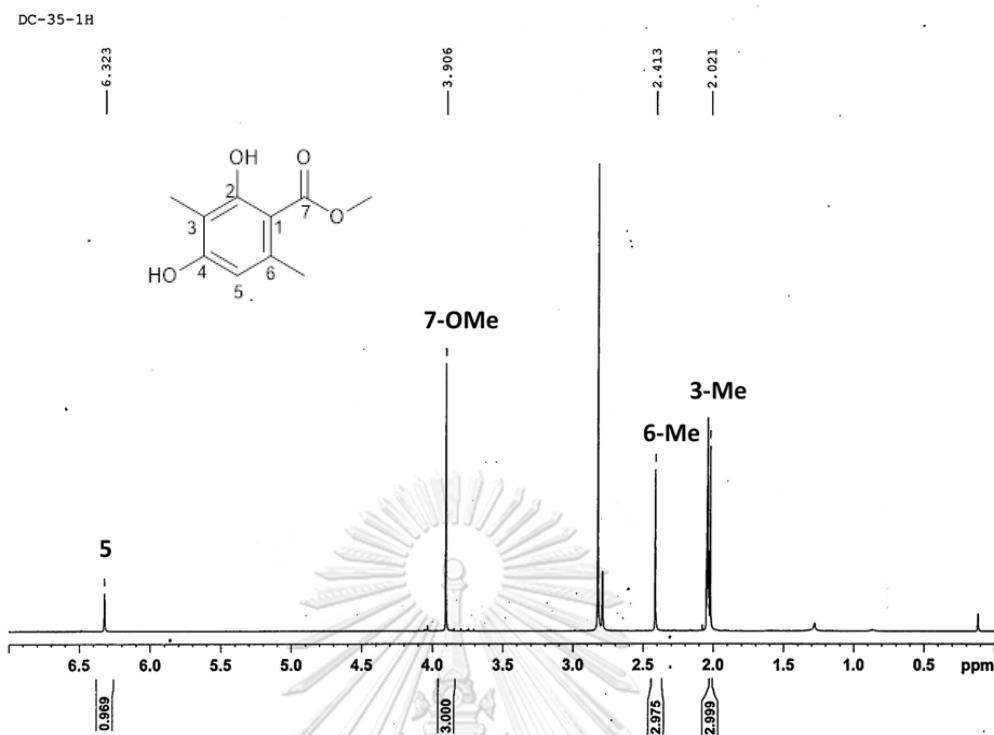


Figure 34 $^1\text{H-NMR}$ (300 MHz) spectrum of compound DC3 (acetone- d_6)

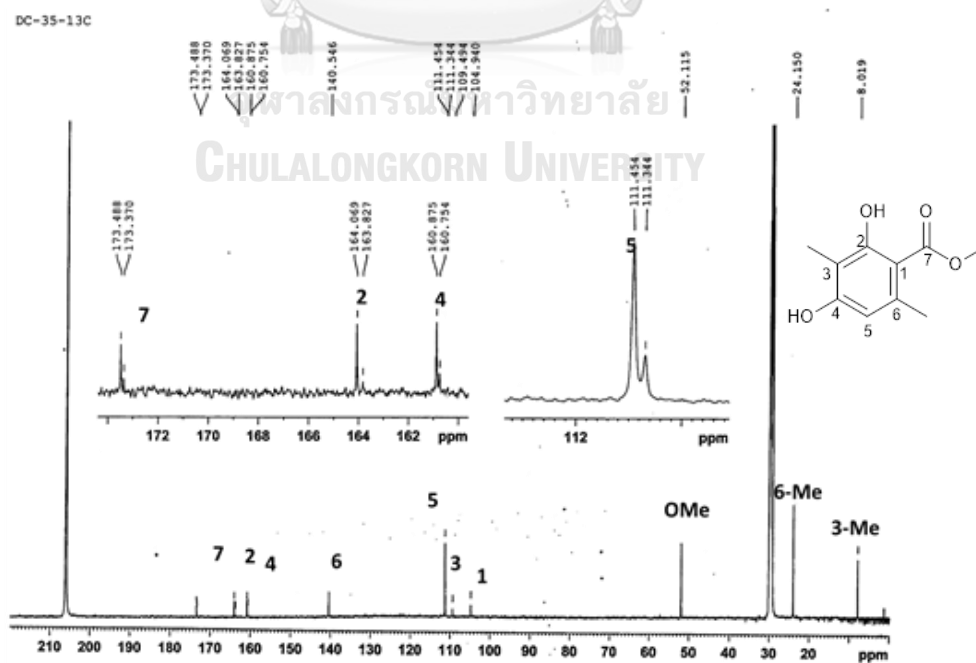


Figure 35 $^{13}\text{C-NMR}$ (75 MHz) spectrum of compound DC3 (acetone- d_6)

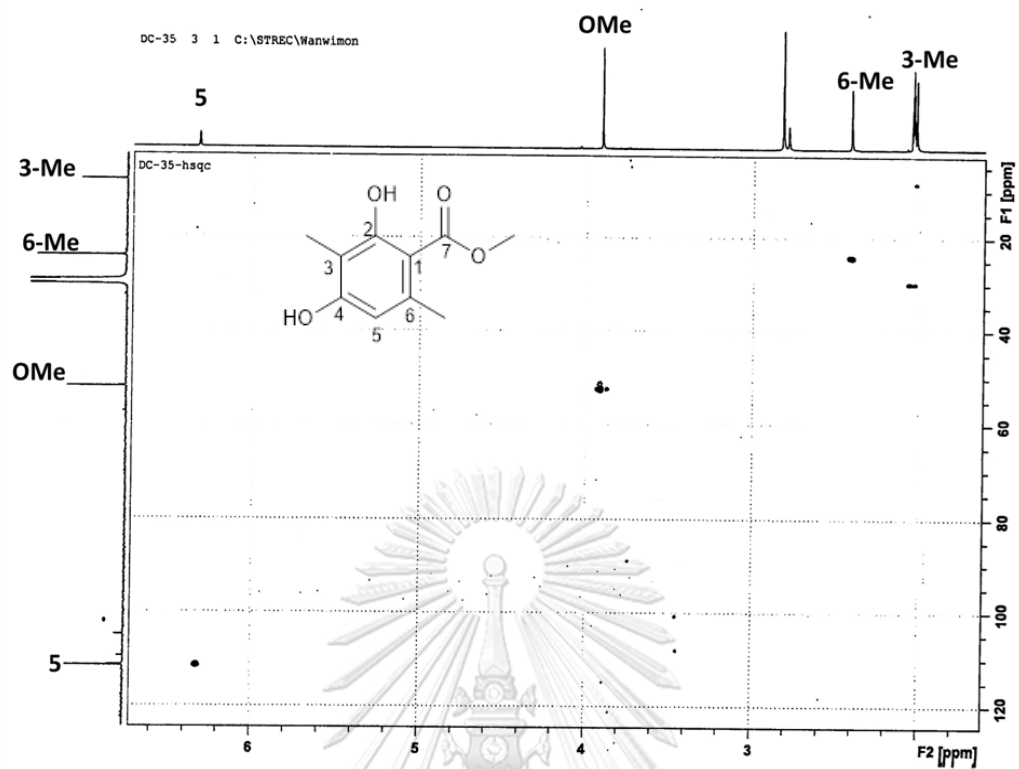


Figure 36 HSQC spectrum of compound DC3

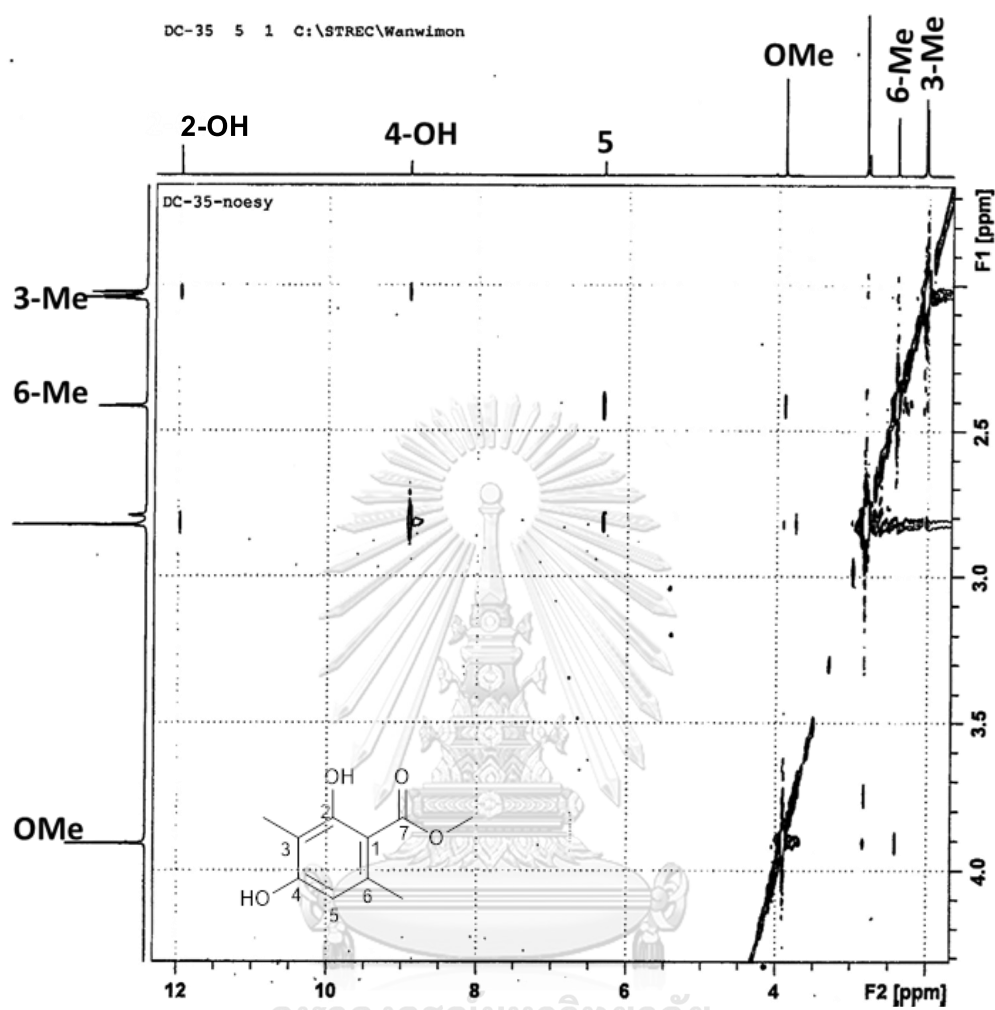


Figure 37 NOESY spectrum of compound DC3

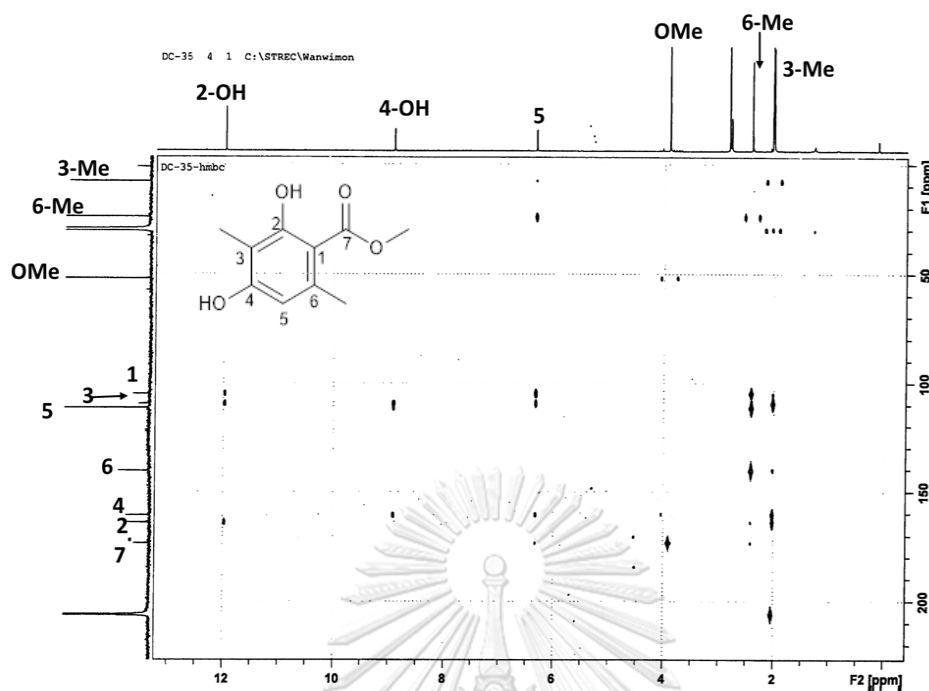
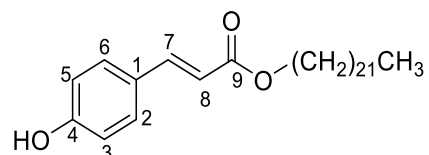


Figure 38 HMBC spectrum of compound DC3

2.2.4 Identification of compound DC4 (*n*-docosyl 4-hydroxy-*trans*-cinnamate)

Compound DC4 showed a protonated molecular ion $[M+H]^+$ at m/z 473.4060 (calcd. for $C_{31}H_{53}O_3$ 473.3994) in the high resolution APCI mass spectrum (Figure 39), suggesting the molecular formula $C_{31}H_{52}O_3$. The 1H -NMR data of DC4 were similar to those of compound DC2 [39] except the absence of the methoxy group in DC4. The 1H -NMR spectrum of compound DC4 (Figure 40) suggested a cinnamoyl structure, displaying signals for *trans* olefinic protons at δ 6.33 (1H, d, $J = 16.2$ Hz, H-8) and 7.59 (1H, d, $J = 16.2$ Hz, H-7)] and a *p*-substituted aromatic ring [δ 6.88 (2H, d, $J = 8.4$ Hz, H-3, H-5) and 7.54 (2H, d, $J = 8.4$ Hz, H-2, H-6)]. This cinnamoyl moiety was esterified with a long chain aliphatic alcohol, as evident from the resonances of the downfield methylene protons at δ 4.13 (2H, t, $J = 6.6$ Hz, OCH_2), twenty pairs of methylene

protons at δ 1.20 – 1.40 (40H, complex multiplets) and terminal methyl protons at δ 0.86 (3H, t, $J = 6.6$ Hz). Results from comparison of the ^1H NMR and MS data of compound DC4 with literature values (**Table 13**) (Chowdhury *et al.*, 2013) indicated that compound DC4 was *n*-docosyl 4-hydroxy-*trans*- cinnamate [345].



n-docosyl 4-hydroxy-*trans*- cinnamate [345]



Table 13 NMR spectral data of compound DC4 as compared with *n*-docosyl 4-hydroxy-*trans*-cinnamate

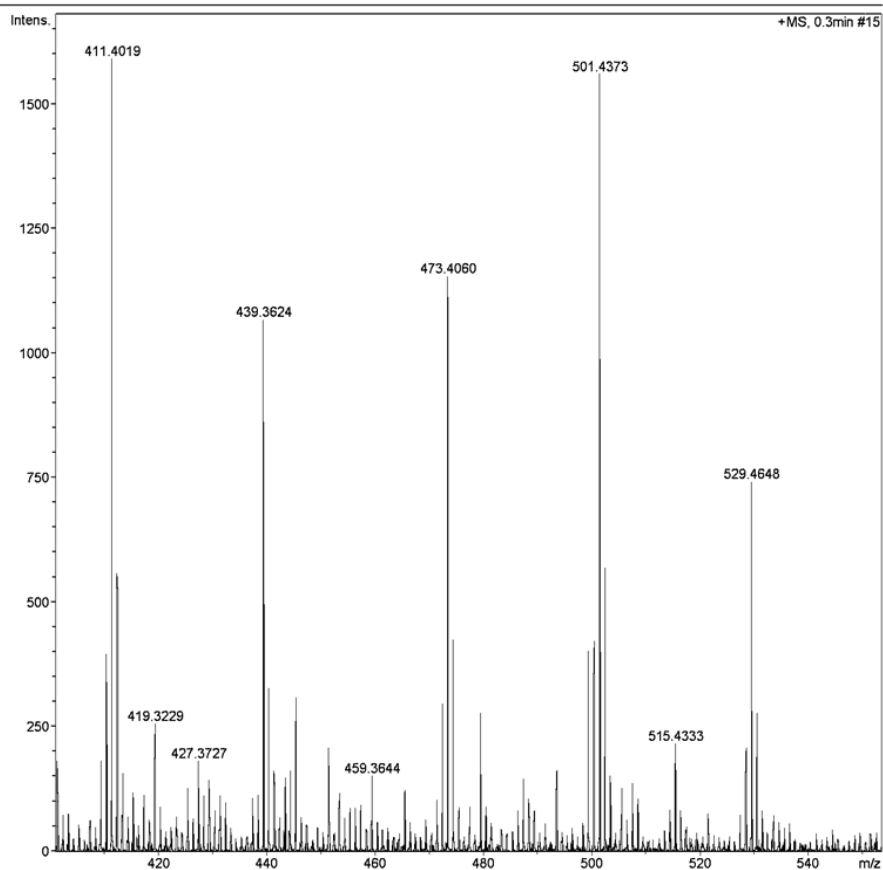
Position	Compound DC4 (acetone- <i>d</i> ₆)	<i>n</i> -docosyl 4-hydroxy- <i>trans</i> -cinnamate (CDCl ₃)*
	δ_{H} (mult., <i>J</i> in Hz)	δ_{H} (mult., <i>J</i> in Hz)
1	-	-
2	7.54 (1H, d, 8.4)	7.41(1H, d, 8.4)
3	6.88 (1H, d, 8.4)	6.83 (1H, d, 8.4)
4	-	-
5	6.88 (1H, d, 8.4)	6.83 (1H, d, 8.4)
6	7.54 (1H, d, 8.4)	7.41(1H, d, 8.4)
7	7.59 (1H, d, 16.2)	7.61 (1H, d, 16)
8	6.33 (1H, d, 16.2)	6.28 (1H, d, 16)
9	-	-
CH ₂ O-	4.13 (2H, t, 6.9)	-
(CH ₂) ₂₀	1.20-1.40 (40H, multiplets)	-
Me	0.86 (3H, s, 6.6)	-

* (Chowdhury *et al.*, 2013)

Display Report

Analysis Info		Acquisition Date	2/20/2019 3:19:25 PM
Analysis Name	D:\Data\Yp sample\DC3.d	Operator	CTB
Method	tune_low_pos_infusion_20131014.m	Instrument	micrOTOF-Q II 10414
Sample Name	DC3		
Comment			

Acquisition Parameter					
Source Type	APCI	Ion Polarity	Positive	Set Nebulizer	1.6 Bar
Focus	Not active	Set Capillary	4500 V	Set Dry Heater	200 °C
Scan Begin	50 m/z	Set End Plate Offset	-500 V	Set Dry Gas	6.0 l/min
Scan End	1500 m/z	Set Collision Cell RF	150.0 Vpp	Set Divert Valve	Waste



Bruker Compass DataAnalysis 4.0

printed: 2/20/2019 4:50:19 PM

Page 1 of 1

Figure 39 Mass spectrum of compound DC4

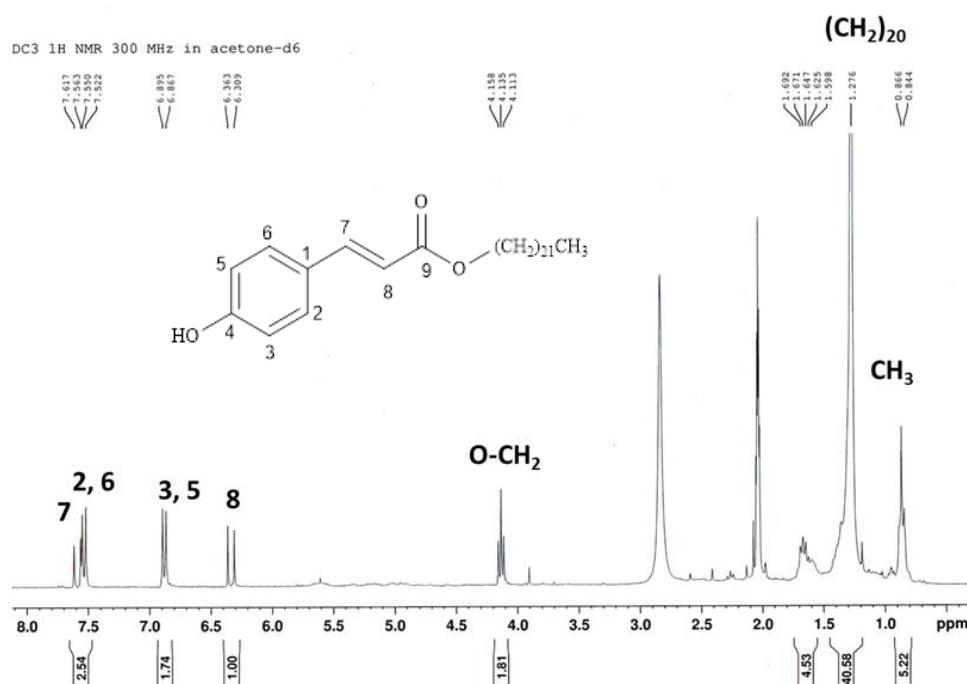


Figure 40 $^1\text{H-NMR}$ (300 MHz) spectrum of compound DC4 (acetone- d_6)

2.2.5 Identification of compound DC5 (vanillin)

The high resolution APCI mass spectrum of compound DC5 (Figure 41) showed a deprotonated molecular ion $[\text{M-H}]^-$ at m/z 151.0394 (calcd. for $\text{C}_8\text{H}_7\text{O}_3$ 151.0395), suggesting the molecular formula $\text{C}_8\text{H}_8\text{O}_3$. The $^{13}\text{C-NMR}$ and DEPT spectra (Figure 42) displayed peaks for aromatic carbons comprising three quaternaries [δ 129.8 (C-1), 148.1 (C-3) and 152.7 (C-4)] and three methines [δ 110.0 (C-2), 115.1 (C-5) and 126.1 (C-6)]. A methoxy group (δ 55.4, 3-OMe) and an aldehyde [δ 190.2 (C-7)] functionality were also present. The $^1\text{H-NMR}$ spectrum (Figure 43) showed a singlet proton signal at δ 9.81 (H-7) which was correlated to the carbon at δ 190.2 (C-7) in the HSQC spectrum (Figure 44). In the HMBC spectrum (Figure 45), H-7 showed 3-bond coupling with C-2 and C-6. The H-6 proton exhibited 3-bond connectivity with a hydroxylated carbon at δ 152.7 (C-4) whereas the methoxyl protons at δ 3.92

displayed 3-bond coupling with C-3 (δ 148.1). The aforementioned NMR data suggested that compound DC5 was vanillin [275]. **Table 14** shows that the ^1H and ^{13}C NMR data of **275** agreed with previously reported values (Ito *et al.*, 2001). Vanillin [275] has been reported as a common constituent in *Dendrobium* species, for example, *D. williamsonii* (Yang *et al.*, 2018).

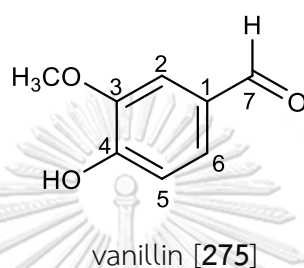


Table 14 NMR spectral data of compound DC5 as compared with vanillin

Position	Compound DC5 (acetone- d_6)		Vanillin (CDCl $_3$)*	
	δ_{H} (mult., J in Hz)	δ_{C}	δ_{H} (mult., J in Hz)	δ_{C}
1	-	129.8	-	129.9
2	7.44 (1H, d, 1.8)	110.0	7.40 (1H, d, 1.6)	108.7
3	-	148.1	-	147.1
4	-	152.7	-	151.6
5	7.00 (1H, d, 7.8)	115.1	7.02 (1H, d, 8.5)	114.4
6	7.46 (1H, dd, 7.8, 1.8)	126.1	7.41 (1H, dd, 8.5, 1.6)	127.5
3-OMe	3.92 (3H, s)	55.4	3.95 (3H, s)	56.1
CHO	9.81 (1H, s)	190.2	9.64 (1H, s)	190.9

* (Ito *et al.*, 2001)

Display Report

Analysis Info
Analysis Name D:\Data\Yp sample\Aj.Taweesak JDC39.d Acquisition Date 2/20/2019 4:09:26 PM
Method tune_low_pos_infusion_20131014.m Operator CTB
Sample Name DC39 Instrument micrOTOF-Q II 10414
Comment

Acquisition Parameter

Source Type	APCI	Ion Polarity	Positive	Set Nebulizer	1.6 Bar
Focus	Not active	Set Capillary	4500 V	Set Dry Heater	200 °C
Scan Begin	50 m/z	Set End Plate Offset	-500 V	Set Dry Gas	8.0 l/min
Scan End	1500 m/z	Set Collision Cell RF	150.0 Vpp	Set Divert Valve	Waste

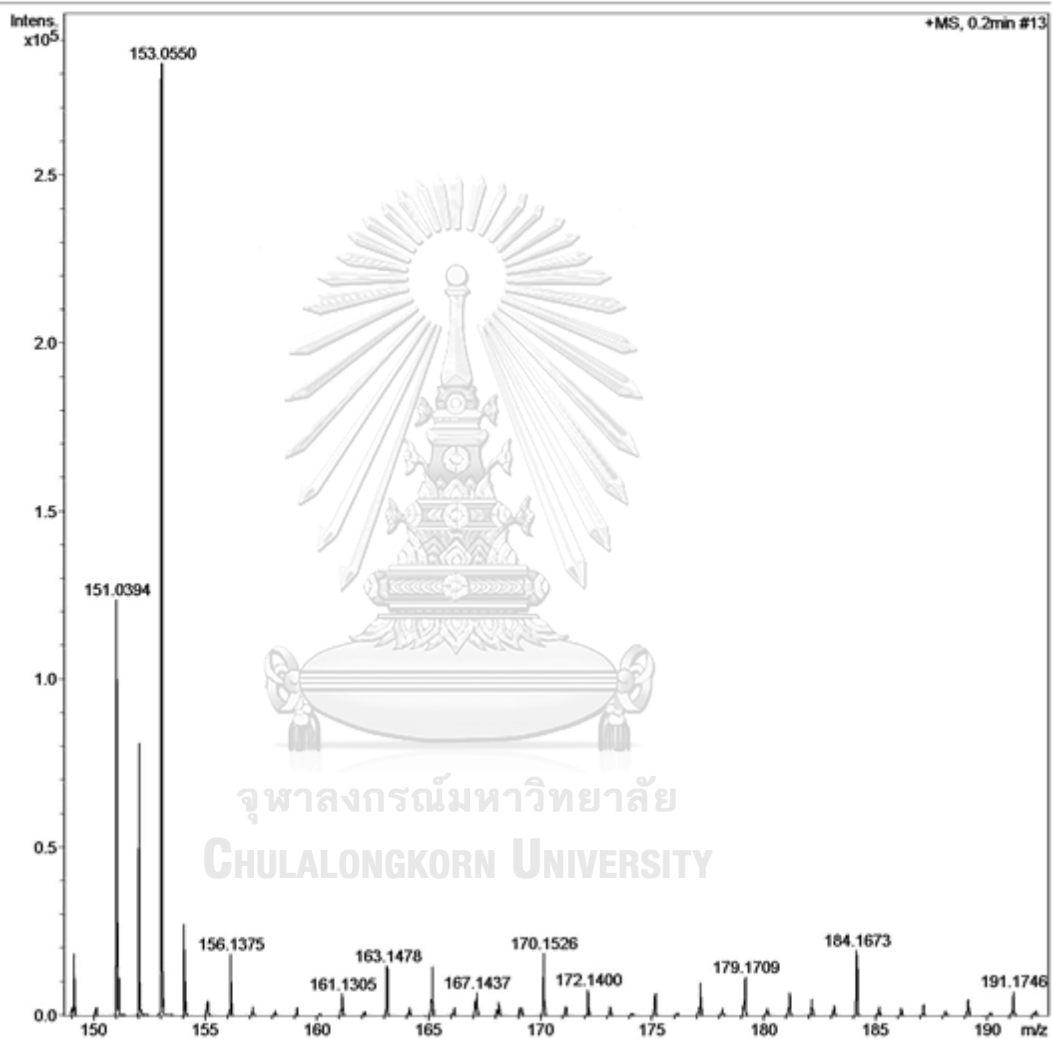
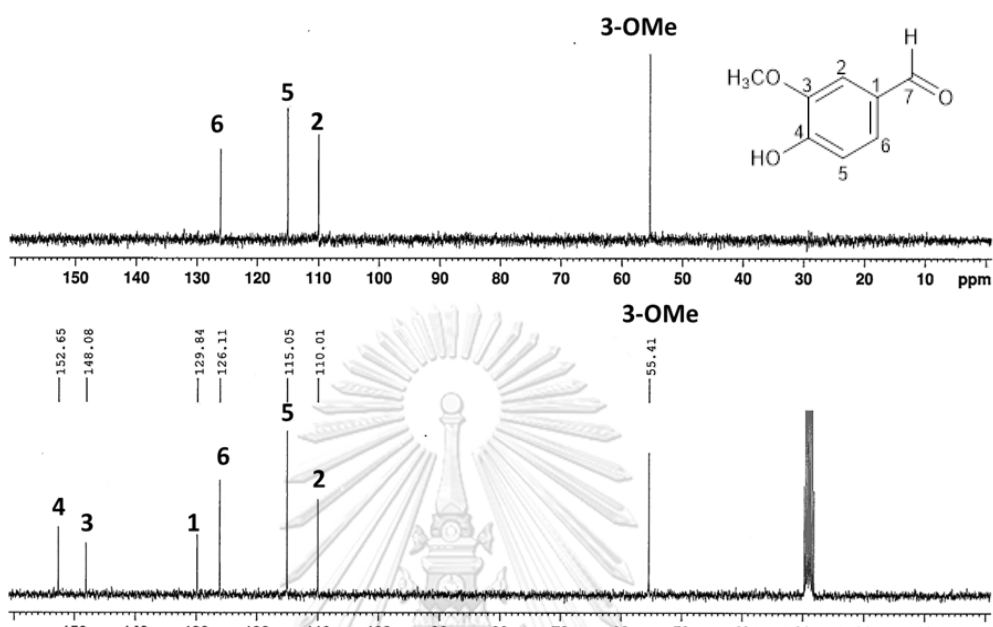
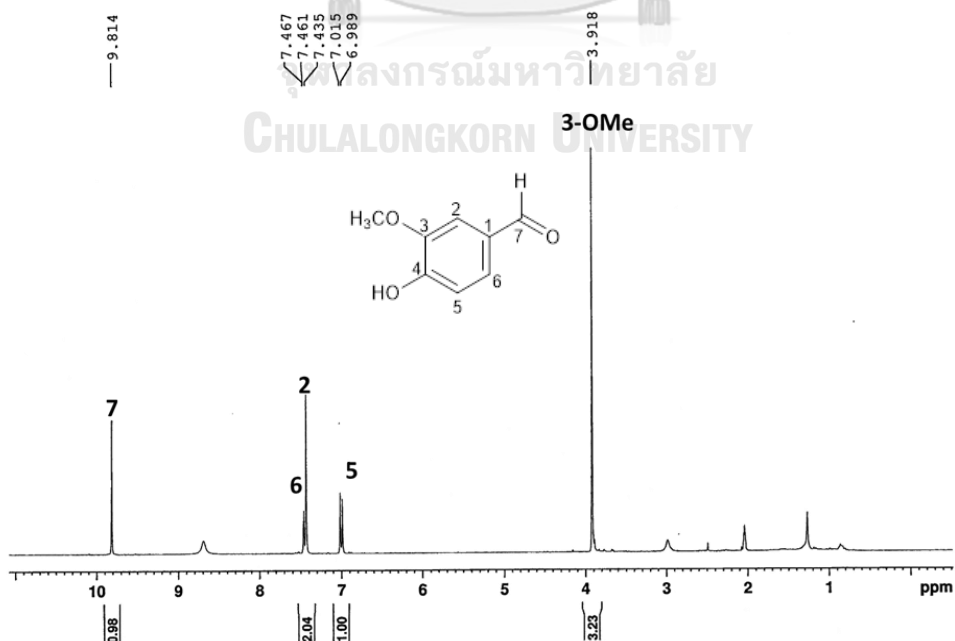


Figure 41 Mass spectrum of compound DC5

DC 39 ^{13}C NMR 75 MHz in acetone- d_6 Figure 42 ^{13}C -NMR (75 MHz) spectrum of compound DC5 (acetone- d_6)DC39 ^1H NMR 300 MHz in acetone- d_6 Figure 43 ^1H -NMR (300 MHz) spectrum of compound DC5 (acetone- d_6)

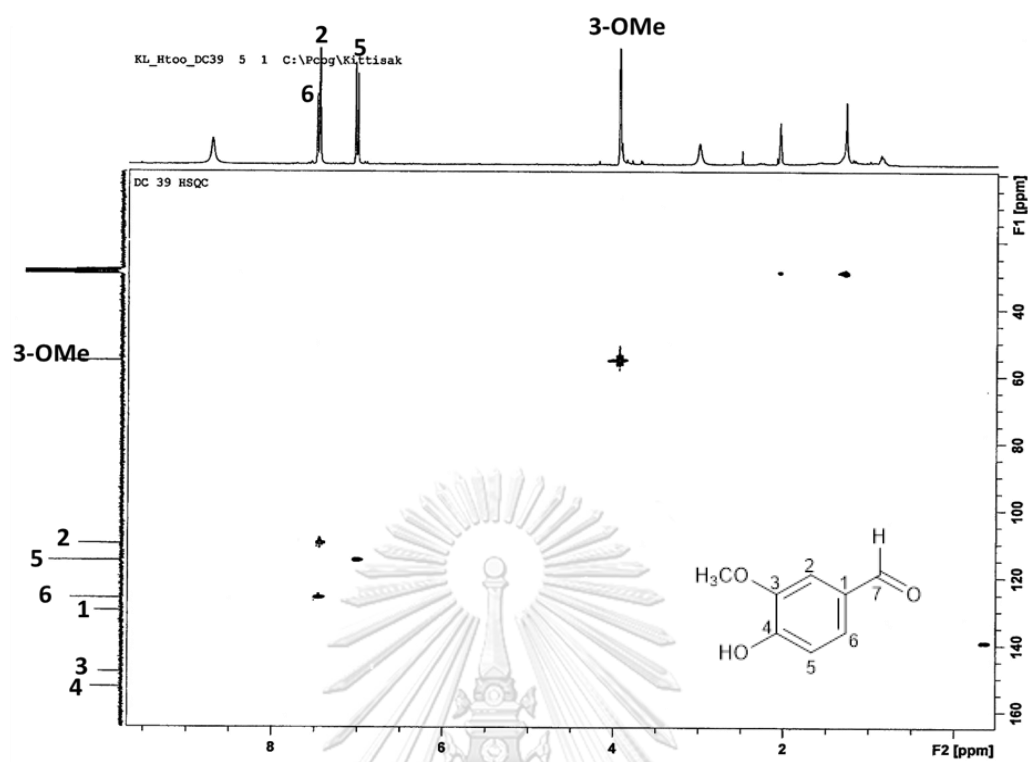


Figure 44 HSQC spectrum of compound DC5

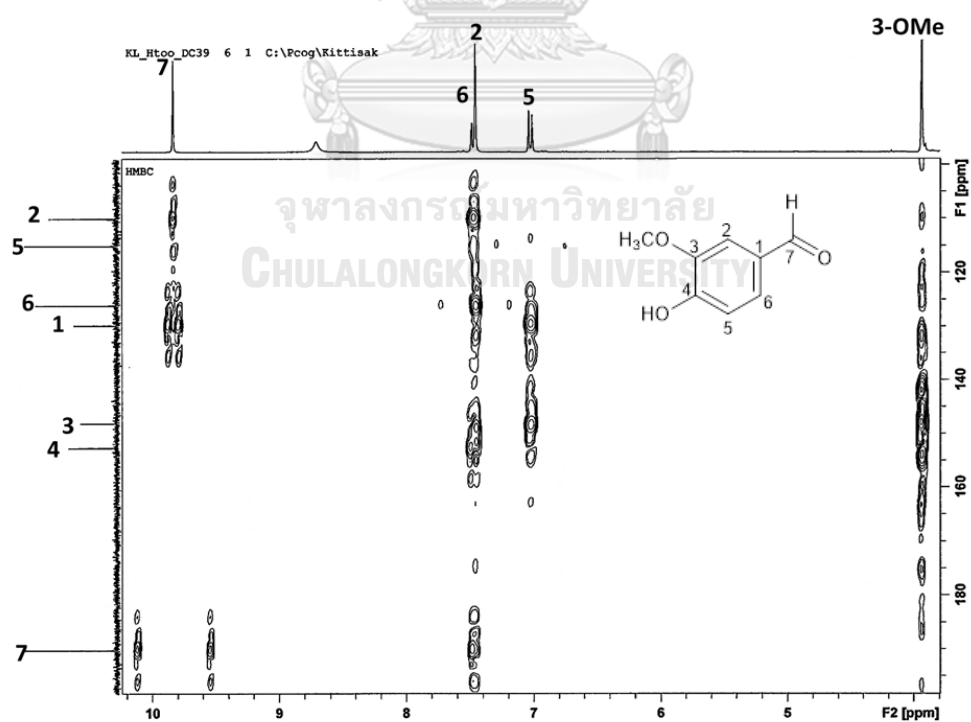


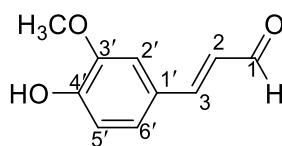
Figure 45 HMBC spectrum of compound DC5

2.2.6 Identification of compound DC6 (coniferyl aldehyde)

The high resolution ESI mass spectrum of compound DC6 (**Figure 46**) showed a sodium-adduct molecular ion $[M+Na]^+$ at m/z 201.0547 (calcd. for $C_{10}H_{10}O_3Na$ 201.0527), suggesting the molecular formula $C_{10}H_{10}O_3$.

The 1H -NMR spectrum (**Figure 47**) exhibited three aromatic protons at δ 7.36 (1H, d, $J = 1.8$ Hz, H-2'), 6.89 (1H, d, $J = 8.1$ Hz, H-5') and 7.19 (1H, dd, $J = 8.1, 1.8$ Hz, H-6'), together with methoxyl protons at δ 3.91 (3H, s). Two *trans* olefinic protons were also present, appearing at δ 7.57 (1H, d, $J = 15.9$ Hz, H-3) and 6.64 (1H, dd, $J = 15.6, 7.8$ Hz, H-2). The latter proton showed vicinal coupling with an aldehyde proton at δ 9.61 (1H, d, $J = 7.8$ Hz) in the COSY spectrum (**Figure 48**). The ^{13}C -NMR spectrum (**Figure 49**) showed signals for six aromatic carbons at δ 127.3 (C-1'), 111.6 (C-2'), 148.9 (C-3'), 151.0 (C-4'), 116.2 (C-5') and 124.7 (C-6'), two olefinic carbons at δ 126.9 (C-2) and 154.2 (C-3), an aldehyde carbonyl carbon (δ 194.0), and a methoxy group (δ 56.3) (**Table 15**). The HSQC spectrum (**Figure 50**) showed a cross peak at δ_H 9.61 / δ_C 194.0 confirming the aldehyde functionality and moreover, provided NMR assignments for protonated carbons. The HMBC correlations (**Figure 51**) from H-3 to C-2' and C-3', and from H-6' to C-3' and C-4' supported 1,3,4 substitution of the aromatic ring and the position of the methoxy group.

On the basis of the above 1H and ^{13}C NMR data and through comparison with literature values (Carpinella *et al.*, 2003), compound DC6 was identified as coniferyl aldehyde [**346**].



coniferyl aldehyde [**346**]

Table 15 NMR spectral data of compound DC6 as compared with coniferyl aldehyde

Position	Compound DC6 (acetone- d_6)		coniferyl aldehyde (CDCl ₃)*	
	δ_H (mult., J in Hz)	δ_C	δ_H (mult., J in Hz)	δ_C
1	9.61 (1H, d, 7.8)	194.0	9.65 (1H, d, 7.7)	193.5
2	6.64 (1H, dd, 15.6, 7.8)	126.9	6.59 (1H, q, 7.8)	126.4
3	7.57 (1H, d, 15.9)	154.2	7.35 (1H, t, 17.9)	153.0
1'	-	127.3	-	126.6
2'	7.36 (1H, d, 1.8)	111.6	7.07 (1H, d, 1.8)	109.4
3'	-	148.9	-	146.9
4'	-	151.0	-	148.9
5'	6.89 (1H, d, 8.1)	116.2	6.96 (1H, d, 8.6)	114.9
6'	7.19 (1H, dd, 8.1, 1.8)	124.7	7.12 (1H, dd, 8.1, 1.8)	124.0
3'-OMe	3.91 (3H, s)	56.3	3.94 (3H, s)	55.9

* (Carpinella *et al.*, 2003)

Mass Spectrum List Report

Analysis Info

Analysis Name OSCUPN201807122002.d
 Method Tune_low_90_04092017.m
 Sample Name DC-47

Acquisition Date 7/22/2018 2:53:45 PM
 Operator Administrator
 Instrument micrOTOF 72

Acquisition Parameter

Source Type ESI Ion Polarity Positive
 Scan Range n/a Capillary Exit 100.0 V
 Scan Begin 50 m/z Hexapole RF 90.0 V
 Scan End 3000 m/z Skimmer 1 70.0 V
 Hexapole 1 25.0 V

Set Corrector Fill 50 V
 Set Pulsar Pull 337 V
 Set Pulsar Push 337 V
 Set Reflector 1300 V
 Set Flight Tube 9000 V
 Set Detector TOF 2295 V

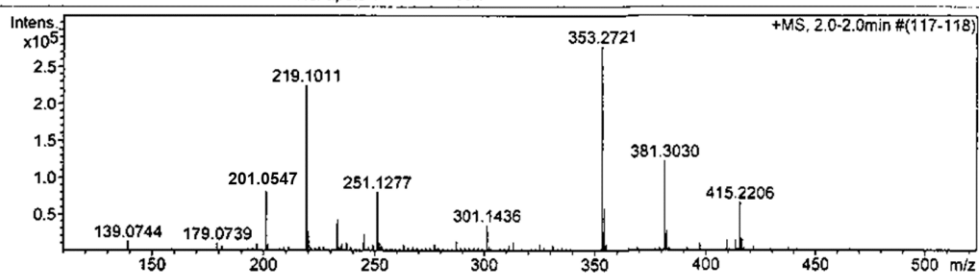


Figure 46 Mass spectrum of compound DC6

DC47 1H NMR 300 MHz in acetone-d₆

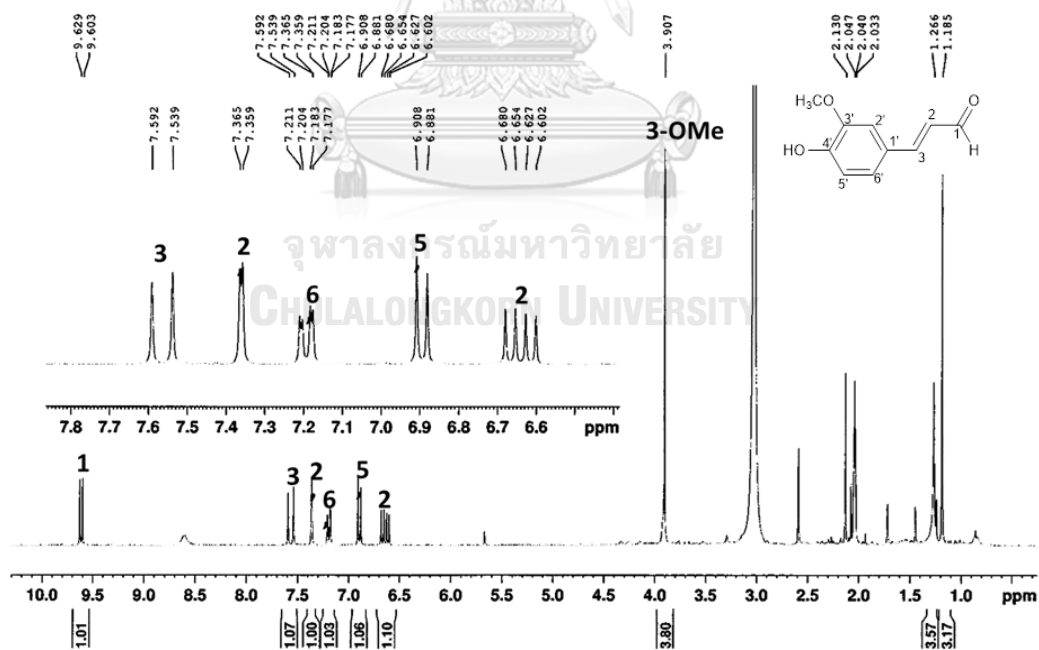


Figure 47 ¹H-NMR (300 MHz) spectrum of compound DC6 (acetone-d₆)

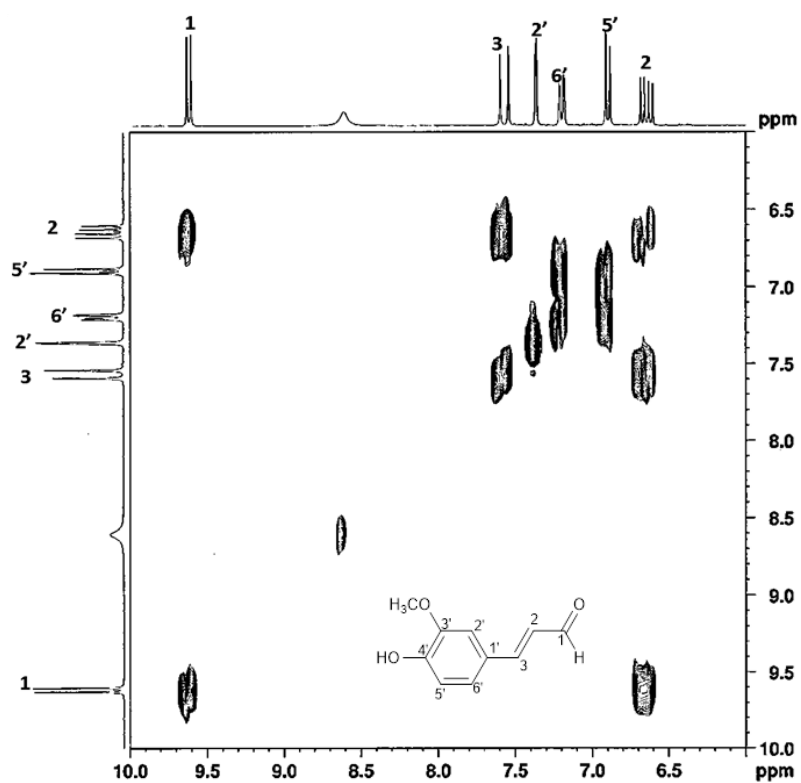
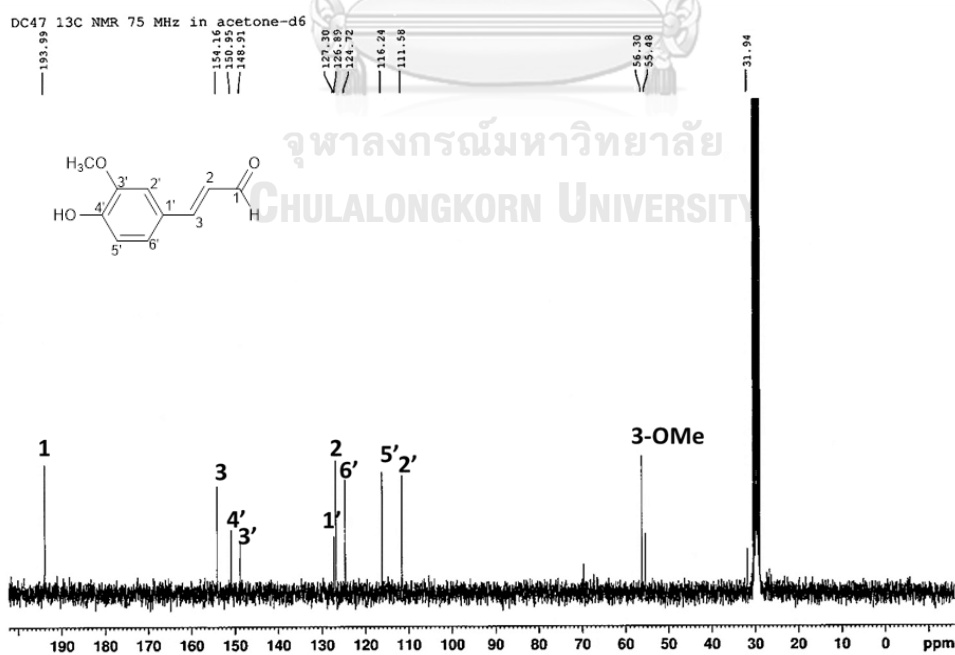


Figure 48 COSY spectrum of compound DC6

Figure 49 ^{13}C -NMR (75 MHz) spectrum of compound DC6 (acetone- d_6)

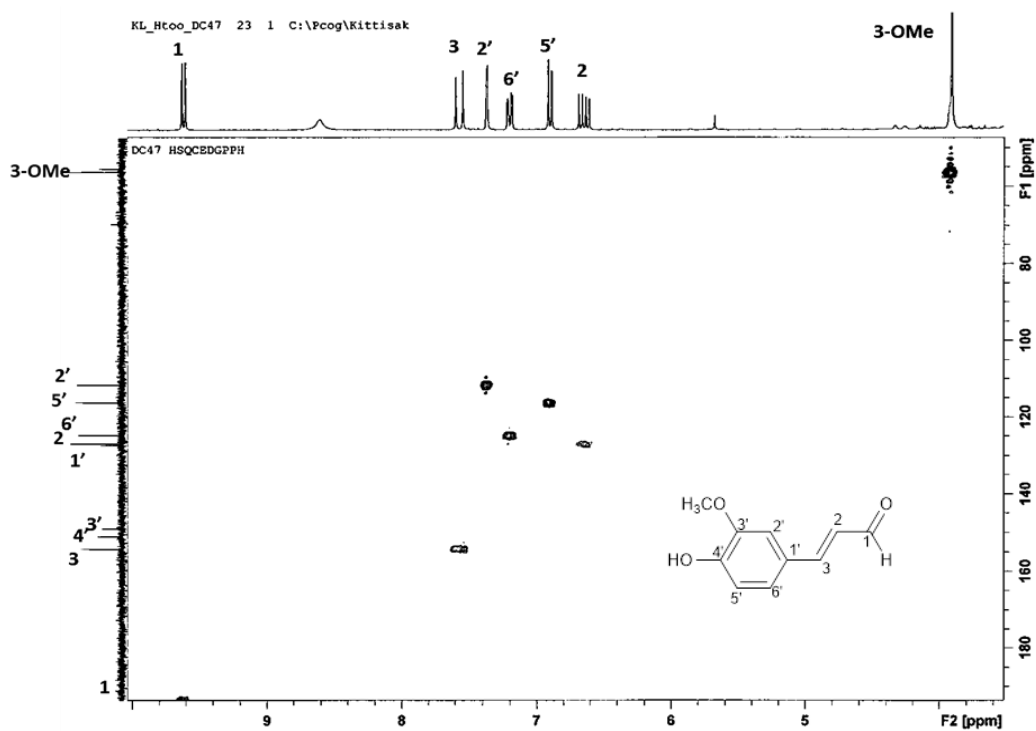


Figure 50 HSQC spectrum of compound DC6

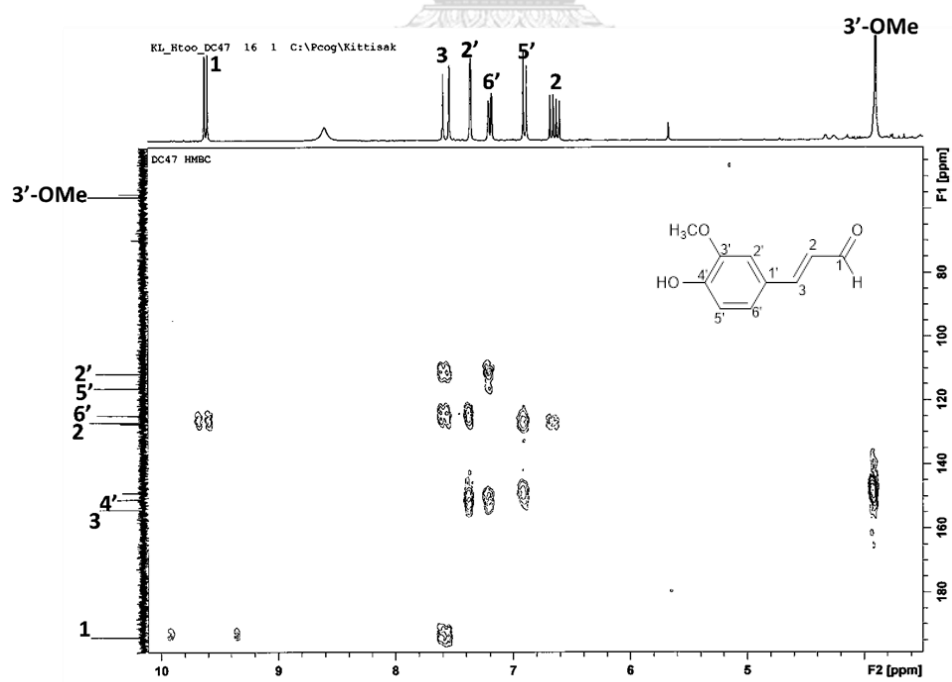


Figure 51 HMBC spectrum of compound DC6

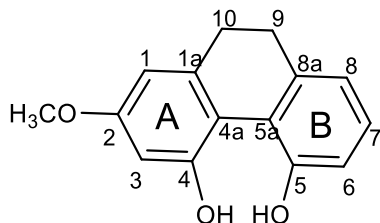
2.2.7 Identification of compound DC7 (4,5-dihydroxy-2-methoxy-9,10-dihydrophenanthrene)

Compound DC7 showed, in the high resolution APCI mass spectrum (**Figure 52**), a protonated molecular ion $[M+H]^+$ at m/z 243.1065 (calcd. for $C_{15}H_{15}O_3$ 243.1021), suggesting the molecular formula $C_{15}H_{14}O_3$.

The 1H -NMR spectrum of compound DC7 (**Figure 53**) revealed the presence of five aromatic protons at δ 6.49 (1H, d, $J = 2.4$ Hz, H-3), 6.51 (1H, d, $J = 2.4$ Hz, H-1), 6.86 (1H, d, $J = 7.5$ Hz, H-8), 6.91 (1H, d, $J = 7.8$ Hz, H-6) and 7.09 (H, dd, $J = 7.8, 7.5$ Hz, H-7), two pairs of methylene protons at δ 2.65 (4H, br s, H₂-9, H₂-10) and methoxyl protons at δ 3.78 (3H, s, 2-OMe). The ^{13}C -NMR and DEPT spectra (**Figure 54**) showed fifteen carbon signals including twelve aromatic carbons [δ 107.3 (C-1), 160.6 (C-2), 102.2 (C-3), 152.7 (C-4), 155.1 (C-5), 116.8 (C-6), 128.0 (C-7), 120.9 (C-8), 143.4 (C-10a), 114.6 (C-4a), 121.8 (C-4b) and 141.8 (C-8a)], two methylene carbons C-9 (δ 32.0) and C-10 (δ 31.5) and a methoxy carbon (δ 55.4). These 1H and ^{13}C NMR data (**Table 16**) suggested that compound DC7 had a dihydrophenanthrene skeleton. The downfield positions of C-2 (δ 160.6), C-4 (δ 152.7) and C-5 (δ 155.1) indicated that each should be an oxygenated carbon. The HSQC spectrum (**Figure 55**) provided assignments for C-9 and C-10. The proton signal at δ 6.51 (d, $J = 2.4$ Hz) was assigned to H-1 from its 3-bond coupling with C-10 in the HMBC spectrum (**Figure 56**). The position of 2-OMe on ring A was deduced from the 2-bond correlation of C-2 with H-1.

The results from comparison of the NMR data with reported values (Matsuda *et al.*, 2004) indicated that compound DC7 was 4,5-dihydroxy-2-methoxy-9,10-dihydrophenanthrene [103]. This compound has been previously found in several species of *Dendrobium* species, for instance, *D. nobile* (Yang *et al.*, 2007), *D.*

aurantiacum Rchb.f. var. *denneanum* (Ying *et al.*, 2009), *D. denneanum* (Lin *et al.*, 2013) and *D. devonianum* (Wu *et al.*, 2019).



4,5-dihydroxy-2-methoxy-9,10-dihydrophenanthrene [103]

Table 16 NMR spectral data of compound DC7 as compared with 4,5-dihydroxy-2-methoxy-9,10-dihydrophenanthrene

Position	Compound DC7 (acetone- d_6)		4,5-dihydroxy-2-methoxy-9,10-dihydrophenanthrene (CD ₃ OD)*	
	δ_H (mult., J in Hz)	δ_C	δ_H (mult., J in Hz)	δ_C
1	6.51(1H, d, 2.4)	107.3	6.47 (1H, d, 2.6)	107.3
2	-	160.6	-	160.8
3	6.49 (1H, d, 2.4)	102.2	6.43 (d, 2.6)	102.1
4	-	152.7	-	152.8
5	-	155.1	--	154.9
6	6.91 (1H, d, 7.8)	116.8	6.82 (1H, dd, 8.2, 1.8)	116.8
7	7.09 (1H, dd, 7.8, 7.5)	128.0	7.05 (1H, dd 8.2, 8.2)	128.0
8	6.86 (1H, d, 7.5)	120.9	6.83 (1H, dd, 8.2, 1.8)	120.9
9	2.65 (2H, br s)	32.0	2.63 (2H, br s)	32.4
10	2.65 (2H, br s)	31.5	2.63(2H, br s)	31.9
10a	-	143.4	-	143.7
4a	-	114.6	-	115.0
4b	-	121.8	-	122.1
8a	-	141.8	-	141.9
2-OMe	3.78 (3H, s)	55.4	3.77 (3H, s)	55.5

* (Matsuda *et al.*, 2004)

Display Report

Analysis Info		Acquisition Date	2/20/2019 3:23:47 PM
Analysis Name	D:\Data\Yp sample\DC40.d	Operator	CTB
Method	tune_low_pos_infusion_20131014.m	Instrument	micrOTOF-Q II 10414
Sample Name	DC40		
Comment			

Acquisition Parameter					
Source Type	APCI	Ion Polarity	Positive	Set Nebulizer	1.6 Bar
Focus	Not active	Set Capillary	4500 V	Set Dry Heater	200 °C
Scan Begin	50 m/z	Set End Plate Offset	-500 V	Set Dry Gas	8.0 l/min
Scan End	1500 m/z	Set Collision Cell RF	150.0 Vpp	Set Divert Valve	Waste

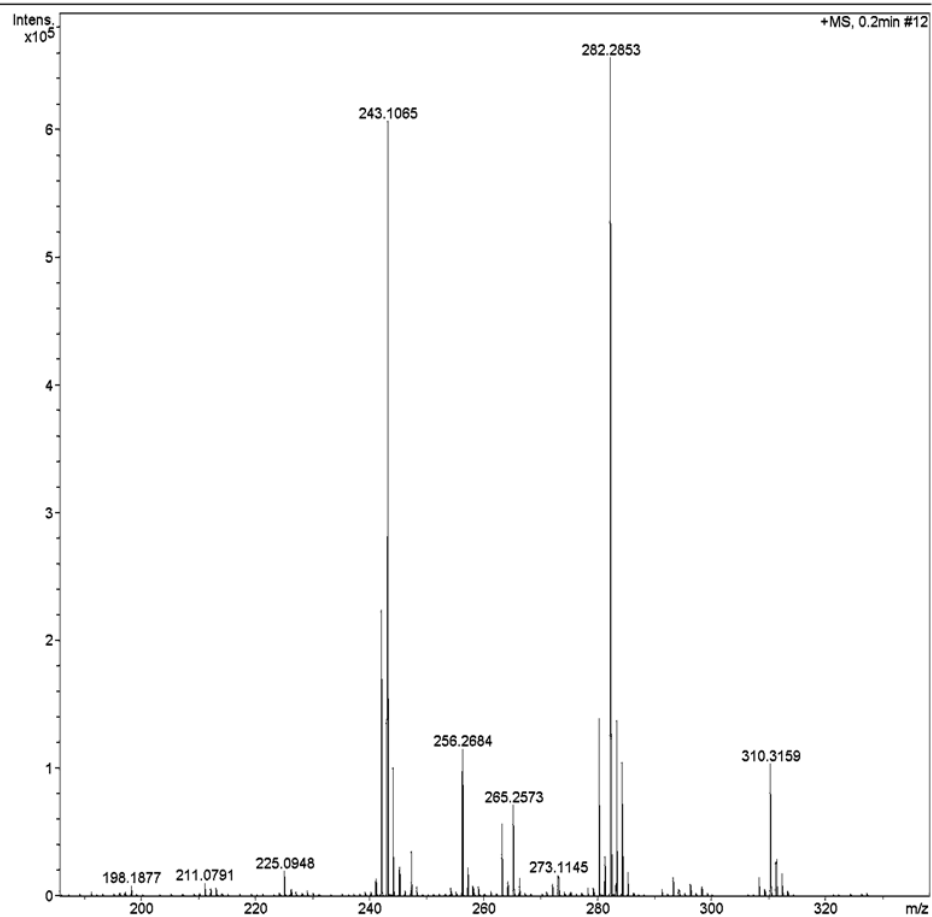


Figure 52 Mass spectrum of compound DC7

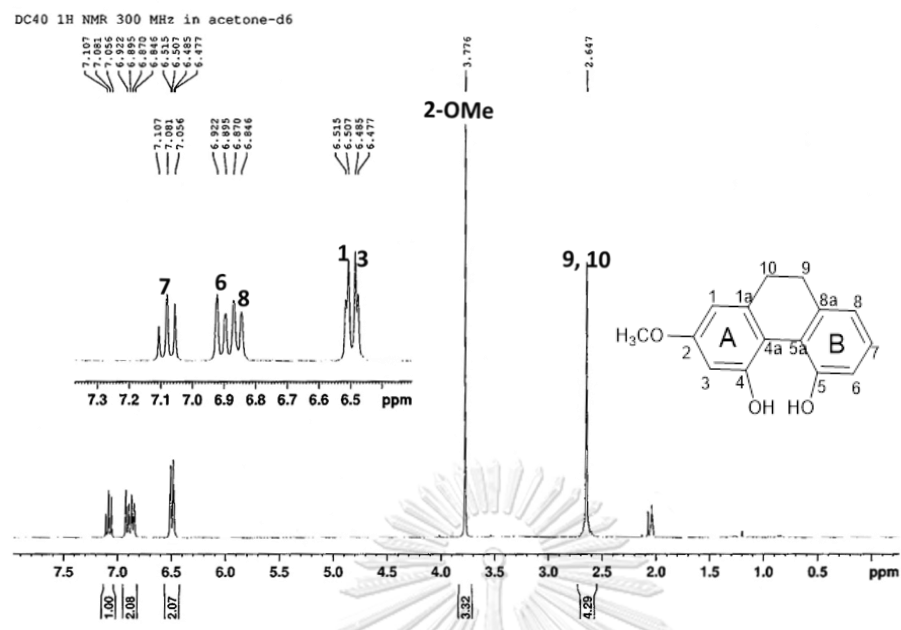


Figure 53 ¹H-NMR (300 MHz) spectrum of compound DC7 (acetone-d₆)

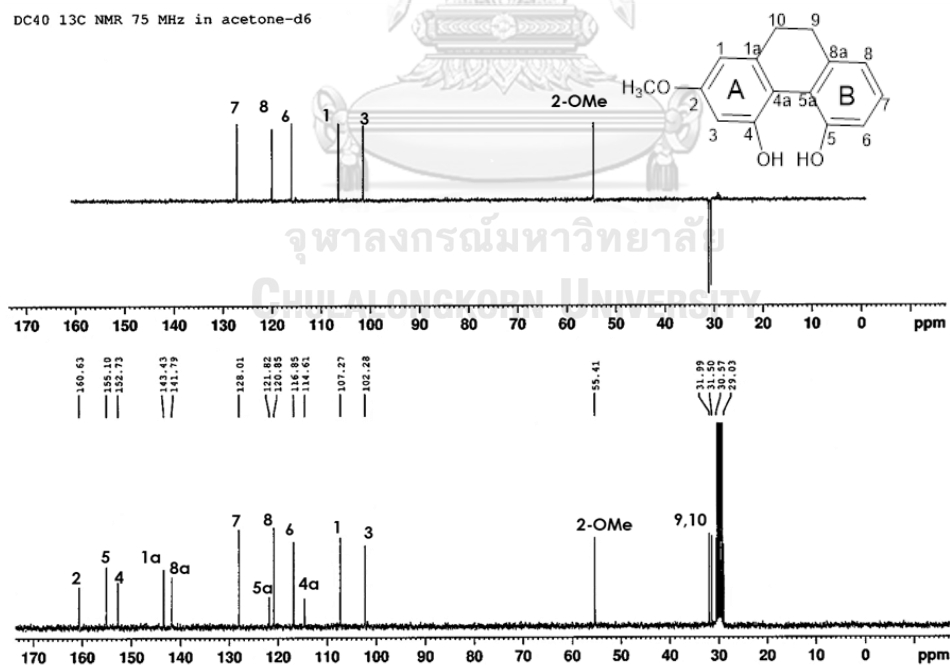


Figure 54 ¹³C-NMR (75 MHz) and DEPT-35 spectra of compound DC7 (acetone-d₆)

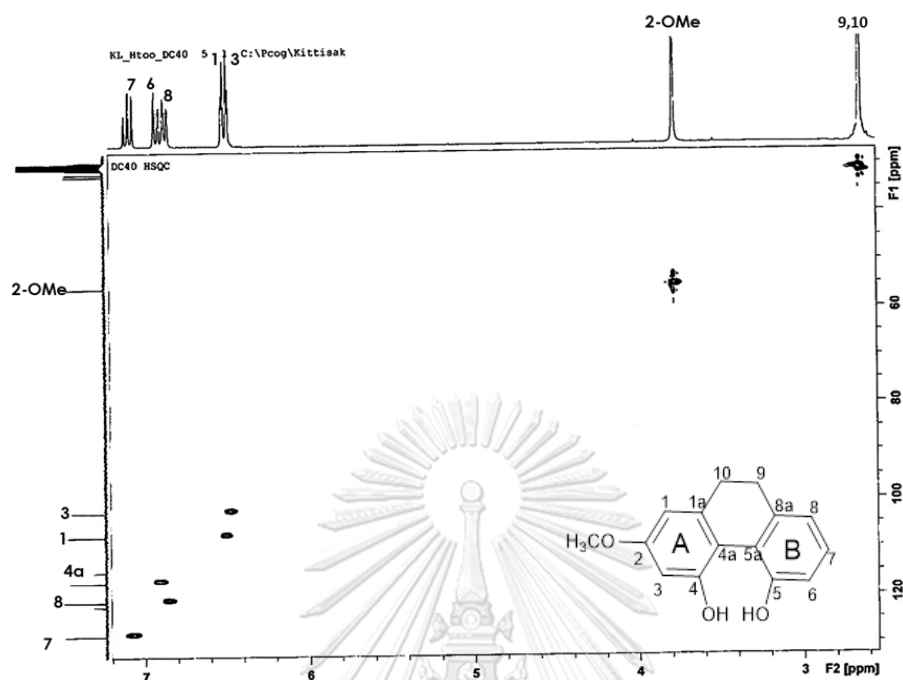


Figure 55 HSQC spectrum of compound DC7

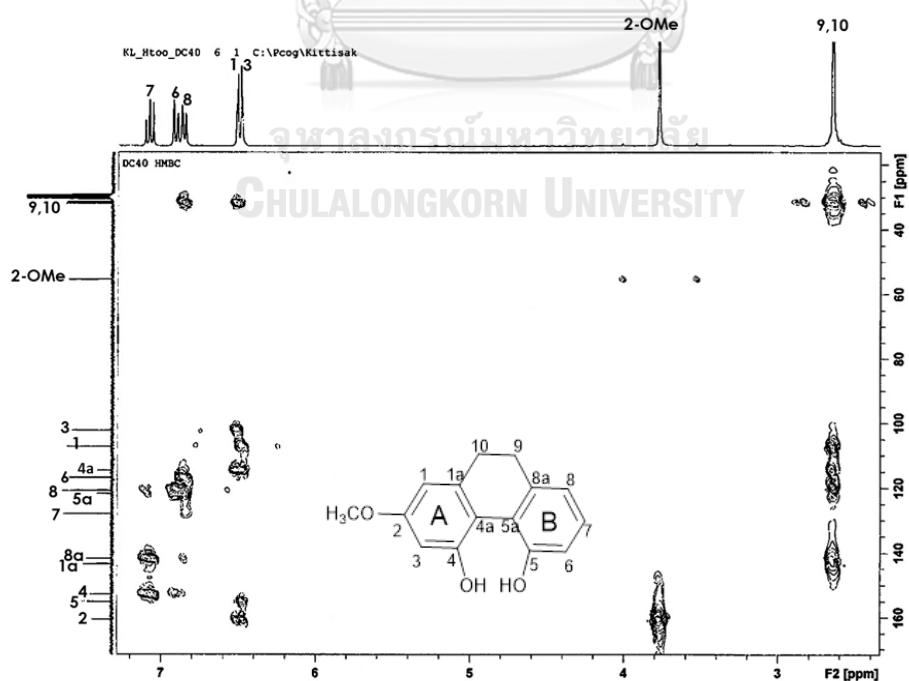
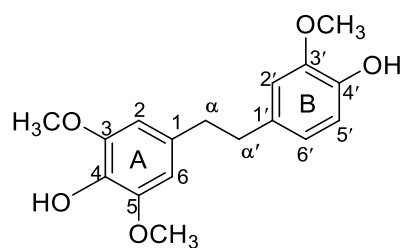


Figure 56 HMBC spectrum of compound DC7

2.2.8 Identification of compound DC8 (moscatilin)

The high resolution ESI mass spectrum of compound DC8 (**Figure 57**) showed a sodium-adduct molecular ion $[M+Na]^+$ at m/z 327.1215 (calcd. for $C_{17}H_{20}O_5Na$ 327.1208), suggesting the molecular formula $C_{17}H_{20}O_5$. The 1H -NMR spectrum of compound DC8 (**Figure 58**) showed five aromatic protons at δ 6.46 (2H, s, H-2, H-6), 6.62 (1H, dd, $J = 8.1, 1.8$ Hz, H-6'), 6.70 (1H, d, $J = 8.1$ Hz, H-5') and 6.77 (1H, d, $J = 1.8$ Hz, H-6') and two pairs of methylene protons at δ 2.77 (4H, s, $H_2-\alpha$, $H_2-\alpha'$), characteristic signals of a bibenzyl skeleton. The chemical shift equivalence of H-2 and H-6 suggested symmetric substitution on the A ring. In addition, 1,3,4-substitution on ring B was evident from the appearance of H-2', H-5' and H-6'. Additional proton resonances accounting for three methoxy groups were observed at δ 3.74 (9H, s, 3-OMe, 5-OMe, 3'-OMe). The ^{13}C -NMR spectrum (**Figure 59**) showed signals for a bibenzyl skeleton, consisting of twelve aromatic carbons (δ 134.0 (C-1), 106.7 (C-2), 148.4 (C-3), 134.8 (C-4), 148.4 (C-5), 106.7 (C-6), 133.1 (C-1'), 112.9 (C-2'), 148.0 (C-3'), 145.4 (C-4), 115.5 (C-5) and 121.5 (C-6) and two methylene carbons at δ 38.4 (C- α') and 38.9 (C- α). The corresponding carbon resonances for the three methoxy groups showed at δ 56.1 (3'-OMe) and 56.4 (3-OMe, 5-OMe). All of these NMR data indicated that compound DC8 was identical with moscatilin [59] (Klongkumnuankarn *et al.*, 2015).

Occurrence of moscatilin [59] has been reported from several members of *Dendrobium*. Examples are *D. brymerianum* (Klongkumnuankarn *et al.*, 2015), *D. devonianum* (Sun *et al.*, 2014), *D. draconis* (Sritularak *et al.*, 2011b), *D. formosum* (Inthongkaew *et al.*, 2017), *D. loddigesii* (Chen *et al.*, 1994a; Ito *et al.*, 2010), *D. officinale* (Zhao *et al.*, 2018), *D. palpebrae* (Kyokong *et al.*, 2018), *D. wardianum* (Zhang *et al.*, 2017), *D. parishii* (Kongkatitham *et al.*, 2018) and *D. scabrilingue* (Sarakulwattana *et al.*, 2018).



moscatilin [59]

Table 17 NMR spectral data of compound DC8 as compared with moscatilin

Position	Compound DC8 (acetone- d_6)		moscatilin (acetone- d_6)*	
	δ_H (mult., J in Hz)	δ_C	δ_H (mult., J in Hz)	δ_C
1	-	134.0	-	133.1
2	6.46 (1H, s)	106.7	6.48 (1H, s)	106.7
3	-	148.4	-	148.3
4	-	134.8	-	134.8
5	-	148.4	-	148.3
6	6.46 (1H, s)	106.7	6.48 (1H, s)	106.7
1'	-	133.1	-	134.1
2'	6.77 (1H, d, 1.8)	112.9	6.78 (1H, d, 2.0)	112.9
3'	-	148.0	-	147.9
4'	-	145.4	-	145.3
5'	6.70 (1H, d, 8.1)	115.5	6.75 (1H, d, 8.0)	115.4
6'	6.62 (1H, dd, 8.1, 1.8)	121.5	6.64 (1H, dd, 8.0, 2.0)	121.6
α	2.77 (2H, s)	38.9	2.78 (2H, m)	38.8
α'	2.77 (2H, s)	38.4	2.78 (2H, m)	38.3
3-OMe	3.74 (6H, s)	56.4	3.75 (3H, s)	56.5
5-OMe	3.74 (6H, s)	56.4	3.75 (3H, s)	56.5
3'-OMe	3.74 (3H, s)	56.1	3.76 (3H, s)	56.1

* (Klongkumnuankarn *et al.*, 2015)

Mass Spectrum List Report

Analysis Info			
Analysis Name	OSCUCS201806292005.d	Acquisition Date	6/29/2018 10:21:32 AM
Method	Tune_low_POS_Natee20130403.m	Operator	Administrator
Sample Name	DC-29	Instrument	micrOTOF 72
	DC-29		
Acquisition Parameter			
Source Type	ESI	Ion Polarity	Positive
Scan Range	n/a	Capillary Exit	130.0 V
Scan Begin	50 m/z	Hexapole RF	150.0 V
Scan End	3000 m/z	Skimmer 1	45.0 V
		Hexapole 1	24.3 V
		Set Corrector Fill	50 V
		Set Pulsar Pull	337 V
		Set Pulsar Push	337 V
		Set Reflector	1300 V
		Set Flight Tube	9000 V
		Set Detector TOF	2295 V

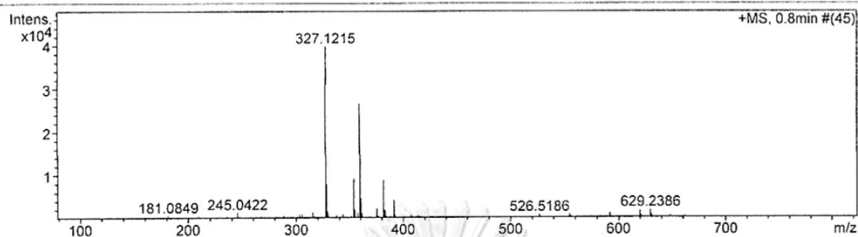


Figure 57 Mass spectrum of compound DC8

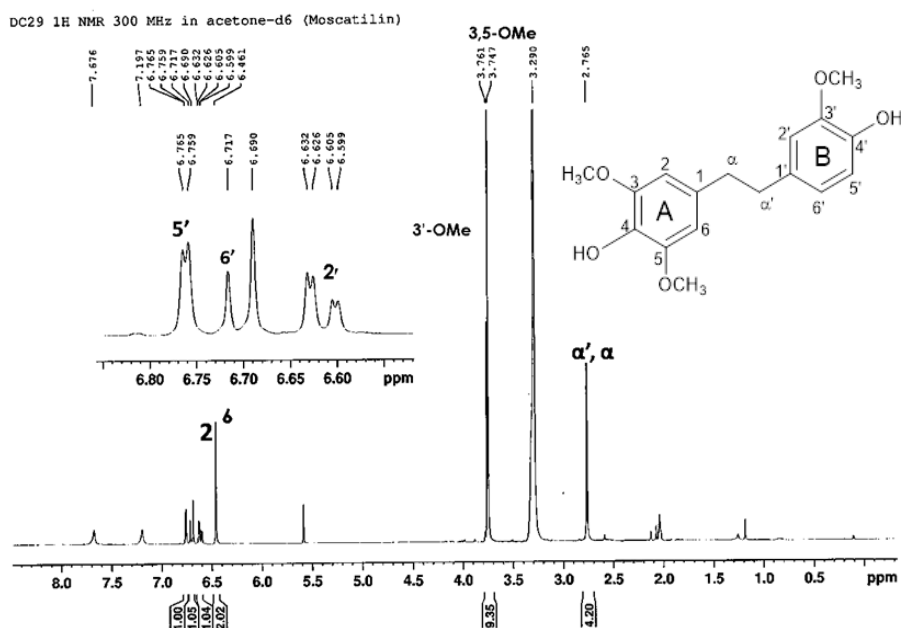


Figure 58 ¹H-NMR (300 MHz) spectrum of compound DC8 (acetone-d₆)

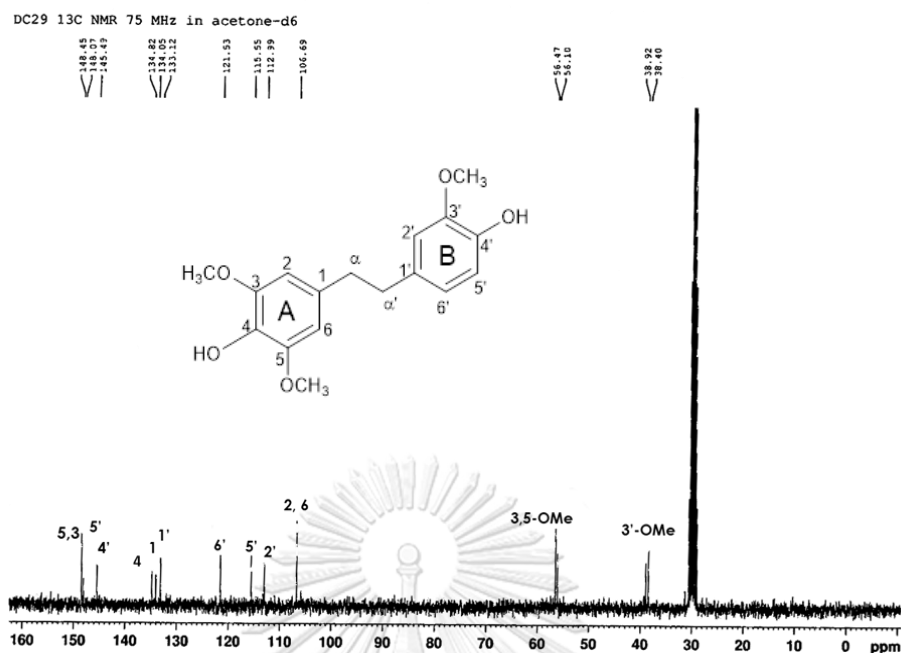


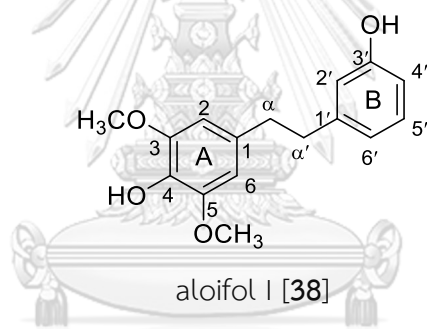
Figure 59 ¹³C-NMR (75 MHz) spectrum of compound DC8 (acetone-*d*₆)

2.2.9 Identification of compound DC9 (aloifol I)

Compound DC9 showed a sodium-adduct molecular ion $[M+Na]^+$ at m/z 297.1102 (calcd. for $C_{16}H_{18}O_4Na$ 297.1102) in the high resolution ESI mass spectrum (Figure 60), suggesting the molecular $C_{16}H_{18}O_4$. The ¹H NMR spectrum of compound DC9 (Figure 61) exhibited signals for two pairs of methylene protons [δ 2.80 (4H, m, H₂- α , H₂- α')] and six aromatic protons [δ 6.48 (2H, s, H-2, H-6), 6.66 (3H, m, H-2', H-4', H-6') and 7.07 (1H, dd, $J = 7.8, 7.5$ Hz, H-5')], which were suggestive of a bibenzyl skeleton. The bibenzyl structure was confirmed by the resonances of twelve aromatic carbons (δ 133.0 (C-1), 106.7 (C-2), 148.4 (C-3), 134.8 (C-4), 148.4 (C-5), 106.7 (C-6), 144.4 (C-1'), 116.2 (C-2'), 158.1 (C-3'), 113.5 (C-4'), 129.9 (C-5') and 120.4 (C-6'), and two methylene carbons at δ 38.7 (C- α) and 38.5 (C- α') observed in the ¹³C NMR and DEPT spectra (Figure 62). These structural features were confirmed by the correlation peaks for protonated carbons in the HSQC spectrum (Figure 63).

Compound DC9 possessed two chemically equivalent methoxy groups on ring A, as indicated from the HSQC cross peak at δ_{H} 3.76 (6H, s, 3-OMe, 5-OMe) / δ_{C} 56.5. The appearance of H-2', H-4', H-5' and H-6' suggested that an OH group was located at C-3'. This was confirmed by the HMBC correlations from H₂- α' to C-2' and C-6' (Figure 64). Based on the above NMR data, DC9 was identified as aloifol I [59]. The NMR and MS data of DC9 were superimposable with earlier reported values (Juneja *et al.*, 1987) as shown in Table 18.

Similar to moscatilin [59], aloifol I [38] has also been found as a common constituent in many *Dendrobium* species, for instance, *D. williamsonii* (Yang *et al.*, 2017a), *D. longicornu* (Hu *et al.*, 2008a), *D. sinense* (Chen *et al.*, 2014), *D. moniliforme* (Zhao *et al.*, 2016) and *D. scabrilingue* (Sarakulwattana *et al.*, 2018).



จุฬาลงกรณ์มหาวิทยาลัย
CHULALONGKORN UNIVERSITY

Table 18 NMR spectral data of compound DC9 as compared with aloifol I

Position	Compound DC9 (acetone- d_6)		Aloifol I (CDCl $_3$)*	
	δ_H (mult., J in Hz)	δ_C	δ_H (mult., J in Hz)	δ_C
1	-	133.0	-	132.8
2	6.48 (1H, s)	106.7	6.27 (1H, s)	105.4
3	-	148.4	-	146.8
4	-	134.8	-	132.9
5	-	148.4	-	146.8
6	6.48 (1H, s)	106.7	6.27 (1H, s)	105.4
1'	-	144.4	-	143.3
2'	6.66 (1H, br s)	116.2	6.62 (1H, m)	115.2
3'	-	158.1	-	155.9
4'	6.66 (1H, br d, 7.5)	113.5	6.62 (1H, m)	112.9
5'	7.07 (1H, dd, 7.5, 7.8)	129.9	7.03 (1H, t, 7.5)	129.2
6'	6.66 (1H, br d, 7.5)	120.4	6.62 (1H, m)	120.5
α, α'	2.80 (4H, s)	38.7 (α) 38.5 (α')	2.75 (4H, s)	36.7 (α) 37.7 (α')
3-OMe, 5-OMe	3.76 (6H, s)	56.5	3.72 (6H, s)	56.2

* (Juneja *et al.*, 1987)

Mass Spectrum List Report

Analysis Info		Acquisition Date	
Analysis Name	OSCUCS201806292002.d	6/29/2018	10:11:31 AM
Method	Tune_low_POS_Natee20130403.m	Operator	Administrator
Sample Name	DC-9	Instrument	micrOTOF 72
DC-9			
Acquisition Parameter		Set Corrector Fill	
Source Type	ESI	Ion Polarity	Positive
Scan Range	n/a	Capillary Exit	130.0 V
Scan Begin	50 m/z	Hexapole RF	150.0 V
Scan End	3000 m/z	Skimmer 1	45.0 V
		Hexapole 1	24.3 V
		Set Pulsar Pull	337 V
		Set Pulsar Push	337 V
		Set Reflector	1300 V
		Set Flight Tube	9000 V
		Set Detector TOF	2295 V

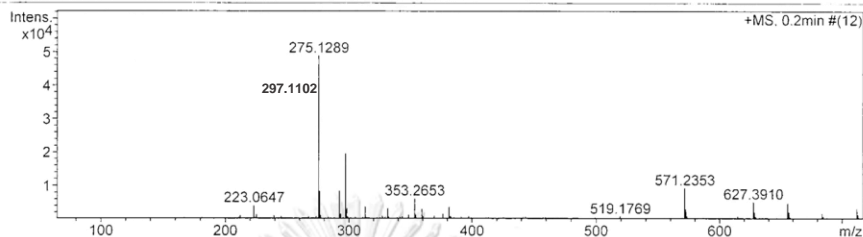
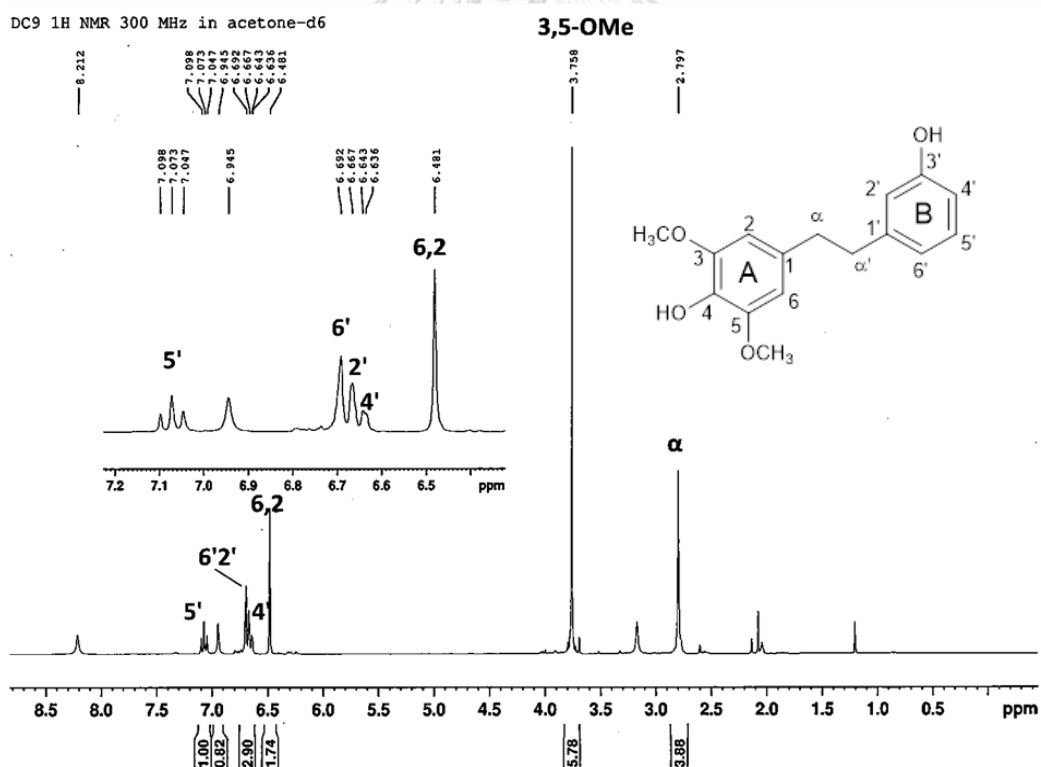


Figure 60 Mass spectrum of compound DC9

Figure 61 ¹H-NMR (300 MHz) spectrum of compound DC9 (acetone-d₆)

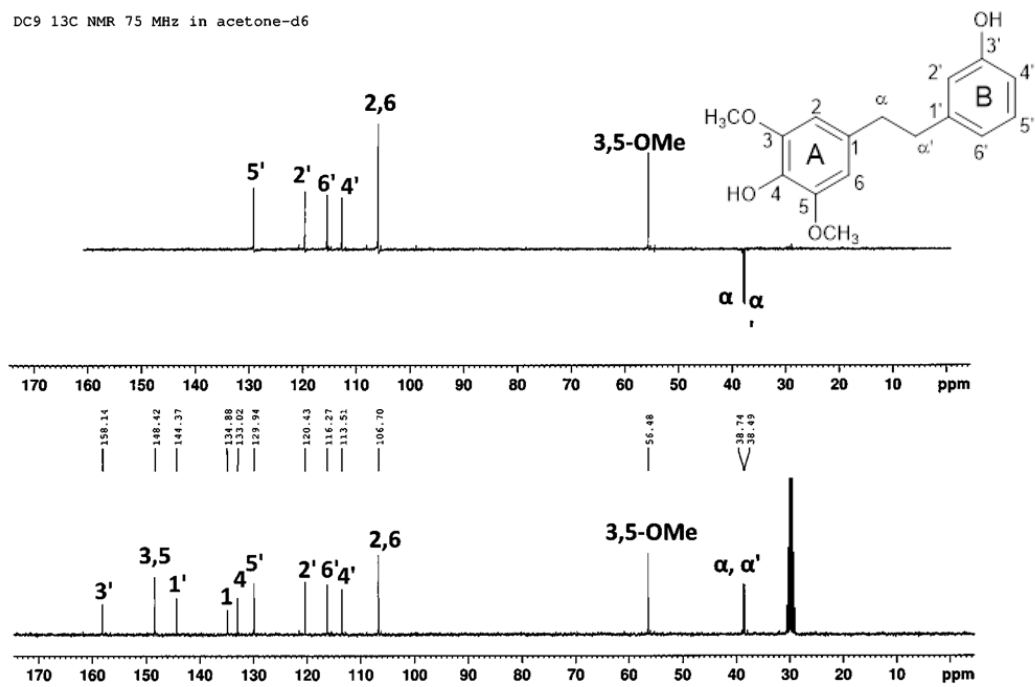


Figure 62 ¹³C-NMR (75 MHz) spectrum of compound DC9 (acetone-d₆)

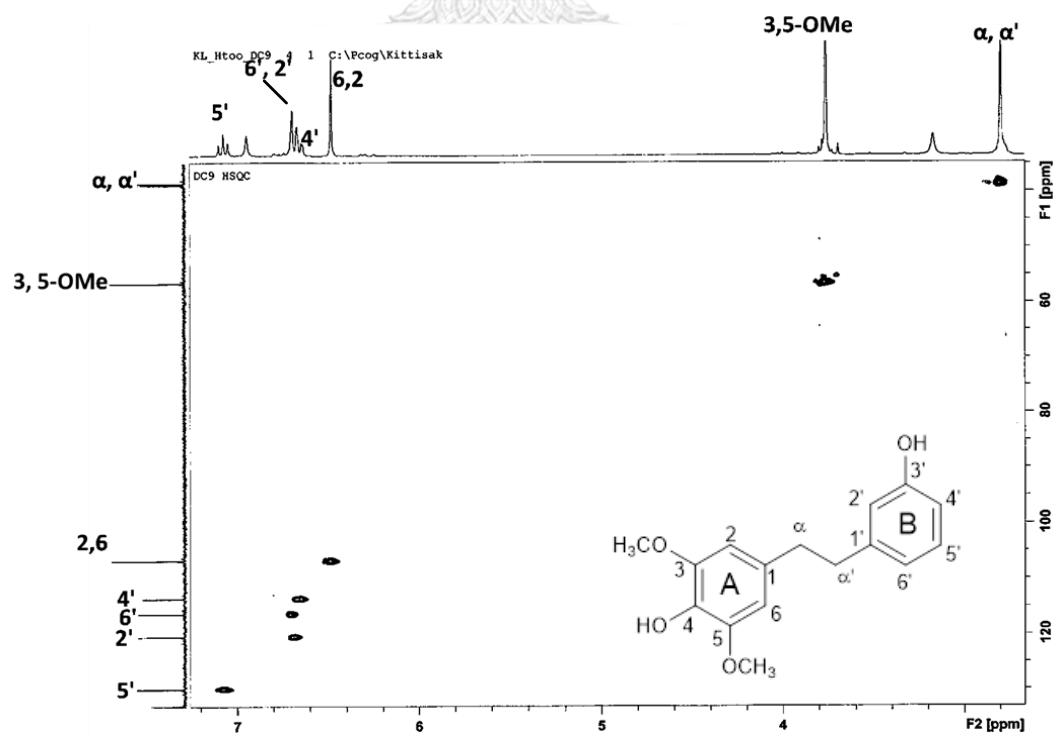


Figure 63 HSQC spectrum of compound DC9

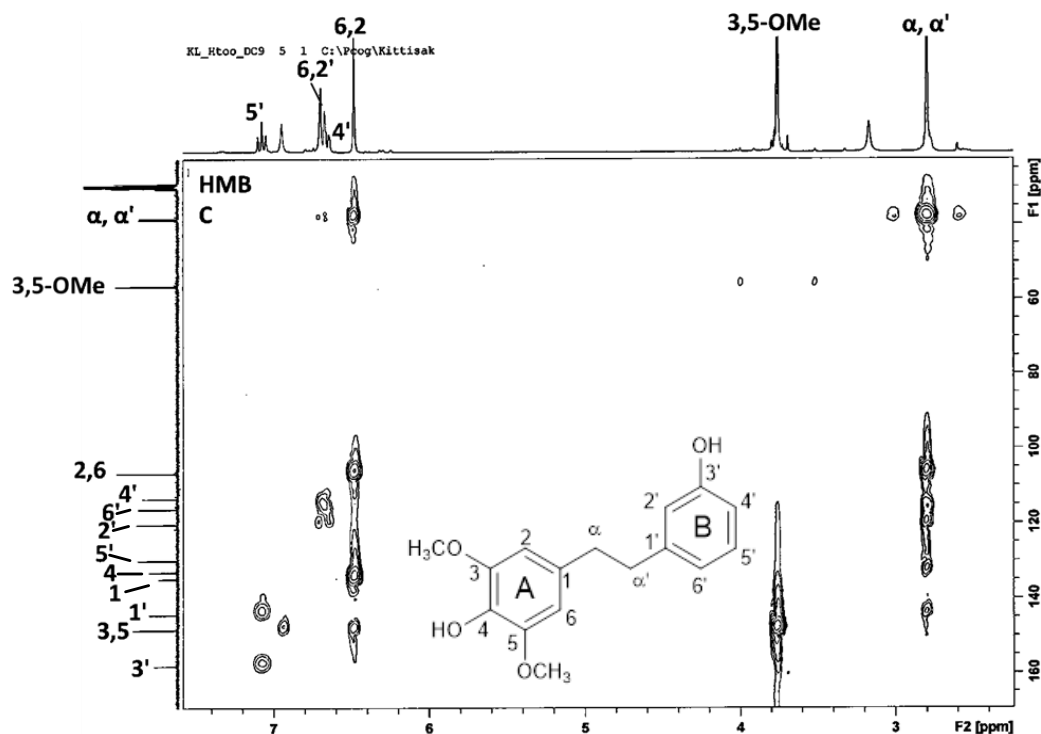


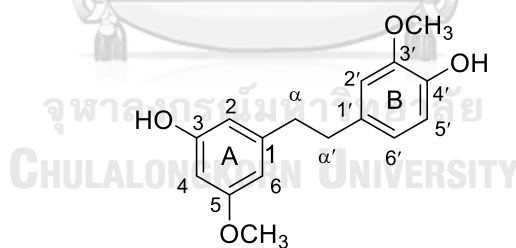
Figure 64 HMBC spectrum of compound DC9

2.2.10 Identification of compound DC10 (gigantol)

The high resolution ESI mass spectrum of compound DC10 (Figure 65) showed a sodium-adduct molecular ion $[M+Na]^+$ at m/z 297.1178 (calcd. for $C_{16}H_{18}O_4Na$ 297.1102), suggesting the molecular formula $C_{16}H_{18}O_4$. The 1H NMR spectrum (Figure 66 and Table 19) showed characteristic signals for a bibenzyl skeleton. The 1,3,5-trisubstitution of ring A was suggested from the triplet signal at δ 6.22 (1H, t, $J = 2.1$ Hz, H-4) and the triplet-like overlapping signals of two protons at δ 6.29 (2H, br t, $J = 2.1$ Hz, H-2, H-6). The 1,3,4-trisubstitution of ring B was deduced from the doublet of doublets at δ 6.68 (1H, dd, $J = 7.8, 1.8$ Hz, H-6') and two doublets at δ 6.71 (1H, d, $J = 7.8$ Hz, H-5') and 6.80 (1H, d, $J = 1.8$ Hz, H-2'). Two methoxy groups appeared at δ 3.70 (3H, s, 5-OMe) and 3.78 (3H, s, 3'-OMe), and two pairs of methylene protons resonated at δ 2.77 (4H, s, H- α , H- α'). The ^{13}C -NMR

spectrum (**Figure 67**) showed twelve aromatic, two methylene and two methoxy carbons, suggesting a bibenzyl nucleus (**Table 19**). The methoxy group at δ 3.70 was placed at C-5 based on the cross peak of these protons with H-6 (δ 6.29) and H-4 (δ 6.24) in the NOESY spectrum (**Figure 68**). The methoxyl protons at δ 3.78 (3'-OMe) displayed a NOESY cross peak with H-2' (δ 6.80). Results from the comparison of the NMR data of compound DC10 with previously described values (Chen *et al.*, 2008d) indicated that compound DC10 was gigantol [**54**].

Earlier reports have shown that gigantol is a bibenzyl commonly found in the genus *Dendrobium*. Examples are *D. brymerianum* (Klongkumnuankarn *et al.*, 2015), *D. devonianum* (Sun *et al.*, 2014), *D. draconis* (Sritularak *et al.*, 2011b), *D. formosum* (Inthongkaew *et al.*, 2017), *D. officinale* (Zhao *et al.*, 2018), *D. palpebrae* (Kyokong *et al.*, 2018), *D. venustum* (Sukphan *et al.*, 2014) and *D. scabrilingue* (Sarakulwattana *et al.*, 2018).



gigantol [**54**]

Table 19 NMR spectral data of compound DC10 as compared with gigantol

Position	Compound DC10 (acetone- d_6)		Gigantol (CDCl ₃)*	
	δ_H (mult., J in Hz)	δ_C	δ_H (mult., J in Hz)	δ_C
1	-	144.6	-	144.5
2	6.29 (1H, br t, 2.1)	98.9	6.30 (1H, dd, 2.0, 2.0)	98.7
3	-	158.4	-	158.2
4	6.22 (1H, t, 2.1)	108.1	6.26 (1H, dd, 2.0, 2.0)	107.9
5	-	161.0	-	160.8
6	6.29 (1H, br t, 2.1)	105.5	6.33 (1H, dd, 2.0, 2.0)	105.3
α	2.77 (2H, s)	38.2	2.79 (2H, s)	37.9
α'	2.77 (2H, s)	37.1	2.78 (2H, s)	36.9
1'	-	133.3	-	133.1
2'	6.80 (1H, d, 1.8)	114.7	6.80 (1H, d, 2.0)	114.6
3'	-	147.2	-	147.0
4'	-	144.4	-	144.2
5'	6.71 (1H, d, 7.8)	112.1	6.74 (1H, d, 8.0)	111.9
6'	6.68 (1H, dd, 7.8, 1.8)	120.8	6.66 (1H, dd, 8.0, 2.0)	120.6
3'-OMe	3.78 (s)	54.5	3.78 (s)	54.3
5-OMe	3.70 (s)	55.3	3.69 (s)	55.2

* (Chen *et al.*, 2008d)

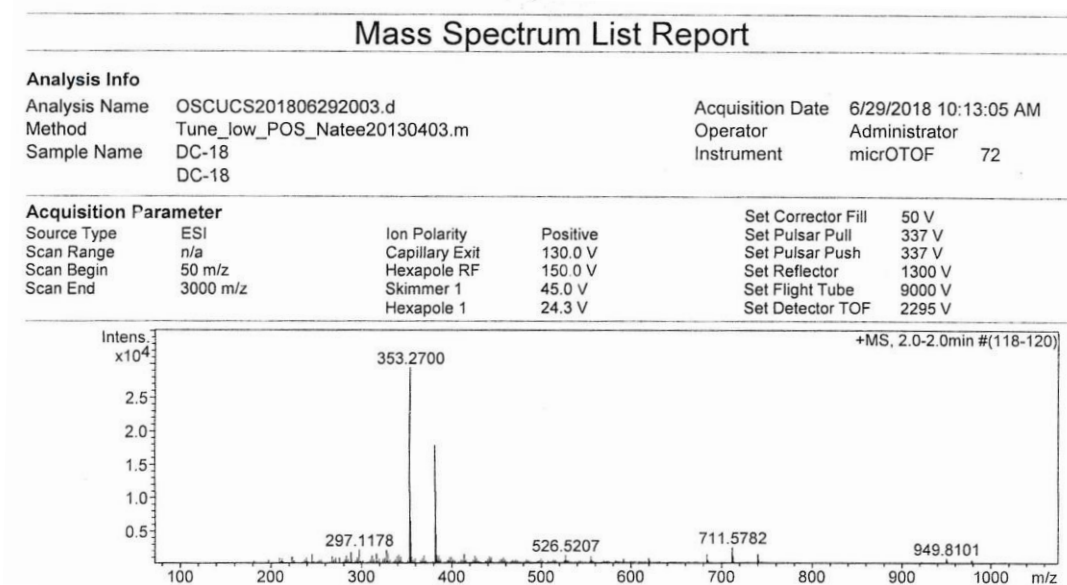


Figure 65 Mass spectrum of compound DC10

DC18 1H NMR in acetone-d₆

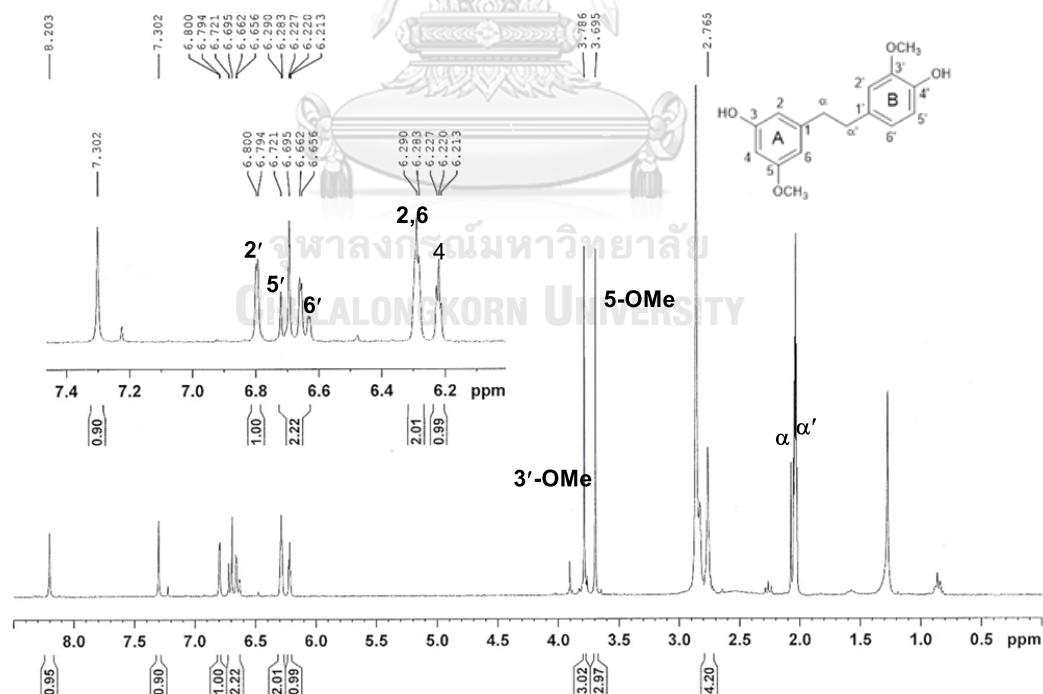


Figure 66 ¹H-NMR (300 MHz) spectrum of compound DC10 (acetone-d₆)

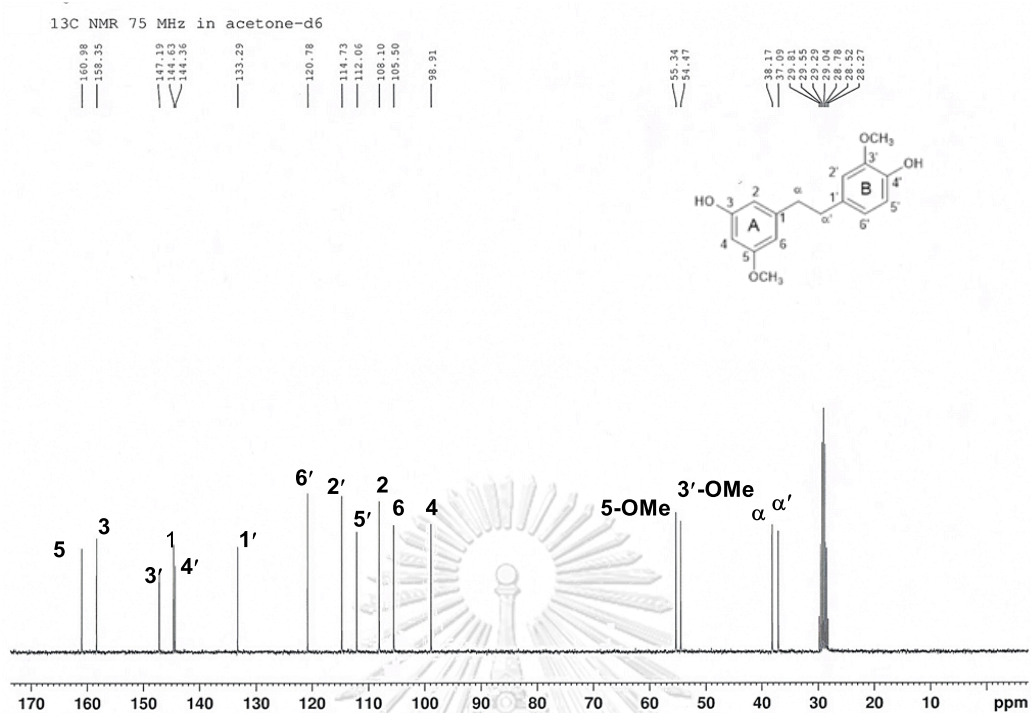


Figure 67 ¹³C-NMR (75 MHz) spectrum of compound DC10 (acetone-d₆)

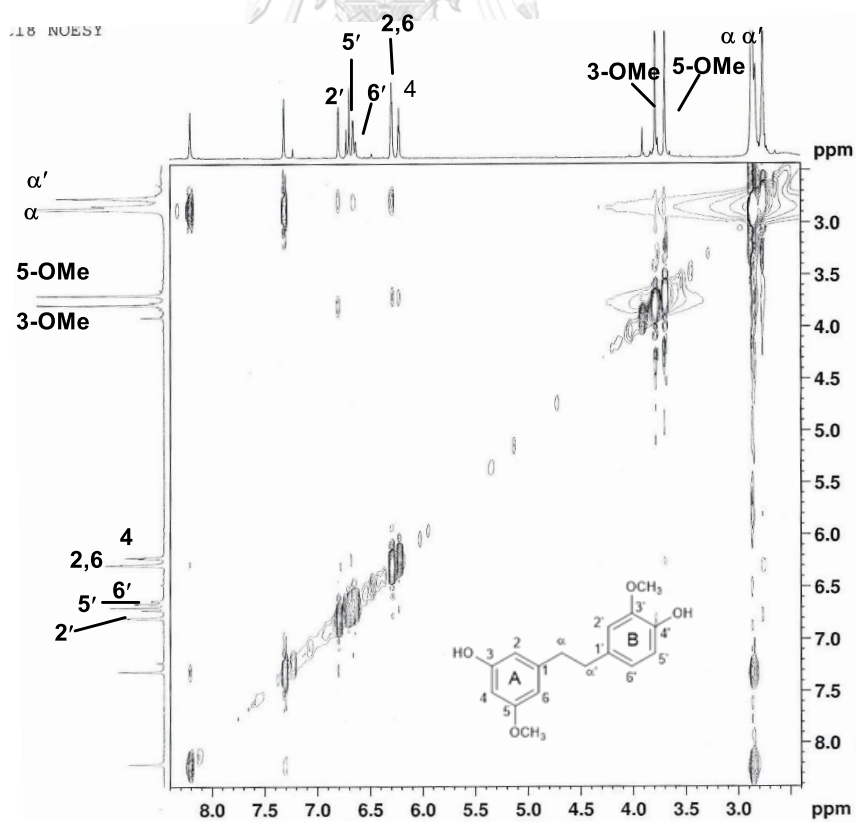


Figure 68 NOESY spectrum of compound DC10

2.2.11 Identification of compound DC11 (batatasin III)

The high resolution ESI mass spectrum of compound DC11 (**Figure 69**) showed a $[M+Na]^+$ ion at m/z 267.1024 (calcd. for $C_{15}H_{16}O_3Na$ 267.0997), suggesting the molecular formula $C_{15}H_{16}O_3$.

The 1H -NMR spectrum (**Figure 70** and **Table 20**) displayed signals for seven aromatic protons at δ 6.31 (1H, br t, $J = 2.1$ Hz, H-2), 6.23 (1H, br t, $J = 2.1$ Hz, H-4), 6.31 (1H, br t, $J = 2.1$ Hz, H-6), 6.62 (1H, br s, H-2'), 6.63 (1H, dd, $J = 8.7, 1.8$ Hz, H-4'), 7.07 (1H, dd, $J = 8.1, 7.5$ Hz, H-5') and 6.65 (1H, br d, $J = 7.5$ Hz, H-6') and two pairs of methylene protons at δ 2.78 (4H, m, $H_2-\alpha, H_2-\alpha'$), suggesting a bibenzyl structure. In support of this, the ^{13}C -NMR and DEPT spectra (**Table 20** and **Figure 71**) exhibited twelve aromatic carbons [δ 145.1 (C-1), 108.8 (C-2), 161.9 (C-3), 99.8 (C-4), 159.3 (C-5), 106.1 (C-6), 144.3 (C-1'), 116.2 (C-2'), 158.3 (C-3'), 113.6 (C-4'), 130.0 (C-5') and 120.4 (C-6')] and two methylenes at δ 38.6 (C- α) and 38.2 (C- α'). Compound DC11 also had a methoxy substituent as indicated by the cross peak at δ_H 3.70 (3H, s, 3-OMe) / δ_C 55.3 in the HSQC spectrum (**Figure 72**). The 1,3,5-substitution of ring A of compound DC11 was suggested from the signals at δ 6.23 (1H, br t, $J = 2.1$ Hz, H-4) and 6.31 (2H, br t, $J = 2.1$ Hz, H-2, H-6). Ring B should have *meta*-substitution, as indicated from the appearance of H-5' at δ 7.07 (1H, dd, $J = 8.1, 7.5$ Hz), and H-4' at 6.63 (1H, dd, $J = 8.7, 1.8$ Hz) and H-6' at 6.65 (1H, br d, $J = 7.5$ Hz). The methoxy group was located at C-3 of ring A, based on the NOESY correlations from these methoxyl protons (δ 3.70) to H-2 (δ 6.31) and H-4 (δ 6.23) (**Figure 73**). This suggested that an OH group was present at C-3' of ring B. From these NMR data, compound DC11 was identified as batatasin III [**41**] (Majumder *et al.*, 1997). Further analysis of the HSQC (**Figure 72**) and HMBC (**Figure 74**) spectra confirmed the structure of DC11 and provided complete ^{13}C NMR assignments.

Batatasin III has been found in several species of *Dendrobium* species, for example *D. aphyllum* (Yang *et al.*, 2015), *D. cariniferum* (Chen *et al.*, 2008c), *D. chrysotoxum* (Li *et al.*, 2009), *D. draconis* (Sritularak *et al.*, 2011b), *D. formosum* (Inthongkaew *et al.*, 2017), *D. infundibulum* (Na Ranong *et al.*, 2019), *D. gratiosissimum* (Zhang *et al.*, 2008a), *D. loddigesii* (Ito *et al.*, 2010), *D. venustum* (Sukphan *et al.*, 2014).

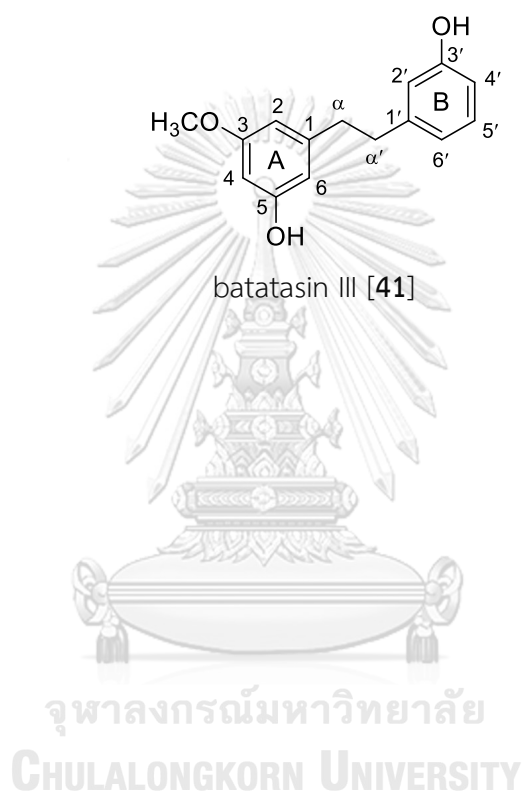


Table 20 NMR spectral data of compound DC11 as compared with batatasin III

Position	Compound DC11 (acetone- <i>d</i> ₆)		batatasin III (CDCl ₃)*	
	δ_{H} (mult., <i>J</i> in Hz)	δ_{C}	δ_{H} (mult., <i>J</i> in Hz)	δ_{C}
1		145.1		145.0
2	6.31 (1H, br t, 2.1)	108.8	6.24 (1H, dd)	108.8
3	-	161.9	-	161.9
4	6.23 (1H, br t, 2.1)	99.8	6.20 (1H, dd, 2.0, 2.2)	99.9
5	-	159.3	-	159.2
6	6.31 (1H, br t, 2.1)	106.1	6.24 (1H, dd)	106.3
1'	-	144.3	-	144.3
2'	6.62 (1H, br s)	116.2	6.63 (1H, m)	116.2
3'	-	158.3	-	158.2
4'	6.63 (1H, dd, 8.7, 1.8)	113.6	6.63 (1H, m)	113.6
5'	7.07 (1H, dd, 8.1, 7.5)	130.0	7.08 (1H, dd, 7.5, 8.0)	130.0
6'	6.65 (1H, br d, 7.5)	120.4	6.63 (1H, m)	120.4
α, α'	2.78 (4H, m)	38.6 (α) 38.2 (α')	2.79 (4H, m)	37.3 (α), 36.9 (α')
3-OMe	3.70 (3H, s)	55.3	3.70 (3H, s)	55.6

* (Majumder *et al.*, 1997)

Mass Spectrum List Report

Analysis Info

Analysis Name OSCUCS201806292001.d
 Method Tune_low_POS_Natee20130403.m
 Sample Name DC-5
 DC-5

Acquisition Date 6/29/2018 10:08:28 AM
 Operator Administrator
 Instrument micrOTOF 72

Acquisition Parameter

Source Type ESI
 Scan Range n/a
 Scan Begin 50 m/z
 Scan End 3000 m/z
 Ion Polarity Positive
 Capillary Exit 130.0 V
 Hexapole RF 150.0 V
 Skimmer 1 45.0 V
 Hexapole 1 24.3 V

Set Corrector Fill 50 V
 Set Pulsar Pull 337 V
 Set Pulsar Push 337 V
 Set Reflector 1300 V
 Set Flight Tube 9000 V
 Set Detector TOF 2295 V

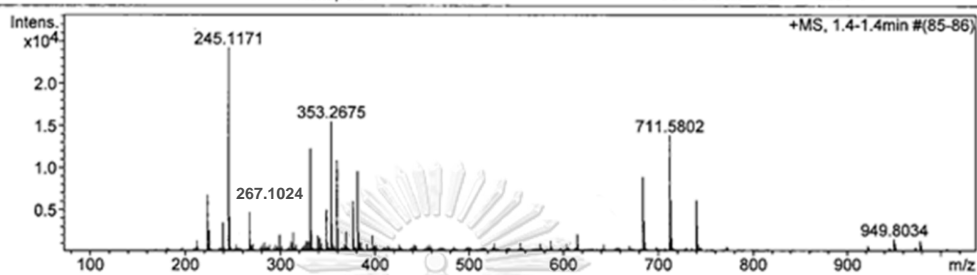


Figure 69 Mass spectrum of compound DC11

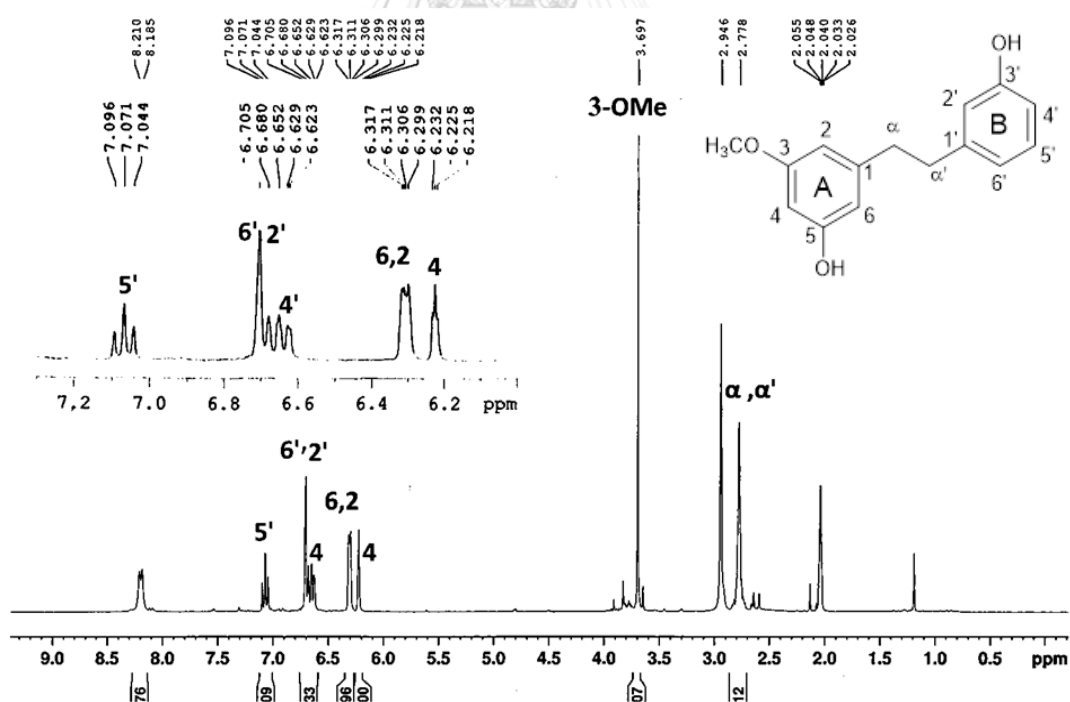


Figure 70 $^1\text{H-NMR}$ (300 MHz) spectrum of compound DC11 (acetone- d_6)

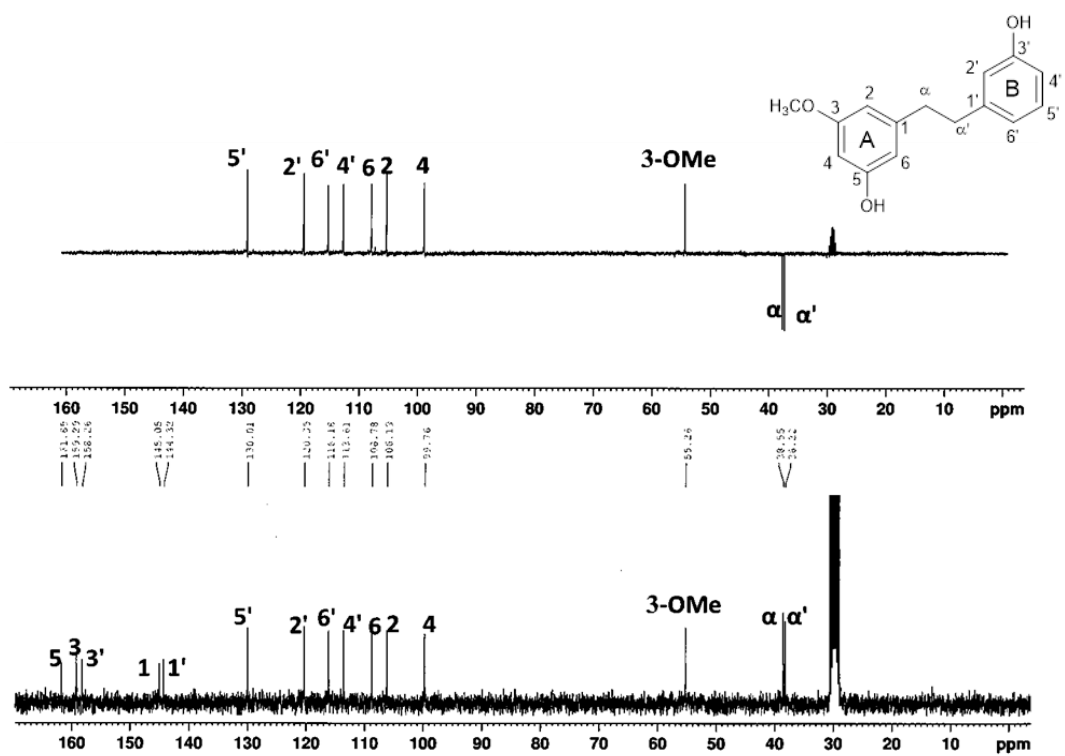


Figure 71 ^{13}C -NMR (75 MHz) and DEPT-135 spectra of compound DC11 (acetone- d_6)

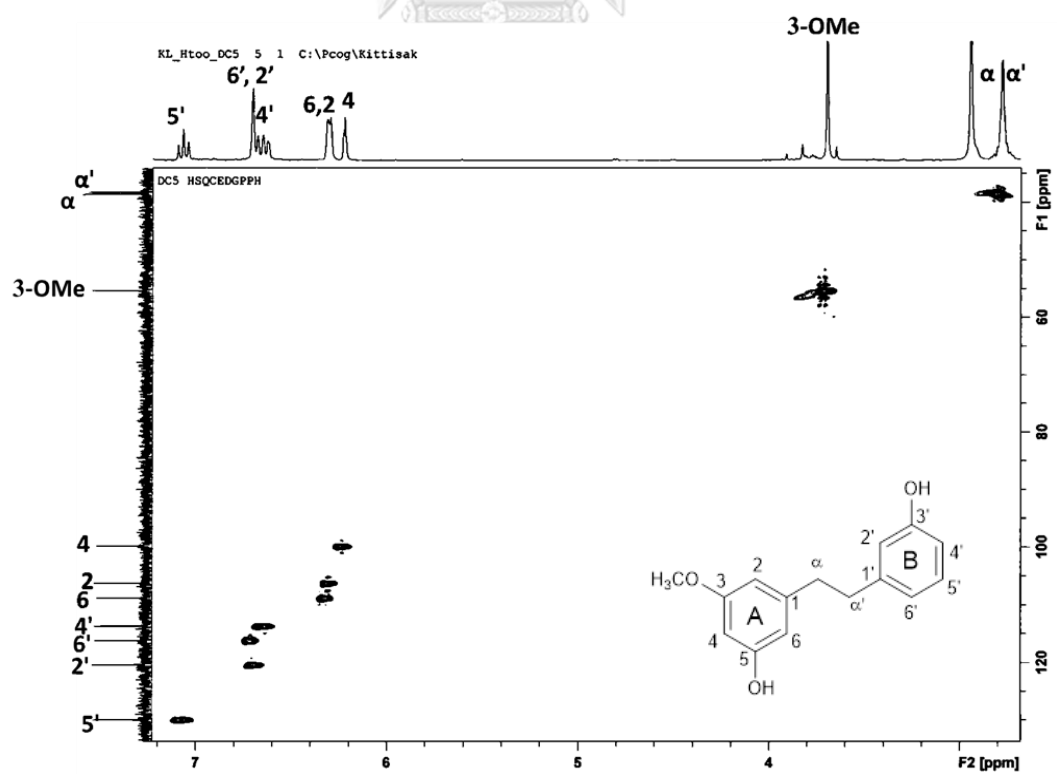


Figure 72 HSQC spectrum of compound DC11

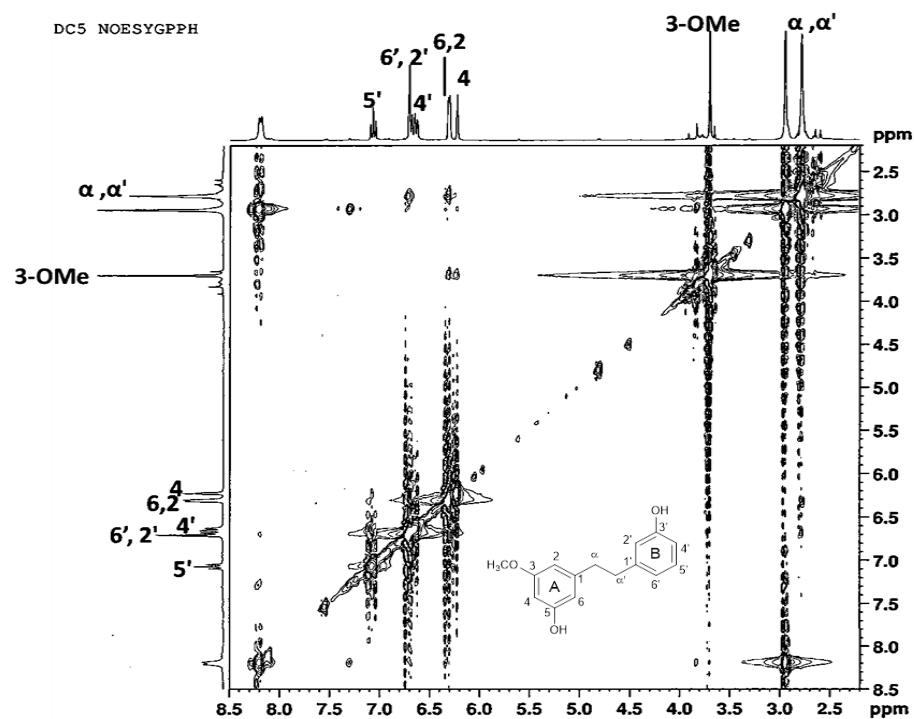


Figure 73 NOESY spectrum of compound DC11

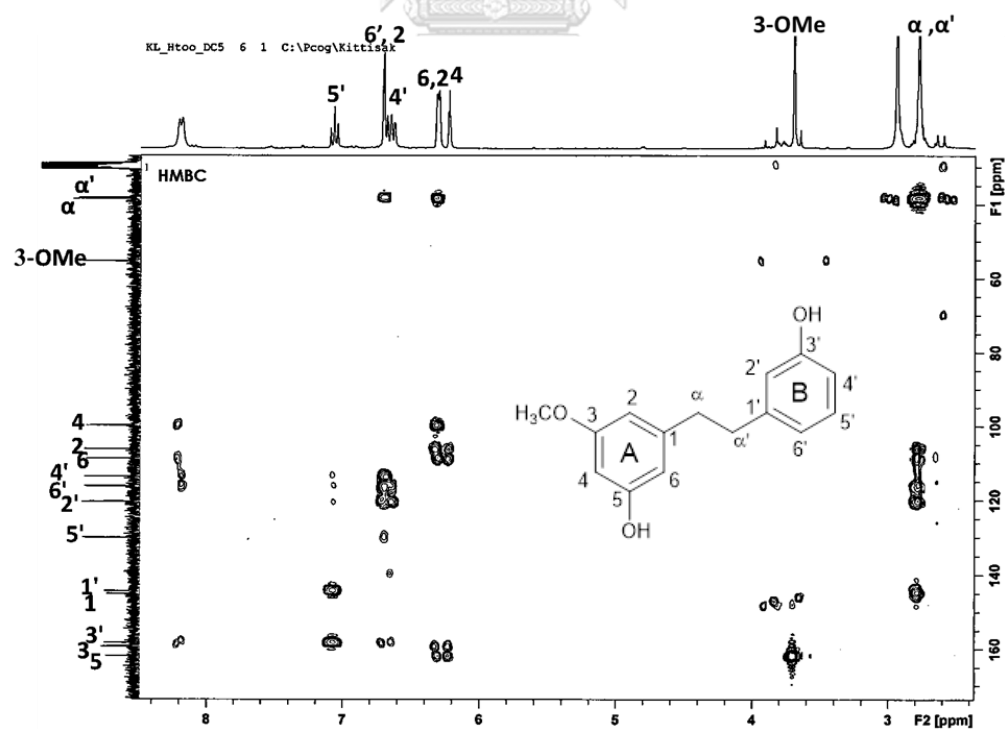
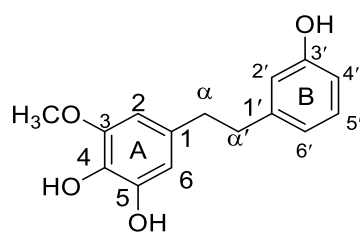


Figure 74 HMBC spectrum of compound DC11

2.2.12 Identification of compound DC12 (dendrosinen B)

Compound DC12 was collected as a brown amorphous solid. The high resolution ESI mass spectrum (**Figure 75**) showed a sodium-adduct molecular ion $[M+Na]^+$ at m/z 283.0998 (calcd. for $C_{15}H_{16}O_4Na$ 283.0946), suggesting the molecular formula $C_{15}H_{16}O_4$. The ^{13}C -NMR and DEPT spectra (**Figure 76**) showed characteristic signals for a bibenzyl structure, including twelve aromatic carbons at δ 133.6 (C-1), 104.5 (C-2), 148.7 (C-3), 132.7 (C-4), 146.1 (C-5), 109.6 (C-6), 144.5 (C-1'), 116.2 (C-2'), 158.2 (C-3'), 113.5 (C-4'), 130.0 (C-5') and 120.4 (C-6') and two methylene carbons at δ 38.4 (C- α) and 38.7 (C- α'). The 1H NMR spectrum (**Table 21** and **Figure 77**) exhibited six aromatic protons at δ 6.35 (d, $J = 1.8$ Hz, H-2), 6.37 (d, $J = 1.8$ Hz, H-6), 6.63 (dd, $J = 7.2, 1.5$ Hz, H-4'), 7.06 (dd, $J = 7.2, 8.1$ Hz, H-5'), 6.67 (d, $J = 8.1$ Hz, H-6'). In the aliphatic region, resonances for the ethylene bridge at δ 2.75 (4H, m, H₂- α , H₂- α') and a methoxy substituent at δ 3.75 (3H, s, 3-OMe) were observed. This methoxy group was placed at C-3 of ring A, as suggested by the NOESY correlation (**Figure 78**) between these methoxyl protons and H-2 (δ 6.35). The remaining substituents were three phenolic groups which were placed at C-4, C-5 and C-3'. All protonated carbons were then assigned from the correlation peaks in the HSQC spectrum (**Figure 79**). The position of OH at C-3' was deduced from the HMBC correlations from H-2' to C-3' and C- α' (**Figure 80**). From these spectroscopic properties, compound DC12 was identified as dendrosinen B [**73**]. Its NMR and MS were in good agreement with literature values (Chen *et al.*, 2014). Dendrosine B was also previously found in *D. infundibulum* (Na Ranong *et al.*, 2019) and *D. sinense* (Chen *et al.*, 2014).



dendrosinen B [**73**]

Table 21 NMR spectral data of compound DC12 as compared with dendrosinen B

Position	Compound DC12 (acetone- <i>d</i> ₆)		Dendrosinen B (CD ₃ OD)*	
	δ_{H} (mult., <i>J</i> in Hz)	δ_{C}	δ_{H} (mult., <i>J</i> in Hz)	δ_{C}
1	-	133.6	-	134.0
2	6.35 (1H, d, 1.8)	104.5	6.24 (1H, d, 1.8)	105.0
3	-	148.7	-	149.4
4	-	132.7	-	133.1
5	-	146.1	-	146.2
6	6.37(1H, d, 1.8)	109.6	6.30 (1H, d, 1.9)	109.9
1'	-	144.5	-	144.8
2'	6.65 (1H, d, 1.5)	116.2	6.59 (1H, d, 1.6)	116.4
3'	-	158.2	-	158.2
4'	6.63 (1H, dd, 7.2, 1.5)	113.5	6.57 (1H, dd, 7.8, 1.6)	113.6
5'	7.06 (1H, dd, 7.2, 8.1)	130.0	7.06 (1H, t, 7.6)	130.2
6'	6.67 (1H, d, 8.1)	120.4	6.63 (1H, d, 7.4)	120.9
α	2.75 (2H, m)	38.4	2.72 (2H, m)	38.8
α'	2.75 (2H, m)	38.7	2.76 (2H, m)	39.2
3-OMe	3.75 (3H, s)	56.3	3.76 (3H, s)	56.5

* (Chen *et al.*, 2014)

Mass Spectrum List Report

Analysis Info

Analysis Name	OSCUCS201806292004.d	Acquisition Date	6/29/2018 10:17:19 AM
Method	Tune_low_POS_Natee20130403.m	Operator	Administrator
Sample Name	DC-21	Instrument	micrOTOF 72
	DC-21		

Acquisition Parameter

Source Type	ESI	Ion Polarity	Positive	Set Corrector Fill	50 V
Scan Range	n/a	Capillary Exit	130.0 V	Set Pulsar Pull	337 V
Scan Begin	50 m/z	Hexapole RF	150.0 V	Set Pulsar Push	337 V
Scan End	3000 m/z	Skimmer 1	45.0 V	Set Reflector	1300 V
		Hexapole 1	24.3 V	Set Flight Tube	9000 V
				Set Detector TOF	2295 V

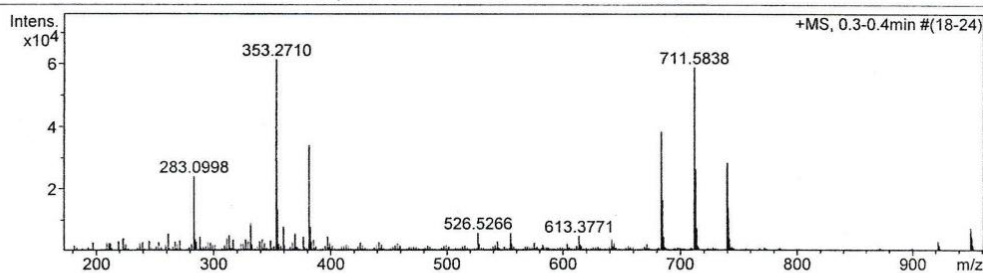


Figure 75 Mass spectrum of compound DC12

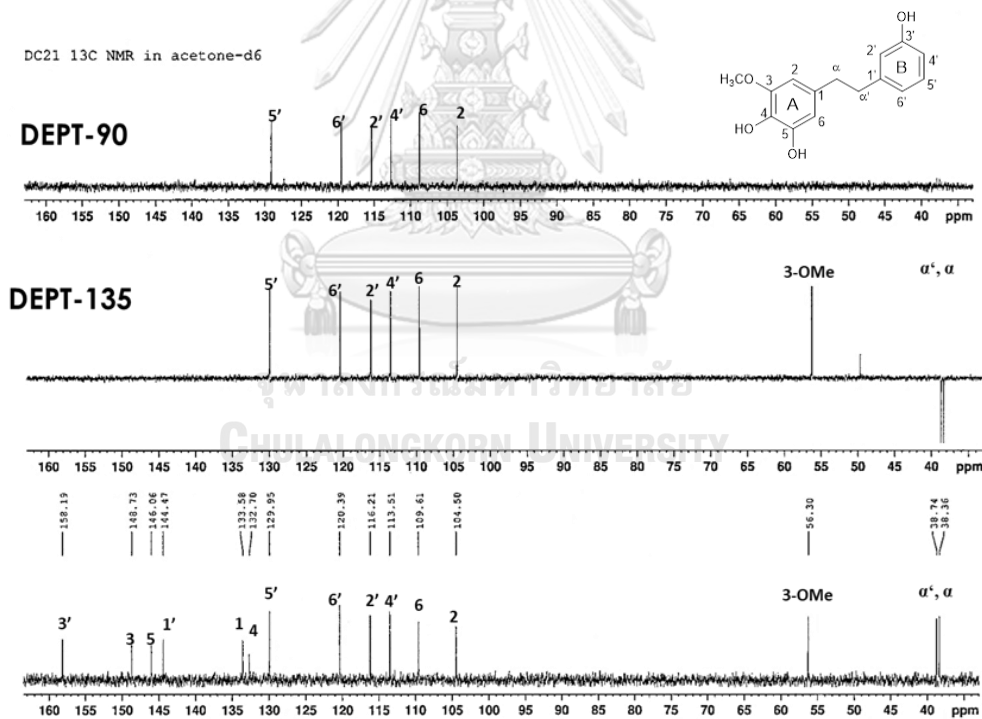


Figure 76 ¹³C-NMR (75 MHz) and DEPT-135 spectra of compound DC12 (acetone-d₆)

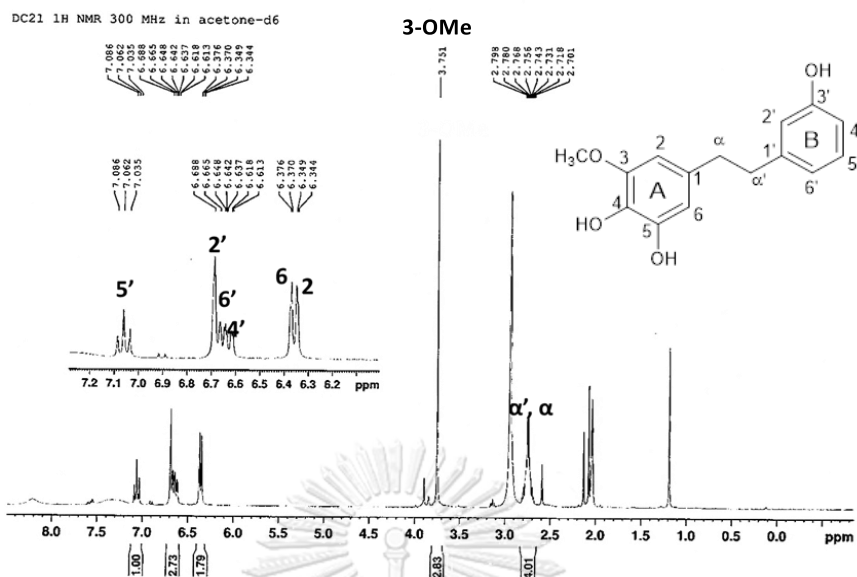


Figure 77 ¹H-NMR (300 MHz) spectrum of compound DC12 (acetone-d₆)

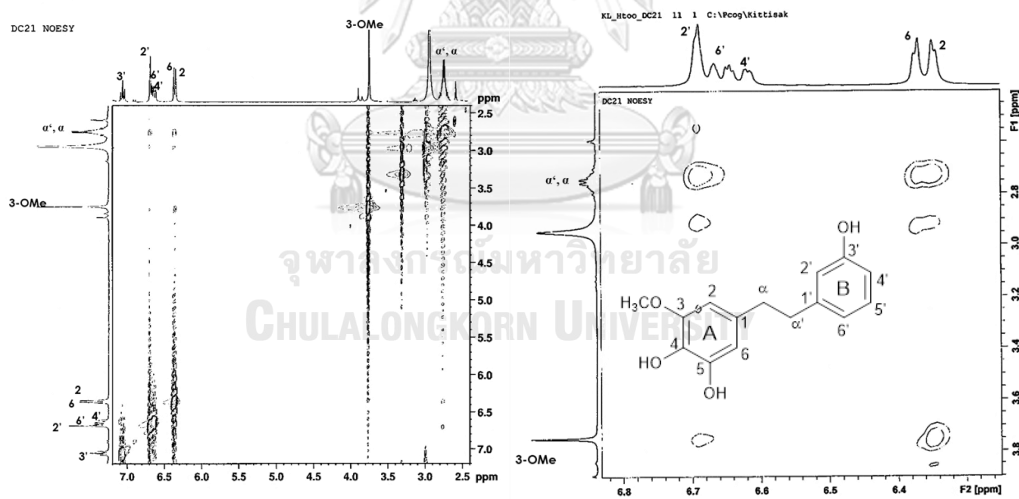
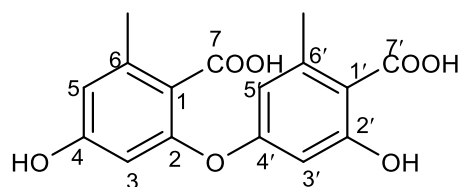


Figure 78 NOESY spectrum of compound DC12

2.2.13 Identification of compound DC13 (diorcinolic acid)

Compound DC13 was collected as a brownish white powder. The high resolution APCI mass spectrum (**Figure 81**) showed a deprotonated molecular ion $[M-H]^-$ at m/z 317.0752 (calcd. for $C_{16}H_{13}O_7$ 317.0661), suggesting the molecular formula $C_{16}H_{14}O_7$. The 1H -NMR spectrum (**Table 21** and **Figure 82**) exhibited signals for four aromatic protons [δ 6.27 (1H, d, $J = 2.5$ Hz, H-3), 6.36 (1H, d, $J = 2.5$ Hz, H-5), 6.47 (1H, d, $J = 2.0$ Hz, H-5') and 6.55 (1H, d, $J = 2.0$ Hz, H-3')] and two methyl groups [δ 2.58 (3H, s, 6'-Me) and 2.64 (3H, s, 6-Me)]. The ^{13}C -NMR spectrum (**Table 22** and **Figure 83**) showed twelve aromatic carbons at δ 105.0 (C-1), 165.2 (C-2), 101.8 (C-3), 166.8 (C-4), 112.7 (C-5), 144.7 (C-6), 116.5 (C-1'), 163.9 (C-2'), 108.4 (C-3'), 152.8 (C-4'), 115.2 (C-5') and 144.5 (C-6'). In addition, resonances for two carbonyl carbons [δ 170.7 (C-7) and 176.1 (C-7')] and two methyl groups [δ 24.4 (6-Me) and 23.7 (6'-Me)] were also observed. The ^{13}C NMR assignments for protonated carbons were then obtained by examination of the HSQC spectrum (**Figure 84**), and the positions of the substituents were deduced from correlation peaks displayed in the HMBC spectrum (**Figure 85**). Important HMBC correlations were found from 6-Me protons (δ 2.64) to C-5 (δ 112.7), and from 6'-Me protons (δ 2.58) to C-5' (δ 115.2). Besides, three-bond connectivities were observed from C-1 (δ 105.0) to H-3 (δ 6.27) and H-5 (δ 6.36), and from C-1' (δ 116.5) to H-3' (δ 6.55) and H-5' (δ 6.47). Based on the above spectroscopic data, compound DC13 was identified as diorcinolic acid [347]. The structure of compound DC13 was confirmed by comparing its NMR data with earlier reported values (Duong, 2019). It should be mentioned that diorcinolic acid [347] was previously recorded as a typical depside type constituent of lichens (Huneck & Yoshimura, 1996).



diorcinolic acid [347]

Table 22 NMR spectral data of compound DC13 as compare with diorcinolic acid

Position	Compound DC13 (acetone- d_6)		diorcinolic acid (acetone- d_6)*	
	δ_H (mult., J in Hz)	δ_C	δ_H (mult., J in Hz)	δ_C
1	-	105.0	-	104.1
2	-	165.2	-	165.7
3	6.27 (1H, d, 2.5)	101.8	6.29 (1H, d, 2.5)	100.8
4	-	166.8	-	163.0
5	6.36 (1H, d, 2.5)	112.7	6.38 (1H, d, 2.5)	111.8
6	-	144.7	-	143.8
7	-	170.7	-	169.8
6-Me	2.64 (3H, s)	24.4	2.59 (3H, s)	23.6
1'	-	116.5	-	116.1
2'	-	163.9	-	164.4
3'	6.55 (1H, d, 2.0)	108.4	6.53 (1H, d, 2.0)	107.3
4'	-	152.8	-	151.6
5'	6.47 (1H, d, 2.0)	115.2	6.44 (1H, d, 2.0)	114.1
6'	-	144.5	-	143.5
7'	-	176.1	-	174.7
6'-Me	2.58 (3H, s)	23.7	2.65 (3H, s)	22.8

* (Duong, 2019)

Display Report

Analysis Info

Analysis Name D:\Data\Yp sample\DC64-2.d
Method tune_low_pos_infusion_20131014.m
Sample Name DC64-2
Comment

Acquisition Date 2/20/2019 4:05:25 PM

Operator CTB
Instrument micrOTOF-Q II 10414

Acquisition Parameter

Source Type	APCI	Ion Polarity	Positive	Set Nebulizer	1.6 Bar
Focus	Not active	Set Capillary	4500 V	Set Dry Heater	200 °C
Scan Begin	50 m/z	Set End Plate Offset	-500 V	Set Dry Gas	8.0 l/min
Scan End	1500 m/z	Set Collision Cell RF	150.0 Vpp	Set Divert Valve	Waste

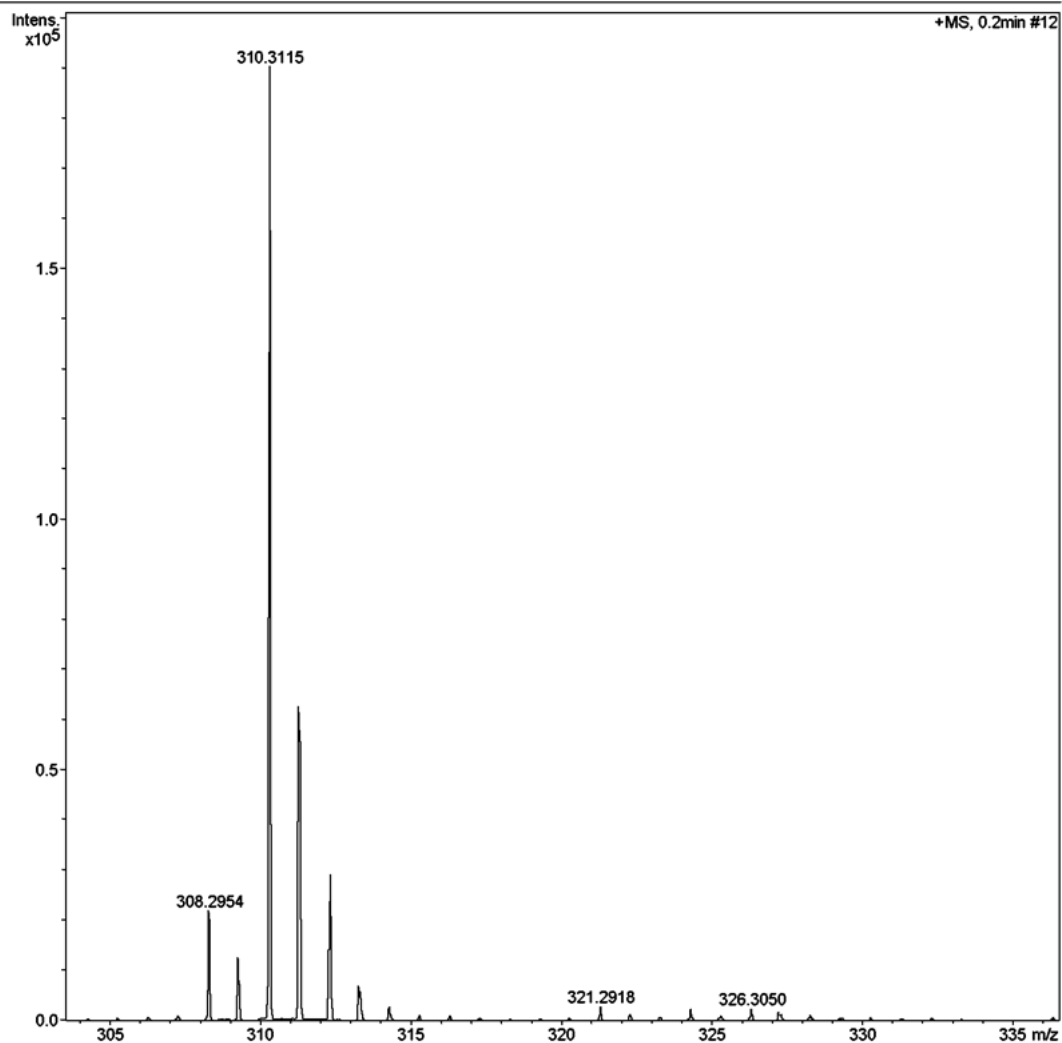


Figure 81 Mass spectrum of compound DC13

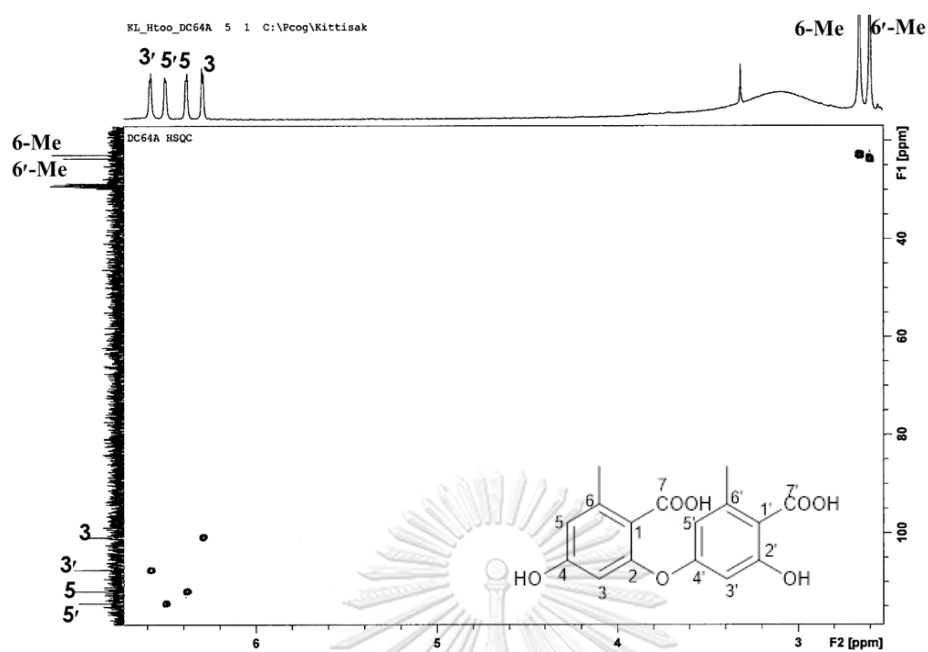


Figure 84 HSQC spectrum of compound DC13



Figure 85 HMBC spectrum of compound DC13

2.3 Biological activity of isolated compounds

All the thirteen compounds isolated from *D. christyanum* were evaluated for α -glucosidase inhibitory activity. Six compounds, including *n*-eicosyl *trans*-ferulate [343], vanillin [275], moscatilin [59], aloifol I [38], batatasin III [41] and dendrosinen B [73] showed no inhibition of the enzyme. The other seven compounds displayed stronger activity than acarbose, as evidenced by their lower IC₅₀ values (Table 22). The α -glucosidase inhibitory activities of methyl haematommate [342] and diorcinolic acid [347] were reported for the first time in this study whereas those of atraric acid [344], *n*-docosyl 4-hydroxy-*trans*- cinnamate [345], coniferyl aldehyde [346], 4,5-dihydroxy-2-methoxy-9,10- dihydrophenanthrene [103] and gigantol [54] were earlier described (Karunaratne *et al.*, 2014; Sarakulwattana *et al.*, 2018).

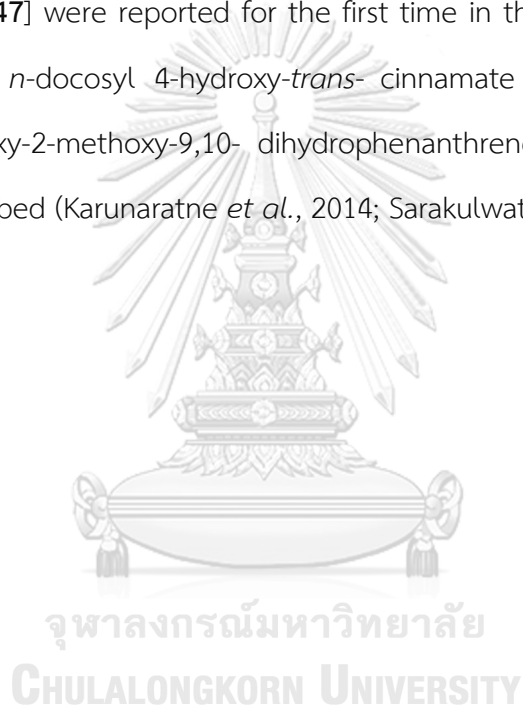


Table 23 α -Glucosidase inhibitory activity of compounds isolated from *D.**christyanum*

compounds	% inhibition at 100 $\mu\text{g/ml}$	IC ₅₀ (μM)
methyl haematommate [342]	97.9 \pm 0.1	18.7 \pm 2.1
<i>n</i> -eicosyl <i>trans</i> -ferulate [343]	NA	-
atraric acid [344]	93.1 \pm 1.1	47.8 \pm 3.3
<i>n</i> -docosyl 4-hydroxy- <i>trans</i> - cinnamate [345]	101.1 \pm 3.4	4.6 \pm 0.2
vanillin [274]	NA	-
coniferyl aldehyde [346]	92.5 \pm 3.2	66.4 \pm 4.7
4,5-dihydroxy-2-methoxy-9,10-dihydrophenanthrene [103]	84.5 \pm 2.1	133.1 \pm 10.8
moscatilin [59]	NA	-
aloifol I [38]	NA	-
gigantol [54]	85.1 \pm 2.1	79.9 \pm 14.2
batatasin III [41]	NA	-
dendrosinen B [73]	NA	-
diorcinolic acid [347]	97.1 \pm 1.4	31.8 \pm 2.4
acarbose	21.9 \pm 1.5	724.7 \pm 46

NA= no activity

For the glucose uptake stimulatory effects in rat L6 myotubes (Mitsumoto *et al.*, 1991), almost all of the isolates were investigated, except for methyl haematommate [342] and gigantol [54] because of their inadequate quantity. Each test sample was prepared in three different concentrations (1, 10 and 100 $\mu\text{g/ml}$)

(Figure 86), and evaluated for cytotoxicity and glucose uptake enhancing activity.

Percentages of cell viability above 80 % were considered as non-cytotoxicity (ISO-10993-5, 2009), as shown in Table 24. When tested at 100 $\mu\text{g/ml}$, *n*-docosyl 4-hydroxy-*trans*- cinnamate [345] (0.212 mM), vanillin [275] (0.657 mM) and coniferyl aldehyde [346] (0.561 mM) enhanced the glucose uptake by L6 myotubes by 31.6 ± 4.4 %, 97.1 ± 8.7 % and 56.4 ± 2.5 %, respectively, without toxicity. Furthermore, aloifol I [38] (0.036 mM) and batatasin III [41] (0.041 mM) showed enhancement of 11.3 ± 2.5 % and 30.2 ± 6.7 %, respectively (Table 23 and Figure 86).

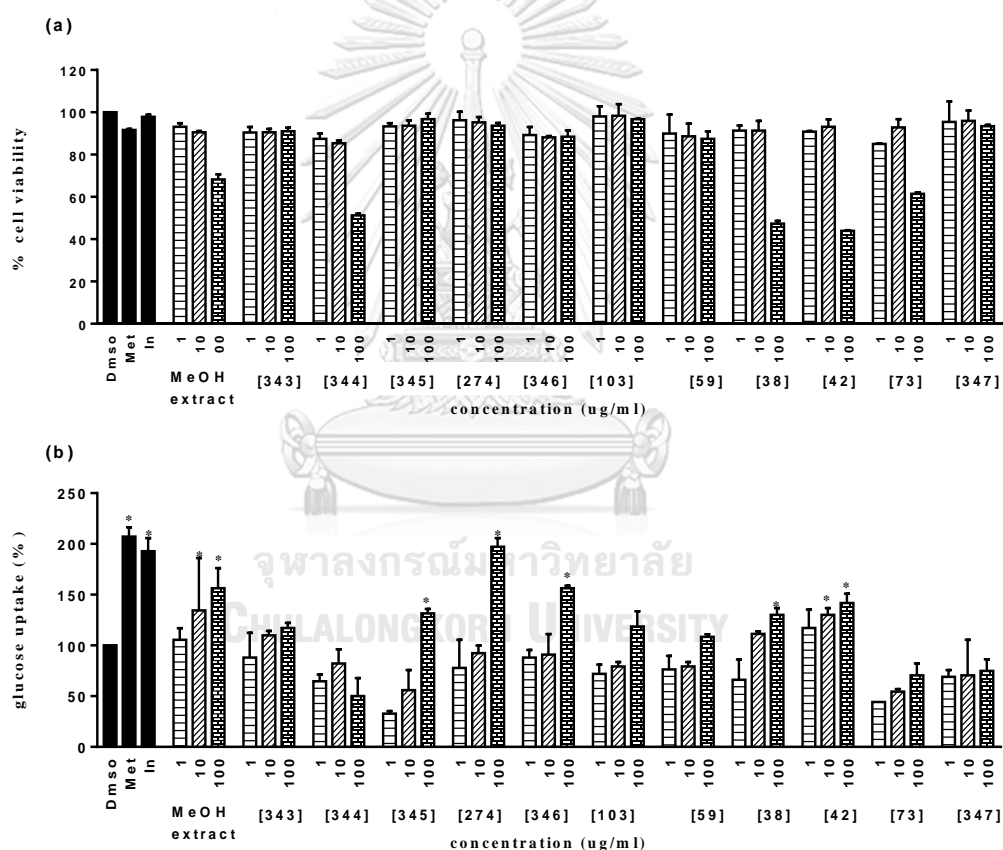


Figure 86 Cytotoxicity (a) and glucose uptake stimulatory activity (b) of extract and isolated compounds

*($p < 0.05$) Significantly different when compared to the control (DMSO)

DMSO (control); Met = metformin, In = insulin (positive control)

Table 24 Glucose uptake stimulatory activity of compounds isolated from *D.**christyanum*

Sample	Percentage of glucose uptake	Percent enhancement
DMSO	100	0
Metformin (2 mM)	207.3 ± 9.1*	107.3 ± 9.1
Insulin (500 nM)	192.7 ± 13.1*	92.7 ± 13.1
MeOH extract		
1 µg/ml	105.5 ± 11.5	NA
10 µg/ml	134.5 ± 51.7*	34.5 ± 51.7
100 µg/ml	156.4 ± 19.7*	56.4 ± 19.7
<i>n</i> -eicosyl <i>trans</i> -ferulate [343]		
1 µg/ml (0.002 mM)	88.0 ± 24.3	NA
10 µg/ml (0.021 mM)	109.8 ± 4.4	NA
100 µg/ml (0.211 mM)	117.1 ± 5.0	NA
Atraric acid [344]		
1 µg/ml (0.005 mM)	64.7 ± 6.7	NA
10 µg/ml (0.051 mM)	82.2 ± 14.0	NA
100 µg/ml (0.510 mM)	NT	NA
<i>n</i> -docosyl 4-hydroxy- <i>trans</i> -cinnamate [345]		
1 µg/ml (0.002 mM)	32.7 ± 2.5	NA
10 µg/ml (0.021 mM)	56.0 ± 19.7	NA
100 µg/ml (0.212 mM)	131.6 ± 4.4*	31.6 ± 4.4
Vanillin [275]		
1 µg/ml (0.006 mM)	77.8 ± 27.7	NA
10 µg/ml (0.066 mM)	92.4 ± 7.6	NA
100 µg/ml (0.657 mM)	197.1 ± 8.7*	97.1 ± 8.7
Coniferyl aldehyde [346]		
1 µg/ml (0.005 mM)	88.0 ± 7.6	NA
10 µg/ml (0.056 mM)	90.9 ± 20.2	NA
100 µg/ml (0.561 mM)	156.4 ± 2.5*	56.4 ± 2.5

Sample	Percentage of glucose uptake	Percent enhancement
4,5-Dihydroxy-2-methoxy -9,10-dihydrophenanthrene [103]		
1 µg/ml (0.004 mM)	72.0 ± 9.1	NA
10 µg/ml (0.041 mM)	79.3 ± 4.4	NA
100 µg/ml (0.413 mM)	118.5 ± 15.1	NA
Moscatilin [59]		
1 µg/ml (0.003 mM)	76.4 ± 13.3	NA
10 µg/ml (0.033 mM)	79.3 ± 4.4	NA
100 µg/ml (0.329 mM)	108.4 ± 2.5	NA
Aloifol I [38]		
1 µg/ml (0.003 mM)	66.2 ± 20.0	NA
10 µg/ml (0.036 mM)	111.3 ± 2.5	11.3 ± 2.5
100 µg/ml (0.365 mM)	NT	NA
Batatasin III [41]		
1 µg/ml (0.004 mM)	117.1 ± 18.2	NA
10 µg/ml (0.041 mM)	130.2 ± 6.7*	30.2 ± 6.7
100 µg/ml (0.409 mM)	NT	NA
Dendrosinen B [73]		
1 µg/ml (0.004 mM)	44.4 ± 0.0	NA
10 µg/ml (0.038 mM)	54.5 ± 2.5	NA
100 µg/ml (0.384 mM)	NT	NA
Diorcinolic acid [347]		
1 µg/ml (0.003 mM)	69.1 ± 6.7	NA
10 µg/ml (0.031 mM)	70.5 ± 34.9	NA
100 µg/ml (0.314 mM)	74.9 ± 11.5	NA

* ($p < 0.05$) Significantly different when compared to the control (DMSO)

NT = not tested due to toxicity

NA = not applicable

3. Phytochemical and biological studies of *Gastrochilus bellinus*

3.1 Preliminary biological activity evaluation

The air-dried samples of *Gastrochilus bellinus* (3.6 kg) were extracted with MeOH. The obtained MeOH extract was partitioned with EtOAc, *n*-BuOH and water to give corresponding fractions after removal of the solvent. Each of the extract and fractions was screened for α -glucosidase inhibitory activity. Although the initial MeOH extract showed only 4.3 % inhibition, the EtOAc fraction showed 77.7% inhibition of the enzyme. Thus, the EtOAc fraction was further studied to identify the constituents responsible for α -glucosidase inhibitory activity.

Table 25 α -Glucosidase inhibitory activity of extracts from *Gastrochilus bellinus*

Fraction	% inhibition at 100 μ g/ml
MeOH	4.3 \pm 3.5
EtOAc	77.7 \pm 2.4
BuOH	3.1 \pm 1.6
acarbose	21.9 \pm 1.5

3.2 Chemical investigation

Separation of the EtOAc fraction of *Gastrochilus bellinus* resulted in the isolation of four new compounds which included three phenanthropyrans, i.e. [348], [349] and [350], and a phenanthrene derivative [351].

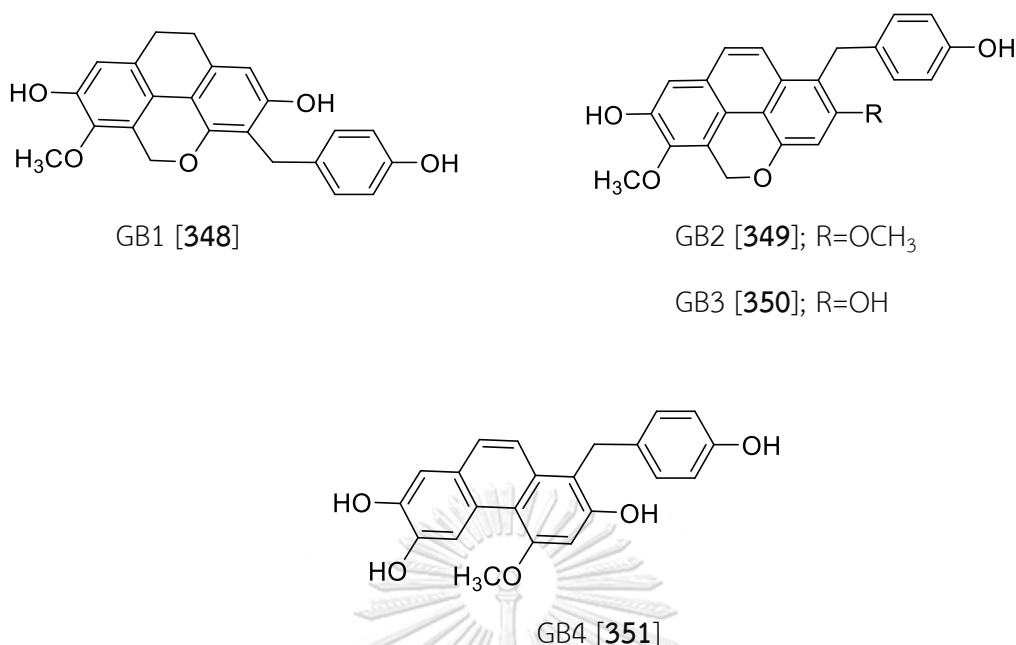


Figure 87 Structures of compounds isolated from *Gastrochilus bellinus*

3.2.1 Structure elucidation of compound GB1

Compound GB1 was collected as a brown amorphous solid. The high resolution APCI mass spectrum (**Figure 88**) showed a protonated molecular ion $[M+H]^+$ at m/z 377.1360 (calcd. for C₂₃H₂₁O₅ 377.1389), suggesting the molecular formula C₂₃H₂₀O₅. The UV spectrum of GB1 in MeOH showed maximal absorptions at 206 and 284 nm (**Figure 89**). The IR spectrum (**Figure 90**) displayed bands at 3360, 1659 and 1633 cm⁻¹. The ¹H-NMR spectrum (**Figure 91**) exhibited two pairs of methylene protons at δ 2.72 (4H, br s, H₂-9, H₂-10), two aromatic singlets signals at δ 6.40 (1H, s, H-1) and 6.69 (1H, s, H-8), two aromatic doublet peaks at δ 7.15 (2H, d, J = 8.4 Hz, H-2', H-6') and 6.66 (2H, d, J = 8.4 Hz, H-3', H-5'), one methoxy signals at δ 3.79 (3H, s, 6-OMe), a pair of methylene protons at 3.88 (2H, s, H- α'). The two-proton singlet at δ 5.17 (2H, s) indicated the presence of oxymethylene protons of the 9,10-dihydrophenanthropyran. The proton signals at δ 7.15 (2H, d, J = 8.4 Hz, H-2', H-6') and 6.66 (2H, d, J = 8.4 Hz, H-3', H-5') suggested a *para*-substituted aromatic ring. The

^{13}C -NMR spectrum (**Figure 92**) revealed 23 carbon signals. As expected, an oxygen-bearing methylene carbon appeared at δ 63.3 (C-11). The HSQC spectrum (**Figure 93**) displayed correlations for protonated carbons. The HMBC spectrum (**Figure 94**) showed that H₂-11 (δ 5.17) had 3-bond correlation with C-6 (δ 141.7) and C-4 (δ 150.8). The HMBC correlation from H- α' (δ 3.88) to C-4 (δ 150.8) and C-2'/6' (δ 129.4) connected the 9,10-dihydrophenanthropyran with the 4-hydroxy benzyl skeleton. The NOESY spectrum (**Figure 95**) displayed NOE correlation of H- α' (δ 3.88) with H-2' (δ 7.15) and H-6' (δ 7.15).

Based on the NMR data, GB1 was determined as a new dihydrophenanthropyran derivative [349].

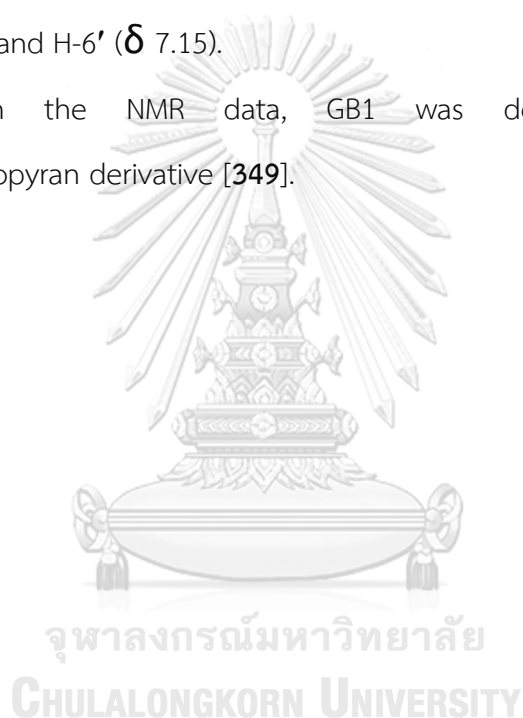
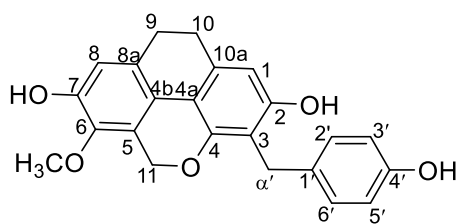


Table 26 NMR spectral data of compound GB1

Position	δ_{H} (mult., J in Hz)	δ_{C}	HMBC (correlation with ^1H)
1	6.40 (1H, s)	108.0	10
2	-	154.8	α'
3	-	114.5	1, α'
4	-	150.8	α' , 11
4a	-	111.8	1, 10
4b	-	119.6	8, 9, 11
5	-	121.3	11*
6	-	141.7	8, 11, 6-OMe
7	-	148.4	-
8	6.69 (1H, s)	114.9	9
8a	-	128.6	10
9	2.72 (1H, br s)	27.1	8
10	2.72 (1H, br s)	27.6	1
10a	-	132.4	9
11	5.17 (2H, s)	63.3	-
α'	3.88 (2H, s)	27.6	2', 6'
1'	-	132.6	α' *, 3', 5'
2'	7.15 (1H, d, 8.7)	129.4	α' , 6'
3'	6.66 (1H, d, 8.7)	114.6	5'
4'	-	155.2	2', 6'
5'	6.66 (1H, d, 8.7)	114.6	3'
6'	7.15 (1H, d, 8.7)	129.4	α' , 2'
6-OMe	3.79 (s)	60.4	-

*= two-bond coupling



[348]

Display Report

Analysis Info		Acquisition Date	2/14/2020 10:32:40 AM
Analysis Name	D:\Data\SEC\Gbel-15A.d	Operator	CTB
Method	tune_low.m	Instrument	micrOTOF-Q II 10414
Sample Name	Gbel-15A		
Comment			

Acquisition Parameter			
Source Type	APCI	Ion Polarity	Positive
Focus	Not active	Set Capillary	4500 V
Scan Begin	50 m/z	Set End Plate Offset	-500 V
Scan End	3000 m/z	Set Collision Cell RF	150.0 Vpp
		Set Nebulizer	1.6 Bar
		Set Dry Heater	200 °C
		Set Dry Gas	8.0 l/min
		Set Divert Valve	Waste

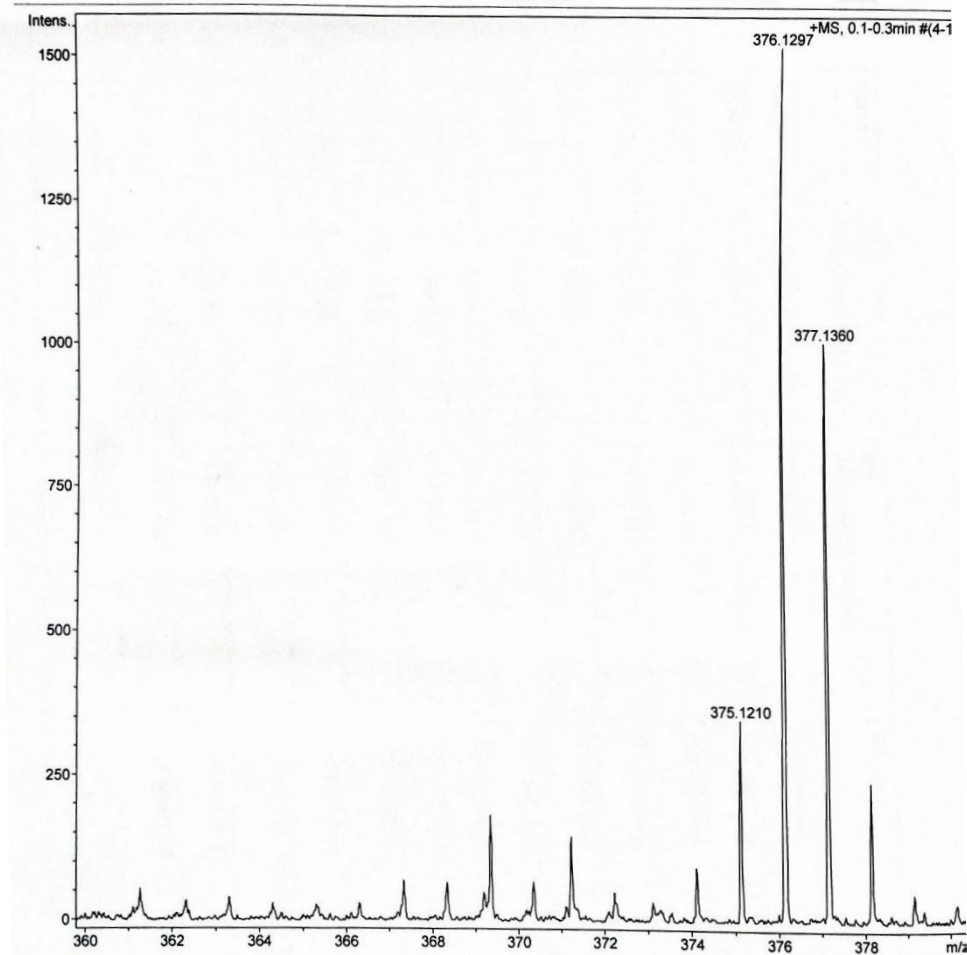


Figure 88 Mass spectrum of compound GB1

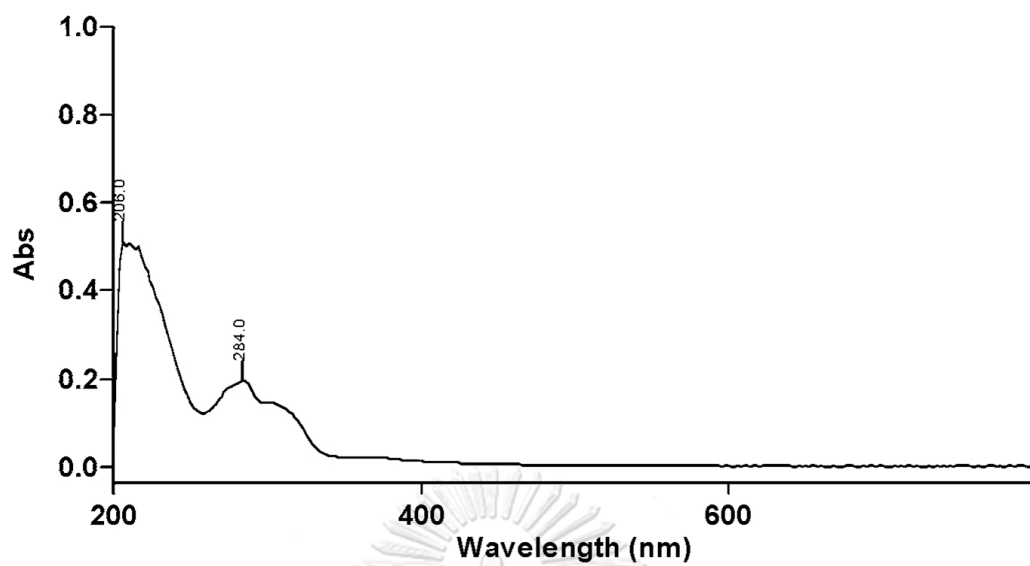


Figure 89 UV spectrum of compound GB1

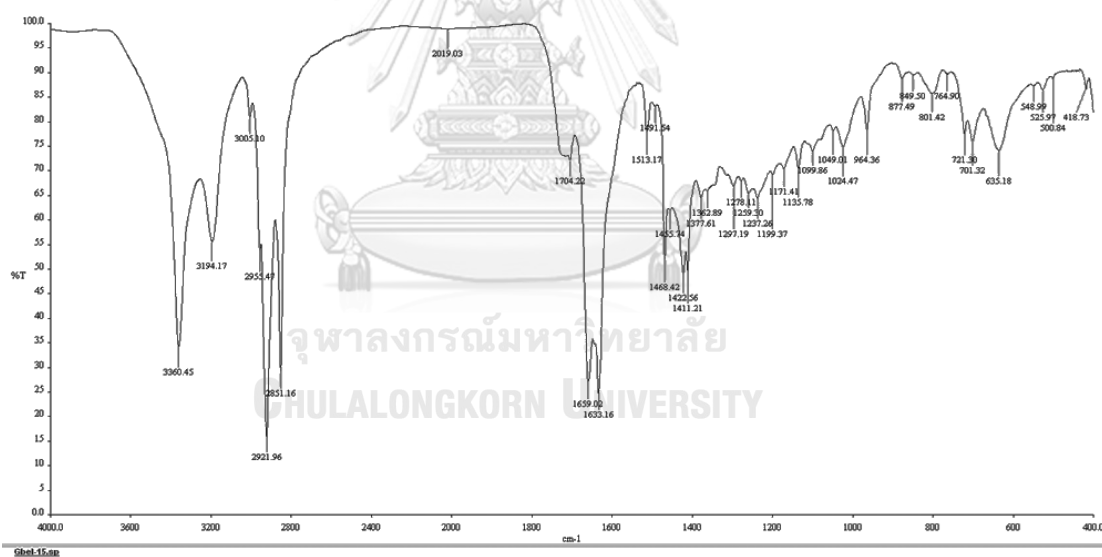
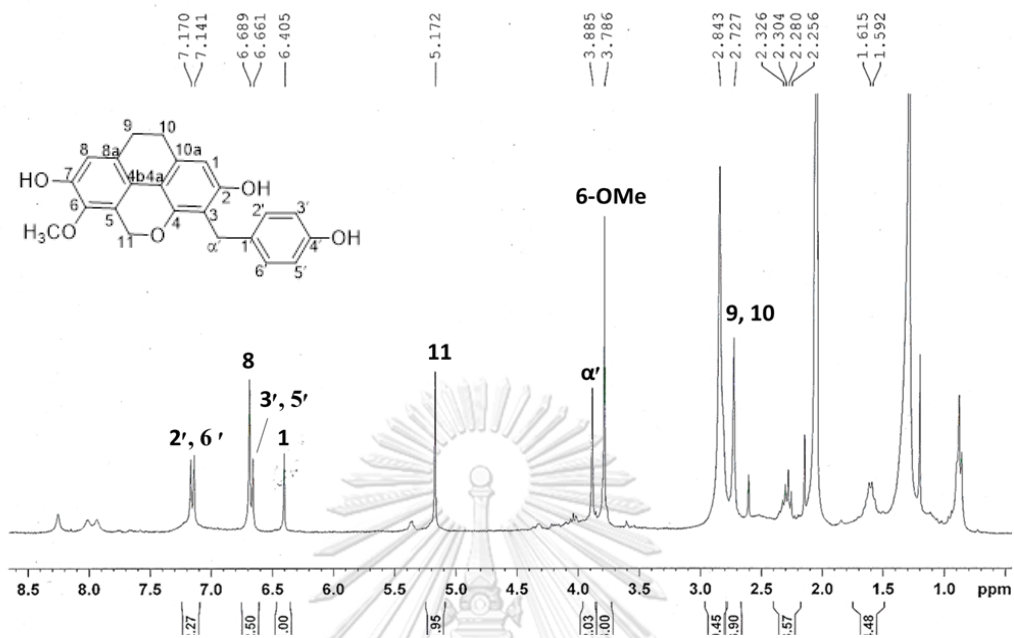
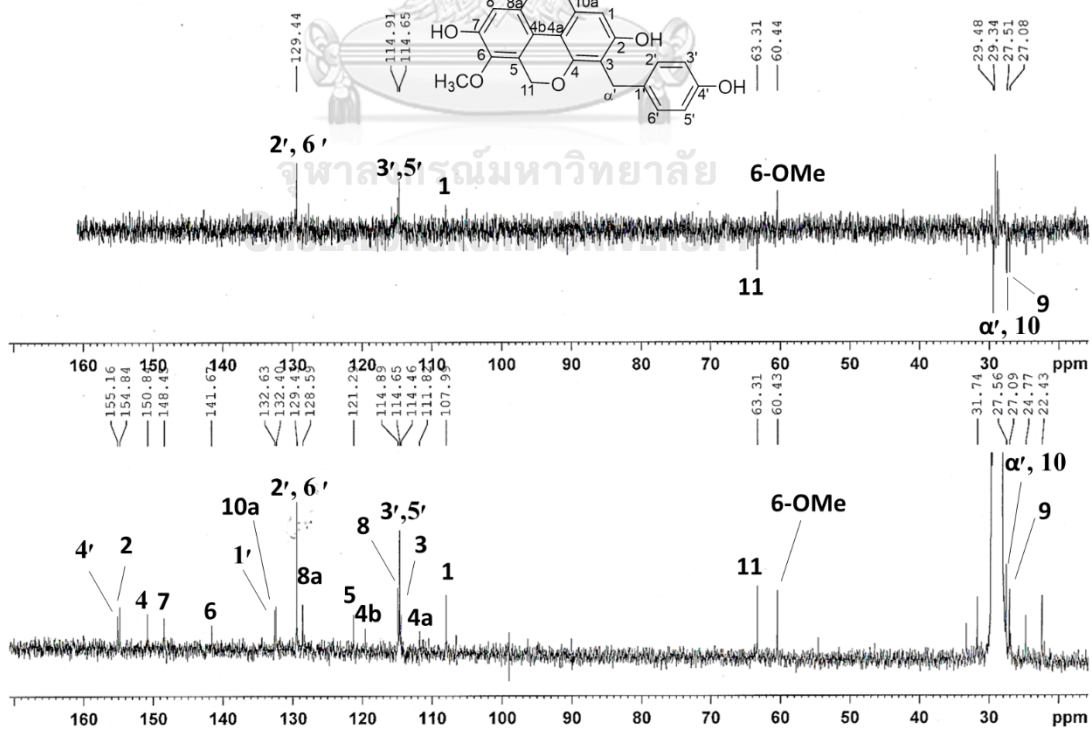


Figure 90 IR spectrum of compound GB1

Gbel15A 1H NMR 300 MHz in acetone-d6

Figure 91 ¹H-NMR (300 MHz) spectrum of compound GB1 (acetone-d₆)

Gbel15A 13C NMR 75 MHz in acetone-d6

Figure 92 ¹³C-NMR (75 MHz) and DEPT-135 spectra of compound GB1 (acetone-d₆)

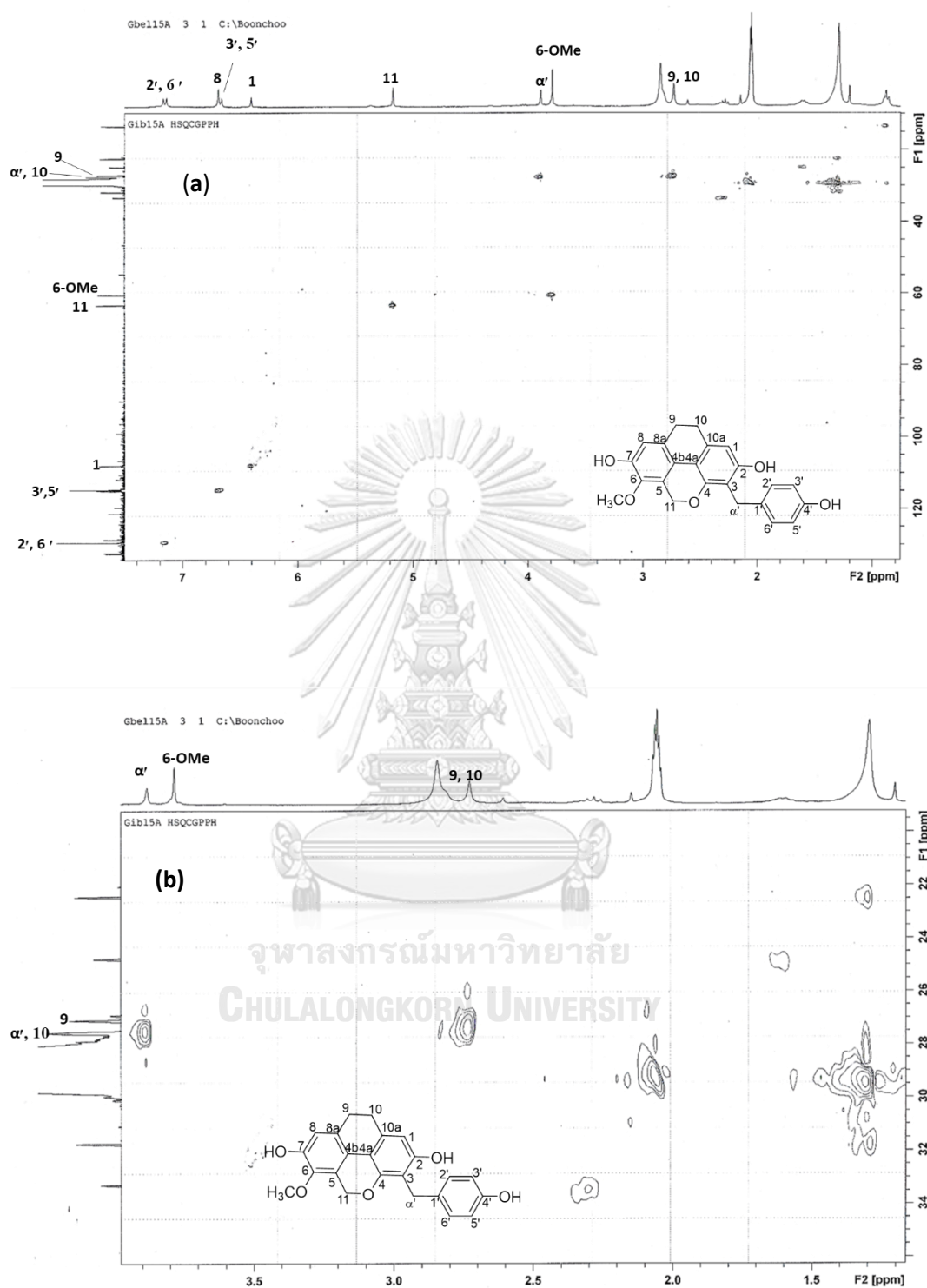


Figure 93 HSQC spectrum of compound GB1

(a) full spectrum; (b) expansion [δ_{H} 1.2-3.9 ppm, δ_{C} 20-36 ppm]

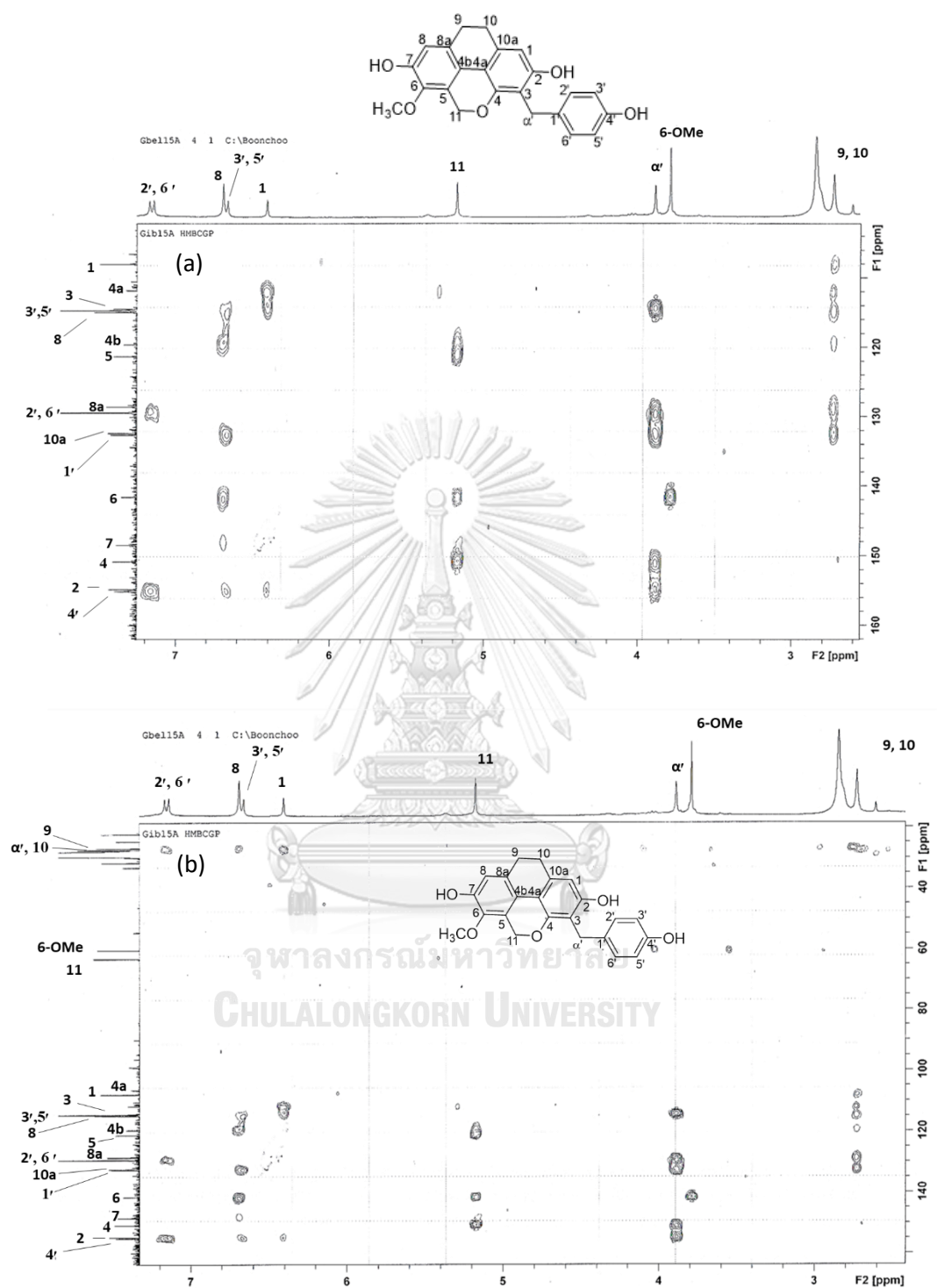


Figure 94 HMBC spectrum of compound GB1

(a) full spectrum; (b) expansion [δ_{H} 2.4-7.2 ppm, δ_{C} 100-160 ppm]

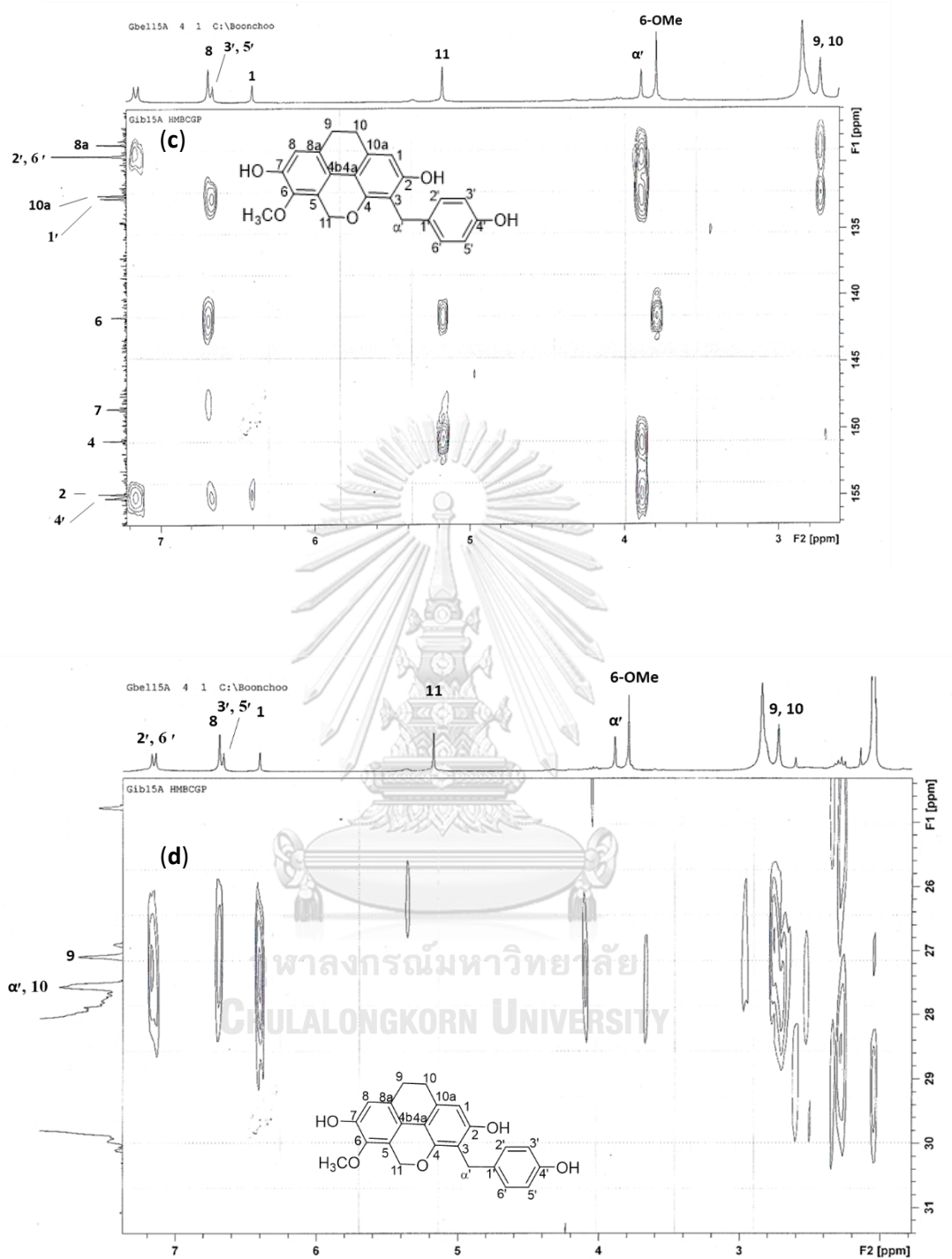


Figure 94 HMBC spectrum of compound GB1 (continued)

(c) expansion [δ_H 2.6-7.2 ppm, δ_C 125-157 ppm];

(d) expansion [δ_H 1.8-7.4 ppm, δ_C 22-33 ppm]

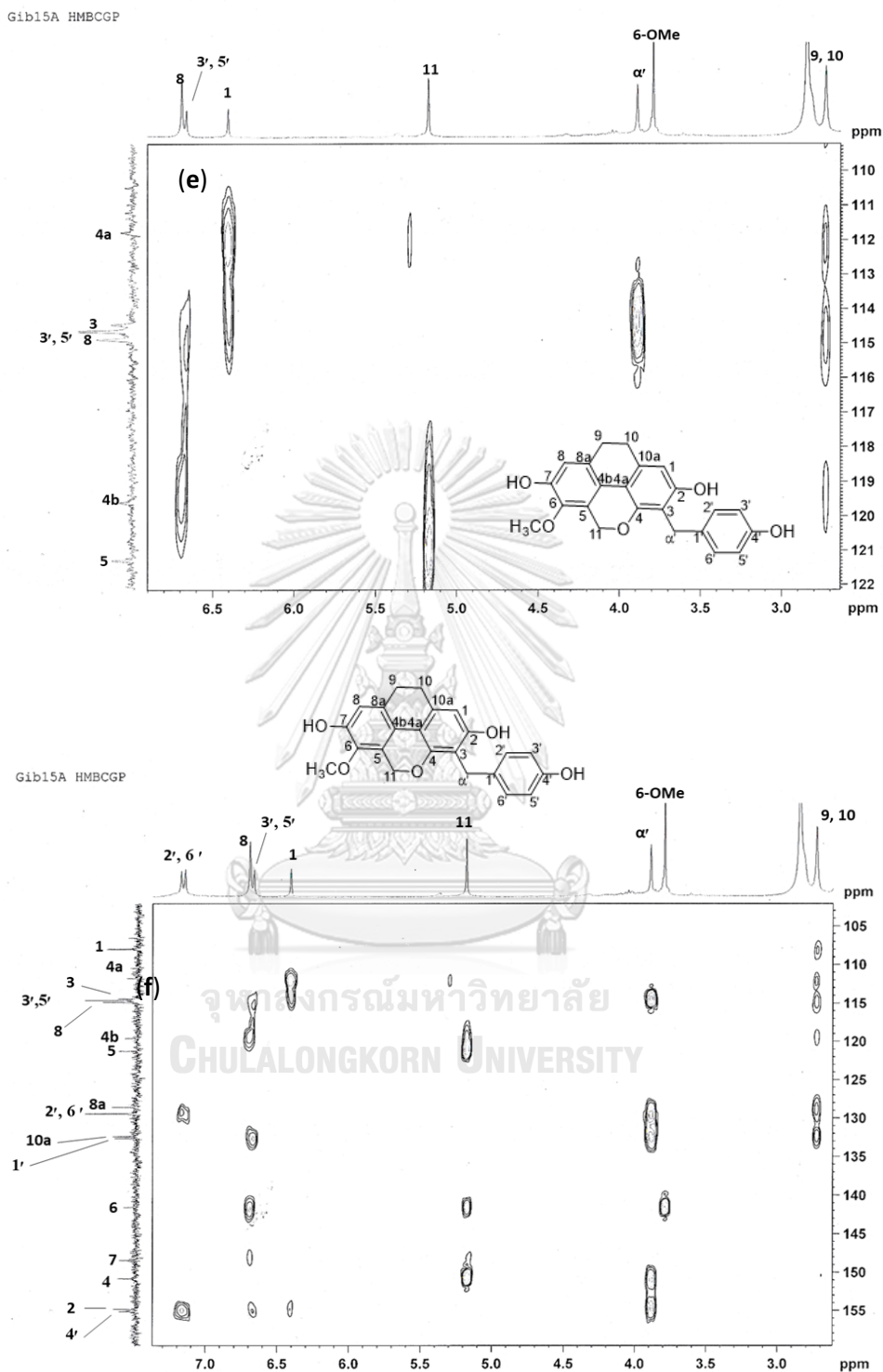


Figure 94 HMBC spectrum of compound GB1 (continued),

(e) expansion [δ_{H} 2.5-7.0 ppm, δ_{C} 108-122 ppm];

(f) expansion [δ_{H} 2.5-7.4 ppm, δ_{C} 109-150 ppm]

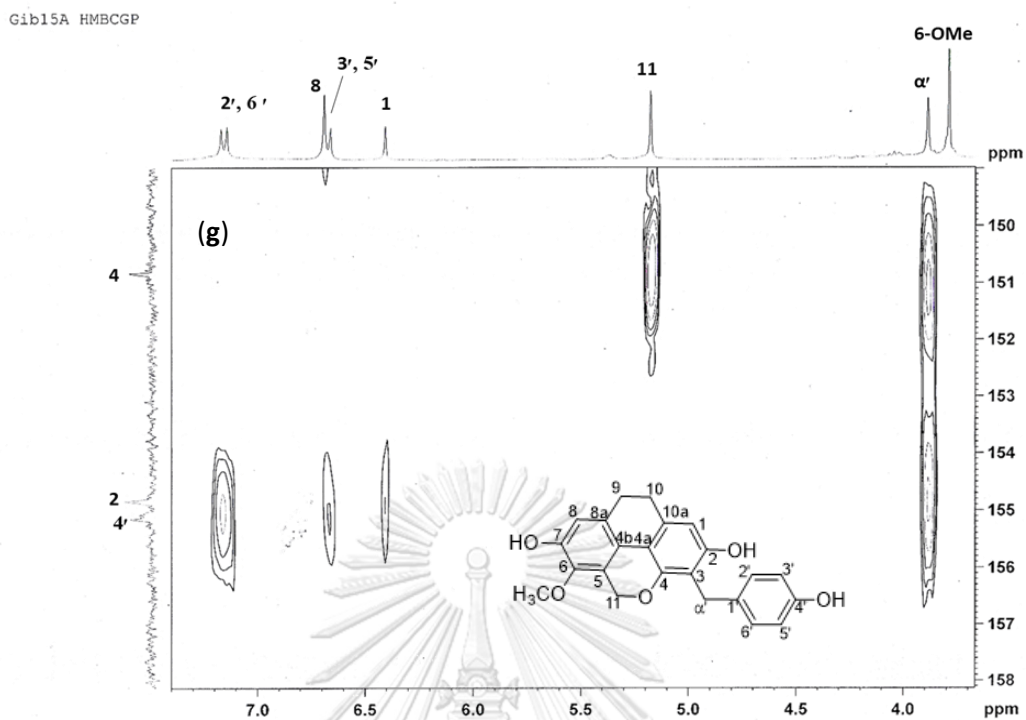


Figure 94 HMBC spectrum of compound GB1 (continued)

(g) expansion [δ_H 3.5-7.5 ppm, δ_C 149-158 ppm]

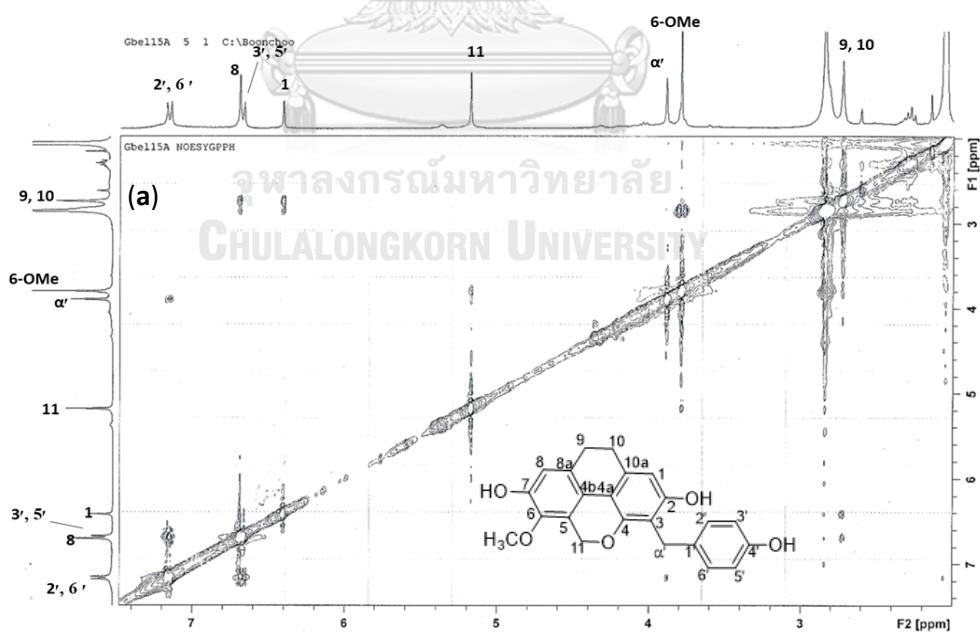


Figure 95 NOESY spectrum of compound GB1

(a) full spectrum

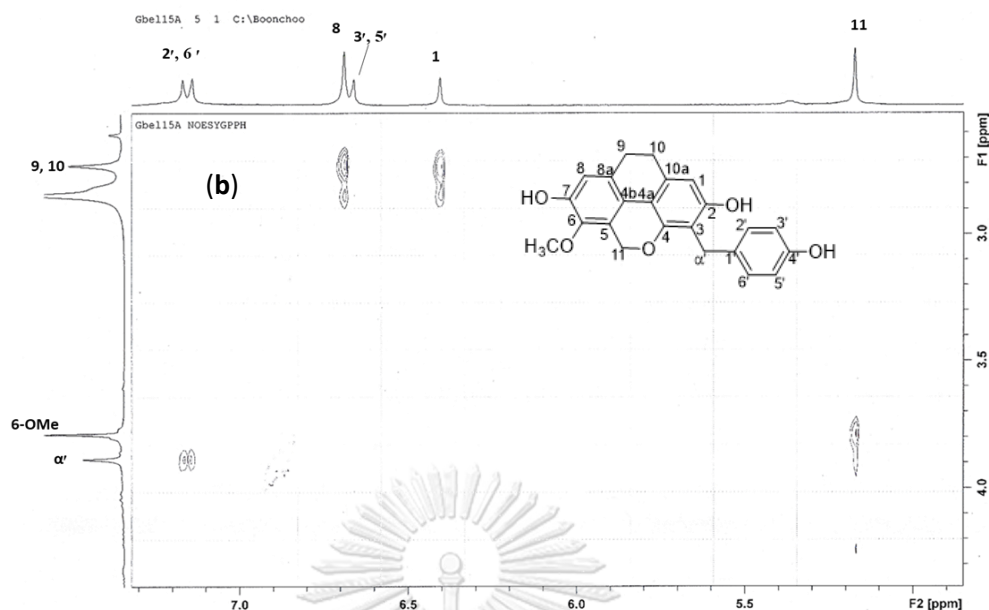


Figure 95 NOESY spectrum of compound GB1 (continued)

(b) expansion [$F_1 \delta_H$ 2.5-4.5 ppm, $F_2 \delta_H$ 4.8-7.3 ppm]

3.2.2 Structure elucidation of compound GB2

Compound GB2 was obtained as a brown amorphous solid. The high resolution APCI mass spectrum of GB2 (**Figure 96**) showed a protonated molecular ion $[M+H]^+$ at m/z 389.1351 (calcd. for $C_{24}H_{21}O_5$ 389.1389), suggesting the molecular formula $C_{24}H_{20}O_5$. The UV spectrum of GB2 (MeOH) showed maximum absorptions at 205, 225, 270 and 380 nm (**Figure 97**), which were similar to those of 1-(4'-hydroxybenzyl)-imbricatin (Dong *et al.*, 2013). The IR spectrum (**Figure 98**) displayed strong absorption bands at 3360, 1658 and 1633 cm^{-1} .

The 1H -NMR spectrum (**Figure 99**) exhibited olefinic protons with *cis*-configuration at δ 7.55 (1H, d, $J = 9.3$ Hz, H-9) and 7.78 (1H, d, $J = 9.3$ Hz, H-10), aromatic protons at δ 6.91 (1H, s, H-3), 7.25 (1H, s, H-8), 7.01 (2H, d, $J = 8.4$ Hz, H-2', H-6') and 6.66 (2H, d, $J = 8.4$ Hz, H-3', H-5'). A pair of oxymethylene protons appeared at δ 5.64 (2H, s), indicating the presence of a phenanthropyran structure. In

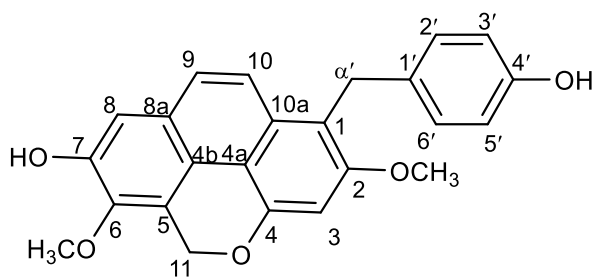
addition, resonances for two methoxy groups at δ 3.94 (3H, s, 2-OMe) and 3.93 (3H, s, 6-OMe), a pair of methylene protons at 4.29 (2H, s, H- α') were also observed. The coupling system of protons at δ 7.01 (2H, d, J = 8.4 Hz, H-2', H-6') and 6.66 (2H, d, J = 8.4 Hz, H-3', H-5') suggested a *p*-substituted aromatic ring. The ^{13}C -NMR and DEPT spectra (**Figure 100**) revealed twenty-four carbon signals representing twenty olefinic/aromatic and four aliphatic carbons. The signal at δ 63.8 (C-11) was reminiscent of an oxymethylene group. The HSQC spectrum (**Figure 101**) displayed 1-bond C-H couplings. The HMBC spectrum (**Figure 102**) showed that H-11 (δ 5.64) had 3-bond correlation with C-6 (δ 143.3) and C-4 (δ 151.5). The HMBC connectivities from H- α' (δ 4.29) to C-1 (δ 116.1), C-2 (δ 156.2), C-10a (δ 129.5), C-1' (δ 132.4), C-2' (δ 129.0) and C-6' (δ 129.0) confirmed the linkage between the phenanthropyran core structure and the *p*-hydroxybenzyl moiety. In support of the connection of the two units, NOESY correlations were found from H- α' (δ 4.29) to H-2' (δ 7.01) and H-10 (δ 7.78) (**Figure 103**). The methoxy groups were placed at C-2 and C-6 from the NOESY peaks between H-3 (δ 6.91) and 2-OMe protons, and between H-11 (δ 5.64) and 6-OMe protons (δ 3.93).

Based on the above NMR data, compound GB2 was characterized as a new compound with the structure as shown [349]. It can be considered as a phenanthropyran derivative possessing an unusual *p*-hydroxybenzyl moiety at C-1. All the ^1H and ^{13}C NMR data of 349 are summarized in **Table 27**.

Table 27 NMR spectral data of compound GB2

Position	δ_{H} (mult., J in Hz)	δ_{C}	HMBC (correlation with ^1H)
1	-	116.1	3, 10, α' *
2	-	156.2	3*, α' , 2-OMe
3	6.91 (1H, s)	98.2	-
4	-	151.5	3*, 11
4a	-	112.1	3, 10
4b	-	118.1	8, 9, 11
5	-	120.1	11*
6	-	143.3	8, 11, 6-OMe
7	-	149.6	8*
8	7.25 (1H, s)	110.9	9
8a	-	125.2	10
9	7.55 (1H, d, 9.3)	125.8	8
10	7.78 (1H, d, 9.3)	122.6	-
10a	-	129.5	9, α'
11	5.64 (2H, s)	63.8	-
α'	4.29 (2H, s)	28.9	2, 2' , 6'
1'	-	132.4	α' *, 3' , 5'
2'	7.01 (1H, d, 8.4)	129.0	α' , 6'
3'	6.66 (1H, d, 8.4)	114.9	5'
4'	-	155.2	2' , 6'
5'	6.66 (1H, d, 8.4)	114.9	3'
6'	7.01 (1H, d, 8.4)	129.0	α' , 2'
2-OMe	3.94 (3H, s)	55.8	-
6-OMe	3.93 (3H, s)	60.4	-

*= two-bond coupling



[349]

Display Report

Analysis Info		Acquisition Date	2/14/2020 10:37:03 AM
Analysis Name	D:\Data\SEC\Gbel-20.d	Operator	CTB
Method	tune_low.m	Instrument	microTOF-Q II 10414
Sample Name	Gbel-24		
Comment			

Acquisition Parameter					
Source Type	APCI	Ion Polarity	Positive	Set Nebulizer	1.6 Bar
Focus	Not active	Set Capillary	4500 V	Set Dry Heater	200 °C
Scan Begin	50 m/z	Set End Plate Offset	-500 V	Set Dry Gas	8.0 l/min
Scan End	3000 m/z	Set Collision Cell RF	150.0 Vpp	Set Divert Valve	Waste

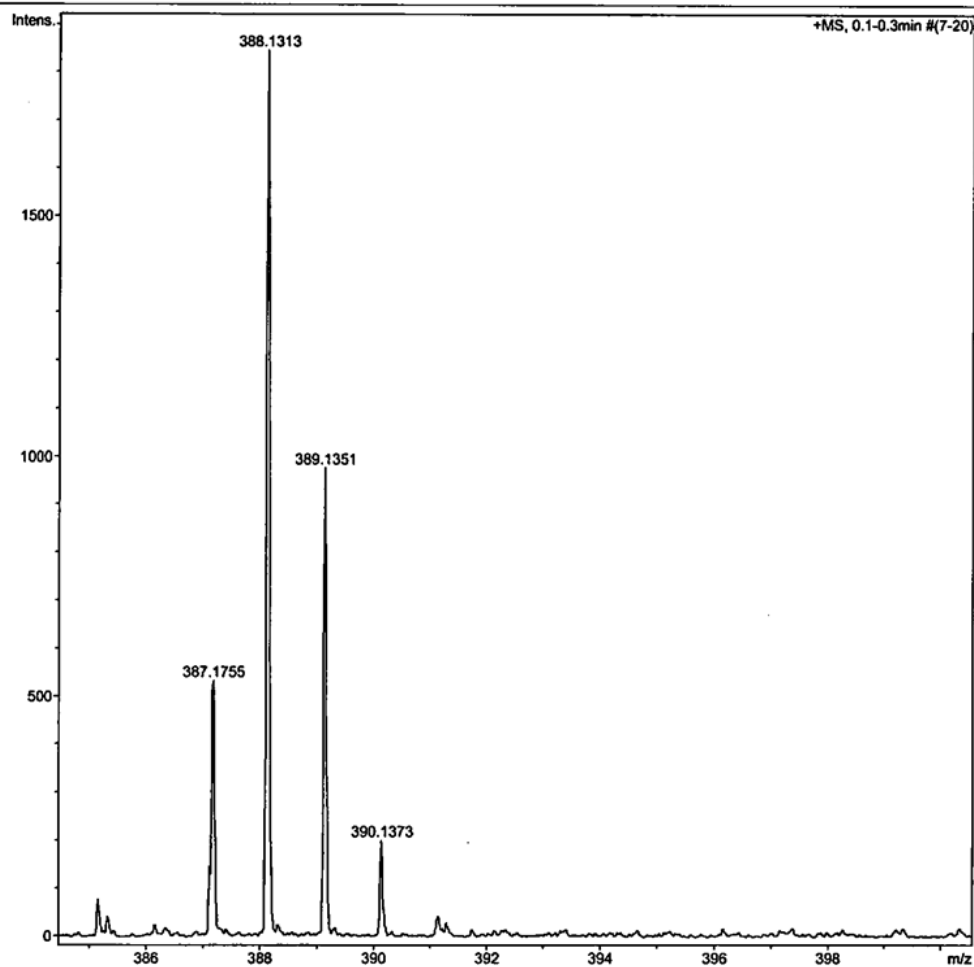


Figure 96 Mass spectrum of compound GB2

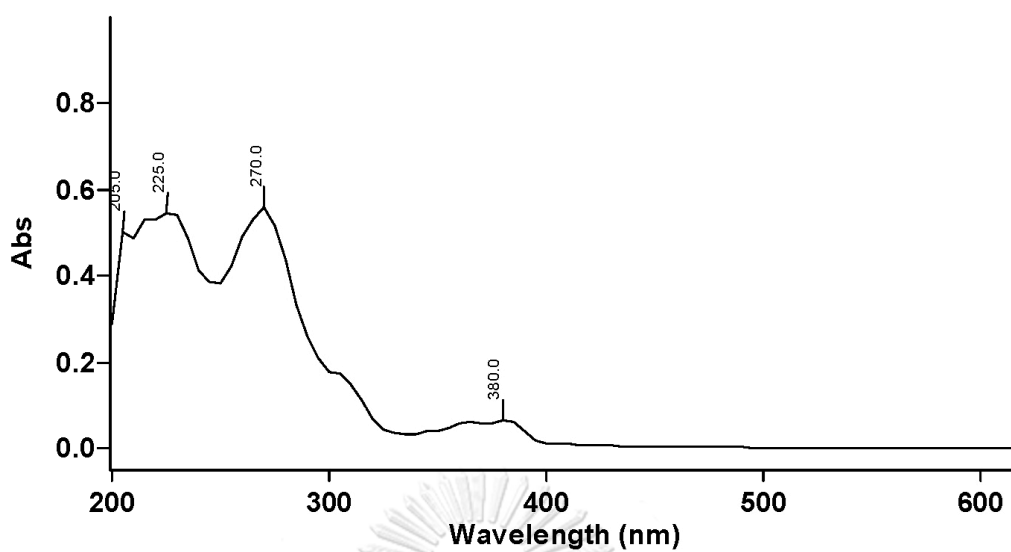


Figure 97 UV spectrum of compound GB2

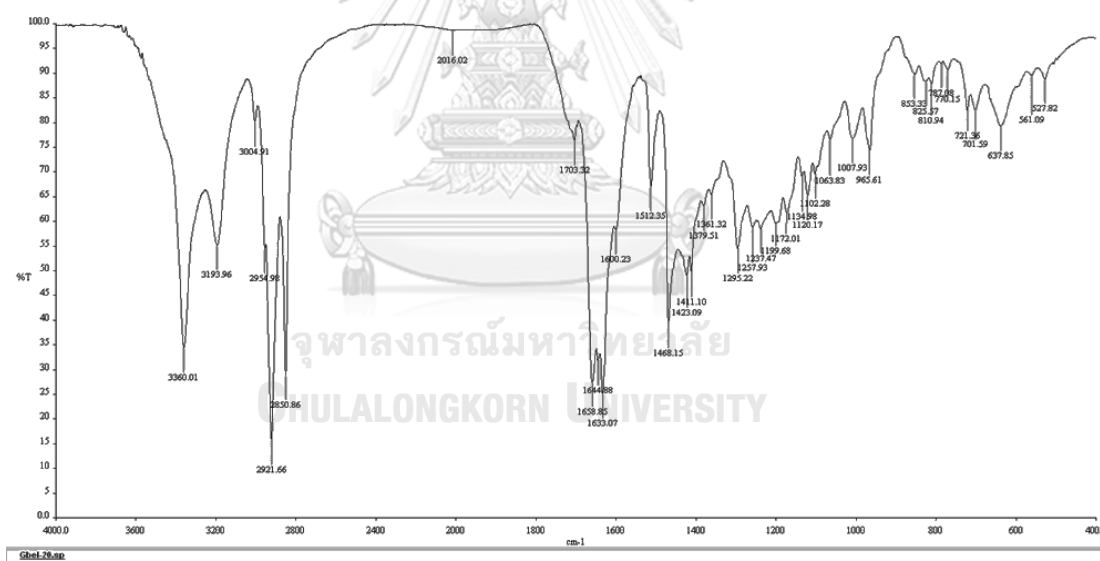


Figure 98 IR spectrum of compound GB2

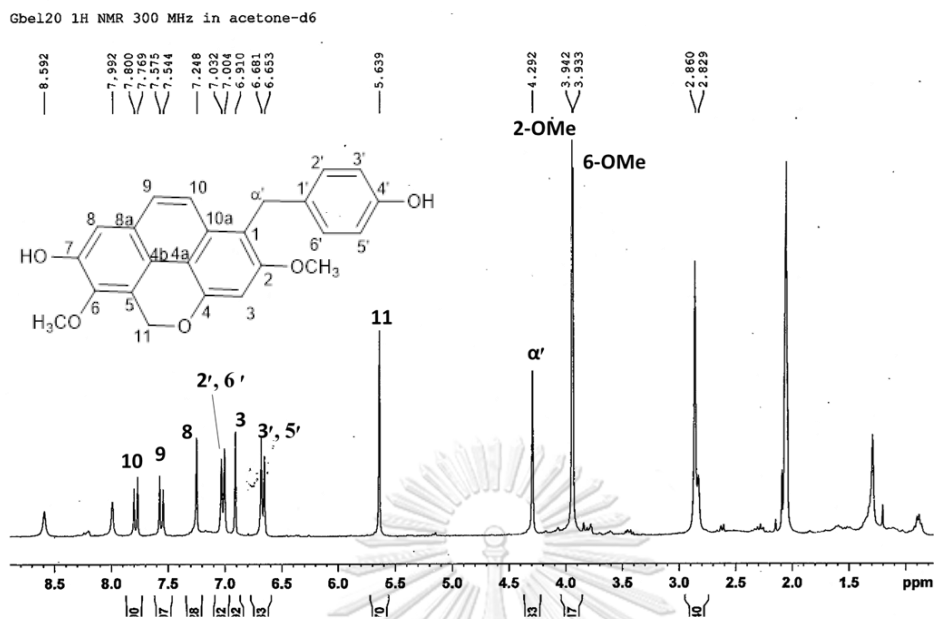


Figure 99 ¹H-NMR (300 MHz) spectrum of compound GB2 (acetone-d₆)

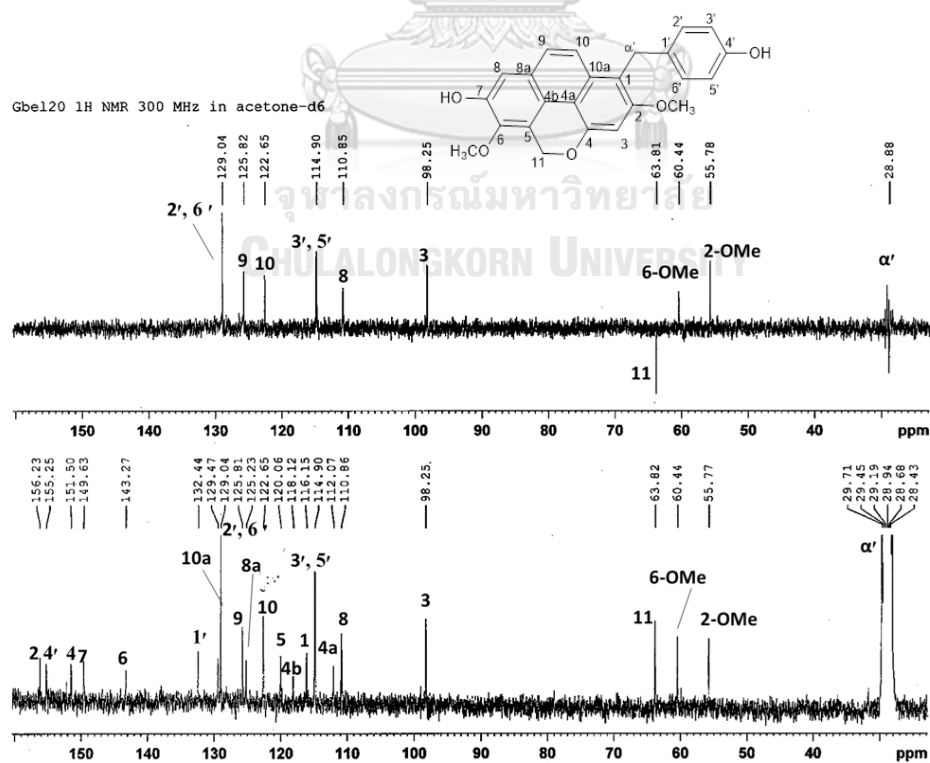


Figure 100 ¹³C-NMR (75 MHz) and DEPT-135 spectra of compound GB2 (acetone-d₆)

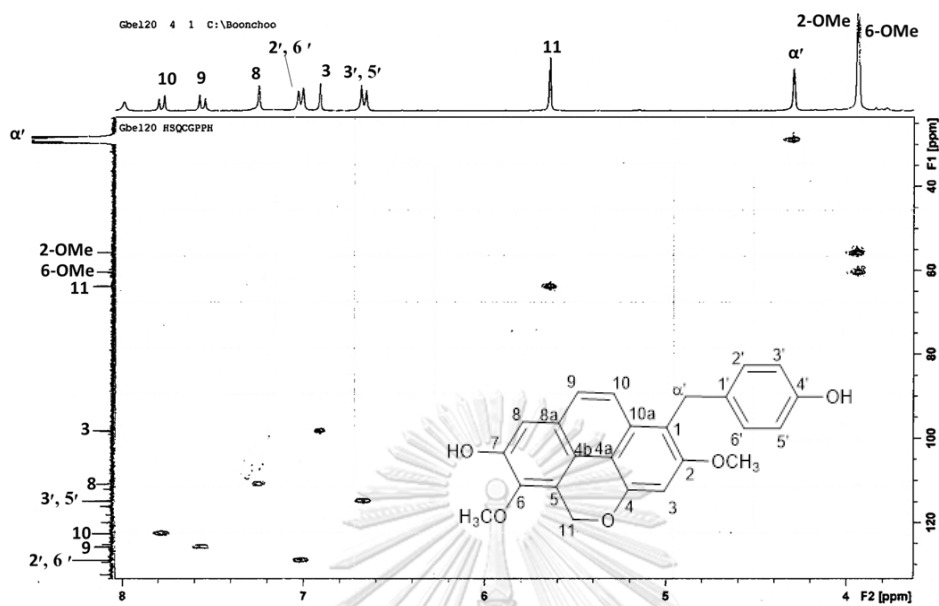


Figure 101 HSQC spectrum of compound GB2

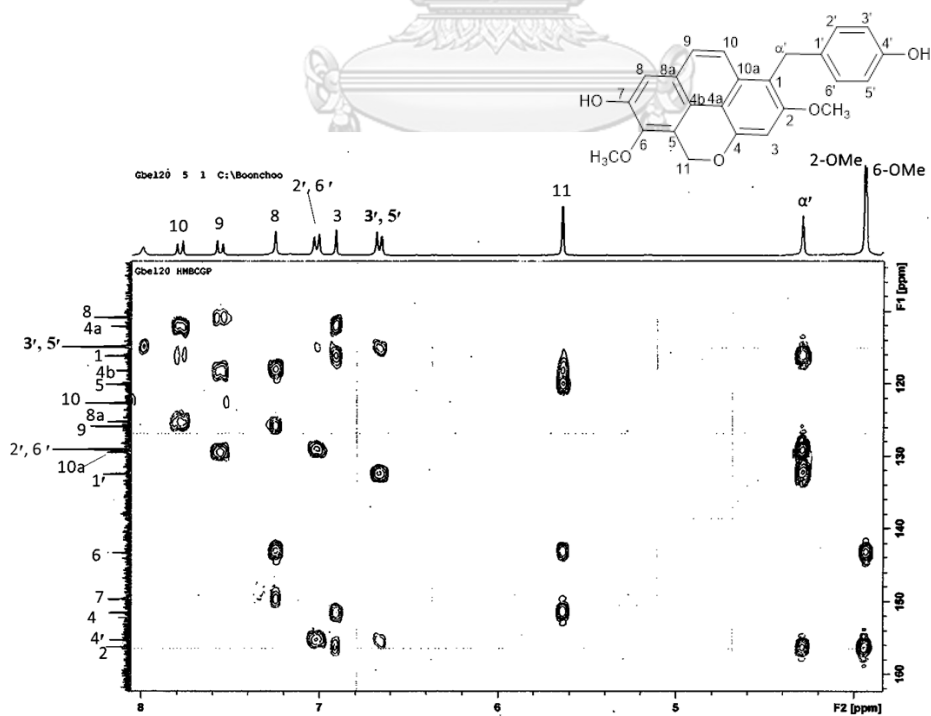


Figure 102 HMBC spectrum of compound GB2

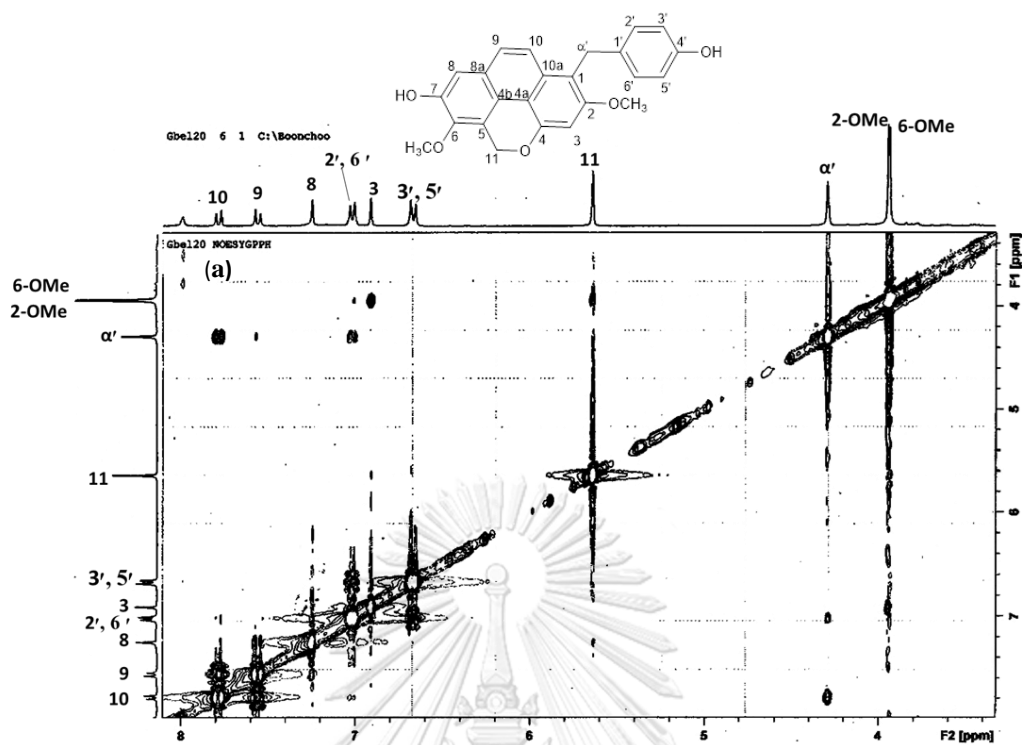


Figure 103 NOESY spectrum of compound GB2

(a) full spectrum

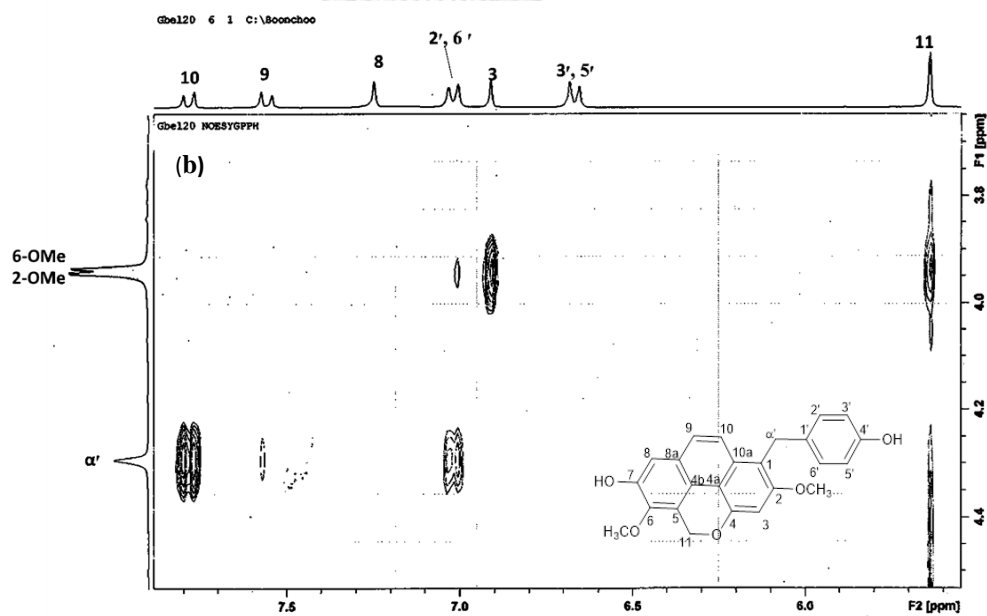


Figure 103 NOESY spectrum of compound GB2 (continued)

(b) Expansion [$F_1 \delta_H$ 3.6-4.5 ppm, $F_2 \delta_H$ 5.5-8.0 ppm]

3.2.2 Structure elucidation of compound GB3

Compound GB3 was collected as a brown amorphous solid. The high resolution APCI mass spectrum (**Figure 104**) showed a protonated molecular ion $[M+H]^+$ at m/z 375.1214 (calcd. for $C_{23}H_{19}O_5$ 375.1232), suggesting the molecular formula $C_{23}H_{18}O_5$. The UV maximal absorptions at 225, 270, 365 and 380 nm of compound GB3 (**Figure 105**) were similar to those of GB2, suggesting the same basic skeleton. The IR spectrum (**Figure 106**) displayed strong absorption bands at 3354, 1652 and 1614 cm^{-1} . The 1H and ^{13}C NMR and DEPT spectra of compound GB3 (**Figures 107 and 108**) exhibited signals similar to those of GB2 except that GB3 had only one methoxy group that showed a cross peak at δ_H 3.92 (3H, s, 6-OMe)/ δ_C 60.4 in the HSQC spectrum (**Figure 109**). The position of the methoxy group was deduced from the NOESY cross peak between these methoxyl protons and H-11. In the HMBC spectrum (**Figure 110**), H-11 (δ 5.60) showed 3-bond correlation with C-6 (δ 143.2) which was also correlated to the 6-OMe protons. The HMBC correlation from H- α' (δ 4.29) to C-2, C-2', C-6' and C-10a confirmed the linkage between the phenanthropyran structure and the *p*-hydroxybenzyl moiety.

Based on the aforementioned NMR data, compound GB3 was characterized as a new compound with the structure [350] as shown. It could be considered as a de-2-O-methyl derivative of GB2.

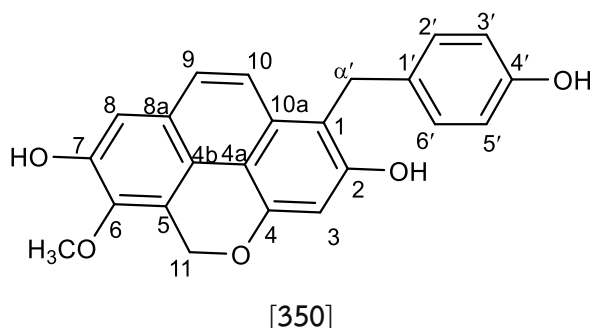


Table 28 NMR spectral data of compound GB3

Position	δ_{H} (mult., J in Hz)	δ_{C}	HMBC (correlation with ^1H)
1	-	114.0	3, 10, α' *
2	-	153.7	3*, α'
3	6.79 (1H, s)	101.8	-
4	-	151.0	3*, 11
4a	-	111.9	3, 10
4b	-	118.4	8, 9, 11
5	-	119.9	11*
6	-	143.2	8, 11, 6-OMe
7	-	149.4	8*
8	7.23 (1H, s)	110.7	9
8a	-	125.0	10
9	7.53 (1H, d, 9.3)	125.5	8
10	7.75 (1H, d, 9.3)	122.6	-
10a	-	129.9	9, α'
11	5.60 (2H, s)	63.7	-
α'	4.31 (2H, s)	29.0	2', 6'
1'	-	132.6	α' *, 3', 5'
2'	7.07 (1H, d, 8.4)	129.1	α' , 6'
3'	6.67 (1H, d, 8.4)	114.9	5'
4'	-	155.2	2', 6'
5'	6.67 (1H, d, 8.4)	114.9	3'
6'	7.07 (1H, d, 8.4)	129.1	α' , 2'
6-OMe	3.92 (3H, s)	60.4	-

*= two-bond coupling

Display Report

Analysis Info		Acquisition Date	2/14/2020 10:40:04 AM
Analysis Name	D:\Data\SEC\Gbel-21.d	Operator	CTB
Method	tune_low.m	Instrument	micrOTOF-Q II 10414
Sample Name	Gbel-21		
Comment			

Acquisition Parameter					
Source Type	APCI	Ion Polarity	Positive	Set Nebulizer	1.6 Bar
Focus	Not active	Set Capillary	4500 V	Set Dry Heater	200 °C
Scan Begin	50 m/z	Set End Plate Offset	-500 V	Set Dry Gas	8.0 l/min
Scan End	3000 m/z	Set Collision Cell RF	150.0 Vpp	Set Divert Valve	Waste

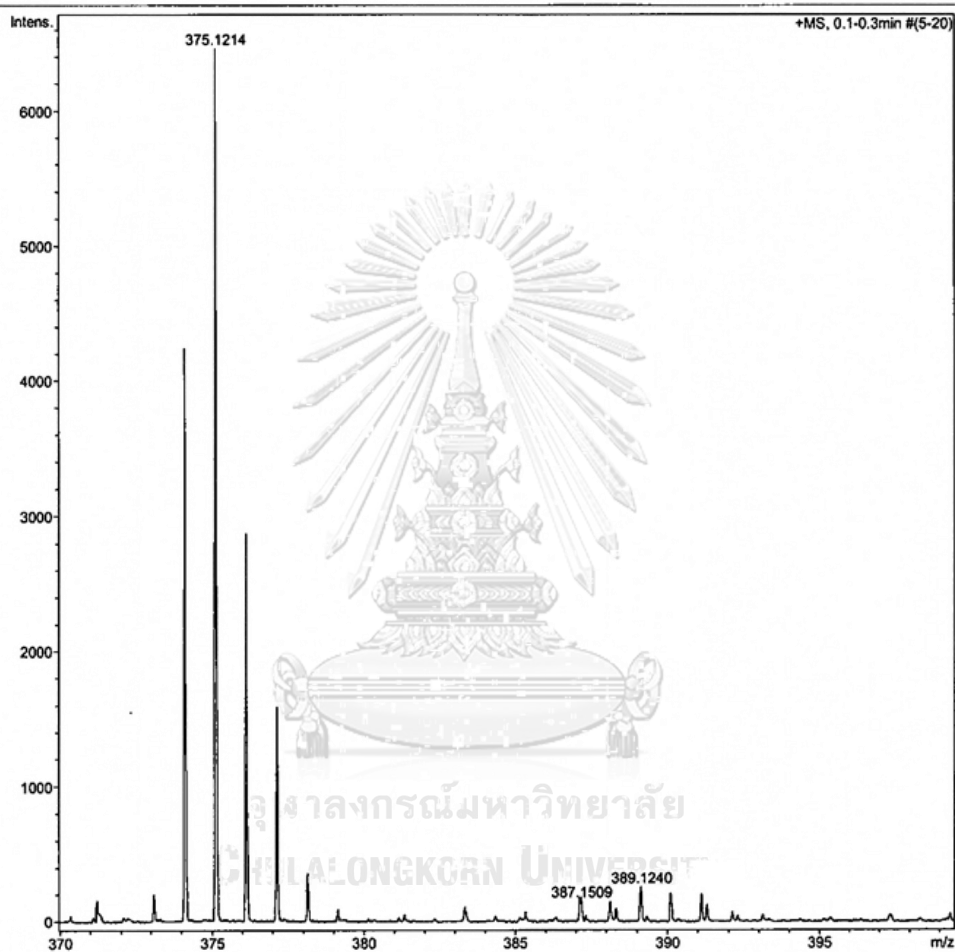


Figure 104 Mass spectrum of compound GB3

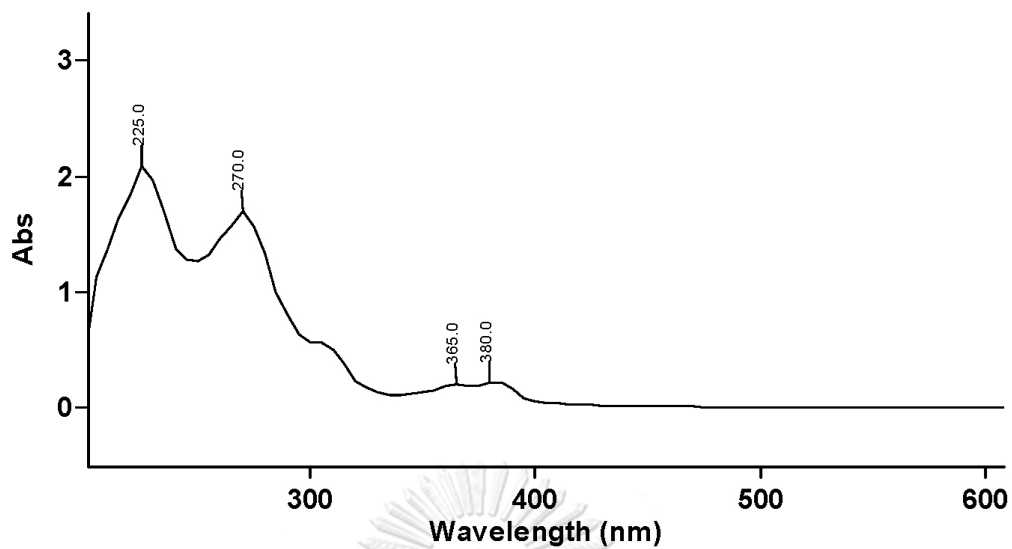


Figure 105 UV spectrum of compound GB3

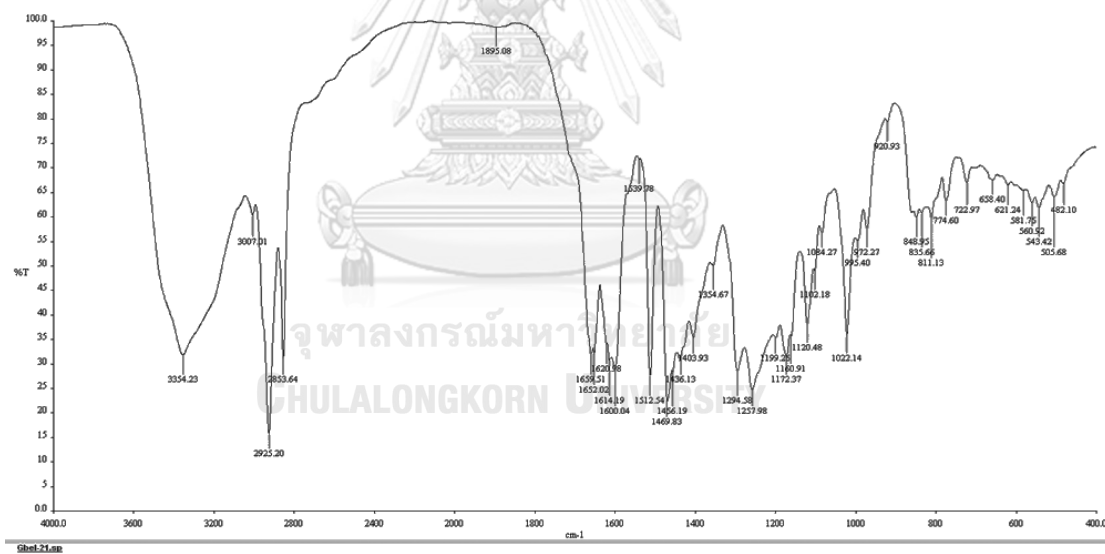


Figure 106 IR spectrum of compound GB3

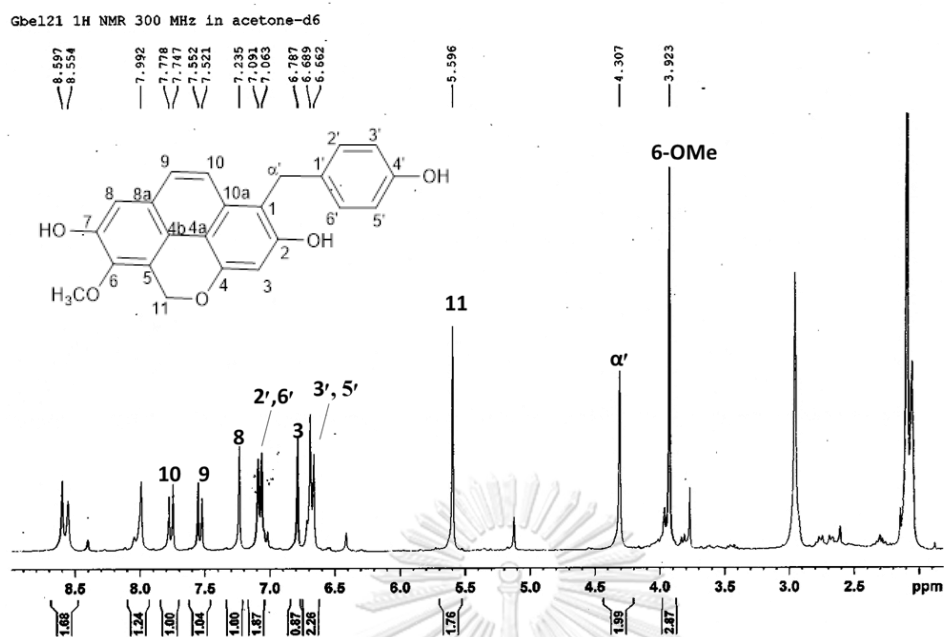


Figure 107 ¹H-NMR (300 MHz) spectrum of compound GB3 (acetone-*d*₆)

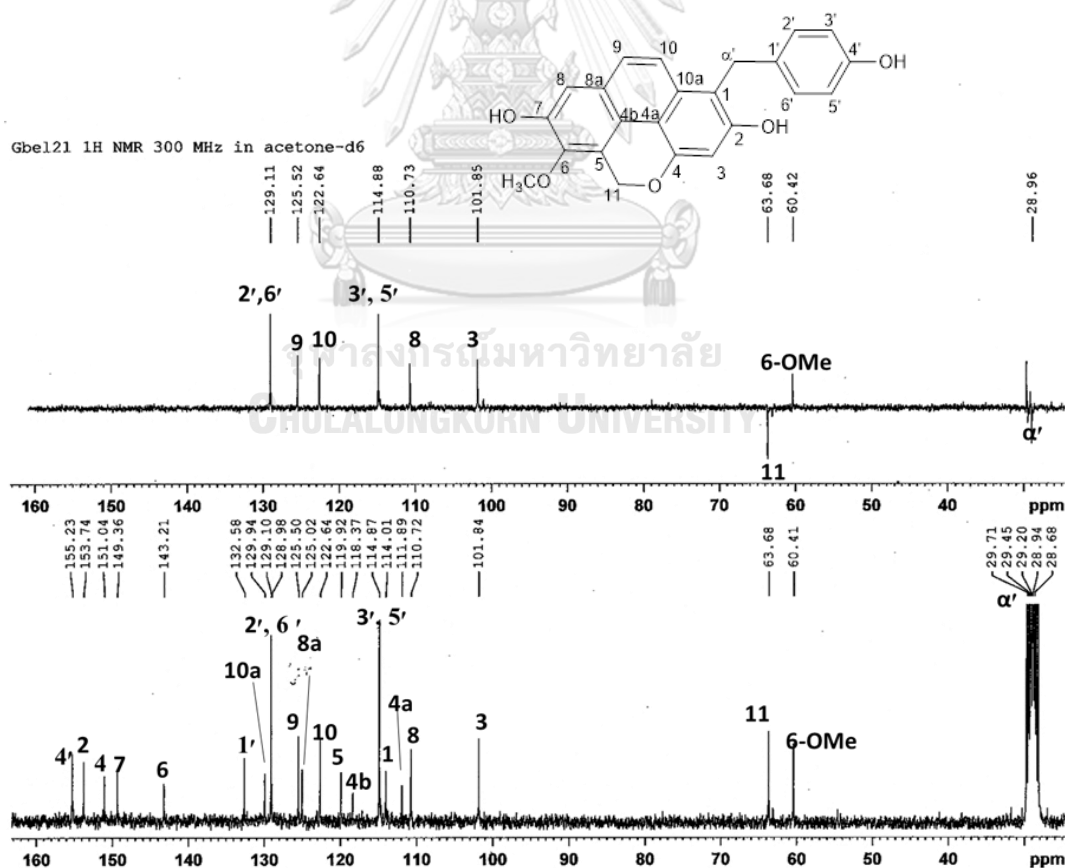


Figure 108 ¹³C-NMR (75 MHz) and DEPT-135 spectra of compound GB3 (acetone-*d*₆)

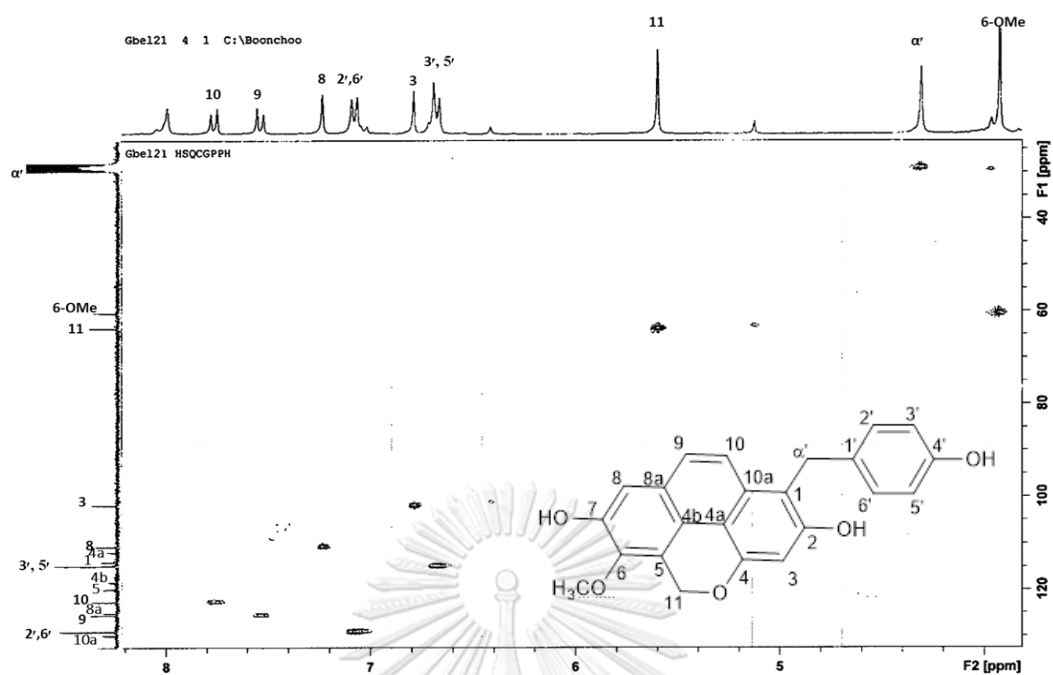


Figure 109 HSQC spectrum of compound GB3

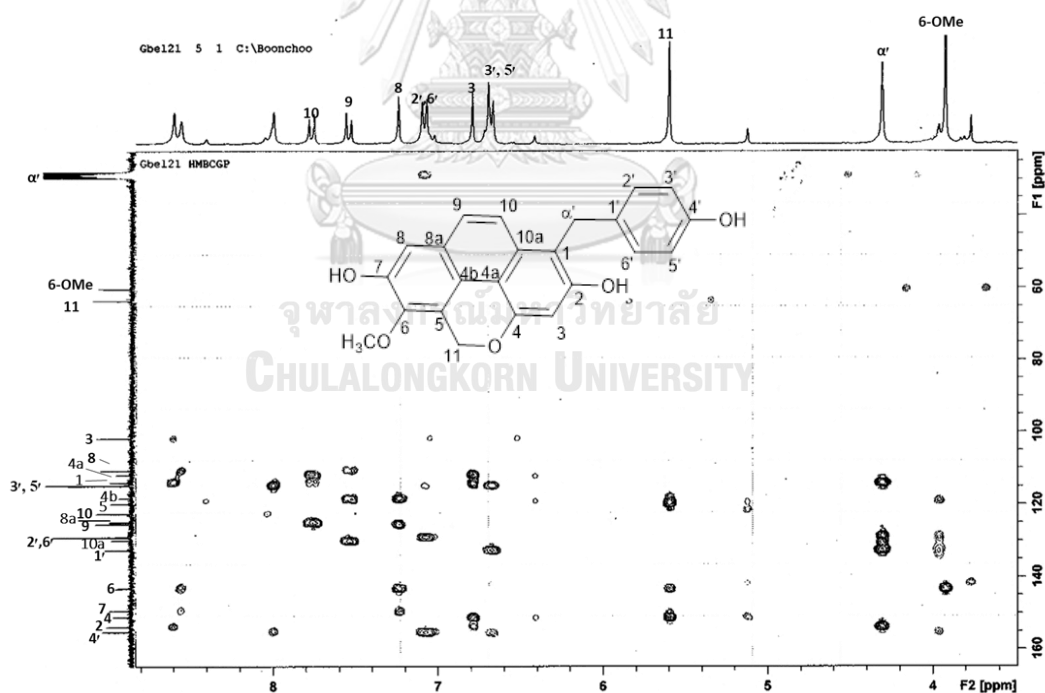


Figure 110 HMBC spectrum of compound GB3

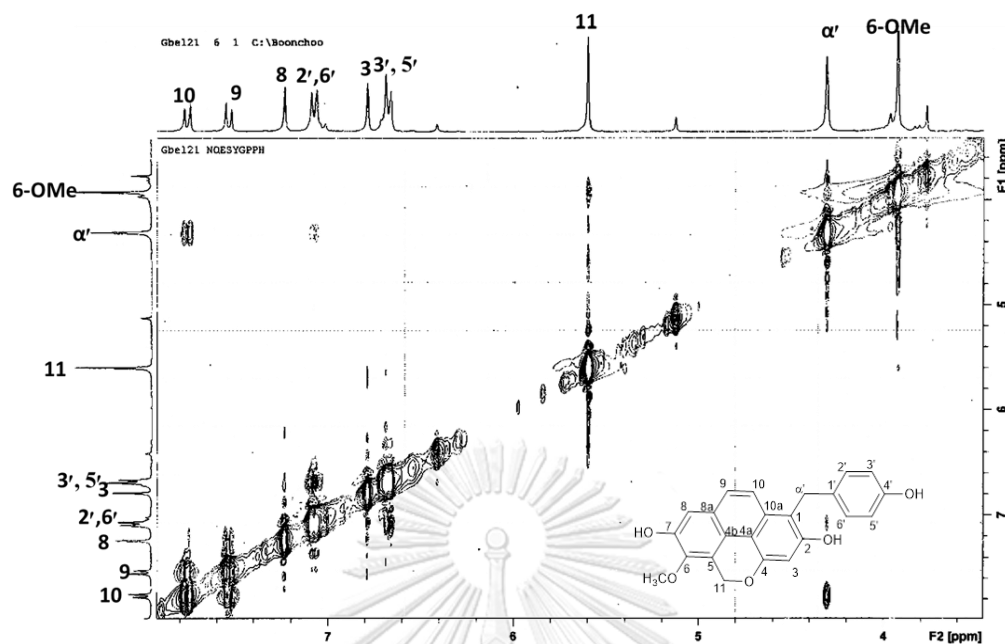


Figure 111 NOESY spectrum of compound GB3

3.2.3 Structure elucidation of compound GB4

Compound GB4 was collected as a brown amorphous solid. The high resolution APCI mass spectrum (Figure 112) showed a protonated molecular ion $[M+H]^+$ at m/z 363.1211 (calcd. for $C_{22}H_{19}O_5$ 363.1232), suggesting the molecular formula $C_{22}H_{18}O_5$. The UV spectrum (Figure 113) of compound GB4 in MeOH showed maximal absorptions at 230, 265, 355, 370 nm, suggesting a phenanthrene core structure (Ito *et al.*, 2001). The IR spectrum (Figure 114) displayed absorption bands at 3360 cm^{-1} for OH and $2921, 1616\text{ cm}^{-1}$ for aromatic rings. The $^1\text{H-NMR}$ spectrum (Figure 115) exhibited proton signals similar to those of GB3. However, in GB4 the signal for the oxymethylene protons of the pyran ring was absent and replaced by a highly deshielded aromatic proton at δ 9.12 (s, H-5). This suggested that GB4 was a phenanthrene having a *p*-hydroxybenzyl unit attached to C-1, similar to GB3. The ^{13}C NMR and DEPT spectra (Figure 116) showed only one signal for a methylene carbon

at (δ 29.4) which was correlated to the methylene protons at 4.34 (2H, s, H- α') in the HSQC spectrum (Figure 117). The HMBC spectrum (Figure 118) displayed 3-bond correlations from H-5 (δ 9.12) to C-7 (δ 144.0) and C-8a (δ 126.4), and from H- α' (δ 4.34) to C-2, C-10a and C-2' (6'), confirming the proposed phenanthrene-benzyl skeleton. In the NOESY spectrum (Figure 119), the methoxyl protons at δ 4.06 (3H, s, 4-OMe) displayed a cross peak with the proton at δ 6.94 (1H, s, H-3). A NOESY correlation was also observed between H- α' (δ 4.29) and H-10 (δ 7.64).

From all the NMR and MS data, it was concluded that compound GB4 was a new phenanthrene with a *p*-hydroxybenzyl substituent and had the structure [351] as shown.

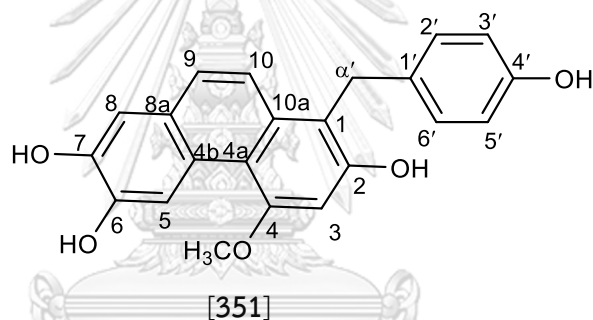


Table 29 NMR spectral data of compound GB4

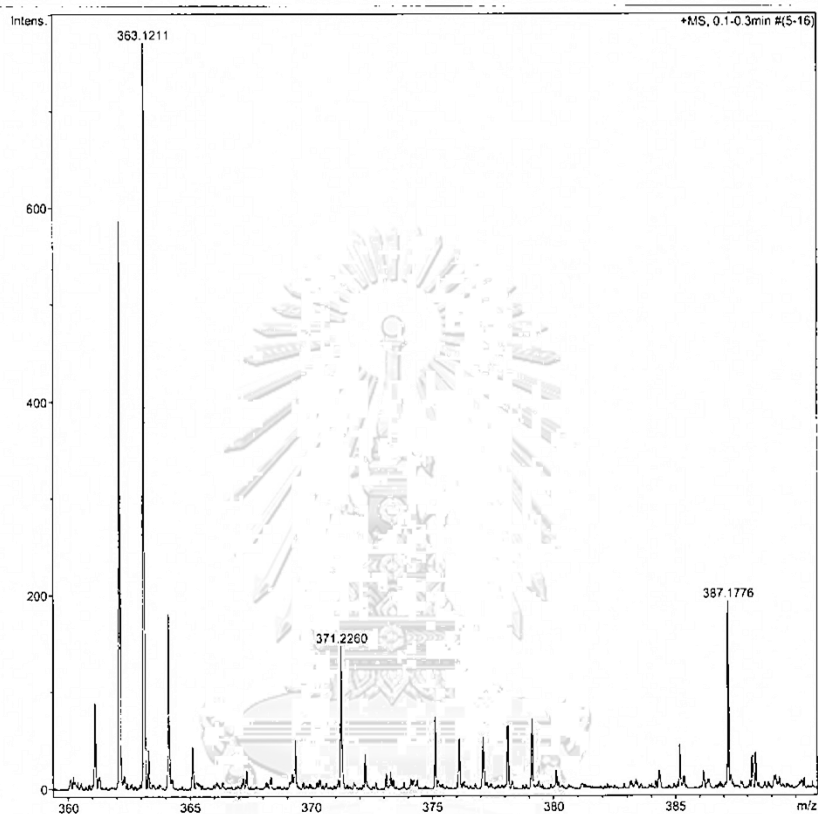
Position	δ_{H} (mult., J in Hz)	δ_{C}	HMBC (correlation with ^1H)
1	-	113.2	3, α' *
2	-	152.4	3*, α'
3	6.94 (1H, s)	98.7	-
4	-	157.7	3*, 4-OMe
4a	-	114.9	3, 5, 10
4b	-	125.3	8, 9
5	9.12 (1H, s)	112.8	-
6	-	145.2	8
7	-	144.0	5
8	7.21 (1H, s)	111.4	9
8a	-	126.4	5, 10
9	7.48 (1H, d, 9.0)	127.1	8
10	7.64 (1H, d, 9.0)	120.5	-
10a	-	133.3	9, α'
α'	4.34 (2H, s)	29.4	2', 6'
1'	-	132.6	α' *, 3', 5'
2'	7.03 (1H, d, 8.4)	129.0	α' , 6'
3'	6.66 (1H, d, 8.4)	114.8	5'
4'	-	155.2	2', 6'
5'	6.66 (1H, d, 8.4)	114.8	3'
6'	7.03 (1H, d, 8.4)	129.0	α' , 2'
4-OMe	4.06 (3H, s)	54.9	-

*= two-bond coupling

Display Report

Analysis Info		Acquisition Date	2/14/2020 10:41:56 AM
Analysis Name	D:\Data\SEC\Gbel-24.d	Operator	CTB
Method	tune_low.m	Instrument	micrOTOF-Q II 10414
Sample Name	Gbel-24		
Comment			

Acquisition Parameter					
Source Type	APCI	Ion Polarity	Positive	Set Nebulizer	1.6 Bar
Focus	Not active	Set Capillary	4500 V	Set Dry Heater	200 °C
Scan Begin	50 m/z	Set End Plate Offset	-500 V	Set Dry Gas	8.0 l/min
Scan End	3000 m/z	Set Collision Cell RF	150.0 Vpp	Set Divert Valve	Waste



Bruker Compass DataAnalysis 4.0 printed: 2/14/2020 11:23:51 AM Page 1 of 1

Figure 112 Mass spectrum of compound GB4

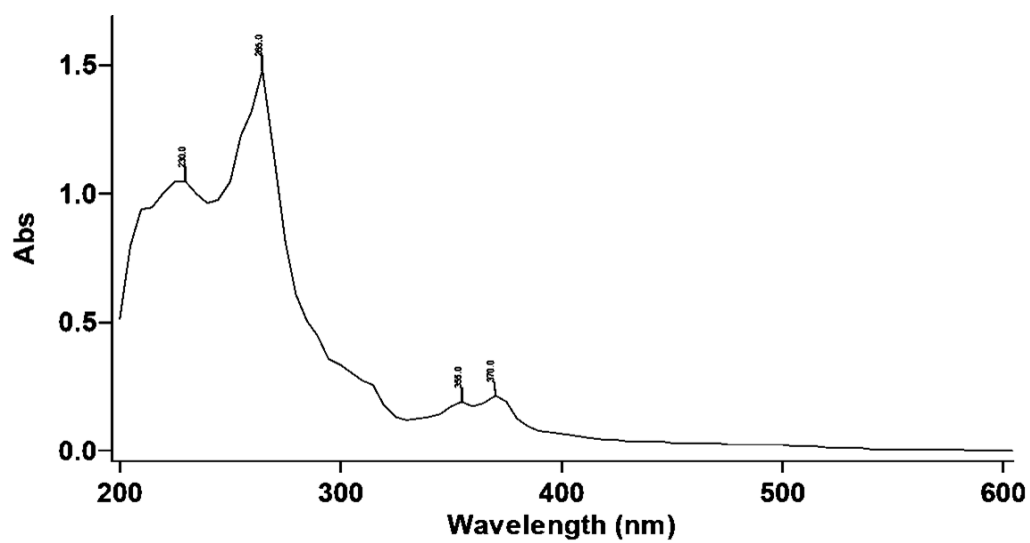


Figure 113 UV spectrum of compound GB4

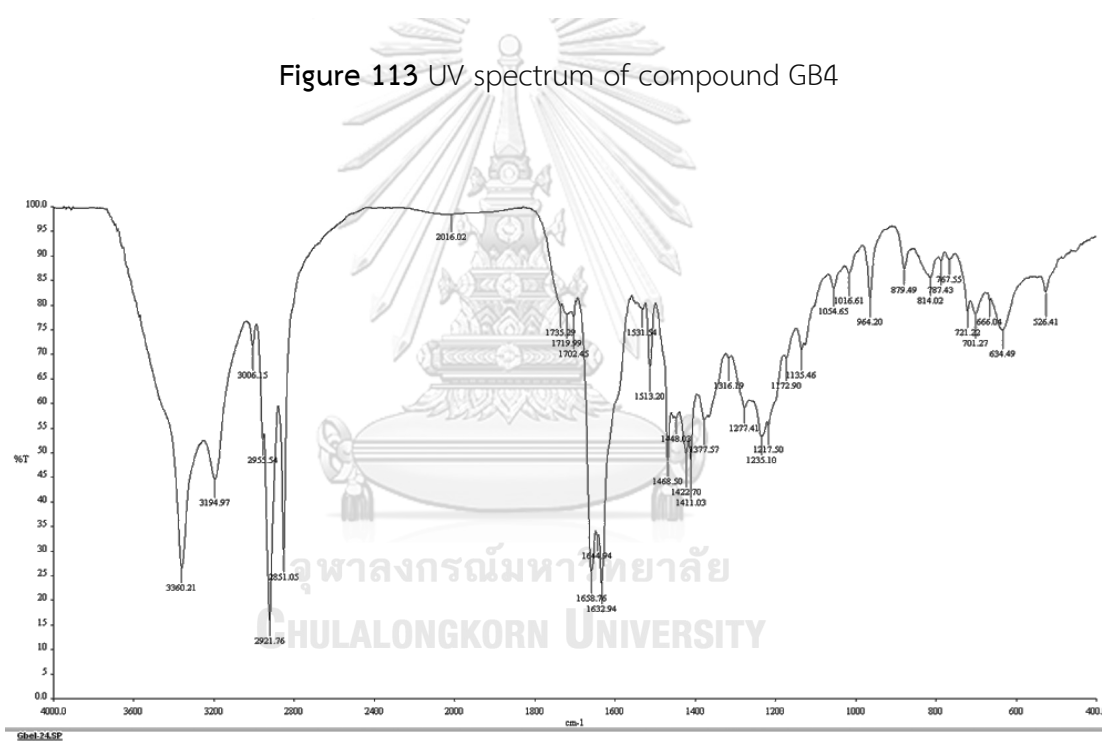


Figure 114 IR spectrum of compound GB4

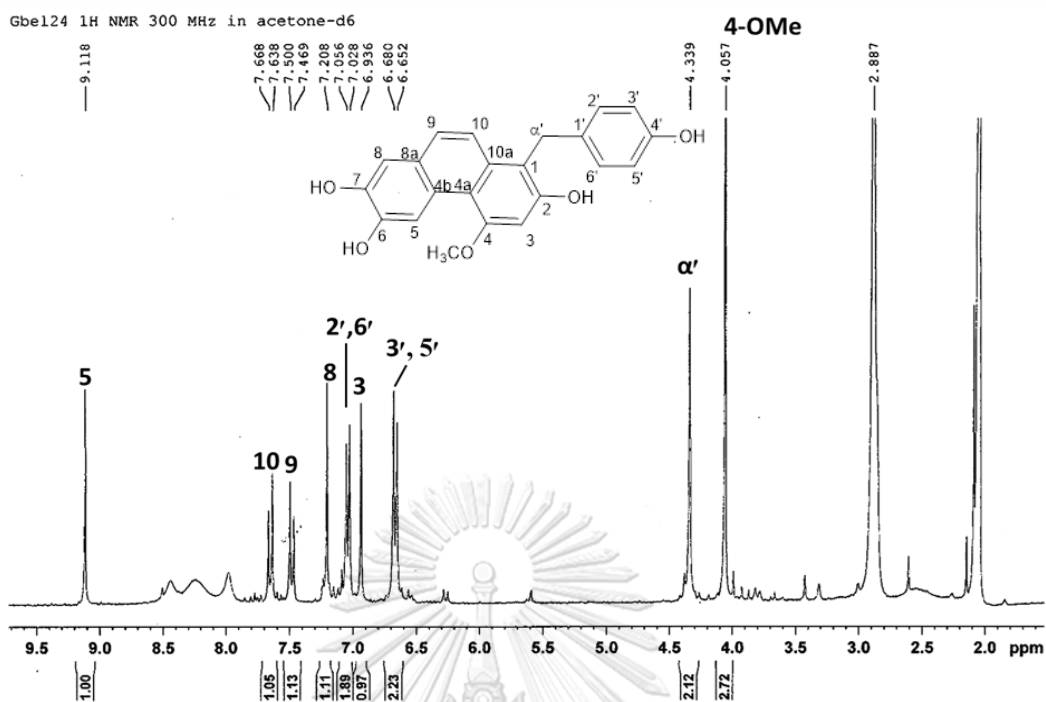


Figure 115 ¹H-NMR (300 MHz) spectrum of compound GB4 (acetone-d₆)

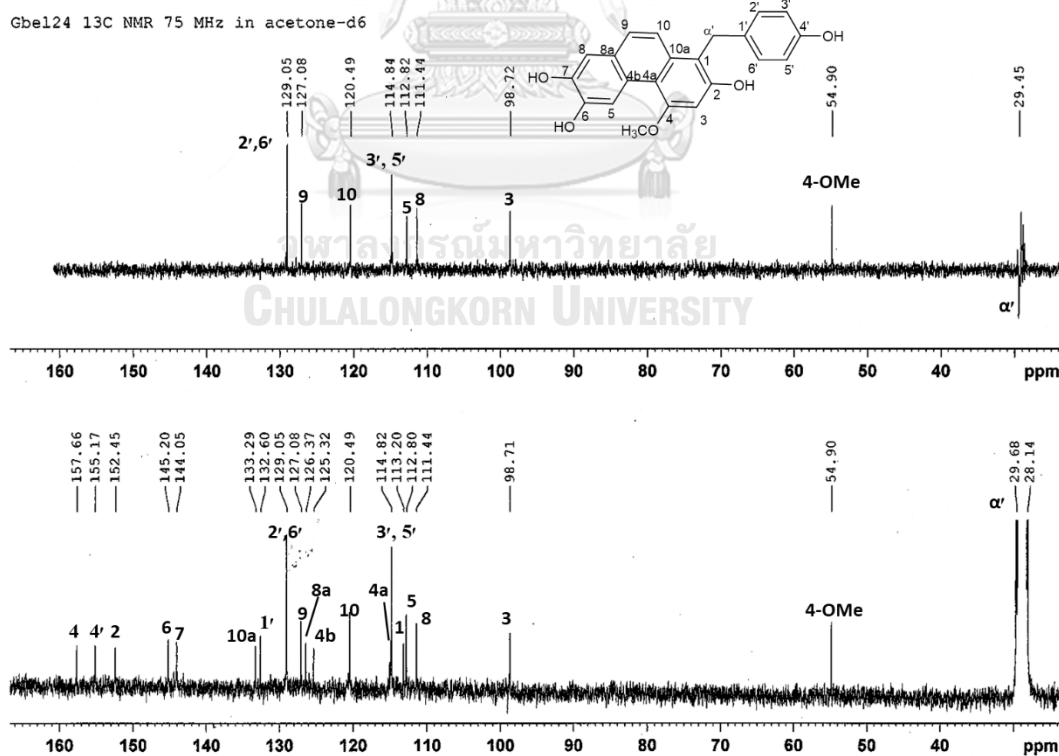


Figure 116 ¹³C-NMR(75 MHz) and DEPT-135 spectra of compound GB4 (acetone-d₆)

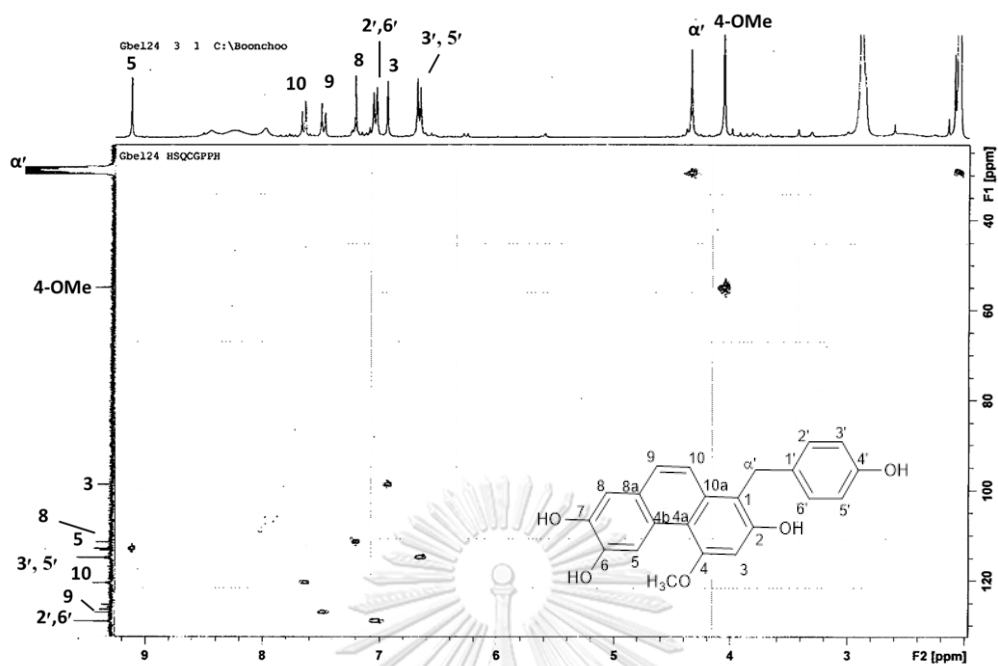


Figure 117 HSQC spectrum of compound GB4

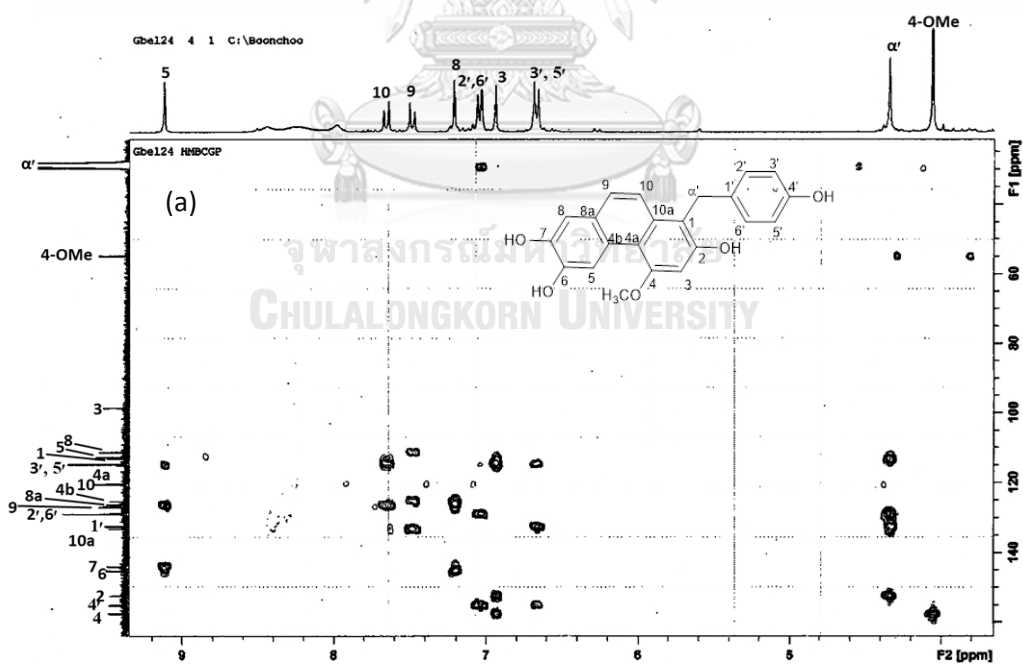


Figure 118 HMBC spectrum of compound GB4

(a) full spectrum

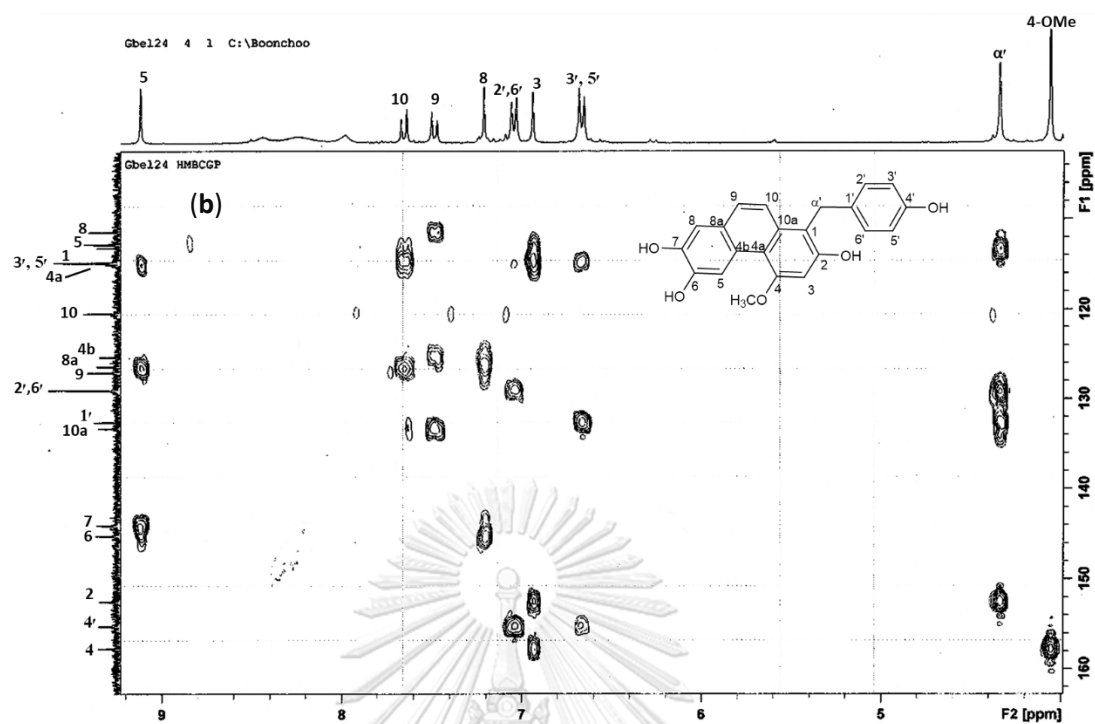


Figure 118 HMBC spectrum of compound GB4 (continued)

(b) expansion [δ_{H} 3.8–9.2 ppm, δ_{C} 110–160 ppm]

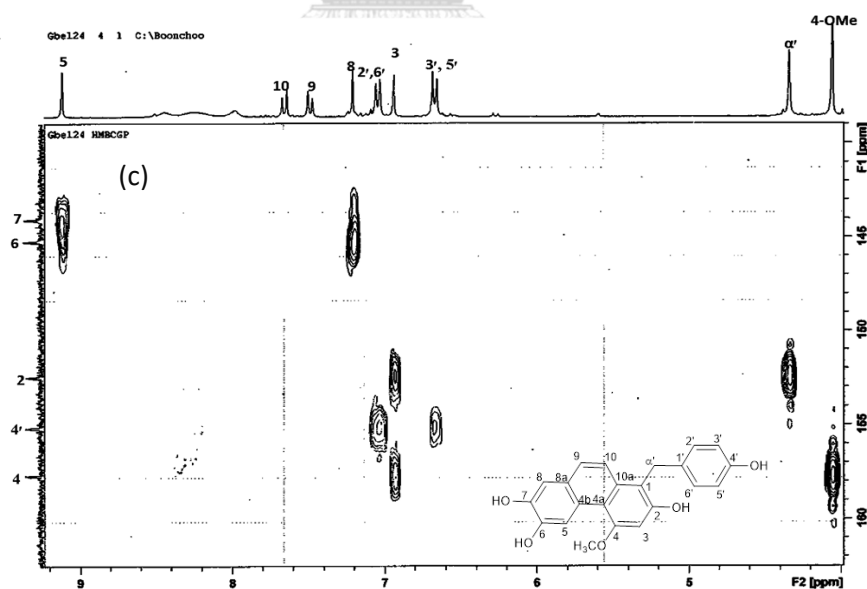


Figure 118 HMBC spectrum of compound GB4 (continued)

(c) expansion [δ_{H} 3.8–9.2 ppm, δ_{C} 104–162 ppm]

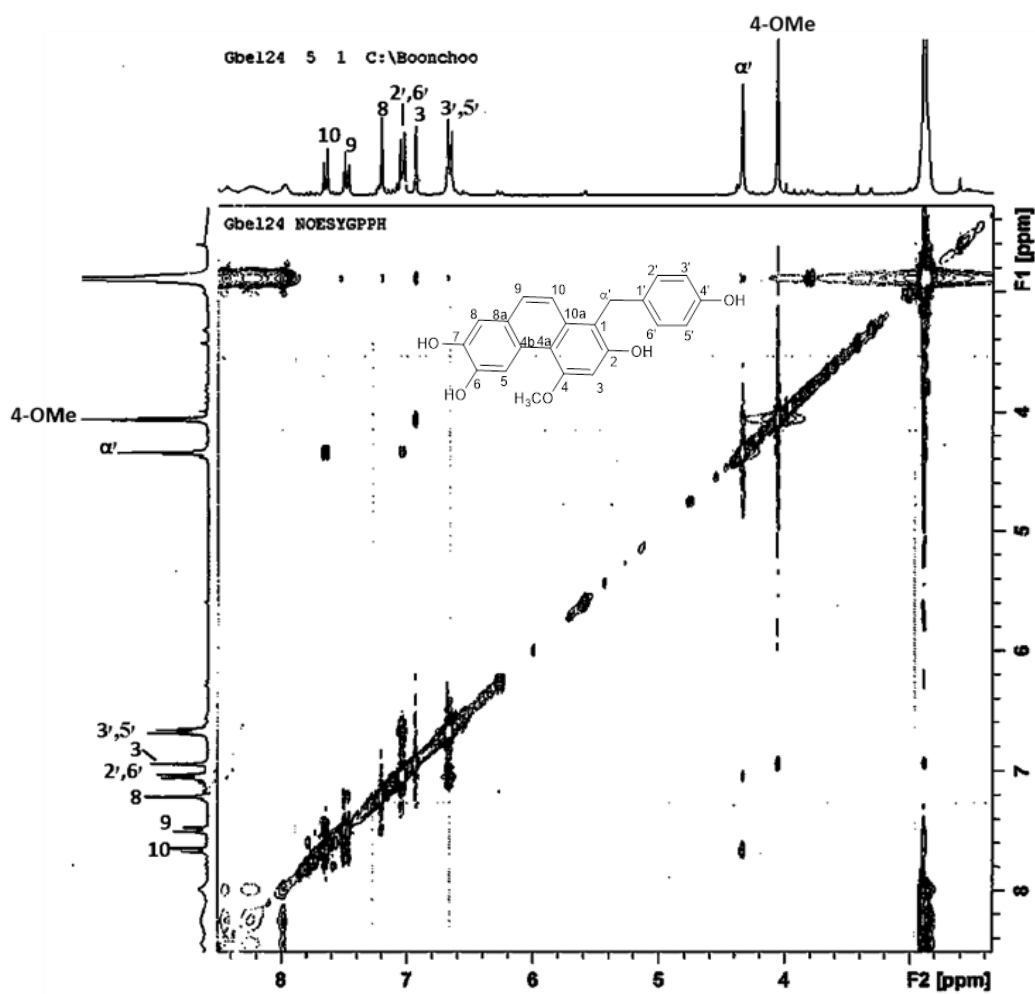


Figure 119 NOESY spectrum of compound GB4

3.3 Biological activity of isolated compounds

All the four new compounds from *G. bellinus* were evaluated for α -glucosidase inhibitory activity. Compounds [348], [349] and [350] displayed enzyme inhibition with IC_{50} values of 88.7 ± 4.1 , 97.8 ± 3.1 and 45.9 ± 2.8 μ M, respectively. Compound [351] was lack of such activity.

Table 30 α -Glucosidase inhibitory activity of compounds isolated from *Gastrochilus bellinus*

compounds	% inhibition at 100 μ g/ml	IC_{50} (μ M)
[348]	94.0 ± 1.9	88.7 ± 4.1
[349]	99.8 ± 1.9	97.8 ± 3.1
[350]	85.6 ± 0.6	45.9 ± 2.8
[351]	30.6 ± 1.3	-
acarbose	21.9 ± 1.5	724.7 ± 46

4. Phytochemical and biological studies of *Huberantha jenkinsii*

4.1 Preliminary biological activity evaluation

The MeOH extract of *H. jenkinsii* was separated by partitioning to give EtOAc, BuOH and water fractions which were subjected to screening for α -glucosidase inhibitory activity (Table 31). The EtOAc fraction at 100 μ g/ml showed 88.9 % inhibition in comparison with acarbose (21.9 ± 1.5 % inhibition at 100 μ g/ml), and therefore, was further studied in detail to isolate and characterize the constituents responsible for the activity.

Table 31 α -Glucosidase inhibitory activity of extracts from *Huberantha jenkinsii*

Fraction	% inhibition at 100 $\mu\text{g/ml}$
MeOH	32.7 \pm 1.1
EtOAc	88.9 \pm 9.0
BuOH	6.7 \pm 2.0
acarbose	21.9 \pm 1.5

4.2 Chemical investigation

Separation of the EtOAc extract of *Huberantha jenkinsii* stem by repeated chromatography led to the isolation of two new 8-oxoprotoberberine alkaloids, i.e. [352] and [353], and five known compounds including mangiferin [337], allantoin [354], oxylopinine [355], *N-trans-feruloyl*tyramine [10] and *N-trans-p-coumaroyl* tyramine [356] (Figure 120).

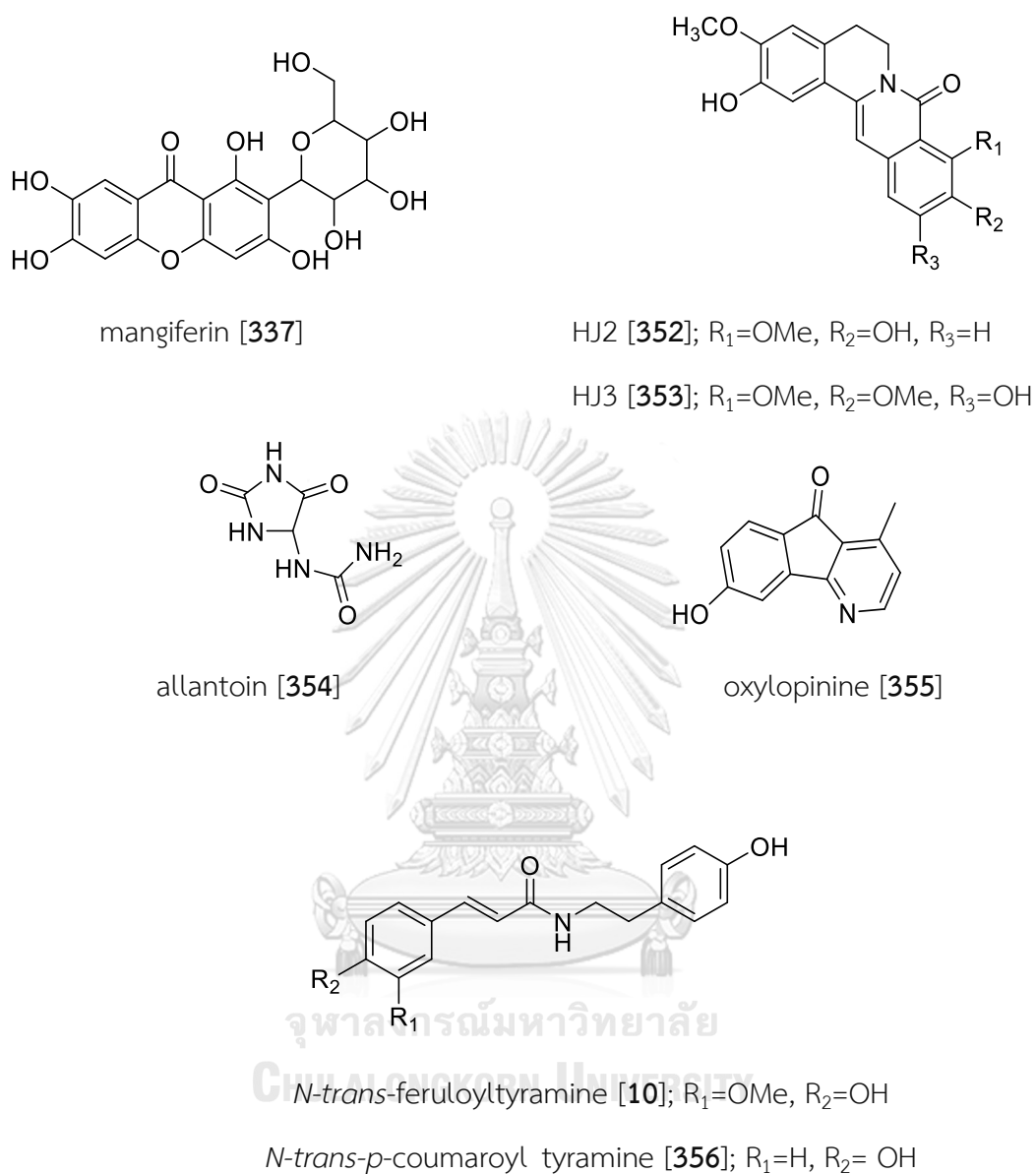


Figure 120 Structures of compounds isolated from *Huberantha jenkinsii*

4.2.1 Identification of compound HJ1 (mangiferin)

Compound HJ1 was collected as a white powder. The high resolution ESI mass spectrum (**Figure 121**) showed a sodium-adduct molecular ion $[M+Na]^+$ at m/z 445.0747 (calcd. for $C_{19}H_{18}O_{11}Na$ 445.0747), suggesting the molecular formula

$C_{19}H_{18}O_{11}$. The 1H -NMR spectrum (**Figure 122**) exhibited three singlet aromatic proton signals at δ 7.36 (1H, s, H-8), 6.85 (1H, s, H-5) and 6.36 (1H, s, H-4), and resonances for a glucose unit at δ 3.13–3.69 (4H, overlapped, Glc-H-3', Glc-H-4', Glc-H-5', Glc-H-6'), 4.04 (1H, t, $J = 9.0$ Hz, Glc-H-2') and 4.58 (1H, d, $J = 9.0$ Hz, Glc-H-1'). The vicinal coupling between H-1' and H-2' was clearly observed in the COSY spectrum (**Figure 123**). The ^{13}C -NMR spectrum (**Figure 124** and **Table 32**) displayed twelve aromatic carbons at δ 162.3 (C-1), 108.1 (C-2), 164.3 (C-3), 93.4 (C-4), 156.7 (C-4a), 101.7 (C-4b), 103.0 (C-5), 151.3 (C-6), 144.2 (C-7), 108.4 (C-8), 112.1 (C-8a) and 154.6 (C-8b), and a ketone carbon at δ 179.5, indicating a xanthone structure. The ^{13}C NMR signals for the glucose unit appeared at δ 73.5 (C-1'), 70.7 (C-2'), 79.5 (C-3'), 71.1 (C-4'), 82.1 (C-5') and 61.9 (C-6'). The HSQC spectrum (**Figure 125**) exhibited a correlation peak for C-1' at a relatively upfield position at δ_C 73.53 / δ_H 4.58 (1H, d, $J=9.9$ Hz) suggesting that HJ1 was a C-glycoside. Compound HJ1 was penta-substituted because there were only three aromatic methine carbon peaks shown in the HSQC spectrum. A phenolic group was present at C-1, as evident from the most downfield proton signal at δ 13.76. In the HMBC spectrum, this phenolic proton showed 2-bond and 3-bond coupling with C-1 (δ 162.3) and C-2, (δ 108.1), respectively. The HMBC correlations (**Figure 126**) from these two carbons to the anomeric proton (H-1') placed the sugar unit at C-2 and confirmed that HJ1 was a xanthone C-glycoside. The proton at δ 7.36 (1H, s) was assigned to H-8 from its 3-bond coupling with the keto carbonyl carbon. A phenolic group was present at C-3, as indicated from the HMBC correlation from the proton at δ 6.36 (1H, s, H-4) to C-2 (δ 108.1) and two oxygenated carbons at δ 164.3 (C-3) and δ 156.7 (C-4a). Two phenolic groups were located at C-6 and C-7, as deduced from the HMBC correlation from the proton at δ 6.8 (1H, s, H-5) to the oxygenated carbons at δ 151.3 (C-6), 144.2 (C-7) and 154.6 (C-8b).

From the above data and through the comparison of its ^1H and ^{13}C spectral data with previously reported values (Djemgou *et al.*, 2010), compound HJ1 was identified as mangiferin [337]. This compound has been earlier found in *H. nitidissima* (Toussirot *et al.*, 2014).

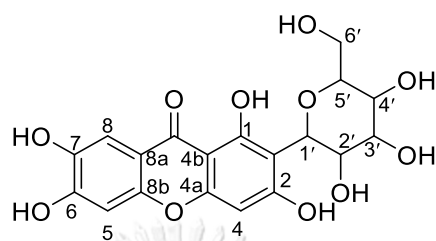


Table 32 NMR spectral data of compound HJ1 as compared with mangiferin

Position	Compound HJ1 (DMSO- d_6)		Mangiferin (DMSO- d_6)*	
	δ_H (mult., J in Hz)	δ_C	δ_H (mult., J in Hz)	δ_C
1	13.76 (1-OH)	162.3	13.80 (1-OH)	161.7
2	-	108.1	-	107.5
3	-	164.3	-	163.8
4	6.36 (1H, s)	93.7	6.40(1H, s)	93.3
4a	-	156.7	-	156.2
4b	-	101.7	-	101.2
5	6.85 (1H, s)	103.0	6.86(1H, s)	102.4
6	-	151.3	-	150.9
7	-	144.2	-	143.9
8	7.36 (1H, s)	108.4	7.41(1H, s)	107.8
8a	-	112.1	-	111.4
8b	-	154.6	-	154.6
CO	-	179.5	-	179.0
1'	4.58 (1H, d, 9.9, Glc-H-1'),	73.5	4.60 (d, 8.3)	73.1
2'	4.04 (1H, t, 9.0, Glc-H-2')	70.7	4.03 (t, 9.5)	70.3
3'		79.4		79.0
4'		71.1	3.16 (3H, m)	70.6
5'	3.13-3.69 (4H, overlapped, Glc- H-3' - Glc-H-6')	82.1		81.5
6'		61.9	3.40 (1H, dd, 11.0, 2.1) 3.60 (1H, dd, 11.0, 4.6)	61.4

* (Djemgou *et al.*, 2010)

Mass Spectrum List Report

Analysis Info

Analysis Name OSHTS28012020005_1.d
 Method Tune_wide_POS_Tawatchai_05Feb2016.m
 Sample Name Hu-9
 Hu-9

Acquisition Date 1/28/2020 3:37:46 PM
 Operator Administrator
 Instrument micrOTOF 72

Acquisition Parameter

Source Type	ESI	Ion Polarity	Positive	Set Corrector Fill	50 V
Scan Range	n/a	Capillary Exit	200.0 V	Set Pulsar Pull	337 V
Scan Begin	50 m/z	Hexapole RF	400.0 V	Set Pulsar Push	337 V
Scan End	3000 m/z	Skimmer 1	70.0 V	Set Reflector	1300 V
		Hexapole 1	25.0 V	Set Flight Tube	9000 V
				Set Detector TOF	2295 V

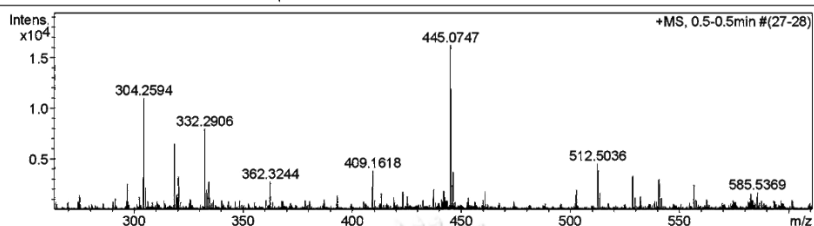


Figure 121 Mass spectrum of compound HJ1

HU9 ¹H NMR 300 MHz in DMSO-d₆

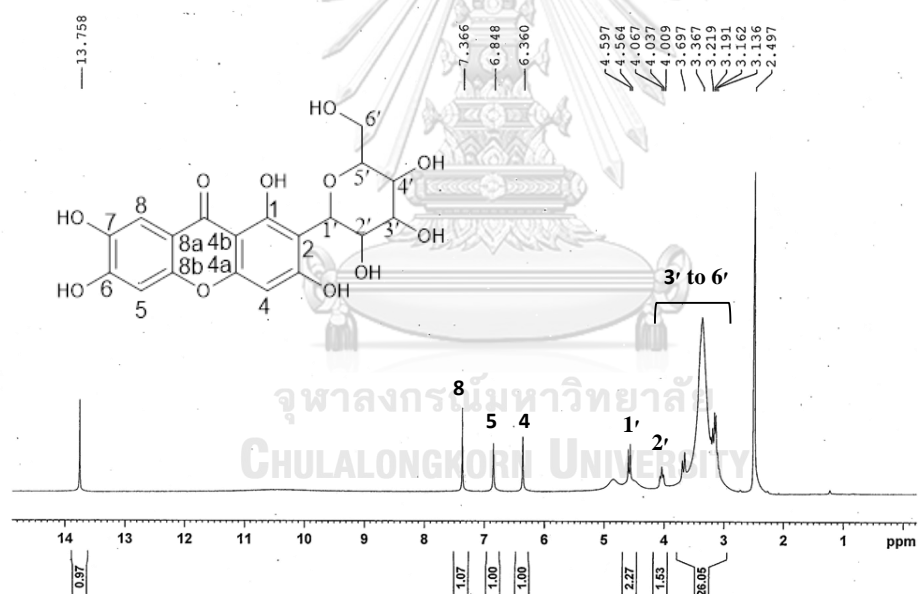


Figure 122 ¹H-NMR (300 MHz) spectrum of compound HJ1 (acetone-d₆)

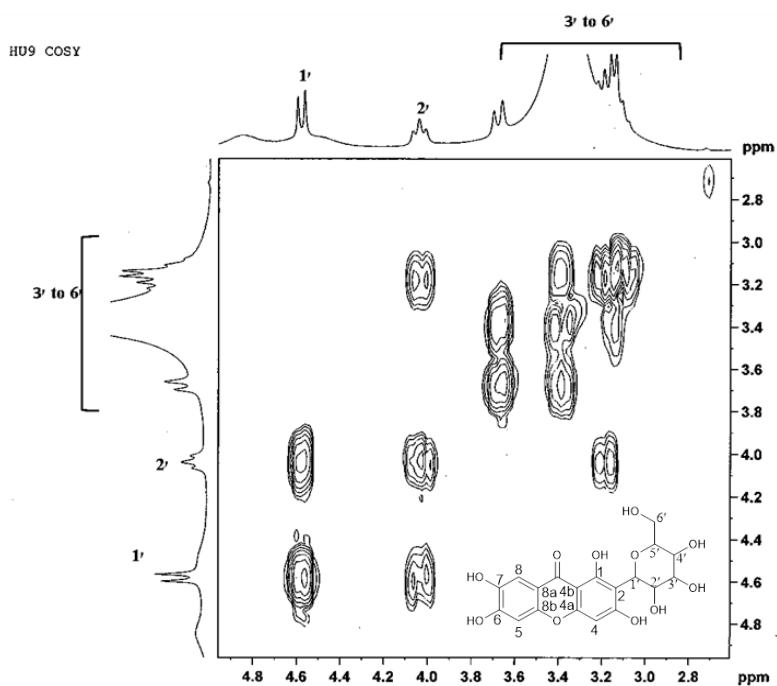
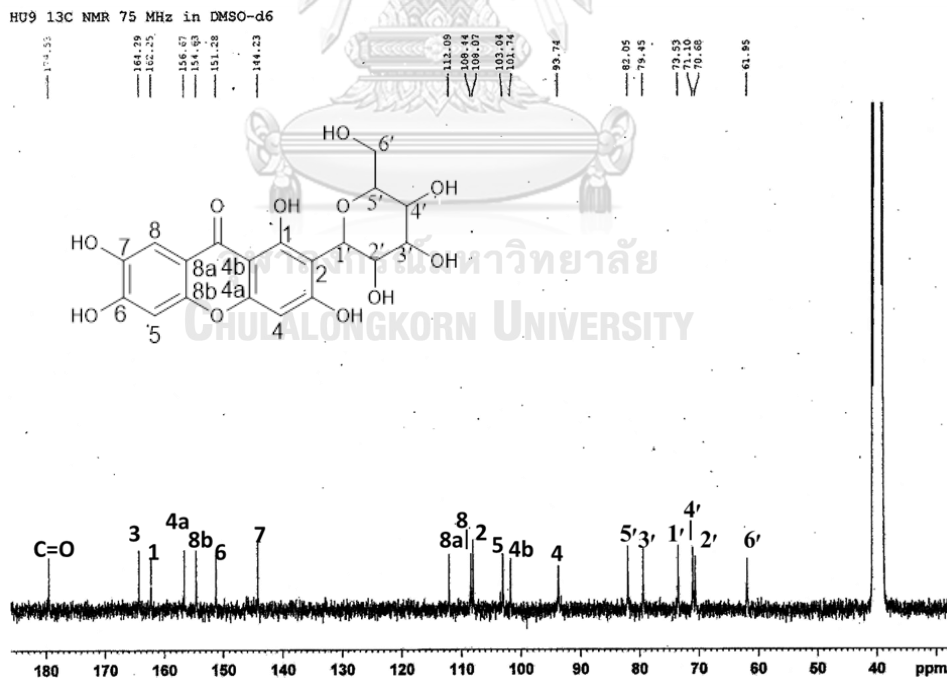


Figure 123 COSY spectrum of compound HJ1

Figure 124 ^{13}C -NMR (75 MHz) spectrum of compound HJ1 (acetone-d_6)

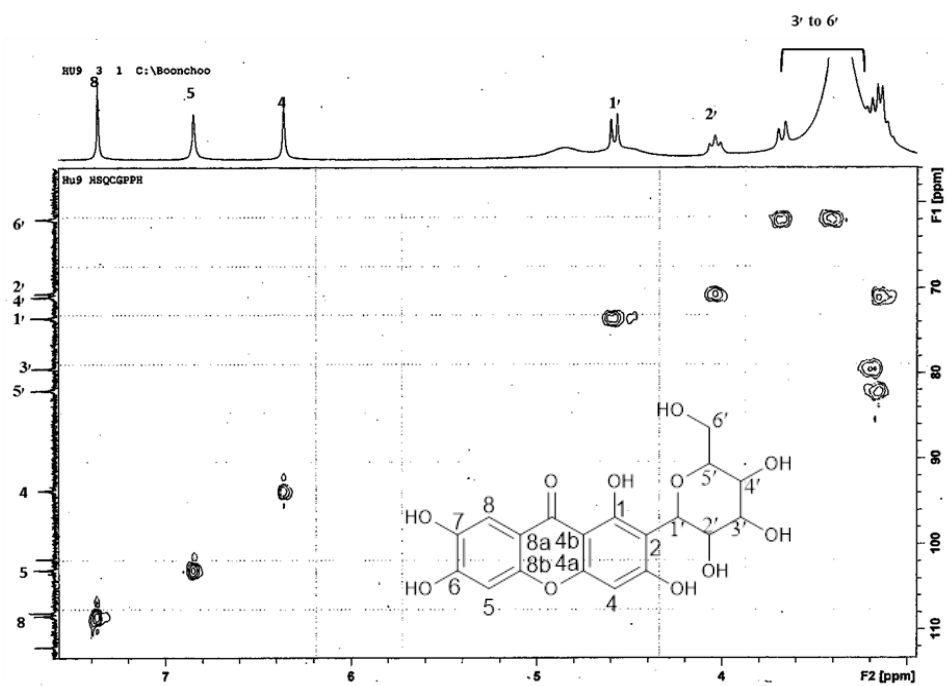


Figure 125 HSQC spectrum of compound HJ1

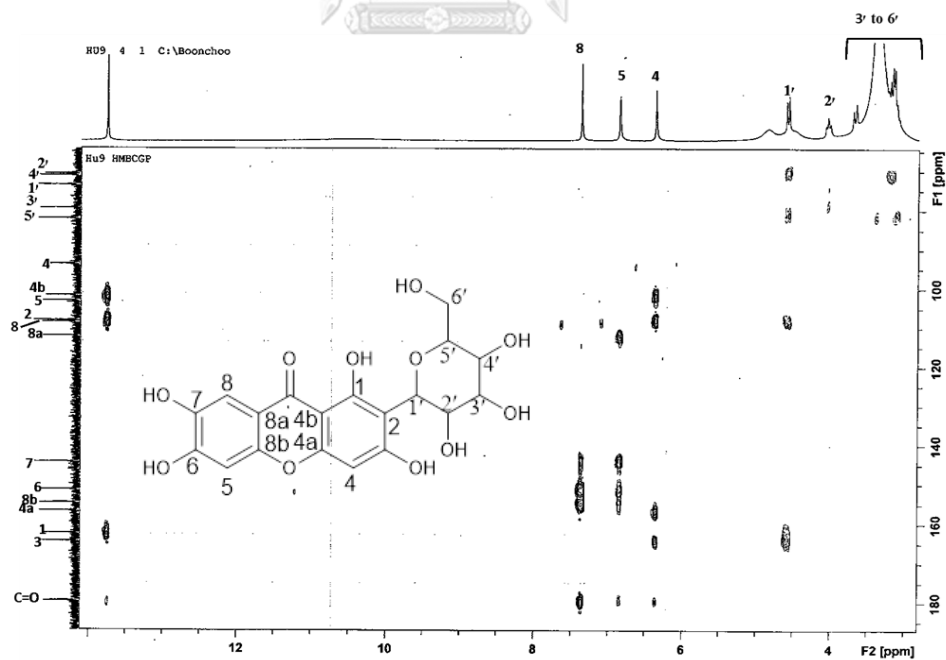


Figure 126 HMBC spectrum of compound HJ1

4.2.2 Structure elucidation of compound HJ2

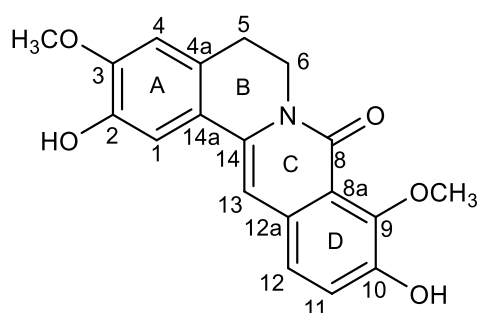
Compound HJ2 was obtained as a brownish white powder, and the molecular formula was determined by HR-ESI-MS to be $C_{19}H_{17}NO_5$ from the deprotonated molecular ion at m/z 338.1029 $[M-H]^-$, (calcd. for $C_{19}H_{16}NO_5$ 338.1028) (**Figure 127**). It gave an orange color with Dragendorff's reagent and showed strong blue fluorescent spot under UV light, characteristic of 8-oxoprotoberberine alkaloids (Patra *et al.*, 1987). The UV spectrum (**Figure 128**) displayed maximal absorptions at 205, 225, 335 and 370 nm, typical of the oxoprotoberberine skeleton (Costa *et al.*, 2010; Le & Cho, 2008). The IR spectrum (**Figure 129**) showed absorption bands for hydroxy (3353 cm^{-1}), conjugated amide (1667 cm^{-1}), and aromatic (1540 and 1513 cm^{-1}) functionalities.

The ^1H NMR spectrum (**Figure 130** and **Table 33**) showed five aromatic protons at δ 7.33 (1H, s, H-1), 6.90 (1H, s, H-4), 7.27 (1H, d, $J = 8.4$ Hz, H-11), 7.33 (1H, d, $J = 8.4$ Hz, H-12) and 6.91 (1H, s, H-13). In the aliphatic region, proton signals for two methoxy groups appeared at δ 3.91 (3H, s, 9-OMe), 3.89 (3H, s, 3-OMe) and two pairs of methylene protons showed at δ 2.91 (2H, t, $J = 6.0$ Hz, H₂-5) and 4.20 (2H, dd, $J = 6.5, 6.0$ Hz, H₂-6). The assignments of H-4, H-5 and H-6 were obtained by a COSY experiment (**Figure 131**) in which H-5 (δ 2.91) showed correlation with H-4 (δ 6.90) and H-6 (δ 4.20). The ^{13}C NMR (**Figure 132**) and HSQC (**Figure 133**) spectra displayed peaks of protonated carbons. H-4 at δ 6.90 (1H, s) showed a NOESY cross peak with H₂-5 (δ 2.91, 2H, t, $J = 6.0$ Hz) (**Figure 134**) and HMBC correlation to C-5 (**Figure 135**). This proton also showed NOESY correlation with methoxyl protons at δ 3.89, placing this methoxy group at C-3. The HMBC connectivity from these methoxyl protons to C-3 (δ 149.4) confirmed this assignment. A hydroxy group was present at C-2, as indicated from the HMBC correlation from the proton at δ 7.33 (H-1) to the oxygenated carbons C-2 (δ 146.7) and C-3 (δ 149.4) and to C-14 (δ 136.1) which was

at the junction of rings B and C. Further analysis of the NOESY spectrum revealed a correlation between H-13 (δ 6.91, 1H, s) and H-12 (δ 7.33, 1H, d, $J = 8.4$ Hz). This implied that the second methoxy group should be located at C-9 or C-10. The 3-bond coupling between H-12 (δ 7.33) and the oxygenated carbon at δ 149.5 (C-10), together with the HMBC between the methoxyl protons at δ 3.91 and the carbon at δ 147.0 (C-9), indicated that this methoxy group must be at C-9.

Based on the above spectroscopic properties, compound HJ1 was characterized as a new oxoprotoberberine alkaloid with the structure [352]. It should be noted that this chemical structure has been mentioned as an intermediate for the synthesis of isocorypalmine (Gadhiya *et al.*, 2015), but so far no chemical, physical or spectroscopic properties have been described.

8-Oxoprotoberberine alkaloids have quite limited distribution. Up to the present, they have been found in the families Annonaceae, e.g. *Polyalthia longifolia* var. *pendula* (Faizi *et al.*, 2003), *Polyalthia cerasoides* (González *et al.*, 1997) and *Milium cuneata* (Promchai *et al.*, 2016); Menispermaceae, e.g. *Stephania suberosa* (Patra *et al.*, 1987), *Coscium fenestratum* (Pinho *et al.*, 1992) and *Sinomenium acutum* (Cheng *et al.*, 2012); Meliaceae, e.g. *Amoora cucullate* (Chumkaew *et al.*, 2019) and Rutaceae, e.g. *Phellodendron amurense* (Min *et al.*, 2007).



HJ2 [352]

Table 33 NMR spectral data of compound HJ2

Position	δ_{H} (mult., J in Hz)	δ_{C}	HMBC (correlation with ^1H)
1	7.33 (1H, s)	111.8	-
2		146.7	1*, 4
3		149.4	1, 4*
4	6.90 (1H, s)	111.4	2*,
4a		128.1	1,6
5	2.91 (2H, t, 6.0)	28.6	6*
6	4.20 (2H, dd, 6.5, 6.0)	40.1	5*
8	-	159.9	6
8a	-	119.5	12, 13
9	-	147.0	11
10	-	149.5	12
11	7.27 (1H, d, 8.4)	122.6	12*
12	7.33 (1H, d, 8.4)	123.7	11*, 13
12a	-	132.9	11
13	6.91 (1H, s)	101.5	12
14	-	136.1	1, 6
14a	-	123.6	4,5,13
9-OMe	3.91 (3H, s)	62.2	-
3-OMe	3.89 (3H, s)	56.3	-

*= Two-bond coupling

Mass Spectrum List Report

Analysis Info

Analysis Name OSHTS12112019001_2.d
Method Tune_low_Neg_PIN012018.m
Sample Name HuS-5a
21122019

Acquisition Date 12/21/2019 3:35:08 PM
Operator Administrator
Instrument micrOTOF 72

Acquisition Parameter

Source Type	ESI	Ion Polarity	Negative	Set Corrector Fill	75 V
Scan Range	n/a	Capillary Exit	-150.0 V	Set Pulsar Pull	372 V
Scan Begin	50 m/z	Hexapole RF	90.0 V	Set Pulsar Push	372 V
Scan End	3000 m/z	Skimmer 1	-50.0 V	Set Reflector	1300 V
		Hexapole 1	-25.0 V	Set Flight Tube	9000 V
				Set Detector TOF	2295 V

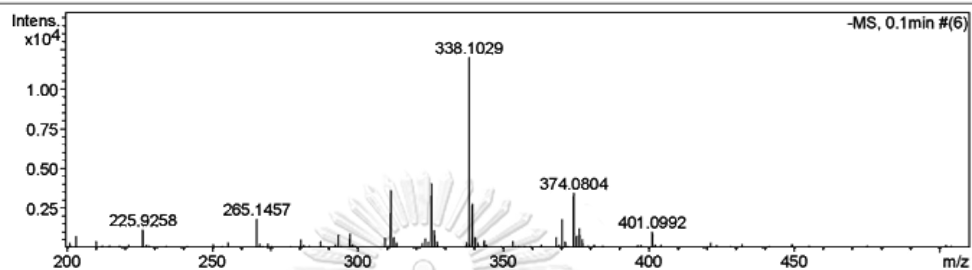


Figure 127 Mass spectrum of compound HJ2

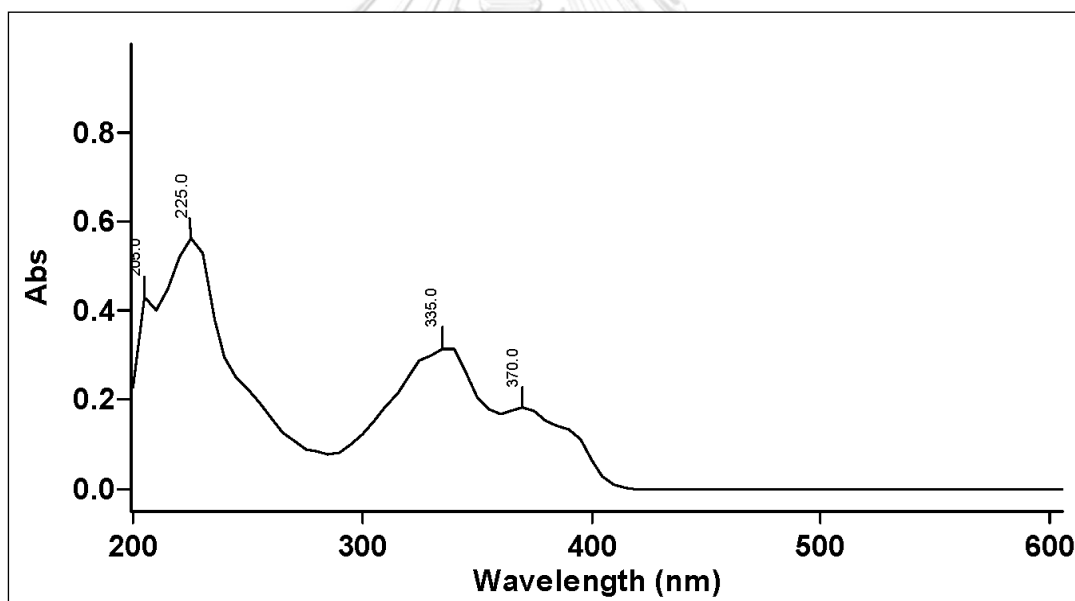


Figure 128 UV spectrum of compound HJ2

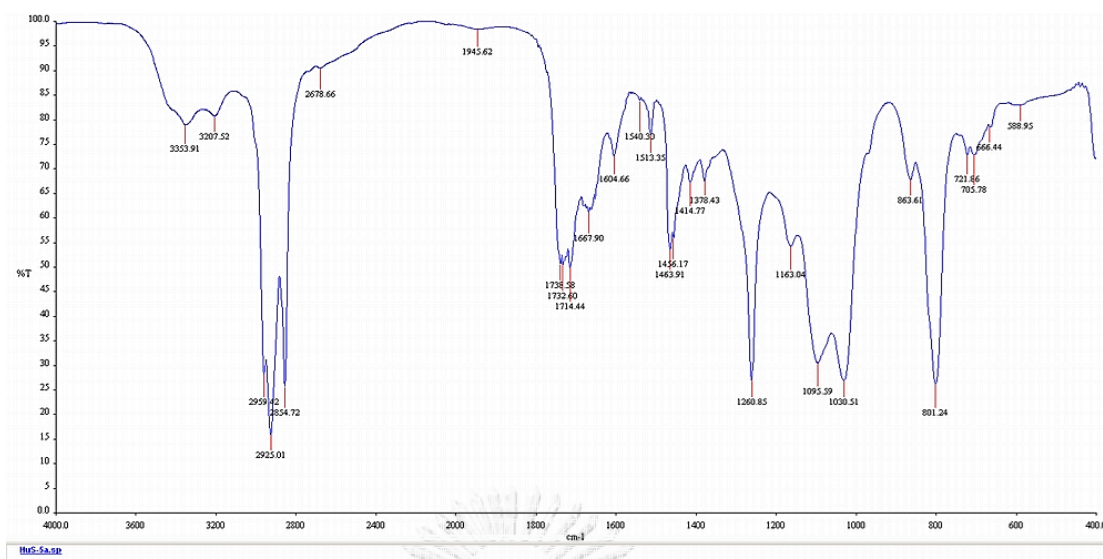
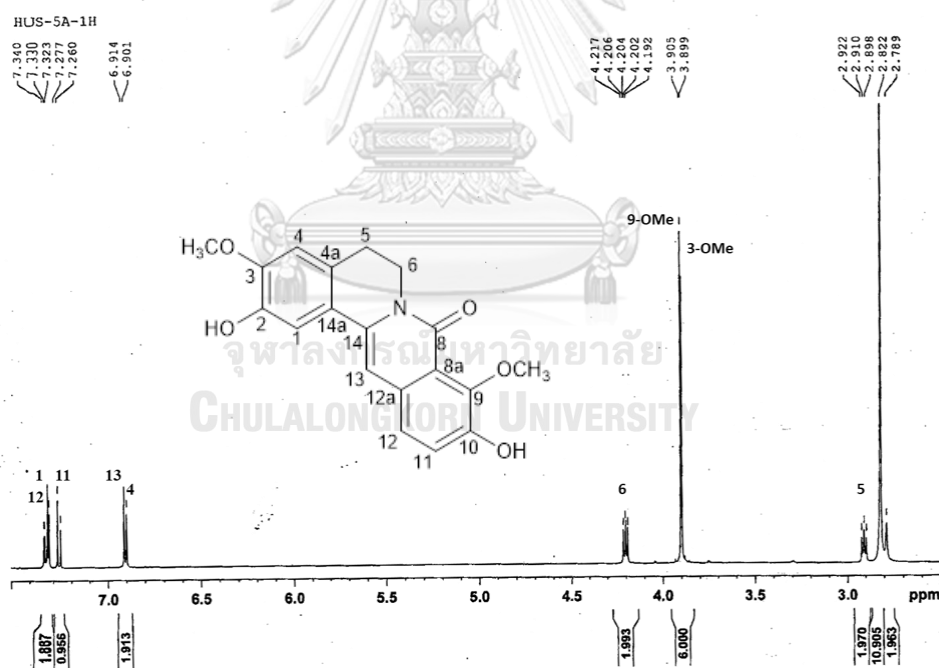


Figure 129 IR spectrum of compound HJ2

Figure 130 $^1\text{H-NMR}$ (500 MHz) spectrum of compound HJ2 (acetone- d_6)

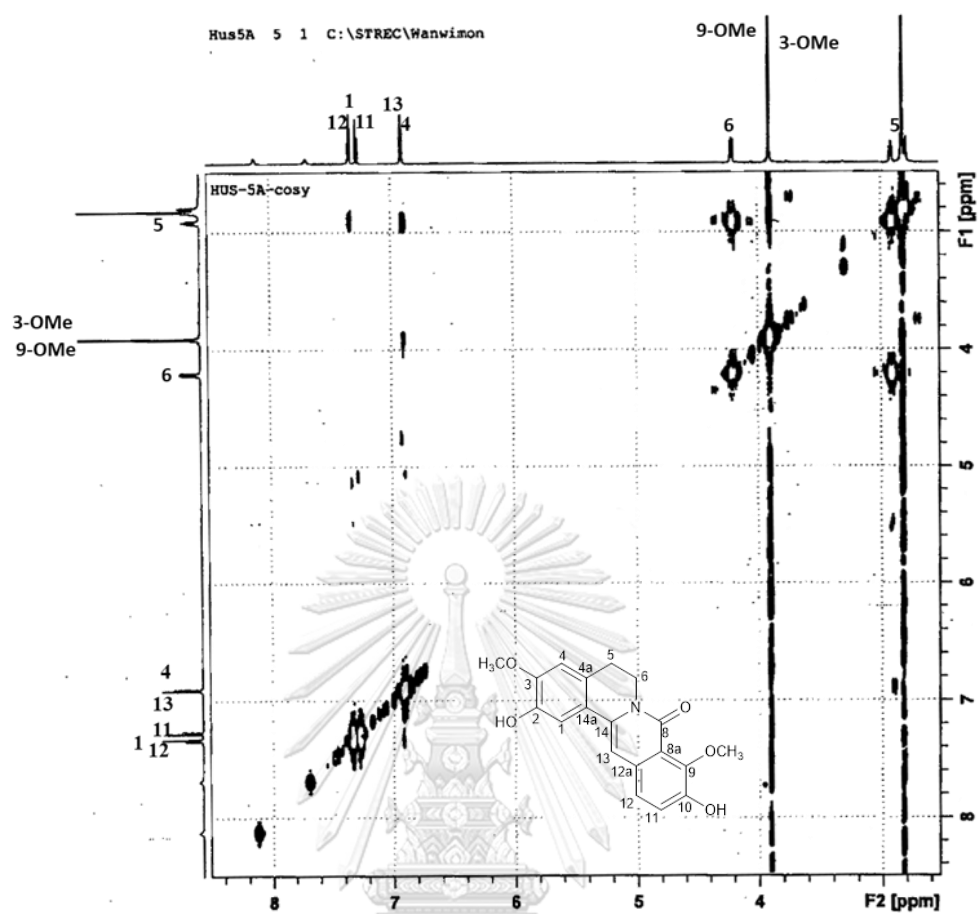


Figure 131 COSY spectrum of compound HJ2

จุฬาลงกรณ์มหาวิทยาลัย

CHULALONGKORN UNIVERSITY

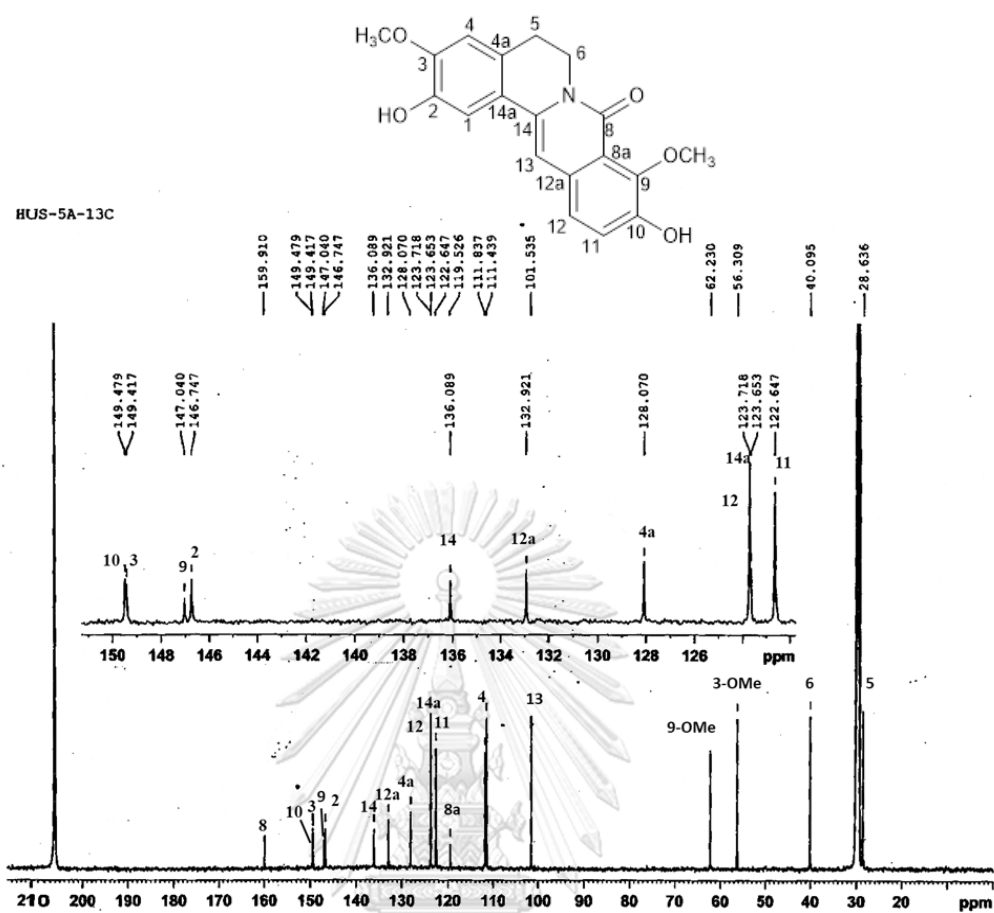


Figure 132 ^{13}C -NMR (125 MHz) spectrum of compound HJ2 (acetone- d_6)

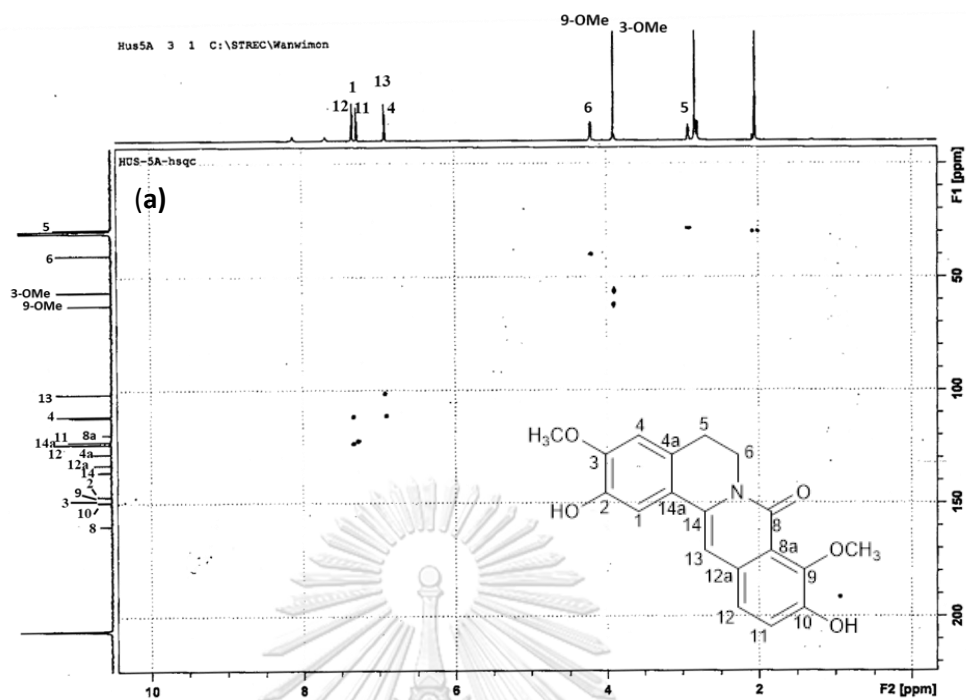


Figure 133 HSQC spectrum of compound HJ2

(a) full spectrum

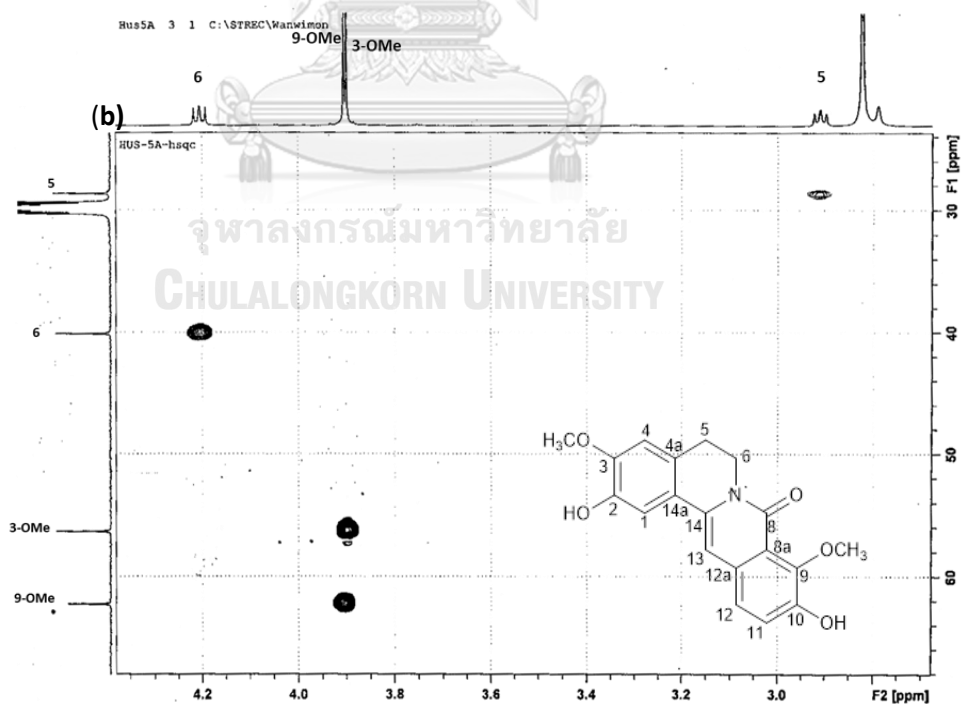


Figure 133 HSQC spectrum of compound HJ2 (continued)

(b) expansion [δ_{H} 2.8-4.4 ppm, δ_{C} 22-58 ppm]

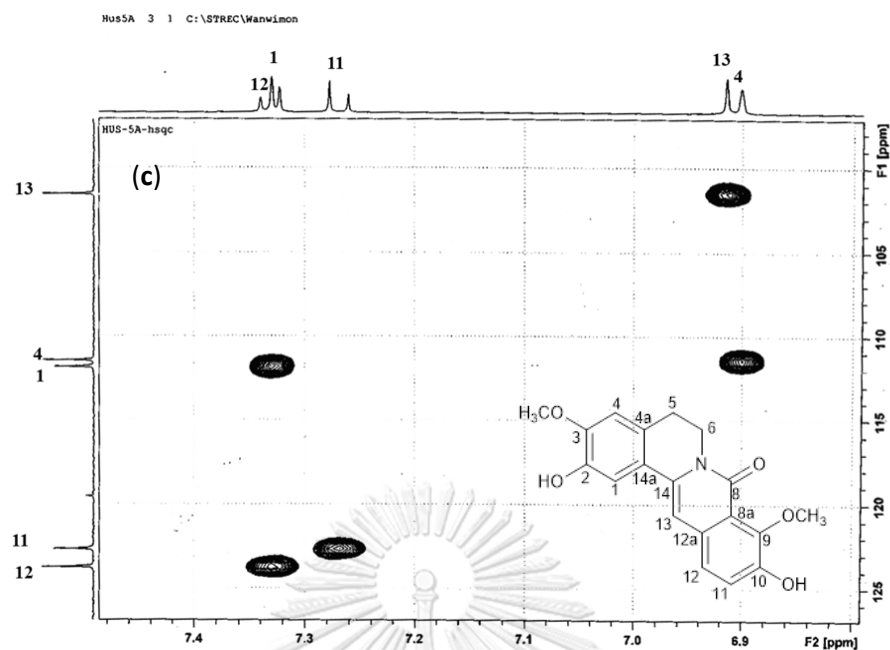


Figure 133 HSQC spectrum of compound HJ2 (continued)

(c) [expansion δ_{H} 6.8-7.5 ppm, δ_{C} 96-126 ppm]

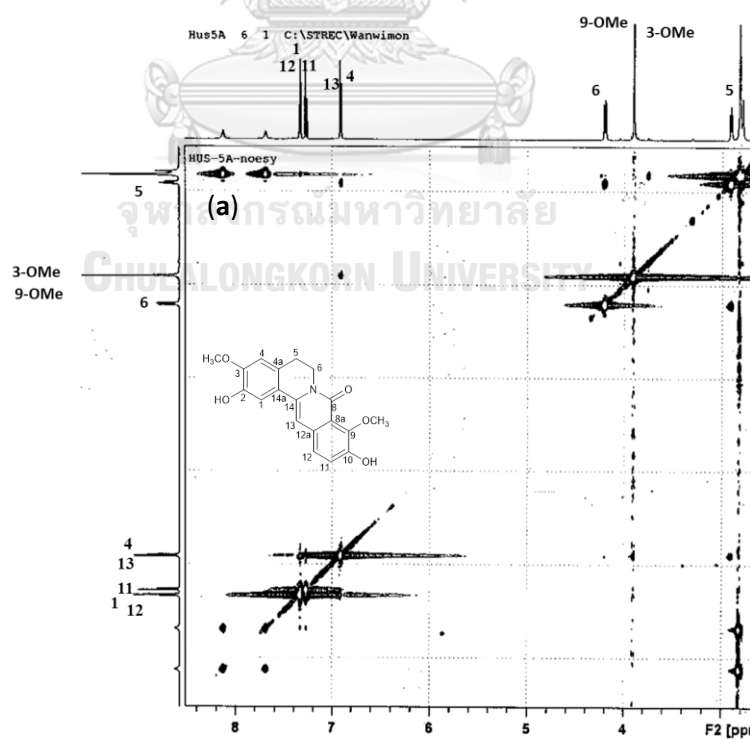


Figure 134 NOESY spectrum of compound HJ2

(a) full spectrum

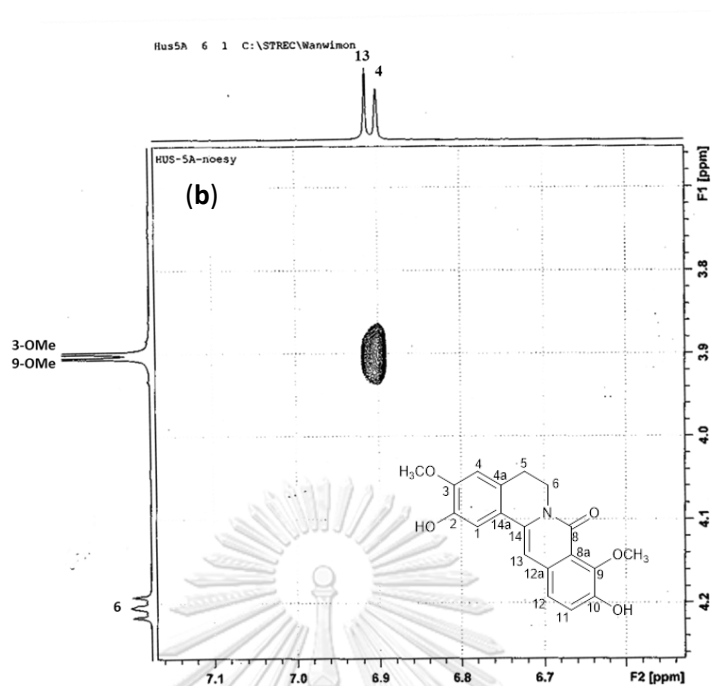


Figure 134 NOESY spectrum of compound HJ2 (continued)

(b) [expansion $F_1 \delta_H$ 3.7-4.3 ppm, $F_2 \delta_H$ 6.5 -7.2 ppm]

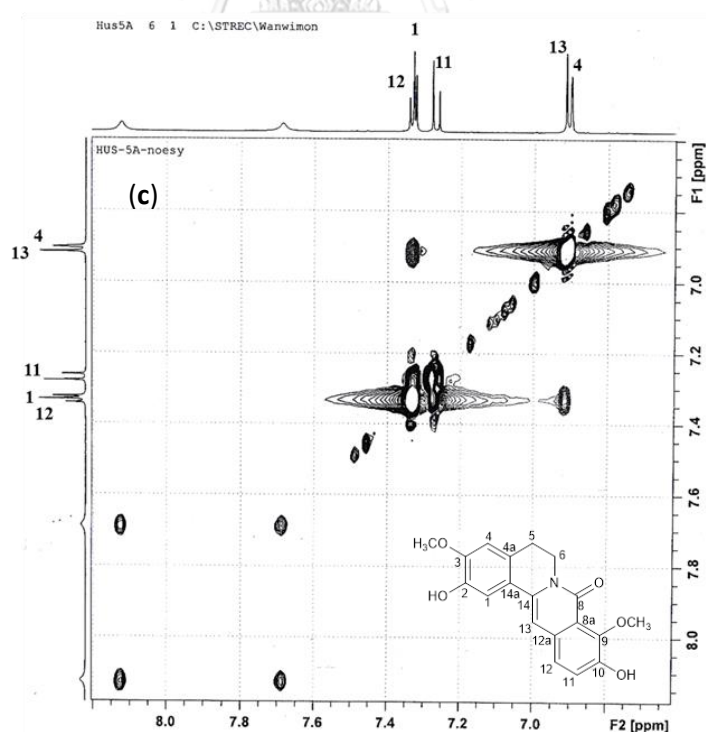


Figure 134 NOESY spectrum of compound HJ2 (continued)

(c) expansion [$F_1 \delta_H$ 6.6-8.2 ppm, $F_2 \delta_H$ 6.6 -8.2 ppm]

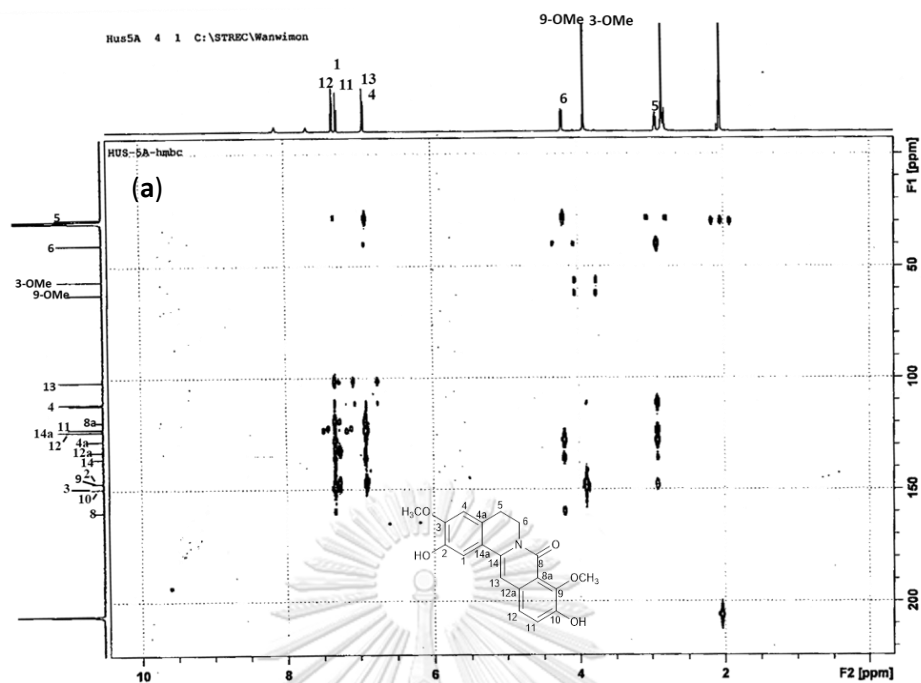


Figure 135 HMBC spectrum of compound HJ2
(a) full spectrum

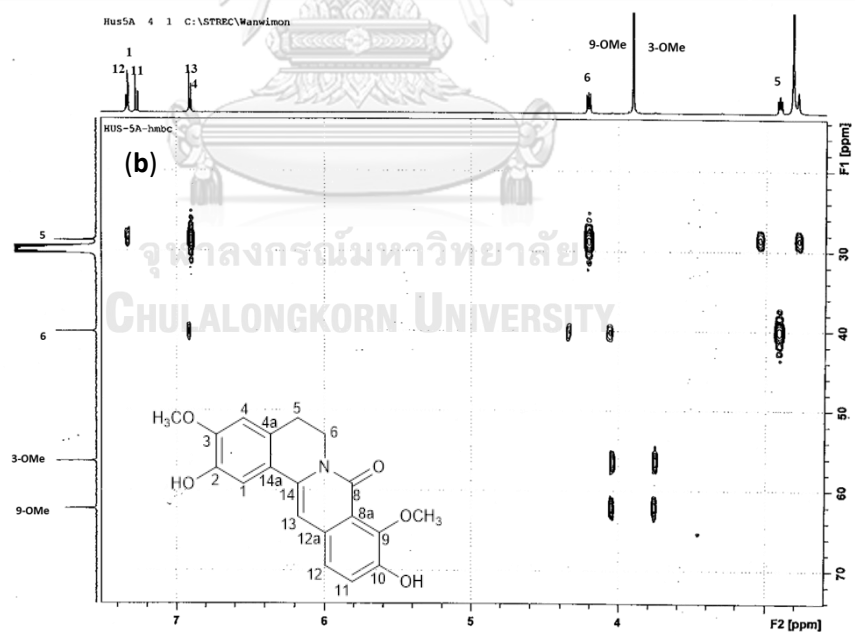


Figure 135 HMBC spectrum of compound HJ2 (continued)
(b) expansion [δ_{H} 2.6-7.5 ppm, δ_{C} 15-74 ppm]

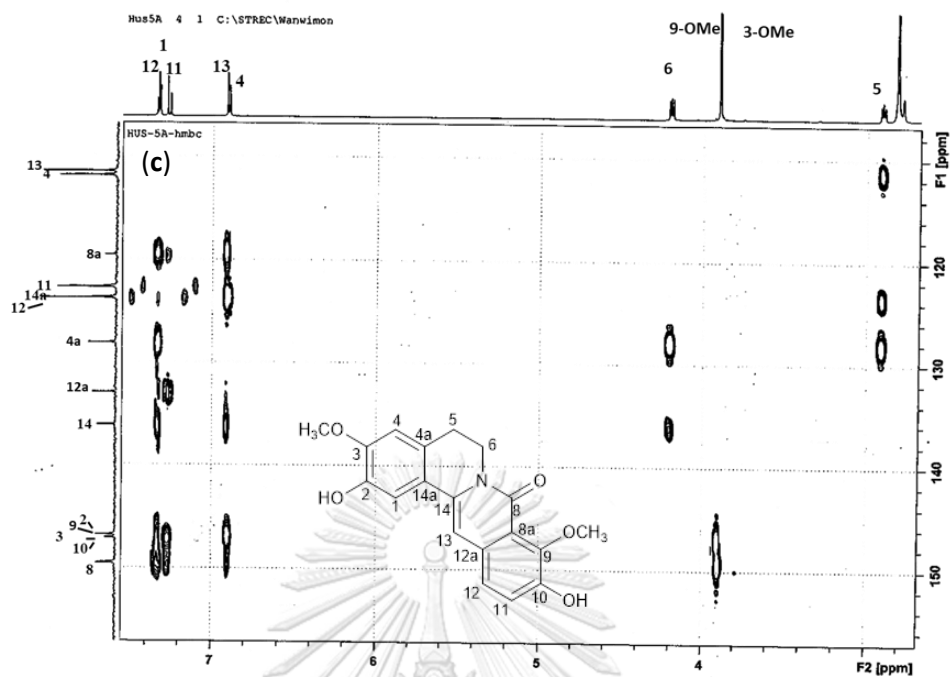


Figure 135 HMBC spectrum of compound HJ2 (continued)

(c) expansion [δ_{H} 2.6-7.6 ppm, δ_{C} 108-158 ppm];

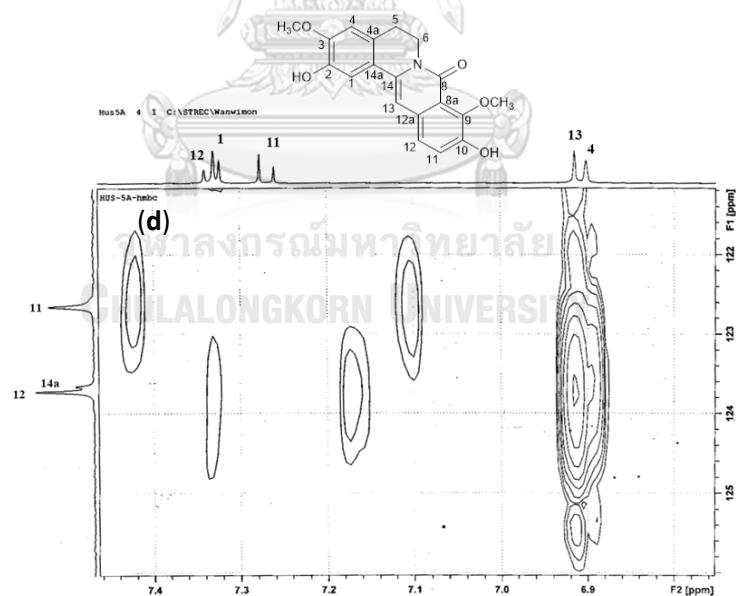


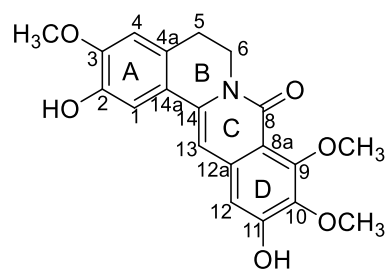
Figure 135 HMBC spectrum of compound HJ2 (continued)

(d) expansion [δ_{H} 6.6-7.5 ppm, δ_{C} 121-126 ppm]

4.2.3 Structure elucidation of compound HJ3

Compound **HJ3** was isolated as a brown powder. The molecular formula was determined by HR-ESI-MS to be $C_{20}H_{19}NO_6$ from the $[M-H]^-$, m/z 368.1129 (calcd. for $C_{20}H_{18}NO_6$ 368.1134) (**Figure 136**). The UV spectrum (**Figure 137**) showed maximal absorptions at 230, 260, 335 and 365 nm, similar to those of HJ2, suggesting an 8-oxoprotoberberine structure. The IR spectrum also indicated the presence of hydroxyl (3359 cm^{-1}), conjugated amide (1658 cm^{-1}), and aromatic (1561 and 1510 cm^{-1}) functionalities (**Figure 138**). The COSY spectrum (**Figure 139**) showed vicinal coupling between H₂-5 (δ 2.89) and H₂-6 (δ 4.16) protons. The molecular mass of compound HJ3 was 30 a.m.u higher than that of compound HJ2, suggesting that compound HJ3 possessed an additional methoxy group. This was supported by the NMR signals for three methoxy groups at δ 3.90 (3H, s, 9-OMe), 3.90 (3H, s, 3-OMe) and 3.88 (3H, s, 10-OMe) in the ^1H NMR spectrum (**Figure 140**) and at δ 61.9 (9-OMe), 61.5 (3-OMe) and 56.3 (10-OMe) in the ^{13}C NMR spectrum (**Figure 141**), and corresponding HSQC correlation peaks (**Figure 142**). This postulation was supported by the absence of the signal for H-11 and the appearance of H-12 as a singlet at δ 6.85 (1H, s) in HJ3. On ring A, a methoxy group was located at C-3, as evident from the NOESY (**Figure 143**) correlations from the methoxyl protons at δ 3.90 to the H-4 proton at δ 6.90. The protons of the other two methoxy groups did not show NOESY correlation with any aromatic proton, implying that they were located at C-9 and C-10. This was supported by the HMBC (**Figure 144**) correlations from H-12 to C-10 (δ 141.5) and C-11 (δ 155.2).

Thus, HJ3 was characterized as a new 8-oxoprotoberberine with the structure as shown [353].



HJ3 [353]



Table 34 NMR spectral data of compound HJ3

Position	δ_{H} (mult., J in Hz)	δ_{C}	HMBC (correlation with ^1H)
1	7.33 (1H, s)	112.0	-
2	-	146.7	1*, 4
3	-	149.6	1, 4*
4	6.90 (1H, s)	111.4	2*,
4a	-	128.4	1,6
5	2.89 (2H, dd, 6.5, 6.0)	28.7	6*
6	4.16 (2H, dd, 6.5, 6.0)	39.7	5*
8	-	159.7	6
8a	-	113.1	12, 13
9	-	155.4	-
10	-	141.5	12
11	-	155.2	12*
12	6.85 (1H, s)	107.3	13
12a	-	136.9	-
13	6.80 (1H, s)	100.7	12
14	-	137.9	1, 6
14a	-	123.4	4, 5, 13
9-OMe	3.90 (3H,s)	61.9	-
3-OMe	3.90 (3H,s)	61.5	-
10-OMe	3.88 (3H,s)	56.3	-
2-OH	7.72	-	-
11-OH	8.70	-	-

*= Two-bond coupling

Mass Spectrum List Report

Analysis Info

Analysis Name OSHTS12112019002.d
Method Tune_low_Neg_PIN012018.m
Sample Name HuS-6
21122019

Acquisition Date 12/21/2019 3:37:20 PM
Operator Administrator
Instrument micrOTOF 72

Acquisition Parameter

Source Type	ESI	Ion Polarity	Negative	Set Corrector Fill	75 V
Scan Range	n/a	Capillary Exit	-150.0 V	Set Pulsar Pull	372 V
Scan Begin	50 m/z	Hexapole RF	90.0 V	Set Pulsar Push	372 V
Scan End	3000 m/z	Skimmer 1	-50.0 V	Set Reflector	1300 V
		Hexapole 1	-25.0 V	Set Flight Tube	9000 V
				Set Detector TOF	2295 V

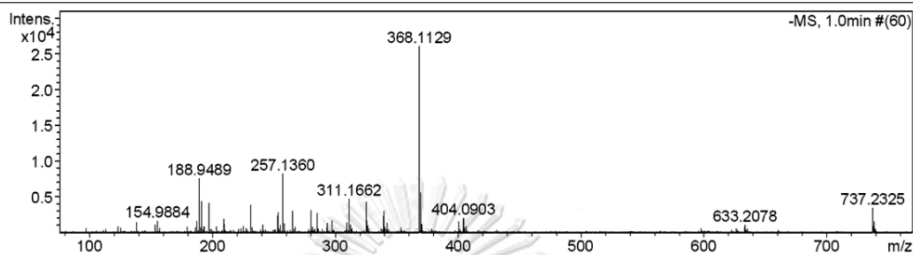


Figure 136 Mass spectrum of compound HJ3

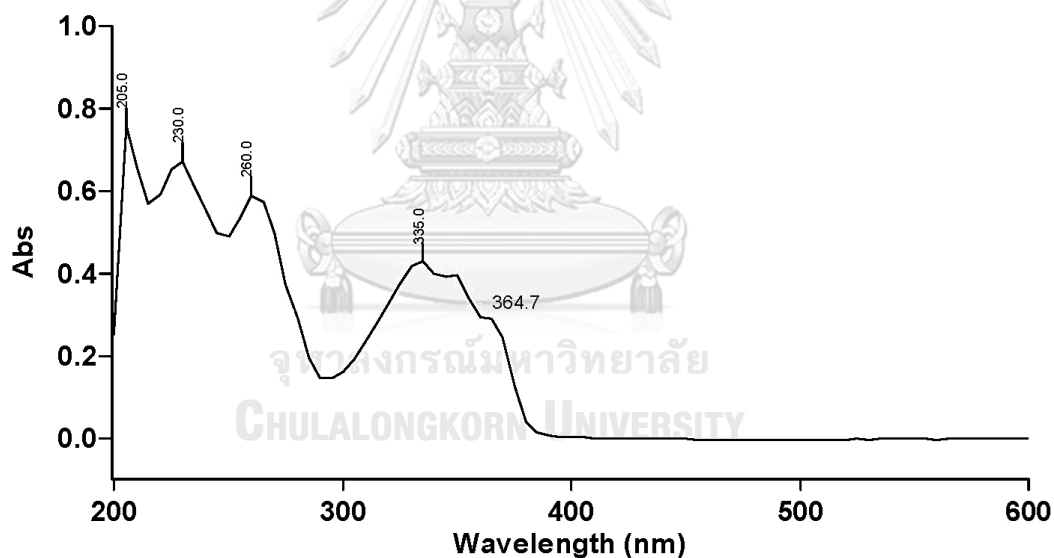


Figure 137 UV spectrum of compound HJ3

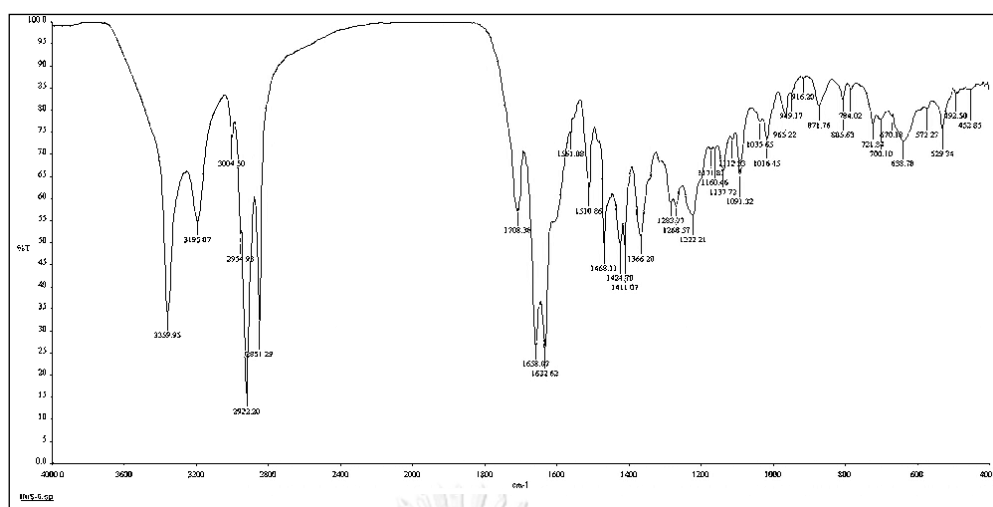


Figure 138 IR spectrum of compound HJ3

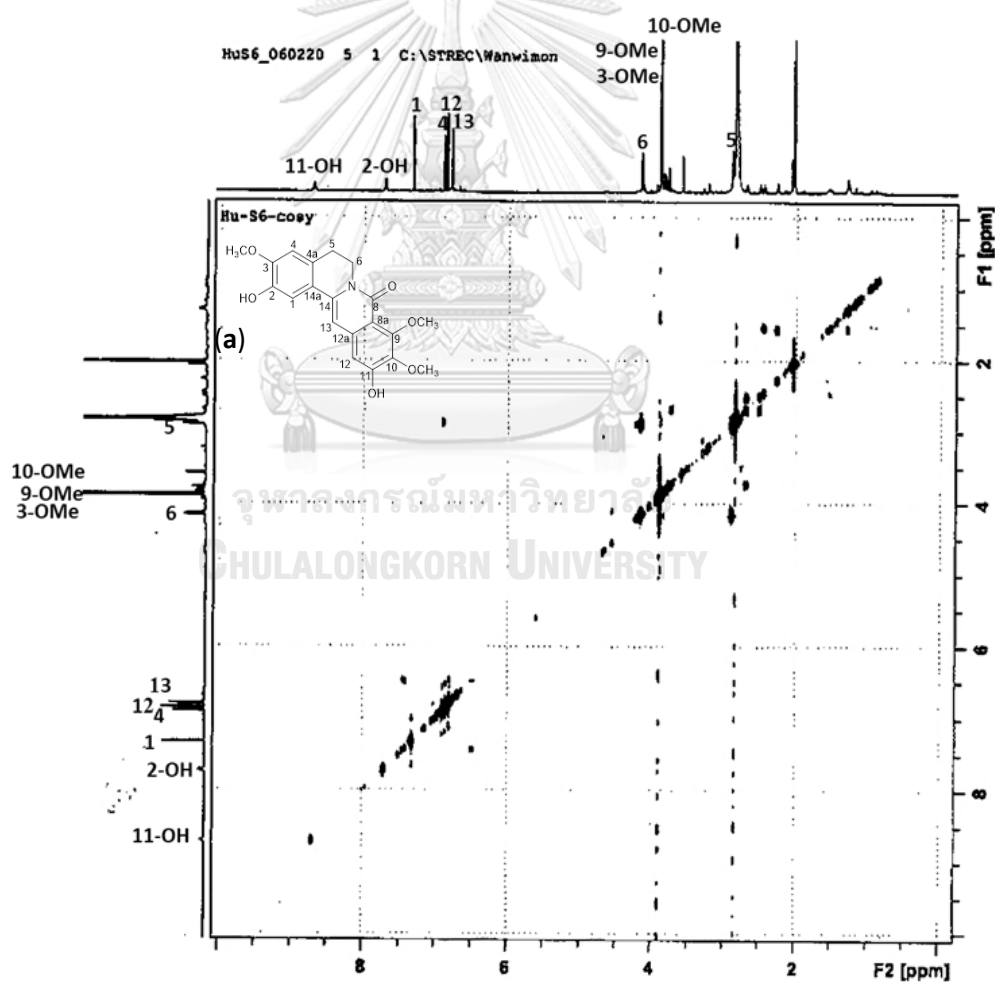


Figure 139 COSY spectrum of compound HJ3

(a) full spectrum

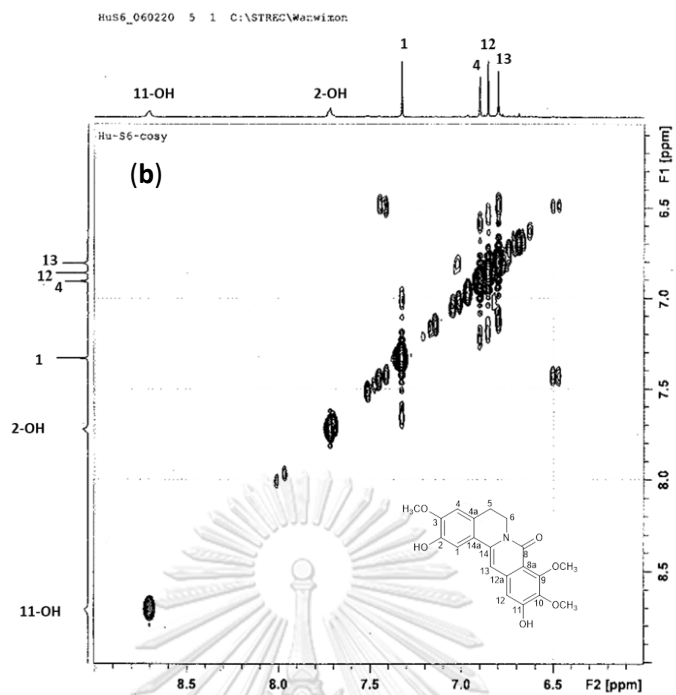
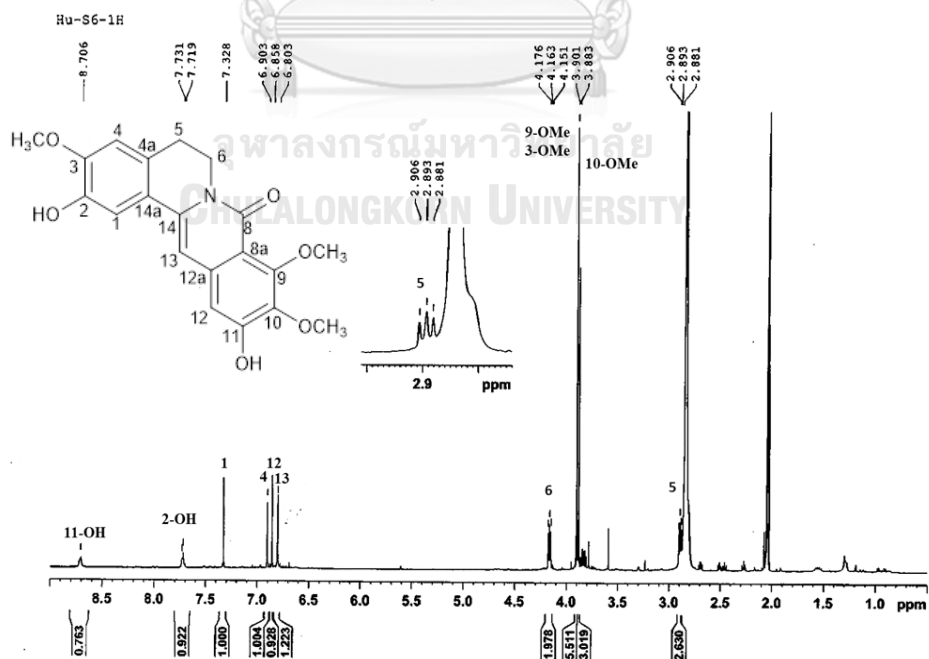


Figure 139 COSY spectrum of compound HJ3 (continued)

(b) expansion [δ_{H} 6.0 -9.0 ppm]Figure 140 $^1\text{H-NMR}$ (500 MHz) spectrum of compound HJ3 (acetone- d_6)

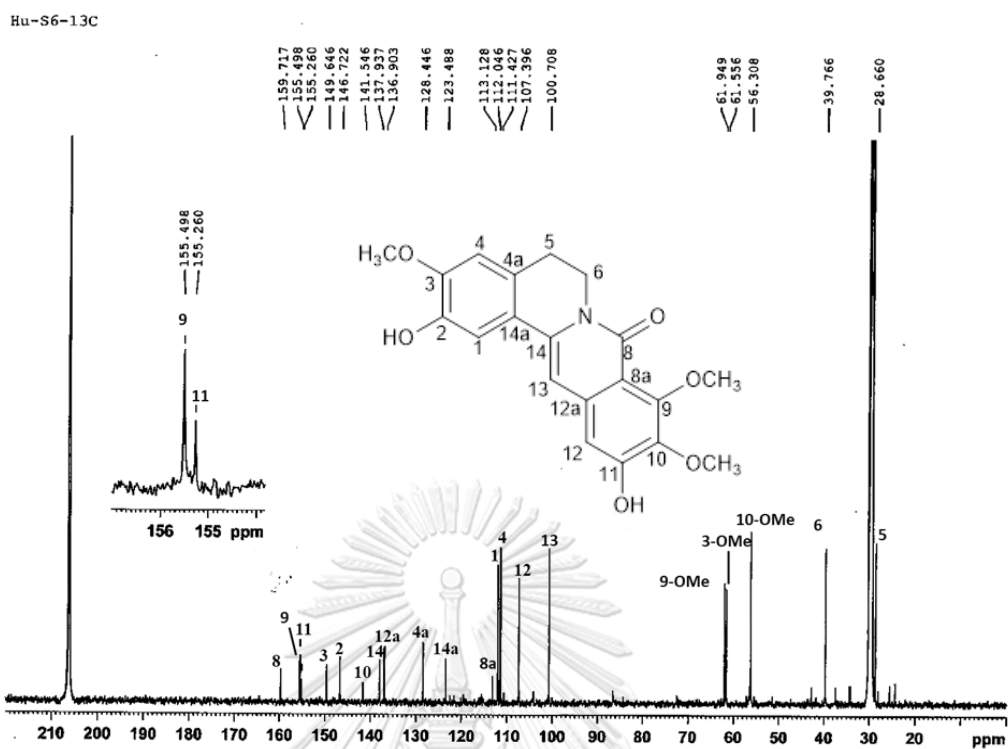


Figure 141 ^{13}C -NMR (125 MHz) spectrum of compound HJ3 (acetone- d_6)

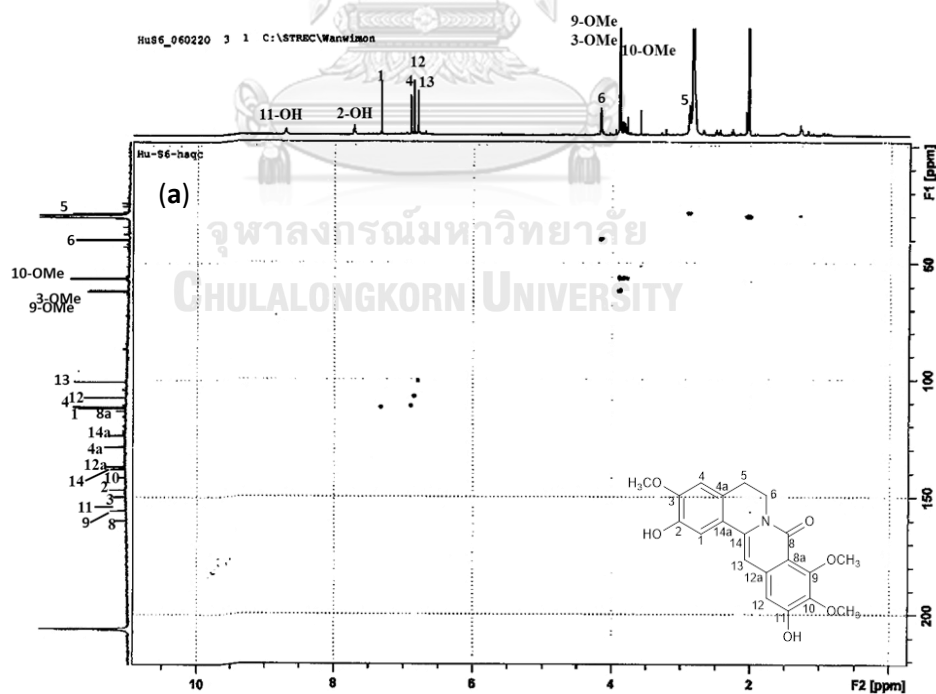
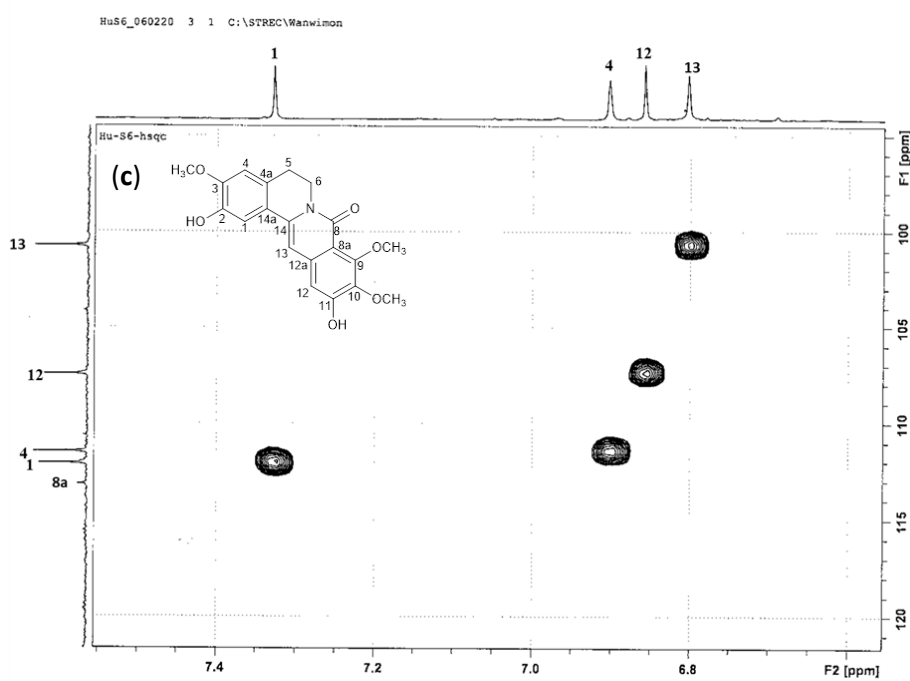
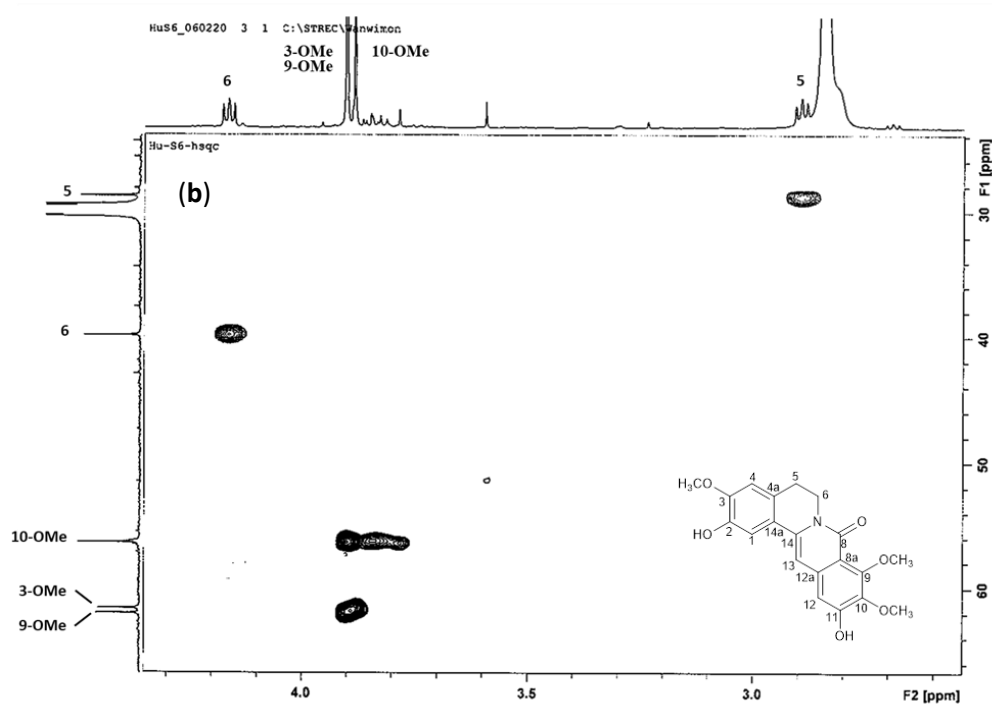


Figure 142 HSQC spectrum of compound HJ3

(a) full spectrum



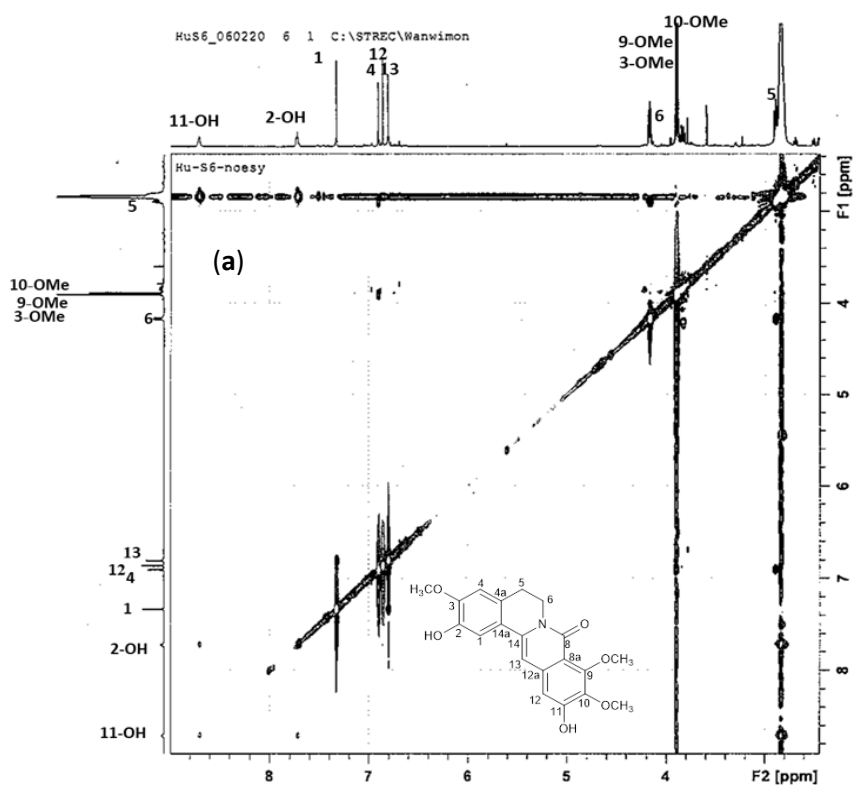


Figure 143 NOESY spectrum of compound HJ3

(a) full spectrum

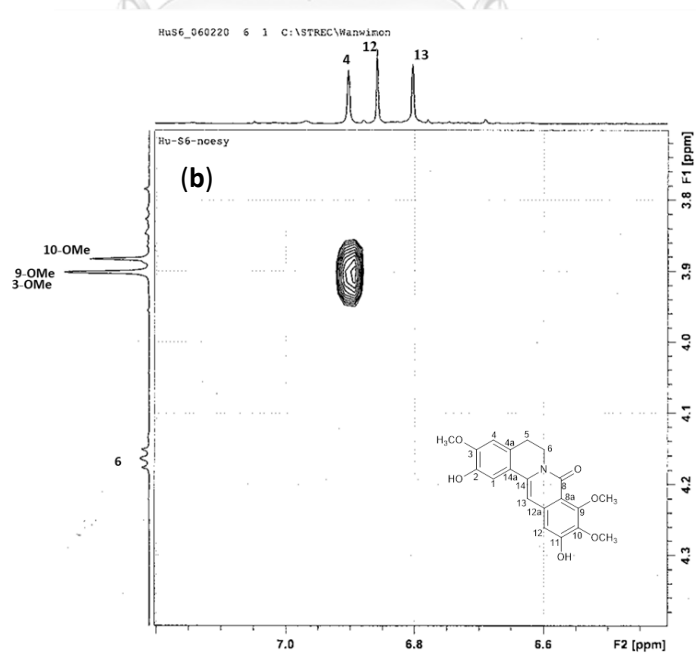


Figure 143 NOESY spectrum of compound HJ3 (continued)

(b) expansion [$F_1 \delta_H$ 3.7 - 4.4 ppm, $F_2 \delta_H$ 6.4 - 7.2 ppm]

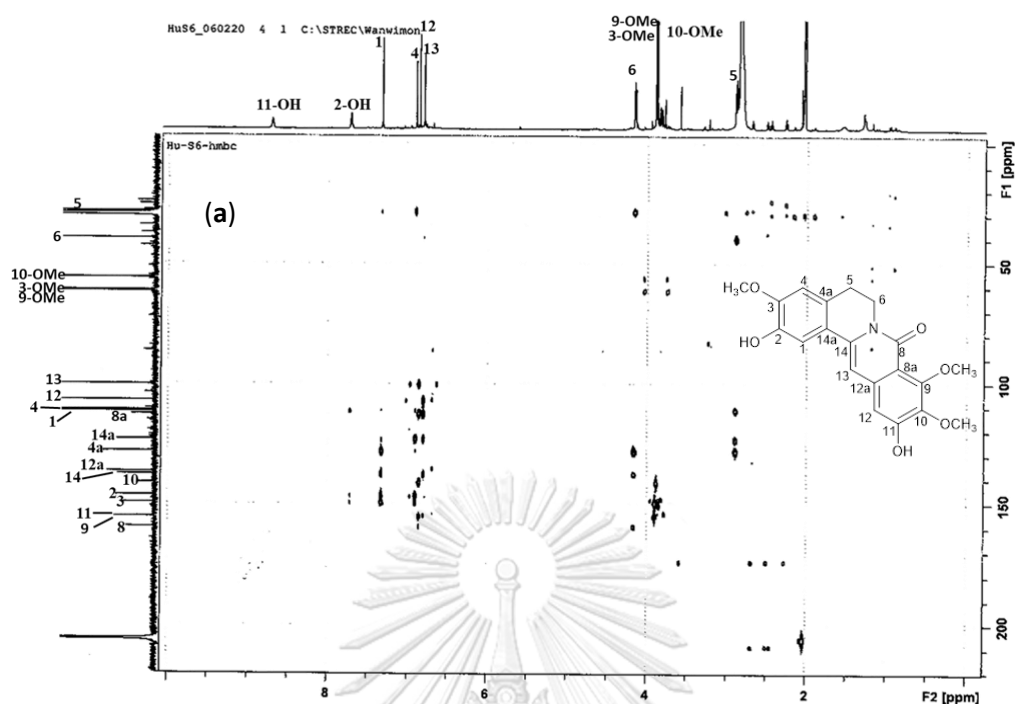


Figure 144 HMBC spectrum of compound HJ3

(a) full spectrum

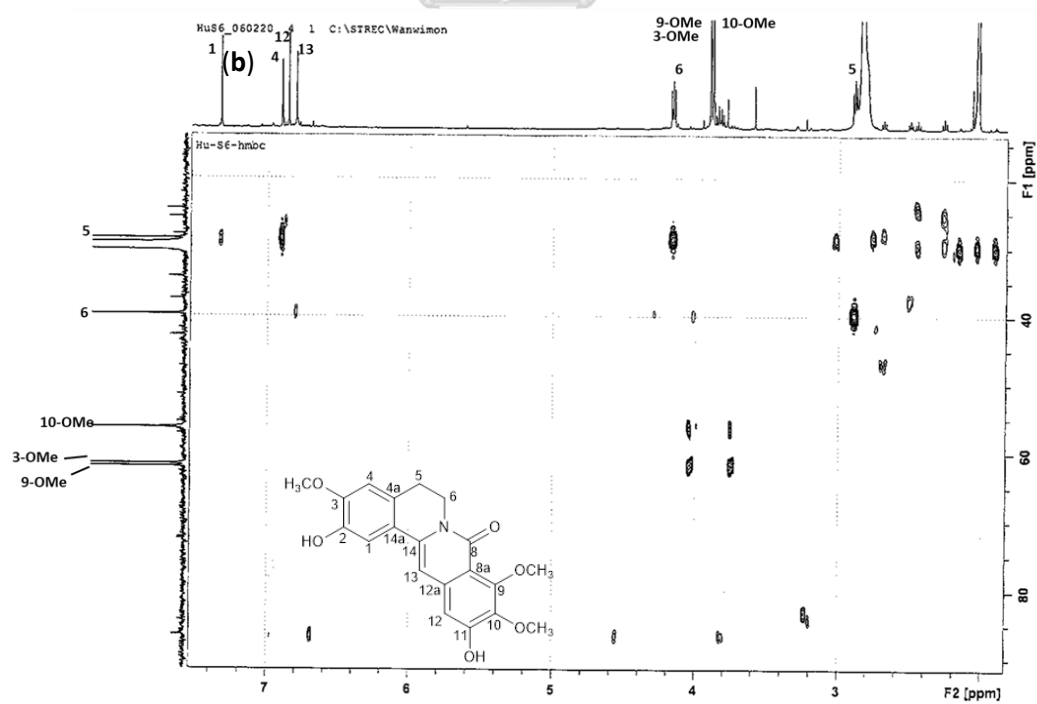


Figure 144 HMBC spectrum of compound HJ3 (continued)

(b) expansion [δ_{H} 2-7.4 ppm, δ_{C} 18-84 ppm]

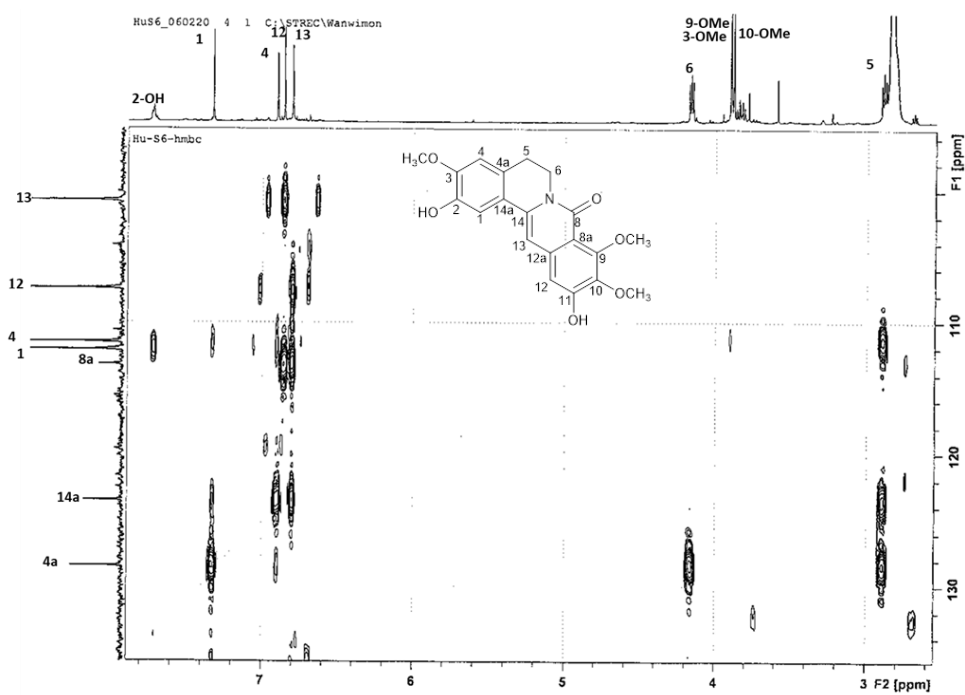


Figure 144 HMBC spectrum of compound HJ3 (continued)

(c) expansion [δ_{H} 2.6-7.8 ppm, δ_{C} 96-134 ppm]

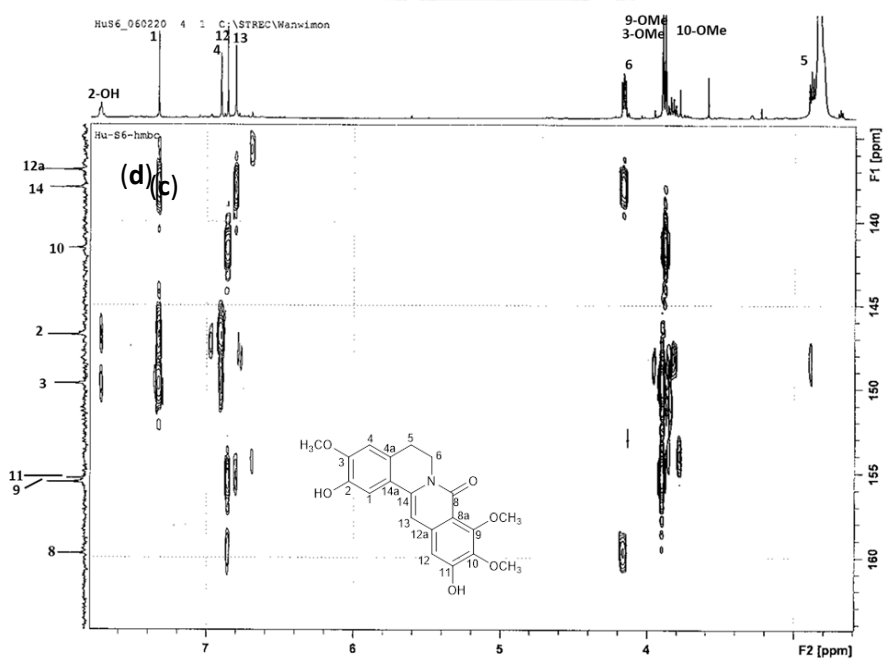


Figure 144 HMBC spectrum of compound HJ3 (continued)

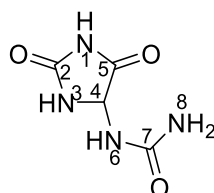
(d) expansion [δ_{H} 2.6-7.8 ppm, δ_{C} 135-164 ppm]

4.2.4 Identification compound HJ4 (allantoin)

Compound HJ4 was isolated as yellowish brown crystals. The high resolution ESI mass spectrum (**Figure 145**) showed a sodium-adduct molecular ion $[M+Na]^+$ at m/z 181.0330 (calcd. for $C_4H_6N_4O_3Na$ 181.0338), suggesting the molecular formula $C_4H_6N_4O_3$.

The 1H -NMR spectrum (**Figure 146**) exhibited three 1H singlets and two 1H doublets (**Table 35**). The ^{13}C -NMR spectrum (**Figure 147**) showed three carbonyl peaks at δ 157.2 (C-2), 157.8 (C-7) and 174.1 (C-5), and an upfield peak at δ 62.9 (C-4). According to the HSQC spectrum (**Figure 148**), the carbon at δ 62.9 was deduced as methine carbon due to the correlation with the proton at δ 5.24 (1H, s, H-4). Therefore, the remaining singlet protons should be attached to hetero atoms. The HMBC spectrum (**Figure 149**) showed 3-bond correlation from NH-3 [δ 6.88 (1H, d, J = 8.1 Hz)] to C-5 (δ 174.1) and C-2 (δ 157.2), and from H-4 [δ 8.05 (1H, s)] to C-7 (δ 157.79). The NOESY spectrum (**Figure 150**) displayed NOE cross peaks for the following pairs of protons: H-6 and H-8, H-3 and H-4, H-4 and H-6. By comparison of the spectral data with reported values (Rasheed *et al.*, 2004), compound HJ5 was identified as allantoin [**354**].

Allatoin [**354**] has been isolated from *Pisonia grandis* R. Br. (Sripathi *et al.*, 2011), rice garin (Wang *et al.*, 2012), *Cleome viscosa* L. (Lakshmanan *et al.*, 2019) and *Portulaca oleraceae* L. (Rasheed *et al.*, 2004).



allantoin [**354**]

Table 35 NMR spectral data of compound HJ4 as compared with allantoin

Position	Compound HJ4 (DMSO- <i>d</i> ₆)		Allantoin (DMSO- <i>d</i> ₆)*	
	δ_{H} (mult., <i>J</i> in Hz)	δ_{C}	δ_{H} (mult., <i>J</i> in Hz)	δ_{C}
1	10.53 (1H, s)	-	10.5 (1H, s)	-
2	-	157.2	-	157.1
3	8.05 (1H, s)	-	8.05 (1H, s)	-
4	5.24 (1H, d, 8.1)	62.9	5.3 (1H, d, 8.1)	62.7
5	-	174.1	-	174.0
6	6.88 (1H, d, 8.1)	-	6.9 (1H, d, 8.1)	-
7	-	157.8	-	157.6
8	5.78 (2H, s)	-	5.8 (2H, s)	-

* (Rasheed *et al.*, 2004)

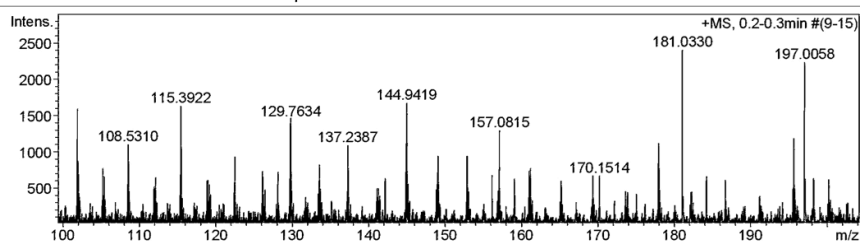
Mass Spectrum List Report

Analysis Info

Analysis Name	OSHTS28012020004.d	Acquisition Date	1/28/2020 3:08:49 PM
Method	Tune_low_90_04092017.m	Operator	Administrator
Sample Name	HuS-17	Instrument	microTOF 72
	HuS-17		

Acquisition Parameter

Source Type	ESI	Ion Polarity	Positive	Set Corrector Fill	50 V
Scan Range	n/a	Capillary Exit	120.0 V	Set Pulsar Pull	337 V
Scan Begin	50 m/z	Hexapole RF	90.0 V	Set Pulsar Push	337 V
Scan End	3000 m/z	Skimmer 1	70.0 V	Set Reflector	1300 V
		Hexapole 1	25.0 V	Set Flight Tube	9000 V
				Set Detector TOF	2285 V

**Figure 145** Mass spectrum of compound HJ4

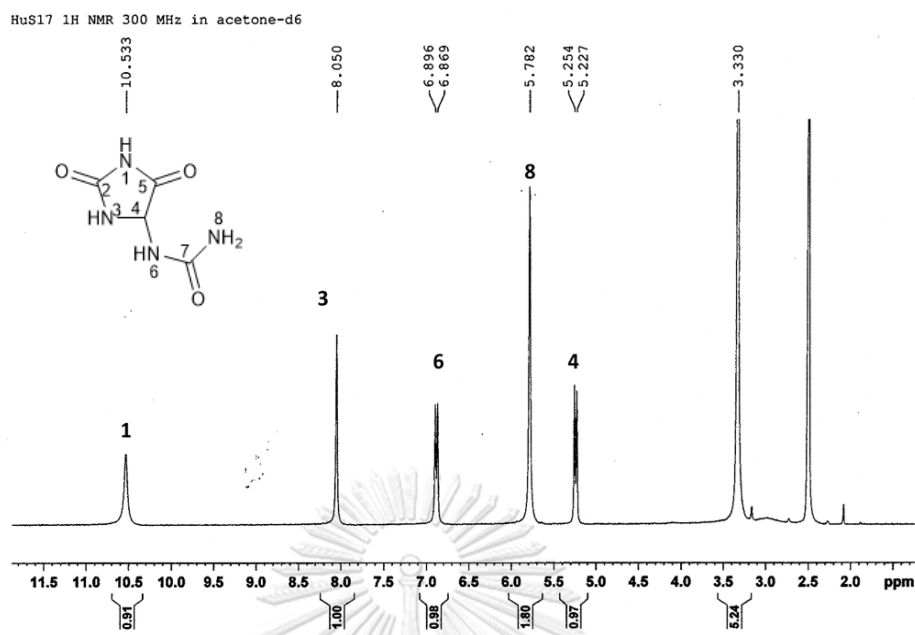


Figure 146 $^1\text{H-NMR}$ (300 MHz) spectrum of compound HJ4 ($\text{DMSO-}d_6$)

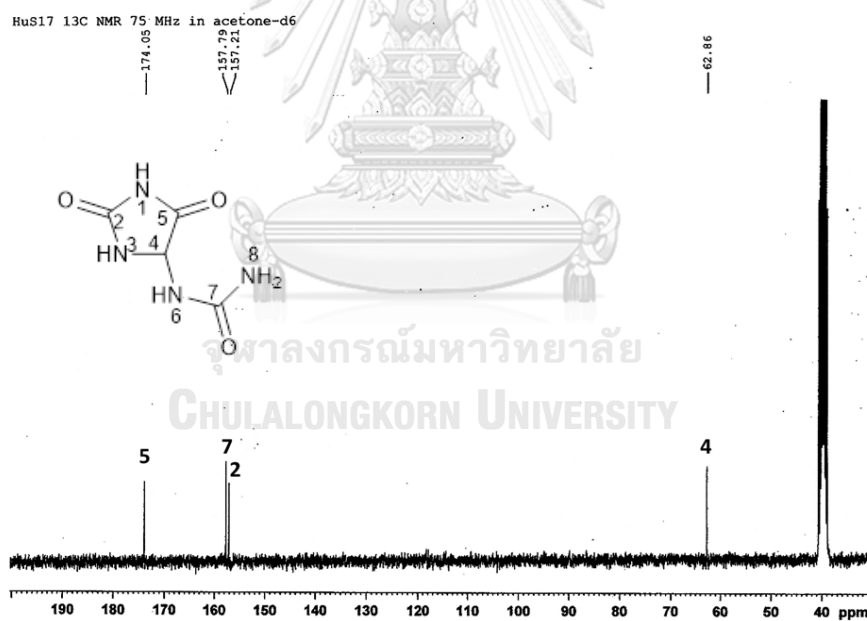


Figure 147 $^{13}\text{C-NMR}$ (75 MHz) spectrum of compound HJ4 ($\text{DMSO-}d_6$)

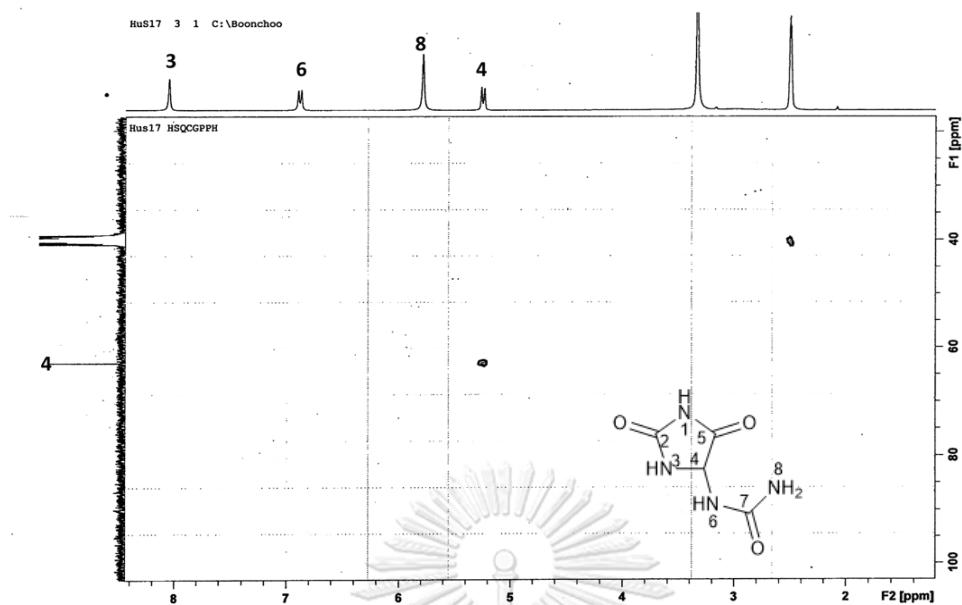


Figure 148 HSQC spectrum of compound HJ4

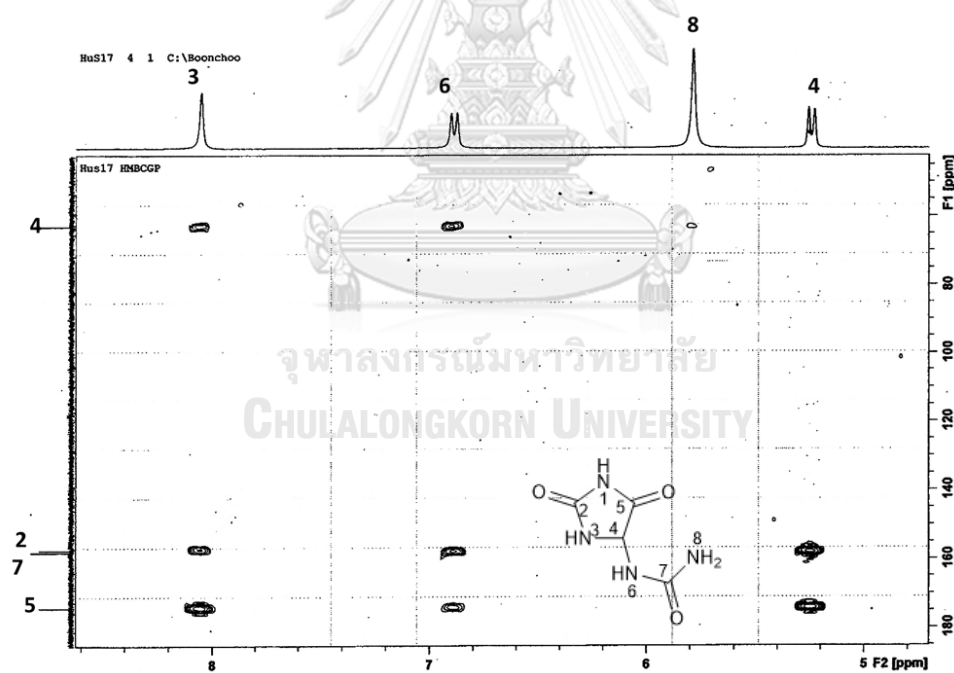


Figure 149 HMBC spectrum of compound HJ4

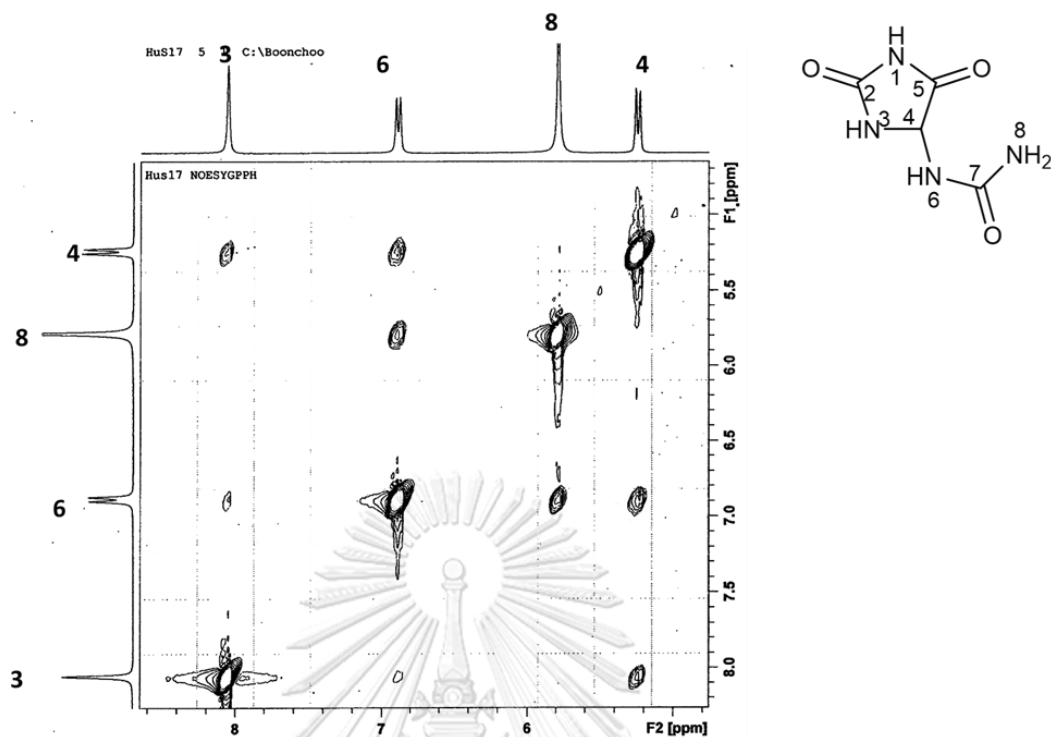


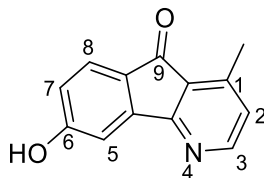
Figure 150 NOESY spectrum of compound HJ4

4.2.5 Identification of compound HJ5 (oxylopinine)

Compound HJ5 was isolated as a yellow powder. The molecular formula was determined by HR-ESI-MS (**Figure 151**) to be $C_{13}H_9NO_2$ from the $[M+H]^+$ m/z 212.0693 (calcd. for $C_{13}H_{10}NO_2$ 212.0712).

In the 1H -NMR spectrum (**Figure 152**), an AB coupling system for pyridine ring was observed at δ 7.11 (1H, d, $J = 5.1$ Hz, H-2) and 8.42 (1H, d, $J = 5.4$ Hz, H-3). The aromatic protons at δ 6.91 (1H, dd, $J = 2.1, 8.1$ Hz, H-7) and 7.56 (1H, d, $J = 8.1$ Hz, H-8) showed *ortho*-coupling to each other. The aromatic proton at δ 7.29 (1H, d, $J = 1.8$ Hz, H-5) showed *meta*-coupling with H-7 (δ 6.91). The ^{13}C -NMR spectrum (**Table 36** and **Figure 153**) displayed 13 carbons including a carbonyl at δ 164.1 (CO) and a methyl at δ 15.9 (3-Me). The HSQC spectrum (**Figure 154**) showed protonated carbons. The HMBC spectrum (**Figure 155**) showed correlations that suggested compound HJ5 as an azafluorene derivative with a carbonyl group connecting an aromatic ring to the heterocyclic pyridine ring.

By comparison of these spectral data with previous literature data (Tadic *et al.*, 1988), compound HJ5 was identified as oxylopinine [355]. Oxylopinine were firstly found in *Oxandra xylopioides* (El-Shanawany *et al.*, 1985). It was also reported as a constituent of *Saccopetalum prolificum* (Wang *et al.*, 2000), *Polyalthia obliqua* (Wu *et al.*, 2016) and *Unonopsis spectabilis* (Laprévôte *et al.*, 1988).



oxylopinine [355]

Table 36 NMR spectral data of compound HJ5 as compared with oxylopinine

Position	Compound HJ5		oxylopinine*	
	δ_{H} (mult., <i>J</i> in Hz)	δ_{C}	δ_{H} (mult., <i>J</i> in Hz)	δ_{C}
1	-	146.5	-	147.0
2	7.11 (1H, d, 5.1)	126.0	7.13 (1H, d)	125.7
3	8.42 (1H, d, 5.4)	152.5	8.35 (1H, d)	152.2
4a	-	164.1	-	164.3
4b	-	146.0	-	145.9
5	7.29 (1H, d, 1.8)	107.8	7.24 (1H, d)	105.9
6	-	164.1	-	165.7
7	6.91 (1H, d, 2.1, 8.1)	116.9	6.82 (1H, t)	116.4
8	7.56 (1H, d, 8.1)	125.7	7.56 (1H, d)	126.1
8a	-	127.1	-	127.1
9	-	192.0	-	191.9
9a	-	126.4	-	127.9
3-Me	2.59 (3H, s)	15.9	2.62 (3H, s)	17.3

* (Tadic *et al.*, 1988)

Mass Spectrum List Report

Analysis Info

Analysis Name OSHTS28012020002.d
 Method Tune_low_120_04092017.m
 Sample Name HuS-3A
 HuS-3A

Acquisition Date 1/28/2020 3:02:21 PM
 Operator Administrator
 Instrument micrOTOF 72

Acquisition Parameter

Source Type	ESI	Ion Polarity	Positive	Set Corrector Fill	50 V
Scan Range	n/a	Capillary Exit	150.0 V	Set Pulsar Pull	337 V
Scan Begin	50 m/z	Hexapole RF	180.0 V	Set Pulsar Push	337 V
Scan End	3000 m/z	Skimmer 1	60.0 V	Set Reflector	1300 V
		Hexapole 1	23.0 V	Set Flight Tube	9000 V
				Set Detector TOF	2295 V

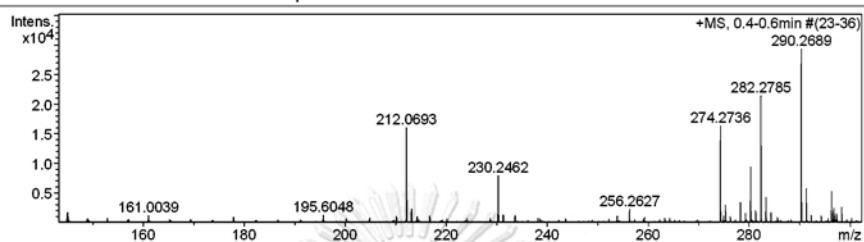


Figure 151 Mass spectrum of compound HJ5

HuS3A 1H NMR 300 MHz in acetone-d6

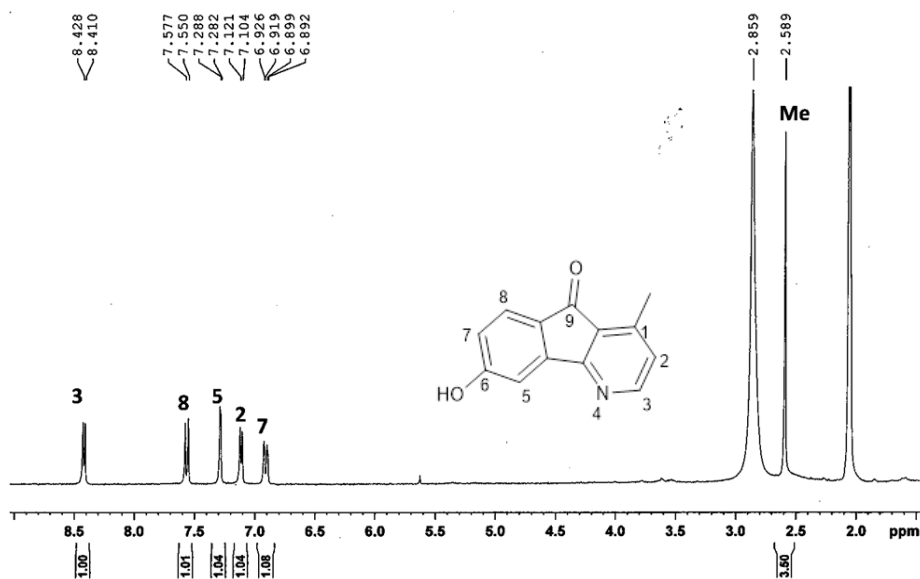
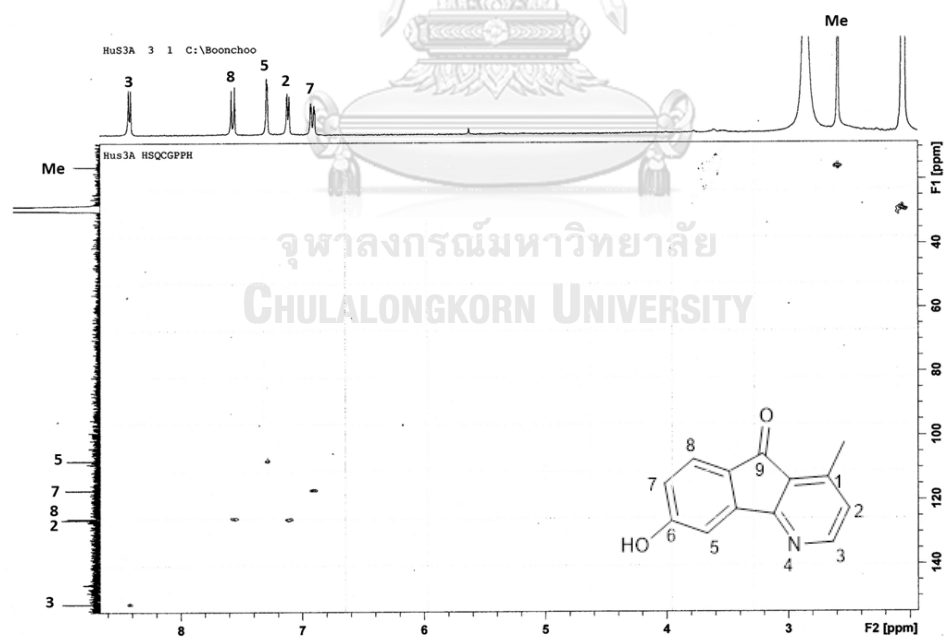
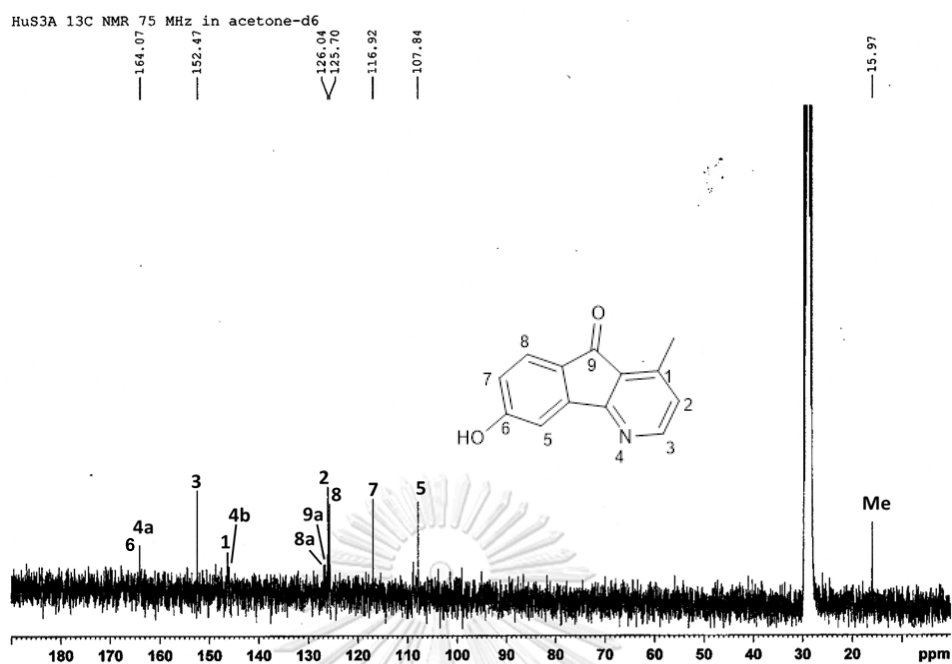


Figure 152 ^1H -NMR (300 MHz) spectrum of compound HJ5 (acetone- d_6)



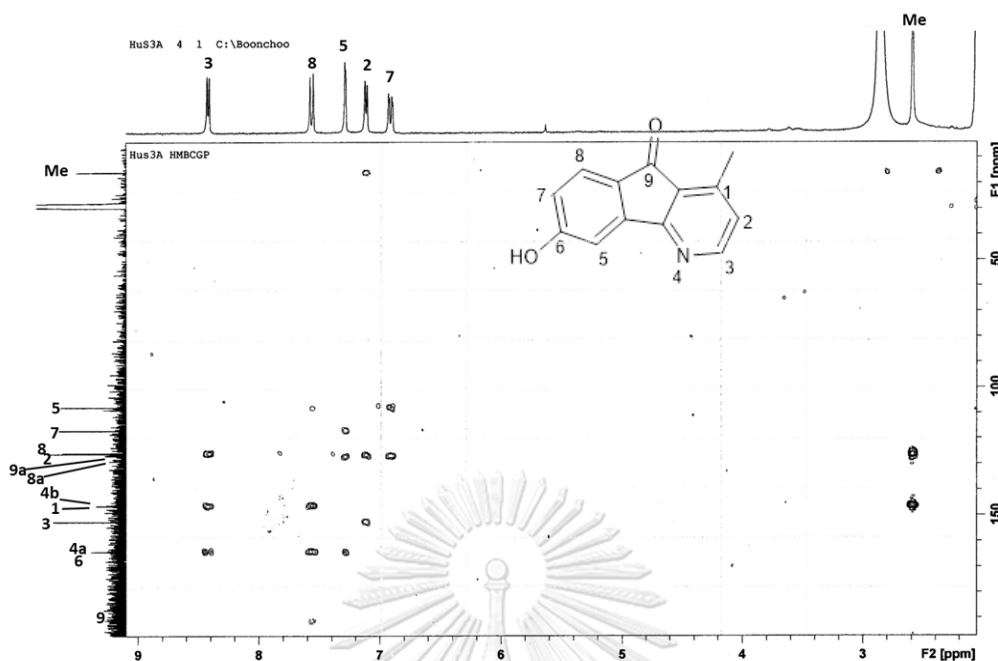


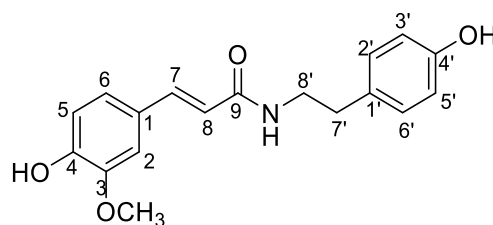
Figure 155 HMBC spectrum of compound HJ5

4.2.6 Identification of compound HJ6 (*N-trans-feruloyltyramine*)

Compound HJ6 was isolated as a brownish white powder. The molecular formula for compound HJ6 was determined by HR-ESI-MS (Figure 156) to be $C_{18}H_{19}NO_4$ from the $[M+H]^+$ m/z 314.1395 (calcd. for $C_{18}H_{20}NO_4$ 314.1392). In the 1H NMR spectrum (Figure 157) the presence of a *para*-substituted aromatic ring was suggested from the signals of *ortho*-coupled protons at δ 7.06 (2H, dd, $J = 8.5, 2.1$ Hz, H-2', H-6') and 6.77 (2H, dd, $J = 8.4, 2.1$ Hz, H-3', H-5'). In addition, three aromatic proton signals at δ 6.82 (1H, d, $J = 8.5$ Hz), 7.06 (1H, dd, $J = 8.5, 2.0$ Hz) and 7.14 (1H, d, $J = 2.0$ Hz) suggested the presence of another aromatic ring with tri-substitution. Resonances for a methoxy group and four methylene protons showed at δ 3.85 (3H, s) and 2.74 (2H, t, $J = 7.5$ Hz, H-2) and 3.48 (2H, t, $J = 7.5$ Hz, H-8'), respectively. Two doublets for olefinic protons appeared at δ 6.5 and 7.5 with $J = 15.5$ Hz, indicating a *trans* configuration.

The ^{13}C NMR and DEPT spectra (**Figure 158**) included 18 signals suggesting two aromatic rings with two olefinic carbons [δ 139.7 (C-7) and 118.9 (C-8)], two methylene groups [δ 41.1 (C-8') and 34.8 (C-7')], a carbonyl [δ 165.9 (C-9)] and a methoxy group (δ 55.3). The HSQC spectrum (**Figure 159**) showed C-H 1-bond couplings. In the HMBC spectrum (**Figure 160**), the olefinic proton H-7 (δ 7.5) showed 3-bond correlation with C-2 (δ 110.4) and C-6 (δ 121.7). The other olefinic proton H-8 (δ 6.5) had a cross peak with C-1 (δ 127.3). The NOESY spectrum (**Figure 161**) revealed the location of the methoxy group at C-3 from the NOE cross peak between H-2 (δ 7.06) and 3-OMe (δ 3.86).

Finally, compound HJ6 was identified as *N-trans-feruloyltyramine* [**10**] through comparison its NMR data with reported literature (Al-Taweel *et al.*, 2012). *N-trans-feruloyltyramine* [**10**] has been previously found in the family Annonaceae, for example *Pseuduvaria fragrans* (Panidthananon *et al.*, 2018), *Annona glabra* (Chang *et al.*, 2000) and *Polyalthia suberosa* (Tuchinda *et al.*, 2000), and other plants such as *Porcelia macrocarpa* (Chaves & Roque, 1997), *Corydalis pallida* (Kim *et al.*, 2005) and *Celtis africana* (Al-Taweel *et al.*, 2012).



N-trans-feruloyltyramine [**10**]

Table 37 NMR spectral data of compound HJ6 as compared with *N-trans*-feruloyltyramine

Position	Compound HJ6		<i>N-trans</i> -feruloyltyramine*	
	δ_{H} (mult., <i>J</i> in Hz)	δ_{C}	δ_{H} (mult., <i>J</i> in Hz)	δ_{C}
1	-	127.3	-	128.2
2	7.14 (1H, d, 2.0)	110.4	7.13 (d, 1H, 1.2)	111.5
3	-	147.7	-	149.3
4	-	148.3	-	149.8
5	6.82 (1H, d, 8.5)	115.2	6.81(1H, d, 8.5)	116.4
6	7.06 (1H, dd, 8.5, 2.0)	121.7	7.05 (1H, dd, 8.5, 1.2)	123.2
7	7.5 (1H, d, 15.6)	139.7	7.44 (1H, d, 15.5)	142.0
8	6.5 (1H, d,15.5)	118.9	6.41 (1H, d, 15.5)	118.7
9	-	165.9	-	169.2
1'	-	130.2	-	131.3
2'	7.06 (1H, dd, 8.5, 2.1)	129.6	7.07 (2H, d, 8.4)	130.7
3'	6.77 (1H, dd, 8.4, 2.1)	115.2	6.73 (2H, d, 8.4)	116.2
4'	-	155.9	-	156.9
5'	6.77 (1H, dd, 8.4, 2.1)	115.2	6.73 (2H, d, 8.4)	116.2
6'	7.06 (1H, dd, 8.5, 2.1)	129.6	7.07 (2H, d, 8.4)	130.7
7'	2.74 (2H, t, 7.5)	34.8	2.76 (2H, t, 7.5)	35.8
8'	3.48 (2H, t, 7.5)	41.1	3.47 (2H, t, 7.5)	42.5
3-OMe	3.86 (3H, s)	55.3	3.85 (3H, s,)	56.4

* (Al-Taweel *et al.*, 2012)

Mass Spectrum List Report

Analysis Info

Analysis Name OSHTS28012020001.d
 Method Tune_low_120_04092017.m
 Sample Name HuS-1
 HuS-1

Acquisition Date 1/28/2020 2:59:54 PM
 Operator Administrator
 Instrument micrOTOF 72

Acquisition Parameter

Source Type	ESI	Ion Polarity	Positive	Set Corrector Fill	50 V
Scan Range	n/a	Capillary Exit	150.0 V	Set Pulsar Pull	337 V
Scan Begin	50 m/z	Hexapole RF	180.0 V	Set Pulsar Push	337 V
Scan End	3000 m/z	Skimmer 1	60.0 V	Set Reflector	1300 V
		Hexapole 1	23.0 V	Set Flight Tube	9000 V
				Set Detector TOF	2295 V

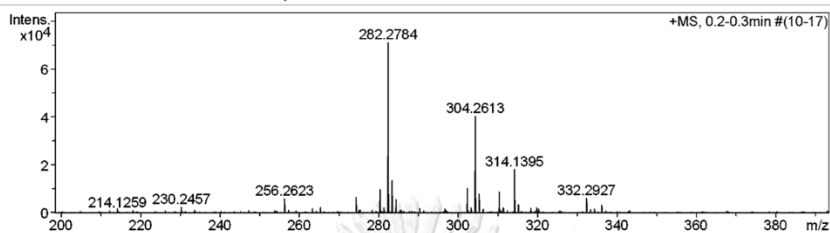


Figure 156 Mass spectrum of compound HJ6

HuS1 1H NMR 300 MHz in acetone-d₆

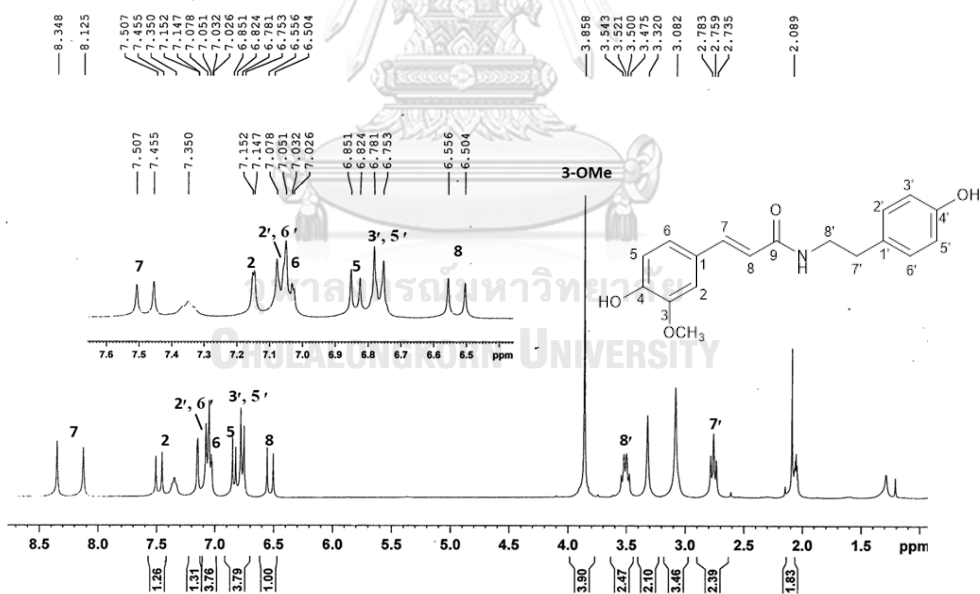


Figure 157 ¹H-NMR (300 MHz) spectrum of compound HJ6 (acetone-d₆)

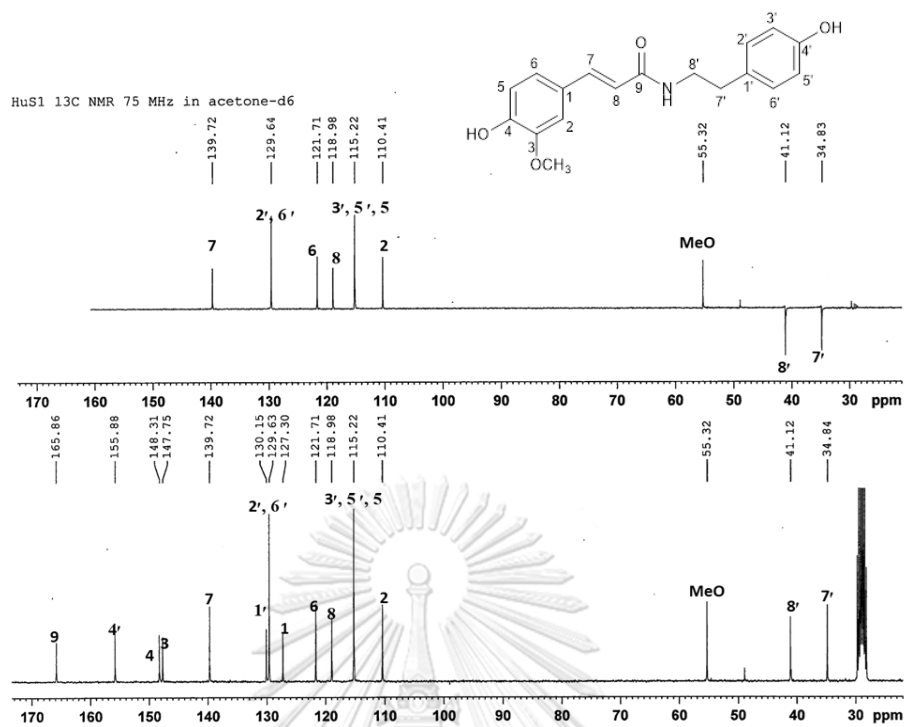


Figure 158 ¹³C-NMR (75 MHz) and DEPT-135 spectra of compound HJ6 (acetone-d₆)

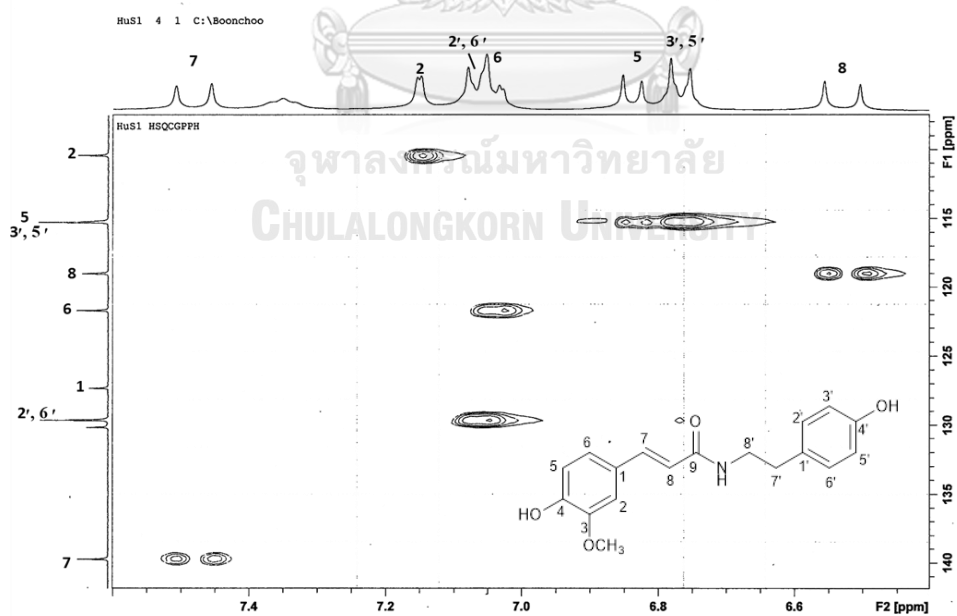


Figure 159 HSQC spectrum of compound HJ6

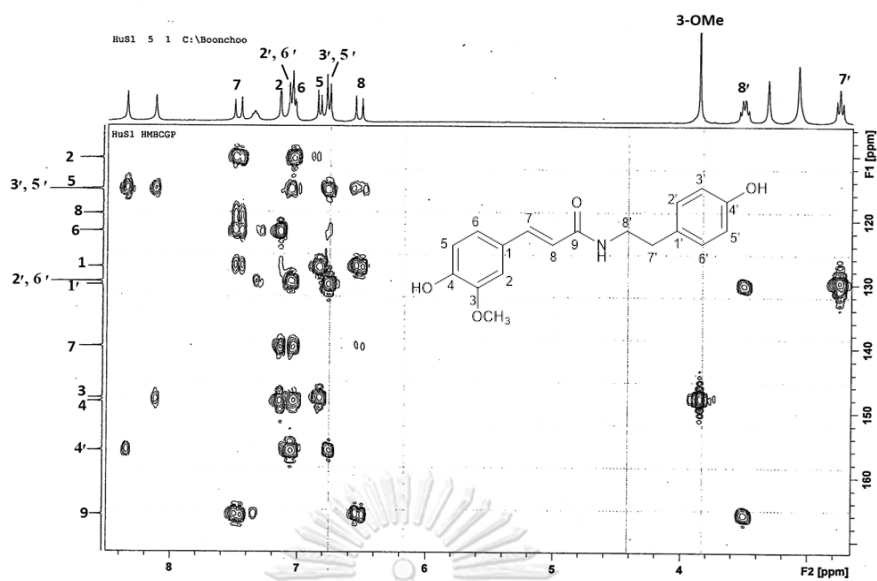


Figure 160 HMBC spectrum of compound HJ6

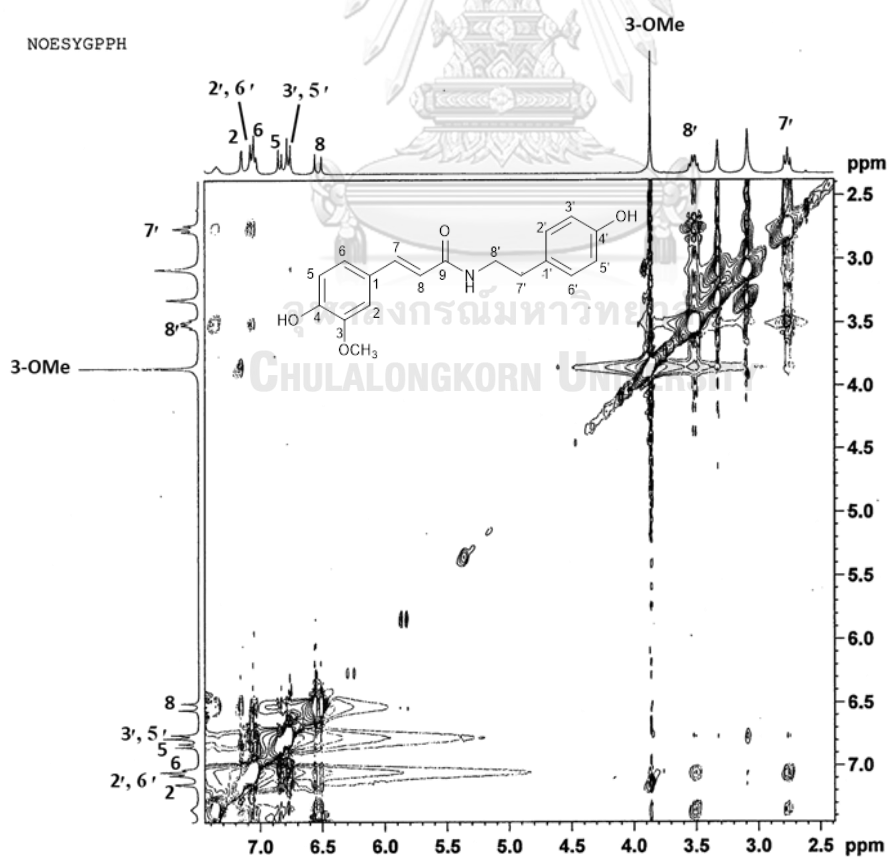


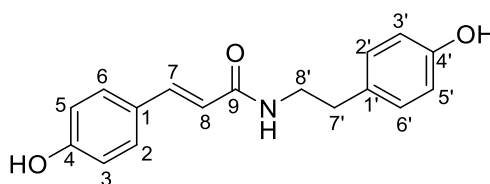
Figure 161 NOESY spectrum of compound HJ6

4.2.7 Identification of compound HJ7 (N-trans-p-coumaroyl tyramine)

Compound HJ7 was isolated as a brownish white powder. The molecular formula for compound HJ7 was determined by HR-ESI-MS to be $C_{17}H_{17}NO_3$ from the $[M+H]^+$, m/z 284.1277 (calcd. for $C_{17}H_{18}NO_3$ 284.1287) (Figure 162).

The 1H -NMR spectrum (Figure 163) exhibited two 2H doublets at δ 7.42 (2H, d, $J = 8.7$ Hz, H-2, H-6) and 6.85 (2H, dd, $J = 8.4, 2.1$ Hz, H-3, H-5). This suggested that compound HJ7 possessed an aromatic ring which had symmetric *para*-substitution, different from compound HJ6. The signals for the other aromatic ring was similar to those of compound HJ6. The ^{13}C -NMR spectrum (Table 38 and Figure 164) and the HSQC spectrum (Figure 165) further confirmed that compound HJ7 was a coumaroyl derivative having seventeen carbon signals for twelve aromatic carbons, two olefinic carbons, one carbonyl and two methylene carbons. In the HMBC spectrum (Figure 166) the olefinic proton H-7 (δ 6.48) showed 3-bond correlation with C-2 (δ 129.2) and C-6 (δ 129.2). The other olefinic proton H-8 (δ 7.47) had a cross peak with C-1 (δ 126.9).

Through comparison of the above data with reported values (Al-Taweel *et al.*, 2012), compound HJ7 was identified as *N*-trans-*p*-coumaroyl tyramine [356]. This compound has been found in several plants such as *Celtis africana* (Al-Taweel *et al.*, 2012), *Hypocoum parviflorum* (Hussain *et al.*, 1980) and also in Annonaceae family such as *Pseuduvaria fragrans* (Panidthananon *et al.*, 2018), *Annona cherimola* (Chen *et al.*, 1998), *Annona glabra* (Chang *et al.*, 2000) and *Polyalthia suberosa* (Tuchinda *et al.*, 2000).



N-trans-*p*-coumaroyl tyramine [356]

Table 38 NMR spectral data of compound HJ7 as compared with *N-trans-p*-coumaroyl tyramine

Position	Compound HJ7 (acetone- d_6)		<i>N-trans-p</i> -coumaroyl tyramine(pyridine- d_6)*	
	δ_H (mult., J in Hz)	δ_C	δ_H (mult., J in Hz)	δ_C
1	-	126.9	-	127.7
2	7.42 (1H, d, 8.7)	129.2	7.41 (1H, d, 8.4)	130.5
3	6.85 (1H, dd, 8.4, 2.1)	115.2	6.80 (1H, d, 8.4)	116.2
4	-	158.8	-	160.5
5	6.85 (1H, dd, 8.4, 2.1)	115.2	6.80 (1H, d, 8.4)	116.2
6	7.42 (1H, d, 8.7)	129.2	7.41 (1H, d, 8.4)	130.5
7	6.48 (1H, d, 15.6)	118.8	6.38 (1H, d, 15.5)	118.4
8	7.47 (1 H, d,15.6)	139.2	7.44 (1H, d, 15.5)	141.8
9	-	165.7	-	169.2
1'	-	130.2	-	131.3
2'	7.06 (1H, dd, 8.5, 2.1)	129.6	7.06 (1H, d, 8.6)	130.7
3'	6.77 (1H, dd, 8.4, 2.1)	115.7	6.73 (1H, d, 8.6)	116.7
4'	-	155.8	-	156.9
5'	6.77 (1H, dd, 8.4, 2.1)	115.7	6.73 (1H, d, 8.6)	116.7
6'	7.06 (1H, dd, 8.5, 2.1)	129.6	7.06 (1H, d, 8.6)	130.7
7'	2.74 (2H, t, 7.5)	34.8	2.75 (2H, t, 7.5)	35.8
8'	3.48 (2H, t, 7.5)	41.1	3.46 (2H, t, 7.5)	42.5

* (Al-Taweel *et al.*, 2012)

Mass Spectrum List Report

Analysis Info		Acquisition Date	1/26/2020 3:04:36 PM
Analysis Name	OSHTS28012020003.d	Operator	Administrator
Method	Tune_low_120_04092017.m	Instrument	microTOF 72
Sample Name	HuS-7		
	HuS-3A		

Acquisition Parameter			
Source Type	ESI	Ion Polarity	Positive
Scan Range	n/a	Capillary Exit	120.0 V
Scan Begin	50 m/z	Hexapole RF	180.0 V
Scan End	3000 m/z	Skimmer 1	60.0 V
		Hexapole 1	23.0 V
		Set Corrector Fill	50 V
		Set Pulsar Pull	337 V
		Set Pulsar Push	337 V
		Set Reflector	1300 V
		Set Flight Tube	9000 V
		Set Detector TOF	2295 V

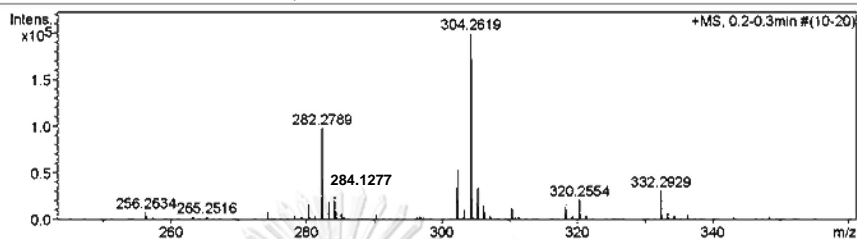


Figure 162 Mass spectrum of compound HJ7

HuS7 1H NMR 300 MHz in acetone-d6

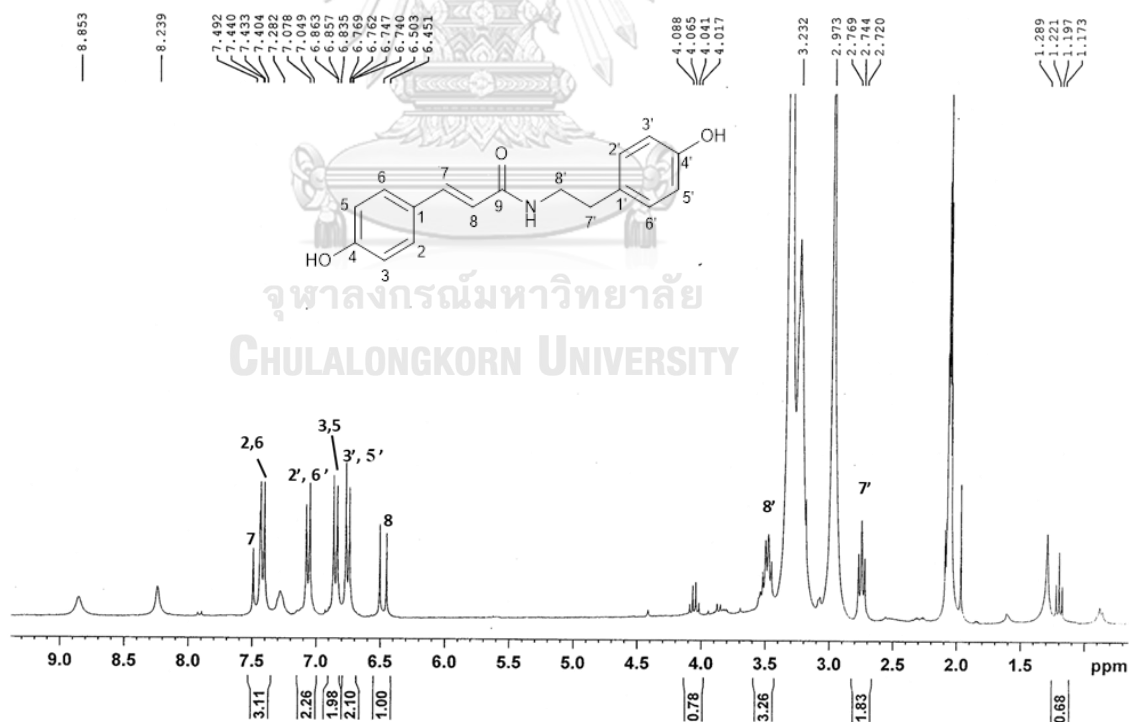


Figure 163 $^1\text{H-NMR}$ (300 MHz) spectrum of compound HJ7 (acetone- d_6)

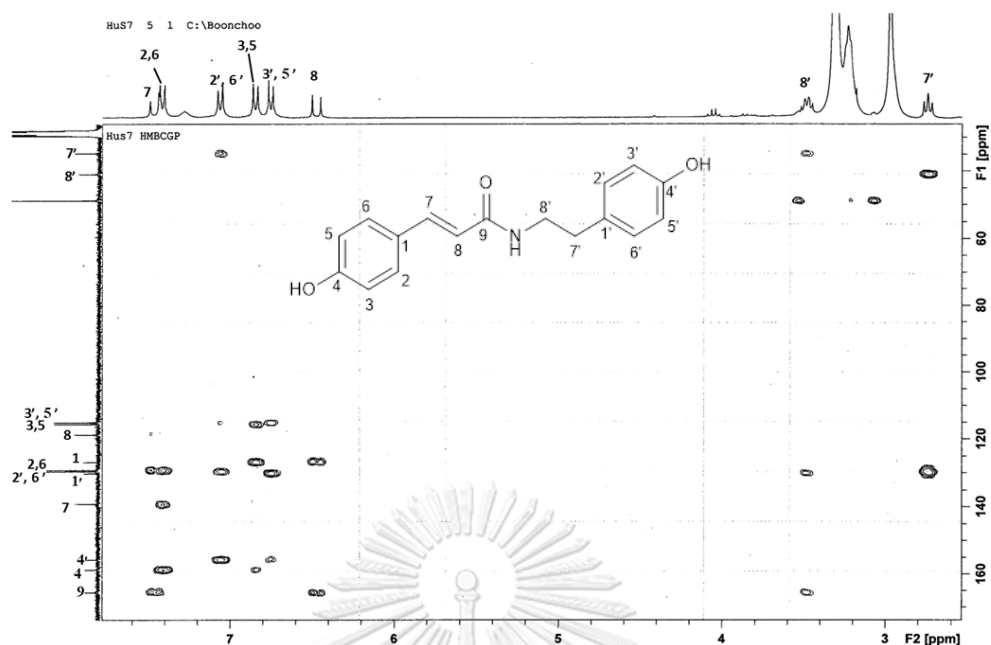


Figure 166 HMBC spectrum of compound HJ7

4.3 Biological activity of isolated compounds

Only five compounds isolated from *H. jenkinsii* were evaluated for α -glucosidase inhibitory activity. Compounds [352] and [353] were not included in the assay due to their insufficient quantity. *N-trans-feruloyl*tyramine [10] and *N-trans-p-coumaroyl* tyramine [356] showed IC_{50} values of 30.6 ± 2.9 and 0.6 ± 0.1 μ M, respectively in comparison with acarbose (IC_{50} at 724.7 ± 46 μ M). These values agreed with previously reported values (Panidthananon *et al.*, 2018). Mangiferin [337] showed an IC_{50} value of 253.6 ± 14.2 μ M. The α -glucosidase inhibitory activity of mangiferin was previously reported (Kulkarni & Rathod, 2018; Sekar *et al.*, 2019; Shi *et al.*, 2017). Allantoin [354] and oxylopinine [355] did not show α -glucosidase inhibition.

Table 39 α -Glucosidase inhibitory activity of compounds isolated from *H. jenkinsii*

compounds	% inhibition at 100 $\mu\text{g/ml}$	IC ₅₀ (μM)
mangiferin [337]*	96.9 \pm 1.0	253.6 \pm 14.2
HJ2 [352]	ND	ND
HJ3 [353]	ND	ND
allantoin [354]	NA	-
oxylopinine [355]	NA	NA
<i>N-trans</i> -feruloyltyramine [10]	92.2 \pm 1.1	30.6 \pm 2.9
<i>N-trans-p</i> -coumaroyl tyramine [356]	99.7 \pm 0.2	0.6 \pm 0.1
acarbose	21.9 \pm 1.5	724.7 \pm 46

* = tested at 300 $\mu\text{g/ml}$

ND= not detected, NA- not active.

Further studies were conducted on mangiferin [337], allantoin [354], oxylopinine [355], *N-trans*-feruloyltyramine [10] and *N-trans-p*-coumaroyl tyramine [356] for their glucose uptake enhancing potential. Each compound was prepared in three concentrations, i.e. 1, 10 and 100 $\mu\text{g/ml}$. (Table 40 and Figure 167) and then evaluated for cytotoxicity and glucose uptake stimulatory activity in L6 myotube cells. Under this condition, all the tested compounds did not show toxicity, except for *N-trans*-feruloyltyramine [10] which was toxic at 100 $\mu\text{g/ml}$. All compounds appeared to possess glucose uptake potential, but none had potency comparable to that of insulin (Table 40 and Figure 167).

Table 40 Glucose uptake stimulatory activity of compounds isolated from *H. jenkinsii*

Sample	Percentage of glucose uptake	Percent enhancement
DMSO	100	0
Metformin (2 mM)	443.9 ± 19.3*	343.9 ± 19.3
Insulin (500 nM)	246.6 ± 35.8*	146.6 ± 35.8
mangiferin [337]		
1 µg/ml	221.6 ± 48.0*	121.6 ± 48.0
10 µg/ml	228.4 ± 2.3*	128.4 ± 2.3
100 µg/ml	308.1 ± 10.7*	208.1 ± 10.7
allantoin [354]		
1 µg/ml	213.5 ± 21.3*	113.5 ± 21.3
10 µg/ml	260.8 ± 15.3*	160.8 ± 15.3
100 µg/ml	347.3 ± 15.3*	247.3 ± 15.3
oxylopinine [355]		
1 µg/ml	195.9 ± 30.0*	95.9 ± 30.0
10 µg/ml	231.1 ± 23.9*	131.1 ± 23.9
100 µg/ml l	332.4 ± 6.6*	232.4 ± 6.6
<i>N-trans-feruloyl</i> tyramine [10]		
1 µg/ml	175.7 ± 30.6*	75.7 ± 30.6
10 µg/ml	191.9 ± 49.8*	91.9 ± 49.8
100 µg/ml	ND	ND
<i>N-trans-p-coumaroyl</i> tyramine [356]		
1 µg/ml	229.7 ± 6.9*	129.7 ± 6.9
10 µg/ml	267.6 ± 62.0*	167.6 ± 62.2
100 µg/ml	321.6 ± 22.5*	221.6 ± 22.5

ND = not determined due to toxicity

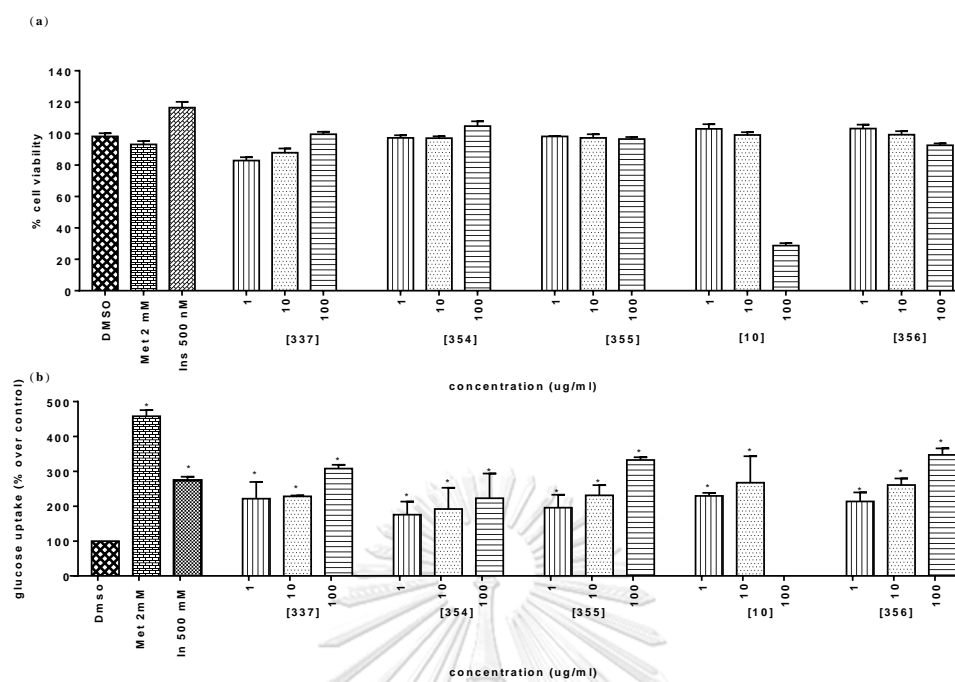


Figure 167 Cytotoxicity (a) and glucose uptake stimulatory activity (b) of isolated compounds

*($p < 0.05$) Significantly different when compared to the control (DMSO)

DMSO (control); Met = metformin, In = insulin (positive control)

CHAPTER V

CONCLUSION

This research primarily aimed to isolate the chemical constituents of four plants, including *Cissus javana*, *Dendrobium christyanum*, *Gastrochilus bellinus* and *Huberantha jenkinsii* and study their α -glucosidase inhibitory potential. A total of 27 compounds have been isolated and structurally characterized, comprising six new and twenty-one known naturally occurring compounds. The isolated compounds were investigated for α -glucosidase inhibitory activity. In addition, some compounds were further studied for the ability to stimulate cellular glucose uptake, as a secondary biological activity that may enhance their antidiabetic potential.

From *Cissus javana*, three known compounds including bergenin [31], stigmast-4-en-3-one [35], β -sitosterol [33] were isolated. In this investigation, bergenin [31] did not inhibit the enzyme α -glucosidase, but at a concentration of 100 $\mu\text{g/ml}$ showed 50.5 % enhancement of cellular glucose uptake. Under the same experimental condition, the two steroidal compounds, stigmast-4-en-3-one [35] and β -sitosterol [33], displayed significant enzyme inhibition (98.6 % and 40.6 % inhibition, respectively) in comparison with acarbose (21.9 % inhibition). However, the two compounds were not studied for cellular glucose uptake stimulatory activity due to their poor solubility in the test system. The results from this study constituted the first report of chemical and biological studies of the roots of *Cissus javana* and provided additional evidence for the antidiabetic potential of bergenin.

Repeated chromatographic separation of an extract prepared from the whole plant of *Dendrobium christyanum* led to the isolation of thirteen known compounds. They could be classified as alkyl cinnamate esters (*n*-eicosyl *trans*-ferulate [343], *n*-docosyl 4-hydroxy-*trans*-cinnamate [345]), a phenanthrene (4,5-dihydroxy-2-methoxy-

9,10-dihydrophenanthrene [103]), bibenzyls (moscatilin [59], aloifol I [38], gigantol [54], batatasin III [41], dendrosinen B [73]), a phenyl propanoid (coniferyl aldehyde [346]) and benzoic acid derivatives (methyl haematommate [342], atraric acid [344], vanillin [275] and diorcinolic acid [347]).

Among the isolates from this plant, methyl haematommate [342] and *n*-docosyl 4-hydroxy-*trans*-cinnamate [345] showed potent α -glucosidase inhibitory action with IC_{50} values of 18.7 ± 2.1 and 4.6 ± 0.2 μ M, respectively. When evaluated at the concentration of 100 μ g/ml, *n*-docosyl 4-hydroxy-*trans*-cinnamate [345] (0.212 mM), vanillin [275] (0.657 mM) and coniferyl aldehyde [346] (0.561 mM) could enhance glucose uptake by L6 myotubes by 31.6 ± 4.4 %, 97.1 ± 8.7 % and 56.4 ± 2.5 %, respectively, without toxicity. Furthermore, aloifol I [38] (0.036 mM) and batatasin III [41] (0.041 mM) showed 11.3 ± 2.5 % and 30.2 ± 6.7 % enhancement of cellular glucose uptake, respectively. The dual biological activity observed for these isolates may result in the increase of antidiabetic potential. This study is the first report of phytochemical and biological investigations of *Dendrobium christyanum*.

Prior to the present research, *Gastrochilus bellinus* was not investigated. Separation of the extract of *Gastrochilus bellinus* by repeated chromatography resulted in the isolation of four new compounds including three phenanthropyrans, [348], [349] and [350], and a phenanthrene derivative [351]. All isolates showed recognizable α -glucosidase inhibitory activity (IC_{50} values of GB1 [348], GB2 [349] and GB3 [350] = 88.7 ± 4.1 , 97.8 ± 3.1 and 45.9 ± 2.8 μ M, respectively) except for GB4 [351] (30.6 ± 1.3 % inhibition at 100 μ g/ml).

Huberantha jenkinsii was subjected to phytochemical investigation, and this led to the isolation of two new 8-oxoprotoberberine alkaloids [352] and [353], and five known compounds including mangiferin [337], allantoin [354], oxylopinine [355], *N-trans*-feruloyltyramine [10] and *N-trans-p*-coumaroyl tyramine [356]). Mangiferin [337] was obtained as the major component and showed potent α -glucosidase

inhibition (IC_{50} $253.6 \pm 14.2 \mu\text{M}$) as compared with acarbose (IC_{50} $724.7 \pm 46 \mu\text{M}$) and recognizable cellular glucose uptake enhancement ($208.1 \pm 10.7\%$ enhancement at 0.237 mM as compared with insulin ($146.6 \pm 35.8 \%$ enhancement at 500 nM). *N-trans-Feruloyltyramine* [10] and *N-trans-p-coumaroyl tyramine* [356] also showed strong inhibition of the enzyme α -glucosidase ($IC_{50} = 30.6 \pm 2.9$ and $0.6 \pm 0.1 \mu\text{M}$, respectively). They also showed some degree of glucose uptake stimulatory activity.

In summary, this dissertation describes the isolation of phytochemicals with α -glucosidase inhibitory potential from four plants belonging to three different plant families. The isolated compounds were found to be secondary metabolites with diverse structures. Some of the isolates showed strong α -glucosidase inhibitory activity, and several also displayed cellular glucose uptake enhancing property as a secondary activity, which may help increase their antidiabetic potential. The chemical and biological data of the phytochemicals obtained in this study have provided information that should be useful for the development of new antidiabetic agents from natural sources.

REFERENCES



จุฬาลงกรณ์มหาวิทยาลัย
CHULALONGKORN UNIVERSITY

- Al-Taweel, A. M., Perveen, S., El-Shafae, A. M., Fawzy, G. A., Malik, A., Afza, N., Iqbal, L., & Latif, M. (2012). Bioactive phenolic amides from *Celtis africana*. *Molecules*, *17*(3), 2675-2682.
- Asem B. D., Laitonjam W. S., Oinam I.S. & Jeena T.H. (2014). Isolation of compounds from the aqueous methanol extract of *Cissus javana* DC. leaves and determination of its trace element content through wet digestion. *Asian Journal of Chemistry*; *26*(13), 3820 -3822.
- Assob, J. C., Kamga, H. L., Nsagha, D. S., Njunda, A. L., Nde, P. F., Asongalem, E. A., ... & Penlap, V. B. (2011). Antimicrobial and toxicological activities of five medicinal plant species from Cameroon Traditional Medicine. *BMC Complementary and Alternative Medicine*, *11*(1), 70.
- Baldé, A. M., Claeys, M., Pieters, L., Wray, V., & Vlietinck, A. (1991). Ferulic acid esters from stem bark of *Pavetta owariensis*. *Phytochemistry*, *30*(3), 1024-1026.
- Beltrame, F. L., Pessini, G. L., Doro, D. L., Dias Filho, B. P., Bazotte, R. B., & Cortez, D. A. G. (2002). Evaluation of the antidiabetic and antibacterial activity of *Cissus sicyoides*. *Brazilian Archives of Biology and Technology*, *45*(1), 21-25.
- Bi, Z. M., Wang, T., & Xu, L. F. (2004). Chemical constituents of *Dendrobium moniliforme*. *Acta Botanica Sinica*, *46*(1), 124-126.
- Bischoff, H. (1994). Pharmacology of alpha-glucosidase inhibition. *European Journal of Clinical Investigation*, *24 Suppl 3*, 3-10.
- Bourgeois, G., Suire, C., Vivas, N., & Vitry, C. (1999). Atraric acid, a marker for epiphytic lichens in the wood used in cooperage: Identification and quantification by GC/MS/(MS). *Analisis*, *27*(3), 281-283.
- Brahmkshatriya, H. R., Shah, K. A., Ananthkumar, G. B., & Brahmkshatriya, M. H. (2015). Clinical evaluation of *Cissus quadrangularis* as osteogenic agent in maxillofacial fracture: A pilot study. *Ayurveda*, *36*(2), 169-173. doi:10.4103/0974-8520.175542

- Brindis, F., Gonzalez-Trujano, M. E., Gonzalez-Andrade, M., Aguirre-Hernandez, E., & Villalobos-Molina, R. (2013). Aqueous extract of *Annona macrophyllata*: A potential alpha-glucosidase inhibitor. *Biomed Research International*, 2013, 591313. doi:10.1155/2013/591313
- Carpinella, M. C., Giorda, L. M., Ferrayoli, C. G., & Palacios, S. M. (2003). Antifungal effects of different organic extracts from *Melia azedarach* L. On phytopathogenic fungi and their isolated active components. *Journal of Agricultural and Food Chemistry*, 51(9), 2506-2511.
- Chan, Y. Y., Wang, C. Y., Hwang, T. L., Juang, S. H., Hung, H. Y., Kuo, P. C., Chen, P. J., & Wu, T. S. (2018). The constituents of the stems of *Cissus assamica* and their bioactivities. *Molecules* (Basel, Switzerland), 23(11), 2799. doi:10.3390/molecules23112799
- Chand, M. B., Paudel, M. R., & Pant, B. (2016). The antioxidant activity of selected wild orchids of nepal. *Journal of Coastal Life Medicine*, 4(9), 731-736.
- Chang, C. C., Ku, A. F., Tseng, Y. Y., Yang, W. B., Fang, J. M., & Wong, C. H. (2010). 6,8-di-glycosyl flavonoids from *Dendrobium huoshanense*. *Journal of Natural Products*, 73, 229-232.
- Chang, F. R., Chen, C. Y., Hsieh, T. J., Cho, C. P., & Wu, Y. C. (2000). Chemical constituents from *Annona glabra* L. *Journal of the Chinese Chemical Society*, 47(4B), 913-920.
- Chang, S. J., Lin, T. H., & Chen, C. C. (2001). Constituents from the stems of *Dendrobium clavatum* var. *Aurantiacum*. *Journal of Chinese Medicine*, 12(3), 211-218.
- Chanvorachote, P., Kowitdamrong, A., Ruanghirun, T., Sritularak, B., Mungmee, C., & Likhitwitayawuid, K. (2013). Anti-metastatic activities of bibenzyls from *Dendrobium pulchellum*. *Natural Product Communications*, 8(1), 115-118.

- Chaowasku, T., Johnson, D. M., Van Der Ham, R. W., & Chatrou, L. W. (2012). Characterization of *Hubera* (Annonaceae), a new genus segregated from *Polyalthia* and allied to *Miliusa*. *Phytotaxa*, 69, 33-56.
- Chaowasku, T., Johnson, D. M., van der Ham, R. W. J. M., & Chatrou, L. W. (2015). Huberantha, a replacement name for *Hubera* (Annonaceae: Malmeoideae: Miliuseae). *Kew Bulletin*, 70(2). doi:10.1007/s12225-015-9571-z
- Chatsumpun, N., Sritularak, B., & Likhitwitayawuid, K. (2017). New biflavonoids with alpha-glucosidase and pancreatic lipase inhibitory activities from *Boesenbergia rotunda*. *Molecules*, 22(11). doi:10.3390/molecules22111862
- Chaudhury, A., Duvoor, C., Dendi, R., Sena, V., Kraleti, S., Chada, A., Ravilla, R., Marco, A., Shekhawat, N. S., & Montales, M. T. (2017). Clinical review of antidiabetic drugs: Implications for type 2 diabetes mellitus management. *Frontiers in Endocrinology*, 8, 6.
- Chaves, M. H., & Roque, N. F. (1997). Amides and lignanamides from *Porcelia macrocarpa*. *Phytochemistry*, 46(5), 879-881.
- Chen, C. Y., Chang, F.R., Yen, H. F., & Wu, Y. C. (1998a). Amides from stems of *Annona cherimola*. *Phytochemistry*, 49(5), 1443-1447.
- Chen, C. C., Wu, L. G., Ko, F. N., & Teng, C. M. (1994). Antiplatelet aggregation principles of *Dendrobium loddigesii*. *Journal of Natural Products*, 57(9), 1271-1274.
- Chen, X. J., Mei, W. L., Cai, C. H., Guo, Z. K., Song, X. Q., & Dai, H. F. (2014). Four new bibenzyl derivatives from *Dendrobium sinense*. *Phytochemistry Letters*, 9, 107-112. doi:10.1016/j.phytol.2014.04.012
- Chen, X. J., Mei, W. L., Zuo, W. J., Zeng, Y. B., Guo, Z. K., Song, X. Q., & Dai, H. F. (2013). A new antibacterial phenanthrenequinone from *Dendrobium sinense*. *Journal of Asian Natural Products Research*, 15(1), 67-70. doi:10.1080/10286020.2012.740473

- Chen, Y., Li, J., Wang, L., & Liu, Y. (2008a). Aromatic compounds from *Dendrobium aphyllum*. *Biochemical Systematics and Ecology*, 36(5), 458-460. doi:<https://doi.org/10.1016/j.bse.2007.11.004>
- Chen, Y., Li, Y., Qing, C., Zhang, Y., Wang, L., & Liu, Y. (2008b). 1,4,5-trihydroxy-7-methoxy-9h-fluoren-9-one, a new cytotoxic compound from *Dendrobium chrysotoxum*. *Food Chemistry*, 108(3), 973-976. doi:10.1016/j.foodchem.2007.12.007
- Chen, Y., Liu, Y., Jiang, J., Zhang, Y., & Yin, B. (2008c). Dendronone, a new phenanthrenequinone from *Dendrobium cariniferum*. *Food Chemistry*, 111(1), 11-12. doi:10.1016/j.foodchem.2008.03.017
- Chen, Y., Xu, J., Yu, H., Qing, C., Zhang, Y., Wang, L., Liu, Y., & Wang, J. (2008d). Cytotoxic phenolics from *Bulbophyllum odoratissimum*. *Food Chemistry*, 107(1), 169-173.
- Cheng, J. J., Tsai, T.-H., & Lin, L.-C. (2012). New alkaloids and cytotoxic principles from *Sinomenium acutum*. *Planta Medica*, 78(17), 1873-1877.
- Chiasson, J. L., Josse, R. G., Gomis, R., Hanefeld, M., Karasik, A., Laakso, M., & Group, S. N. T. R. (2002). Acarbose for prevention of type 2 diabetes mellitus: The stop-NIDDM randomised trial. *The Lancet*, 359(9323), 2072-2077.
- Chowdhury, N., Al Hasan, A., Tareq, F. S., Ahsan, M., & Azam, A. Z. (2013). 4-hydroxy-trans-cinnamate derivatives and triterpene from *Barleria cristata*. *Dhaka University Journal of Pharmaceutical Sciences*, 12(2), 143-145.
- Chumkaew, P., Teerapongpisan, P., Pechwang, J., & Srisawat, T. (2019). New oxoprotoberberine and aporphine alkaloids from the roots of *Amoora cucullata* with their antiproliferative activities. *Records of Natural Products*, 13(6), 498.
- Costa, E. V., Pinheiro, M. L. B., Barison, A., Campos, F. R., Salvador, M. J., Maia, B. H. L., Cabral, E. C., & Eberlin, M. N. (2010). Alkaloids from the bark of *Gutteria*

- hispid* and their evaluation as antioxidant and antimicrobial agents. *Journal of Natural Products*, 73(6), 1180-1183.
- Dahmen, J., & Leander, K. (1978). Amotin and amoenin, two sesquiterpenes of the picrotoxane group from *Dendrobium amoenum*. *Phytochemistry*, 17(11), 1949-1952.
- De Abreu, H. A., Lago, I. A. d. S., Souza, G. P., Piló-Veloso, D., Duarte, H. A., & Alcântara, A. F. D. C. (2008). Antioxidant activity of (+)-bergenin—a phytoconstituent isolated from the bark of *Sacoglottis uchi* Huber (Humireaceae). *Organic & Biomolecular Chemistry*, 6(15), 2713-2718.
- Diabetes Control and Complications Trial Research Group. (1993). The effect of intensive treatment of diabetes on the development and progression of long-term complications in insulin-dependent diabetes mellitus. *The New England Journal of Medicine*, 329(14), 977-986.
- Djemgou, P. C., Hussien, T. A., Hegazy, M. E. F., Ngandeu, F., Neguim, G., Tane, P., & Mohamed, A. E. H. H. (2010). C-glucoside xanthone from the stem bark extract of *Bersama engleriana*. *Pharmacognosy Research*, 2(4), 229.
- Don, G. D., Xinqi, C., Zhanhe, J., & Wood, J. J. (2009). *Flora of China* (Vol. 25, pp. 491–498).
- Dong, F. W., Fan, W. W., Xu, F. Q., Wan, Q. L., Su, J., Li, Y., Zhou, L., Zhou, J., & Hu, J.-M. (2013). Inhibitory activities on nitric oxide production of stilbenoids from *Pholidota yunnanensis*. *Journal of Asian Natural Products Research*, 15(12), 1256-1264.
- Du, Y. T., Rayner, C. K., Jones, K. L., Talley, N. J., & Horowitz, M. (2018). Gastrointestinal symptoms in diabetes: Prevalence, assessment, pathogenesis, and management. *Diabetes Care*, 41(3), 627-637.

- Duong, H. T. (2019). Phenolic compounds from *Pamotrema dilatatum* growing in Lam Dong province. *Science and Technology Development Journal*, 22(1), 114-119.
- Duong, H. T., Huynh, C. B. L., Ha, P. X., Ton, Q. T., & Nguyen, P. K. P. (2011). Some phenolic compounds of lichen *Pamotrema planatilobatum* (Hale) Hale (Parmeliaceae). *Science and Technology Development Journal*, 14(4), 5-10.
- eFloras. (2008). Retrieved 28 February 2020 from Missouri Botanical Garden, St. Louis, MO & Harvard University Herbaria Published on the Internet <http://www.efloras.org>
- El-Shanawany, M., Slatkin, D., Schiff, P., & El-Shabrawy, A. (1985). Oxylopidine and oxylopinine new alkaloids from *Oxandra xylopioides* Diels. *Bulletin of Pharmaceutical Sciences. Assiut*, 8(1), 172-191.
- Faizi, S., Khan, R. A., Azher, S., Khan, S. A., Tauseef, S., & Ahmad, A. (2003). New antimicrobial alkaloids from the roots of *Polyalthia longifolia* var. *pendula*. *Planta Medica*, 69(04), 350-355.
- Fan, Wang, W., Wang, Y., Qin, G., & Zhao, W. (2001). Chemical constituents from *Dendrobium densiflorum*. *Phytochemistry*, 57, 1225-1258.
- Fan, W. W., Xu, F. Q., Dong, F. W., Li, X. N., Li, Y., Liu, Y. Q., Zhou, J., & Hu, J. M. (2013). Dendrowardol C, a novel sesquiterpenoid from *Dendrobium wardianum* Warner. *Natural Products and Bioprospecting*, 3(3), 89-92. doi:10.1007/s13659-013-0024-9
- Fatma, N. (2013). Phytogeographical distribution of indian Vitaceae: A report. *International Journal of Science and Research*, 5(3), 2113-2117.
- Fernandes, G., & Banu, J. (2012). Medicinal properties of plants from the genus *Cissus*: A review. *Journal of Medicinal Plants Research*, 6(16), 3080-3086.
- Gadhiya, S., Ponnala, S., & Harding, W. W. (2015). A divergent route to 9,10-oxygenated tetrahydroprotoberberine and 8-oxoprotoberberine alkaloids:

- Synthesis of (\pm)-isocorypalmine and oxypalmatine. *Tetrahedron*, 71(8), 1227-1231.
- Gao, H., Huang, Y. N., Gao, B., Li, P., Inagaki, C., & Kawabata, J. (2008). Inhibitory effect on alpha-glucosidase by *Adhatoda vasica* Nees. *Food Chemistry*, 108(3), 965-972. doi:10.1016/j.foodchem.2007.12.002
- González, M. C., Zafra-Polo, C., Blázquez, M. A., Serrano, A., & Cortes, D. (1997). Cerasodine and cerasonine: New oxoprotoberberine alkaloids from *Polyalthia cerasoides*. *Journal of Natural Products*, 60(2), 108-110.
- Hakamata, W., Kurihara, M., Okuda, H., Nishio, T., & Oku, T. (2009). Design and screening strategies for α -glucosidase inhibitors based on enzymological information. *Current Topics in Medicinal Chemistry*, 9(1), 3-12.
- Honda, C., & Yamaki, M. (2000). Phenanthrenes from *Dendrobium plicatile*. *Phytochemistry*, 53, 987-990.
- Hu, J. M., Chen, J. J., Yu, H., Zhao, Y. X., & Zhou, J. (2008a). Five new compounds from *Dendrobium longicornu*. *Planta Medica*, 74(5), 535-539. doi:10.1055/s-2008-1074492
- Hu, J. M., Chen, J. J., Yu, H., Zhao, Y. X., & Zhou, J. (2008b). Two novel bibenzyls from *Dendrobium trigonopus*. *Journal of Asian Natural Products Research*, 10(7-8), 653-657. doi:10.1080/10286020802133605
- Hu, J. M., Fan, W. W., Dong, F. W., Miao, Z. H., & Zhou, J. (2012). Chemical components of *Dendrobium chrysotoxum*. *Chinese Journal of Chemistry*, 30(6), 1327-1330.
- Hu, J. M., Zhao, Y. X., Miao, Z. H., & Zhou, J. (2009). Chemical components of *Dendrobium polyanthum*. *Bulletin of the Korean Chemical Society*, 30(9), 2098-2100.
- Hu, Y., Zhang, C., Zhao, X., Wang, Y., Feng, D., Zhang, M., & Xie, H. (2016). (\pm)-Homocrepidine A, a pair of anti-inflammatory enantiomeric

- octahydroindolizine alkaloid dimers from *Dendrobium crepidatum*. *Journal of Natural Products*, 79(1), 252-256. doi:10.1021/acs.jnatprod.5b00801
- Huang, P. K., Lin, S. R., Riyaphan, J., Fu, Y. S., & Weng, C. F. (2019). Polyalthia clerodane diterpene potentiates hypoglycemia via inhibition of dipeptidyl peptidase 4. *International Journal of Molecular Sciences*, 20(3). doi:10.3390/ijms20030530
- Huneck, S., & Yoshimura, I. (1996). Identification of lichen substances. In *Identification of lichen substances* (pp. 11-123): Springer.
- Hussain, S. F., Gözler, B., Shamma, M., & Gözler, T. (1980). Feruloyltyramine from *Hypocoum*. *Phytochemistry*, 21(12), 2979-2980.
- Hwang, J. S., Lee, S. A., Hong, S. S., Han, X. H., Lee, C., Kang, S., J., Lee, D., Kim, Y., Hong, J., T., Lee, M. K., & Hwang, B. Y. (2010). Phenanthrenes from *Dendrobium nobile* and their inhibition of the LPS-induced production of nitric oxide in macrophage raw 2647 cells. *Bioorganic & Medicinal Chemistry Letters* 20(12), 3785-3787. doi: 10.1016/j.bmcl.2010.04.054
- Inthongkaew, P., Chatsumpun, N., Supasuteekul, C., Kitisripanya, T., Putalun, W., Likhitwitayawuid, K., & Sritularak, B. (2017). α -glucosidase and pancreatic lipase inhibitory activities and glucose uptake stimulatory effect of phenolic compounds from *Dendrobium formosum*. *Revista Brasileira de Farmacognosia*, 27(4), 480-487.
- ISO-10993-5. (2009). *Biological evaluation of medical devices. Part 5: Tests for cytotoxicity: In vitro methods* (3rd ed.): Switzerland.
- Ito, J., Chang, F. R., Wang, H. K., Park, Y. K., Ikegaki, M., Kilgore, N., & Lee, K. H. (2001). Anti-AIDS agents. 48. Anti-HIV activity of moronic acid derivatives and the new melliferone-related triterpenoid isolated from *Brazilian propolis*. *Journal of Natural Products*, 64(10), 1278-1281.

- Ito, M., Matsuzaki, K., Wang, J., Daikonya, A., Wang, N. L., Yao, X. S., & Kitanaka, S. (2010). New phenanthrenes and stilbenes from *Dendrobium loddigesii*. *Chemical and Pharmaceutical Bulletin*, *58*, 628-633.
- Juneja, R., Sharma, S., & Tandon, J. (1987). Two substituted bibenzyls and a dihydrophenanthrene from *Cymbidium aloifolium*. *Phytochemistry*, *26*(4), 1123-1125.
- Karunaratne, V., Thadhani, V. M., Khan, S. N., & Choudhary, M. I. (2014). Potent α -glucosidase inhibitors from the lichen *Cladonia* species from Sri Lanka. *Journal of the National Science Foundation of Sri Lanka*, *42*(1), 95-98.
- Kashima, Y., Yamaki, H., Suzuki, T., & Miyazawa, M. (2013). Structure-activity relationships of bergenin derivatives effect on α -glucosidase inhibition. *Journal of enzyme inhibition and medicinal chemistry*, *28*(6), 1162-1170.
- Khin, D., Myint (2000). *Government of the Union of Myanmar ministry of forestry survey on the lesser known species of medicinal plants of East Yoma and the socio-economic status of the local communities* (pp. 6).
- Kim, H. R., Min, H. Y., Jeong, Y. H., Lee, S. K., Lee, N. S., & Seo, E. K. (2005). Cytotoxic constituents from the whole plant of *Corydalis pallida*. *Archives of Pharmacal Research*, *28*(11), 1224.
- Kim, J. H., Oh, S. Y., Han, S. B., Uddin, G. M., Kim, C. Y., & Lee, J. K. (2015). Anti-inflammatory effects of *Dendrobium nobile* derived phenanthrenes in LPS-stimulated murine macrophages. *Archives of Pharmacal Research*, *38*(6), 117-1126.
- Klongkumnuankarn, P., Busaranon, K., Chanvorachote, P., Sritularak, B., Jongbunprasert, V., & Likhitwitayawuid, K. (2015). Cytotoxic and antimigratory activities of phenolic compounds from *Dendrobium brymerianum*. *Evidence-Based Complementary And Alternative Medicine*, *2015*, 350410. doi:10.1155/2015/350410

- Kolak, U., TOPÇU, G., Birteksöz, S., Ötük, G., & Ulubelen, A. (2005). Terpenoids and steroids from the roots of *Salvia blepharochlaena*. *Turkish Journal of Chemistry*, 29(2), 177-186.
- Kongkatitham, V., Muangnoi, C., Kyokong, N., Thaweeseest, W., Likhitwitayawuid, K., Rojsitthisak, P., & Sritularak, B. (2018). Anti-oxidant and anti-inflammatory effects of new bibenzyl derivatives from *Dendrobium parishii* in hydrogen peroxide and lipopolysaccharide treated RAW264.7 cells. *Phytochemistry Letters*, 24, 31-38. doi:10.1016/j.phytol.2018.01.006
- Kress, W., DeFilipps, R., Farr, E., & Kyi, D. (2003). A checklist of the trees, shrubs, herbs, and climbers of Myanmar. United states nat. Herb. 45: 1-590. National Museum of Natural History. *Smithsonian Institution, Washington DC*.
- Kulkarni, V. M., & Rathod, V. K. (2018). Exploring the potential of *Mangifera indica* leaves extract versus mangiferin for therapeutic application. *Agriculture and Natural Resources*, 52(2), 155-161.
- Kumar, R., Patel, D. K., Prasad, S. K., Laloo, D., Krishnamurthy, S., & Hemalatha, S. (2012). Type 2 antidiabetic activity of bergenin from the roots of *Caesalpinia digyna* rottler. *Fitoterapia*, 83(2), 395-401.
- Kumar, S., Narwal, S., Kumar, V., & Prakash, O. (2011). Alpha-glucosidase inhibitors from plants: A natural approach to treat diabetes. *Pharmacognosy Reviews*, 5(9), 19-29. doi:10.4103/0973-7847.79096
- Kyokong, N., Muangnoi, C., Thaweeseest, W., Kongkatitham, V., Likhitwitayawuid, K., Rojsitthisak, P., & Sritularak, B. (2018). A new phenanthrene dimer from *Dendrobium palpebrae*. *Journal of Asian Natural Products Research*, 1-7. doi:10.1080/10286020.2018.1429416
- Lakshmanan, G., Sivaraj, C., Ammar, A., Gopinath, S., Saravanan, K., Gunasekaran, K., & Murugesan, K. (2019). Isolation and structural elucidation of allantoin a

- bioactive compound from *Cleome viscosa* L.: A combined experimental and computational investigation. *Pharmacognosy Journal*, 11(6s),1391-1400.
- Lam, Y., Ng, T. B., Yao, R. M., Shi, J., Xu, K., Sze, S. C., & Zhang, K. Y. (2015). Evaluation of chemical constituents and important mechanism of pharmacological biology in *Dendrobium* plants. *Evidence-Based Complementary and Alternative Medicine*, 2015, 841752. doi:10.1155/2015/841752
- Langcake, P., & Pryce, R. J. (1976). The production of resveratrol by *Vitis vinifera* and other members of the Vitaceae as a response to infection or injury. *Physiological Plant Pathology*, 9(1), 77-86. doi:[https://doi.org/10.1016/0048-4059\(76\)90077-1](https://doi.org/10.1016/0048-4059(76)90077-1)
- Laprévôte, O., Roblot, F., Hocquemiller, R., & Cavé, A. (1988). Alcaloïdes des annonacées, 87. Azafluorénones de *l'unonopsis spectabilis*. *Journal of Natural Products*, 51(3), 555-561.
- Lassak, E.V., McCarthy, T., (1997). *Australian Medicinal Plants*. Reed Books, Victoria, Australia, P. 230.
- Le, T. N., & Cho, W.-J. (2008). First total synthesis of the phenolic 7,8-dihydro-8-oxoprotoberberine alkaloid, cerasonine. *Chemical and Pharmaceutical Bulletin*, 56(7), 1026-1029
- Lee, M. S., & Thuong, P. T. (2010). Stimulation of glucose uptake by triterpenoids from *Weigela subsessilis*. *Phytotherapy Research*, 24(1), 49-53. doi:10.1002/ptr.2865
- Li, Qing, C., Fang, T. T., Liu, Y., & Chen, Y. G. (2009a). Chemical constituents of *Dendrobium chrysotoxum*. *Chemistry of Natural Compounds*, 45(3), 414-416. doi:10.1007/s10600-009-9329-7
- Li, Wang, C. L., Wang, Y. J., Guo, S. X., Yang, J. S., Chen, X. M., & Xiao, P. G. (2009b). Three new bibenzyl derivatives from *Dendrobium candidum*. *Chemical and Pharmaceutical Bulletin*, 57(2), 218-219. doi:10.1248/cpb.57.218

- Li, Wang, C. H., Wang, Y. J., Wang, F. F., Guo, S. X., Yang, J. S., & G, X. P. (2009c). Four new bibenzyl derivatives from *Dendrobium candidum*. *Chemical and Pharmaceutical Bulletin*, 57(9), 997-999.
- Li, Yin, B. L., Liu, Y., Wang, L. Q., & Chen, Y. G. (2009d). Mono-aromatic constituents of *Dendrobium longicornu*. *Chemistry of Natural Compounds*, 45(2), 234-236.
- Li, C. B., Wang, C., Fan, W. W., Dong, F. W., Xu, F. Q., Wan, Q. L., Luo, H. R., Liu, Y. Q., Hu, J. M., & Zhou, J. (2013). Chemical components of *Dendrobium crepidatum* and their neurite outgrowth enhancing activities. *Natural Products and Bioprospecting*, 3(2), 70-73. doi:10.1007/s13659-012-0103-3
- Li, X. H., Guo, L., Yang, L., Peng, C., He, C. J., Zhou, Q. M., Xiong, L., Liu, J., & Zhang, T. M. (2014). Three new neolignan glucosides from the stems of *Dendrobium aurantiacum* var. *denneanum*. *Phytochemistry Letters*, 9, 37-40. doi:10.1016/j.phytol.2014.03.013
- Li, Y., Wang, C. L., Guo, S. X., Yang, J. S., & Xiao, P. G. (2008). Two new compounds from *Dendrobium candidum*. *Chemical and Pharmaceutical Bulletin*, 56(10), 1477-1479.
- Li, Y. P., Qing, C., Fang, T. T., Liu, Y., & Chen, Y. G. (2009). Chemical constituents of *Dendrobium chrysotoxum*. *Chemistry of Natural Compounds*, 45(3), 414-416.
- Limpanit, R., Chuanasa, T., Likhitwitayawuid, K., Jongbunprasert, V., & Sritularak, B. (2016). Alpha-glucosidase inhibitors from *Dendrobium tortile*. *Records of Natural Products*, 10(5), 609.
- Lin, T. H., Chang, S. J., Chen, C. C., Wang, J. P., & Tsao, L. T. (2001). Two phenanthraquinones from *Dendrobium moniliforme*. *Journal of Natural Products*, 64(8), 1084-1086.
- Lin, Y., Wang, F., Yang, L. J., Chun, Z., Bao, J. K., & Zhang, G. L. (2013). Anti-inflammatory phenanthrene derivatives from stems of *Dendrobium denneanum*. *Phytochemistry*, 95, 242-251.

- Lino, C., Sales, T., Gomes, P., do Amaral, J. F., Alexandre, F., Silveira, E., Ferreira, J., de Sousa, D., de Queiroz, M., & de Sousa, F. (2007). Anti-diabetic activity of a fraction from *Cissus verticillata* and tyramine, its main bioactive constituent, in alloxan-induced diabetic rats. *American Journal of Pharmacology and Toxicology*, 2(4), 178-188.
- Liu, Q., Zhou, S. S., Li, R., Tan, Y. H., Zyaw, M., Xing, X. K., & Gao, J. Y. (2020). Notes on the genus *Gastrochilus* (Orchidaceae) in Myanmar. *PhytoKeys*, 138, 113-123. doi:10.3897/phytokeys.138.38781
- Liu, Y., Jiang, J. H., Zhang, Y., & Chen, Y. G. (2009). Chemical constituents of *Dendrobium aurantiacum* var. *denneanum*. *Chemistry of Natural Compounds*, 45(4), 525-527.
- Lu, Y., Kuang, M., Hu, G.-P., Wu, R. B., Wang, J., Liu, L., & Lin, Y. C. (2014). Loddigesiinols G–J: Alpha-glucosidase inhibitors from *Dendrobium loddigesii*. *Molecules*, 19(6), 8544-8555.
- Macabeo, A. P. G., Rubio, P. Y. M., Alejandro, G. J. D., & Knorn, M. (2015). An alpha-glucosidase inhibitor from *Drepananthus philippinensis*. *Procedia Chemistry*, 14, 36-39.
- Majumder, P., Roychowdhury, M., & Chakraborty, S. (1997). Bibenzyl derivatives from the orchid *Bulbophyllum protractum*. *Phytochemistry*, 44(1), 167-172.
- Majumder, P. L., & Chatterjee, S. (1989). Crepidatin, a bibenzyl derivative from the orchid *Dendrobium crepidatum*. *Phytochemistry*, 28, 1986-1988.
- Majumder, P. L., Guha, S., & Sen, S. (1999). Bibenzyl derivatives from the orchid *Dendrobium amoenum*. *Phytochemistry*, 52, 1365-1369.
- Majumder, P. L., & Pal, S. (1992). Rotundatin, a new 9,10-dihydrophenanthrene derivative from *Dendrobium rotundatum*. *Phytochemistry*, 31(9), 3225-3228.

- Majumder, P. L., & Pal, S. (1993). Cumulatin and tristin, two bibenzyl derivatives from the orchids *Dendrobium cumulatum* and *Bulbophyllum triste*. *Phytochemistry*, *52*, 1561-1565.
- Majumder, P. L., & Sen, R. C. (1987). Moscatilin, a bibenzyl derivative from the orchid *Dendrobium moscatum*. *Phytochemistry*, *26*, 2121-2124.
- Matsuda, H., Morikawa, T., Xie, H., & Yoshikawa, M. (2004). Antiallergic phenanthrenes and stilbenes from the tubers of *Gymnadenia conopsea*. *Planta Medica*, *70*(09), 847-855.
- Meesakul, P., Pyne, S. G., & Laphookhieo, S. (2018). Potent alpha-glucosidase inhibitory activity of compounds isolated from the leaf extracts of *Uvaria hamiltonii*. *Natural Product Research*, 1-5. doi:10.1080/14786419.2018.1538996
- Méndez-López, L. F., Garza-González, E., Ríos, M. Y., Ramírez-Cisneros, M., Alvarez, L., González-Maya, L., Sánchez-Carranza, J. N., & Camacho-Corona, M. d. R. (2020). Metabolic profile and evaluation of biological activities of extracts from the stems of *Cissus trifoliata*. *International Journal of Molecular Sciences*, *21*(3), 930.
- Meng, C. W., He, Y. L., Peng, C., Ding, X. J., Guo, L., & Xiong, L. (2017). Picrotoxane sesquiterpenoids from the stems of *Dendrobium nobile* and their absolute configurations and angiogenesis effect. *Fitoterapia*, *121*, 206-211. doi:10.1016/j.fitote.2017.07.017
- Min, Y. D., Kwon, H. C., Yang, M. C., Lee, K. H., Choi, S. U., & Lee, K. R. (2007). Isolation of limonoids and alkaloids from *Phellodendron amurense* and their multidrug resistance (MDR) reversal activity. *Archives of Pharmacal Research*, *30*(1), 58-63.
- Mitsumoto, Y., Burdett, E., Grant, A., & Klip, A. (1991). Differential expression of the GLUT1 and GLUT4 glucose transporters during differentiation of L6 muscle

- cells. *Biochemical and Biophysical Research Communications*, 175(2), 652-659.
- Mittraphab, A., Muangnoi, C., Likhitwitayawuid, K., Rojsitthisak, P., & Sritularak, B. (2016). A new bibenzyl-phenanthrene derivative from *Dendrobium signatum* and its cytotoxic activity. *Natural Product Communications*, 11(5), 657-659.
- Miyazawa, M., Shimamura, H., Nakamura, S. I., Sugiura, W., Kosaka, H., & Kameoka, H. (1999). Moscatilin from *Dendrobium nobile*, a naturally occurring bibenzyl compound with potential antimutagenic activity. *Journal of Agricultural and Food Chemistry*, 47(5), 2163-2167.
- Mohammed, A., Victoria Awolola, G., Ibrahim, M. A., Anthony Koorbanally, N., & Islam, M. S. (2019). Oleanolic acid as a potential antidiabetic component of *Xylopiya aethiopica* (Dunal) A. Rich. (Annonaceae) fruit: Bioassay guided isolation and molecular docking studies. *Natural Product Research*, 1-4. doi:10.1080/14786419.2019.1596094
- Mughal, M. A., Memon, M. Y., Zardari, M. K., Tanwani, R. K., & Ali, M. (2000). Effect of acarbose on glycemic control, serum lipids and lipoproteins in type 2 diabetes. *Journal-Pakistan Medical Association*, 50(5), 152-156.
- Na Ranong, S., Likhitwitayawuid, K., Mekboonsonglarp, W., & Sritularak, B. (2019). New dihydrophenanthrenes from *Dendrobium infundibulum*. *Natural Product Research*, 33(3), 420-426.
- Nanakorn, W., & Indharamusika, S. (1999). *Ex-situ conservation of native thai orchids at queen Sirikit botanic garden*. Paper presented at the Proceedings of International Conference on Biodiversity and Bioresources: Conservation and Utilization.
- Nishioka, T., Kawabata, J., & Aoyama, Y. (1998). Baicalein, an α -glucosidase inhibitor from *Scutellaria baicalensis*. *Journal of Natural Products*, 61(11), 1413-1415.

- Nkobole, N., Houghton, P. J., Hussein, A., & Lall, N. (2011). Antidiabetic activity of *Terminalia sericea* constituents. *Natural Product Communications*, 6(11), 1934578X1100601106.
- Nyemb, J. N., Djankou, M. T., Talla, E., Tchinda, A. T., Ngoudjou, D. T., Iqbal, J., & Mbafor, J. T. (2018). Antimicrobial, α -glucosidase and alkaline phosphatase inhibitory activities of bergenin, the major constituent of *Cissus populnea* roots. *Medicinal Chemistry*, 08(02). doi:10.4172/2161-0444.1000492
- Nyemb, J. N., Ndoubalem, R., Talla, E., Tchinda, A. T., Ndjonga, D., Henoumont, C., Laurent, S., & Mbafor, J. T. (2018). DPPH antiradical scavenging, anthelmintic and phytochemical studies of *Cissus poulnea* rhizomes. *Asian Pacific Journal of Tropical Medicine*, 11(4), 280.
- Nyunt, K. S., Elkhateeb, A., Tosa, Y., Nabata, K., Katakura, K., & Matsuura, H. (2012). Isolation of antitrypanosomal compounds from *Vitis repens*, a medicinal plant of myanmar. *Natural Product Communications*, 7(5), 1934578X1200700516.
- Oyenihi, O. R., Oyenihi, A. B., Adeyanju, A. A., & Oguntibeju, O. O. (2016). Antidiabetic effects of resveratrol: The way forward in its clinical utility. *Journal of Diabetes Research*, 2016.
- Pan, H., Chen, B., Li, F., & Wang, M. (2012). Chemical constituents of *Dendrobium denneanum*. *Chinese Journal Application Environmental Biology*, 18(3), 378-380.
- Pan, L. H., Feng, B. J., Wang, J. H., Zha, X. Q., & Luo, J. P. (2013). Structural characterization and anti-glycation activity *in vitro* of a water-soluble polysaccharide from *Dendrobium huoshanense*. *Journal of Food Biochemistry*, 37(3), 313-321.
- Panidthananon, W., Chaowasku, T., Sritularak, B., & Likhitwitayawuid, K. (2018). A new benzophenone c-glucoside and other constituents of *Pseuduvaria fragrans*

- and their alpha-glucosidase inhibitory activity. *Molecules*, 23(7). doi:10.3390/molecules23071600
- Patra, A., Montgomery, C. T., Freyer, A. J., Guinaudeau, H., Shamma, M., Tantisewie, B., & Pharadai, K. (1987). The protoberberine alkaloids of *Stephania suberosa*. *Phytochemistry*, 26(2), 547-549.
- Paudel, M. R., Rajbanshi, N., Sah, A. K., Acharya, S., & Pant, B. (2018). Antibacterial activity of selected *Dendrobium* species against clinically isolated multiple drug resistant bacteria. *African Journal of Microbiology Research*, 12(18), 426-432.
- Phechrmeekha, T., Sritularak, B., & Likhitwitayawuid, K. (2012). New phenolic compounds from *Dendrobium capillipes* and *Dendrobium secundum*. *Journal of Asian Natural Products Research*, 14(8), 748-754. doi:10.1080/10286020.2012.689979
- Pinho, P. M., Pinto, M. M., Kijjoa, A., Pharadai, K., Díaz, J. G., & Herz, W. (1992). Protoberberine alkaloids from *Coscinium fenestratum*. *Phytochemistry*, 31(4), 1403-1407.
- The plant list (2010). Retrieved 28 February, 2020 <http://www.theplantlist.org/>
- Prasad, C. V., Anjana, T., Banerji, A., & Gopalakrishnapillai, A. (2010). Gallic acid induces GLUT-4 translocation and glucose uptake activity in 3T3-L1 cells. *FEBS letters*, 584(3), 531-536.
- Prasad, R., & Koch, B. (2014). Antitumor activity of ethanolic extract of *Dendrobium formosum* in T-cell lymphoma: An *in vitro* and *in vivo* study. *BioMed research international*, 2014, 753451-753451. doi:10.1155/2014/753451
- Promchai, T., Jaidee, A., Cheenpracha, S., Trisuwan, K., Rattanajak, R., Kamchonwongpaisan, S., Laphookhieo, S., Pyne, S. G., & Ritthiwigrom, T. (2016). Antimalarial oxoprotoberberine alkaloids from the leaves of *Milusa cuneata*. *Journal of Natural Products*, 79(4), 978-983.

- Punthakee, Z., Goldenberg, R., & Katz, P. (2018). Definition, classification and diagnosis of diabetes, prediabetes and metabolic syndrome. *Canadian Journal of Diabetes*, 42, S10-S15. doi:10.1016/j.jcjd.2017.10.003
- Qin, X. D., Qu, Y., Ning, L., Liu, J. K., & Fan, S. K. (2011). A new picrotoxane-type sesquiterpene from *Dendrobium findlayanum*. *Journal of Asian Natural Products Research*, 13, 1047-1050.
- Rasheed, A., Afifi, F. U., Shaedah, M., & Taha, M. O. (2004). Investigation of the active constituents of *Portulaca oleraceae* L. (Portulacaceae) growing in Jordan. *Pakistan Journal of Pharmaceutical Sciences*, 17(1), 37-45.
- Rungwichaniwat, P., Sritularak, B., & Likhitwitayawuid, K. (2014). Chemical constituents of *Dendrobium williamsonii*. *Pharmacognosy Journal*, 6(3), 36-41. doi:10.5530/pj.2014.3.6
- Sabeerali, A., Manikandan, S., & Alagu Lakshmanan, G. (2016). Review on phytochemical and pharmacological activities of the genus *Cissus* Linn. *International Journal of Pharmaceutical Research*, 8(4), 1.
- Sani, Y., Musa, A., Tajuddeen, N., Abdullahi, S., Abdullahi, M., Pateh, U., & Idris, A. (2015). Isoliquiritigenin and beta-sitosterol from *Cissus polyantha* tuber glycid and brandt. *Journal of Medicinal Plants Research*, 9(35), 918-921.
- Sarakulwattana, C., Mekboonsonglarp, W., Likhitwitayawuid, K., Rojsitthisak, P., & Sritularak, B. (2018). New bisbibenzyl and phenanthrene derivatives from *Dendrobium scabrilingue* and their α -glucosidase inhibitory activity. *Natural Product Research*, 1-8.
- Sawangjit, R., Puttarak, P., Saokaew, S., & Chaiyakunapruk, N. (2017). Efficacy and safety of *Cissus quadrangularis* L. In clinical use: A systematic review and meta-analysis of randomized controlled trials. *Phytotherapy Research*, 31(4), 555-567. doi:10.1002/ptr.5783

- Schleich, S., Papaioannou, M., Baniahmad, A., & Matusch, R. (2006). Activity-guided isolation of an antiandrogenic compound of *Pygeum africanum*. *Planta Medica*, 72(06), 547-551.
- Sekar, V., Chakraborty, S., Mani, S., Sali, V., & Vasanthi, H. (2019). Mangiferin from *Mangifera indica* fruits reduces post-prandial glucose level by inhibiting α -glucosidase and α -amylase activity. *South African Journal of Botany*, 120, 129-134.
- Sesti, G. (2006). Pathophysiology of insulin resistance. *Best practice & research Clinical Endocrinology & Metabolism*, 20(4), 665-679.
- Shi, Z. L., Liu, Y. D., Yuan, Y. Y., Song, D., Qi, M. F., Yang, X. J., Wang, P., Li, X. Y., Shang, J. H., & Yang, Z. X. (2017). *In vitro* and *in vivo* effects of norathyriol and mangiferin on α -glucosidase. *Biochemistry Research International*, 2017.
- Singh, G., Rawat, P., & Maurya, R. (2007). Constituents of *Cissus quadrangularis*. *Natural Product Research*, 21(6), 522-528. doi:10.1080/14786410601130471
- Smitinand, T. (2001). *Thai plant names* (Revised Edition ed.). Bangkok: Forest Herbarium-Royal Forest Department.
- Sripathi, S. K., Gopal, P., & Lalitha, P. (2011). Allantoin from the leaves of *Pisonia grandis* R. Br. *International Journal of Pharmacy and Life Sciences*, 2(6), 815-817.
- Sritularak, B., Duangrak, N., & Likhitwitayawuid, K. (2011a). A new bibenzyl from *Dendrobium secundum*. *Zeitschrift für Naturforschung C*, 66(5), 205-208.
- Sritularak, B., Anuwat, M., & Likhitwitayawuid, K. (2011b). A new phenanthrenequinone from *Dendrobium draconis*. *Journal of Asian Natural Product Research*, 13(3), 251-255. doi:10.1080/10286020.2010.546354
- Sritularak, B., & Likhitwitayawuid, K. (2009). New bisbibenzyls from *Dendrobium falconeri*. *Helvetica Chimica Acta*, 92, 740-744.

- Sukphan, P., Sritularak, B., Mekboonsonglarp, W., Lipipun, V., & Likhitwitayawuid, K. (2014). Chemical constituents of *Dendrobium venustum* and their antimalarial and anti-herpetic properties. *Natural Product Communications*, 9(6), 825-827.
- Sun, J., Zhang, F., Yang, M., Zhang, J., Chen, L., Zhan, R., Li, L., & Chen, Y. (2014). Isolation of alpha-glucosidase inhibitors including a new flavonol glycoside from *Dendrobium devonianum*. *Natural Product Research*, 28(21), 1900-1905. doi:10.1080/14786419.2014.955495
- Sun, S., Kadouh, H. C., Zhu, W., & Zhou, K. (2016). Bioactivity-guided isolation and purification of α -glucosidase inhibitor, 6-O-D-glycosides, from Tinta Cão grape pomace. *Journal of Functional Foods*, 23, 573-579.
- Suresh, K., & Sunil, S. (2010). Anti-diabetic potential of *Vitis vinifera* root extract against streptozotocin induced diabetic rats. *International Journal of Medical Sciences (India)*, 3(1/2), 19-23.
- Tadic, D., Cassels Niven, B., & Cavé, A. (1988). Spectral properties of ring-C-oxygenated 4-azafluorenes and 4-azafluorenones. The structures of natural onychine derivatives. *Heterocycles*, 27(1), 407-420.
- Talapatra, B., Das, A. K., & Talapatra, S. K. (1989). Defuscin, a new phenolic ester from *Dendrobium fuscescens*: Conformation of shikimic acid. *Phytochemistry*, 28(1), 290-292.
- Tanagornmeatar, K., Chaotham, C., Sritularak, B., Likhitwitayawuid, K., & Chanvorachote, P. (2014). Cytotoxic and anti-metastatic activities of phenolic compounds from *Dendrobium ellipsophyllum*. *Anticancer Research*, 34, 6573-6580.
- Teixeira da Silva, J. A., & Ng, T. B. (2017). The medicinal and pharmaceutical importance of *Dendrobium* species. *Applied Microbiol Biotechnology*, 101(6), 2227-2239. doi:10.1007/s00253-017-8169-9

- Toussirot, M., Nowik, W., Hnawia, E., Lebouvier, N., Hay, A. E., de la Sayette, A., Dijoux-Franca, M. G., Cardon, D., & Nour, M. (2014). Dyeing properties, coloring compounds and antioxidant activity of *Hubera nitidissima* (Dunal) Chaowasku (Annonaceae). *Dyes and Pigments*, 102, 278-284. doi:10.1016/j.dyepig.2013.11.010
- Tuchinda, P., Pohmakotr, M., Munyoo, B., Reutrakul, V., & Santisuk, T. (2000). An azanthracene alkaloid from *Polyalthia suberosa*. *Phytochemistry*, 53(8), 1079-1082.
- Turner, I. M., & Utteridge, T. M. (2016). Whither *Polyalthia* (Annonaceae) in Peninsular Malaysia? Synopses of *Huberantha*, *Maasia*, *Monoon* and *Polyalthia* ss. *European Journal of Taxonomy*(183), 1-26.
- Veerraju, P., Rao, N. S. P., Rao, L. J., Rao, K. V. J., & Rao, P. R. M. (1989). Amoenumin, a 9,10-dihydro-5H-phenanthro-(4,5-b,c,d)-pyran from *Dendrobium amoenum*. *Phytochemistry*, 28, 950-951.
- Viana, G. S. B., Medeiros, A. C. C., Lacerda, A. M. R., Leal, L. K. A. M., Vale, T. G., & Matos, F. J. D. A. (2004). Hypoglycemic and anti-lipemic effects of the aqueous extract from *Cissus sicyoides*. *BMC Pharmacology*, 4, 9-9. doi:10.1186/1471-2210-4-9
- Wang, H., Zhao, T., & Che, C. T. (1985). Dendrobine and 3-hydroxy-2-oxodendrobine from *Dendrobium nobile*. *Journal of Natural Products*, 48, 796-801.
- Wang, L., Zhang, C. F., Wang, Z. T., Zhang, M., & Xu, L. S. (2009). Five new compounds from *Dendrobium crystallinum*. *Journal of Asian Natural Products Research*, 11, 903-911.
- Wang, M. L., Du, J., Chen, R. Y., & Yu, D. Q. (2000). Alkaloids from the roots of *saccopetalum prolificum*. *Chinese Chemical Letters*, 11(2), 129-130.

- Wang, P., Kong, C. H., Sun, B., & Xu, X. H. (2012). Distribution and function of allantoin (5-ureidohydantoin) in rice grains. *Journal of Agricultural and Food Chemistry*, 60(11), 2793-2798.
- Wang, X. N., Yu, W. T., & Lou, H. X. (2005). Antifungal constituents from the Chinese moss *Homalia trichomanoides*. *Chemistry & Biodiversity*, 2(1), 139-145.
- Wang, Y. H., Zhang, Z. K., He, H. P., Wang, J. S., Zhou, H., Ding, M., & Hao, X. J. (2007). Stilbene C-glucosides from *Cissus repens*. *Journal of Asian Natural Products Research*, 9(7), 631-636. doi:10.1080/10286020600979548
- Wei, W., Feng, L., Bao, W. R., Ma, D. L., Leung, C. H., Nie, S. P., & Han, Q. B. (2016). Structure characterization and immunomodulating effects of polysaccharides isolated from *Dendrobium officinale*. *Journal of Agricultural and Food Chemistry*, 64(4), 881-889. doi:10.1021/acs.jafc.5b05180
- Wilcox, G. (2005). Insulin and insulin resistance. *The Clinical Biochemist Reviews*, 26, 19-29.
- Worldview International Foundation. (2016). *Final report on collection of seed from the endangered orchids*: Worldview International Foundation, Norway.
- Wu, H. S., Xu, J. H., Chen, L. Z., & Sun, J. J. (2004). Studies on anti-hyperglycemic effect and its mechanism of *Dendrobium candidum*. *Zhongguo Zhong Yao Za Zhi*, 29(2), 160-163.
- Wu, L. J., Zheng, C. J., Wang, L. K., Han, C. R., Song, X. P., Chen, G. Y., Zhou, X. M., Wu, S. Y., Li, X. B., & Bai, M. (2016). One new berberine from the branches and leaves of *Polyalthia obliqua* hook. F. & thomson. *Natural Product Research*, 30(20), 2285-2290.
- Wu, L., Lu, Y., Ding, Y., Zhao, J., Xu, H., & Chou, G. (2019). Four new compounds from *Dendrobium devonianum*. *Natural Product Research*, 33(15), 2160-2168.

- Xia, E. Q., Deng, G. F., Guo, Y. J., & Li, H. B. (2010). Biological activities of polyphenols from grapes. *International Journal of Molecular Sciences*, *11*(2), 622-646. doi:10.3390/ijms11020622
- Xie, Y., Deng, P., Zhang, Y., & Yu, W. (2009). Studies on the chemical constituents from *Cissus assamica*. *Zhong Yao Cai*, *32*(2), 210-213.
- Xiong, L., Cao, Z. X., Peng, C., Li, X. H., Xie, X. F., Zhang, T. M., Zhou, Q. M., Yang, L., & Guo, L. (2013). Phenolic glucosides from *Dendrobium aurantiacum* var. *denneanum* and their bioactivities. *Molecules*, *18*(6), 6153-6160.
- Xu, F. Q., Fan, W. W., Zi, C. T., Dong, F. W., Yang, D., Zhou, J., & Hu, J. M. (2017). Four new glycosides from the stems of *Dendrobium fimbriatum* Hook. *Natural Product Research*, *31*(7), 797-801. doi:10.1080/14786419.2016.1247076
- Xu, F. Q., Xu, F. C., Hou, B., Fan, W. W., Zi, C. T., Li, Y., Dong, F. W., Liu, Y. Q., Sheng, J., Zuo, Z. L., & Hu, J. M. (2014). Cytotoxic bibenzyl dimers from the stems of *Dendrobium fimbriatum* Hook. *Bioorganic & Medicinal Chemistry Letters*, *24*, 5268-5273.
- Yamaki, M., & Honda, C. (1996). The stilbenoids from *Dendrobium plicatile*. *Phytochemistry*, *43*(1), 207-208.
- Yang, L.C., Wang F., Liu M. (1998). A study of an endothelin antagonist from a Chinese anti-snake venom medicinal herb. *Cardiovascular Pharmacology*, *31* (1), 249-250.
- Yang, Liu, S. J., Luo, H. R., Cui, J., Zhou, J., Wang, X. J., Sheng, J., & Hu, J. M. (2015). Two new dendrocandins with neurite outgrowth-promoting activity from *Dendrobium officinale*. *Journal of Asian Natural Products Research*, *17*(2), 125-131. doi:10.1080/10286020.2014.942294
- Yang, Qin, L. H., Bligh, S. W., Bashall, A., Zhang, C. F., Zhang, M., Wang, Z. T., & Xu, L. S. (2006a). A new phenanthrene with a spiro lactone from *Dendrobium*

- chrysanthum* and its anti-inflammatory activities. *Bioorganic & Medicinal Chemistry*, 14(10), 3496-3501. doi:10.1016/j.bmc.2006.01.004
- Yang, L., Wang, Z., & Xu, L. (2006b). Phenols and a triterpene from *Dendrobium aurantiacum* var. *denneanum* (orchidaceae). *Biochemical Systematics and Ecology*, 34(8), 658-660. doi:10.1016/j.bse.2006.03.003
- Yang, D., Liu, L. Y., Cheng, Z. Q., Xu, F. Q., Fan, W. W., Zi, C. T., Dong, F. W., Zhou, J., Ding, Z. T., & Hu, J. M. (2015). Five new phenolic compounds from *Dendrobium aphyllum*. *Fitoterapia*, 100, 11-18.
- Yang, H., Chou, G. X., Wang, Z. T., Guo, Y. W., Hu, Z. B., & Xu, L. S. (2004). Two new compounds from *Dendrobium chrysotoxum*. *Helvetica Chimica Acta*, 87(2), 394-399.
- Yang, H., Sung, S. H., & Kim, Y. C. (2007). Antifibrotic phenanthrenes of *Dendrobium nobile* stems. *Journal of Natural Products*, 70, 1925-1929.
- Yang, M., Chen, L. J., Zhang, Y., & Chen, Y. G. (2017a). Two new picrotoxane-type sesquiterpenoid lactones from *Dendrobium williamsonii*. *Journal of Asian Natural Products Research*, 1-5. doi:10.1080/10286020.2017.1394294
- Yang, M., Zhang, Y., Chen, L., & Chen, Y. (2017b). A new (propylphenyl) bibenzyl derivative from *Dendrobium williamsonii*. *Natural Product Research*, 32(14), 1699-1705.
- Ye, Q. H., Zhao, W. M., & Qin, G. W. (2003). New fluorenone and phenanthrene derivatives from *Dendrobium chrysanthum*. *Natural Product Research*, 17(3), 201-205. doi:10.1080/1057563021000040817
- Ye, Q., Mei, Y., Yang, P., Cheng, L., & Kong, D. (2016). A new 9,10-dihydrophenanthrene glycoside from *Dendrobium primulinum*. *Chemistry of Natural Compounds*, 52(3), 381-383. doi:10.1007/s10600-016-1653-0
- Ye, Q., Qin, G., & Zhao, W. (2002). Immunomodulatory sesquiterpene glycosides from *Dendrobium nobile*. *Phytochemistry*, 61, 885-890.

- Ye, Q., & Zhao, W. (2002). New alloaromadendrane, cadinene and cyclocopacamphane type sesquiterpene derivatives and bibenzyls from *Dendrobium nobile*. *Planta Medica*, *68*, 723-729.
- Ye, Q. H., Zhao, W. M., & Qin, G. W. (2004). Lignans from *Dendrobium chrysanthum*. *Journal of Asian Natural Products Research*, *6*(1), 39-43.
- Yin, Z., Zhang, W., Feng, F., Zhang, Y., & Kang, W. (2014). **A**lpha-glucosidase inhibitors isolated from medicinal plants. *Food Science and Human Wellness*, *3*(3-4), 136-174.
- Ying, L., Jin-He, J., Yan, Z., & Ye-Gao, C. (2009). Chemical constituents of *Dendrobium aurantiacum* var. *denneanum*. *Chemistry of Natural Compounds*, *45*(4), 525.
- Zhang, Liu, S. J., Yang, L., Yuan, M. Y., Li, J. Y., Hou, B., Li, H. M., Yang, X. Z., Ding, C. C., & Hu, J. M. (2017). Sesquiterpene amino ether and cytotoxic phenols from *Dendrobium wardianum* Warner. *Fitoterapia*, *122*, 76-79. doi:10.1016/j.fitote.2017.08.015
- Zhang, Wang, M., Wang, L., Iinuma, M., Zhang, M., Xu, L.-S., & Wang, Z.-T. (2008a). Chemical constituents of *Dendrobium gratiosissimum* and their cytotoxic activities. *Indian Journal of Chemistry*, *47B*(6), 952-956.
- Zhang, G. N., Zhong, L. Y., Bligh, S. W. A., Guo, Y. L., Zhang, C. F., Zhang, M., Wang, Z. T., & Xu, L. S. (2005). Bi-bicyclic and bi-tricyclic compounds from *Dendrobium thysiflorum*. *Phytochemistry*, *66*, 1113-1120. doi:10.1016/j.phytochem.2005.04.001
- Zhang, X., Gao, H., Han, H. Y., Liu, H. W., Wang, N. L., Yao, X. S., & Wang, Z. (2007a). Sesquiterpenes from *Dendrobium nobile*. *Chinese Traditional and Herbal Drugs*, *38*(12), 1771-1774.
- Zhang, X., Gao, H., Wang, N. L., & Yao, X. S. (2006). Three new bibenzyl derivatives from *Dendrobium nobile*. *Journal of Asian Natural Products Research*, *8*(1-2), 113-118. doi:10.1080/10286020500480654

- Zhang, X., Tu, F. J., Yu, H. Y., Wang, N. L., Wang, Z., & Yao, X. S. (2008b). Copacamphane, picrotoxane and cyclocopacamphane sesquiterpenes from *Dendrobium nobile*. *Chemical and Pharmaceutical Bulletin*, *56*(6), 854-857.
- Zhang, X., Xu, J. K., Wang, J., Wang, N. L., Kurihara, H., Kitanaka, S., & Yao, X. S. (2007b). Bioactive bibenzyl derivatives and fluorenones from *Dendrobium nobile*. *Journal of Natural Products*, *70*, 24-28.
- Zhang, X., Xu, J. K., Wang, N. L., Kurihara, H., & Yao, X. S. (2008c). Antioxidant phenanthrenes and lignans from *Dendrobium nobile*. *Journal of Chinese Pharmaceutical Sciences*, *17*, 314-318.
- Zhang, Y., Zhang, L., Liu, J., Liang, J., Si, J., & Wu, S. (2017). *Dendrobium officinale* leaves as a new antioxidant source. *Journal of Functional Foods*, *37*, 400-415. doi:<https://doi.org/10.1016/j.jff.2017.08.006>
- Zhang, Y. Y., Wang, P., Song, X. Q., Zuo, W. J., Wang, H., Chen, L. L., Mei, W. L., & Dai, H. F. (2018). Chemical constituents from *Dendrobium hainanense*. *Journal of Asian Natural Products Research*, 1-8. doi:10.1080/10286020.2018.1475476
- Zhao, C., Liu, Q., Halaweish, F., Shao, B., Ye, Y., & Zhao, W. (2003). Copacamphane, picrotoxane, and alloaromadendrane sesquiterpene glycosides and phenolic glycosides from *Dendrobium moniliforme*. *Journal of Natural Products*, *66*(8), 1140-1143. doi:10.1021/np0301801
- Zhao, G. Y., Deng, B. W., Zhang, C. Y., Cui, Y. D., Bi, J. Y., & Zhang, G. G. (2018). New phenanthrene and 9, 10-dihydrophenanthrene derivatives from the stems of *Dendrobium officinale* with their cytotoxic activities. *Journal Of Natural Medicines*, *72*(1), 246-251. doi:10.1007/s11418-017-1141-2
- Zhao, N., Yang, G., Zhang, Y., Chen, L., & Chen, Y. (2016). A new 9,10-dihydrophenanthrene from *Dendrobium moniliforme*. *Natural Product Research*, *30*(2), 174-179. doi:10.1080/14786419.2015.1046379

- Zhao, W., Ye, Q., Tan, X., Jiang, H., Li, X., Chen, K., & Kinghorn, A. D. (2001). Three new sesquiterpene glycosides from *Dendrobium nobile* with immunomodulatory activity. *Journal of Natural Products*, 64(9), 1196-1200.
- Zhao, X., Sun, P., Qian, Y., & Suo, H. (2014). *D. Candidum* has *in vitro* anticancer effects in HCT-116 cancer cells and exerts *in vivo* anti-metastatic effects in mice. *Nutrition Research and Practice*, 8(5), 487-493. doi:10.4162/nrp.2014.8.5.487
- Zhao, Y., Son, Y. O., Kim, S. S., Jang, Y. S., & Lee, J. C. (2007). Antioxidant and anti-hyperglycemic activity of polysaccharide isolated from *Dendrobium chrysotoxum* Lindl. *BMB Reports*, 40(5), 670-677.
- Zhou, X. M., Zheng, C. J., Wu, J. T., Chen, G. Y., Chen, J., & Sun, C. G. (2016). Five new lactone derivatives from the stems of *Dendrobium nobile*. *Fitoterapia*, 115, 96-100. doi:10.1016/j.fitote.2016.10.002
- Zhou, X. M., Zheng, C. J., Wu, J. T., Chen, G. Y., Zhang, B., & Sun, C. G. (2017). A new phenolic glycoside from the stem of *Dendrobium nobile*. *Natural Product Research*, 31(9), 1042-1046. doi:10.1080/14786419.2016.1266352

VITA

NAME	Ms. Htoo Tint San
DATE OF BIRTH	17 July 1990
PLACE OF BIRTH	Yangon, Myanmar
INSTITUTIONS ATTENDED	University of Pharmacy (Yangon), Myanmar Faculty of Pharmaceutical Sciences, Chulalongkorn University,
HOME ADDRESS	54/1, 5th street, 14/1 ward, South Okkalapa, Yangon, Myanmar
PUBLICATION	<ol style="list-style-type: none"> 1. San, H. T., Boonsongcheep, P., Putalun, W., Mekboonsonglarp, W., Sritularak, B., & Likhitwitayawuid, K. (2020). α-Glucosidase inhibitory and glucose uptake stimulatory effects of phenolic compounds from <i>Dendrobium christyanum</i>. <i>Natural Product Communications</i>, 15(3), 1934578X20913453. 2. San, H. T., Boonsongchee, P., Putalun, W., Sritularak, B., & Likhitwitayawuid, K. (2020). Bergenin from <i>Cissus javana</i> DC.(Vitaceae) root extract enhances glucose uptake by rat L6 myotubes. <i>Tropical Journal of Pharmaceutical Research</i>, 19(5), 1081-1086. 3. San, H. T., Chaowasku, T., Mekboonsonglarp, W., Rodsiri, R., Sritularak, B., Buraphaka, H., Putalun, W., & Likhitwitayawuid, K. (2020) .Constituents of <i>Huberantha jenkinsii</i> and their biological activities. <i>Molecules</i> [accepted] 4. San, H. T., Mekboonsonglarp, W., Sritularak, B., & Likhitwitayawuid, K. (2020). α-Glucosidase Inhibitors from <i>Gastrochilus bellinus</i> [in preparation]



จุฬาลงกรณ์มหาวิทยาลัย
CHULALONGKORN UNIVERSITY